THE CONTRIBUTION OF VASCULAR ADHESION PROTEIN-1 TO GLUCOSE AND LIPID HOMEOSTASIS IN THE LIVER

BY

SUMERA KARIM

A thesis submitted to the
University of Birmingham
For the degree of
DOCTOR OF PHILOSOPHY

Institute of Biomedical Research
The School of Immunity & Infection
College of Medical & Dental Sciences
University of Birmingham
May 2013

ABSTRACT

NAFLD is characterized by simple steatosis, which can progress to chronic inflammation and fibrosis. Vascular Adhesion Protein-1 (VAP-1) is an adhesion molecule with semicarbazide-sensitive amine oxidase (SSAO) activity, which is also expressed as a soluble protein in serum (sVAP-1) and elevated in inflammatory liver diseases such as NAFLD. VAP-1 has been shown to modulate glucose and lipid uptake in muscle and adipose tissue and thus we investigated whether it may contribute to glucose and lipid homeostasis in human liver tissue. Recreating the multicellular liver environment using an *ex-vivo* model we have shown that activation of VAP-1 by its substrate methylamine leads to activation of NF-κB, glucose uptake and lipid accumulation in the human liver with changes in transporter expression of GLUT4, GLUT10 and GLUT13, as well as FABP2, LRP1, FATP2, FATP3, FATP4 and FATP6. We have also documented changes in transporter expression profiles in human disease. In conclusion, we demonstrate for the first time global alterations in cellular expression of glucose and lipid transporter proteins in NASH. We confirm that VAP-1 is elevated in disease and that SSAO activity of VAP-1 results in enhanced hepatic glucose and lipid accumulation with changes in transporter expression. Thus we propose that bioactive metabolites of SSAO activity contribute to the metabolic derangement evident in fatty liver disease.

Work arising from this thesis

Published Manuscripts

An in vitro model of human acute ethanol exposure that incorporates CXCR3 and CXCR4 dependent recruitment of immune cells,
Sumera Karim, Evaggelia Liaskou, Samuel Hadley, Janine Youster, Jeffrey Faint, David H Adams, Patricia F Lalor, Toxicological Sciences, January 2013 132 (1): 131-141

Hepatic expression and cellular distribution of the glucose transporter family, **Sumera Karim**, David H Adams, Patricia F Lalor, World Journal of Gastroenterology, 2012 December 14; 18 (46): 6771-6781

Published Abstracts

Digestive Disorders Federation (DDF) combined meeting for BSG, AUGIS, BAPEN and BASL. Joint Meeting, June 7–20 2012, Arena and Convention Centre (ACC), Liverpool, UK. Poster presentation. (Awarded poster of distinction), published in Gut 2012; 61:Suppl 2 A86-A87.

The liver meeting, 62nd annual meeting of the American association for the study of liver diseases (ASSLD), November 4-8 2011, Moscone West Convention Center, San Francisco, CA. Poster presentation. Published in Hepatology, 2011, Volume 54, Number 4, 1174A.

British association for the study of liver (BASL), 7-9 September 2011, Royal College of physicians, London. Poster presentation. Published in special addition of GUT 2011; 60: Supplement 2, A40-A41

American society for Mass Spectrometry, 59th Annual Meeting. June 5-9th 2011, Denver, Colorado. (Poster presentation). Published in Journal for the American Society for Mass Spectrometry, Volume 22, Supplement 1.

International presentations

International society for Hepatic Sinusoidal Research, 16th International Symposium on cells of the Hepatic Sinusoid, Sinusoidal cells and the metabolic syndrome. September 22-24, 2011. Florence, Italy.

Manuscripts In preparation

Dysregulated hepatic expression of glucose transporters in NASH: The contribution of amine oxidase activity to hepatic glucose uptake.
Sumera Karim, Evaggelia Liaskou, Janine Fear, Abhilok Garg, Lee Claridge, Gary Reynolds, Sirpa Jalkanen, David H Adams, Philip N. Newsome and Patricia F Lalor.

Use of MALDI Image analysis to determine disease-specific expression of variant forms of L-FABP in non-alcoholic fatty liver disease.
Josephine Bunch, **Sumera Karim**, Joscelyn Sarsby, Anna Bradford, Evangelia Liaskou, Janine Fear, Patricia F. Lalor.

The formation of atheroma is linked to steatohepatitis and hyper triglyceridaemia by inflammatory signalling through the lymphotoxin-β receptor.
Mathew J. Harrison, Cécile Bénézech, **Sumera Karim**, Carl F. Ware, Patricia. F. Lalor, Jorge H. Caamaño, G. Ed Rainger.

Multivariate and correlation analysis of MALDI mass spectrometry imaging data reveals features in human Non-Alcoholic Steatohepatitis (NASH) liver samples.
Andrew D. Palmer, Alan M. Race, Rian L. Griffiths, Rory T. Steven, **Sumera Karim**, Patricia F Lalor, Iain Styles, Josephine Bunch.

Learn from yesterday, live for today, hope for tomorrow. The important thing is not to stop questioning.

Albert Einstein

Dedication

I dedicate this thesis to mum and my late father Abdul Karim.

ACKNOWLEDGEMENTS

I would like to take this opportunity and show my gratitude to my supervisor Dr PF Lalor and co supervisor Professor P Newsome who gave me the opportunity to do this PhD and also to Professor DH Adams. In particular I would like to say a special thank you to Dr PF Lalor for her excellent guidance throughout my PhD and for supporting me not only academically but also personally. I am eternally grateful to her. Thank you also to my past and present industrial supervisors for their support and advice on microarrays.

This PhD would not have been possible without my funding bodies, so a special thank you to BBSRC and my industrial sponsors for funding my PhD. Professor S Jalkanen for providing VAP-1 constructs and our collaborators from chemistry Dr J Bunch and Rian Griffiths. A big thank you to everyone in the liver labs for all their support in particular Ben James and Dr Evangelia Liaskou who showed me many of the techniques when I started and Dr Lee Claridge for providing the mouse samples used in this study.

I feel I have had an amazing journey both scientifically and personally and although there are many lows and highs during a PhD the highs certainly make up for the lows. Last but not least I would like to thank my family, firstly my mum who has always been there for me, who has never let me down and who's supported me in everything I have ever done. I would like to thank my husband and my best friend Naveed Liaquat who has believed in me and has supported me and has always found a way to cheer me up, to the rest of my family thank you for your continued support and encouragement and finally thank you to my beautiful son Ismaeel Sabih Naveed for being a good little boy whilst mummy was writing up.

TABLE OF CONTENTS

LIST OF FIGURES

LIST OF TABLES

LIST OF ABBREVIATIONS

AA	Amino Acid
Acetyl-CoA	Acetyl Coenzyme A
ACS	Acyl CoA Activity
AFLD	Alcoholic Fatty Liver Disease
ALD	Alcoholic Liver Disease
ALT	Alanine Transaminase
AMP	Adenosine Monophosphate
AO	Amine Oxidase
ASH	Alcoholic Steatohepatitis
AST	Aspartate Transaminase
ATP	Adenosine Triphosphate
BACS	Bile Acid CoA Synthetase
BAPN	β-Aminopropanitrile
BEA	2-Bromoethylamine
BEC	Biliary Epithelial Cells
BMI	Body Mass Index
BSA	Bovine Serum Albumin
C	Chlorgyline
CAV1	Caveolin 1
CHCA	α-Cyano-4-Hydroxycinnamic Acid
ChREPP	Carbohydrate-Responsive Element-Binding Protein
CPS1	Carbamoyl Phosphate Synthase 1
CPT1	Carnitine Palmitoyltransferase I
DAB	3,3'Diaminobenzidine Tetrahydrochloride
DCA	Deoxycholic Acid
DHB	2,5,Dhydroxybenzoic acid
DMEM	Dulbecco's Modified Eagle's Medium
DMSO	Dimethyl Sulfoxide
DNL	De Novo Lipogenesis
DPM	Disintegrations Per Minute
DPX	Depex
ECM	Extra Cellular Matrix
EDTA	Ethylene Diaminotetraacetic Acid
EGF	Epidermal Growth Factor
EGTA	Ethylene Glycol Tetraacetic Acid
ELISA	Enzyme-Linked Immunosorbent Assay
ER	Endoplasmic Reticulum
FA	Fatty Acid
FABP	Fatty Acid Binding Protein
FATP	Fatty Acid Transporter Protein

FCS	Fetal Calf Serum
FFA	Free Fatty Acid
FAD	Flavin-Adenine-Dinucleotide
FOXO-1	Forkhead Box Protein O1
FP	Focusing Potential
FXRα	Farnesoid X Receptor Alpha
G-6-P	Glucose-6-Phosphate
GC	Gas Chromatography
GLP-1	Glucagon-Like-Peptide-1
GLP-2	Glucagon Like Peptide-2
GRP78	Glucose Regulated Protein
GS	Glycogen Synthase
GSC	Group Specific Component
GSK3	Glycogen Synthase Kinase 3
H&E	Hematoxylin and Eosin
HCC	Hepatocellular Carcinoma
HDL	High Density Lipoproteins
HEA	Human Epithelial Antibody
HEPES	4-(2-hydroxyethyl)-1-Piperazineethanesulfonic Acid
HFD	High Fat Diet
HFE	Hemochromatosis
HGF	Hepatocyte Growth Factor
HIAA	5-Hydroxyindoleacetic Acid
HSC	Hepatic Stellate Cells
HSEC	Hepatic Sinusoidal Endothelial Cells
HSL	Hormone-Sensitive Lipase
IBD	Inflammatory Bowel Disease
ICAM-1	Intercellular Adhesion Molecule 1
IFC	Integrated Fluidic Circuit
IL-8	Interleukin 8
IL-6	Interleukin-6
IR	Insulin Resistance
IRS	Insulin Receptor Substrates
JAK-STAT	Janus Kinase Signal Transducer and Activator of Transcription
JNK	Jun N-terminal Kinase
K	Potassium
kDA	kiloDalton
KO	Knock Out
LCFA	Long Chain Fatty Acid
LCP1	Lymphocyte Cytosolic Protein 1
LDL	Low-Density Lipoprotein
LESA	Liquid Extraction Surface Analysis Mass Spectrometry
LOX	Lysyl Oxidase

LPS	Lipopolysaccharide
LRPs	Receptor Related Proteins
MAdCAM-1	Mucosal Addressin Cell Adhesion Molecule-1
MALDI-MS	Matrix-Assisted Laser Desorption Ionisation - Mass Spectrometry Imaging
MALDI-MSI	Matrix-Assisted Laser Desorption Ionization Mass Spectrometry Imaging
MAOA	Monoamine Oxidase A
MAOB	Monoamine Oxidase B
MetS	Metabolic Syndrome
MnSOD	Manganese Superoxide Dismutase
MRI	Magnetic Resonance Imaging
MTP	Mitochondrial Transfer Protein
MTT	Methyl Thiazol Tetrazolium
NADPH	Nicotinamide Adenine Dinucleotide Phosphate
NAFLD	Non-Alcoholic Fatty Liver Disease
NASH	Non-Alcoholic Steatohepatitis
NEFA	Non-Esterified Fatty Acid
NF-κB	Nuclear Factor kappa B
NK	Natural Killer
NO	Nitrogen Oxide
OA	Oleic Acid
OCT	Optimal Cutting Temperature Polymer
P	Pargyline
PA	Palmitic acid
PBC	Primary Biliary Cirrhosis
PBMC	Peripheral Blood Mono Nuclear Cells
PBS	Phosphate Buffered Saline
PC	Phosphocholine
PCA	Principal Components Analysis
PCLS	Precision Cut Liver Slices
PEPCK	Phosphoenolpyruvate Carboxykinase
PI3-K	Phosphoinositide 3-Kinase
PM	Plasma Membrane
PPARGC1A	Peroxisome Proliferator-Activated Receptor Gamma Coactivator 1-Alpha
PPARα	Peroxisome Proliferator-Activated Receptor Alpha
PPARδ	Peroxisome Proliferator-Activated Receptor Delta
RBC	Red Blood Cells
ROS	Reactive Oxygen Species
RT	Retention Times
RTC	Rat Tail Collagen
SA	3,5,dimethoxy-4-Hydroxycinnamic Acid
sCD36	Soluble CD36
SLC2A	Solute Carrier 2A Protein

SREBP	Sterol Regulatory Element-Binding Protein
SSAO	Semicarbazide-Sensitive Amine Oxidase
sVAP-1	Soluble Vascular Adhesion Protein
TAG	Triglyceride
TBS	Tris-Buffered Saline
TCA	Tricarboxylic Acid Cycle
TGFβ	Transforming Growth Factor β
TMB	Tetramethylbenzidine
TNFα	Tumour Necrosis Factor-Alpha
TPQ	Topa Quinone
UDCA	Ursodeoxycholic Acid
UK	United Kingdom
VAP-1	Vascular Adhesion Protein 1
VEGF	Vascular Endothelial Growth Factor
VLDLPs	Very Low Density Lipoproteins
VSMC	Vascular Smooth Muscle Cells
WHO	World Health Organisation
WT	Wild Type

CHAPTER 1

1 GENERAL INTRODUCTION

1.1 Overview

1.1.1 The Human Liver

The liver is the largest visceral organ in the body weighing approximately 1.5kg in an average adult and a remarkable organ with regenerative capacity. It is enclosed in a coating of the visceral peritoneum and wrapped in a tough fibrous capsule (Martini, 2006). It lies just under the diaphragm protected by the rib cage in the right upper quadrant of the abdominal cavity (Sheila Sherlock, 2002). The liver consists of two lobes the right and left, which are separated on the anterior, posterior and inferior surface by the falciform ligament, ligamentum venosum and ligamentum teres (Martini, 2006). The right lobe is the largest lobe of the two, which is further, subdivided in to two smaller lobes the caudate lobe on the posterior surface and the quadrate lobe on the inferior surface (Sheila Sherlock, 2002).

Each lobe of the liver is further divided in to approximately 100,000 liver lobules forming the functional units of the liver (Martini, 2006). The liver has a dual blood supply arising from the hepatic artery which carries approximately 20-30% of blood flow to the liver and is rich in oxygen (Greenway and Stark, 1971) and the hepatic portal vein which supplies almost 70-80% of blood which is rich in nutrients from the small intestine (Greenway and Stark, 1971). These branch into smaller vessels allowing the blood to flow through the sinusoids and subsequently to the central vein of a single lobule before drainage into the hepatic vein.

In a cross section of the liver the lobules appear to be hexagonal in shape and at each corner there is the hepatic triad consisting of a branch of the hepatic artery, branch of the portal vein and a branch of the bile duct, which is lined with Biliary Epithelial Cells (BEC). The portal triad also contains the lymphatic vessels and the Vagus nerve.

1.1.2 The Liver Acinus

The liver acinus (Figure 1.1) is the main metabolic functional unit of the liver (Rappaport et al., 1954) and is best described as a diamond shape as it lies along two portal triads and spreads away towards two central veins. It is divided in to three zones based on the flow of blood. Thus, Zone 1 is closest to the flow of blood from the portal triad (periportal) rich in oxygen, nutrients and hormones, Zone 2 is located between Zone 1 and Zone 3 (transition zone) and Zone 3 is closest to blood leaving the hepatocytes via the central vain (centrilobular Zone) low in oxygen and rich in waste products for example metabolites and carbon dioxide. This zonation of the liver can change, based on metabolic alterations such as post birth, in the fetal liver and during starvation (Katz, 1992).

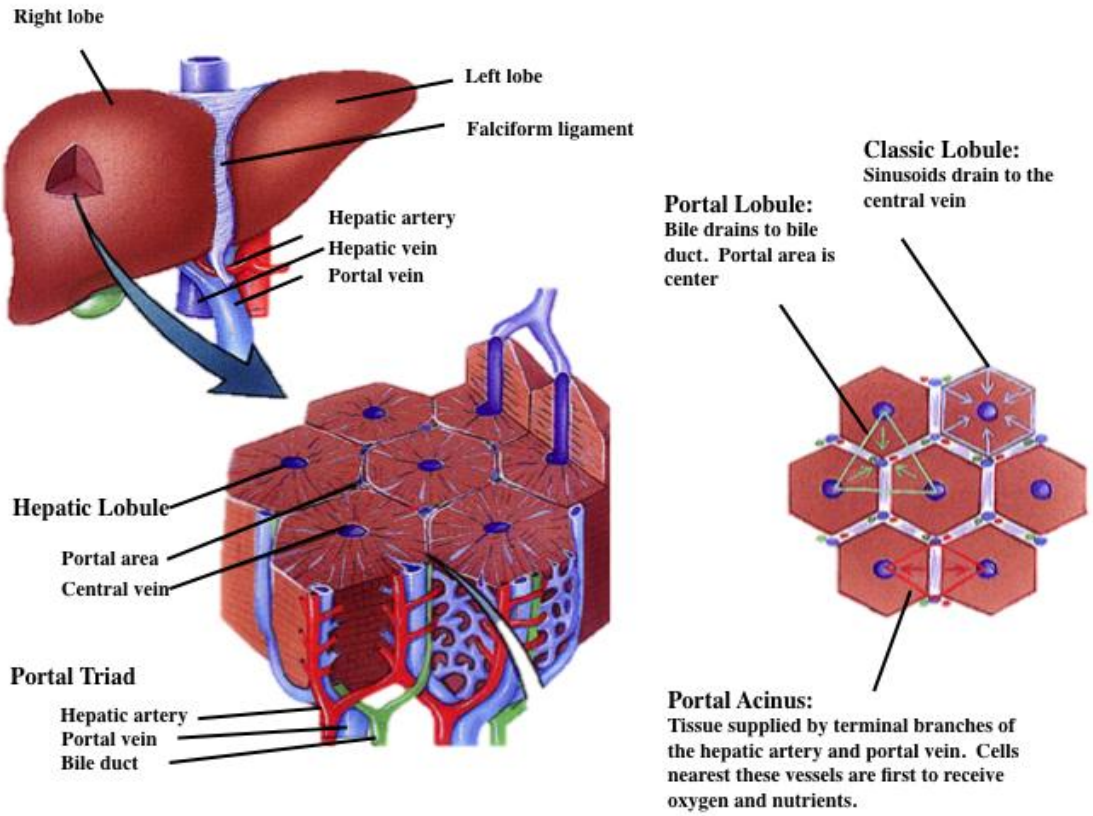

Figure 1.1: Structure and morphology of the liver
The liver is made up of two lobes the right and left that the falciform ligament separates. The right lobe is subdivided in to two smaller lobes the caudate lobe on the posterior surface and the quadrate lobe on the inferior surface (not shown). The liver has a dual blood supply arising from the hepatic portal vein and the hepatic artery. The lobes of the liver are further divided in to smaller lobules, which are hexagonal in shape at each corner there is the hepatic triad consisting of a branch of the hepatic artery, branch of the portal vein and a branch of the bile duct. The liver acinus is a diamond shape (shown in red) it lays along two portal triads and spreads away towards two central veins. Image adapted from: http://medcell.med.yale.edu/systems_cell_biology/liver_and_pancreas/images/liver_cartoon.jpg

The liver lobule/acinus contains many cell types, which can be classified into parenchymal epithelial cells, the hepatocytes which compromise approximately 80% of the liver volume (Wisse et al., 1996) and non-parenchymal cells which include non epithelial cells which occupy 6.5% of the liver volume (Wisse et al., 1996).

1.1.3 Liver cells

The different cell types are distinctly located in the liver for example each lobule consists of hepatocytes arranged in plates, and each plate is separated by sinusoids lined with Hepatic Sinusoidal Endothelial Cells (HSEC). The Kupffer Cells (KC) are attached to the endothelium and the Hepatic Stellate Cells (HSCs) reside between the hepatocytes and HSEC in the space of Disse (space between the hepatocytes and HSEC). Lymphocytes, dendritic and other immune cells are often present in the sinusoidal lumen and within the parenchyma and the functions of each in the normal liver and pathological conditions are discussed below.

1.1.3.1 Hepatocytes and Biliary epithelium

Hepatocytes are multifaceted cells, which are found in layers packed on top of each other, with microvilli on their sinusoidal face. Hepatocytes are the predominant and main functional cells of the liver containing large amounts of mitochondria, which provide energy for their numerous functions. There is a functional heterogeneity of these cells across the acinus, for example there are respectively more mitochondria in Zone 1 hepatocytes compared to Zone 3 (Loud, 1968) and increased activities of gluconeogenic and amino acid metabolism enzymes (Katz et al., 1977a), (Katz et al., 1977b), (Welsh, 1972), (Katz, 1992). In contrast Zone 3 hepatocytes have high expression of glycolytic and liponeogenic enzymes (Katz, 1992). Thus it has been proposed Zone 1 hepatocytes have a main role in oxidative energy metabolism whilst Zone 3 have a favored role in glucose uptake, glycolysis and liponeogenesis (Jungermann, 1988). Hepatocytes are in close contact with HSEC, which line the sinusoids.

The other major epithelial component of the liver is the biliary epithelium. These cells are BEC and function to modify bile and are also involved in the immune response by secreting

chemokines (Wu et al., 2004). BEC are affected in Primary Biliary Cirrhosis (PBC) which is a destructive autoimmune disease targeting the biliary ducts and is associated with inflammation and fibrosis (Popov and Popova, 1986), (Reshetnyak, 2006). Furthermore bile acids have been considered as signaling molecules and have been implicated in glucose and lipid homeostasis by activating Farnesoid X Receptor α (FXRα) (Houten et al., 2006).

1.1.3.2 Hepatic Sinusoidal Endothelial cells

HSEC are thin flat shaped cells, and are the first hepatic cells to come into contact with sinusoidal blood. They are considered unique and specialized compared to other endothelial cells as they lack a basement membrane (Wisse, 1970), allowing the free movement of fluid and substances from the sinusoids (Wisse et al., 1996). They contain fenestrations which are approximately 100-200 nm in diameter (Cogger et al., 2006) which behave like "sieves" as they allow only the movement of particles which are less than the diameter of the fenestrae. These are involved in clearance of chylomicron remnants (Fraser et al., 1978), and HSEC have roles as scavengers by engulfing pathogens by receptor mediated endocytosis and also in immune modulation (Connolly et al., 2010), (Lalor et al., 2002).

HSEC fenestrations are important in regulating lipoprotein transfer from the blood into hepatocytes and defenestration can affect systemic lipoprotein levels and prevent steatosis in hepatocytes (Cogger et al., 2006). Furthermore chronic exposure to alcohol impairs the fenestrae in alcoholic cirrhosis (Horn et al., 1987) leading to hyperlipoproteinaemia (Clark et al., 1988). HSEC have roles in controlling vascular tone (Iwakiri and Groszmann, 2006) and thus damage can lead to portal hypertension. Furthermore Reactive Oxygen Species (ROS)

can deplete levels of Nitrogen Oxide (NO) released by endothelial cells and thus have impact on vascular tone (Gryglewski et al., 1986), and subsequent HSEC dysfunction.

1.1.3.3 Hepatic Stellate Cells (HSCs)

HSCs are described as star shaped cells and in the quiescent state have a role in vitamin A regulation and storage (Blomhoff and Blomhoff, 2006), they are involved in liver regeneration (Chen et al., 2012), regulation of blood flow in the sinusoids (Reynaert et al., 2008), and regulate the extracellular matrix (ECM) turnover. As a result of liver injury HSCs transform from the quiescent to the activated state, which disrupts normal ECM turnover as HSCs produce and deposit increased collagen, which eventually leads to fibrosis, and cirrhosis (Bataller and Brenner, 2005). They also exacerbate the immune response by secreting cytokines and chemokines and induce KC activation (Chang et al., 2012).

1.1.3.4 Kupffer cells

Kupffer cells are asymmetrical in shape possessing filopodia which spike through HSEC fenestrae and anchor on to the sinusoidal lining (McCuskey and McCuskey, 1990). They are liver macrophages and are involved in engulfing foreign material or toxic material such as bacteria in the liver and are also involved in the breakdown of old Red Blood Cells (RBCs). Activation of KC by bacteria or for example by cytokines or chemokines secreted by activated HSCs can lead to secretion of pro-inflammatory cytokines such as Tumor Necrosis Factor α (TNFα) which in turn can activate HSCs. This ability means that KC have been implicated in the pathogenesis of Alcoholic Liver Disease (ALD) (Tsukamoto and Lu, 2001)

and Non Alcoholic Fatty Liver Disease (NAFLD) (Solga and Diehl, 2003) and have also been proposed to play a role in liver regeneration (Xu et al., 2012).

1.1.3.5 Lymphocytes and other immune cells

The liver contains resident populations of lymphocytes including 'Pit cells' which are regarded as large granulocyte lymphocytes and as liver exclusive Natural Killer (NK) cells (Wisse et al., 1997). They have defense roles against virally infected cells and have been suggested to be the first line of defense against metastatic cells (Bouwens and Wisse, 1992). Importantly the liver is regarded as an immunologic organ (Racanelli and Rehermann, 2006) and contains additional immune cells such as dendritic cells, macrophages and monocytes (Liaskou et al., 2012).

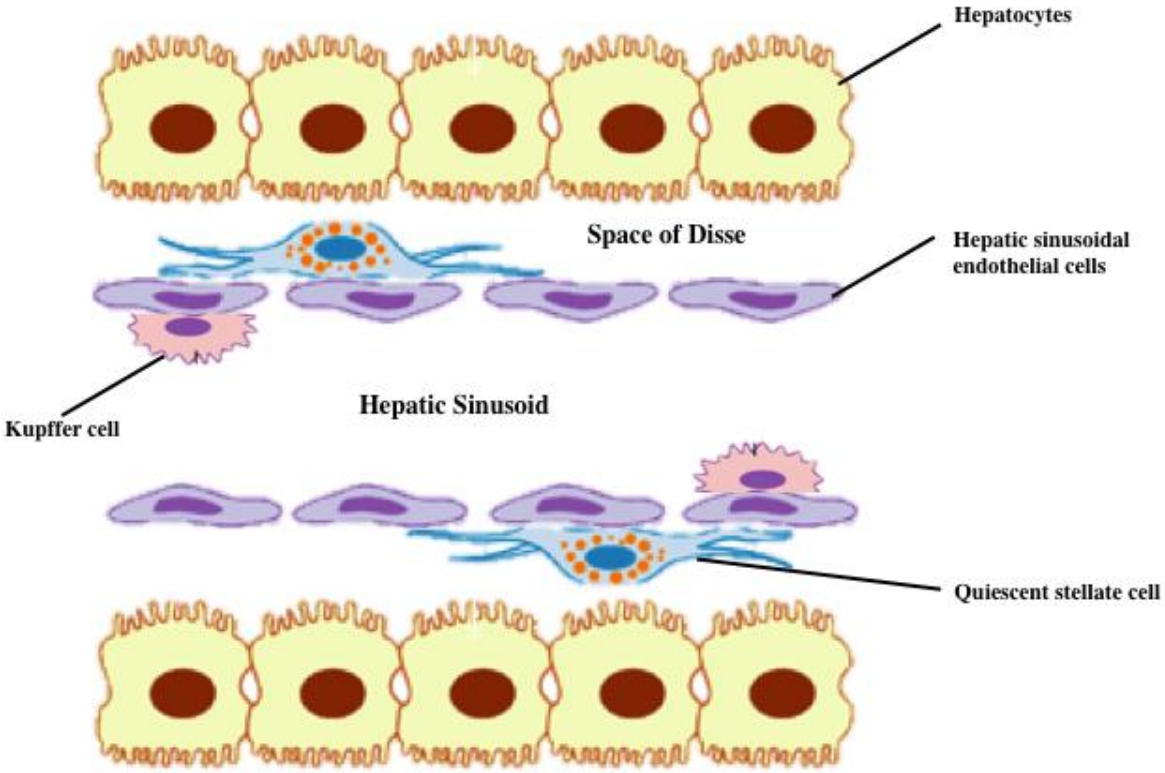

Figure 1.2: Localization of hepatic cells in the liver lobule
In the liver lobule hepatocytes are arranged in plates, and each plate is separated by sinusoids lined with HSEC, which are the first hepatic cells to come into contact with sinusoidal blood. The KC are attached to the endothelium and the quiescent HSCs containing Vitamin A granules (depicted in orange) reside between the hepatocytes and HSEC in the space of Disse (space between the hepatocytes and HSEC). Hepatic lymphocytes or 'Pitt cells' are also often present in the sinusoidal lumen and function as NK cells, along with macrophages and monocytes (not shown). Figure adapted from (Hui and Friedman, 2003).

1.1.4 Functions of the liver

The liver is a central organ in metabolic homeostasis and has many functions. It synthesis and secretes bile, stores vitamins and minerals, it is involved in drug inactivation and waste product removal it also has the ability to absorb, store, metabolize and produce carbohydrates, lipids and amino acids (AAs) and control their subsequent redistribution to other peripheral organs (Martini, 2006). These functions are tightly regulated by hormones insulin, glucagon, glucocorticoids and catecholamines (adrenaline, noradrenaline, dopamine) (Fritsche et al., 2008).

This thesis will consider the role of the liver in glucose and lipid homeostasis, two metabolic pathways which are intricately linked and share mutual metabolites. An imbalance in this system due to insulin resistance (IR) can lead to and contribute to the metabolic syndrome (MetS) and subsequent liver damage and so these functions are discussed in more detail in this thesis.

1.1.5 The role of the liver in glucose homeostasis

1.1.5.1 The postprandial state

During the post and pre-prandial state the pancreas is the major organ involved in secretion of insulin and glucagon from β and α cells, two hormones, which work antagonistically to regulate glucose and lipid homeostasis. As the blood glucose levels raise, glucose passes into the β cells of the pancreas via the glucose transporter GLUT2 (Jorns et al., 1996). Glucose is then phosphorylated by the enzyme glucokinase, and is eventually metabolized via glycolysis, the Tricarboxylic Acid Cycle (TCA) and the electron transport chain to generate Adenosine

Triphosphate (ATP). As the levels of ATP rise, ATP sensitive potassium (K) channels close causing the influx of positive K^+ ions to enter and depolarize the cell. Depolarization of the cell causes an influx of calcium ions, which cause the activation of synaptotagmin, which in turn helps granules containing insulin to fuse with the Plasma Membrane (PM) and secrete insulin in to the bloodstream (Grodsky and Bennett, 1966). Glucagon-like-peptide-1 (GLP-1) can also stimulate insulin secretion.

When insulin binds to its receptor on the plasma membrane of target cells, the insulin receptor, which is a receptor tyrosine kinase, becomes activated and uses insulin receptor substrates (IRS) to initiate signaling. The net result of insulin signaling in target organs such as the liver, muscle and adipose tissue are that it causes peripheral tissue such as muscle and adipose tissue to clear glucose and stops liver producing glucose and releasing it through GLUT2 via internalization of GLUT2 and IRS (Grodsky and Bennett, 1966). Insulin exerts its actions via nuclear transcription factors Sterol Element Regulatory Binding Protein (SREBP)-1c and Carbohydrate Response Element Binding Protein (ChREBP) (Kawaguchi et al., 2001) by increasing the expression of genes involved in lipogenesis (Canbay et al., 2007), (Sirek et al., 2009) and phosphorylating Forkhead Box Protein-O1 (FOXO-1) thus inhibiting gluconeogenesis and glycogenolysis (Puigserver et al., 2003).

1.1.5.2 Hepatic glucose metabolism

1.1.5.2.1 Glycolysis

Glycolysis occurs in the cytosol of cells and essentially involves splitting of sugar *glykos* "sugar" and *lysis* "splitting". It is the essential stage in glucose metabolism providing energy for subsequent metabolic reactions. The initial stage involves phosphorylation of glucose catalyzed by the enzyme glucokinase forming the intermediate Glucose-6-Phosphate (G-6-P), which can be used for glycogen synthesis via glycogenesis, or further metabolized producing two molecules of pyruvate and generation of ATP and Nicotinamide Adenine Dinucleotide Phosphate (NADPH). Pyruvate then enters mitochondria were it becomes Acetyl coenzyme A (Acetyl-CoA), a carrier molecule which is further metabolized in the TCA cycle generating energy for cellular processes.

1.1.5.2.2 Glycogenesis

When glucose exceeds requirement, surplus glucose present in the bloodstream, is used to generate or replenish hepatic glycogen stores, via the conversion of G-6-P to glycogen. G-6-P is an allosteric regulator of Glycogen Synthase (GS), the key enzyme involved in conversion of G-6-P to glycogen. Insulin inhibits glucose synthesis and output by promoting storage of glucose as glycogen within hepatocytes. Glycogenesis is primed by insulin causing dephosphorylation and activation of GS by inactivation of Glycogen Synthase Kinase 3 (GSK3). This leads to inhibition of other key enzymes involved in gluconeogenesis such as Phosphoenolpyruvate Carboxy Kinase (PEPCK) and glucose-6-phosphatase by phosphorylation and subsequent nuclear exclusion of the transcription factor FOXO-1 (Barthel et al., 2005).

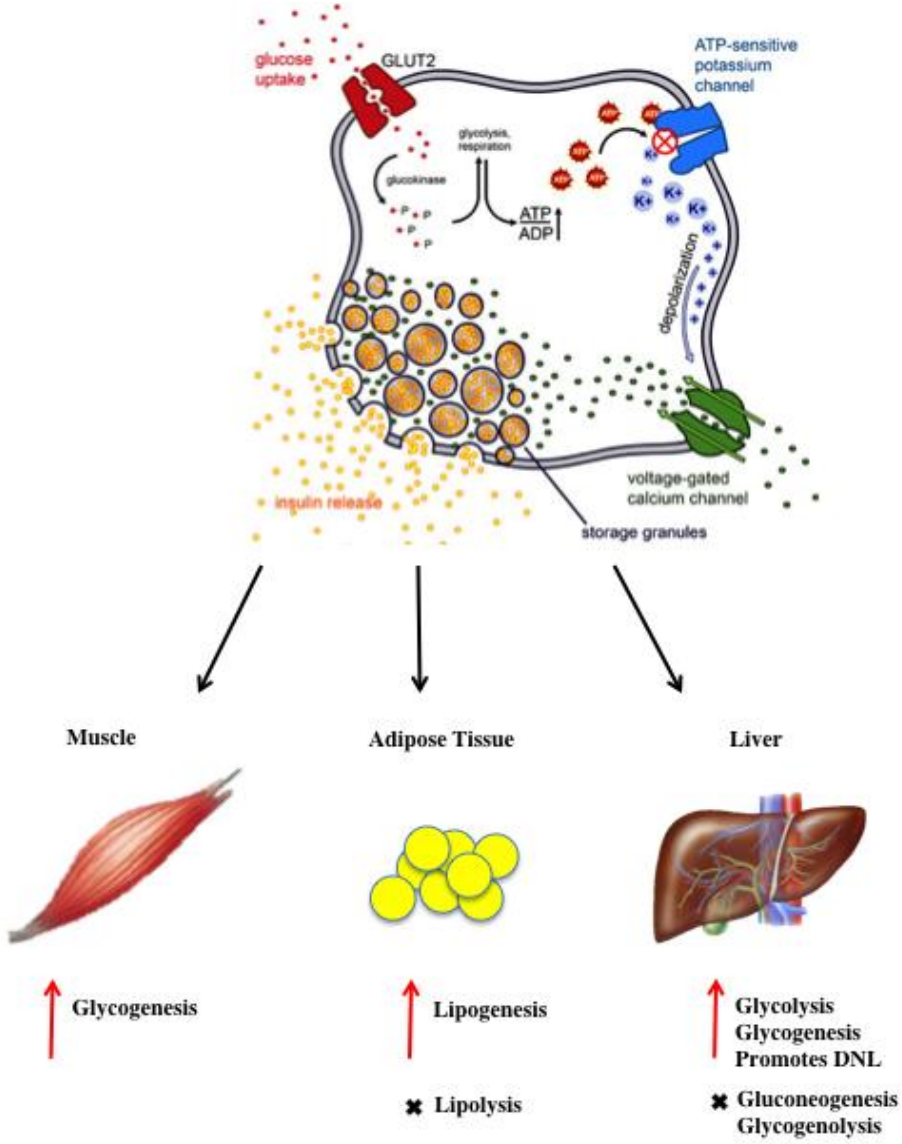

Figure 1.3: Insulin secretion and effect of insulin on peripheral tissues
In the postprandial state, glucose levels rise and glucose enters β cells of the pancreas through GLUT2 and is phosphorylated by glucokinase, and is eventually metabolized generating ATP. As the levels of ATP rise, ATP sensitive potassium (K) channels close, causing the influx of positive K^+ ions to enter which depolarize the cell. Depolarization of the cell causes an influx of calcium ions, causing the activation of synaptotagmin, which in turn helps granules containing insulin to fuse with the plasma membrane and secrete insulin in to the bloodstream. The net effects of insulin when it binds to its receptors on the plasma membrane of target cells are that it promotes muscle glycogenesis, adipose tissue lipogenesis and inhibits lipolysis. Whilst in the liver it promotes glycolysis, glycogenesis, DNL and inhibits gluconeogenesis and glycogenolysis. Figure adapted from http://2011.igem.org/wiki/images/d/da/Insulin_production_model.jpg.

Approximately 400kcal (1700kJ) of glycogen can be stored in the liver (Jeremy M Berg, 2002). However when glycogen stores are fully replenished, excess G-6-P has a variety of fates. It is either metabolized to Acetyl-CoA which is used for De Novo Lipogenesis (DNL) (Bechmann et al., 2012) and the anabolism of bile salts and cholesterol (Jeremy M Berg, 2002), or it enters the pentose-phosphate pathway to generate reducing power in the form of NADPH for the reductive biosynthesis of the above (Jeremy M Berg, 2002). These pathways work intrinsically to restore glucose homeostasis in the fed state.

1.1.5.3 The pre-prandial state

In the pre-prandial state (between meals) when blood glucose levels fall the liver is the main organ involved in glucose release providing energy to peripheral organs. Although muscle has the largest reserves of glycogen it does not possess glucose 6 phosphatase and thus cannot export free glucose out of myocytes (Jeremy M Berg, 2002). Instead, glucagon works antagonistically to insulin by increasing breakdown of fats in the adipose tissue to free fatty acids (FFA) and initiates glycogenolysis and gluconeogenesis. Glucagon stimulates the cyclic Adenosine Monophosphate (AMP) cascade which causes the activation of the enzyme phosphorylase and the inhibition of GS inhibiting glycogen synthesis (Jeremy M Berg, 2002). It also initiates gluconeogenesis and inhibits glycolysis by decreasing levels of fructose-2-6-bisphosphate, an intermediate metabolite that allosterically activates expression of key enzymes involved in glycolysis and thus inhibits Fatty Acid (FA) synthesis by inhibition of pyruvate formation.

1.1.5.3.1 Glycogenolysis

Glycogen phosphorylase is the main enzyme involved in the catalysis of glycogen to glucose-1-phosphate. Glucose-1-phosphate is then converted to G-6-P for glycolysis and glycogenesis, catalyzed by the enzyme phosphoglucomutase (Bechmann et al., 2012). Glucose-6-phosphatase then catalyzes the reaction releasing free glucose out of the hepatocytes available to other peripheral organs for energy. When glycogen stores are exhausted the liver provides glucose via gluconeogenesis.

1.1.5.3.2 Gluconeogenesis

During sustained starvation the liver forms glucose from alternate precursors such a lactate (Raddatz and Ramadori, 2007). For example during strenuous exercise muscle obtains energy via glycogenolysis however this can lead to production of lactate, which cannot be utilized for energy. Thus its transported out of myocytes to the liver were it is converted back to pyruvate and used in the TCA cycle to generate energy in the form of ATP or used for the synthesis of glucose. This is also known as the Cori cycle named after the Nobel prize winners who discovered it (Raju, 1999).

1.1.6 The role of carbohydrate transporters in glucose metabolism

To date 14 members of the GLUT family have been identified which facilitate entry of glucose into and out of cells. These GLUT proteins are required in hepatocytes to facilitate glucose uptake in the post-absorptive state and to permit the exit of glucose formed by glycogenolysis and gluconeogenesis. Moreover glucose has the ability to regulate ChREBP (Yamashita et al., 2001) and thus drive lipogenesis. Despite importance of these in glucose

homeostasis and liver metabolism the significance of these transporters, and their expression patterns in the diseased liver have not been clearly defined (Karim et al., 2012) and thus these transporters are discussed in more detail in Chapter 3.

1.1.7 The role of the liver in lipid homeostasis

1.1.7.1 Hepatic lipid metabolism

As discussed earlier, when the liver glycogen stores reach approximately 5% of the total liver mass (Postic and Girard, 2008) excess glucose is used for synthesis of FAs. The liver also receives Non Esterified Fatty Acids (NEFA) liberated from adipose tissue in plasma via specific transporter proteins as well as chylomicron remnants containing cholesterol, FA, and glycerol (Cooper, 1997). These remnants, are taken up by Low Density Lipoprotein (LDL) receptor related proteins (LRP)s. Cholesterol can be used for membranes, as a precursor for bile acid synthesis, or exported out of the hepatocytes as Very Low-Density Lipoproteins (VLDLs). FAs can be stored within hepatocytes as triglycerides (TAG), in lipid droplets or if surplus to requirement are esterified to TAG, which are exported out of the hepatocytes as VLDLs for transport to adipose tissue. FAs can also be oxidized to produce fuel via β oxidation in mitochondria.

The role of the liver in lipid metabolism begins with emulsification of fats in the small intestine by bile secreted by the liver (Oude Elferink and Groen, 2000). Once in the liver the fate of lipids follows one of two metabolic pathways, esterification or oxidation. Lipids are subject to esterification in the Endoplasmic Reticulum (ER) and β oxidation in the mitochondria. Lipids can also undergo both α and β oxidation in peroxisomes.

Whether lipids undergo esterification or oxidation depends on the nutritional state of the individual. In the fed state, insulin prevents breakdown of fats (Rautou et al., 2010), (Yang et al., 2010) furthermore oxidation of FAs is limited and this is primarily regulated by the concentration of malonyl CoA. In addition during starvation lipoautophagy can liberate FAs from lipid droplets within the hepatocyte (Rautou et al., 2010), (Wang et al., 2010), (Singh et al., 2009), (Liu and Czaja, 2013). In order to be oxidized a FA needs to be able to transverse from the outer membrane of mitochondria to the matrix of the inner membrane of the mitochondria, which contains the enzymes for β oxidation (Reddy and Hashimoto, 2001). Very long chain FAs consisting of $>C_{20}$ undergo β oxidation in the peroxisomes to shorten the carbon length before entering further oxidation in the mitochondria. In mitochondria, the initial stage in β oxidation involves the dehydrogenation of acyl-CoA by acyl-CoA dehydrogenases, and mice lacking these enzymes have been shown to develop micro and macrovesicular steatosis in the liver (Tolwani et al., 2005). The FA then attaches to a carnitine molecule, which facilitates its move to the matrix aided by a carnitine carrier protein. The enzyme carnitine palmitoyltransferase I (CPT 1) then supports the transfer of FA from the cytoplasmic side to the mitochondrial side (Reddy and Hashimoto, 2001). The next stage of β oxidation involves the Mitochondrial Trifunctional Protein (MTP). This protein consists of three enzymes, 2-enoyl-CoA hydratase, 3- hydroxyacyl-CoA dehydrogenase and 3-ketoacyl-CoA thiolase, which further catalyze the oxidation of FAs.

When levels of malonyl CoA are low during the fasting state, β oxidation is favored and this is aided by the flux of FAs through the CPT 1 reaction. Similarly when levels are high as in the fed state esterification is favored (Reddy and Hashimoto, 2001) due to a decrease in FA delivery as a result of CPT 1 inhibition (Reddy and Hashimoto, 2001).

In addition to hormonal control, lipid and glucose metabolism can be directly regulated by FA themselves through regulation of nuclear transcription factors such as Peroxisome Proliferator Activated Receptor δ (PPARδ) which is involved in activating glycolysis by regulating SREBP-1c and Peroxisome Proliferator Activated Receptor α (PPARα), which increases expression of FA transporters, leading to FA uptake, usage and breakdown (Rakhshandehroo et al., 2010).

1.1.8 The role of fatty acid transporters in lipid metabolism

FAs gain entry into the hepatocytes via facilitated carrier proteins such as the Fatty Acid Binding Proteins (FABP), Fatty Acid Transporter Proteins (FATP), Caveolin 1 (CAV1) and CD36 (Musso et al., 2009) also known as Fatty acid Translocase (FAT), whilst the chylomicron remnants gain entry via receptor mediated endocytosis by attaching to LRP proteins (Fritsche et al., 2008). Furthermore these proteins are involved in the intracellular shuttling of FAs to target organelles for oxidation or storage. These transporters are fundamentals for lipid entry and thus metabolism, and yet their role in the liver and liver disease has been under appreciated. This thesis will consider the expression patterns of these proteins in liver cells and their implications in liver disease and therefore they are discussed in more detail in Chapter 3.

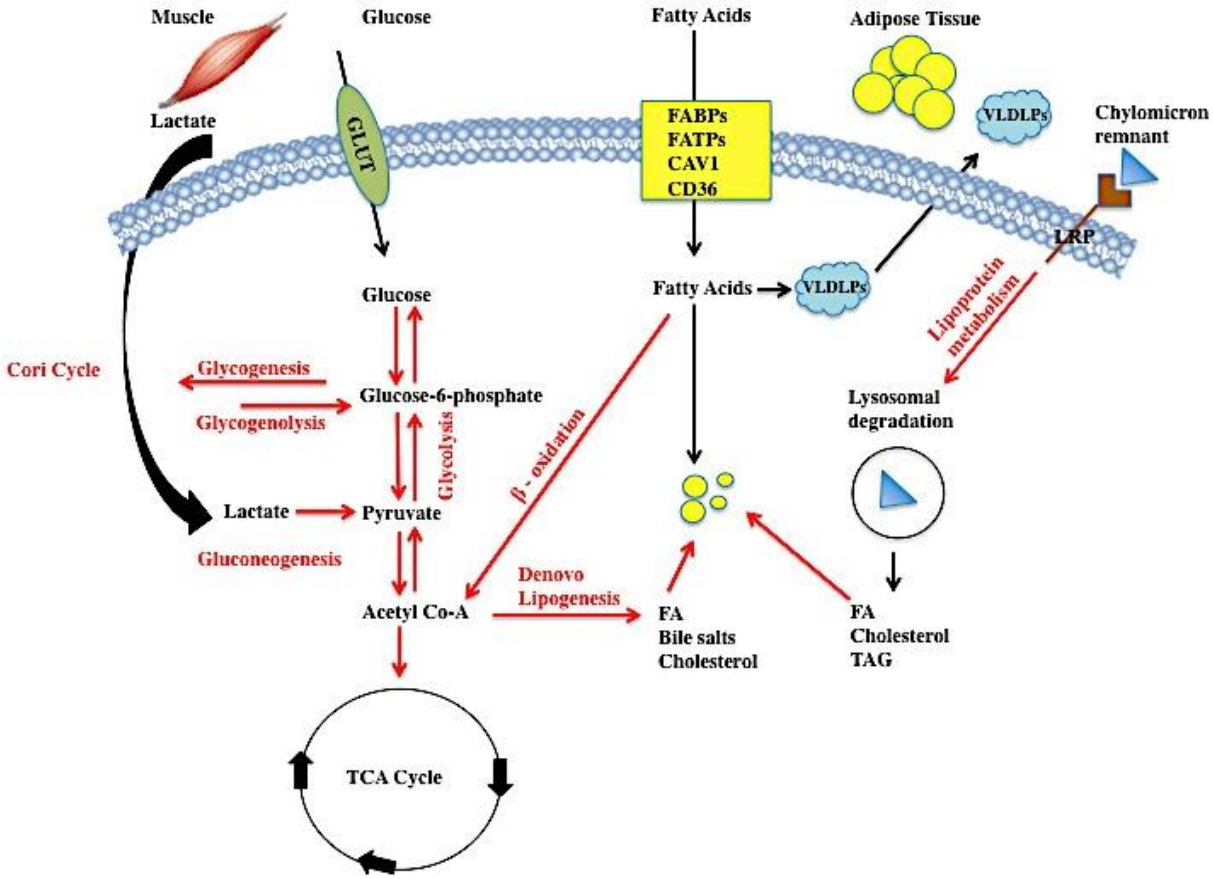

Figure 1.4: Schematic showing the interrelationships between glucose and lipid metabolism

Glucose enters hepatocytes through GLUT proteins it is then metabolized via glycolysis to G-6-P which is an intermediate metabolite which can be used for storage of glucose in the form of glycogen via glycogenesis, and reverted back to free glucose via glycogenolysis depending on the nutritional status for example during starvation or exercise. Hepatocytes can form glucose from lactate released by myocytes during exercise (Cori cycle), this process is known as gluconeogenesis. Further metabolism of G-6-P can produce Acetyl Co-A, which can further be processed in the TCA cycle for generating energy in the form of ATP or used for DNL of FAs, these can be used as precursors for bile salts, cholesterol synthesis or storage as lipid droplets. The hepatocytes can also receive FAs liberated from adipocytes or from the diet; these are taken up via facilitator proteins FABPs, FATPs, CAV1 and CD36. Internalized FAs can be used for synthesis of VLDLPs, which can be exported out of the hepatocyte to peripheral tissues such as adipose tissue, stored as lipid droplets within the hepatocyte or enter β-oxidation. Chylomicron remnants are internalized via receptor mediated endocytosis and subjected to lysosomal degradation releasing FAs, cholesterol and TAG.

1.1.9 Obesity and the Metabolic Syndrome

The prevalence of obesity in the United Kingdom (UK) and across the world is increasing due to poor dietary habits and a sedentary lifestyle. The world health organization (WHO) reports a doubling in worldwide obesity since 1980, with shocking statistics revealed in 1998: 200 million adult males and 300 million adult females were classified as obese. In 2010 the WHO reported 40 million children (under 5) to be overweight (http://www.who.int/mediacentre/factsheets/fs311/en/index.html). The rising trend in obesity is alarming and has led to many health complications, which include the MetS also commonly referred to as syndrome X (Reaven, 1988), (Reaven, 1993). The MetS includes a spectrum of diseases including hypertension, presence of low high-density lipoproteins (HDL), high fasting glucose and an increased abdomen circumference (2001). It is associated with inflammatory markers such as TNFα and Interleukin 6 (IL6) (Sutherland et al., 2004), (Hardy et al., 2013) along with IR which is considered a hallmark of this condition (Alberti and Zimmet, 1998), (Balkau and Charles, 1999). However it must be noted that IR has also been reported in non obese individuals (Ruderman et al., 1998). MetS alarmingly has also been reported in children (Sung et al., 2003), (Wang et al., 2013), (Pastucha et al., 2013). Furthermore individuals with the MetS are more likely to develop cardiovascular disorders, type II diabetes and NAFLD which is becoming a growing problem in the western world and is one of the leading causes of end stage liver disease (Blachier et al., 2013).

1.1.10 Non-Alcoholic Fatty Liver Disease

NAFLD is increasing rapidly in the developing world, with 25%-30% of the general population in western countries said to be suffering from the condition (Bhala et al., 2013). NALFD has also been reported in children, (Franzese et al., 1997), (Akcam et al., 2013), with an estimated prevalence of 2.6% in some cohort studies (Tominaga et al., 1995). NAFLD encompasses hepatic steatosis, which is the accumulation of lipid in the liver and can occur in the absence of alcohol consumption or due to excessive alcohol consumption and is referred as Alcoholic Fatty Liver Disease (AFLD) or ALD (Reddy and Rao, 2006).

NAFLD encompasses a spectrum of diseases, which includes the presence of simple steatosis which is benign (Day, 2005), to the more aggressive form Non Alcoholic Steatohepatitis (NASH) (Ludwig et al., 1980) where inflammation is present. The prevalence of NASH in the general population is said to be around 3%-5% (Vernon et al., 2011). NASH is characterized by steatosis and inflammation which is also characteristic in Alcoholic Steato Hepatitis (ASH); which can progress to fibrosis and eventually cirrhosis and is an important risk factor for the development of Hepatocellular Carcinoma (HCC), (Torres and Harrison, 2012), (Starley et al., 2010), (Tacke and Yoneyama, 2013).

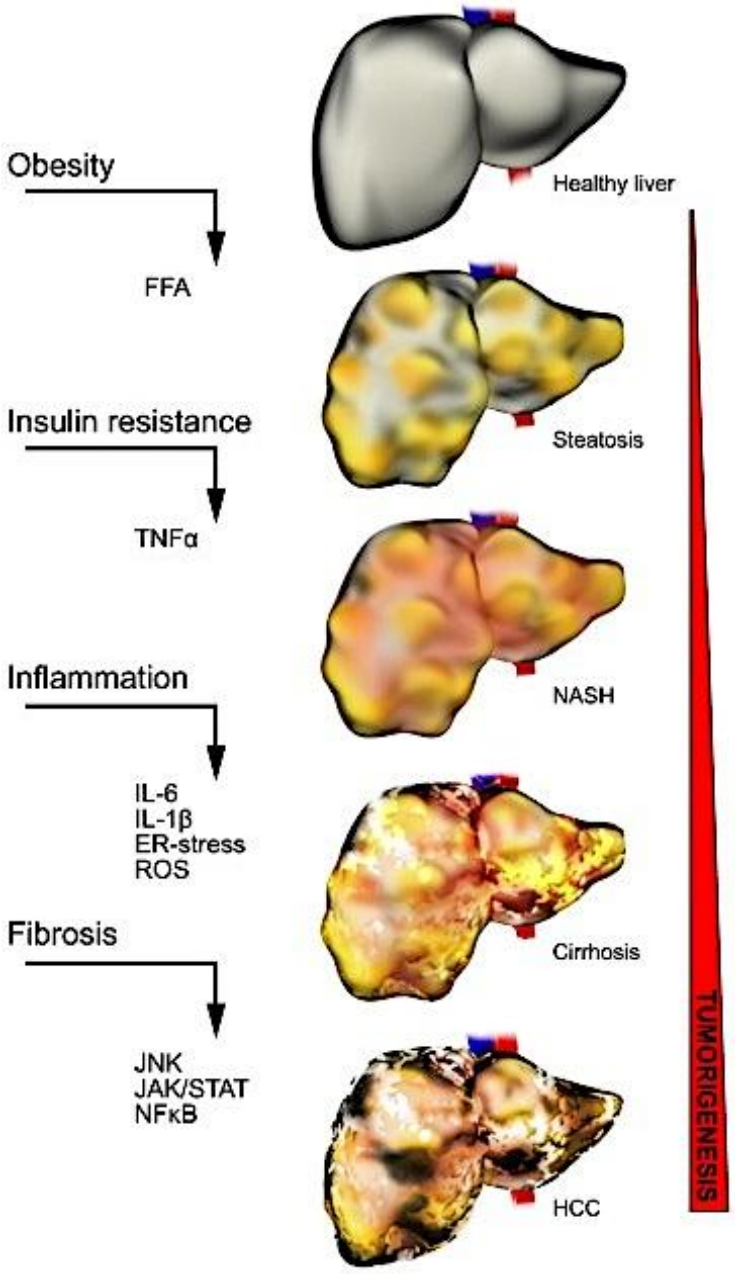

Figure 1.5: Schematic showing disease progression from the healthy liver to HCC
Obesity leads to an overload of FFA in the adipose tissue, and in the IR this leads to increased lipolysis, along with DNL leads to steatosis in the liver. Obesity leads to a rise in TNFα in adipocytes further increasing IR and lipolysis. Overload of FAs leads to formation of ROS, which leads to inflammation and thus development of NASH. Activation of HSCs and Kupffer cells further exacerbates liver damage by deposition of collagen, which leads to fibrosis and cirrhosis through Jun Terminal Kinase (JNK), Janus Kinase Signal Transducer and Activator of Transcription JAK/STAT and Nuclear Factor kappa B (NF-κB) pathways. Figure adapted from (Bechmann et al., 2012)

1.1.10.1 Pathogenesis of NAFLD

The precise causes of NALFD are poorly understood but disease progression has been coined a "two hit hypothesis" with the first hit, were the hepatocytes fill with lipid droplets in the form of TAG. Precursors for these are the FFAs, which can arise from the breakdown of TAG from the diet, from adipose tissue due to inhibition of lipolysis or from DNL from substrates such as glucose (Cazanave and Gores, 2010). The net accumulation is due to increase delivery of substrate to the hepatocytes, increased DNL (Postic and Girard, 2008), decreased oxidation of FAs and decreased export of VLDLPs. The first hit is fairly benign and is often regarded as a protective mechanism where toxic FFAs are esterified to neutral TAG (Yamaguchi et al., 2007). However overload of lipid can eventually prime the liver for the "second hit" or rather "multiple hits" which includes inflammation, oxidative stress, lipid peroxidation and mitochondrial dysfunction impairing lipid oxidation (Fromenty et al., 2004). Furthermore FFAs have been reported to induce oxidative stress (Feldstein et al., 2004). Various factors have been considered to drive disease onset and progression and these are discussed below.

1.1.10.1.1 Free Fatty Acids

Adipose tissue in the fed state can increase in mass, which may lead to increased concentrations of FFAs in serum. These can also increase due to prohibition of lipolysis in the IR state, and thus have been implicated in the pathogenesis of NAFLD. FFA have been shown to cause lipotoxicity by activating JNK dependent apoptosis (Malhi et al., 2006), (Cazanave et al., 2009), inducing endoplasmic reticulum stress (Wei et al., 2006), (Wang et al., 2006), (Wei et al., 2009) and altered lysosomal metabolism (Feldstein et al., 2004), (Feldstein et al., 2006). It is has also been shown that FAs can induce β oxidation enzymes by

binding to PPAR- α, and mice lacking this receptor during starvation have been shown to develop severe liver steatosis (Rao et al., 2002). The nature of available lipids and FFAs also impacts upon pathology. The circulating FFA lipid profile observed in NASH patients (Fong et al., 2000), (Diraison et al., 2003) is principally composed of saturated and monounsaturated FAs Palmitic Acid (PA) and Oleic Acid (OA) (de Almeida et al., 2002). A recent report has shown that medium chain triglycerides reduce lipid content in a rat model of NAFLD by activating PPAR- α and hence stimulating β and ω oxidation (Ronis et al., 2013). Importantly lipids such as ceramides have been implicated in IR (Summers, 2006), (Holland et al., 2007) whilst free cholesterol has been implicated in the pathogenesis of NASH (Van Rooyen et al., 2011) thus esterification of lipids is an important detoxifying mechanism of the liver.

1.1.10.1.2 Adipokines

Adipocytes in addition to secreting FFA also secrete signaling molecules such as cytokines known as adipokines which can exert their own biological effects meaning adipose tissue has also been considered as an endocrine organ (Ahima and Flier, 2000), (Galic et al., 2010), (Duan et al., 2013). For example leptin and adiponectin have been considered as insulin sensitizers, whilst TNF-α, IL-6 and resistin as insulin suppressors (Pittas et al., 2004). Leptin has been reported to have a role in regulating the immune system (Lord, 2002), energy intake and usage and to increase insulin sensitivity in muscle and liver (Unger et al., 1999), (Minokoshi et al., 2002). Hence leptin has been implicated in obesity. In mice for example addition of leptin has shown to decrease weight in the ob/ob mice with a deletion in the leptin gene (Friedman et al., 1991) whilst in human obesity leptin levels are increased (Considine et al., 1996). Leptin is elevated in NASH and associated with steatosis rather than inflammation and fibrosis (Chitturi et al., 2002), whilst levels of adiponectin have been shown to be low in

NASH (Jarrar et al., 2008), (Hui et al., 2004), (Shimada et al., 2007), (Younossi et al., 2008). Lower levels have also been correlated with increased histological severity of disease (Aller et al., 2008), (Targher et al., 2006), furthermore adiponectin expression has been detected in murine hepatocytes, HSEC and HSCs in response to fibrotic stimuli and hence hepatic damage (Wolf et al., 2006), (Yoda-Murakami et al., 2001). Its levels are suppressed by TNF-α (Bruun et al., 2003) whilst adiponectin itself suppresses TNF-α (Xu et al., 2003). In addition elevated levels of resistin and IL-6 have been reported in NASH compared to simple steatosis alone (Senates et al., 2012), (Wieckowska et al., 2008).

1.1.10.1.3 Glucocorticoids

Glucocorticoid hormones have a role in gluconeogenesis (Nordlie et al., 1999), (Pilkis and Granner, 1992) and have been implicated in NAFLD pathogenesis. For example patients with Cushing's syndrome have elevated levels of cortisol (Hatipoglu, 2012) and some of these Cushing's patients have been reported to have hepatic steatosis (Rockall et al., 2003). Enzymes which inactivate cortisol have been reported to be increased in IR states (Tomlinson et al., 2008) and NAFLD (Konopelska et al., 2009) and it has been postulated these enzymes are upregulated in order to retain insulin sensitivity, thereby serving as a protective mechanism (Tomlinson et al., 2008). Certainly a recent report has shown that glucocorticoids enhance the insulin response in hepatocytes (Hazlehurst et al., 2013).

1.1.10.1.4 Genetic factors

Although many factors of the MetS are common in NAFLD, not all NAFLD patients progress to NASH suggesting there are environmental and genetic factors, which may lead to increased

susceptibility of disease progression in some individuals. Certainly ethnic differences in histological severity of NAFLD have been reported. African Americans have less steatosis than Caucasians whilst Asians and Hispanics demonstrate increased severity of disease (Mohanty et al., 2009). Recently genetic polymorphisms in Lymphocyte Cytosolic Protein-1 (LCP1) and Group Specific Component (GSC) have been associated with NAFLD (Adams et al., 2013) and polymorphism of Peroxisome Proliferator-Activated Receptor-γ Coactivator (PGC)-1α gene (PPARGC1A) have been reported to increase the risk of developing NAFLD in obese children (Lin et al., 2013). Similarly gene polymorphisms in MTP, PPAR-α, adiponectin, Manganese Superoxide Dismutase (MnSOD), Hormone Sensitive Lipase (HSL) have also been reported in NASH (Namikawa et al., 2004), (Dongiovanni and Valenti, 2013), (Merriman et al., 2006).

1.1.10.2 Pathophysiology of NAFLD

Hepatic steatosis can exist as macrovesicular steatosis where a large lipid droplet can displace the nuclei of hepatocytes, or co-exist with microvesicular steatosis characterized by multiple lipid droplets in the hepatocyte with a centrally located nuclei (Crabb et al., 2004), (Ludwig et al., 1980), (Schwimmer et al., 2005). Mixed steatosis has been reported for both ASH and NASH (Brunt, 2001) but microvesicular steatosis is considered to be increasingly severe. NASH compromises both steatosis and inflammation (Lee, 1995), with presence of fibrosis, hepatocellular injury and necroinflammation present mainly in Zone 3 (Schwimmer et al., 2005), (Brunt, 2001), (Cortese and Brunt, 2002). Inflammation can be mixed with prescence of neutrophils (Brunt, 2001) and some forms of NASH can also include Mallory bodies (Brunt, 2001). Portal inflammation has been asscoiated with increased disease progression in ALD and NAFLD (Rakha et al., 2010). Despite the underlying causes of ASH and NASH

being different, it is usually difficult to distinguish between the two types histologically. Studies have attempted to differentiate between the two types and have reported glycogenated nuclei to be present in NASH (Itoh et al., 1987) but not ASH (MacSween and Burt, 1986), (French et al., 1993), whilst others have reported features such as cholestasis (French et al., 1993) and sclerosing hyaline necrosis (Goodman and Ishak, 1982) as more prominent in ASH than NASH.

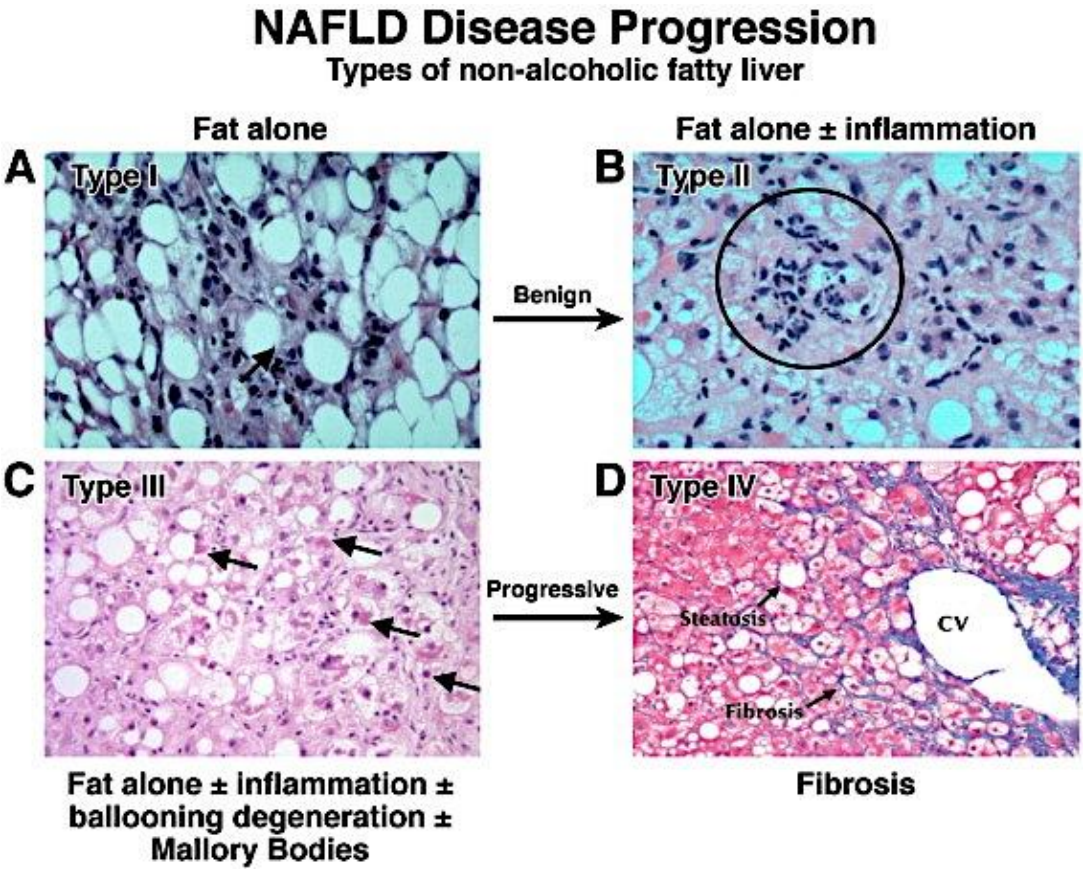

Figure 1.6: Histology of NAFLD disease progression
Arrow in (A) indicate presence of TAG, whilst in (B) circle indicates presence of inflammatory cells as disease progresses there is appearance of ballooning degeneration, Mallory bodies and (D) the progressive form encompassing both steatosis and fibrosis, central vein is depicted as CV (Parekh and Anania, 2007).

1.1.10.3 Diagnosis of NALFD

Most patients with NAFLD are asymptomatic; although some common conditions include right upper quadrant pain, fatigue, malaise and hepatomegaly on physical examination (Lewis and Mohanty, 2010). Thus diagnosis of NAFLD is often difficult or accidental as a result of routine liver function checks in susceptible individuals. Presence of altered Alanine Transaminase (ALT) and Aspartate Transaminase (AST) levels can indicate liver damage and thus an underlying cause, however some individuals with NAFLD have been reported to have normal levels of these enzymes (Browning et al., 2004). Imaging such as ultrasound can be used to identify presence of fat in the liver, but may not permit a clinician to distinguish between simple fatty liver and NASH (Obika and Noguchi, 2012). Furthermore some imaging techniques such as Magnetic Resonance Imaging (MRI) are expensive (Obika and Noguchi, 2012). Thus the gold standard for diagnosing NAFLD, and assessing disease severity and prognosis is the liver biopsy, which is an invasive procedure. However on histology it is difficult to distinguish between ALD, NAFLD and ASH versus NASH as discussed earlier. Thus there is a need for specific biomarkers, which could be less invasive than a biopsy and which could distinguish between NAFLD and NASH. Recent attempts using Gas Chromatography (GC) and exhaled breath samples have been used to distinguish patients with NASH (Verdam et al., 2013), furthermore techniques such as Matrix Assisted Laser Desorption Ionization Mass Spectrometry (MALDI-MS) have been used to identify disease pathogenesis (Gorden et al., 2011), (Feldstein et al., 2010), (Wattacheril et al., 2013) and these are discussed in more detail in Chapter 5.

1.1.10.4 Treatment strategy for NAFLD

Current options for preventing or ameliorating NAFLD include lifestyle modifications such as diet, weight loss and improving insulin sensitivity by taking drugs such as metformin which decreases hepatic glucose release and increases β oxidation (Nakajima, 2012), or GLP-1 analogues which can increase insulin secretion (Cuthbertson et al., 2012), (Iltz et al., 2006). For ALD, abstinence from alcohol is recommended. Treatments targeting NASH include anti-inflammatory and antioxidant therapies such as vitamin E which decreases lipid peroxidation (Chang et al., 2006), and ursodeoxycholic acid (Ratziu et al., 2011). For patients with NASH associated fibrosis, anti fibrotic drugs such as PPARϒ agonists are used (Aithal et al., 2008), (Belfort et al., 2006), whilst for patients with cirrhosis, liver transplantation is the only treatment option. In all many of the treatment strategies currently employed in the management of NAFLD and its related conditions are either associated with side effects or show little benefit (Lago et al., 2007), (Lavine et al., 2011), (Musso et al., 2012), (Adinolfi and Restivo, 2011), (Miller et al., 2005a), (Duvnjak et al., 2009), (Keech et al., 2005). Thus an excellent treatment option for NAFLD would be a target directly in the liver, which would prevent oxidant stress, inflammation and subsequent fibrosis.

One potential molecule, which may be involved in the pathogenesis of NASH, is Vascular-Adhesion Protein-1 (VAP-1), which has adhesive properties, Semicarbazide Sensitive Amine Oxidase (SSAO) activity, and has a reported role in glucose, lipid modulation. This may present a novel target for therapeutic intervention in NAFLD and is the focus of this thesis and so is introduced below with further detail in Chapters 4 and 5.

1.1.11 Vascular Adhesion Protein- 1

VAP-1 (AOC3, EC 1.4.3.6) is a 180 Kilo Dalton (kDA) protein. It is multifunctional and expressed on diverse cell types including endothelial cells, adipocytes, smooth muscle and heart. It localizes within cytoplasmic vesicles (Enrique-Tarancon et al., 1998) and a soluble form is also found in serum (sVAP-1) (Stolen et al., 2004a), (Morin et al., 2001), (Salmi and Jalkanen, 1992), (Salmi et al., 1993), (Salmi and Jalkanen, 2006). The soluble form is cleaved and shed from membrane bound VAP-1 which is controlled by TNFα and insulin in some cells (Abella et al., 2004) and levels increase in inflammatory liver disease (Kurkijarvi et al., 1998), (Kurkijarvi et al., 2000), obesity (Meszaros et al., 1999), diabetes (Salmi et al., 2002), (Boomsma et al., 1999) and congestive heart failure (Boomsma et al., 1997), (Boomsma et al., 2000). Furthermore in experimental diabetes sVAP-1 appears to be shed by endothelial cells and adipose tissue (Stolen et al., 2004b).

VAP-1 is an Amine Oxidase (AO) enzyme. Amine oxidases are classified into two groups depending on the co factor they possess. For example the Flavin-Adenine-Dinucleotide (FAD) containing AO and the copper and 6-Hydroxy-Topa Quinone (TPQ) containing AO. The FAD containing AO include the Mono Amine Oxidase- A (MAO-A) and Mono Amine Oxidase-B (MAO-B), which are found in the outer mitochondrial membrane (Strolin Benedetti et al., 2007). Cloning of VAP-1 revealed it had similarity to the copper containing amine oxidases (Smith et al., 1998). These AO such as Lysyl Oxidase (LOX) are sensitive to inhibition by semicarbazide and thus are also referred to as SSAO (Jalkanen and Salmi, 2001). Thus VAP-1/SSAO is a membrane bound protein, which has one transmembrane spanning domain, the extracellular domain has the active site containing the two co factors copper and TPQ (Jakobsson et al., 2005) and contains multiple glycosylation sites whilst the

intracellular domain is much shorter (Smith et al., 1998), (Salmi and Jalkanen, 1992). The X ray crystal structure of this enzyme revealed that the entrance of substrates to the active site may be regulated by a Leu469 residue which blocks the active site functioning rather like a gate (Airenne et al., 2005), (Jakobsson et al., 2005). A recent study has reported substrates with a long aliphatic chain are better substrates for VAP-1 as the enzyme has higher affinity and catalytic efficiency for them (Bonaiuto et al., 2010).

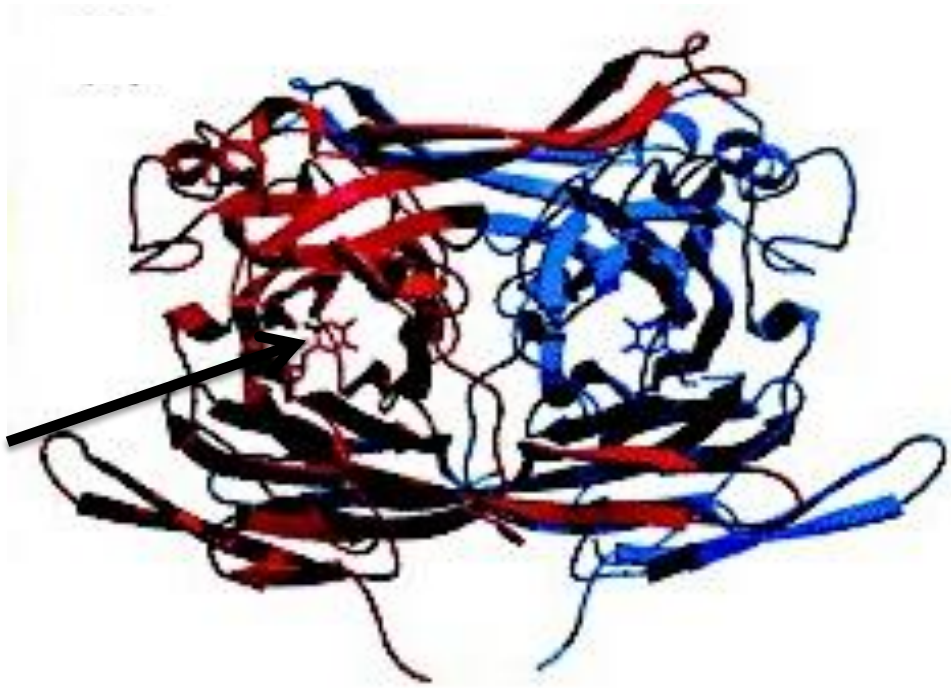

Figure 1.7: Structure of VAP-1
VAP-1 is a homodimeric protein and the figure shows an overall fold of the active domain of VAP-1. Blue and red indicate the monomers, which contain the active site, which is indicated by the black arrow in the red colored monomer on the left. Figure adapted from (Salmi and Jalkanen, 2001).

VAP-1 and other AO generally catalyze the deamination of endogenous and exogenous amines producing an aldehyde and hydrogen peroxide. For example VAP-1 catalyzes the oxidative deamination of both endogenous (methylamine and aminoacetone) (Bonaiuto et al., 2010) and exogenous (benzylamine) primary amines generating aldehydes, ammonia and hydrogen peroxide as products based on the reaction:

$$RCH_2NH_2 + O_2 + H_20 \xrightarrow{SSAO} RCHO + NH_3 + H_20_2$$

(Reviewed in (Klinman and Mu, 1994), (Wilmot et al., 1999)).

These products have been shown to exert biological affects. For example the aldehydes formaldehyde and methylglyoxal produced from methylamine and aminoacetone and also ammonia have been shown to fuel glycation and produce protein cross linking (Yu et al., 1997), (Mathys et al., 2002), (Seiler, 2002), (Yang and Butler, 2002). Furthermore hydrogen peroxide can act as a signaling molecule and also as a ROS (Veal and Day, 2011), (Muzykantov, 2001) (Muzykantov, 2001) and has been shown to mimic the effects of insulin (Mahadev et al., 2001).

1.1.12 VAP-1 is a multifunctional protein

VAP-1 was initially identified in endothelium where it has been reported as an adhesion molecule supporting lymphocyte recruitment to the liver (Salmi and Jalkanen, 1992), (Lalor et al., 2002) and its role as an immunomodulatory molecule is well known. For example in HSEC, the SSAO activity of VAP-1 activates the NF-κB pathway leading to the upregulation of Intracellular Adhesion Molecule-1 (ICAM-1), Vascular Cell Adhesion Molecule-1 (VCAM-1) and E selectin (Lalor et al., 2007) hence supporting leukocyte recruitment. VAP-

1 has also been reported to be involved in neutrophil extravasation during inflammation (Tohka et al., 2001). In addition VAP-1 has been shown to induce expression of Mucosal Addressin Cell Adhesion Molecule-1 (MAdCAM-1) a molecule involved in Inflammatory Bowel Disease (IBD) (Liaskou et al., 2011). Other reported roles include implications in atherogenesis (Yu et al., 2002), angiogenesis (Langford et al., 1999), and the most intriguing in glucose and lipid modulation, the specifics of which are discussed in Chapters 4 and 5 respectively.

Amine Oxidase (AO)	Substrates	Inhibitors
VAP-1/SSAO	Methylamine Aminoacetone Allylamine Benzylamine Beta-Phenyl-Ethylamine Tyramine Dopamine Mescaline Tryptamine Histamine	2-Bromethylamine (BEA) Semicarbazide Hydroxylamine Propargylamine Pyridoxamine (+) Mexiletine B-24 FLA 336 MDL-72145 MDL-72974A Iproniazid Phenelzine Procarbazine Hydralazine Carbidopa Benserazide Aminoguanidine
MAO-A	Benzylamine Tyramine Beta-Phenyl-Ethylamine Serotonin Dopamine Norepinephrine Epinephrine	Chlorgyline (C)
MAO-B	Benzylamine Tyramine Beta-Phenyl-Ethylamine Dopamine	Pargyline (P) MDL-72974A MDL-72145
LOX	Lysine	β-Aminopropionitrile (BAPN)

Table 1.1: Substrates and Inhibitors of Amine Oxidase Enzymes
Table 1.1 shows the preferred substrates and inhibitors of SSAO/VAP-1, MAO-A, MAO-B and LOX. (K Magyar, 2001), (Ochiai et al., 2006), (Jalkanen and Salmi, 2001), (Kagan and Li, 2003).

In all, the mechanisms leading to NAFLD and subsequent progression to NASH fibrosis and in some cases to HCC remain elusive, although initial stages are likely to involve IR, increased flux of FFAs and decreased lipid oxidation. Since the rather benign simple steatosis can develop to the more aggressive NASH leading to chronic inflammation and fibrosis, it is important to understand and elucidate the molecular mechanisms leading to NAFLD so that

therapeutic interventions can be developed. Since VAP-1 is expressed in the hepatic microenvironment, and has been involved in the inflammatory response, glucose and lipid modulation in extra-hepatic tissues and is upregulated in inflammatory liver disease, obesity and type II diabetes it poses as a potential molecule, which may be involved in disease progression. Thus, just as adipose tissue has its own compensatory mechanisms in the form of leptin and adiponectin, VAP-1 may be the livers compensator.

Thus we hypothesized that VAP-1 is able to modulate glucose and lipid uptake in the liver through specific GLUT and possibly lipid transporters and at the same time due to its multiple functions such as immune modulation exacerbates disease pathogenesis. Thus the major aims of this thesis were:

(I) To investigate the expression patterns of genes involved in glucose and lipid transport in hepatic cells and hepatic disease.

(II) To develop an *ex-vivo* model and investigate the role of VAP-1 in glucose modulation in the liver.

(III) To investigate the role of VAP-1 in lipid modulation in the liver using an *ex-vivo* model.

(IV) To use mass spectrometry in the identification of possible lipid biomarkers and disease pathogenesis.

CHAPTER 2

2 MATERIALS & METHODS

2.1 Human Tissue

All human liver tissue used in this study was obtained from patients attending the Liver Unit at the Queen Elizabeth Hospital Birmingham, UK. Normal tissue was collected from donor material surplus to transplantation requirements or from excised non-diseased margin samples from tumor resection specimens. On occasion normal samples were rejected on the basis of excessive steatosis and these samples were designated steatotic. Diseased tissue was also obtained from explanted livers collected during transplantation surgery for, NASH, PBC and ALD. Liver tissue was cut into $2cm^3$ cubes and immediately snap frozen in liquid nitrogen, before storage at -80°C prior to cryosectioning or fixed in formal saline (10%, Adams, Healthcare) for paraffin embedded tissue blocks. Alternately fresh tissue was processed immediately for cell isolation (see section 2.8) or generation of Precision Cut Liver Slices (PCLS), (see section 2.3). Kidney, breast melanoma and adipose tissue were used as positive controls for immunohistochemistry and were obtained from routine clinical procedures surplus to requirement with appropriate ethical approval. Whole blood from patients with hemochromatosis (HFE) attending clinic at the Queen Elizabeth Hospital was collected for isolation of peripheral blood mononuclear cells (PBMC). All human material was collected with local research ethics committee approval (Walsall LREC) and written informed patient consent.

2.2 Murine Tissue

Murine tissue used in this study was obtained from C57BL/6 Wild Type (WT) (Charles River, UK) and VAP-1 Knock Out (KO) (Taconic, Denmark) mice fed on a High Fat Diet (HFD) (Special Diets Services, Essex, UK) for 12 weeks (Project License 40/3201). Mice were sacrificed and the liver was removed and used for the generation of PCLS (see section 2.3) or staining and quantifying steatosis.

2.3 Generation of Precision-Cut Liver Slices (PCLS)

To generate PCLS, 8mm tissue cores were aseptically obtained and placed in DMEM (Invitrogen, UK) at 4°C prior to slicing. A Krumdieck tissue slicer (Alabama Research and Development, USA), (Figure 2.1) was set up aseptically in a class II microflow tissue safety hood according to the manufacturers instructions. Tissue cores were placed into the Krumdieck tissue slicer assembly and aseptic 240μm thick PCLS were cut with a blade cycle speed ranging from 20-70/min depending on the type of tissue used (cirrhotic or normal). PCLS were then immediately transferred to tissue culture media consisting of Williams E media (Sigma, UK) supplemented with 2% Fetal Calf Serum (FCS, Invitrogen, UK), 0.1μM dexamethasone (Sigma, UK), and 0.5μM insulin (Novo-Nordisk) unless otherwise noted for specific assays. PCLS were cultured for up to 48 hours *ex vivo* in static culture at 37°C in 5% CO_2 in a humidified atmosphere (Karim et al., 2013).

In order to assess functional integrity of PCLS before or after specific treatments, slices were fixed in formal saline (10%, Adams, Healthcare) for three days followed by a three-day incubation in 30% sucrose (Sigma) made up in Phosphate Buffered Saline (PBS, Oxoid, UK). PCLS were then embedded in Tissue-Tek® Optimal Cutting Temperature polymer ™ (OCT) compound (Sakura Finetek, UK) in a foil boat, and snap frozen in liquid nitrogen prior to -80°C storage until they were cryosectioned at 15μm for immunohistochemical staining.

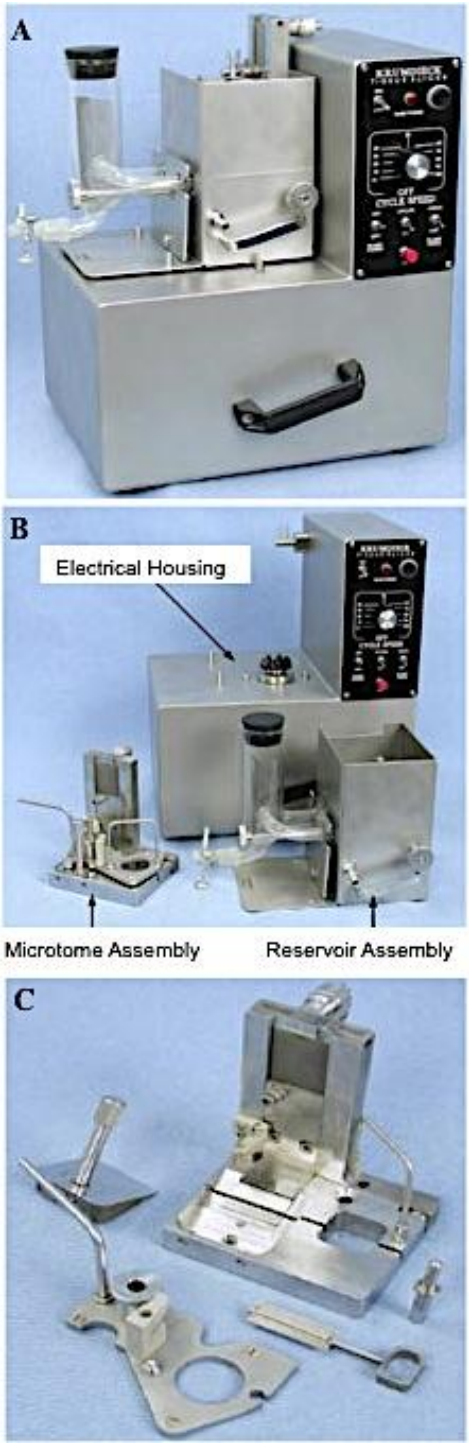

Figure 2.1: Functional components of the Krumdieck tissue slicer
(A) Krumdieck tissue slicer, (B) components of the Krumdieck tissue slicer include the electrical housing indicated by arrow, which rotates to allow the tissue core to be cut and is placed in the microtome assembly (indicated by arrow) which sits in the reservoir assembly to be cut. The reservoir assembly contains sterile PBS and allows cut PCLS to flow in to the glass funnel for collection. (C) Components of the microtome assembly. Figure adapted from (Estes et al., 2007).

2.4 Preparation of tissue sections for immunochemistry

For immunohistochemical staining procedures sections were produced from previously snap frozen human or mouse liver tissue cubes. Tissue blocks were mounted and cut on a BRIGHT (model-OTF) cryostat into 5-10μm sections which were then mounted on glass microscope slides (Xtra Slides, Leica UK), fixed in acetone (Fisher Scientific, Loughborough, UK) and stored at -20°C wrapped in foil. Some tissue sections were also taken from formalin fixed paraffin embedded tissue blocks which had been fixed in formal saline (10%, Adams, Healthcare) and tissue was embedded in paraffin and sectioned into 5-10μm sections using a rotary microtome (Leica microsystems) tissue was floated in a water bath and transferred on to glass slides and stored at room temperature.

2.5 Sectioning of liver tissues for Matrix Assisted Laser Desorption Ionization Mass Spectrometry Imaging (MALDI-MSI)

Serial tissue sections of normal, steatotic, NASH, ALD and PBC liver samples or WT and VAP-1 KO mice livers were cut using a cryostat (Leica) at 5μm and were mounted with water rather than OCT compound. Sections were placed on glass slides (Xtra Slides, Leica UK) for Hematoxylin and Eosin (H&E) staining. Sections were also placed on steel MALDI plates (AB Sciex, Warrington, UK) for MALDI imaging (section 2.29).

2.6 Immunohistochemical staining of human liver specimens

Fixed liver sections from patients stored at -20°C were defrosted at room temperature in foil for 15 minutes. The sections were then fixed in acetone for five minutes and endogenous peroxidase activity was blocked with 1-2 drops of peroxidase block (Dako) for 20 minutes or 0.3% H_20_2 (diluted in methanol) for 10 minutes. This was carried out in a humidified

chamber to prevent evaporation of solutions. The sections were washed twice with Tris Buffered Saline pH 7.6 (TBS) + Tween 20 (Sigma) and treated with 1- 2 drops of horse serum (Vector ImmPress Kit, Vector labs UK) for 30 minutes. The horse serum was drained and the sections were incubated for 1 hour with 100µl of primary antibody or respective control antibodies diluted in TBS pH 7.6 as indicated in Table (2.1). Sections were washed twice with TBS pH 7.6 and incubated with 100µl of secondary antibody (Vector ImmPress Kit, Vector labs UK) for 30 minutes, and were further washed twice with TBS pH 7.6 and incubated in 3,3' diaminobenzidine tetrahydrochloride (DAB) substrate (Vector, laboratories) for five minutes. The sections were washed in distilled water for 5 minutes, counterstained with Mayer's haematoxylin (Leica, Biosystems, Peterborough) for 1 minute and then washed in running tap water. The sections were mounted with Depex (DPX) mountant (Shandon, UK) and were left to dry for 24 hours before microscopic observation. On occasion paraffin-embedded, formalin-fixed human liver sections were used for immunohistochemical staining. Here all staining methods were as above with the addition of a dewaxing step and antigen retrieval. Briefly slides were deparaffinised in xylene (Sigma) (2 washes, 3 minutes each) and rehydrated through a series of alcohol changes (100% ethanol, 2 washes three minutes each, 95% ethanol three minutes, 70% ethanol three minutes) and finally washed in running tap water. To unmask the antigenic epitope, heat mediated antigen retrieval was performed were slides where incubated in warm Ethylenediaminetetraacetic acid (EDTA) buffer for approximately 10 minutes to allow exposure of antigenic sites.

2.6.1 Immunofluorescent staining

Analyses of protein expression in formalin-fixed sections cut from PCLS were demonstrated using immunofluorescent staining. Firstly antigen retrieval was carried out in EDTA buffer

(as described above, section 2.6). Sections were then washed in EnVision buffer (Dako) and non-specific binding to sections was inhibited by treatment with 2% casein blocking solution for 10 minutes (Vector Laboratories). Primary antibody or appropriate isotype-matched negative control antibody was applied for 1 hour, followed by a 5-minute wash with Envision buffer. The appropriate FITC-conjugated secondary antibody was then added for 30 minutes. The sections were then washed twice with buffer and mounted using VECTASHIELD mounting media (VECTOR Laboratories). Images were obtained using Zeiss LSM Zen conofocal.

Antigen	Isotype	Concentration	Source
GLUT1[1]	IgG2a	1µg/ml- 5µg/ml	ABCAM
GLUT2[2]	IgG	5µg/ml	ABCAM
GLUT4[1]	IgG2b	10µg/ml	ABCAM
GLUT9[2]	IgG	10µg/ml	ABCAM
GLUT10[2]	IgG	2.5µg/ml	ABCAM
FABP1[1]	IgG1	1µg/ml	Cambridge Bioscience
FABP4[1]	IgG1	10µg/ml	ABCAM
LRP8[2]	IgG	2µg/ml	Cambridge Bioscience
Caveolin 1[1]	IgG2b	0.2µg/ml	ABCAM
VAP-1[1]	IgG2a	5µg/ml	Biotie therapeutics
		Negative control antibodies	
	IgG2a	1µg/ml-5µg/ml	R&D
	IgG2b	0.2µg/ml	R&D
	IgG	2.5µg/ml-10µg/ml	ABCAM
		Secondary antibodies	
Immunopress secondary antibodies		1-2 drops on tissue section	Vector laboratories
2° Antibody, Anti mouse Alexa 488 FITC green	IgG2b	1/500	Invitrogen

Table 2.1: Antibodies used for immunohistochemial detection of proteins
Antibodies used in frozen and paraffin embedded human tissues. [1] denotes mouse anti human monoclonal antibodies whilst [2] denotes rabbit anti human polyclonal antibodies. Immunopress secondary antibodies contained both mouse and rabbit antibodies.

2.7 Histological staining to investigate liver morphology, steatosis and fibrosis

Fresh frozen, unfixed liver sections from normal, steatotic, NASH, ALD and PBC patients or from WT and VAP-1 KO mice fed on a HFD stored at -20°C were defrosted at room temperature in foil for 30 minutes. For morphological analysis, they were stained using standard H&E methodology (Leica, UK) with sequential baths in the reagent series indicated in Figure 2.2 for various time points as indicated.

To examine samples for the degree of steatosis present, we used lysochrome Oil Red O (ORO). Here a working solution of ORO made fresh in isopropanol (5g/L, Sigma UK) was further diluted to 60% v/v in distilled water. Sections were defrosted at room temperature in foil for 30 minutes, fixed in formal saline for 5 minutes, and were then washed in distilled water for 10 minutes before staining as illustrated in Figure 2.2.

Serial acetone-fixed frozen sections from the same patients were also stained with Sirius Red, (0.1% w/v, Sigma Aldrich in 1.3% saturated picric acid, Sigma) to allow visualisation of the extent of fibrosis present, according to standard protocols. Sections were defrosted at room temperature and then subjected to Sirius Red staining as illustrated in Figure 2.2.

Following completion of staining protocols, the slides were then mounted using DPX (Shandon, UK) and a 24x40mm coverslip (SurgiPath, UK) was placed on the sections. The sections were left to dry for 24 hours before visualising using a Zeiss Axiovert microscope, and representative images were captured using Axiovision software.

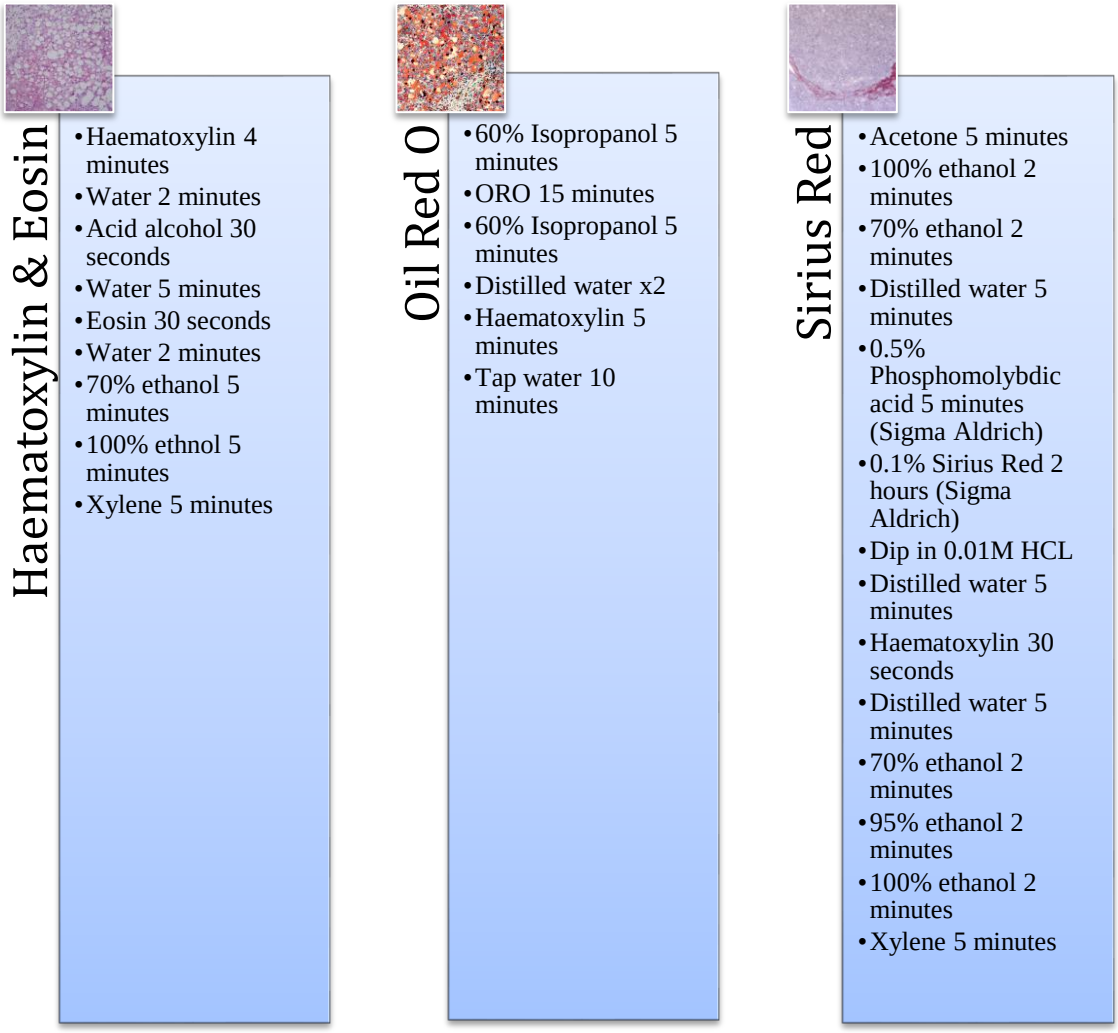

Figure 2.2: Protocol for histological staining procedures for H&E, ORO and Sirius Red staining.

2.8 Cell Isolation, Culture and Maintenance

2.8.1 Isolation and culture of HSEC, BEC and Fibroblasts from human liver tissue

In order to isolate cells from tissue samples, 5-10cm thick (approximately 50g) slices of human liver tissue were used. The tissue was chopped finely using scalpels and transferred to a sterile beaker containing 20ml of PBS. 5ml of 0.2% Collagenase solution (Sigma, Poole UK) was added and the tissue slice was incubated for 20 minutes in 5% CO_2 at 37°C until the tissue was well digested. The liver suspension was then passed through a fine mesh and washed with 200ml of PBS. The filtrate was then divided in to eight universal tubes and centrifuged at 550g for five minutes. The supernatant was discarded and the pellets were rewashed in PBS until the supernatants were relatively clear. To obtain the non-parenchymal cell populations the cell pellets were then resuspended in 3ml of PBS and layered over a 77% and 33% Percoll^{TM} (Amersham Biosciences) gradient and subjected to density gradient centrifugation at 869g, for 25 minutes. The non-parenchymal cell population was collected from the gradient interface, washed in PBS and centrifuged at 550g for 5 minutes.

Next the BEC were magnetically selected using positive selection by addition of mouse anti Human Epithelial Antibody (HEA) (50µg/ml, Progen, Biotec) and pan mouse Dynabeads ® (4 x 10^8 beads/ml, Dynal, UK). These were then seeded in to a Rat Tail Collagen (RTC, Sigma) coated T25cm^2 flask (Corning, UK) and cultured in BEC media consisting of: equal volumes of complete Dulbecco's Modified Eagle Medium (DMEM, GIBCO®, Invitrogen) and HAMS-F1 (GIBCO®, Invitrogen) containing 2mM L-Glutamine, 100U/ml Penicillin and 100µg/ml Streptomycin (Sigma, Dorset, UK). The medium was supplemented with 10% human serum (H+D supplies, UK), 2µg/ml hydrocortisone (Solu- Cortef Pharmacia), 125µl insulin (per 100ml) and 10ng/ml of cholera toxin (Sigma), Hepatocyte Growth Factor (HGF)

and Vascular Endothelial Growth Factor (VEGF), (both Peprotech, UK). This was then followed by positive selection of HSEC using mouse anti-human CD31 antibody (10µg/ml, Dako, ELY, UK) with magnetic selection using Dynabeads as above. HSEC were then seeded in to an RTC-coated T25cm^2 flask (Corning, UK). HSEC were maintained in a humidified atmosphere at 5% CO_2 in complete endothelial basal media (Invitrogen, Paisley, UK) containing 2mM L-Glutamine, 100U/ml Penicillin and 100µg/ml Streptomycin (Sigma, Dorset, UK). The medium was supplemented with 10% human serum (H+D supplies, UK) and 10ng/ml of both HGF and VEGF (both Peprotech, UK). The HSEC and BEC depleted supernatant from the cell preparation was then centrifuged at 550g for 5 minutes. The pellet which contained predominantly hepatic fibroblasts was resuspended in fibroblast growth media consisting of complete DMEM (GIBCO®, Invitrogen) containing 2mM L-Glutamine, 100U/ml Penicillin and 100µg/ml Streptomycin (Sigma, Dorset, UK) and supplemented with 16% FCS (H+D supplies, UK) seeded in to a T25cm^2 flask (Corning, UK) and cultured at 37°C in humidified atmosphere at 5% CO_2.

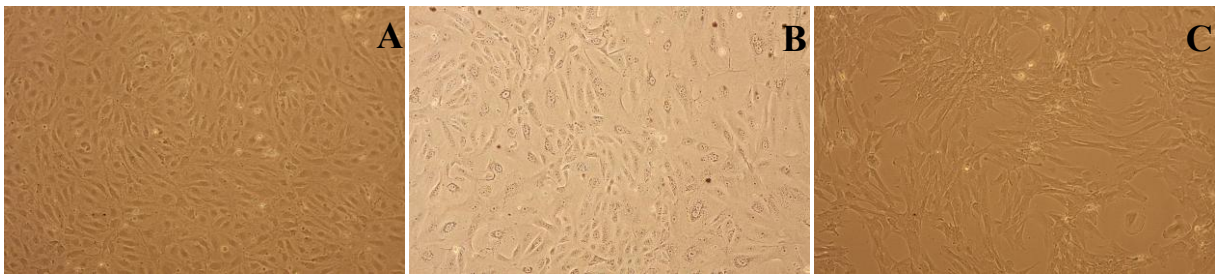

Figure 2.3: Representative phase contrast pictures of HSEC, BEC and fibroblast cells in culture.
Typical images of (A) HSEC, (B) BEC and (C) Fibroblasts isolated from human liver. Images taken using canon camera, connected to a phase contrast microscope, original magnification X10.

2.8.2 Isolation and culture of primary hepatocytes

Hepatocyte isolation was carried out according to established protocols within our laboratory (Bhogal et al., 2011). Briefly liver wedges (50-413g) were cut and placed in cold DMEM (Gibco, Paisley, UK). The wedge was perfused with PBS to remove blood from the liver and for the identification of two suitable vessels for cannulation and perfusion of buffers. Two 20-gauge cannulae (Becton-Dickinson, UK) were sutured into the vessels using a 3/0 prolene (Covidien, Hampshire, UK) purse string suture. The liver wedge was then perfused with wash buffer 10mM 4-(2-hydroxylethyl)-1-piperazineethanesulfonic acid (HEPES) pH7.2 (Sigma, Dorset, UK) at room temperature using a flow rate of 75ml/min. The liver wedge was then perfused with a chelating solution consisting of 10mM HEPES, 0.5mM Ethylene Glycol Tetra-Acetic Acid (EGTA) pH7.2, (Sigma), followed by a further perfusion with wash buffer. The liver wedge was then perfused with a recirculating enzymatic buffer at 37°C for 1-19min at a flow rate of 75ml/min consisting of 0.5% w/v Collagenase A from Clostridium Histolyticum (Roche, UK), 0.25% w/v 4.5units/mg Protease type XIV from Streptomyces Griseus (Sigma), 0.125% w/v 451units/mg Hyaluronidase from bovine testes (Sigma) and 0.05% w/v 552units/mg Deoxyribonuclease from bovine pancreas (Sigma). All enzymes were dissolved in Hank's Balanced Salt Solution (HBSS) (Gibco, Paisley, UK) supplemented with 5mM calcium and magnesium chloride. The liver was then mechanically disrupted and the suspension was filtered through a nylon mesh of 250μm (John Staniar Ltd, UK) followed by a nylon mesh of 60μm (John Staniar Ltd, UK). Cell suspensions were washed three times at 50xg for 10 minutes at 4°C in supplemented media, and cells were plated on to type 1 RTC plates for two hours after which the media was removed and replaced with Arginine-free Williams E media (Sigma) supplemented with hydrocortisone (2μg/ml), Insulin (0.124U/ml),

Glutamine (2mM), Penicillin (20,000units/l), streptomycin (20mg/l) and Ornithine (0.4 mmol/l), (Bhogal et al., 2011).

2.8.3 Isolation and culture of peripheral blood mononuclear cells (PBMC)

Approximately 25mls of blood from patients with HFE attending clinic at the Queen Elizabeth Hospital was layered on to 25mls of lympholyte (Cedarlane laboratories) separation gradient and centrifuged for 20 minutes at 900g with the brake at zero. Mixed PBMC were collected from the gradient interface and washed three times in PBS, centrifuged for 550g for 5 minutes. The pellet was resuspened in PBS and centrifuged further at 88g for 10 minutes to remove platelets. PBMCs were used fresh for isolation of RNA using the RNEasy mini kit (Qiagen, Crawley, UK) according to the manufacturers instructions.

2.9 Culture and maintenance of hepatocyte cell lines

The human hepatoma-derived hepatocyte cell lines Huh7.5 and HepG2 were used in this study and were available in house. The Huh7.5 and HepG2 cell line were resuscitated from liquid nitrogen storage and thawed using warm FCS to prevent any toxic effects from dimethyl sulfoxide (DMSO), which was a constituent of the freezing medium used. The cell suspension was then topped up with PBS and centrifuged at 550g for 5 minutes. The cell pellet was seeded in to a T75cm^2 flask (Corning, UK) cultured in complete DMEM, (GIBCO®, Invitrogen) containing 2mM L-Glutamine, 100U/ml Penicillin and 100µg/ml Streptomycin (Sigma, Dorset, UK). The medium was also supplemented with 10% FCS (Invitrogen, Paisley, UK) and 1ml of non-essential AAs (GIBCO®, Invitrogen). The cells were maintained in a 5% CO_2 humidified atmosphere at 37°C.

2.10 Maintenance of cells by freezing and storing

Primary cells or cell lines were stored long term in liquid nitrogen at the gaseous phase. Cultured cells were detached enzymatically with trypsin (Invitrogen), centrifuged at 550g for 5 minutes and resuspended in 95%FCS+5%DMSO (Sigma-Aldrich). The cell suspension was then placed in cryovials (Corning), which were placed in a Mr Frosty^{TM} (Wessington Cryogenics, Tyne & Wear, UK) containing isopropanol (Sigma). The Mr Frosty^{TM} was then transferred to -80°C for 24 hours which allowed gradual freezing of cells at a rate of 1°C per minute. After 24 hours the cryovials were stored at the gaseous phase of liquid nitrogen at -157°C. On requirement cells were removed from nitrogen storage and placed on ice to thaw, and the cell pellet was diluted in PBS, centrifuged at 550g for 5 minutes and seeded and cultured in the appropriate cell media.

2.11 Adenoviral Transfection of Human HSEC with VAP-1 Constructs

To stably express VAP-1 in HSEC, adenoviral constructs encoding WT hVAP-1 (enzymatically active), hVAP-1 (Y471F), which is enzymatically inactive, and a LacZ control virus (see table 2.2) were transfected in HSEC according to established protocols (Liaskou et al., 2011). HSEC were grown to confluency in 12 well plates. Media containing human serum was removed prior to transfection, cells were washed with PBS and cells were incubated in endothelial basal media containing 10% (v/v) FCS for one hour. The medium was discarded, cells washed again before adenoviral transfection at a multiplicity of infection of 600 for four hours. Cell numbers in confluent wells were calculated according to the formula below:

$$N = \frac{\text{Average number of cells from 2 fields X } 100cm^2 \text{ X } 3.8cm^{2\,*}}{0.1496\,^{*}}$$

* Approximate growth area in single well of a 12 well plate (Corning, UK)

* Cells counted in a field of $0.1496mm^2$ at X10 magnification

After incubation with viruses, the media was removed; cells washed again and complete HSEC media was added to the cells overnight. The cells were then incubated at 37°C in a humidified atmosphere containing 5% CO_2. The next day cells were washed prior to experimental use. To confirm the presence of hVAP-1, single color flow cytometry was performed.

Adenoviral Constructs	Concentration (PFU/ml)	Lot number
Padre hVAP-1	1.4×10^{10}	842
Padre hVAP-1	1.2×10^{10}	1252
hVAP-1_Y471F	2.6×10^{10}	1025
hVAP-1_Y471F	2.2×10^{10}	1241
LacZ	4.2×10^{10}	950
LacZ	1.4×10^{10}	1156

Table 2.2: Adenoviral constructs used for HSEC transfection
* Constructs were a kind gift from Professor Sirpa Jalkanen, Medcity laboratory, Turku, Finland.

2.12 Single Color Flow Cytometry

To confirm the presence of hVAP-1 positivity after transfection, single color flow cytometry was performed. Transfected HSEC were washed in PBS, detached with trypsin and spun at 550g for 5 minutes. The pellets were resuspended in Fluorescence Activated Cell Sorting (FACS) buffer (PBS + 10% FCS) and incubated with mouse anti human VAP-1 antibody (TK8-14 FITC conjugated) and matched isotype control (IgG1 FITC) conjugated antibodies

for approximately 40 minutes in the dark at 4°C, washed in FACS buffer and samples were run on the Cyan FACS analyzer.

Antibody (FITC conjugated)	Clone	Concentration	Source
VAP-1	TK8-14	10μg/ml	Biotie, Finland
IgG1	DAK-G01	10μg/ml	Dako

Table 2.3: Antibodies used for single color flow cytometry

2.13 Determination of cell and PCLS function and viability in culture

2.13.1 Treatment of cells and PCLS with palmitic and oleic acid

Huh7.5 and HSEC were liberated from a confluent T75cm^2 flask using Trypsin (Invitrogen) and seeded in to a 24 well or 48 well plate as required. They were cultured in the appropriate media (see sections 2.8 and 2.9) for 24 hours until confluent. Cells or PCLS were then treated with PA or OA (both Sigma, UK) at 250μm, 500μm or 1500μm (PA made up in methanol and OA in ethanol 25mM and stored under nitrogen gas) for 3, 6 and 24 hours. Control wells were treated with methanol or ethanol alone. For cells duplicate plates were treated identically and then fixed and stained with Hoechst dye (2.5μg/ml, Invitrogen, UK) to permit cell quantification and signal normalisation after treatment. Cell counts were calculated according to the methodology described below in section 2.17. The data from cells treated with ORO and Hoechst dye was manipulated to express the amount of ORO normalised to amount of lipid taken up per 100,000 cells. Treated cells were fixed in formal saline for 5 minutes, washed in PBS three times and then stored in PBS at 4ºC until use for analysis whilst PCLS were fixed in formal saline (10%, Adams, Healthcare) for three days followed by a three-day incubation in 30% sucrose (Sigma) made up in PBS.

2.13.2 Quantification of lipid accumulation in fatty acid treated cells and PCLS using ORO labelling

Following FA treatment, cells or PCLS were treated with ORO to permit quantification of lipid accumulation. Cells or PCLS were treated with 60% isopropanol (Sigma) for five minutes followed by a 45-minute incubation with ORO; this was then followed by a 5-minute incubation with 60% isopropanol (Sigma) and then cells and PCLS were washed in distilled water. Finally the ORO reagent was solubilised out of treated cells or PCLS, in order for spectrophotometric quantification, 300µl of isopropanol (Sigma) was added to each well, and the plate was placed on a plate shaker for 5 minutes. 100µl of solubilised supernatant from each well or an isopropanol control was added to triplicate wells in a 96 well plate, and the plate was read at an absorbance of 520nm. Each PCLS was weighed and results normalised and expressed as amount of lipid taken up per 500mg of tissue. For cells the data was manipulated to express the amount of ORO normalised to amount of lipid taken up per 100,000 cells as described in section (2.17).

2.13.3 Use of MTT to assess viability of PCLS and cultured cells

In order to assess the viability of either cells cultured in 24 well plates or PCLS in culture a Methyl Thiazol Tetrazolium (MTT) assay was used (Sigma). Control or pretreated cultured cells seeded in to a 24 well plate at a density of 1.0×10^5 per well, or PCLS were incubated with MTT. PCLS were cultured for 1.5 hours at 37°C Williams E media containing 2mg/ml MTT, whilst cells were treated with 300µl of 0.4mg/ml MTT made up in DMEM without phenol red (Invitrogen UK) and incubated for 1 hour until the development of a purple insoluble formazan product was visualised. Thereafter PCLS and cells were washed with PBS and the resulting formazan product was extracted by treatment with DMSO (Sigma

Aldrich) for 5 minutes. Absorbance of replicate samples was read at 570nm using a microplate reader (Biotek Proview) using KC4^{TM} software, (Wolf Laboratories). The absorbance of DMSO alone was also read as a background control. All results were expressed as means of replicate samples. Signal from PCLS was normalized to per 500mg of tissue, and percentage viability of cultured cells and PCLS was calculated using the following formula:

$$\% \text{ Viability} = \frac{\text{Mean absorbance of sample}}{\text{Mean absorbance of control}} \times 100$$

2.14 Assessment of lipid accumalation in PCLS and hepatic cells after VAP-1 treatment

In order to study the effects of VAP-1 activity on lipid uptake in an intact organ culture system and isolated cells PCLS and Huh7.5 were used. PCLS were cultured in Williams E media (Sigma, UK) supplemented with 2% FCS (Invitrogen, UK). Insulin and dexamethasone were removed from the culture media unless added as treatments separately. Huh7.5 cells were cultured in the appropriate media as described (section 2.9). PCLS and Huh7.5 cells were stimulated with treatments alone as indicated in Table 2.4 or in combination with each other for approximately 18 hours followed by a 6-hour incubation with either 250μm OA or 250μm PA. Media alone was added in as a control.

Reagent	Concentration	Source
Insulin	0.10IU	Novo-nordisk
Methylamine	200µm	Sigma
Benzylamine	200µm	Sigma
rVAP-1	500ng	Biotie therapeutics
H_20_2	10µm	ProLABO BDH
BEA	400µm	Sigma
BAPN	250µm	Sigma
Chlorgyline	200µm	Sigma
Pargyline	200µm	Sigma

Table 2.4: Reagents used for glucose and lipid uptake assays

2.15 Assessment of triglyceride secretion from PCLS after VAP-1 interventions

To quantify and detect secretion of TAG after VAP-1 interventions and subsequent treatment with PA at 250µm, a TAG secretion assay (Cayman chemical calorimetric assay (CAT10010303) was carried out according to the manufacturers instructions.

2.16 Assessment of glucose uptake in PCLS and hepatic cells after VAP-1 treatment using 2- Deoxy-D- Glucose [3H (G)] uptake assay

In order to study the effects of VAP-1 treatment on glucose uptake in the intact liver and isolated liver cell populations, PCLS and single populations of HSEC (transfected see section 2.11), Huh7.5 and HepG2 were used. PCLS were cultured and stimulated in 500µl of low glucose DMEM (Invitrogen) (glucose concentration 1000mg/L) media consisting of 2% FCS (Invitrogen, UK) for approximately 2.5 hours. Cells were cultured for 24 hours in the appropriate media as indicated in sections 2.11 and 2.9 in 12 or 24 well plates. Thereafter the complete media was removed; cells were washed with PBS and incubated with treatments for 2.5 hours in low glucose DMEM (Invitrogen) containing growth factors or FCS as appropriate for each cell type. For HSEC human serum was replaced with 0.5% Bovine Serum Albumin (BSA) as human serum contains VAP-1. Treatments used are as indicated in

Table 2.4 were PCLS or cells were treated alone with each reagent or in combination with other treatments as indicated in specific figures. PCLS and cells were then washed in PBS at least three times and were further incubated for 30 minutes in low glucose DMEM containing 0.1mM 2 Deoxy-glucose (Sigma) and 2µci/ml 2-Deoxy-D-Glucose [3H (G)] (Sigma). PCLS and cells were washed three times with ice cold PBS to stop the reaction and each PCLS was lysed in approximately 400µl of 1N NaOH (Sigma) for 30 minutes on a plate shaker, whilst cells were lysed in 400µl of 0.2% Triton X-100 (Sigma) and visualised microscopically to ensure cell liberation. The lysates were then mixed with 4ml of scintillation fluid (Fisher Scientific, UK) and sent for scintillation counting on a Packard T2500 liquid scintillation counter (Perkin Elmer). Samples were run on a five-minute program to give tritium Disintegrations Per Minute (DPM) values. Each PCLS was weighed and results expressed and normalized to 500mg of tissue.

2.17 Validation of Hoechst dye for cell quantification

Here cells were seeded at densities ranging from 8.0×10^3 -8.0×10^5 in 24 well plates and fixed with methanol for five minutes. Hoechst dye (Bisbenzamide 33342, Invitrogen UK) which specifically incorporates in AT rich regions of double stranded DNA in cell nuclei was used to determine cell number at a final concentration of 2.5µg/ml. 500µl of Hoechst dye was added to each well for five minutes, cells were washed and fluorescence was measured on a plate reader (excitation 355nm, emission 465nm) as above. Background fluorescence signals were also determined from control wells containing PBS alone. Plotting an XY scatter graph of the absorbance values obtained for each cell density generated a standard curve. A regression equation was generated so that in future experiments cell number could be determined from the cell number calibration. Experiments were repeated three times using

different cell isolates and in each case the standard curve was used only if the R^2 value was ≥ 0.9.

These calibration curves were then used in conjunction with ORO staining to express the amount of ORO taken per 100,000 cells. Graphical representations showing ORO uptake per 100,000 cells were plotted by dividing the cell number by 100,000. The absorbance values were then multiplied by this corrected value as were the SEM values and a graph showing ORO uptake per 100,000 cells plotted.

2.18 Determination of PCLS function and viability in culture

2.18.1 Quantification of Albumin production for the assessment of hepatocyte synthetic function in PCLS

Hepatocyte function was assessed by measuring albumin production by Enzyme-Linked Immunosorbent Assay (ELISA) using optimal concentrations of coating antibody (0.5mg/ml goat anti-human albumin antibody) and detection antibody (1mg/ml HRP-conjugated goat anti-human albumin antibody: both Bethyl Industries, USA) and albumin standards (Bethyl Industries, USA). Briefly the coating antibody was diluted 1/200 in coating buffer 0.05M (5.3g/l) Na_2CO_3 pH 9.6 and 100µl was applied to each well of a Nunc 96 well maxisorp immunoplate and incubated for 1 hour at room temperature. The wells were then washed three times with 400µl of wash solution (Tween20 containing 0.2% FCS), prior to the addition of 200µl of blocking solution to prevent unspecific binding of primary antibody (50mM Tris. 0.14M NaCl, 1% BSA) pH 8. The wells were incubated at room temperature for 30 minutes, followed by three washes with washing buffer.

Standards (ranging from 400ng/ml-6.25ng/ml), samples and a negative control (uPA-SCID plasma) were diluted in sample buffer (50mM Tris. 0.14M NaCl, 1% BSA, 0.05% Tween20) pH 8 and 100µl of each was placed in triplicates on the plate and incubated for 1 hour at room temperature. This was then followed by five washes with washing buffer prior to the addition of the detection antibody which was diluted 1/100 in sample buffer and 100µl was added to each well for 1 hour at room temperature. The wells were washed a further five times with washing buffer and the binding of detection antibody was visualized with Tetramethylbenzidine (TMB) substrate (Sigma). The reaction was stopped with the addition of 100µl of 1M sulphuric acid (H_2SO_4) and the plate was read at an absorbance of 490nm on a Synergy HT plate reader using the KC4 program. The albumin concentration in samples was determined by comparison to the standard concentration curve.

2.18.2 Assessment of glycogen storage in PCLS

PCLS were cultured in complete media for up to 48 hours before representative samples were cryopreserved and sectioned (see section 2.3). For assessment of glycogen content, sections were stained using ready-made working concentrations of Periodic Acid Schiff Stain (Leica, UK) using standard methodology. Briefly the sections were washed in excess distilled water, followed by a 5-minute incubation in 500µl of periodic acid, rinsed in tap water and incubated with 500ul of Schiff's reagent for ten minutes. The sections were then rinsed twice with distilled water for up to 5 minutes before being dehydrated through graded alcohol twice for 3 minutes and clearance series three times, for two minutes. Sections were mounted using a non-aqueous mountant (Thermoscientific) and left to day for 24 hours before microscopic observation

using a Zeiss Axiovert microscope and representative images were captured using Axiovision software.

2.18.3 Assessment of nuclear integrity in PCLS using Hoechst dye

Nuclear integrity was assessed using Bisbenzimide (Hoescht dye, 2.5ug/ml, Sigma UK) staining followed by fluorescent microscopic imaging. PCLS frozen sections were incubated for five minutes with 500µl of 2.5ug/ml Hoechst dye. The sections were then rinsed with PBS and mounted with VECTASHIELD mounting media (VECTOR Laboratories) and imaged by fluorescent microscopy. Image J was used to assess the percentage of staining as a proportion of that seen at control time points.

2.19 Determination of the enzymatic activity of VAP-1 in whole tissues by the Amplex Ultra Red method

In order to quantify endogenous VAP-1 activity in normal and diseased tissue, approximately 2cm/2cm tissue blocks of normal, steatotic, NASH, ALD and PBC livers were snap frozen in liquid nitrogen and stored at -80°C. Frozen tissue blocks were then digested in 0.2% Triton X-100 (Sigma-Aldrich) containing protease inhibitor cocktail using gentleMACS^{TM} tubes (Miltenyi Biotec). Tissue lysates were briefly spun at 13148g for 20 minutes, and the supernatant was collected and placed on ice whilst protein concentration in a sample of the lysate was measured using a Bio-Rad DC Protein Assay according to the manufacturers instructions. A protein standard curve using dilutions of BSA (Sigma) was generated to calculate the concentration of protein in each sample. Total protein samples from all tissues were then diluted to a final protein concentration of 8mg/ml and stored at -20°C.

The Amplex ultra red assay was then used to quantify VAP-1 activity in these protein lysates. Briefly the reaction works as follows: upon addition of substrates such as MA or BA to VAP-1, enzymatic activity leads to the production of formaldehyde, ammonia and hydrogen peroxide. The hydrogen peroxide produced in this reaction reacts with the Amplex Red reagent (10-acetyl-3, 7-dihydroxyphenoxazine) in the presence of horseradish peroxidase (HRP) in a 1:1 stoichiometric ratio, producing Amplex UltroxRed, a brightly fluorescent product with a long wavelength spectrum, which can be quantified spectrophotometrically. Protein lysates were added in triplicates to a 96 well flat bottom plate. Benzylamine (2mM) was added in the presence or absence of the specific VAP-1 inhibitor BEA (400μM). Chlorgyline and Pargyline inhibitors for MAOA and MAOB were also added in to wells containing BA alone to block non-specific activity. The fluorometric reaction was initiated by the addition of the Amplex red reagent consisting of 1/100 Amplex ultra red (20mM stock, Invitrogen) and 1/100 HRP (200U/ml stock, Invitrogen). The reaction was measured continuously in a fluorescence microplate reader (Biotek Proview) for approximately 3 hours using excitation of 530nm and emission detection at 590nm using KC4^{TM} software, (Wolf Laboratories). PBS was added as a negative control to some wells and 30% hydrogen peroxide as a positive control.

2.20 Analysis of gene expression in cultured cells and whole liver using microarrays and quantitative PCR (qPCR)

2.20.1 RNA extraction

2.20.1.1 RNA extraction from primary cells and cell lines

Microarray analysis and qPCR was carried out to see what the basal expression of glucose and fatty acid transporters was in cultures of primary hepatocytes, HSEC, Huh7.5, HepG2, BEC, fibroblasts and PBMC cells and in normal, steatotic, NASH, ALD and PBC patients to see whether firstly what the expression patterns were and weather these changed in disease, and between different cell types. In addition to see whether the activity of VAP-1 altered expression of any of these transporters. Specific arrays such as the human NF-κB signaling pathway PAHS-025A (Qiagen) was used to analyze the expression of genes involved in the NF-κB signal transduction pathway in PCLS which had been treated with VAP-1+MA for 2.5 hours.

For the microarray analysis Huh7.5 and HSEC were grown in culture and total cellular RNA from samples was extracted from all cell populations, whilst for qPCR analysis total RNA was isolated from HSEC, BEC, fibroblasts, primary hepatocytes, HepG2, PBMC cells and normal, steatotic, NASH, ALD and PBC explanted livers. To determine whether there were any changes in lipid transporter expression after FA treatment RNA was also extracted from Huh7.5, which had been treated with 250μm OA or PA using the RNEasy mini kit (Qiagen, Crawley, UK) according to the manufacturers instructions.

Briefly Media from confluent T75cm_2 flasks containing cells was removed and the flasks were washed with 10ml of PBS. Then 5ml of trypsin (Invitrogen) was added to the flask to detach cells. The detachment of cells was visualized under a phase contrast microscope. The trypsin was neutralised with 20ml of PBS and the cell suspension was centrifuged at 550g for 5 minutes. The pellet was resuspended in PBS and then further centrifuged to remove residual trypsin; the pellet was resuspended in 200µl of PBS and 1ml in RNA later (Ambion). The sample was stored at 4°C for 24 hours and then transferred to -80°C storage. The RNA samples were also treated with DNAase treatment with RNAase free DNAase (Qiagen, UK) as part of the protocol instructions. This was done to eliminate possible genomic contamination, which may interfere with downstream reactions.

2.20.1.2 RNA extraction from human liver tissue

Tissue blocks from normal, steatotic, NASH, ALD and PBC patients, roughly 2cm/2cm, had previously been preserved in RNA later and stored at -80°C. Tissue blocks were removed from -80°C storage and placed on ice, approximately 30mg of tissue was excised and used to isolate RNA as previously described (see section 2.20.1.1). RNA was also extracted from untreated PCLS and PCLS treated with 200µm MA for approximately 4.5hours; here the PCLS were submerged in buffer RLT+β-mercaptoethanol immediately after treatment for RNA extraction. The concentration of the eluted RNA from all samples was checked as well as the purity and integrity before further use using the NanoDrop spectrophotometer (Thermo Fisher Scientific). The 260/280nm and 260/230nm ratios were calculated and samples with a value of 2 at 260/280nm ratio were indicative of relatively pure RNA. For samples, which were used for microarray analysis, the RNA integrity was confirmed using Agilent 2100 Bioanalyser (Palo Alto, CA, USA).

2.20.2 cDNA synthesis

All RNA samples were transcribed into cDNA with approximately 1µg of total RNA using the first strand cDNA synthesis kit (Roche) according to the manufacturer's protocol unless otherwise stated for example for specific arrays such as the Fluidigm ® 96.96 Dynamic Array ™ Integrated Fluidic Circuit; the minimum amount of RNA which could be used was 125ng/ul and all RNA samples were diluted to 125ng/µl and approximately 1µl of total RNA was transcribed to cDNA using the superscript TM III first strand synthesis supermix kit (Invitrogen) according to the manufactures instructions. Samples used for the human NF-κB signaling pathway PAHS-025A (Qiagen) were transcribed using the RT^2 First Strand Kit (SABiosciences, Qiagen) according to the manufacturers instructions. The concentration of cDNA from all samples was checked as well as the purity and integrity before further use, using the NanoDrop spectrophotometer (Thermo Fisher Scientific).

2.20.3 Microarray Analysis

Transcriptome analysis was carried out for all samples using Agilent Human Whole Genome Oligo Arrays (catalogue number G4112F) in accordance with the Agilent One-Color Microarray-Based Gene Expression Analysis Protocol. Key consumables were purchased from Agilent Technologies UK Ltd (Wokingham, Berkshire, UK) unless otherwise stated.

2.20.3.1 Labelling

RNA from each sample (200 to 1000ng depending on amount and concentration available) and the appropriate amount of Agilent One-Color RNA Spike-In RNA were labeled with reagents supplied in the Agilent Quick Amp one-color Labeling Kit, according to manufacturer's instructions, and with final reagent concentrations and volumes as follows:

Primers were annealed to template by mixing 1.2 µl T7 Promoter Primer, RNA and spike-in control in a volume of 11.5µl. Samples were then denatured at 65ºC for 10min followed by incubation at 4ºC for 5min. First Strand Buffer (1X stock), DTT (10mM), dNTP (0.5mM), MMLV (1µl) and RNaseOut (0.5 µl) were then added to make up the cDNA synthesis reaction (20µl), which was incubated for 2h at 40 ºC. After 15 min denaturation at 65ºC, the reaction was made up to 80µl with the addition of Cyanine 3-CTP (0.3mM), Transcription Buffer (1X), DTT (10mM), NTP (8µl), PEG (4%), RNaseOUT (0.5µl), Inorganic Phosphatase (0.6µl), and T7 RNA Polymerase (0.8µl) and incubated for 2h at 40ºC to synthesize the fluorescently- labeled cRNA. The labeled cRNA was then purified with the RNeasy Mini Kit (Qiagen Ltd, Crawley, UK) according to the manufacturer's protocol.

2.20.3.2 Hybridisation and Scanning

The labeled cRNA was then hybridized to the Agilent human whole genome Oligo Array slides (Agilent array ID 014850) using reagents from the Agilent Hybridization Kit (catalogue number 5188-5242) with a slight modification to manufacturer's protocol: 2µg (instead of 1.65µg) of the labeled sample RNA was used for hybridization. Hybridization was performed for 17 hours at 65ºC with 10-rpm rotation on a mixer platform. Slides were washed for 1 min at 22ºC in Wash Solution 1 (catalogue number 5188-5325), followed by 1 minute in Wash Solution 2, which was pre-warmed, to 37ºC (catalogue number 5188-5326), 30 seconds in acetonitrile (Fisher catA/0630/PB15), and 30 seconds in Agilent Stabilization and Drying Solution (catalogue number 5185-5979). Slides were then scanned with the Agilent Microarray Scanner System. Data was extracted using the Agilent Feature Extraction Software (v.9.1), and analyzed using Gene Spring (GX.12.5).

2.20.3.3 Data analysis

Genes or spots, which were not reliably detected, were filtered/removed and the data sets were normalized based on percentile shift normalization. Percentile shift normalization is a global normalization, where all the spot intensities in an array are adjusted to enable comparison with other arrays. This normalization computes the 75th percentile of the log transformed expression values for each array independently, across all spots, then subtracts this value from the log transformed expression value of each spot. To detect GLUT and fatty acid transporters, heat maps were generated for genes which were detected in >75% of all samples tested. Heat maps, are a visual tool to aid assessment of the expression patterns of genes across different samples.

Data was represented by the per gene normalization method. For example the median expression of a given gene is found across all samples and then expression is relative to the median expression of that gene in all samples tested.

2.20.4 Quantitative real-time PCR

2.20.4.1 Pre amplification of cDNA for Fluidigm® 96.96 Dynamic Array™ Integrated Fluidic Circuit

To validate our results from the microarray data the Fluidigm ® 96.96 Dynamic Array ™ Integrated Fluidic Circuit (IFC) was used. Here all cDNA samples had to be preamplified with the TaqMan PreAmp Master Mix (Applied Biosystems). Briefly all 20X Taqman assays to be used in the array were pooled and diluted to 0.2X in Tris-EDTA buffer 100X (Sigma). High expressers such as the house keeping genes β-actin and GAPDH were excluded from the

preamp stage. Taqman fluorogenic 5' nuclease assays using gene-specific 5'FAM labeled probes were used in this array.

Reagent	µl/reaction
TaqMan PreAmp Master mix (2X) (Applied Biosystems)	2.5
0.2X pooled TaqMan assay	1.25
cDNA	1.25
Final volume (µl)	5

Table 2.5: Preamp reaction mix

The Preamp thermocycling parameters were as follows: 95°C for 10 minutes, 14 cycles at 95°C for 15 seconds followed by 60°C for 4 minutes. The PreAmplified template was diluted (at least 1:5 dilution) with 20µl of 1X Tris-EDTA buffer 100X (Sigma) and stored at -20°C until further use.

2.20.4.2 Fluidigm® 96.96 Dynamic Array™ Integrated Fluidic Circuit chip preparation

The 96.96 syringes containing 150µl of control line fluid were gently inserted into the dynamic array. The plate was then primed for 20 minutes on the IFC loader (136X script), before 5µl of each sample and probe were dispensed on to the 96.96 dynamic array on respective inlets on the plate. The plate was loaded on the IFC for 1 hour and 30 minutes on the load mix (136x) script. When the load mix script had finished the plate was removed from the IFC controller, the blue protective film from the underside of the plate was removed, any dust particles or debris on the plate were removed and the plate was then run in the fluidigm for two hours and 10 minutes. All samples were run in triplicate and therefore three 96.96 Dynamic Array plates were used.

Gene	Gene symbol	Taqman Assay ID	Agilent Probe ID
GLUT1	SLC2A1	Hs00892681_m1*	A_23_P571
GLUT2	SLC2A2	Hs01096904_m1*	A_24_P405705
GLUT3	SLC2A3	Hs00359840_m1*	A_24_P81900
GLUT4	SLC2A4	Hs00168966_m1*	A_32_P151263
GLUT5	SLC2A5	Hs00161720_m1*	A_24_P111054
GLUT6	SLC2A6	Hs01115485_m1*	A_23_P169249
GLUT7	SLC2A7	Hs01013553_m1*	-
GLUT8	SLC2A8	Hs00205863_m1*	A_24_P175435
GLUT9	SLC2A9	Hs01115485_m1*	A_24_P118211
GLUT10	SLC2A10	Hs00368843_m1*	A_24_P271323
GLUT11	SLC2A11	Hs00368843_m1*	A_23_P404565
GLUT12	SLC2A12	Hs00376943_m1*	A_23_P395001
GLUT13	SLC2A13	Hs00369423_m1*	A_23_P10211
FABP1	FABP1	Hs00155026_m1*	A_23_P79562
FABP2	FABP2	Hs01573164_g1*	A_23_P391711
FABP3	FABP3	Hs00269758_m1*	A_24_P62783
FABP4	FABP4	Hs01086177_m1*	A_23_P8820
FABP5	FABP5	Hs02339439_g1	A_24_P673063
FABP6	FABP6	Hs01031183_m1*	A_23_P43846
FABP7	FABP7	Hs00361426_m1*	A_23_P134139
FATP1	SLC27A1	Hs01587917_m1*	A_24_P382489
FATP2	SLC27A2	Hs00186324_m1*	A_23_P140450
FATP3	SLC27A3	Hs00225680_m1*	A_24_P179816
FATP4	SLC27A4	Hs00192700_m1	A_24_P257971
FATP5	SLC27A5	Hs00202073_m1*	A_23_P4611
FATP6	SLC27A6	Hs00204034_m1*	A_23_P41789
CAV1	CAV1	Hs00971716_m1*	A_23_P134454
CD36	CD36	Hs00169627_m1*	A_24_P925505
LRP1	LRP1	Hs00233856_m1*	A_23_P124837
LRP2	LRP2	Hs00189742_m1*	A_23_P28295
LRP8	LRP8	Hs00182998_m1*	A_23_P200222

Table 2.6: Probe identifiers for Fluidigm® 96.96 Dynamic Array™ and Agilent microarrays
*All Taqman probes from Applied Biosystems

For the human NF-κB signaling pathway PAHS-025A (Qiagen) the RT^2 SYBR® green qPCR Mastermix (SABiosciences, Qiagen) was used according to the manufacturers instructions and the PCR conditions were 95°C for 10 minutes required to activate hotstart taqDNA Polymerase, followed by 95°C for 15 seconds and 40 cycles at 60°C for 1 minute, qPCR was performed using the 700HT (Applied Biosystems) real time PCR machine.

2.21 Whole tissue lipid analysis using Mass Spectrometry (MS) and Gas Chromatography (GC)

Mass spectrometric techniques were used in order to assess spatial location and distribution of phospholipids and FFA in normal, steatotic, NASH, ALD and PBC livers as well as PCLS treated with VAP-1 and its substrates. In order to assess whether certain lipids were associated with disease pathogenesis such as in NASH livers and whether these correlate to mouse models of steaotohepatitis and fatty liver disease (WT and VAP-1 KO mice fed on a HFD), and acute treatments of PCLS with VAP-1 were investigated.

2.22 Extraction of lipids from liver tissue and PCLS for analysis by GC and MALDI-MS dried droplet analysis

Tissue blocks from normal, steatotic, NASH, ALD and PBC explanted livers or PCLS treated with VAP-1 interventions which had previously been snap frozen in liquid nitrogen were removed from -80°C storage. Each block of tissue was weighed and approximately 0.13-0.15g of tissue was removed from each block for lipid extraction using a modified version of the Folch's methodology (Folch et al., 1957). Briefly, each block of tissue was finely chopped on a glass petri dish on ice and transferred to 1ml of 2:1 (CHCl3: MeOH) (Fisher Scientific, Leicestershire, UK) mixture. The tissue and chloroform: methanol mixture was then made up to 20 fold its volume with 2:1 (CHCl3: MeOH) and homogenized vigorously. The samples were then filtered into a separating funnel through fat free filter paper (Whatman®). The organic extract containing the lipids were washed in deionized distilled water, which formed two separate phases, the aqueous phase at the top, and the organic phase (chloroform: methanol containing lipid) formed the bottom layer. The organic phase was decanted and retained whilst the aqueous phase was discarded. The organic phase was then

rewashed for a second time with deionized distilled water. This method was also used for the extraction of lipids from treated PCLS samples. The final extracts were then collected and stored in glass vials at -80°C until further use.

For GC analysis the 2:1 (CHCl3: MeOH) solvent was evaporated off from 500µl of each liver lipid extract sample. 750µl of hexane (Fisher Scientific, Leicestershire, UK) was added followed by 500µl of 250mM KOH in MeOH (Fisher Scientific, Leicestershire, UK). This mixture was then shaken for two minutes and left to stand for two minutes. This resulted in the formation of two layers of which the upper layer was pipetted into a vessel for GC injection. Samples along with a standard containing 37 methyl esters were run on a DB225 column and GC was performed with Rian Griffiths (Chemistry Department, University of Birmingham) using established methodology. Chromatograms for each sample were obtained with Retention Times (RT); these were then compared to retention times to the known standard to assign a lipid identity to each peak.

2.23 Identification of lipid species in tissue extracts using MALDI-MS dried droplet analysis

MALDI-MS dried droplet analysis allows acquisition of lipid spectra from digested lipid extracts, here 10 replicate spots (approximately 0.5µl) of lipid sample from each liver were pipetted on to a steel MALDI multi-well plate (AB Sciex, Warrington, UK) and allowed to dry. This was then followed by the addition of 0.5µl α-Cyano-4-Hydroxycinnamic Acid (CHCA) matrix (25mg/ml, Sigma) which was prepared in 80% MeOH with 0.1% TFA (both Sigma). Complex extract samples were analyzed on a hybrid quadrupole time of flight mass

spectrometer (Qstar XL, Applied Biosystems, Warrington, UK), fitted with an orthogonal MALDI ion source (pulsed N_2 laser, 337nm, operated at 20Hz, 200μm core diameter fiber delivered). All data were acquired in positive refelectron mode. Spot analyses were interrogated using a circular laser pattern, summing 30 scans per spectrum. Ion transmission was optimized and a Focusing Potential (FP) of 60 and declustering potential DP2 of 20 were used in all experiments. Data processing was performed using MATLAB (MathWorks Inc), and Principle Component Analysis (PCA) was performed to reduce the dimensionality of the data. For all MALDI data sets the spectra were collated to generate a total spectrum and peak intensities of interest were extracted from each individual spectrum. Lipid maps (http://www.lipidmaps.org) and lipid libraries were used to identify lipid species as well as MS/MS fragmentation analysis to confirm lipid identities. Experiments where performed by Sumera Karim and Rian Griffiths.

2.24 Identification and localization of lipids in tissue extracts using MALDI imaging

MALDI imaging was used to visualize the spatial distribution of lipids within intact tissue sections. Liver sections (5μm) from normal, steatotic, NASH, ALD and PBC explanted livers or from WT and VAP-1 KO mice livers were cut onto steel MALDI plates (AB Sciex, Warrington, UK) for MALDI imaging as described in section 2.5. CHCA matrix (see above) was then applied to each tissue section using an artist's brush (Draper Air Tools Airbrush kit, Hampshire, UK) with Badger Airbrush propellant (Badger, Illinois, USA). Tissue samples were analyzed on a hybrid quadrupole time of flight mass spectrometer (Qstar XL, Applied Biosystems, Warrington, UK), as described above. For all MALDI imaging data sets, the spectra were collated to generate a total spectrum and peak ion images for peaks of interest were generated in MATLAB. H&E and MALDI ion image overlays were produced to see if

lipids correlated to anatomical regions, these were generated using GNU image manipulation program 2.6.

2.25 Statistical Analysis

Data was analyzed using students T test to compare means of two samples unless otherwise stated for specific assays for example a two way ANOVA with no replication was used to examine differences between time and concentration in the lipid uptake assays using Graphpad Prism version 5.0a, for gene array data a one-way ANOVA (unequal variance) with Benjamini Hochberg was used with a p value cut of at $p<0.05$ using gene spring (GX.12.5) and are indicated in specific figures. Statistical significance accepted as * ≤ 0.05, ** ≤ 0.01, *** ≤ 0.001.

CHAPTER 3

3 HEPATOCELLULAR EXPRESSION OF GLUCOSE AND LIPID TRANSPORTERS

3.1 Introduction

In a climate of rising obesity and increasing incidence of fatty liver disease in the Western world, this thesis sets out to examine potential roles of novel mediators that may impact upon hepatic glucose and lipid homeostasis. As stated in the introductory chapter, factors which may give rise to excess TAG within the hepatocyte leading to NALFD, include:

- Increased uptake of FFAs and glucose by liver cells. This may occur in response to an overload of dietary fats and possibly due to altered expression of FA and carbohydrate transport proteins.
- Decreased β-oxidation in mitochondria (Nakamuta et al., 2005)
- Increased DNL
- Decreased FA efflux caused by decrease in the production of apolipoprotein B which is involved in the transport of cholesterol low-density lipoproteins (LDL) and triglycerides to the rest of the body (Utzschneider and Kahn, 2006), (Chitturi and Farrell, 2001).

This thesis will consider lipid and glucose uptake paths, and also how disease induced alterations in transporter proteins may impact on pathogenesis. Upon investigation, of published data regarding basal expression of carbohydrate and lipid transporters in the human liver, we were surprised by the lack of available information. Therefore we begin by documenting expression in health and disease. Since both glucose and lipid uptake requires presence of active transport systems, we felt it was important to look at expression patterns of each.

Hepatocytes and other non-parenchymal cells require energy for cellular processes and this energy can be generated from carbohydrates and FFAs entering the cell. Carbohydrates enter using members of a specific family of 14 integral membrane transporter proteins also known as solute carrier 2A (SLC2A) proteins. These proteins are divided in to three classes (class 1-3) (Olson and Pessin, 1996), (Joost and Thorens, 2001), class I consisting of GLUT1, 2, 3, 4 and 14, class II GLUT5, 7, 9, 11 and class III 6, 8, 10, 12, 13. The GLUT proteins are classified according to their transport characteristics whether they are inducible or intrinsic and sequence similarities (Bell et al., 1990) and some are sensitive to stimuli such as insulin.

3.1.1 Hepatic expression and function of carbohydrate transporters

To date the expression of GLUT1, GLUT2 (Wu et al., 2008), (Nordlie et al., 1999), GLUT9 (Keembiyehetty et al., 2006) and GLUT10 (McVie-Wylie et al., 2001) has been reported on the hepatocytes (Karim et al., 2012). However it is clear that expression patterns of the different family members differs between species, and tissue and cell type specific differences have been described (Karim et al., 2012) and are summarized in Table 3.1.

Class	GLUT Isoform	Human subcellular expression/localization	Animal/other hepatic expression	References
Class I	GLUT1	Cytoplasmic hepatocyte expression in some HCC	Expressed on hepatocytes, endothelial cells KC and rat cholangiocytes. Also found on sinusoidal membrane of rat and porcine hepatocytes	(Spolarics et al., 1993, Lazaridis et al., 1997, Aschenbach et al., 2009, Shinoda et al., Roh et al., 2004, Bilir et al., 1993)
	GLUT2	Human liver	In rats localises on sinusoidal membrane+ malignant hepatocytes	(Axelrod and Pilch, 1983, Thorens et al., 1990), (Leturque et al., 2009)
	GLUT3	Human liver	Porcine liver, rat hepatocyte plasma membrane	(Aschenbach et al., 2009), (Ciaraldi et al., 1995, Kurata et al., 1999, Shinoda et al.)
	GLUT4		Porcine liver. Rat HSCs	(Aschenbach et al., 2009, Tang and Chen, 2010)
Class II	GLUT5	Normal liver tissue hepatocytes (cytoplasmic)	Porcine livers	(Aschenbach et al., 2009, Godoy et al., 2006)
	GLUT9	Majority of expression in hepatocytes of normal liver and HCC with granular cytoplasmic expression more in pericentral areas		(Takanaga et al., 2008)
	GLUT11		Porcine liver	(Aschenbach et al., 2009)
Class III	GLUT6		Hepatoma cell lines	(Kayano et al., 1990)
	GLUT8		Mouse perivenous hepatocytes, porcine liver	(Aschenbach et al., 2009, Gorovits et al., 2003)
	GLUT10	Human liver	Porcine liver, zebra fish livers	(Aschenbach et al., 2009, Chiarelli et al., 2011, McVie-Wylie et al., 2001)
	GLUT12	Normal and cirrhotic human liver lysates	Bovine liver	(Miller et al., 2005b), (http://www.abcam.com/GLUT12-antibody-ab100993.html)

Table 3.1: Summary of reported human and animal hepatic expression of GLUT proteins

GLUT1 expression is suggested to be low in hepatocytes compared to endothelium and KC in animal models (Spolarics et al., 1993). Cholangiocytes also express GLUT1 to facilitate the absorption of glucose from bile (Lazaridis et al., 1997). Cellular distribution remains controversial however, with hepatocyte sinusoidal membrane localization reported in rat and porcine hepatocytes (Aschenbach et al., 2009), (Shinoda et al.) and zonal expression patterns (Tal et al., 1991) and membrane localization reported under basal conditions restricted to hepatocytes proximal to the hepatic venule (Bilir et al., 1993). In contrast cytoplasmic GLUT1 expression has been noted in some HCC, with suggestions that this may be used as a marker for distinguishing cholangiocarcinomas from HCC (Roh et al., 2004).

Whilst some degree of GLUT1 expression in the liver is likely, GLUT2 is considered the major GLUT transporter in the liver (Axelrod and Pilch, 1983), (Gould and Holman, 1993). In rats it has been reported to localize to the sinusoidal membrane domain of normal (Leturque et al., 2009), (Thorens et al., 1990) and malignant hepatocytes. GLUT2 is more important for glucose efflux during gluconeogenesis (Leturque et al., 2009) than glucose uptake, and this is supported by studies in murine hepatocytes where upon insulin stimulation both GLUT2 and the insulin receptor co localize and internalize in the endosomal fraction (Leturque et al., 2009), (Eisenberg et al., 2005), (Gonzalez-Rodriguez et al., 2008). There is also evidence to suggest that other GLUTS may play a role in the exit of glucose from the liver since in mice lacking GLUT2 the rate of hepatic glucose production is not impaired (Guillam et al., 1998).

GLUT3 is expressed in porcine livers (Aschenbach et al., 2009), and in rat hepatocytes it is localized to the plasma membrane with the bile canicular membrane being more enriched

with GLUT3 than the sinusoidal membrane (Shinoda et al.). In humans immunohistochemical staining of primary and metastatic lesions suggests an increase in hepatic expression during carcinogenesis (Kurata et al., 1999). Although there has been some speculation that the low level of human GLUT3 expression in the liver reflects expression upon a specific subset of cells (Ciaraldi et al., 1995) to date there is no data documenting specific cellular expression.

GLUT5 is localized to the cytoplasmic regions of human hepatocytes (Godoy et al., 2006), as is GLUT9 which is found as granular structures in HCC (Godoy et al., 2006) and in normal liver is found in pericentral hepatocytes. Hepatocytic expression is supported by data from the tumor cell line HepG2 cells where GLUT9 together with GLUT1 has been found in the plasma membrane. The membranous distribution in cancer cells suggests a transport role in glucose influx (Takanaga et al., 2008), and studies showing that GLUT9 inactivation in mouse leads to hyperuricosuria suggest a wider substrate specificity (Preitner et al., 2009) with confirmed ability to transport urate (Vitart et al., 2008). In contrast GLUT10 may have roles in antioxidant defense. It is expressed in liver of several species (McVie-Wylie et al., 2001), (Aschenbach et al., 2009), (Chiarelli et al., 2011) but its cellular localization is yet to be confirmed. Its localization in mitochondria of smooth muscle cells and adipocytes, ability to transport antioxidant vitamin C (Lee et al., 2010) and contribution towards mitochondrial respiration in the cardiovascular system (Willaert et al., 2012) suggest it may play important protective roles in the fatty liver.

The expression patters of GLUT1, GLUT2, GLUT3, GLUT5, GLUT9 and GLUT10 in the liver are reasonably well documented; in contrast there is little information on GLUT4,

GLUT6, GLUT7, GLUT11, GLUT12, GLUT13 and GLUT14 expression in the liver. GLUT4 is the main inulin sensitive member of the family and hence this property distinguishes it from other members of the GLUT family. It is mainly expressed in insulin sensitive tissues such as skeletal, cardiac, brown and white adipose tissue (Zhao and Keating, 2007), whilst the liver is generally considered to lack significant expression of GLUT4 (Nevado et al., 2006) its mRNA has been detected in porcine liver (Aschenbach et al., 2009). In contrast, GLUT6 mRNA has been documented in hepatoma cell lines with a lack in normal liver (Kayano et al., 1990) whilst GLUT7 was initially reported as a hepatic microsomal glucose transporter found in the endoplasmic reticulum, which facilitated the release of glucose formed in the process of gluconeogenesis and glycogenolysis for export into the blood (Gould and Holman, 1993), (Waddell et al., 1992). However this long standing view has recently been challenged by Ann Burchell who has shown that neither human nor rat liver contain mRNA comparable to the clone termed GLUT7 (Burchell, 1998). Similarly GLUT8 mRNA has only been described in porcine (Aschenbach et al., 2009) and mouse livers were it is detected in perivenous hepatocytes (Gorovits et al., 2003) and might function in regulating glycolytic flux.

Finally whilst there are some reports of mammalian hepatic mRNA expression for GLUT11 (Aschenbach et al., 2009) and GLUT12 (Miller et al., 2005b), and a single report of GLUT12 protein expression in human liver tissue (http://www.abcam.com/GLUT12-antibody-ab100993.pdf) there is little convincing data for expression patterns of these, and none for GLUT13 and GLUT14 in the human liver. Therefore this chapter will focus on documenting disease specific and cellular expression of the GLUT transporters 1-13.

Over the last two decades the identification of lipid transport systems such as the FABP family, FATP family and the lipoprotein binding CD36/FAT have been reported. Its important to understand which proteins regulate FA uptake in the liver. In obesity related conditions such as the MetS, IR leads to inhibition of lipolysis in adipose tissue this leads to an increase in circulating FFA, which are taken up by cells. There is a fine balance between FFA uptake, storage and oxidation, which is regulated by specific transport proteins. These proteins also direct intracellular trafficking of FA (FABPs and FATPs). For FA to be targeted for storage or β-oxidation to the mitochondria they need to be activated via FATPs by their Acyl CoA activity- (ACS). When there is a deregulation in these proteins it can lead to excess storage of lipids within cells, which eventually can cause IR, ER stress and apoptosis. Furthermore these transport proteins have tissue specific expression and function for example in the liver they are involved in storage and oxidation of lipids, in the intestine they aid in absorption of dietary lipids, in macrophages and adipose tissue they order storage and lipid mediated gene expression and in neuronal tissue maintain the phospholipid bilayer. In addition other proteins such as CD36 have been found to localize with GLUT4 in caveolae rich regions and (Lisanti et al., 1994), (Gonzalez-Munoz et al., 2009) the LRPs have been associated with elevated TAG levels (Shen et al., 2012).

It is likely that these FATP and FABP may play an important role in the pathogenesis of metabolic diseases such as NASH and so we were also interested to study them in this chapter. Multiple families and classes of receptors play a role in fatty acid homeostasis and a brief detail of the major family members is below.

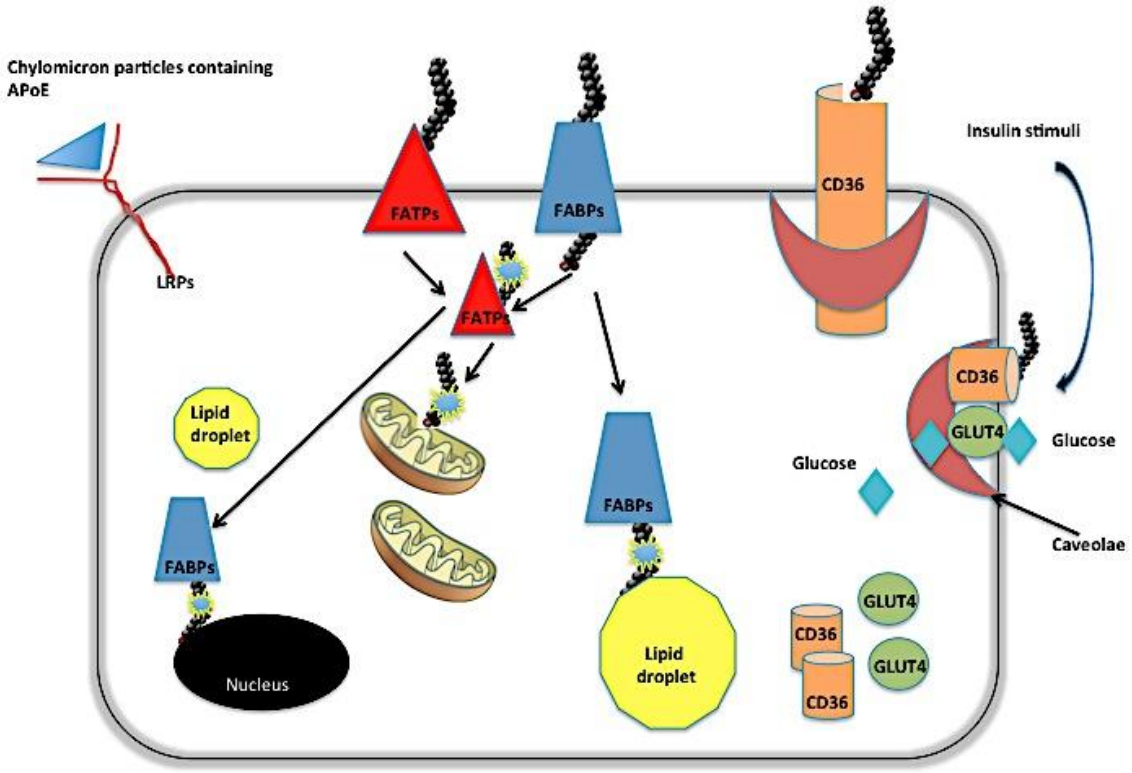

Figure 3.1: Roles of GLUT and fatty acid trafficking proteins
In the post prandial state, insulin stimulation triggers CD36 and GLUT4 mobilization to the cell surface from intracellular storage sites, this leads to glucose and lipid uptake. CD36 is also found at the cell membrane. FA can also be taken up by FABPs, which are found on the cell membrane and also intracellularly were they can transport FAs activated by FATPs to either the mitochondria for β-oxidation or storage in lipid droplets. Activated FA can also be transported to nuclear receptors such as PPARs and NF-κB hence regulating genes which are involved in metabolic and inflammatory processes (Musso et al., 2009), (Tan et al., 2002), (Helledie et al., 2000), (Wolfrum et al., 2001).

3.1.2 Hepatic expression and function of lipid transporters

3.1.2.1 Fatty Acid Transport Proteins (FATPs)

The FATP family (SLC27A) contains 6 integral membrane proteins involved in long chain fatty acid uptake (LCFA) uptake. These are found in all tissues, although the distribution at different sites varies (Musso et al., 2009). Therefore we begin by reviewing the current literature on specific expression of lipid transporters in the liver.

FATP1 expression is insulin regulated in adipose tissue were it translocates and colocalises with GLUT4 on the cell membrane to facilitate LCFA uptake (Stahl et al., 2002). Thus the protein is predominant in white adipose tissue, skeletal muscle and the heart (Musso et al., 2009). However a recent study has reported FATP1 mRNA expression in chicken liver (Wang et al., 2011) and it is expressed in HepG2 cells although to lesser extent than the other FATP (Sandoval et al., 2008). In contrast FATP2 is abundantly expressed in the liver (Musso et al., 2009), (Moya et al., 2012) consistent with a role in peroxisomal FA processing (Falon 2010). However it is likely a multifunctional protein with roles in LCFA transport and FA biosynthesis, in peroxisomes of mouse liver (Falcon et al., 2010). In Huh7.5 and HepG2 cells its found only in the endoplasmic reticulum (Krammer et al., 2011) whist the most abundant expression appears to be in the adrenal gland, brain, ovary, and testis.

In the context of hepatic lipid transport, FATP5 is the predominant isoform expressed in the liver (Auinger et al., 2010), and found on the plasma membrane of hepatocytes most proximal to the sinusoids (Musso et al., 2009) consistent with a role in uptake of circulating lipids. A further member of the family, FATP6 is reported as being absent in liver (Gimeno et al.,

2003) and is rather selectively expressed in the heart (Musso et al., 2009) where it transports LCFA (Auinger et al., 2012).

3.1.2.2 Fatty Acid Binding Proteins (FABPs)

The second family of fatty acid trafficking proteins considered in this thesis is the FABP family, which consists of nine membrane transport proteins that can bind FA as well as eicosanoids (Makowski and Hotamisligil, 2005), (Makowski and Hotamisligil, 2004). They are also found in the cytosol were its speculated they may aid in FA transport to nuclear receptors such as PPARs and NF-κB hence regulating genes which are involved in metabolic and inflammatory processes (Musso et al., 2009), (Tan et al., 2002), (Helledie et al., 2000), (Wolfrum et al., 2001). Again differential cell and tissue specific expression patterns have been reported and are linked to organ-specific functions.

FABP1/L-FABP is expressed in the pancreas, small intestine, kidney and the liver (Musso et al., 2009) were its reported to constitute 2-5% of total cytosolic protein (Atshaves et al., 2010). Moreover in mice lacking FABP1 there is strong association with IR, increased lipogenesis and TAG secretion (Newberry et al., 2003). Similarly a recent study has shown that polymorphisms of FABP1 make an individual more susceptible to NAFLD (Peng et al., 2012b) and also to developing type II diabetes (Mansego et al., 2012).

FABP2 is reported to be mainly expressed in the small intestine and has been considered as a candidate gene for diabetes (Humphreys et al., 1994). It binds saturated LCFA with high affinity and unsaturated LCFA with lower affinity and is involved in the intracellular transport of LCFA and their acyl CoA esters (Bass et al., 1985), (www.uniprot.org). There

are no studies documenting liver specific expression of FABP2 although certain polymorphisms of the gene have been associated with NAFLD. Certainly mice lacking FABP2 are more susceptible to dietary induced fatty liver disease, independent of FABP1 expression (Agellon et al., 2007).

No human hepatic protein expression data exists for FABP3 which is considered the 'heart specific' isoform, however mRNA expression of FABP3 has been reported in porcine livers (Li et al., 2010) and is also found at lower levels in mammary gland, skeletal muscle and blastocyts (Musso et al., 2009). In contrast FABP4 is expressed in adipocytes and macrophages (Musso et al., 2009) and has also been documented in the nucleus and cytoplasm of murine endothelial cells and in hepatic and portal vein branches (Elmasri et al., 2009b).

FABP5 is expressed in the liver and is also found in abundance in the skin and to a lesser extent in the mammary gland, eyes, tongue, adipocytes and kidney (Musso et al., 2009). It binds LCFA with high affinity and has a lower affinity for short chain FAs and those containing double bonds (www.uniprot.org).

FABP6 and FABP7 are both expressed in the ileum (Musso et al., 2009), but whilst a role for bile acid transport is attributed to FABP6, decreased lipid uptake occurs in response to FABP7 blockade in murine cells (Ahn et al., 2012). Hepatic expression of these proteins is less well documented although FABP6 mRNA is present in zebra fish livers with a 55.3% sequence homology to human FABP6 and FABP7, mRNA is present in murine kupffer cells (Abdelwahab et al., 2003). The remaining members of this family are also little studied, with

FABP8 expression documented in myelin and FABP9 in testis (Musso et al., 2009) and the suggestion that hepatic expression of FABP10 increases in response to food intake in chickens (Hughes and Piontkivska, 2011). However a mammalian orthologue of this gene does not exist and similarly FABP11 mRNA has only been documented in fish (Agulleiro et al., 2007), (Karanth et al., 2008), (Torstensen et al., 2011).

3.1.2.3 Additional transport proteins

We also felt it was important to look at other transport proteins like the LRPs since LRPs have been associated with elevated TAG levels and fibrogenesis in the liver (Pieper-Furst et al., 2011), (Shen et al., 2012) and also CAV1 and CD36 as there is growing evidence suggesting these proteins work jointly together to aid FA and glucose uptake (Souto et al., 2003). Since caveolae contain VAP-1, which regulates glucose and lipid uptake through GLUT4 and CD36 translocation (Pilch et al., 2007), (Karlsson et al., 2002) we considered documentation of CD36 and Caveolin expression may be of benefit. Caveolins are constituents of caveolae, the small infoldings of plasma membranes, which have multiple roles including endocytosis and intracellular signaling. Caveolins are important for the formation of the caveoli, can bind cholesterol and FAs (Dugail and Postic, 2010), (Trigatti et al., 1999), (Murata et al., 1995) and are important in lipid droplet formation, cell signaling and protein trafficking (Pol et al., 2004). There are three caveolin family members which all localize with caveoli plasma membrane facing the cytoplasmic interface of the cell, but the distribution varies with cell type although Caveolin 1 and Caveolin 2 are normally co-expressed (Dugail and Postic, 2010). Epithelial, endothelial cells and adipocytes express Caveolin 1 with Caveolin 3 expressed in cardiac and skeletal myocytes (Dugail and Postic, 2010). Within the liver, Caveolin 1 is expressed at low levels in endothelium and HSCs and

increases in cirrhotic liver. (Yokomori et al., 2002). In particular, fatty hepatocytes have increased expression inside and around the lipid droplets as well as increased expression in the inner membrane of their mitochondria (Mastrodonato et al., 2011).

CD36/FAT is ubiquitously expressed (Greenwalt et al., 1992), (Febbraio et al., 2001). Within the liver however, its expression in hepatocytes has been reported to be low (Musso et al., 2009), but it is expressed on HSEC were it acts as a scavenger receptor (class B) for oxidized lipid (Lalor et al., 2006). Two properties discriminate it from the FABP and FATP family, firstly there are no tissue specific isoforms and secondly it has diverse functions other than FA uptake (Musso et al., 2009). CD36 allows FAs bound to albumin to dissociate and sequester on the outer side of the plasma membrane, creating a diffusion gradient which allows the FA to flip flop across the inner leaflet, and it has been suggested the movement of these FA through the plasma membrane and to the cytosol is through contact with FABP (Glatz and Storch, 2001). CD36 has been shown to localize in caveolae (Lisanti et al., 1994) and in murine fibroblasts Caveolin1 is needed for CD36 translocation to the cell membrane (Ring et al., 2006). Furthermore decreased expression of Caveolin 1 in adipocytes has been shown to result in decreased caveolae on the plasma membrane resulting in decreased expression of IRS and GLUT4 leading to decreased glucose uptake (Gonzalez-Munoz et al., 2009). Muscle CD36 localizes with Caveolin 3 (Vistisen et al., 2004) and in the heart insulin stimulation causes simultaneous GLUT4 and CD36 translocation (Schwenk et al., 2010). Furthermore a soluble form of CD36 (sCD36) has been found to positively correlate with IR, fatty liver and atherosclerosis in non diabetic subjects (Handberg et al., 2012).

The final types of receptors we where interested in are the LRP family. LRP1, LRP2 and LRP8 are endocytic receptors, which bind multiple ligands (Lillis et al., 2008) and are involved in cholesterol homeostasis. LRP1/CD29 is expressed in the liver parenchymal and KC (Lillis et al., 2008) and in rat HSEC (Oie et al., 2011). It binds apolipoprotein E (Beisiegel et al., 1989) and is involved in clearance of chylomicron particles and their degradation (Lillis et al., 2008) and reduced hepatic LRP1 has been associated with atherosclerosis (Espirito Santo et al., 2004). LRP2/Megalin C has been associated with fibrogenesis in mice liver (Pieper-Furst et al., 2011) and LRP8 polymorphisms are related to increased TAG levels in patients with coronary artery disease (Shen et al., 2012). However as with the proteins we have discussed previously, little evidence of hepatocellular expression and changes in disease have been reported. We have summarized the current state of knowledge in Table 3.2 below:

Fatty acid transport protein family	Isoform	Substrates	Human Subcellular expression/ localization	Animal/other hepatic expression	References
FATP	FATP1	LCFA		HepG2 cells, chicken livers	(Stahl et al., 2002, Wang et al., 2011, Sandoval et al., 2008)
	FATP2	Activates Long and branched chain FA	Hepatocytes in HepG2 and Huh7 cells is only found in the ER	Peroxisomes of mouse liver	(Musso et al., 2009, Moya et al., 2012, Krammer et al., 2011), www.uniprot.org (Falcon et al., 2010)
	FATP4	FFA, very LCFA	ER of Huh7 and HepG2		(Herrmann et al., 2001, Krammer et al., 2011)
	FATP5		Cell membrane of hepatocytes facing HSEC	Hepatocytes of mice	(Auinger et al., 2010, Musso et al., 2009, Doege et al., 2006)
	FATP6	Translocation of LCFA across PM			(Gimeno et al., 2003)
FABP	FABP1	FA and eicosanoids	Hepatocytes, also found as a cytosolic protein		(Atshaves et al., 2010, Charlton et al., 2009a)
	FABP2	Intracellular transport of LCFA and their acyl CoA esters. High affinity for saturated LCFA and low affinity for unsaturated LCFA			www.uniprot.org
	FABP3			Porcine livers	(Li et al., 2010)
	FABP4	Binds LCFA and retinoic acid	Human fatty liver	Mice, hepatic portal vein branches, endothelial cell cytoplasm and nucleus	www.uniprot.org (Elmasri et al., 2009b), (Westerbacka et al., 2007)
	FABP5	High affinity for FA, especially long chain compared to short and those containing double bonds.	Human fatty liver		(Musso et al., 2009), www.uniprot.org, (Westerbacka et al., 2007)
	FABP6			Zebra fish livers	(Alves-Costa et al., 2008)
	FABP7			Mice kupffer cell cytoplasm	(Abdelwahab et al., 2003)
CD36		Oxidized lipid, HDL, cholesterol esters	Hepatocytes, HSEC		(Lalor et al., 2006) (Musso et al., 2009)
Caveolin	Caveolin1	Cholesterol and FA	HSEC, HSCs		(Yokomori et al., 2002), (Dugail and Postic, 2010)
LRPs	LRP1	Chylomicron particles	Parenchymal and Kupffer cells	Rat HSEC	(Lillis et al., 2008), (Oie et al., 2011)

Table 3.2: Summary of reported human and animal hepatic expression of fatty acid trafficking proteins.

In summary, we are interested in novel mechanisms linked to glucose and lipid uptake in the liver such as VAP-1/SSAO, which may contribute to hepatic steatosis. Currently there is little detailed description of the expression patterns of GLUT proteins or indeed fatty acid trafficking proteins in normal or diseased livers (see summary Tables 3.1 and 3.2). These proteins have vital roles in glucose and lipid uptake for example GLUT5 is important in the transport of fructose and has been associated with NAFLD (Vila et al., 2008). Decreased Caveolin 1 expression is linked to GLUT4 which results in decreased glucose uptake (Gonzalez-Munoz et al., 2009). FABP4 and FABP5, are associated with IR and NAFLD (Westerbacka et al., 2007) and polymorphisms in FABP1 have been linked to NAFLD (Peng et al., 2012b). CD36 null mice show increased insulin sensitivity and decreased muscle TAG content (Goudriaan et al., 2003), (Hajri et al., 2002) and LRP2 has been associated with fibrogenesis in mice liver (Pieper-Furst et al., 2011). Furthermore there is evidence to suggest these proteins work together to achieve glucose and lipid homeostasis, for example GLUT4 and its association with FATP1 and CD36 (Stahl et al., 2002), (Schwenk et al., 2010). Taken together it is clear that these transporters have significant implications in disease pathogenesis and yet their hepatic expression in disease is unknown.

Therefore the major aims of this chapter were:

Aims:

I) To document the expression of GLUT transporters GLUT1-13 in normal and diseased liver tissue.

II) To document the expression of lipid trafficking proteins FATP, FABP, CD36, Caveolin 1 and LRPs in normal and diseased liver tissue.

III) To characterize the specific hepatocellular expression of GLUT transporters and lipid trafficking proteins by using histological and cell-based transcriptome analysis.

3.2 Methods

For methods pertinent to this chapter please refer to the general methods p60-65.

3.3 Results

3.3.1 Microarray analysis reveals expression of GLUT receptors in human liver

In this thesis we wanted to examine the expression patterns of carbohydrate and fatty acid trafficking proteins in human liver, parenchymal and non-parenchymal cells. We began by using microarrays to measure gene expression in normal liver, HSEC and hepatocytes (represented by the cell line Huh7.5). Heat maps were generated using GeneSpring (GX.12.5) which showed transcripts were present for all GLUTS in normal liver, HSEC and Huh7.5 with the exception of GLUT7 (Figure 3.2 and Figure 3.3A), which was not present. For each heatmap the color code is shown as a key indicating average gene intensity change for all genes sampled. Data for our genes of interest is expressed relative to the median expression of a given gene in all samples tested, and the colour key at zero (Figure 3.2B) indicates median expression of all genes across all samples whilst blue coloration indicates expression lower than median expression and red coloration indicates expression higher than the median.

We found that expression of eight of our key genes significantly ($P<0.05$) differed by more than two-fold between HSEC and Huh.7.5. Thus GLUT2, 53.8fold ($p<3.17E-0.4$), GLUT4 2.9fold ($p<0.018$), GLUT8 10.13fold ($p<6.09E-05$), GLUT11 3.49 ($p<0.026$) were down regulated on HSEC compared to hepatocytes and GLUT3 9.78fold ($p<0.001$), GLUT6 3.99fold ($p<0.004$), GLUT10 7.17fold ($p<6.35E-04$), GLUT12 37.70fold ($p<0.004$) were more abundant in HSEC (Figure 3.3C).

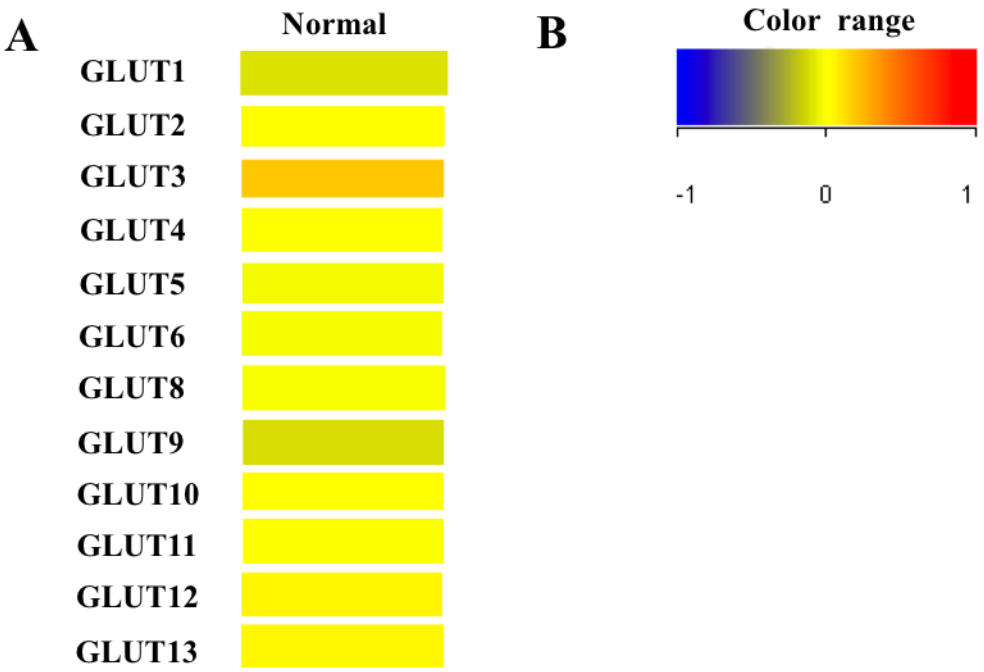

Figure 3.2: Microarray analysis of GLUT receptor expression in normal liver
(A) RNA was extracted from normal livers using Qiagen RNeasy mini kit and assessed for purity and integrity using an Agilent bioanalyser before being run on human oligo arrays (Agilent array ID 014850). Extracted data was analyzed using Gene Spring (GX.12.5). Column represents liver type and rows are the gene of interest, data is expressed relative to the median expression of a given gene in all samples tested. (B) Color key indicates log values (log base 2) were zero indicates median expression of all genes across all samples whilst blue coloration indicates expression lower than median expression and red coloration indicates expression higher than the median. Representative data from N=14 normal livers.

A

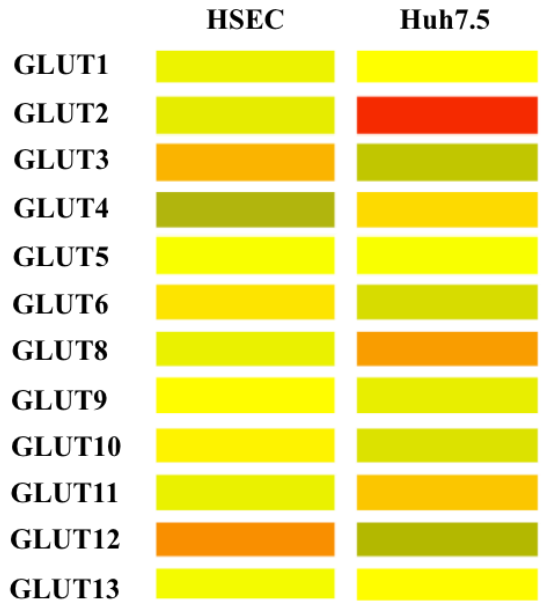

B

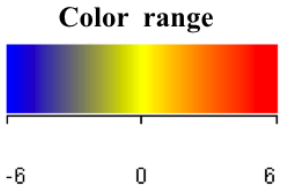

C

GLUT	Expression in HSEC	Fold Change	P-value
GLUT2	Down	53.8	3.17E-04
GLUT3	Up	9.78	0.001
GLUT4	Down	2.90	0.018
GLUT6	Up	3.99	0.004
GLUT8	Down	10.13	6.09E-05
GLUT10	Up	7.17	6.35E-04
GLUT11	Down	3.49	0.026
GLUT12	Up	37.70	0.004

Figure 3.3: Microarray analysis of GLUT receptor expression in HSEC and Huh7.5

(A) RNA was extracted from HSEC and Huh7.5 using Qiagen RNeasy mini kit and assessed for purity and integrity using an Agilent bioanalyser before being run on human oligo arrays (Agilent array ID 014850). Extracted data was analyzed using Gene Spring (GX.12.5). Columns represent cell type and rows are the gene of interest, data is expressed relative to the median expression of a given gene in all samples tested. (B) Color key indicates log values (log base 2) were zero indicates median expression of all genes across all samples whilst blue coloration indicates expression lower than median expression and red coloration indicates expression higher than the median (C) Table of GLUT probes which were >2-fold and $p<0.05$ different between HSEC compared to Huh7.5 using one way ANOVA with Benjamini Hochberg correction, data representative from N=5 HSEC and N=3 Huh7.5.

3.3.2 qPCR confirms expression of GLUT family receptors in human liver

We then used qPCR to measure the mRNA transcript levels of the glucose transporters GLUT1-13 in normal and diseased human liver tissue, and relative expression compared to the averaged pooled CT values of β-actin and GAPDH housekeeping genes was calculated using the Livak method (Livak and Schmittgen, 2001, Schmittgen and Livak, 2008). The use of multiple house keeping genes allowed for accurate quantification and normalization, as the expression patterns of both GAPDH and β-actin were unchanged in disease (for example the average CT values for pooled GAPDH and β-actin were 24.5 in normal and 24.11 in steatotic livers). In agreement with our microarray data, mRNA for all GLUT receptors bar GLUT7 was present in normal liver (Figure 3.4) with GLUT2, GLUT8, GLUT9 and GLUT10 most abundantly expressed. GLUT7 was only expressed in one normal liver and only in two cases of ALD.

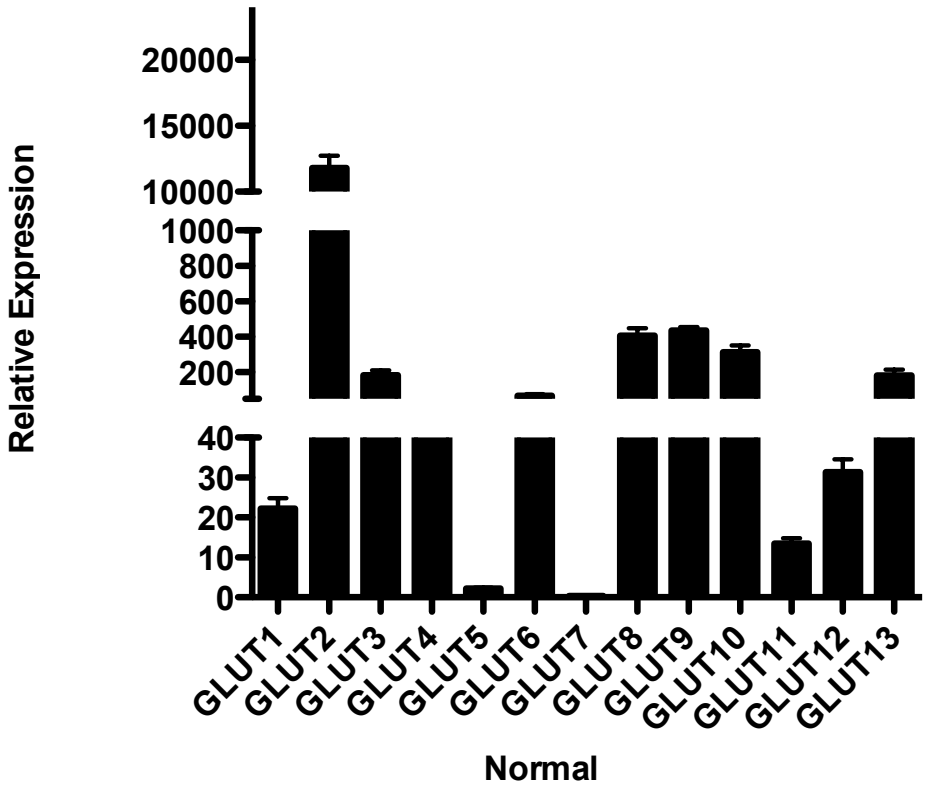

Figure 3.4: Analysis of GLUT receptor expression in human liver by quantitative qPCR analysis
mRNA expression of glucose transporters GLUT1-13 in normal human liver determined using a fluidigm qPCR array®. Results are expressed as means of five normal livers +/- SEM, run on triplicate arrays and normalized to pooled endogenous controls β-actin and GAPDH and log transformed using 2-ΔCt.

Analysis of the fold change in GLUT expression in disease compared to normal liver (Figure 3.5) shows that relative abundance of some receptors significantly changes with disease. Thus whilst there was no dramatic change in the steatotic livers (Figure 3.5A), in contrast for diseased and inflamed livers (eg NASH and ALD) the majority of GLUTS were significantly up regulated compared to normal. GLUT1, GLUT3, GLUT5 and GLUT12 were up regulated in NASH (fold change 4.76, 3.29, 4.20, 3.21 respectively) and in ALD (fold change 7.49, 7.38, 11.24, 4.75 respectively). In contrast in PBC only GLUT1 and GLUT5 were up regulated (fold change 1.75 and 3.62).

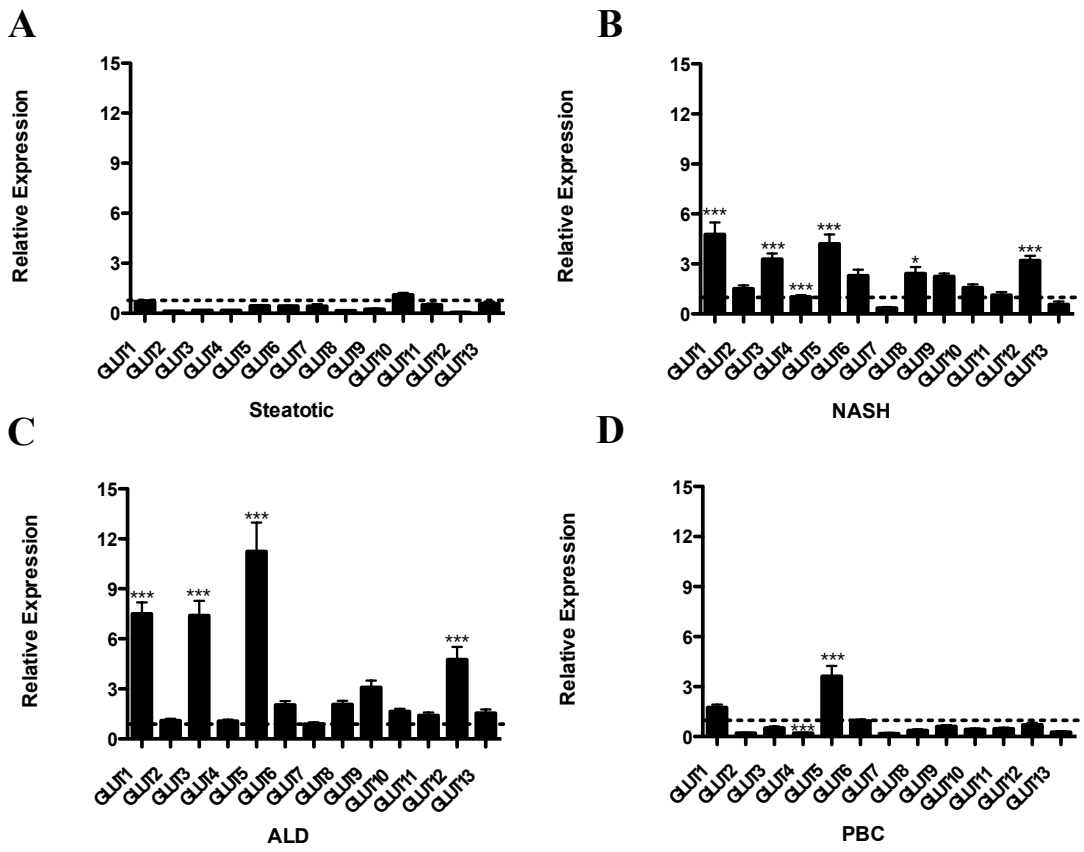

Figure 3.5: Analysis of GLUT receptor expression in human diseased liver by quantitative qPCR analysis

(A) mRNA expression of glucose transporters GLUT1-13 in steatotic liver, (B) NASH, (C) ALD and (D) PBC, using a fluidigm qPCR array® and run on triplicate arrays. Results are expressed as the mean fold change in gene expression normalized to pooled endogenous controls β-actin and GAPDH relative to normal livers defined as 1 +/- SEM with means from five normal livers, four steatotic, three NASH, four ALD and four PBC. Dotted line represents normal expression at 1. Significance expressed as * $p<0.05$, ***$p<0.001$ using a one way ANOVA with Bonferroni correction.

3.3.3 Liver epithelial cells express a varied GLUT receptor profile

Changes in total mRNA expression in tissue can reflect either disease-related changes in proportions of cells, which express a particular receptor, or an up regulation in signal on specific cells. Therefore we then went on to assess the receptor expression profile on isolated cultured liver epithelial and non-epithelial cells using qPCR. Primary hepatocytes abundantly expressed GLUT1, GLUT2, GLUT6, GLUT8, GLUT9 and GLUT10, (Figure 3.6A). The hepatocyte cell lines Huh7.5 and HepG2 reflected GLUT expression seen in primary hepatocytes to some extent with abundant GLUT1, GLUT2, GLUT6 and GLUT8 present. However cell lines expressed more GLUT4, Huh.7.5 had lower GLUT6 and GLUT9 than primary cells (Figure 3.6A) and HepG2 cells had higher GLUT1, GLUT3, GLUT9 and GLUT10 (Figure 3.6A). In contrast primary BEC, Figure 3.6B did not express GLUT2, GLUT4, GLUT7 or GLUT12 with GLUT1, GLUT3 and GLUT6 being most abundant in this cell type.

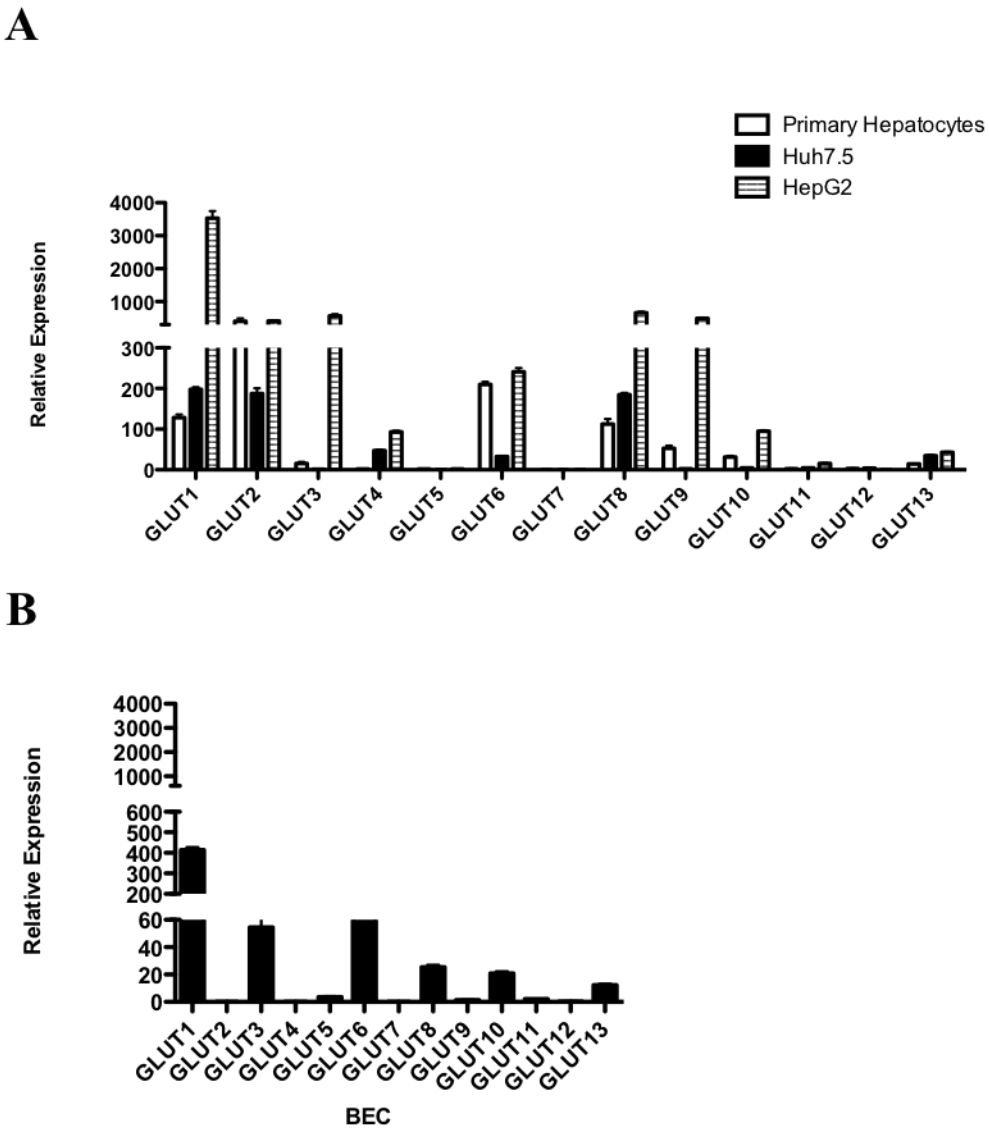

Figure 3.6: Analysis of GLUT receptor expression in human liver epithelial cells by quantitative qPCR analysis

(A) mRNA expression of glucose transporters GLUT1-13 in primary hepatocytes, Huh7.5 and HepG2 and (B) BEC determined using a fluidigm qPCR array®. Results are expressed as means of three primary hepatocytes, three Huh7.5, three HepG2 and three BEC +/- SEM, run on triplicate arrays and normalized to pooled endogenous controls β-actin and GAPDH log transformed using 2-Δct.

3.3.4 GLUT receptor profile in non-epithelial cells

Finally we assessed GLUT family expression in, non-epithelial (non-parenchymal) cells. HSEC most abundantly expressed GLUT1, GLUT3, and GLUT6 (Figure 3.7A), and in contrast to hepatocytes had higher GLUT3 and GLUT12 and decreased GLUT9 expression. This pattern was similar in liver-derived fibroblasts, although these had lower signals for GLUT12 and GLUT8 compared to HSEC. We also assessed expression in peripheral blood leukocytes, since diseased livers would contain elevated numbers of inflammatory cells. These cells expressed GLUT1, GLUT2 and interestingly GLUT5, which was present at negligible levels in primary hepatocytes, HepG2, BEC (Figure 3.6A, and B), and fibroblasts (Figure 3.7B) and absent in Huh 7.5 (Figure 3.6A). Of note mRNA for GLUT5 was more abundantly expressed in NASH (Figure 3.5B), ALD (Figure 3.5C) and PBC livers (Figure 3.5D) when compared to normal.

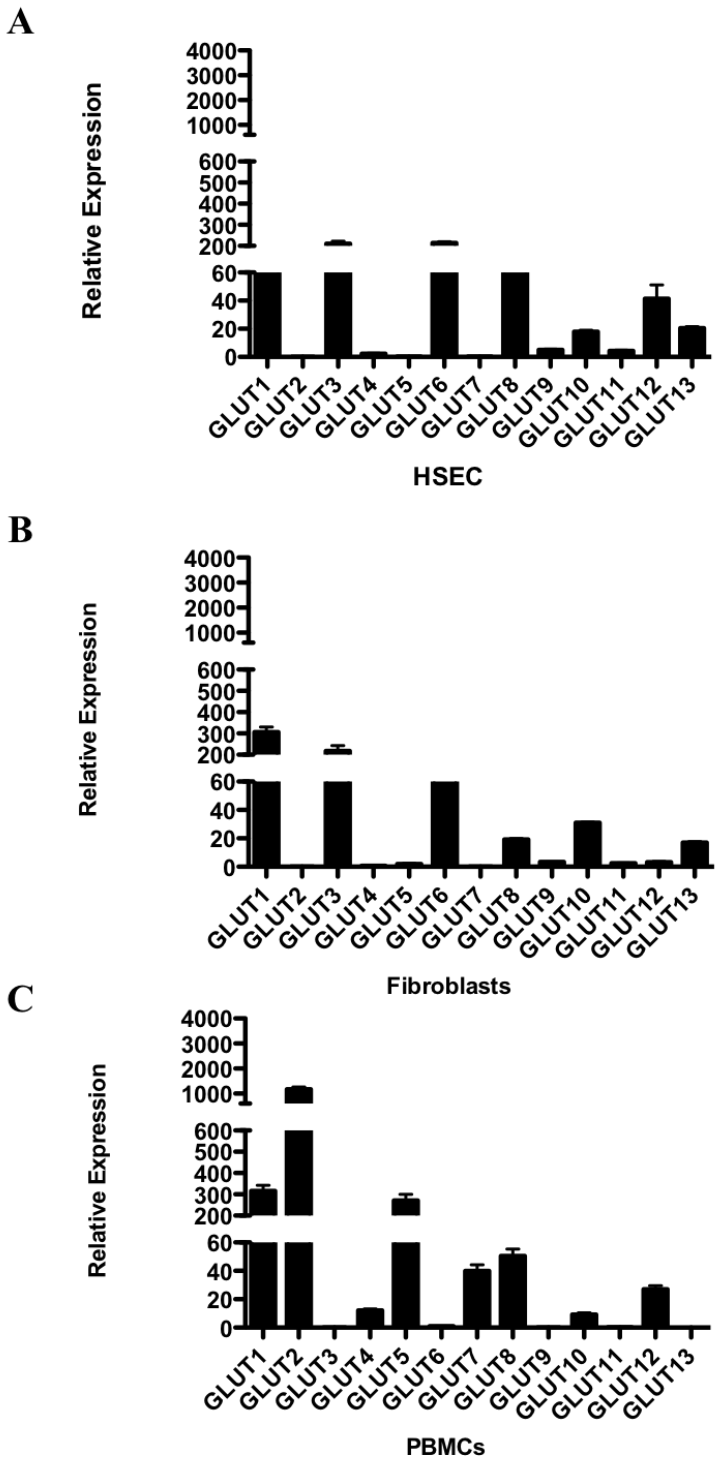

Figure 3.7: Analysis of GLUT receptor expression in human liver non-epithelial cells and PBMCs by quantitative qPCR analysis

(A) mRNA expression of glucose transporters GLUT1-13 in HSEC (B) fibroblasts and (C) PBMCs using a fluidigm qPCR array®. Results are expressed as means of four HSEC, four fibroblasts and two PBMCs +/- SEM, run on triplicate arrays and normalized to pooled endogenous controls β-actin and GAPDH log transformed using 2-Δct.

3.3.5 Immunohistochemical detection of GLUT protein expression in normal and diseased livers

Next we wished to determine whether our mRNA expression patterns were reflected by protein expression in liver tissue sections. Ideally antibodies for all isoforms would have been screened, but commercial availability restricted our analysis to GLUT1, GLUT2, GLUT4, GLUT9 and GLUT10.

GLUT1 protein was expressed in normal, steatotic, NASH, ALD and PBC livers (Figure 3.8). In particular there was uniform strong membranous staining in the hepatocytes of normal liver, and staining of bile ducts (Figure 3.8A). There was a tendency for increased staining for GLUT1 in hepatocytes in Zones 2 and 3 in normal liver whilst in the steatotic liver, occasional patches of intense staining were noted (shown by arrow Figure 3.8B). The ALD and NASH livers again showed a typical membranous hepatocyte-staining pattern, although the intensity of staining was greater (Figure 3.8D). The ALD and NASH livers also showed staining in some periportal inflammatory cells (Figure 3.8C and D). This was also present in the PBC livers, but here the uniform intense membranous pattern of hepatocyte staining was not present (Figure 3.8E) and instead staining was localized to occasional areas of parenchyma. Isotype-matched control antibody staining was negative for all liver diseases (see representative example from NASH liver in 3.8F).

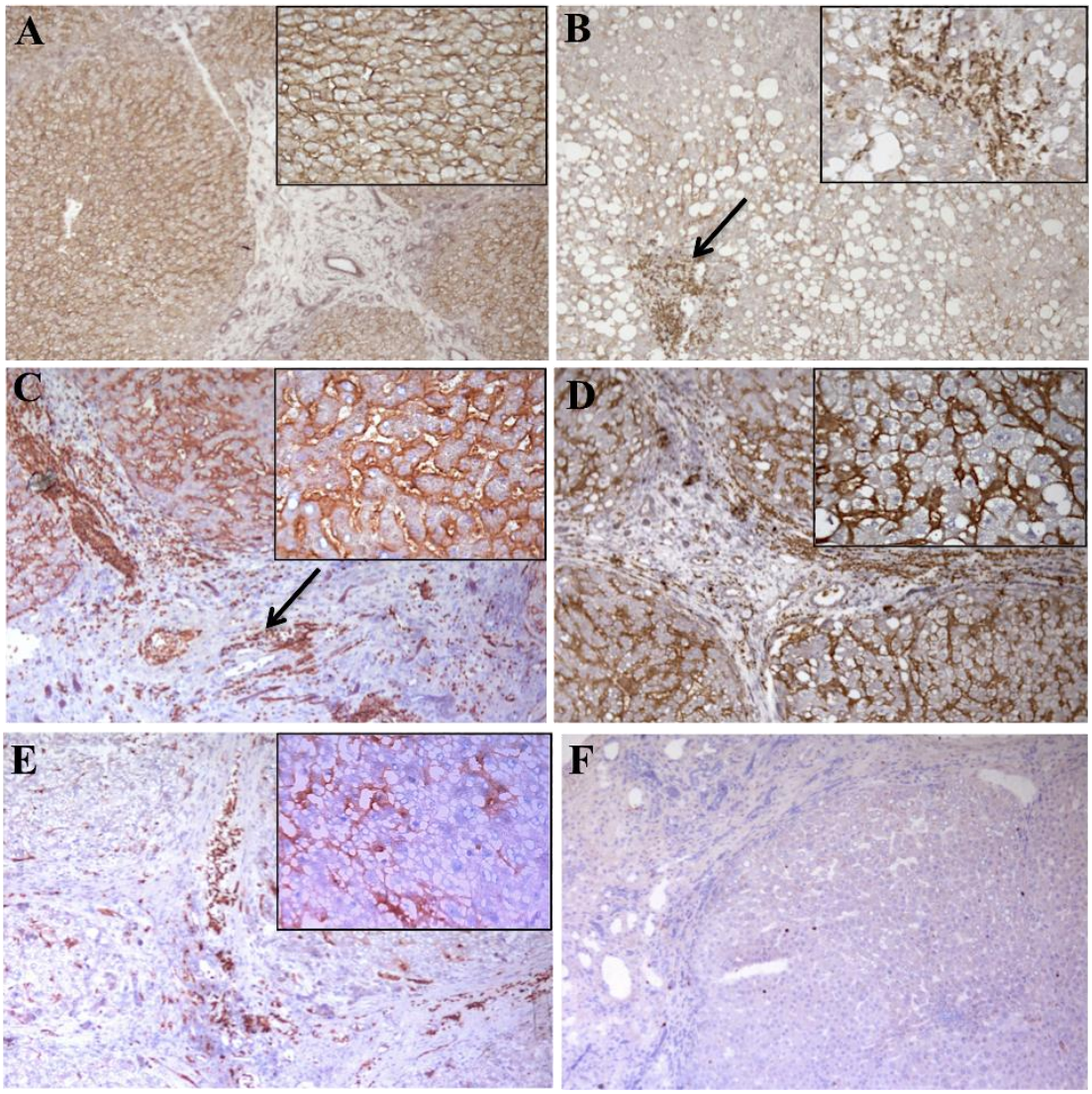

Figure 3.8: Immunohistochemical analysis of GLUT1 protein expression in normal human and diseased livers

Immunohistochemical staining for GLUT1 in acetone fixed frozen sections from (A) normal, (B) steatotic, (C) NASH, (D) ALD, (E) PBC and (F) staining of isotype matched control antibody in NASH liver. Fields were captured at 10X original magnification with inset pictures captured at 40X original magnification. Images shown are representative of N=3 for each disease and arrows in (B) indicate patches of intense staining whilst arrows in (C) indicate staining of periportal inflammatory cells.

GLUT2 was also present in all livers with clear membranous hepatocyte staining of central lobular areas in particular (Figure 3.9A, B, D and E). Interestingly this typical membranous staining pattern was lost in NASH livers, which showed a more diffuse cytoplasmic staining pattern where the protein appeared to be localized within the hepatocytes (Figure 3.9C). The BEC were negative for GLUT2 staining indicated by arrows in Figure 3.9B and only some inflammatory cells were positively stained. Isotype-matched control antibody staining was negative for all liver diseases (see representative example from steatotic liver in Figure 3.9F).

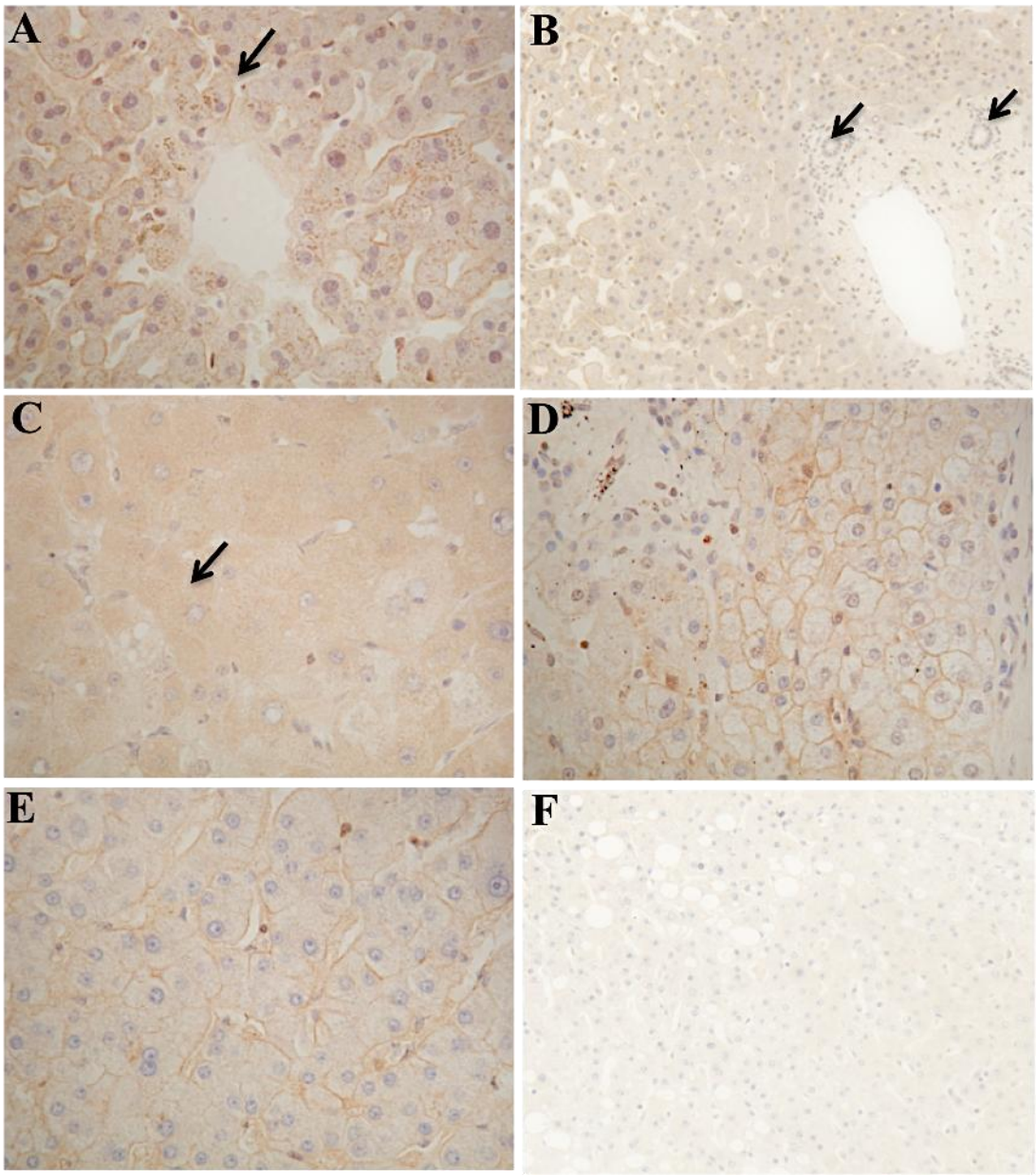

Figure 3.9: Immunohistochemical analysis of GLUT2 protein expression in normal and diseased livers

Immunohistochemical staining of GLUT2 in paraffin embedded (A) normal, (B) steatotic, (C) NASH, (D) ALD, (E) PBC and (F) staining of isotype matched control antibody. Fields were captured using at 20X original magnification. Images shown are representative from N=3 for each disease and arrows in (A) indicate membranous staining in central lobular areas, whilst arrows in (B) indicate no staining in bile ducts and arrows in (C) indicate diffuse cytoplasmic staining in hepatocytes.

GLUT4 staining in normal livers was generally found to be weak and diffuse with, a cytoplasmic localization in hepatocytes (Figure 3.10A). The hepatocyte staining appeared more intense in NASH (Figure 3.10C) and ALD (Figure 3.10D) livers. GLUT4 expression was also noted around vessels within the liver. Isotype-matched control antibody staining was negative for all liver diseases (see representative example from steatotic liver in Figure 3.10F). BEC did not express GLUT4 but there was some staining in infiltrating inflammatory cells. Confirmatory immunofluorescent staining for GLUT4 in PCLS from normal liver confirmed the diffuse hepatocyte-staining pattern for GLUT4 (Figure 3.11).

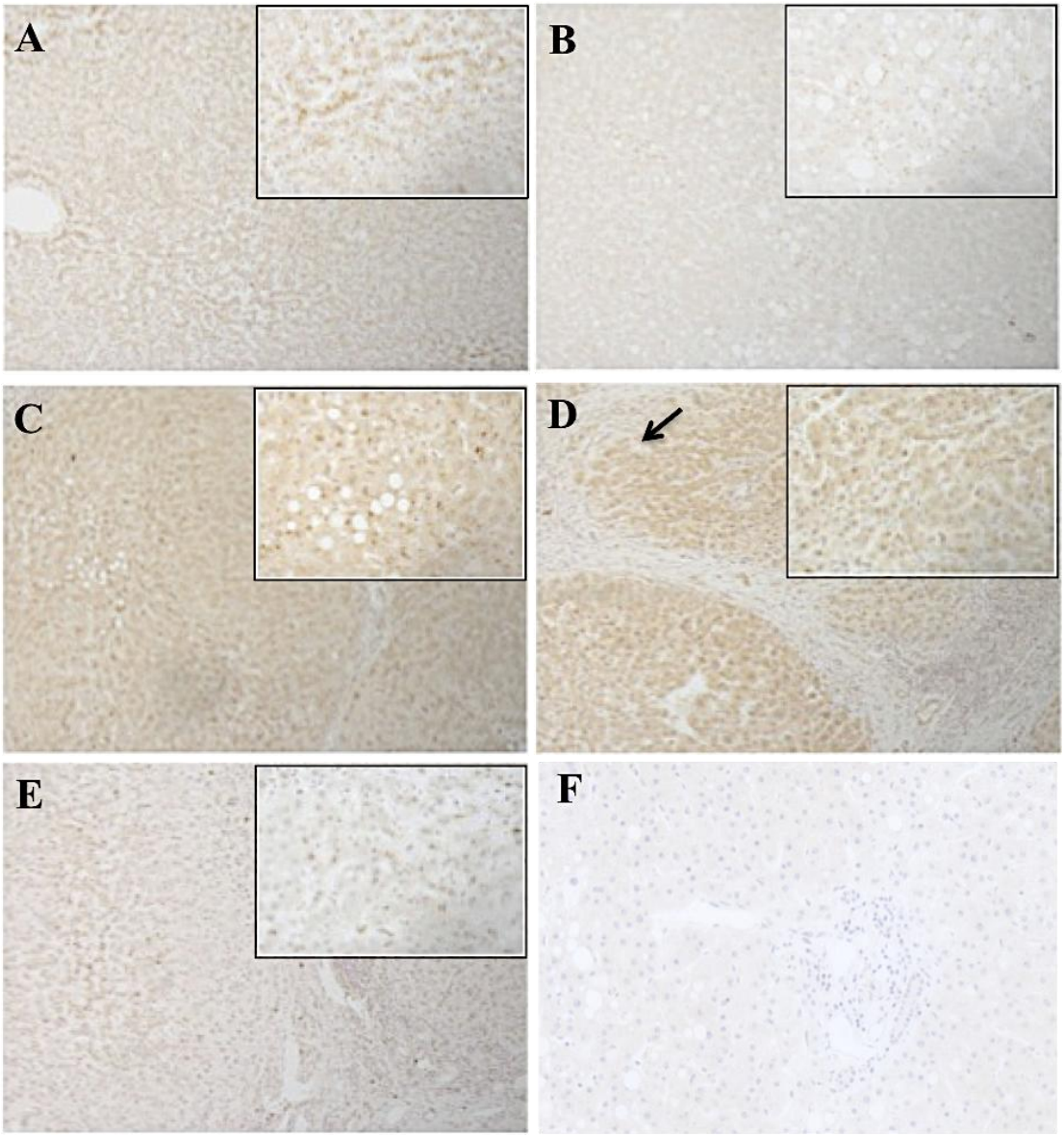

Figure 3.10: Immunohistochemical analysis of GLUT4 protein expression in normal and diseased livers

Immunohistochemical staining of GLUT4 in paraffin embedded (A) normal, (B) steatotic, (C) NASH, (D) ALD (E) PBC and (F) staining of isotype matched control antibody. Fields were captured at 10X original magnification with inset pictures captured at 40X original magnification. Images shown are representative from N=3 for each disease and arrow in (D) indicates diffuse cytoplasmic staining in hepatocytes.

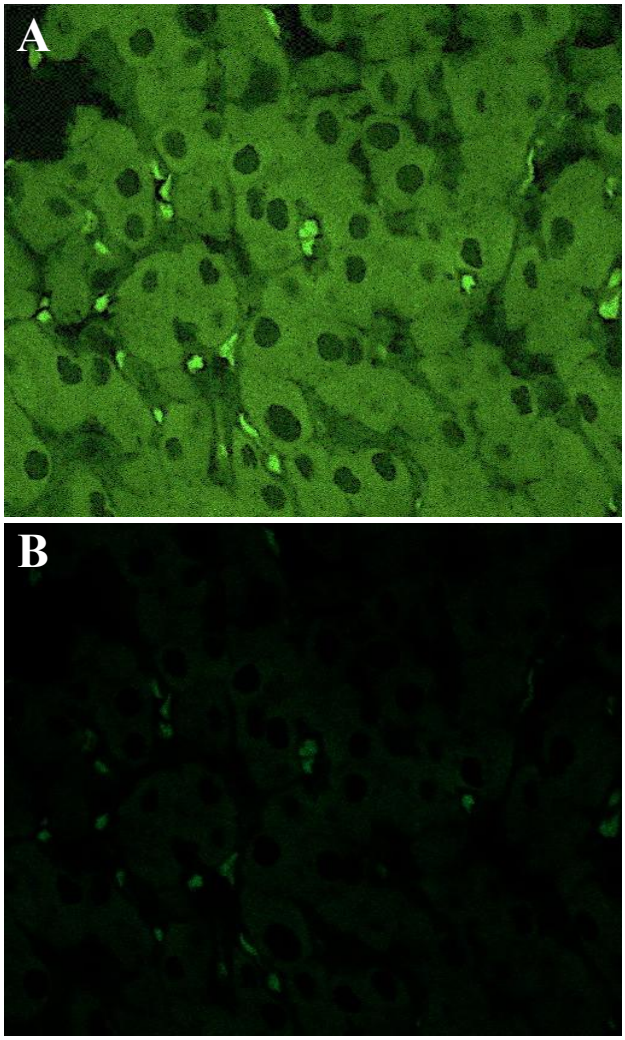

Figure 3.11: Immunofluorescence analysis of GLUT4 protein expression in normal liver

(A) Immunofluorescent staining for GLUT4 in PCLS from a resected normal liver and (B) staining of isotype matched control antibody. Fields were captured at 20X original magnification. Images shown are representative from N=3 livers

Similar to GLUT4, GLUT9 was expressed in all livers (Figure 3.12) with a diffuse cytoplasmic staining pattern, and tendency for increased expression in periportal hepatocytes in disease. We also noted some degree of endothelial staining in normal liver (arrows Figure 3.12A). Whilst our isotype matched controls were negative, we did observe some non-specific staining of RBCs within tissue on occasion (Figure 3.12B). GLUT10 was expressed diffusely in hepatocytes in all livers examined (Figure 3.13) with some strong endothelial staining observed (indicated by arrows in Figure 3.13C and D. We also observed some staining on BECs in normal liver (indicated by arrows in Figure 3.13A) and also in steatotic liver (indicated by arrows in Figure 3.13B), and found some staining in infiltrating cells. Isotype-matched control antibody staining was negative for all liver diseases (see representative example from steatotic liver in Figure 3.13F).

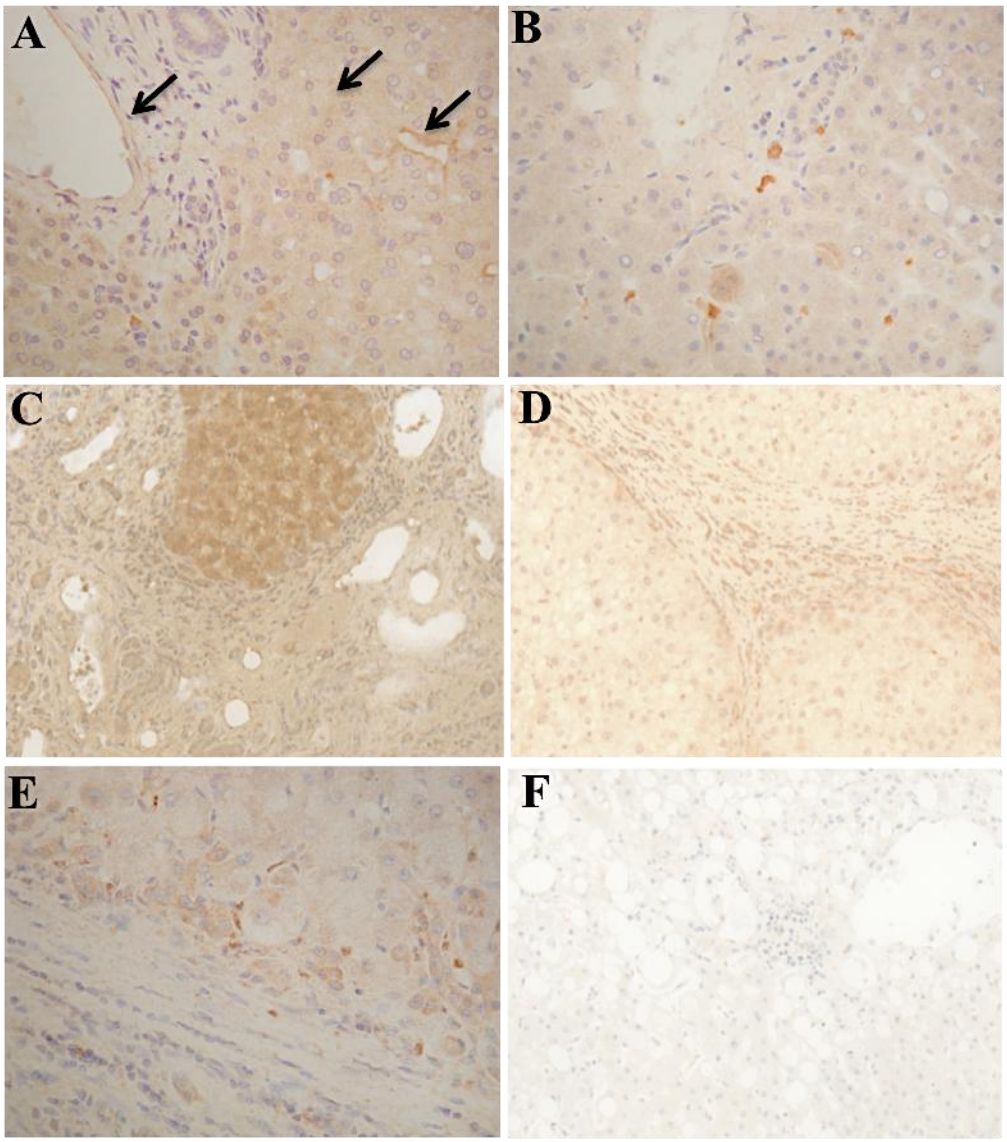

Figure 3.12: Immunohistochemical analysis of GLUT9 protein expression in normal and diseased livers

Immunohistochemical staining of GLUT9 in paraffin embedded (A) normal, (B) steatotic, (C) NASH, (D) ALD, (E) PBC and (F) staining of isotype matched control antibody. Fields were captured at 20X original magnification. Images shown are representative from N=2 for each disease and arrows in (A) indicate endothelial staining.

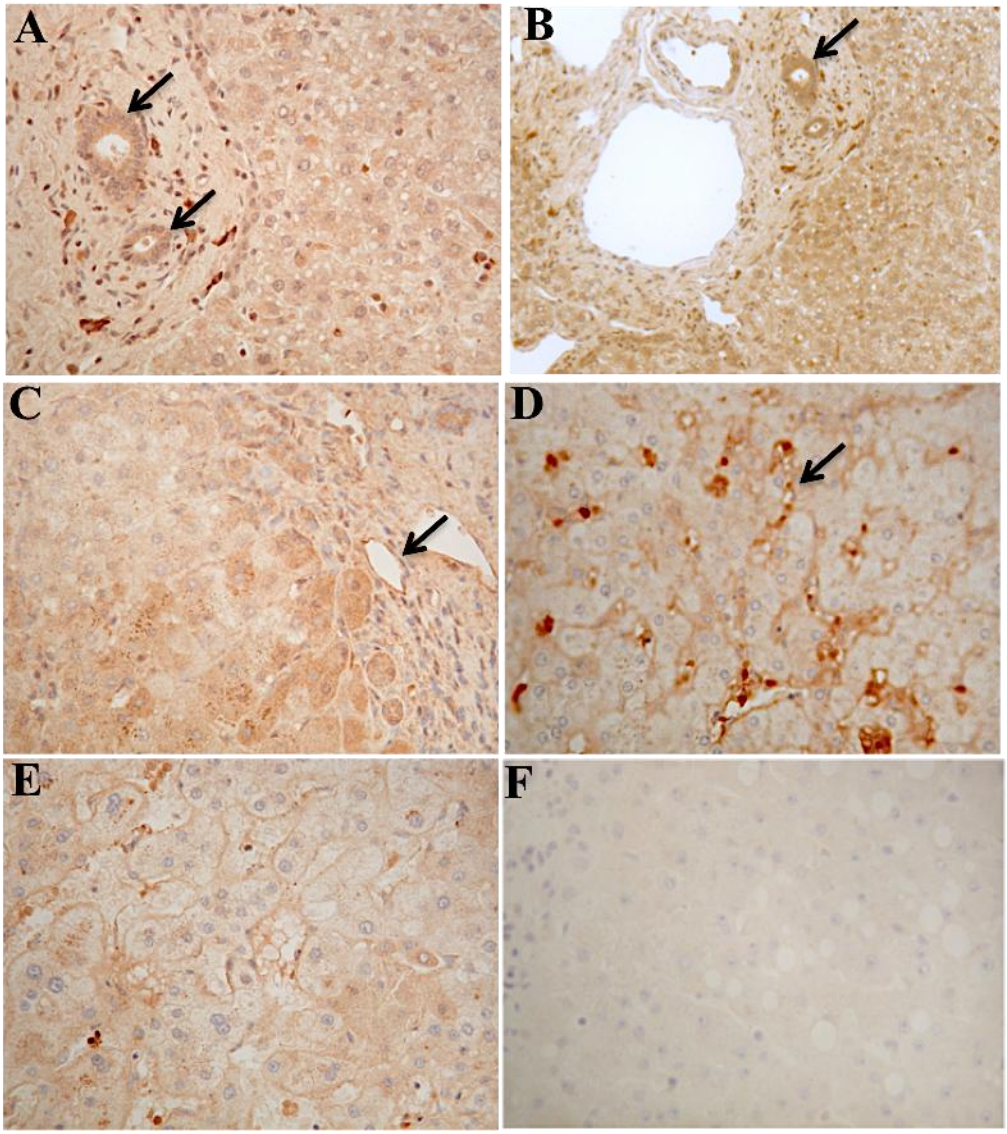

Figure 3.13: Immunohistochemical analysis of GLUT10 protein expression in normal and diseased livers

Immunohistochemical staining of GLUT10 in paraffin embedded (A) normal, (B) steatotic, (C) NASH, (D) ALD, (E) PBC and (F) staining of isotype matched control antibody. Fields were captured at 20X original magnification. Images shown are representative from N=2 for each disease and arrows in (A) and (B) indicate bile duct staining, whilst arrow in (C) and (D) indicate endothelial staining.

3.3.6 Microarray analysis reveals expression of lipid trafficking proteins in human liver

Next we examined the expression patterns of lipid trafficking proteins in human liver. As before we began by using microarrays to measure gene expression in normal liver, HSEC and hepatocytes. Heat maps were generated using GeneSpring (GX.12.5) and transcripts for FABPs 1-7, FATPS 1-5, CAV1, CD36, LRP1, and LRP8 were found in normal liver (Figure 3.14). We also saw transcripts for the same genes in HSEC and Huh7.5, in addition to FATP6 and LRP2 (Figure 3.15). Of note, the hepatocytes abundantly expressed FABP1 with little FABP4 whilst the reverse was true for HSEC, which also had more FATP1 than the hepatocytes. For each heatmap the color code is shown as before (Figure 3.15C).

We found that expression of 14 of our key genes significantly ($P<0.05$) differed by more than two-fold between HSEC and Huh.7.5. Thus FABP1, 28912.47fold ($p<7.49E-08$), FABP3 1.35fold ($p<4.09E-04$), LRP1 6.45fold ($p<0.003$), LRP2 20.24fold ($p<2.00E-04$), LRP8 2.23fold ($p<0.006$), were down regulated on HSEC compared to hepatocytes and FABP4 1412.32fold ($p<5.26E-05$), FABP5 4.71fold ($p<7.61E-06$), CAV1 31.86fold ($p<6.44E-06$), CD36 67.99fold ($p<2.50E-04$), FATP1 57.57fold ($p<1.05E-05$), FATP3 6.12fold ($p<0.002$), FATP4 1.52 fold ($p<2.86E-04$), FATP5 2.40fold ($p<1.77E-06$), were more abundant in HSEC (Figure 3.16).

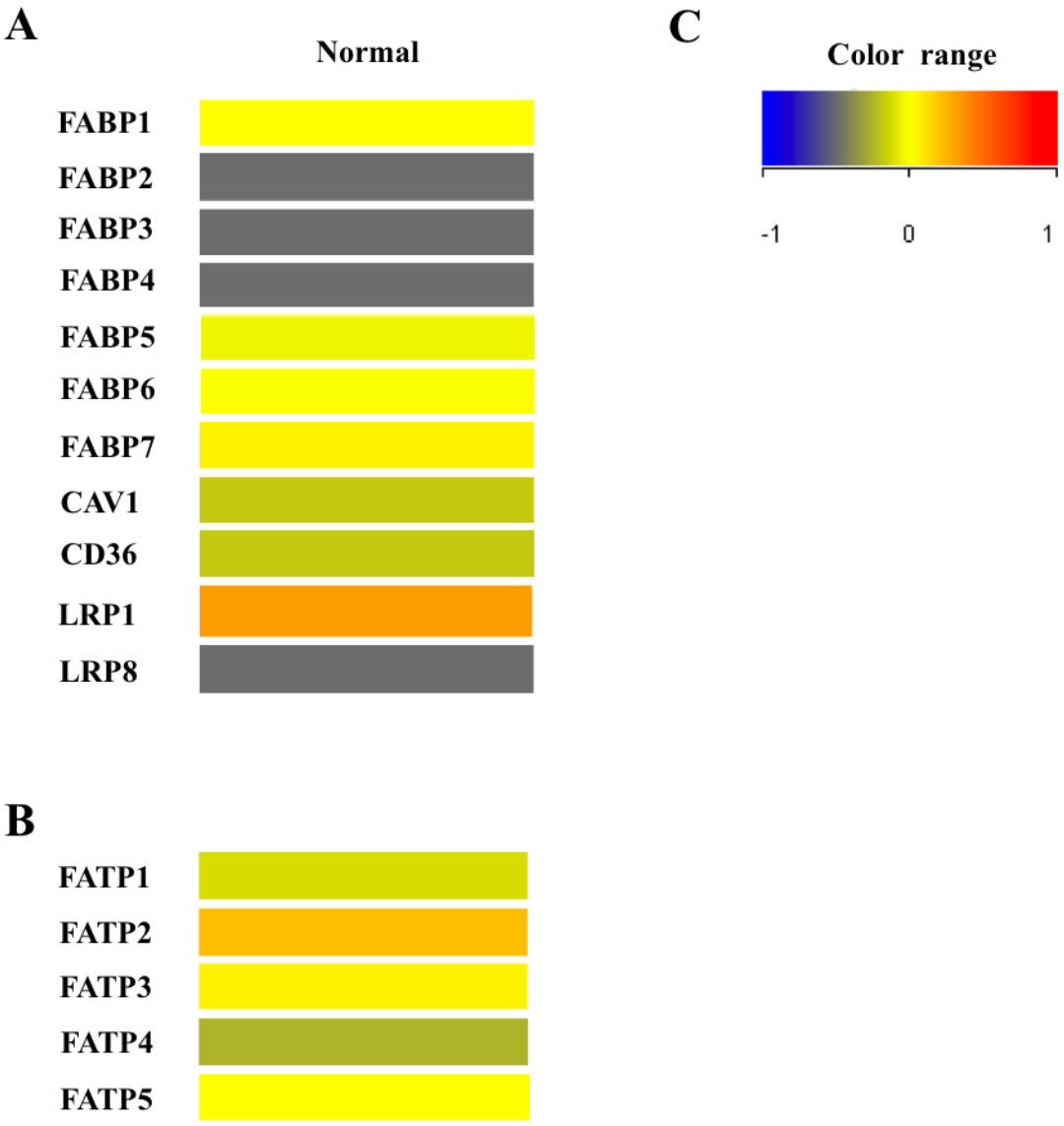

Figure 3.14: Microarray analysis of lipid trafficking receptor expression in normal liver

(A) RNA was extracted from normal livers using Qiagen RNeasy mini kit and assessed for purity and integrity using an Agilent bioanalyser before being run on human oligo arrays (Agilent array ID 014850). Extracted data was analyzed using Gene Spring (GX.12.5). Column represents liver type and rows are the gene of interest for FABP1-7, CAV1, CD36, LRP1, and LRP8, (B) FATP1-5, data is expressed relative to the median expression of a given gene in all samples tested. (C) Color key indicates log values (log base 2) were zero indicates median expression of all genes across all samples whilst blue coloration indicates expression lower than median expression and red coloration indicates expression higher than the median. Data representative from N=14 normal livers.

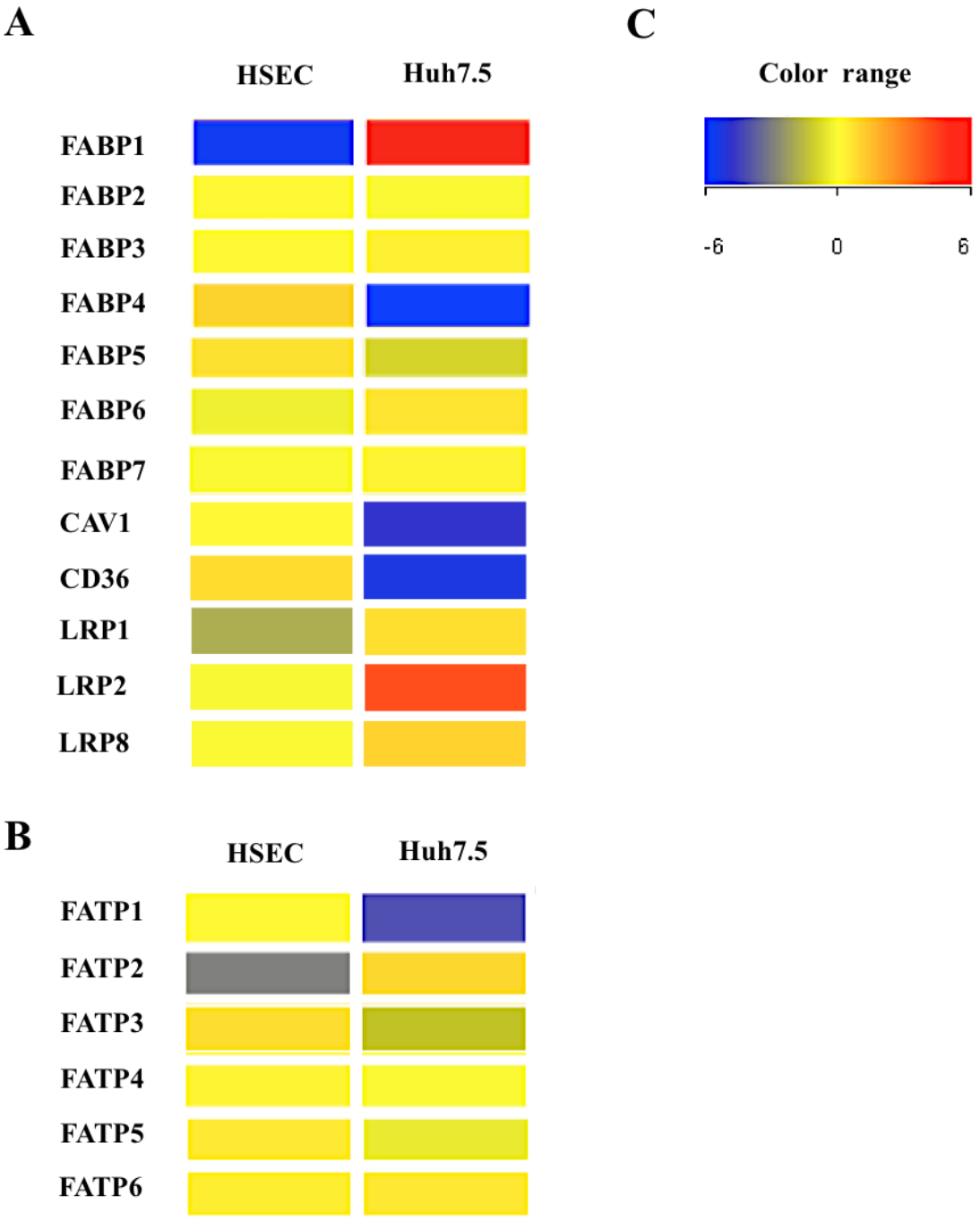

Figure 3.15: Microarray analysis of lipid trafficking receptor expression in HSEC and Huh7.5

(A) RNA was extracted from HSEC and Huh7.5 using Qiagen RNeasy mini kit and assessed for purity and integrity using an Agilent bioanalyser before being run on human oligo arrays (Agilent array ID 014850). Extracted data was analyzed using Gene Spring (GX.12.5). Columns represent cell type and rows are the gene of interest for FABP1-7, CAV1, CD36, LRP1, LRP2 and LRP8, (B) FATP1-6, data is expressed relative to the median expression of a given gene in all samples tested. (C) Color key indicates log values (log base 2) were zero indicates median expression of a given gene across all samples whilst blue coloration indicates expression lower than median expression and red coloration indicates expression higher than the median.

A

Fatty acid trafficking transporters	Expression in HSEC	Fold Change	P-value
FABP1	Down	28912.47	7.49E-08
FABP3	Down	1.35	4.09E-04
FABP4	Up	1412.32	5.26E-05
FABP5	Up	4.71	7.61E-06
CAV1	Up	31.86	6.44E-06
CD36	Up	67.99	2.50E-04
LRP1	Down	6.45	0.003
LRP2	Down	20.24	2.00E-04
LRP8	Down	2.23	0.006

B

FATP	Expression in HSEC	Fold Change	P-value
FATP1	Up	57.57	1.05E-05
FATP2	Down	35.37	7.37E-04
FATP3	Up	6.12	0.002
FATP4	Up	1.52	2.86E-04
FATP5	Up	2.40	1.77E-06

Figure 3.16: Lipid trafficking receptors are differential regulated in HSEC and Huh7.5

RNA was extracted from HSEC and Huh7.5 using Qiagen RNeasy mini kit and assessed for purity and integrity using an Agilent bioanalyser before being run on human oligo arrays (Agilent Array ID 014850). Extracted data was analyzed using Gene Spring (GX.12.5), (A) Table of fatty acid trafficking transporters and (B) Table of FATPs which were >2-fold and $p<0.05$ different between HSEC compared to Huh7.5 using one way ANOVA with Benjamini Hochberg correction, data representative from N=5 HSEC and N=3 Huh7.5.

3.3.7 qPCR confirms expression of FABP receptors in human liver

Then qPCR was used to measure mRNA transcript levels of the fatty acid trafficking proteins FABP1-7, CAV1, CD36, LRP1, LRP2 and LRP8 in normal and diseased liver. mRNA for all FABPs was present in normal liver (Figure 3.17) with the exception of FABP6 and FABP7 which were not expressed (Figure 3.17). The fold change in gene expression of the fatty acid trafficking proteins when compared to normal revealed only one transporter, LRP2 to be up regulated in steatotic livers (fold change 1.48, Figure 3.18A). In contrast in diseased and inflamed livers (e.g. NASH and ALD) the majority of fatty acid trafficking proteins were highly up regulated. FABP4, FABP5, FABP6, CAV1, LRP2 and LRP8 were up regulated in NASH (fold change 34.17, 2.98, 3.26, 2.94, 5.67, and 4.42 respectively, Figure 3.18B) and in ALD FABP2, FABP4, FABP5, FABP6, CAV1, LRP2 and LRP8 were up regulated (fold change 3.73, 51.9, 4.31, 3.79, 4.99, 4.34, and 8.21 respectively, Figure 3.18C). In contrast FABP2, FABP6, LRP8 were up regulated in PBC (fold change 4.38, 8.32 and 4.07 respectively, Figure 3.18D).

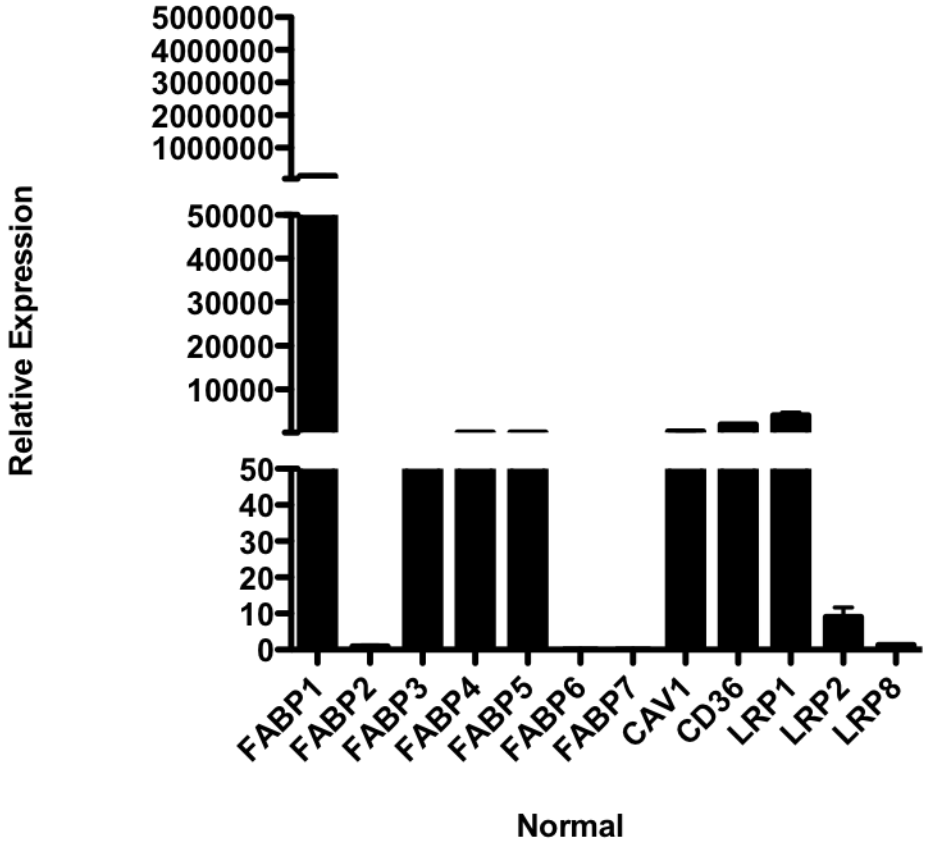

Figure 3.17: Analysis of fatty acid trafficking protein receptor expression in human liver by quantitative qPCR analysis

mRNA expression of the fatty acid trafficking proteins, FABPs1-7, CAV1, CD36, LRP1, LRP2 and LRP8 in normal human liver using a fluidigm qPCR array®. Results are expressed as means of five normal livers, +/- SEM, run on triplicate arrays and normalized to pooled endogenous controls β-actin and GAPDH and log transformed using 2-ΔCt

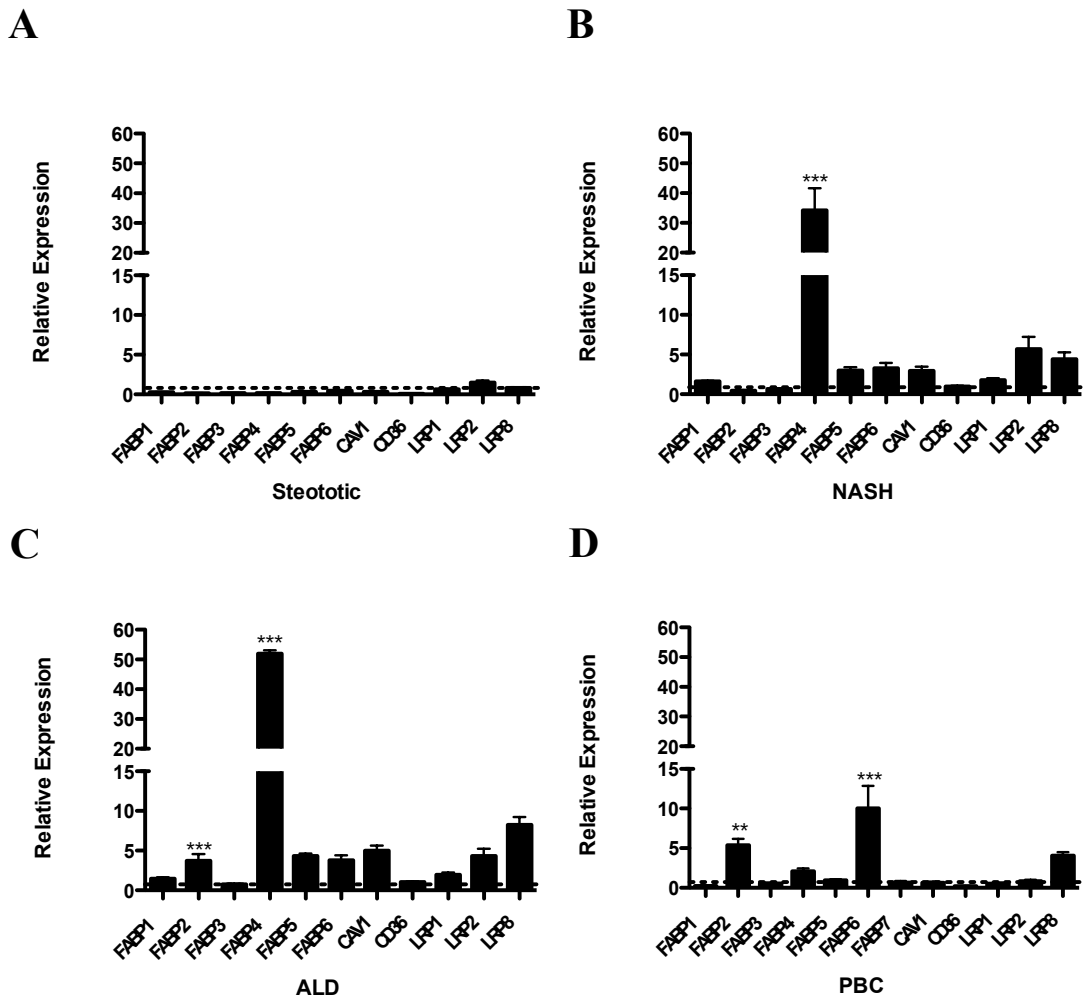

Figure 3.18: Analysis of fatty acid trafficking protein receptor expression in human liver by quantitative qPCR analysis

(A) mRNA expression of the fatty acid trafficking proteins, FABP1-7, CAV1, CD36, LRP1, LRP2 and LRP8 in steatotic liver, (B) NASH, (C) ALD and (D) PBC, using a fluidigm qPCR array® and run on triplicate arrays. Results are expressed as the mean fold change in gene expression normalized to pooled endogenous controls β actin and GAPDH relative to normal livers defined as 1 +/- SEM with means from four normal livers, four steatotic, three NASH, four ALD and four PBC. Dotted line represents normal expression at 1. Significance expressed as **p<0.01, ***p<0.001 using a one way ANOVA with Bonferroni correction.

3.3.8 Liver epithelial cells express FABP

Next we investigated the expression of these transporters in cultured liver epithelial and non-epithelial cells. In primary hepatocytes, FABP1, FABP5, CAV1 and LRP1 (Figure 3.19A) were most abundantly expressed. The hepatocyte cell lines had similar expression except for CAV1, which was not abundantly expressed in HepG2. Primary hepatocytes also expressed FABP4 and FABP3, in contrast to the cell lines except for a negligible amount of FABP3 in Huh7.5 (Figure 3.19A). However both the cell lines expressed more LRP8, Huh7.5 expressed more LRP2 and HepG2 more FABP2 and CD36 than primary hepatocytes (Figure 3.19A). In contrast BEC were found only to express FABP5, CAV1, LRP1 and to a lesser extent LRP8 (Figure 3.19B).

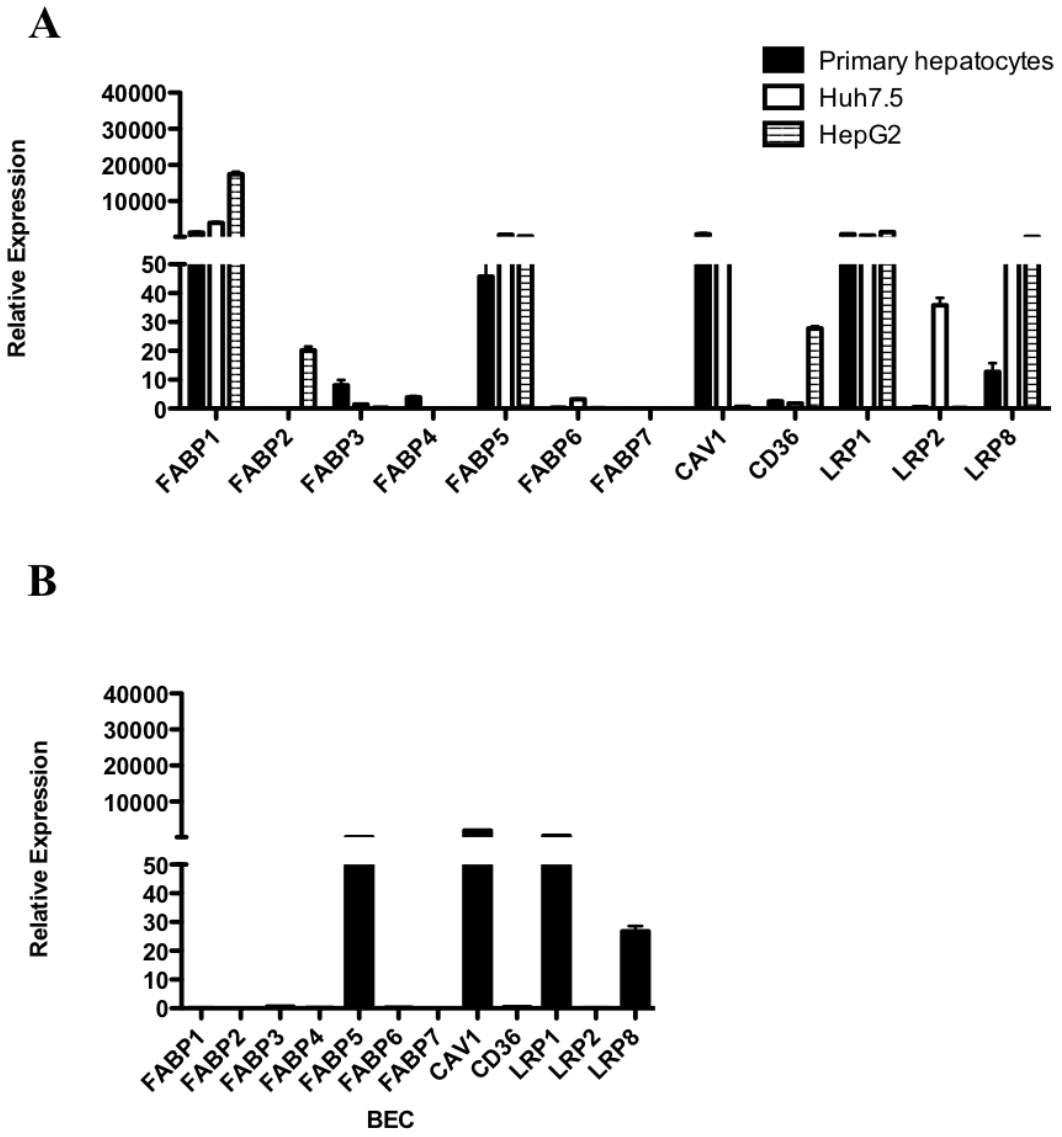

Figure 3.19: Analysis of fatty acid trafficking protein receptor expression in human liver epithelial cells by quantitative qPCR analysis

(A) mRNA expression of the fatty acid trafficking proteins, FABPs1-7, CAV1, CD36, LRP1, LRP2 and LRP8 in primary hepatocytes, Huh7.5 and HepG2 and (B) BEC, using a fluidigm qPCR array®. Results are expressed as means of three primary hepatocytes, three Huh7.5, three HepG2 and three BEC +/- SEM, run on triplicate arrays and normalized to pooled endogenous controls β-actin and GAPDH and log transformed using 2-ΔCt.

3.3.9 FABP receptor profile in non-epithelial cells

Finally non-epithelial cells were examined (Figure 3.20). In comparison to primary hepatocytes, HSEC and liver derived fibroblasts showed increased expression of FABP4, CD36, and LRP8 (Figure 3.20A and B), whilst HSEC expressed more FABP5 and fibroblasts expressed more FABP3. HSEC, fibroblasts and PBMCs did not express FABP6, FABP7 or LRP2 and in contrast to hepatocytes did not express FABP1. Fibroblast had increased expression for FABP3 in comparison to hepatocytes whilst it was not expressed in all other cell types. The cellular expression data was in agreement with our microarray data (Figure 3.15), confirming FABP1 expression is higher in Huh7.5 compared to HSEC. Similarly there was little FABP4 expression in Huh7.5 cells compared to HSEC.

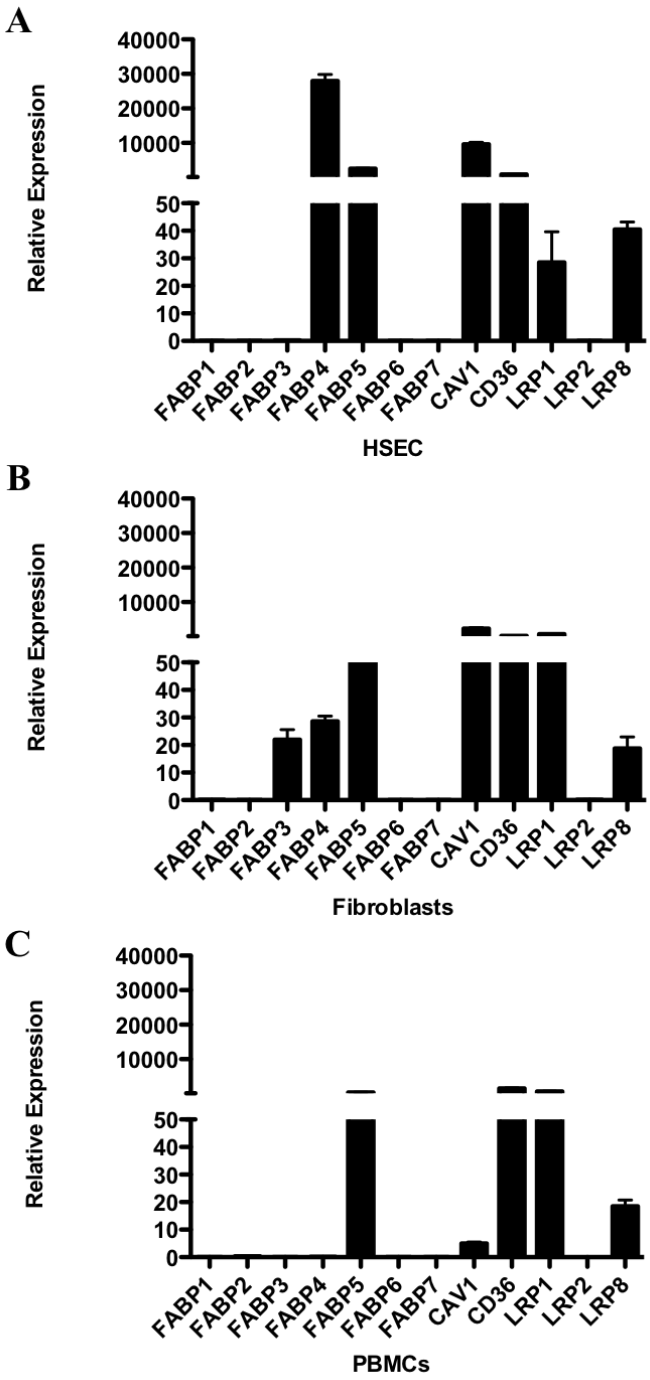

Figure 3.20: Analysis of fatty acid trafficking protein receptor expression in human liver non-epithelial cells and PBMCs by quantitative qPCR analysis
(A) mRNA expression of the fatty acid trafficking proteins, FABPs1-7, CAV1, CD36, LRP1, LRP2 and LRP8 in HSEC, (B) fibroblasts and (C) PBMCs using a fluidigm qPCR array®. Results are expressed as means of four HSEC, four fibroblasts and two PBMCs +/- SEM, run on triplicate arrays and normalized to pooled endogenous controls β-actin and GAPDH and log transformed using 2-ΔCt.

3.3.10 Immunohistochemical detection of fatty acid trafficking protein expression in normal and diseased livers.

We were then able to investigate whether some of these proteins were also expressed at the protein level by immunohistochemical analysis. CAV1 protein expression was found in all livers (Figure 3.21) in support of our qPCR data. In particular there was strong sinusoidal staining in the normal livers and weaker staining around the hepatocyte membrane (Figure 3.21A). There was also stronger staining around the smooth muscle of vessels. The steatotic livers had less staining for CAV1 compared to normal (Figure 3.21B) and the NASH, ALD and PBC showed intense expression of CAV1 in portal and scarred areas (Figure 3.21C, D and E). Interestingly we saw little staining of bile ducts. Protein expression for FABP1, 4 and LRP8 was found in all livers. In particular there was intense staining for all three in NASH livers and a decrease in expression in the steatotic livers. There was an increase in expression around the portal area and no staining on bile ducts for FABP1 whilst there was increased expression around the central vein in normal liver for LRP8 (Figure 3.21-3.24).

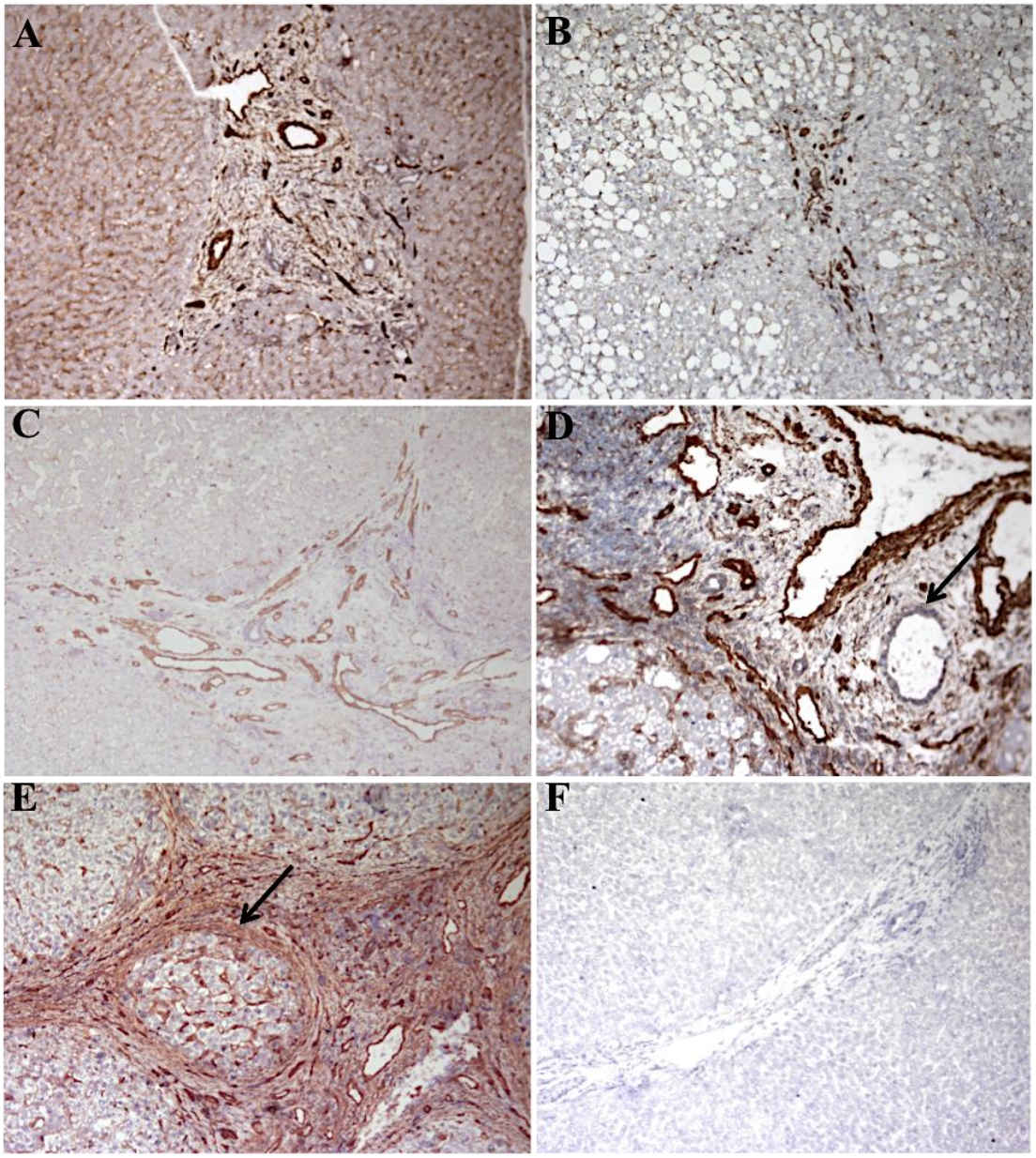

Figure 3.21: Immunohistochemical analysis of Caveolin 1 protein expression in normal human and diseased livers

Immunohistochemical staining for Caveolin 1 in acetone fixed frozen sections from (A) normal, (B) steatotic, (C) NASH, (D) ALD, (E) PBC and (F) staining of isotype matched control antibody. Fields were captured at 10X original magnification. Images shown are representative from N=3 for each disease and arrow in (D) indicates no bile duct staining whilst arrow in (E) indicates intense staining in scarred areas.

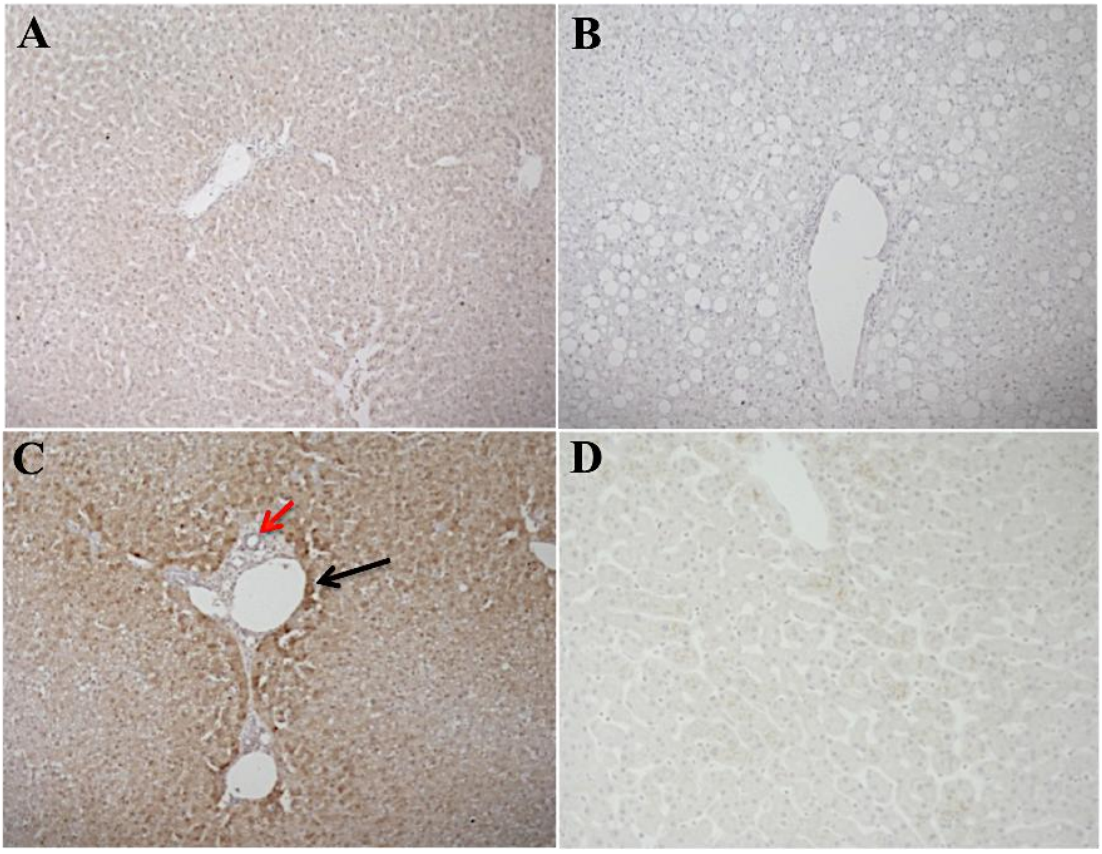

Figure 3.22: Immunohistochemical analysis of FABP1 protein expression in normal human and diseased livers

Immunohistochemical staining for FABP1 in paraffin embedded sections from (A) normal, (B) steatotic, (C) NASH, and (D) staining of isotype matched control antibody. Fields were captured at 10X original magnification. Images shown are representative from N=4 for each disease and red arrow in (C) indicates no bile duct staining whilst black arrow indicates intense staining around the portal area.

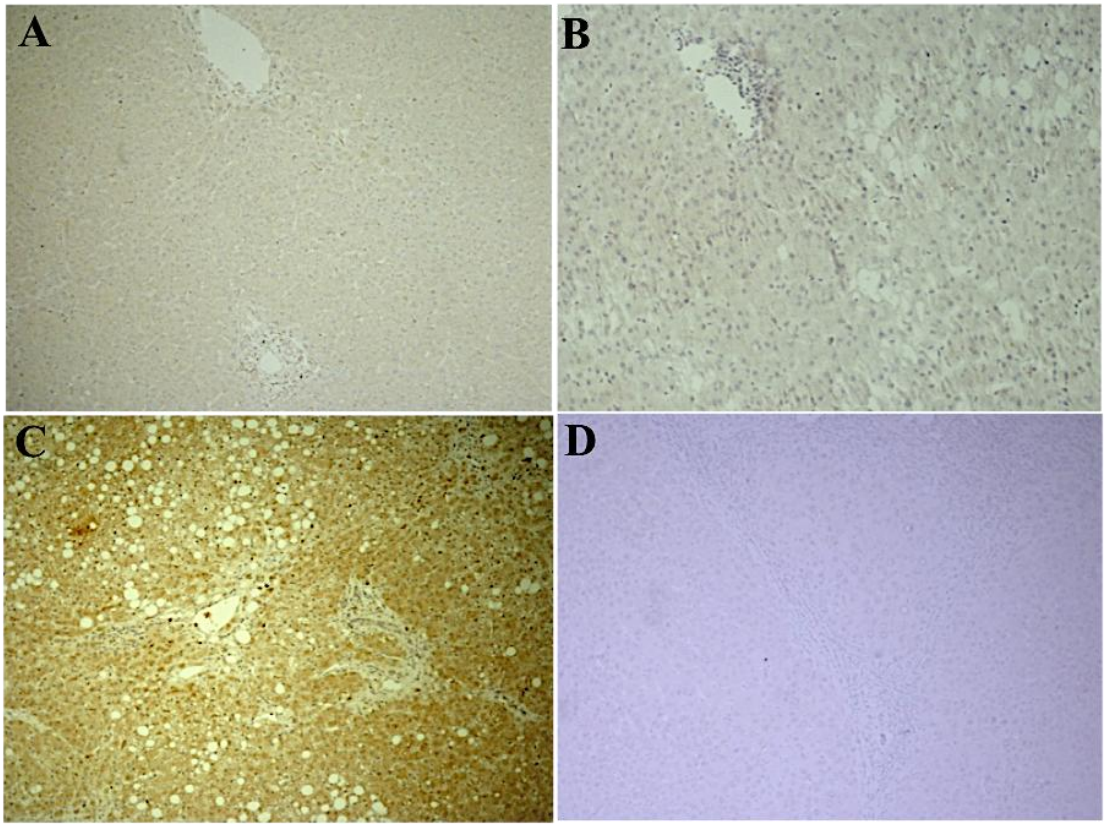

Figure 3.23: Immunohistochemical analysis of FABP4 protein expression in normal human and diseased livers

Immunohistochemical staining for FABP4 in paraffin embedded sections from (A) normal, (B) steatotic, (C) NASH, and (D) staining of isotype matched control antibody. Fields were captured at 10X original magnification. Images shown are representative from N=4 for each disease.

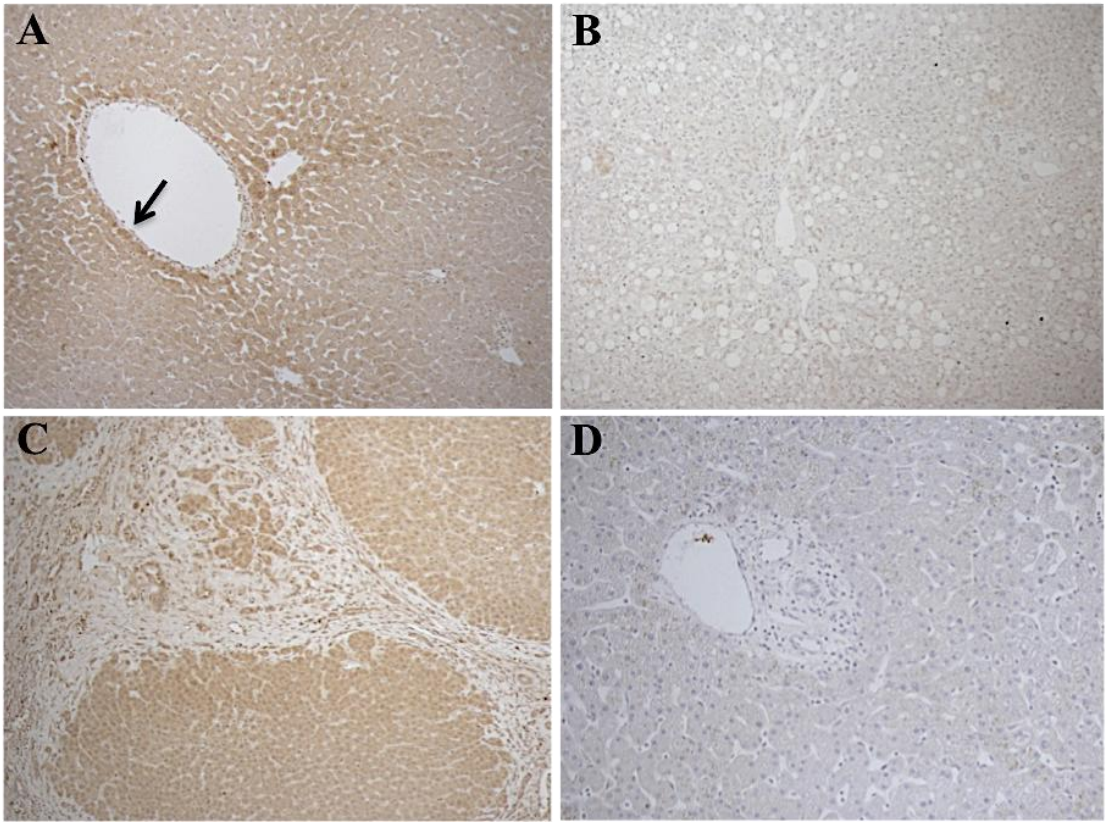

Figure 3.24: Immunohistochemical analysis of LRP8 protein expression in normal human and diseased livers

Immunohistochemical staining for LRP8 in paraffin embedded sections from (A) normal, (B) steatotic, (C) NASH, and (D) staining of isotype matched control antibody. Fields were captured at 10X original magnification. Images shown are representative from N=4 for each disease and arrow in (A) indicates intense staining around central vein.

3.3.11 qPCR confirms expression of FATPs in human liver

We also examined the mRNA profile of the FATPs 1-6. We found expression of FATP1-5 in normal liver (Figure 3.25) with FATP2 and FATP5 most abundantly expressed in normal whilst FATP6 was not expressed. We examined the fold change in gene expression compared to normal and found that FATPs were up regulated in the NASH and ALD livers (Figure 3.26B and C). In NASH FATP1, FATP2, FATP3, FATP4, FATP5 and FATP6 were up regulated (fold change 3.03, 1.33, 3.99, 2.63, 1.22 and 3.60 respectively, Figure 3.26B). In the ALD livers FATP1, FATP2, FATP3, FATP4, FATP5 and FATP6 were up regulated (fold change 3.22, 1.11, 4.37, 2.44, 1.47 and 2.48 respectively, Figure 3.26C).

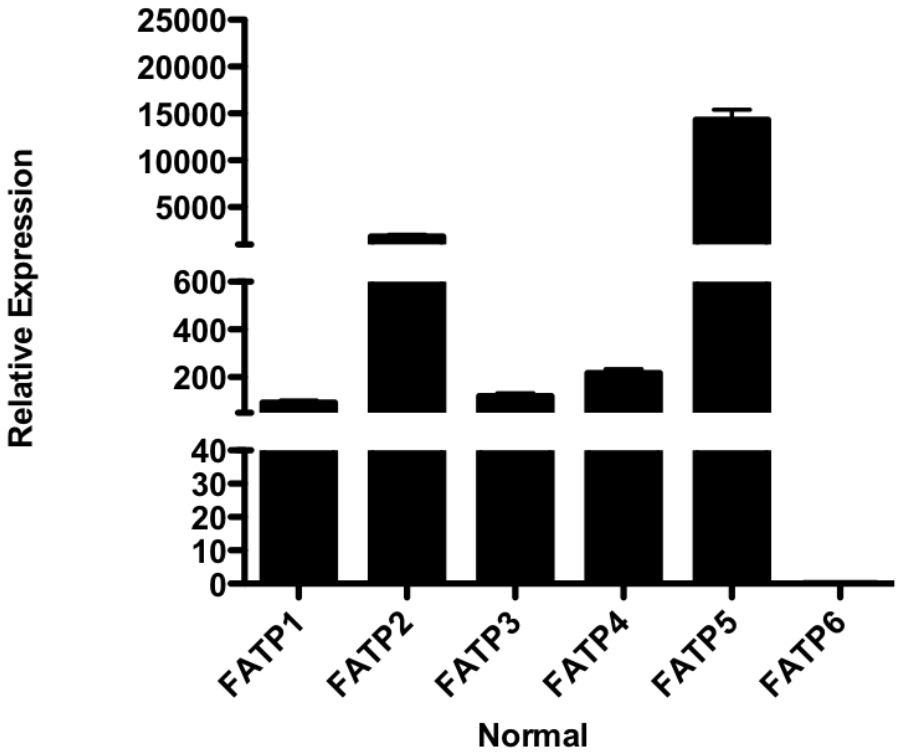

Figure 3.25: Analysis of FATP expression in human liver by quantitative qPCR analysis
mRNA expression of the FATPs 1-6 in normal human liver using a fluidigm qPCR array®. Results are expressed as means of five normal livers, +/- SEM, run on triplicate arrays and normalized to pooled endogenous controls β-actin and GAPDH and log transformed using 2-ΔCt

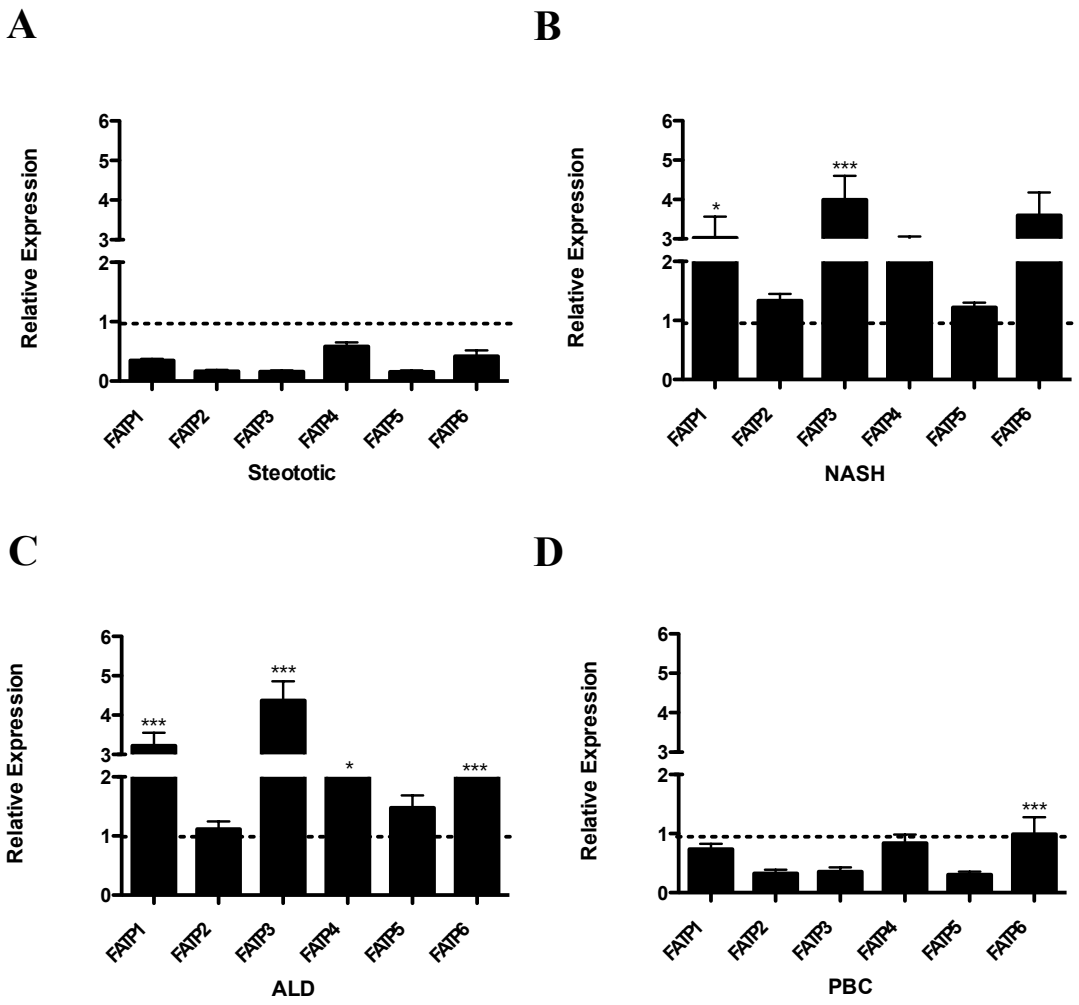

Figure 3.26: Analysis of FATP receptor expression in human liver by quantitative qPCR analysis

(A) mRNA expression of FATPs 1-6 in steatotic liver (B) NASH, (C) ALD and (D) PBC using a fluidigm qPCR array® and run on triplicate arrays. Results are expressed as the mean fold change in gene expression normalized to pooled endogenous controls β-actin and GAPDH relative to normal livers defined as 1 +/- SEM with means from four normal livers, four steatotic, three NASH, four ALD and four PBC. Dotted line represents normal expression at 1. Significance expressed as * $p<0.05$, ***$p<0.001$ using a one way ANOVA with Bonferroni correction.

3.3.12 Liver epithelial cells express FATP receptors

We examined the liver epithelial expression of FATP and found that primary hepatocytes expressed FATP1-5 (Figure 3.27A) with FATP2 and FATP4 most abundantly expressed. Huh7.5 also abundantly expressed FATP4. The HepG2 cells in contrast had more FATP1 and FATP4 (Figure 3.27A) whilst BEC only expressed FATP1 and FATP4 (Figure 3.27B).

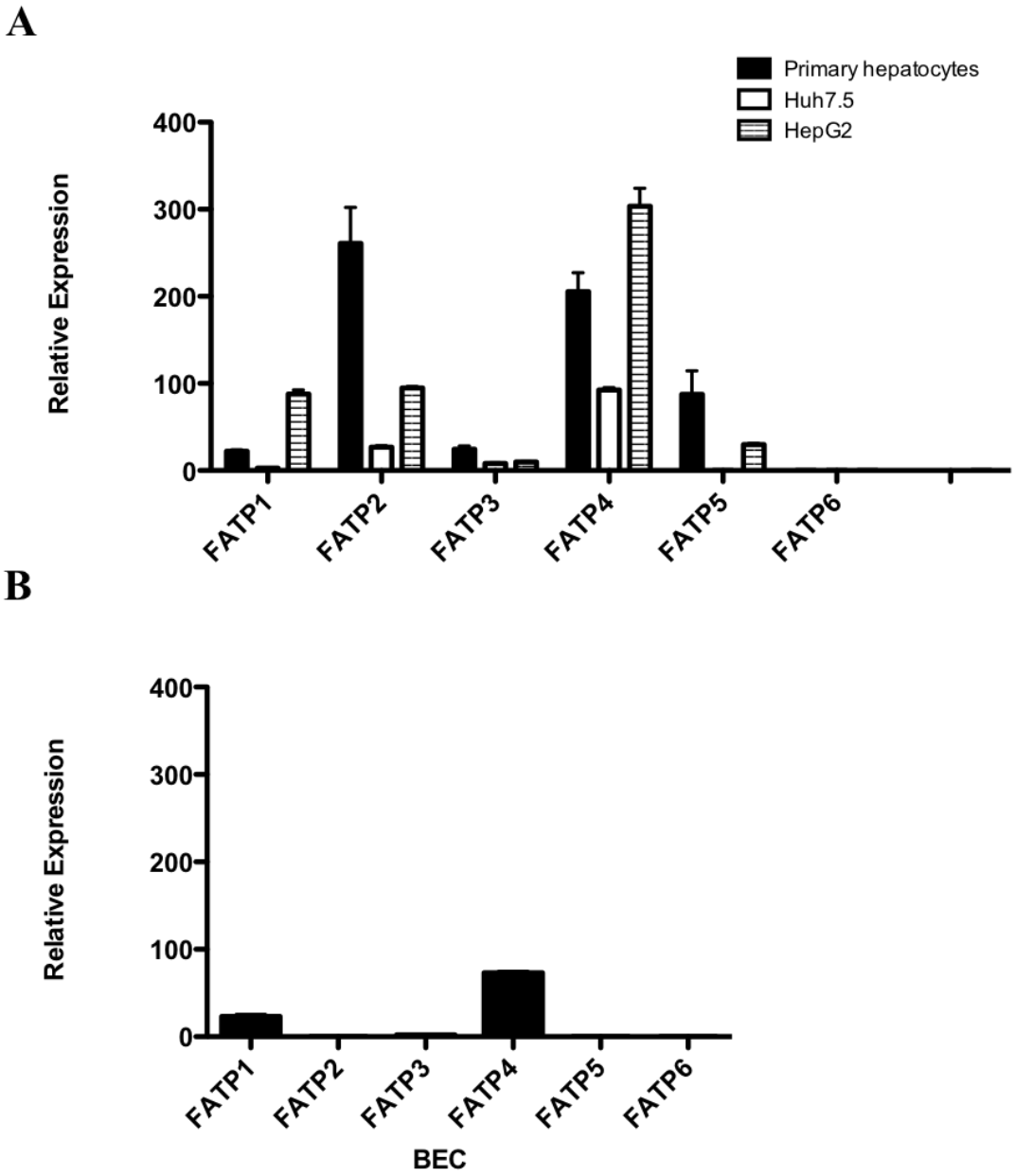

Figure 3.27: Analysis of FATP receptor expression in human liver epithelial cells by quantitative qPCR analysis

(A) mRNA expression of FATPs in primary hepatocytes, Huh7.5 and HepG2 and (B) BEC using a fluidigm qPCR array®. Results are expressed as means of three primary hepatocytes, three Huh7.5, three HepG2 and three BEC +/- SEM, run on triplicate arrays and normalized to pooled endogenous controls β-actin and GAPDH and log transformed using 2-ΔCt.

3.3.13 Liver non-epithelial cells express FATP receptors

The non-epithelial cells such as HSEC expressed FATP1, FATP3 and FATP4 to the highest extent (Figure 3.28A), whilst fibroblasts contained abundant FATP1 and FATP4 with a smaller amount of FATP3 (Figure 3.28B). PBMCs expressed FATP1, FATP3 and FATP4 (Figure 3.28C). This confirms the microarray data (Figure 3.15B) suggesting more FATP1 in HSEC than in Huh 7.5 and increased expression of FATP2 in Huh7.5 compared to HSEC.

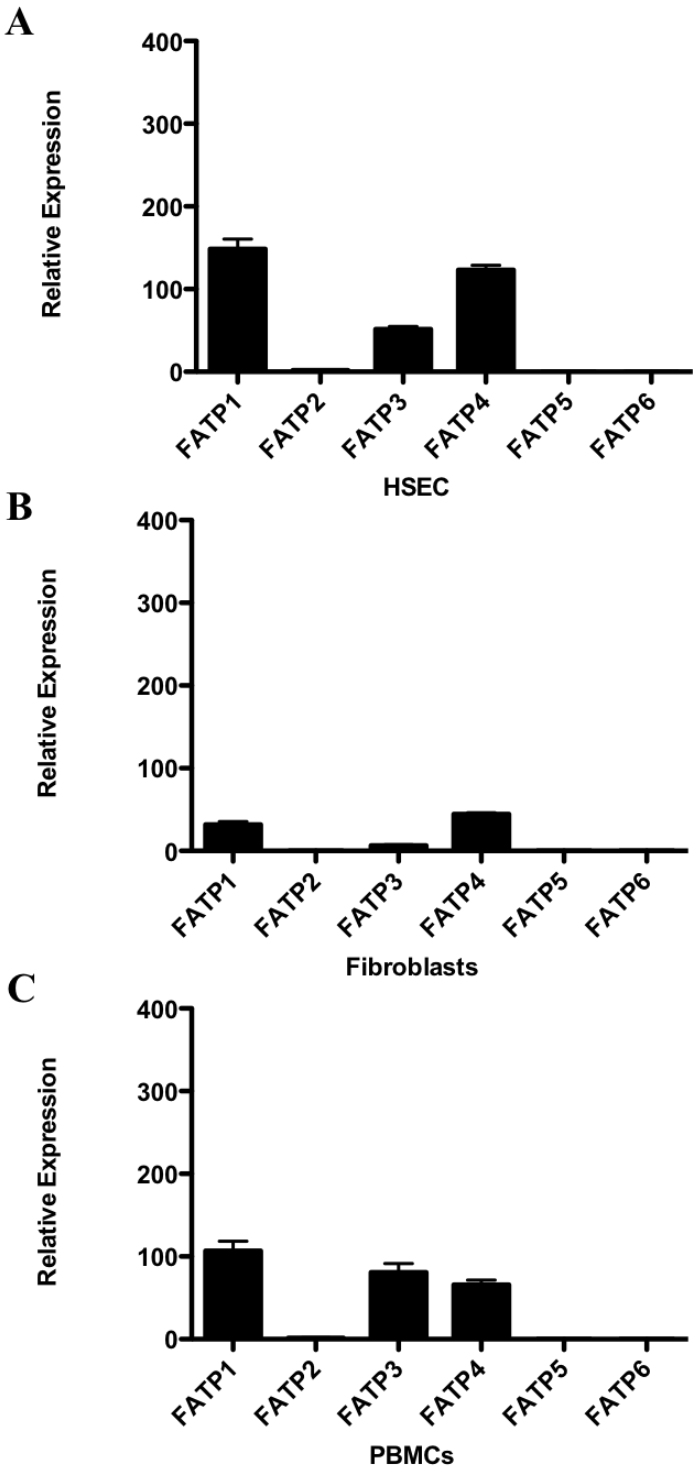

Figure 3.28: Analysis of FATP receptor expression in human liver non-epithelial cells and PBMCs by quantitative qPCR analysis

(A) mRNA expression of FATPs 1-6 in HSEC, (B) fibroblasts and (C) PBMCs using a fluidigm qPCR array®. Results are expressed as means off four HSEC, four fibroblasts and two PBMCs +/- SEM, run on triplicate arrays and normalized to pooled endogenous controls β-actin and GAPDH and log transformed using 2-ΔCt.

3.4 Discussion

Increasing incidence of liver disease in the western world and in particular NAFLD and NASH is a growing concern for healthcare providers. With uncertainty in disease progression many initiating factors are under investigation with a primary concern being the accumulation of lipids, which can either remain benign, or trigger the cascade of events causing NASH. As discussed previously hepatocyte steatosis can result directly from accumulation of FAs or through de novo synthesis from substrates including the carbohydrates glucose and fructose, which make their journey into the cell via specific facilitator proteins. However the expression patterns of these transporters in normal and diseased liver has received little attention.

Therefore we began this thesis by using genomic and immunohistochemical approaches to document hepatocellular expression of a diverse array of carbohydrate and fatty acid transporter proteins in normal and diseased liver and whether changes in disease were attributable to a specific subset of cells. To our knowledge this is the first time such a study has been performed with human tissue and is reflected by our published review of the literature (Karim et al., 2012). Our results show that normal liver expresses all GLUTs 1-13 with the exception of GLUT7. Simple steatosis was characterized by a similar expression pattern where as in more advanced disease where steatosis progresses to inflammation and fibrosis we noted an up regulation in receptor expression. Thus NASH was associated with increased GLUTS 1,3,5,6,8,9,12 mRNA; ALD GLUTS 1,3,5 and 12 and GLUT1 at the protein level, particularly on immune cells. GLUT 2,4,9 and 10 were expressed on hepatocytes whilst GLUT4 was up in NASH and ALD at the protein level. GLUT9 was expressed on HSEC and GLUT10 on HSEC and BEC. We found PBC, which is also

characterized by fibrosis and inflammation, was the most different from the normal situation with an up regulation of GLUT5 expression on BEC, fibroblasts and PBMCs. We noted that on a cellular level whilst many receptors were common there are some specific differences, which could contribute to global changes in disease for example BEC most abundantly expressed GLUTS 1,3 and 6, HSEC 1,3,6,8 and 12, fibroblasts 1,3,6 and 10 and PBMCs 1,2,5,7,8 and 12.

In addition we document expression of FABPs 1-6, CAV1, CD36, LRP1, LRP2 and LRP8 in normal liver with a tendency for more expression of FABP1 on hepatocytes and FABP4 on HSEC. Again simple steatosis was associated with little change in receptor expression whilst NASH and ALD were associated with increased expression of FABP1, FABP4 (most abundant), FABP5 and FABP6, CAV1, and LRP8. In common with our findings for carbohydrate receptors, the profiles of lipid transporters in PBC were most different from the normal situation with changes in FABP2, FABP4, LRP8 and particularly FABP6. Our pilot immunohistochemistry experiments confirmed protein upregulation in NASH for FABP1, FABP4, CAV1 and LRP8. All cells expressed FABP5, CAV1, CD36, LRP1 and LRP8 whilst FABP4 expression was restricted to HSEC, fibroblasts and immune cells and FABP3 to fibroblasts.

In relation to FATP expression, simple steatosis and PBC were associated with downregulation of all FATPs except FATP6 in PBC, whilst NASH and ALD had increased expression for all and in particular FATPs 1,3,4 and 6. Primary hepatocytes and hepatocyte cell lines expressed FATP1-5 and all cells expressed FATP1, whilst BEC did not express FATP3.

Whilst some of these receptor proteins such as FABP4 and FABP5 have previously been shown to be up regulated in NALFD (Westerbacka et al., 2007), to our knowledge, no studies to date have documented the full expression patterns of any of the carbohydrate or fatty acid trafficking proteins in the liver. One reason for the lack of investigation may be the long held view that the passage of glucose and lipids largely involves passive diffusion rather than facilitated transport (Bradbury, 2006), (Bonen et al., 2007) however this longstanding view has been challenged by identification of specific transporters and recent findings which suggest that transport is not merely a passive process. Specific proteins are up regulated in disease for example FABP4 and FABP5 (Westerbacka et al., 2007) and some are involved in active FA uptake for example CD36 (Zhou et al., 2008). Since disease onset and progression can be fueled by many different and specific substrates, and because uptake of these may be driven by an increase in specific receptor expression as part of disease pathogenesis, we felt it was important to characterize hepatocellular expression in health and disease.

3.4.1 Hepatocellular expression of GLUT proteins

The completion of the human genome project has meant that to date, 14 members of the GLUT family have been identified (Karim et al., 2012). We have found mRNA transcripts for 13 GLUTS in the human liver; we have documented expression in specific cultured cell types and have supporting protein expression data for GLUT1, GLUT2, GLUT4, GLUT9 and GLUT10. Previous studies have shown GLUT2 to be the predominant GLUT isoform in the liver (Nordlie et al., 1999) also some evidence of GLUT1 (Wu et al., 2008), GLUT9 (Keembiyehetty et al., 2006) and GLUT10 expression (McVie-Wylie et al., 2001) have been documented. These findings

support our studies, which further demonstrate chronic disease specific increases in expression of GLUT1, GLUT3, GLUT5 and GLUT12 in particular and a marked decrease in hepatocellular expression of many transporters in steatosis.

GLUT1 is ubiquitously expressed in all tissue and cells (Mueckler et al., 1985), (Takata et al., 1990), (Mueckler, 1990) and indeed this was reflected in our study with abundant mRNA in all livers and protein expression around the hepatocyte membrane and strongly in endothelial cells and in infiltrating cells. We demonstrate parenchymal expression in both primary hepatocytes and abundantly in hepatocyte cell lines (Amann et al., 2009), which fits with reported elevated hepatocyte expression in HCC which is linked to advanced stage in tumor progression (Amann et al., 2009). Interestingly silencing of GLUT1 in tumor cells leads to a reduction in glucose uptake and HCC cell migration (Amann et al., 2009), confirming the functional importance of this receptor even in the presence of GLUT2. As expected GLUT2, was expressed both at the mRNA level and also at protein level in all liver types. There was strong membranous staining in the hepatocytes in normal, steatotic, ALD and PBC livers. Interestingly in two cases of NASH we found diffuse cytoplasmic staining for GLUT2 with loss of membrane staining. This phenomenon of GLUT2 internalization has also been reported in enterocytes of mice caused by the action of insulin (Tobin et al., 2008). Other factors have also shown to cause this internalization such as corticoids, stress and Glucagon-Like Peptide-2 (GLP-2) (Kellett and Brot-Laroche, 2005). Further more in support of our findings GLUT2 internalization has also been documented in mice, were insulin stimulation has been shown to cause IR and GLUT2 cointernalization and colocalization in hepatocytes (Eisenberg et al., 2005), (Gonzalez-Rodriguez et al., 2008). Thus it is likely that an

insulin-dependent mechanism may also underlie enhanced cytoplasmic localization in human NASH liver.

We have additionally documented GLUT3, GLUT5 and GLUT12 expression in human liver, all of which were highly up regulated in NASH and ALD, with GLUT5 also particularly abundant in PBC. To date, GLUT3 protein expression in the liver has only been associated with hepatic tumor biology by Kurata et al (Kurata et al., 1999), and indeed Ciaraldi et al speculated that the low level of expression in the normal liver was due to restriction to a specific sub set of cells. Our qPCR data confirms expression in malignant hepatocyte lines, and for the first time we have shown the presence of mRNA transcripts in HSEC, BEC and fibroblasts. Thus enhanced expression in fibrotic and cholestatic diseases may relate to increased relative abundance of biliary and fibroblastic cells in disease. GLUT5 is abundantly expressed in muscle tissue and functions as a fructose transporter (Corpe et al., 2002) but it has previously been shown to be expressed in cytoplasmic regions of hepatocytes (Godoy et al., 2006). Other data suggests it is barely detectable in porcine livers implying both tissue specific and species differences in distribution (Aschenbach et al., 2009). Interestingly increased expression of this protein is also associated with IR in diabetes (Litherland et al., 2004) again pointing to common regulatory mechanisms in NASH.

Similarly subcellular distribution for GLUT12 has been reported to be influenced by insulin (Stuart et al., 2009) and whilst mRNA has been reported in whole liver (Miller et al., 2005b) we found it to be one of the least abundant isoforms in the primary hepatocytes, Huh7.5, fibroblasts and PBMCs. It was not expressed in HepG2 cells or

BEC and compared to other cell types, was most abundantly expressed in HSEC. This was supported by our microarray data were we found significantly more expression in HSEC than Huh7.5. We were unable to quantify or detect its cellular expression during this investigation, but a recent report points to protein expression within normal and cirrhotic human liver lysates (http://www.abcam.com/GLUT12-antibody-ab100993.pdf).

GLUT4 is the main insulin sensitive member of the GLUT family, and thus is abundantly expressed in muscle and adipose tissue. We demonstrate mRNA and protein expression in normal, steatotic, NASH, ALD and PBC livers, with protein expression around the smooth muscle of vessels as expected but also abundant cytoplasmic localization in hepatocytes with no distinct membrane positivity. Control staining in adipocytes confirmed the specificity of our reagent and mRNA expression in HepG2 and Huh7.5 and to lesser extent primary hepatocytes, confirmed this. Interestingly we also noted endothelial expression, as suggested by other studies (Tsukioka et al., 2007) as well as smaller amounts in, fibroblasts and PBMCs. Previous studies of patients with liver cirrhosis, who have a tendency for reduced insulin responses have documented maintained skeletal expression of GLUT4 (Shan et al., 2011) but cirrhotic animals also hint at reduced responsiveness to insulin (Jessen et al., 2006). To our knowledge, ours is the first study to consider hepatic expression in cirrhosis.

We also found a modest increase in GLUT6, GLUT8, GLUT9 and GLUT10 mRNA expression in NASH and ALD. GLUT6 was present in hepatocytes, cell lines were its previously been reported (Kayano et al., 1990) and in BEC, HSEC and fibroblasts

were it has not been previously reported but was most abundantly expressed, thus increased expression of this transporter in disease may reflect the energy demands of non parenchymal cells more than parenchymal.

GLUT8 was expressed in all cell types with high abundance in primary hepatocytes and the hepatocyte cell lines, although it has been detected in porcine liver and mouse hepatocytes there are no known reports in human liver (Gorovits et al., 2003), (Aschenbach et al., 2009). Its significance in NASH and ALD may reflect increase expression of this transporter in perivenous hepatocytes were its been reported to be involved in regulating glycolytic flux (Gorovits et al., 2003).

GLUT9 and GLUT10 were highly expressed in primary hepatocytes and in HepG2, expression of GLUT9 in HepG2 fits with previously reported expression in malignant tissue (Godoy et al., 2006). However its expression patterns have not been documented in diseased livers. Since it was most abundantly expressed in hepatocytes and was one of the least abundant isoforms expressed in all other cell types, disease specific increase in expression is most likely due to hepatocytes. Moreover protein expression of GLUT9 and GLUT10 was similar to GLUT4 were it was diffused and cytoplasmic in the hepatocytes, this data supports previous GLUT9 expression in HCC (Godoy et al., 2006), furthermore we document intense staining pattern for GLUT10 in the NASH and strong endothelial staining in the ALD livers, which was confirmed by our qPCR findings, this suggests disease and cell specific increase in expression, cellular distribution has not been reported previously. Although the precise function of GLUT10 is unknown it has a reported role in transporting antioxidant vitamin C (Lee et al., 2010) thus increased expression in

NASH and ALD may be a protective mechanism to protect the liver from ROS induced damage. It must be noted we found staining in RBCs of ALD livers and this may suggest this is non specific staining, however our IgG control was negative for staining and kidney tissue stained positive, were GLUT9 is known to be expressed. There are no reports linking GLUT9 and RBC expression.

The true extent of expression of GLUT7 is difficult to gauge since we found mRNA in only one case of normal liver out of four and in 2 cases of ALD. We are confident that out reported absences in some patients were genuine since transcripts were detected appropriately in our universal human standard control in the qPCR experiments. Similarly studies with porcine livers support little or no hepatic expression (Aschenbach et al., 2009). However since PBMCs expressed GLUT7, it is possible that hepatic expression reflects the extent of inflammation in some patients. GLUT11 and GLUT13 expression remained relatively unchanged in diseased liver compared to normal suggesting minimal functional roles. However in malignant melanoma GLUT8 and GLUT11 expression has been linked to cell proliferation (McBrayer et al., 2012). Since we see enhanced expression in the tumor cell lines compared to primary hepatocytes this role may be more widespread.

3.4.1.1 Functional Significance of GLUT proteins in liver disease

As discussed previously NASH and ALD are cirrhotic liver diseases, which are associated with inflammation, hypoxia and stress, and where patients may exhibit impaired insulin responses (Shan et al., 2011). We have seen increased expression of GLUT1 and GLUT3 in NASH and ALD and have also reported expression of GLUT1 in PBMCs. Thus an increase in mRNA expression in the NASH and ALD livers in

part may be attributed by the presence of inflammatory cells, or by hypoxia in NASH since its been found that hypoxia induces GLUT1 expression (Amann et al., 2009) and recently increased expression of GLUT3 mRNA and protein in macrophages was found in hypoxic atherosclerotic lesions (Li et al., 2012) suggesting GLUT 1 and GLUT3 expression can be increased in hypoxic conditions. Moreover the significance of GLUT3 increased expression in NASH and ALD may be that it functions as one of the main GLUT transporters in hypoxic conditions or when glucose is the only available energy source its expression increases when glucose is used in the synthesis of lipids. This is supported by findings, which show that when GLUT3 is knocked down in macrophages there is a decrease in glucose uptake and lipid accumulation when there are no other exogenous lipids present (Li et al., 2012). This fits with the insulin resistant, hyperglycemic environment, which characterizes NASH.

Some GLUTS may also be upregulated in diseased liver as a protective mechanism. For example we saw increased expression of GLUT10 in endothelial cells of ALD livers. Mitochondrial GLUT10 in smooth muscle cells has been shown to have a functional role in protecting cells from oxidative damage caused by ROS (Lee et al., 2010), furthermore in adipocytes it has been shown to be insulin stimulated were it can translocate from the Golgi to the mitochondria were its involved in the uptake of vitamin C (Lee et al., 2010) which is also an antioxidant. As metabolism of alcohol and fructose leads to the generation of ROS, which ultimately leads to cellular damage, the increase in expression of GLUT10 in HSEC and also diseased liver may be a mechanism to protect the cell from further damage. Furthermore increased expression of GLUT12 could be a compensatory mechanism in the NASH and ALD

liver when other GLUTS become defective to improve insulin sensitivity and glucose clearance rates as in mice, over expression of GLUT12 has been shown to improve whole body insulin sensitivity and glucose clearance rates (Purcell et al., 2011). Interestingly we also found internalization of GLUT2 a bidirectional transporter in NASH livers this also may be a protective mechanism in the NASH liver when exogenous insulin and glucose levels are high thus preventing glucose release from hepatocytes. Since insulin promotes hepatic lipogenesis its understandable that GLUT2 would internalize to prevent glucose release. Whether the insulin receptor is also internalized with GLUT2 needs further investigation.

The role of GLUT5, a fructose transporter in health and disease has recently received great attention and this is mainly due to increase consumption of high fructose corn syrup, which is used in the manufacturing of food and drinks in the western world. Furthermore in the context of fatty liver and NASH, fructose is very important since it can be utilized for DNL. The significance of increased GLUT5 expression in NASH and ALD is very important in the transition from NALFD to NASH, as an increase in receptor expression would result in an increase in fructose uptake. Hepatic metabolism of fructose can lead to inflammation via the production of free radicals which when the detoxifying mechanisms of the cell are overwhelmed can cause lipid peroxidation, necroinflammtion as observed in NASH and eventually fibrosis and cirrhosis (Lim et al., 2010) through the activation of HSCs and KC. Furthermore GLUT9 can also transport fructose, in addition metabolism of fructose leads to increase synthesis of uric acid (Stirpe et al., 1970) which is also transported by GLUT9. The significance of this in context of NASH, which is commonly associated with the MetS is that uric acid levels have been shown to predict obesity and

hypertension (Masuo et al., 2003). Furthermore in rats with the MetS induced by fructose, an inhibitor of uric acid Allopurinol reversed and prohibited the MetS (Nakagawa et al., 2006). In addition Vilà et al have shown in male rats who ingested fructose in their drinking water leptin signaling was impaired leading to hypertriglyceridemia and hepatic steatosis (Vila et al., 2008). Furthermore the metabolism of alcohol and fructose is similar and we also see an increase in GLUT5 expression in ALD.

GLUT4, GLUT8, GLUT10 and GLUT12 have all been reported to be insulin sensitive. For example insulin stimulated translocation of GLUT8 has been shown in acrosomes of sperm (Schurmann et al., 2002) and mice preimplatation blastocysts (Carayannopoulos et al., 2000), GLUT10 in adipocytes (Lee et al., 2010) and GLUT12 in normal muscle (Stuart et al., 2009), with translocation being dependent on Phosphoinositide 3-Kinase (PI3-K) activation (Stuart et al., 2009). Although there are no reports of insulin stimulated GLUT expression in the liver in our study, the presence of GLUT4 and GLUT10 in the liver within cytoplasmic droplets suggests they may translocate to the cell membrane upon stimulation. Such stimuli could be insulin or the activity of VAP-1, a protein that is increased in liver inflammatory diseases such as ALD and NASH. For example in isolated rat adipocytes, activation of VAP-1 (Enrique-Tarancon et al., 1998), (Marti et al., 1998) causes GLUT4 mobilization to the cell surface, and in cultured vascular smooth muscle cells (VSMCs) VAP-1 substrates such as methylamine have been shown to regulate glucose uptake. Such mechanisms may also act on transporters other than GLUT4, such as GLUT1, (El Hadri et al., 2002) since GLUT4 is not expressed in VSMCs (Low et al., 1992). Furthermore in rat's leptin signaling has been shown to enhance

GLUT4 mediated glucose uptake in HSCs (Tang and Chen, 2010) leading to HSC activation, which may contribute to fibrogenesis in NAFLD. Also VAP-1 and CD36 are found together in caveolae in adipocytes (Souto et al., 2003), (Pilch et al., 2007), and there is speculation caveolae are involved in GLUT4 trafficking (Scherer et al., 1994), (Gustavsson et al., 1996), (Ros-Baro et al., 2001), (Karlsson et al., 2002) suggesting that regulation of glucose and lipid uptake is closely linked.

Furthermore sinusoidal endothelium has been shown to express IRS and its been suggested that endothelial responses to insulin could be a rate limiting factor in glucose uptake (Yang et al., 1989). However the increased expression of GLUT12 in NASH with expression being most abundant in HSEC, suggests that other non-parenchymal cells may play a role in disease pathogenesis. Since hepatocytes and HSEC are physiologically in close contact it is possible that substrates taken up by HSEC may be passed through the sinusoidal endothelial fenestrations and hence exacerbate disease pathogenesis. Additionally GLUT8 and GLUT12 may work jointly, since enterocytes from GLUT8 KO mice fed on a high fructose diet showed increased fructose uptake compared to WT mice and this was associated with increased levels of GLUT12. GLUT8 also inhibits fructose uptake in the jejunum (DeBosch et al., 2012). Thus GLUT8 suppresses fructose uptake and KO models show increased expression of GLUT12 which causes fructose uptake thus GLUT8 controls GLUT12 expression in a fructose induced manner in enterocytes (DeBosch et al., 2012). This suggests that the activity of some GLUTS directly affects other isoforms and that regulation is closely linked, which is likely the case in NASH.

The functional significance of GLUT7 in disease needs further investigation, however GLUT7 has high sequence homology to GLUT5 and can also transport glucose and fructose however the capacity for these substrates is low and thus its been hypothesized (Cheeseman, 2008) that GLUT7 may prefer other as yet unidentified substrates, similar to GLUT9 which transports urate. Its been suggested to be in the hepatic ER and its functional role has been reported to be in the release of glucose produced during gluconeogenesis and glycogenolysis (Gould and Holman, 1993, Waddell et al., 1992).

3.4.1.2 Regulation of GLUT expression in disease

In all it is interesting to note that in simple steatosis many of the GLUT receptors were downregulated. This is perhaps logical since a cell, which has ample fuel, stored in the form of lipid droplets, does not require excess carbohydrate fuel and so GLUT receptors are downregulated. In contrast most receptors were upregulated in both NASH and ALD. A possible reason for this is that many patients with NASH/ALD (Smits et al., 2013), (Strand et al., 2012) also have the MetS, and are IR. Firstly IR would promote an increase in systemic insulin levels this may cause an upregulation of specific transporters such as GLUT4, GLUT8, GLUT10 and GLUT12 which have been reported to be insulin sensitive in an effort to remove the glucose from circulation and improve glucose clearance rates. Secondly the IR state would mean that postprandial circulating levels of many sugars would be high which could induce expression of transporters. Also many of the transporters, as discussed, are also upregulated in hypoxic conditions seen in NASH and ALD. Furthermore systemic IR leads to increased hepatic lipogenesis and thus its plausible that GLUT receptors would be upregulated in an attempt to firstly remove sugars from the bloodstream and

secondly to convert them to lipids via lipogenesis for storage, causing further lipotoxicity and oxidative stress through lipid peroxidation and ROS generation.

These changes are likely to be specific for chronic liver diseases associated with metabolic disturbances since our data suggests that GLUT expression is very different in PBC. One reason for this may be that unlike NASH and ALD it is not a metabolic disease. PBC is a chronic autoimmune disease, which ultimately leads to the destruction of bile ducts. This contrasts with NASH and ALD which are metabolically very similar, and hard to distinguish histologically. We also noted key differences in GLUT expression between hepatocytes and the two-hepatocyte cell lines studied, which are both, derived from differentiated HCCs. It was not surprising to see that many GLUT receptors were highly expressed in the cell lines compared to primary hepatocytes since as discussed previously tumor cells have an increased demand for energy for growth which is fulfilled by an upregulation of GLUT receptors.

3.4.2 Hepatocellular expression of fatty acid trafficking proteins

We have shown for the first time disease specific alterations in lipid transporters. Normal liver expressed FABP1-5, CAV1, CD36, LRP1, LRP2 and LRP8 mRNA and this was similar in simple steatotic livers. In contrast the inflamed and fibrotic livers (NASH, ALD, PBC) again demonstrated altered expression patterns the significance of which is discussed below.

3.4.2.1 FABP expression in the liver

FABP1 was strongly expressed cytoplasmically in hepatocytes of normal liver at the protein level and expression decreased in steatotic liver but increased in NASH. Furthermore at the mRNA level it was one of the most abundant isoforms in the primary hepatocytes and cell lines, with no expression in all other cell types studied. This corroborates previous immunohistochemical studies showing hepatocyte staining in individuals with simple steatosis (Charlton et al., 2009b) but contrasts data in the same investigation showing decrease in progressive forms of NASH with little expression in individuals with severe NASH (Charlton et al., 2009b). This finding is not in agreement with our results, although the cases shown in the Charlton investigation suggest that steatosis was still evident in their 'severe' samples. Thus we would hypothesize that steatosis leads to a decrease in expression, which may not be maintained in individuals, transplanted for end stage disease where extensive cirrhosis, but little steatosis is present. In contrast we found FABP2 and FABP3, expression in NASH to be similar to that in normal, whilst FABP2 was upregulated in ALD and PBC. FABP2 overexpression in cell lines has been linked to reduced lipoprotein export, and is downregulated by insulin but upregulated by Epidermal Growth Factor (EGF) and steroid administration (Levy et al., 2009). Since cirrhotic patients have elevated circulating EGF levels (Tanabe et al., 2008) and may have received treatment with steroidal anti-inflammatory drugs prior to transplantation, this could explain enhanced FABP2 expression in PBC and ALD.

In particular we found the adipocyte (Makowski and Hotamisligil, 2004), (Boord et al., 2002) and macrophage specific FABP4 (Pelton et al., 1999), highly upregulated compared to normal in NASH and ALD livers at the mRNA level and also at the

protein level in NASH, particularly on sinusoidal endothelium, with a decrease in steatotic livers. Endothelial expression is in agreement with identification of this molecule as a useful endothelial phenotypic marker (Herbert et al., 2008), and its regulation by VEGF-A has been demonstrated in cultured endothelial cells, furthermore FABP4 has been shown to be a positive regulator of endothelial cell proliferation (Elmasri et al., 2009a). We did not find any expression in PBMCs although its been reported to be expressed in macrophages where it regulates inflammatory function (Makowski et al., 2005). A single study has reported mRNA expression for FABP4, FABP5 and FATP5 in livers of NAFLD patients with the suggestion that expression of FABP4 and FABP5 increases with percentage of liver fat, (Westerbacka et al., 2007). Of note, livers with NASH or other chronic cirrhotic injuries were not examined in this study and we did not find similar results linked to steatosis in our findings. Others have shown an inverse relationship between FABP4 expression in adipose tissue and liver in obesity (Queipo-Ortuno et al., 2012) and FABP4 and CD36 have also reported to be positively correlated with liver fat content in NAFLD (Greco et al., 2008). It is interesting to note that in our study we found reduced expression of FABP4 in steatotic livers and a strikingly high up regulation in NASH and ALD livers, which are associated with inflammation and fibrosis. FABP4 is also found in the circulation were its shed from adipose tissue (Xu et al., 2007), (Xu et al., 2006) furthermore Xu et al and others have shown plasma FABP4 levels as an early indicator in the development of the MetS independent of obesity and IR (Xu et al., 2007), (Tso et al., 2007), (Stejskal and Karpisek, 2006). Given the reported regulation of adipocyte FABP4 expression by PPARϒ (Li and Gu, 2012), (Rival et al., 2004), and the acquisition of an adipocyte-like phenotype by hepatocytes during steatotic liver injury concurrent with PPARϒ activation (Larter et al., 2008) it is

possible that similar regulatory mechanisms govern expression of FABP4 in hepatocytes.

A similar level of expression was seen in NASH and ALD livers for FABP5, FABP6 and Caveolin 1, all of which were up regulated compared to normal livers. In particular we found FABP6 a bile acid transporter most abundantly expressed in PBC whilst FABP7 expression only in PBC livers and not in any isolated cell types studied including BEC. FABP5 binds LCFA with high affinity and has a lower affinity for short chain FAs and those containing double bonds (www.uniprot.org). Increased expression has been associated with progression of intrahepatic cholangiocarcinomas (Jeong et al., 2012), HFD induced rodent liver injury (Peng et al 2010) and the development of atherosclerotic lesions (Babaev et al., 2011). Furthermore polymorphisms in the FABP5 gene have been associated with type II diabetes (Bu et al., 2011), and again the gene is regulated by PPARγ.

Association with or functioning of FABP6 in PBC has not previously been reported but regulation of expression has been linked to ligation of the Farnesoid X Receptor by bile salts (Liu et al., 2008), and thus a similar mechanism may operate in cholestatic liver injury. In contrast we noted a marked absence of FABP7 mRNA under most circumstances. The protein is found in murine KC where expression decreases in response to Lipopolysaccharide (LPS) (Abdelwahab et al., 2003), and blockade of function in murine hepatoma cell lines, leads to decreased lipid accumulation (Ahn et al., 2012). Thus there is a precedent for hepatocellular expression and so our data either points to species-specific changes in expression or possible deficiencies in our genomic analyses.

3.4.2.1.1 Functional Significance of FABPs in liver disease

FABPs are capable of binding FA and either directing them for storage or oxidation in mitochondria. Furthermore some FABP gene polymorphisms have been associated with risk of developing NAFLD, for example for FABP1 (Peng et al., 2012a) and the Ala54Thr polymorphism of FABP2 (Baier et al., 1995), (Levy et al., 2001), (Musso et al., 2009), (Peng et al., 2009). Links between variant expression patterns and function have yet to be fully defined, however Aller et al suggest that in patients with NAFLD the Ala54Thr polymorphism is not associated with histological changes, or IR. (Aller et al., 2009), Whilst other studies link FABP1 with a new mechanism of lipotoxicity in NAFLD (Charlton et al., 2009b) where expression is mediated by levels of cholesterol (Charlton et al., 2011). Upregulated FABP1 could contribute to NASH by increasing the uptake of LCFA, which it can transport to the nucleus and cause activation of PPARα (Adida and Spener, 2002) thus increasing expression of genes involved in lipid metabolism; however it is also involved in esterification of lipids to TAG (Veerkamp and van Moerkerk, 1993), (Zimmerman and Veerkamp, 2002), whilst the T94A polymorphism of FABP1 has been shown to have a reduced affinity for LCFAs (Gao et al., 2010) and thus would lead to decreased ligand activation of PPARα leading to increased lipid buildup (Peng et al., 2012a).

The significance of increased expression of FABP4 in NASH and ALD is currently unknown, but could relate to exacerbation of the immune response, regulation of cholesterol handling, obesity and IR. Thus in macrophages FABP4 has been shown to regulate cholesterol traffic and is also involved in the cytokine responses during the inflammatory response (Makowski et al., 2005). In addition mice deficient in FABP4 do not develop diet-induced IR (Hotamisligil et al., 1996) and demonstrate reduced

TNFα expression, again linking obesity and IR (Hotamisligil et al., 1996). Thus increased expression of FABP4 in diseased liver could lead to increased uptake of FA further damaging the cell. Since soluble forms of FABP4 have been shown as an early indicator in the development of the MetS, the protein has merit both as a potential biomarker in detecting MetS and therapeutic target for ameliorating NASH. As adipocytes from FABP4 KO mice have decreased lipolysis (Coe et al., 1999, Scheja et al., 1999), therapeutic approaches directed against this isoform, may also improve whole body insulin sensitivity. However it is important to note that whilst FABP4 and FABP5 double KO mice show increased protection from fatty liver, type II diabetes, obesity and IR, (Maeda et al., 2005). In contrast the single KO mice did not demonstrate protection against fatty liver or obesity even though modest increases in insulin sensitivity were noted (Hotamisligil et al., 1996), (Maeda et al., 2003). This reiterates the complex interplay between lipid receptors and suggests that therapeutic approaches may need to consider blockade of multiple pathways for maximal effect.

It would be interesting to see if NASH patients have increase circulating levels of FABP4 in the blood. Soluble forms of other isoforms have also been reported as biomarkers for certain disease, for instance FABP3 Heart (Pelsers et al., 2005), FABP1, hepatocellular injury after transplant (Pelsers et al., 2002), FABP2 intestine (Lieberman et al., 1997) and FABP7 brain (Wunderlich et al., 2005).

The increased expression of FABP6 in PBC may be due to the nature of the disease, since expression of FABP6 is also regulated by bile acids as the bile ducts are damaged this leads to poor drainage of bile acids which can regulate FABP6 expression. Furthermore bile acids can regulate DNL and gluconeogenesis through

activation of farnesoid X receptor (Halilbasic et al., 2012) which may explain why FABP2, FABP4 and LRP8 are also upregulated.

3.4.2.2 FATP expression in the liver

The second family of lipid transporters we studied was the FATPs, and we found a down regulation of all FATPs in steatotic and PBC livers. In contrast NASH and ALD livers showed an up regulation of all the FATPs and in particular FATP1, FATP3, FATP4 and FATP6 were most abundantly expressed. We found expression of FATP2 and FATP5 in primary hepatocytes and cell lines, which support's previous expression data in the liver, and interestingly these were the least up regulated in disease in comparison to the other isoforms. FATP2 is found in the cytoplasm, bile canaliculus and peroxisomes of mouse hepatocytes (Falcon et al., 2010), but restricted to the ER in malignant human hepatocyte cell lines (Krammer et al., 2011), where it is primarily involved in large fluxes of LCFA uptake (Krammer et al., 2011). FATP5 has previously been reported in the liver (Auinger et al., 2010) on the plasma membrane of hepatocytes facing most proximal to the sinusoids (Musso et al., 2009) consistent with a role in uptake of circulating lipids. Its functional significance is illustrated by overexpression studies leading to increased hepatic FA uptake (Doege et al., 2006), and a 50% reduction in FA uptake in hepatocytes from mice lacking FATP5 (Doege et al., 2006). It is also distinctive from other family members as it demonstrates bile acid CoA synthetase (BACS) activity (Musso et al., 2009). This is interesting given our noted reduction in FATP5 in PBC livers, and the observation that bile acids can reduce hepatocyte FA uptake in a FATP5-dependent manner (Nie et al., 2012).

Knockdown of FATP3 in rat hepatocytes results in a decrease in lipogenic transcription factors (Bu et al., 2009), but there is very little data on human hepatic expression patterns of FATP3. However mRNA expression has been found in mouse mammary glands during lactation (Han et al., 2010) and in the lungs (Hirsch et al., 1998), (Stahl et al., 2001). FATP1, FATP3 and FATP4 expression has been reported to be elevated in mice with fatty liver induced by a methionine choline deficient diet whilst FATP2 and FATP5 levels did not change (Rinella et al., 2008). We report for the first time that FATP3 is expressed in the human liver and also highly up regulated in NASH and ALD livers. Since knockdown of FATP3 in rat hepatocytes results in a decrease in lipogenic transcription factors (Bu et al., 2009), disease-induced upregulation could contribute to steatogenesis. In contrast, although FATP6 has been found to colocalise with CD36 in facilitating LCFA uptake in the heart (Gimeno et al., 2003), it is reported as being absent in the liver (Gimeno et al., 2003). Of note we found FATP6 mRNA expression upregulated in NASH and ALD livers, but in the absence of mRNA expression in the individual cell types we studied. This may suggest that expression is only turned on in disease or it is expressed on cells, which we have not studied.

3.4.2.2.1 Functional Significance of FATPs in liver disease

Up regulation of FATPs in diseased liver may have an impact upon the uptake of LCFA, amplifying diet-induced obesity and IR. This is exemplified by FATP4 which has been associated with obesity and IR (Gertow et al., 2004), and evidence that polymorphisms in the FATP5 promoter (rs56225452) are linked with IR, increased ALT activity and dyslipidemia (Auinger et al., 2010). Furthermore FABP1 and FATP4 are overexpressed in rat fatty liver (Feng and Chen, 2005) and in mice livers

FATP2 KO results in improved insulin sensitivity and a reduction in hepatic steatosis (Falcon et al., 2010). Similar findings have also been reported for FATP5 KO mice fed a HFD, which have enhanced insulin sensitivity and do not become obese or accumulate TAG (Hubbard et al., 2006). This suggests potential for targeting such receptors therapeutically to modify disease activity, and indeed reduction in FATP2 expression through transcription factor FOXA activity, results in inhibition of TAG synthesis, accumulation and release (Moya et al., 2012). This fits well with the situation in humans where FOXA1 expression is low in NAFLD (Moya et al., 2012) and we have noted reduced FATP2 expression in fatty livers, suggesting FOXA1 may govern FATP2 expression. However selection of receptor targets for inhibition is key since FATP5 KO mice have defective bile acid conjugation (Hubbard et al., 2006) and therefore cholestasis may present as a problem (Musso et al., 2009). However evidence that uptake of LCFA by FATP5 can be reversibly inhibited by the secondary bile acids Ursodeoxycholic Acid (UDCA) and Deoxycholic Acid (DCA) (Nie et al., 2012) suggests these bile acids may serve as a potential treatment for NAFLD (Nie et al., 2012). Certainly some evidence suggests FATP5 expression is higher in patients with steatosis than patients with NASH (Mitsuyoshi et al., 2009), and although we did not replicate this finding, our evidence of high expression in NASH suggests therapeutic interventions involving FATP5 should be considered on the basis of disease progression (Mitsuyoshi et al., 2009).

Therapeutic strategies directed against FATPs need to consider the daily nutritional variations in patients, and potential functional cooperation between receptors. Pre and post absorptive state specific expression of FATP varies. For example its been proposed that FATP1 has more of a role in LCFA uptake in the post-absorptive state

when insulin levels are high in muscle and adipose tissue (Doege and Stahl, 2006) and that in the pre-absorptive state FATP4 and CD36 are involved in LCFA uptake (Doege and Stahl, 2006, Coburn et al., 2001). In addition FATP1 KO mice do not exhibit LCFA uptake stimulated by insulin in adipose or skeletal muscle tissue (Wu et al., 2006) and are rather directed to the liver (Wu et al., 2006) hence protecting these tissues from diet induced obesity and IR (Wu et al., 2006). The same phenomenon is also true for FATP5 where in FATP5 KO mice, the post-absorptive lipid uptake rate is decreased and lipids are shunted to tissues, which predominantly express other FATPs (Doege et al., 2006). This suggests, that when there are disruptions in FATPs in extra hepatic tissues, circulating lipids are directed to other sites such as the liver, and this overload could contribute to disease pathogenesis in the liver.

3.4.2.3 Expression of additional transport and related proteins in the liver

As expected, we detected mRNA and protein expression for Caveolin 1 a constituent protein of caveolae in all liver types and cells studied. In support of our findings, Caveolin 1 is involved in lipid metabolism in rat hepatocyte peroxisomes (Woudenberg et al., 2010). Furthermore Caveolin 1 has been associated with tumor progression in HCC (Cokakli et al., 2009) and also liver regeneration (Mastrodonato et al., 2012). We found strong endothelial staining in the normal livers with some weaker staining around the hepatocyte membrane. In contrast expression was reduced in simple steatosis while mRNA was up regulated in NASH and ALD livers. However in chronic disease, endothelial staining appeared less consistent and uniform, whilst in PBC livers particularly, Caveolin 1 localized to areas of fibrosis. This supports data from a rat model of cirrhosis where Caveolin 1 protein was similarly increased (Shah et al., 1999).

CD36 a major lipoprotein scavenger receptor was also present in liver as previously reported, and mRNA expression was unchanged in chronically diseased livers but down regulated in steatotic livers. This contrasts other studies, which have reported increase in CD36 expression in NASH (Miquilena-Colina et al., 2011), and may represent patient diversity. CD36 expression has been reported to be elevated in NAFLD patients, which coincides with fat content in the liver (Greco et al., 2008), Our data suggested expression predominates on non-parenchymal cells, which fits with reports of scavenger functions on endothelium (Duryee et al., 2005) and contributions to cholesterol uptake in KC in NASH (Bieghs et al., 2012).

3.4.2.3.1 Functional Significance of additional transport proteins during liver disease

Caveolae are membrane enclosed, cytoplasmic vesicles containing a number of proteins including Caveolin 1 and Caveolin 2, GLUT4, insulin receptors and CD36, which play important roles in glucose and lipid signaling. Hence Caveolin 1 null mice do not become obese on a HFD (Razani et al., 2002) and Caveolin 1 KO mice have decreased lipid droplet formation in hepatocytes (Fernandez et al., 2006). Overexpression of Caveolin 3 in mice reverses a diabetic phenotype and IR by interacting with IRS1, increasing tyrosine phosphorylation and hence increased insulin receptor signal transduction (Dugail and Postic, 2010). Caveolin 1 has been implicated in liver regeneration (Mastrodonato et al., 2012) were its thought to be involved in supplying FAs to regenerating hepatocytes for energy, and this may be mediated though CD36 which is found in caveolae (Lisanti et al., 1994) and interestingly also with VAP-1 (Souto et al., 2003). Thus this may explain increased Caveolin 1 expression in NASH.

Rats fed on a high fructose or HFDs have been shown to have increased CD36 mRNA expression (Janevski et al., 2012) however this does not relate to an increase in hepatic fatty acid composition (Janevski et al., 2012). In contrast mice fed on a HFD have increased CD36 expression and TAG (Koonen et al., 2007), (Handberg et al., 2012), and CD36 null mice show increased insulin sensitivity and decreased muscle TAG content compared to WT (Goudriaan et al., 2003), (Hajri et al., 2002), which is associated with increased plasma NEFA and hepatic IR and TAG, (Goudriaan et al., 2003). Here it was postulated that these NEFA were shunted to the liver where the FABP and FATP family are involved in uptake since CD36 expression is low in hepatocytes (Goudriaan et al., 2003). Furthermore increased CD36 expression in NASH has been associated with increased steatosis (Miquilena-Colina et al., 2011) and onset of inflammation (Bieghs et al., 2012). Thus, the increased expression of LRPs we have reported in NASH and ALD liver may be a compensatory mechanism to increase import of lipoproteins and export of HDL in an IR state. Certainly in the post absorptive state, hepatic LRP1 has been shown to increase clearance of chylomicron remnants when it translocates to the plasma membrane in response to insulin (Laatsch et al., 2009). Furthermore in hepatocytes from mice lacking LRP1, HDL export is reduced (Basford et al., 2011) and LRP8 polymorphisms have been associated with onset of coronary artery disease and myocardial infarction (Shen et al., 2007).

3.4.3 Mechanisms explaining changes in lipid transporter proteins

In all, we found a majority of fatty acid trafficking proteins down regulated in simple steatosis except LRP2, which was modestly elevated probably in an attempt to remove HDL cholesterol from the circulation. In particular many of the fatty acid

trafficking proteins were upregulated in NASH and ALD livers. As discussed earlier IR is a predominant factor in patients with NASH/ALD. Since IR promotes inhibition of adipose tissue lipolysis and increases hepatic lipogenesis, this would result in high serum levels of FFA, which would be taken up by the liver, resulting in lipid storage, and increased hepatic lipogenesis would further overwhelm the cells storage ability. An overload of FA would ultimately lead to hepatocyte cell damage via lipid peroxidation, oxidative stress, and generation of ROS through ER stress and mitochondrial dysfunction. The release of cytochrome C from damaged cells would result in apoptosis/necrosis, thereby activating hepatic KC and HSCs. This cascade of events, which would ultimately overwhelm the detoxifying mechanism of the cell, would add further injury to the liver. The release of cytokines and other inflammatory mediators would result in hepatic upregulation of some of these FABPs, which bind FA. Furthermore cytosolic localization of some receptors may aid FA transport to nuclear receptors such as PPARs and NF-κB hence regulating genes, which are involved in metabolic and inflammatory processes. In addition we found that disease was associated with upregulation of many of the FATPs. This is perhaps expected since for FA to be directed for storage or oxidation in cells they need to be activated via FATPs by their ACS activity. However these receptors are also involved in the transport of LCFA. The increased uptake of FFA beyond the cells storage capability would mean that FATPs would need to be upregulated in an attempt to activate FA and direct them for oxidation however their dual function in transporting LCFA would further exacerbate lipid loading and cellular damage. Increased expression in disease may be due to presence of ligands such as FAs, which can activate nuclear receptors PPAR, which control expression of these genes (Madrazo and Kelly, 2008).

Interestingly PBC livers demonstrated a distinct pattern of transporter expression with FABP6 highly upregulated. This may be explained by the fact that bile acids can regulate FABP6 expression (Liu et al., 2008). FABP expression in cell lines was more similar to primary hepatocytes than the GLUTs and this may be due to preference of cell lines for glucose as fuel rather than lipid. Furthermore as previously discussed activated VAP-1 can modulate glucose uptake via insulin sensitive GLUT4, other GLUTs have also been reported to be insulin sensitive such as GLUT8, GLUT10, GLUT12 and also FATP1 and LRP1, which may also translocate in response to activated VAP-1 hence take up lipids and add further damage to the cell. Elevated expression patterns for many of the transporters in this study may be related to the chronically diseased liver environment, which consists of ROS, hypoxia, cytokines, and elevated VAP-1 activity, which may lead to induction of these mediators leading to, altered expression patterns.

3.4.4 Future work

In all, we have described for the first time the specific hepatocellular expression of key receptors involved in glucose and lipid homeostasis, and have shown that key transporters are up regulated in diseased liver. The upregulation patterns of multiple specific GLUTS and fatty acid trafficking transporters, confirms that the processes regulating carbohydrate and lipid homeostasis are not simple ones, but rather involve many different receptors which are deregulated in disease. Whist we have made significant progress documenting patterns of expression, the functional significance of these needs further investigation.

We were able to support our microarray findings, with confirmatory qPCR findings, which were supported by protein expression where possible. Matching patient tissue was used for both immunohistochemical studies and qPCR analysis and additional samples were used for the microarray analysis. Thus our use of multiple patient samples for each condition strengthens our confidence in the altered expression patterns we report in disease. However using a larger sample number for protein expression and staining (eg for those already tested such as GLUT 9 and 10) would support and validate our findings further. Furthermore the limited availability of a number of antibodies for GLUTS and some fatty acid trafficking proteins such as the FATP has meant that we have not been able to identify all of our transporters at the protein level. Thus protein expression for many transporters remains to be confirmed, and it would be prudent to consider additional techniques such as immunoprecipitation, western blotting and dual staining with phenotypic markers to validate the expression patterns. We also observed key differences between primary hepatocytes and cell lines in transporter expression. Whilst this may reflect malignancy-induced changes it would be important to study greater numbers of primary hepatocytes isolated from different patients, and to consider the impact of disease on hepatocyte phenotype. It is also important to note that our 'simple steatosis' samples were obtained from fatty donor livers, which were rejected for transplant, and much of our 'normal' tissue was collected as uninvolved, non-diseased margins from tumor resection surgery.

Our qPCR analyses were based around the use of Taqman probes, which have been reported to have 100% efficiency in amplification (http://rtsf.msu.edu/Efficiency-AN.pdf) and the use of multiple house keeping genes allowed for accurate

quantification and normalization. All probes and samples were spotted twice on plates and run in triplicate generating at least 18 technical replicates. A human universal standard containing RNA from all organs in the body was also run in parallel with our samples to ensure our probes were working as expected. Thus we are confident that the data generated from this analysis is genuine. However of note, we restricted our cell type analysis to key cell populations but did not consider KC, HSCs, or tissue-derived immune cell populations which contribute to the disease-specific changes observed. For example we did not find expression of FATP6 on any of the cells we studied, however expression was observed in diseased liver. An explanation for this may be that this gene is only switched on in disease, and our cultured cells may not recreate the diseased phenotype *in vitro*, or the expression is restricted to a cell type we did not study. This is exemplified by the experiments where we used PBMCs isolated from peripheral blood for expression analysis. Whilst this data is novel and has implications for immune modulation and leukocyte metabolism, the expression patterns we report may not accurately reflect that of infiltrating cells in the diseased liver as monocytes and lymphocytes differentiate into tissue specific resident cells within the local environment.

Of particular importance is the question of whether increases in mRNA and protein expression leads to an increase in glucose/fructose or indeed lipid uptake in the liver? Therefore functional studies are needed to quantify the functional impact of our reported expression patterns. KO mouse models for selected GLUT and FA trafficking proteins are available and would allow us to assess their importance in disease and energy balance. Cultured cells from diseased livers could also be used in functional assays to assess whether metabolic responses change in disease. In order to

do this however it would be necessary to check whether primary cells *in vitro* such as hepatocytes and fibroblasts from NASH livers for example, reflect the pattern of expression seen in diseased tissue. Polymorphisms for some fatty acid transporters exist such as FABP1 and have been associated with increased disease risk (Charlton et al., 2009b) and thus it would be interesting to see whether patients have polymorphisms in specific isoforms for example such as FABP1, FABP2 and FABP5. Similarly it would be interesting to investigate possible changes in transporter expression at the different stages of NASH progression from mild, moderate to severe to determine whether any key biomarkers or pathogenic signals emerge. This would be particularly important since some of these proteins are found in the serum and have been shown to be elevated in NAFLD for example FABP4 (Koh et al., 2009), thus representing potential diagnostic markers. Availability of liver tissue and difficulties in isolating and culturing primary hepatocytes has made cell lines attractive and are routinely used in laboratories for research. However there are differences between cell lines and primary hepatocytes as shown by our data and thus the use of primary cells and even whole tissue slices representing a mini organ system encompassing a multicellular environment are attractive models for future functional studies in liver research.

CHAPTER 4

4 IS THERE A ROLE FOR VAP-1 IN GLUCOSE HOMEOSTASIS IN THE LIVER?

4.1 Introduction

A contribution of VAP-1 and its substrates to regulation of glucose uptake has been widely documented in the context of adipocytes and smooth muscle cells. For example in isolated rat adipocytes, the SSAO substrates benzylamine and tyramine have been shown to stimulate glucose transport in the presence of vanadate (Enrique-Tarancon et al., 1998). In contrast, in isolated human adipocytes the response to methylamine and benzylamine can occur in the absence of vanadate (Morin et al., 2001). SSAO activity can also enhance glucose uptake in VSMCs (El Hadri et al., 2002) and F422A cells (Fontana et al., 2001). In many cases the mechanism underlying enhanced glucose uptake has been linked to hydrogen peroxide as a metabolite produced during the deamination of amines (Enrique-Tarancon et al., 1998), (Marti et al., 1998), (El Hadri et al., 2002), and is based on tyrosine phosphorylation of IRS-1 and IRS-3 and activation of PI3-K, (Enrique-Tarancon et al., 2000). Furthermore the SSAO stimulated glucose uptake is dependent on translocation of GLUT4 to the cell membrane in rat adipocytes (Enrique-Tarancon et al., 1998) and in VSMCs an increase of GLUT1 at the cell membrane (El Hadri et al., 2002). Importantly this suggests that SSAO activity may regulate different GLUTS in different cells. Of note, SSAO colocalizes in intracellular vesicles with GLUT4 in rat adipocytes, rat skeletal muscle and 3T3-L1 adipocytes (Enrique-Tarancon et al., 1998) suggesting a specific role in glucose uptake. These pathways are summarized in Figure 4.1.

4.1.1 Could VAP-1 activity be of significance in hepatic glucose homeostasis?

Modulation of SSAO activity has proven impacts on systemic hyperglycaemia and glucose tolerance. Hence SSAO substrates, have anti-diabetic effects *in vivo* in streptozotocin-induced diabetic rats, where benzylamine reduces hyperglycemia and improves glucose tolerance (Marti et al., 2001). Overexpression of VAP-1 in mice also improved glucose uptake however this was associated with several diabetic complications (Stolen et al., 2004a).

Our group has published pilot data showing that levels of sVAP-1 and hepatic VAP-1 increase in NASH (Claridge L C, 2009) and also that elevated sVAP-1 is found in many chronic inflammatory liver diseases (Kurkijarvi et al., 1998). Thus it is prudent to investigate whether a similar SSAO-dependent regulation of glucose homeostasis operates in the liver, and to measure whether hepatic cells respond to SSAO activity in the manner reported for other cell types. VAP-1 has potential to contribute to the development of NAFLD and exacerbate disease pathogenesis as observed in NASH both through modulation of glucose function and via effects upon leukocyte recruitment and fibrogenesis (Weston and Adams, 2011).

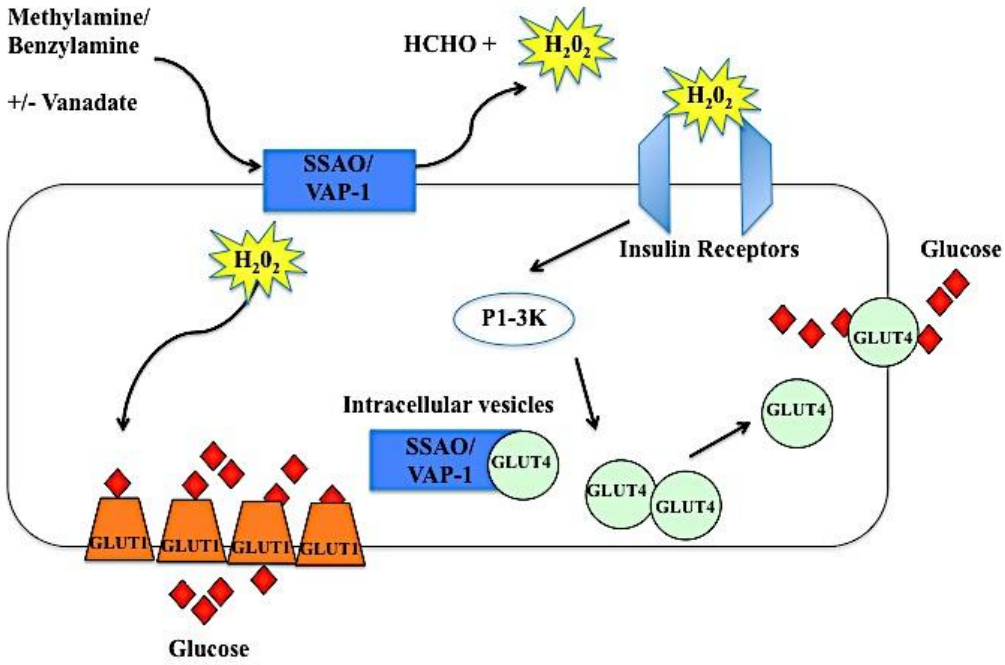

Figure 4.1: Schematic showing VAP-1/SSAO related glucose uptake
Deamination of primary amines by VAP-1/SSAO leads to the production of hydrogen peroxide, which causes tyrosine phosphorylation of insulin substrates and activation of PI3-K leading to GLUT4 mobilization to the cell surface and uptake of glucose in rat adipocytes (Enrique-Tarancon et al., 1998). There is also presence of both SSAO/VAP-1 and GLUT4 in intracellular vesicles. Furthermore SSAO/VAP-1 derived hydrogen peroxide also leads to an accumulation of GLUT1 at the cell membrane in VSMCs (El Hadri et al., 2002).

Thus we hypothesis VAP-1 and its substrates may regulate glucose uptake in the liver by regulating specific GLUTS. Therefore the major aims of this chapter were:

(I) To develop methodology/an *ex vivo* based model to investigate the role of VAP-1 in regulation of glucose uptake in whole liver and cultured hepatic cells.

(II) To investigate the mechanisms underlying SSAO-dependent hepatic responses.

(III) To investigate whether SSAO activity modulates GLUT transporter expression or cellular localization.

4.2 Methods

For methods pertinent to this chapter please refer to the general methods p49-50, p54-59.

4.3 Results

4.3.1 VAP-1 expression and functional activity is increased in diseased liver

Since this thesis sets out to examine the potential role of VAP-1 in glucose and lipid homeostasis in the human liver we began by identifying the expression pattern of this protein, and that of related oxidase enzymes in normal and diseased liver. At the mRNA level we found increased expression in NASH, ALD and PBC livers and a decrease in expression in the steatotic livers compared to normal (Figure 4.2). On a cellular level, primary hepatocytes and BEC did not express VAP-1 mRNA whilst cell lines HepG2 and Huh7.5, HSEC, fibroblasts and PBMCs did (Figure 4.3 and 4.4). We also examined the mRNA expression pattern of other oxidases such as MAOA, MAOB and LOX in the same samples. We generally found an increase in expression of MAOA, MAOB and LOX in NASH and ALD and a decrease in expression in steatotic and PBC livers except for LOX in PBC, which was also, upregulated compared to normal (Figure 4.2). Primary hepatocytes, BEC, HSEC, fibroblasts and PBMCs expressed all three enzymes with hepatocytes most abundantly expressing MAOA; BEC LOX, and HSEC and fibroblasts MAOA and LOX, (Figure 4.3 and Figure 4.4).

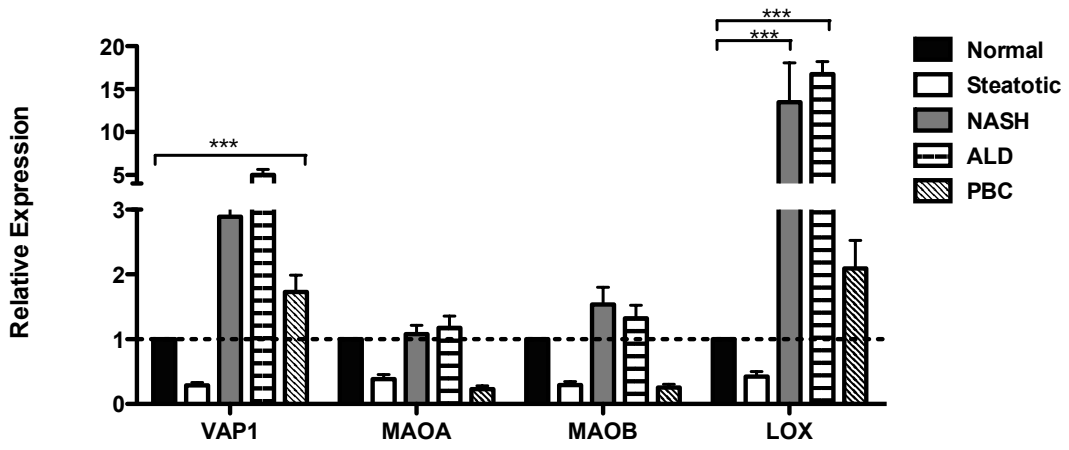

Figure 4.2: Analysis of SSAO and MAO by quantitative qPCR analysis
mRNA expression of MAO and SSAO in normal, steatotic, NASH, ALD and PBC livers using a fluidigm qPCR array®, run on triplicate arrays. Results are expressed as the mean fold change in gene expression normalized to pooled endogenous controls β-actin and GAPDH relative to normal livers defined as 1 +/- SEM with means from five normal livers, four steatotic, three NASH, four ALD and four PBC. Dotted line represents normal expression set at 1. Significance expressed as ***$p<0.001$ using a one way ANOVA with Bonferroni correction.

A

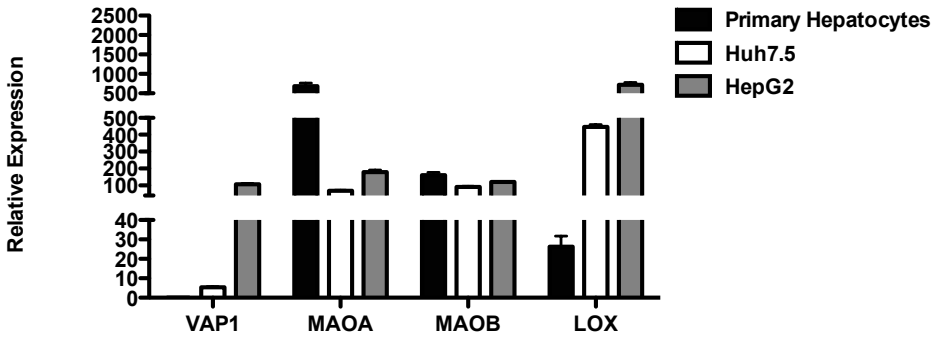

B

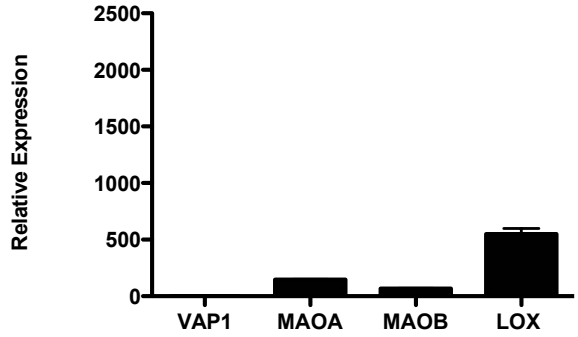

Figure 4.3: Analysis of SSAO and MAO in human liver epithelial cells by quantitative qPCR analysis

(A) mRNA expression of SSAO and MAO in primary hepatocytes, Huh7.5, HepG2 and (B) BEC determined using a fluidigm qPCR array®. Results are expressed as means of three primary hepatocytes, three Huh7.5, three HepG2 and three BEC +/- SEM, run on triplicate arrays and normalized to pooled endogenous controls (β-actin and GAPDH) log transformed using 2-ΔCt.

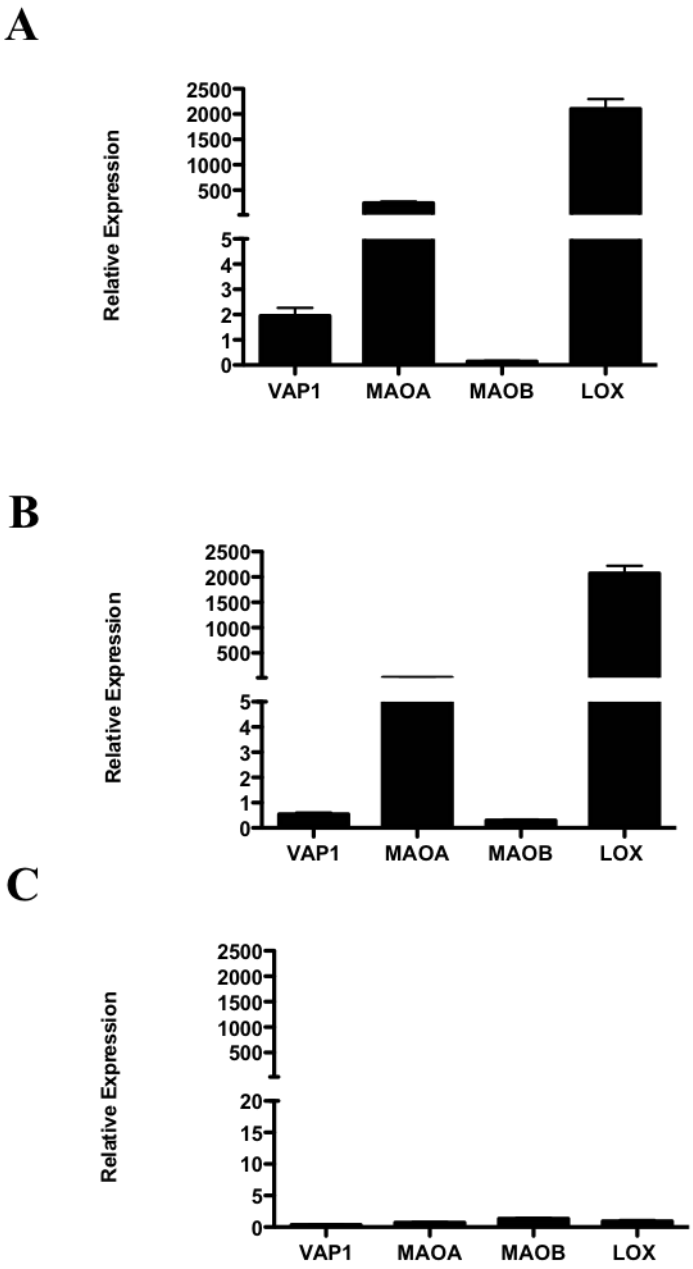

Figure 4.4: Analysis of SSAO and MAO in human liver non-epithelial cells and PBMCs by quantitative qPCR analysis

(A) mRNA expression of SSAO and MAO in HSEC (B) fibroblasts (C) PBMCs using a fluidigm qPCR array®. Results are expressed as means of four HSEC, four fibroblasts and two PBMCs +/- SEM, run on triplicate arrays and normalized to pooled endogenous controls (β-actin and GAPDH) log transformed using 2-ΔCt.

Immunohistochemical detection of VAP-1 localization revealed sinusoidal staining in all livers (shown by arrow in normal liver, Figure 4.5A) and perivascular staining in portal areas. Expression increased in the NASH, ALD and PBC livers in the fibrotic regions (shown by arrows in, Figure 4.5C and E) as well as in the sinusoidal areas, particularly in ALD livers (shown by arrow, Figure 4.5D). We wanted to assess whether the increase in VAP-1 protein in diseased liver paralleled an increase in activity, thus we assessed VAP-1 activity in standardized protein tissue lysates (8mg/ml) from normal and diseased livers using the Amplex red assay and the specificity of our assay was confirmed by addition of BEA see Figure 4.6A. We found an increase in activity in NASH, ALD and PBC livers compared to normal and steatotic livers (Figure 4.6B).

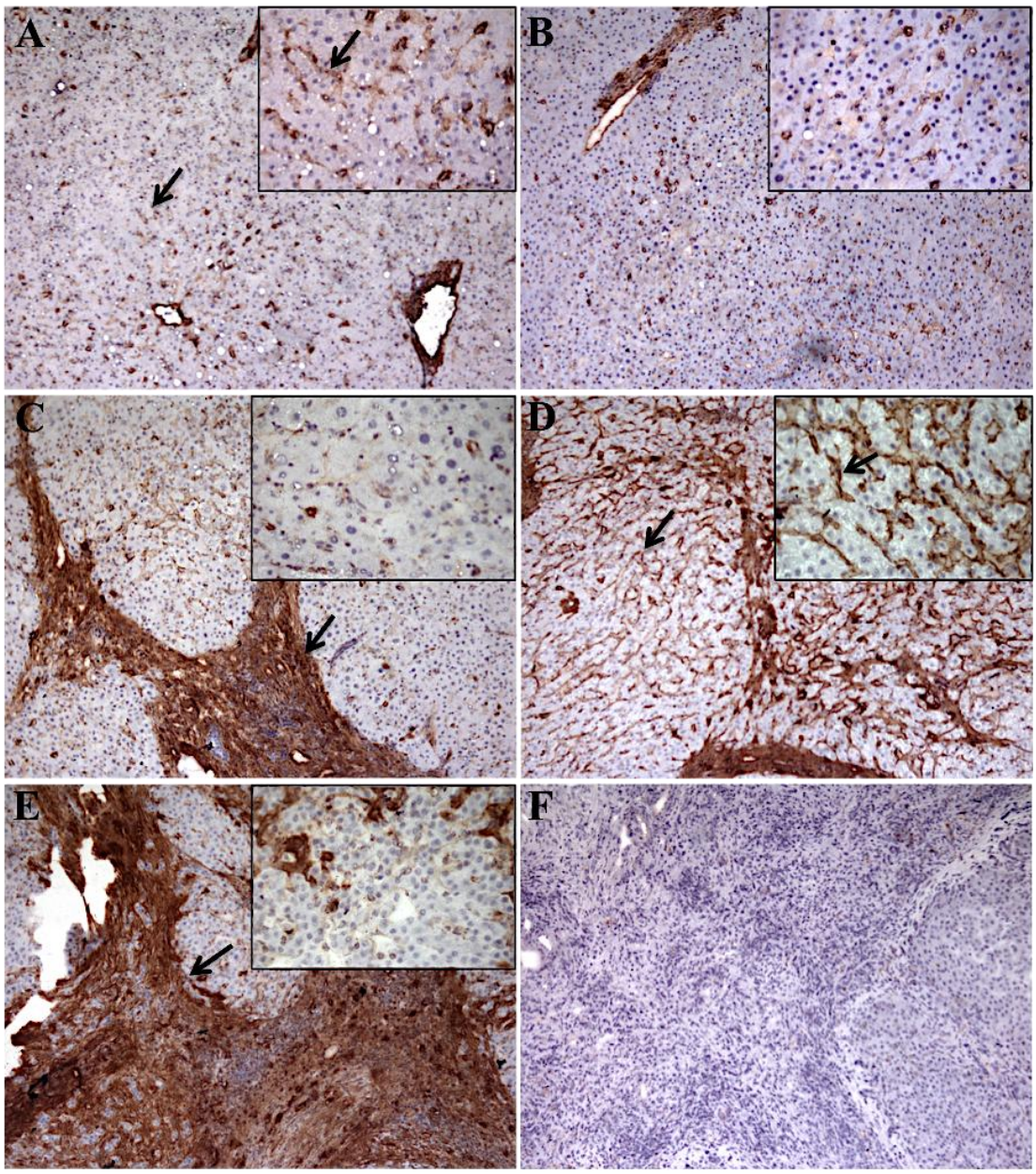

Figure 4.5: Immunohistochemical analysis of VAP-1 protein expression in normal and diseased livers

Immunohistochemical staining of VAP-1 in acetone fixed frozen sections from (A) normal, (B) steatotic, (C) NASH, (D) ALD, and (E) PBC livers and (F) is representative staining with isotype matched control antibody in PBC liver. Fields were captured at 10X original magnification with inset pictures captured at 40X original magnification. Images shown are representative from N=3 for each disease and arrows in (A) indicate sinusoidal staining, arrows in (C) and (E) indicate staining in fibrotic regions and arrows in (D) indicate strong sinusoidal endothelial staining.

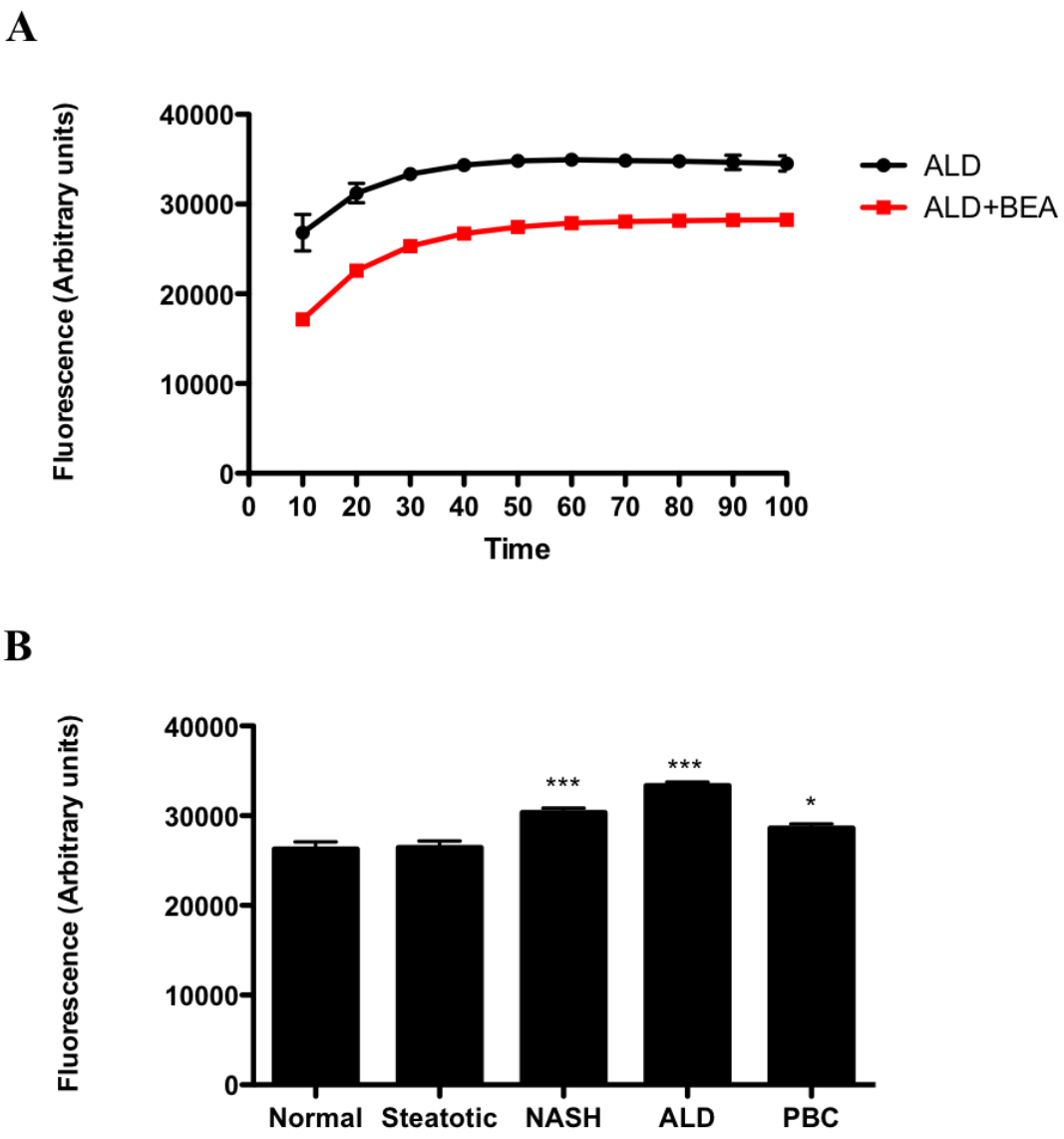

Figure 4.6: Analysis of SSAO activity in normal and diseased human liver lysates (A) Detection of SSAO activity in lysates from normal and diseased tissue. 8mg/ml of equilibrated protein lysates prepared from indicated liver types were added to a 96 well flat bottom plate. Benzylamine (2mM) was added in the presence or absence of the specific VAP-1 inhibitor BEA (400µM). The fluorometric reaction was initiated by the addition of the Amplex red reagent consisting of 1/100 Amplex ultra red and 1/100 HRP. The reaction was measured continuously in a fluorescence microplate reader for approximately 3 hours using excitation of 530nm and emission detection at 590nm. Data is represented as the mean fluorescence reading up to a time point of 100 minutes in ALD with specific inhibition of VAP-1 with BEA shown in red and (B) the mean fluorescence reading at 30 minutes, N=3 for each disease +/- SEM. Significant elevation of SSAO activity in diseased livers expressed as * $p<0.05$, ***$p<0.001$.

4.3.2 VAP-1 and its substrate methylamine regulate glucose uptake in Hepatic cells

The activity of VAP-1 has been shown to regulate glucose uptake in adipose and smooth muscle cells thus, next we went on to assess whether the activity of VAP-1 was able to modulate glucose hemostasis in isolated hepatic cells. Insulin was used as a positive control and Figure 4.7A shows a significant uptake of glucose following insulin treatment of HSEC. Furthermore, pretreatment of HSEC with MA, MA+VAP-1 and hydrogen peroxide all enhanced glucose uptake compared to control in HSEC. Importantly, glucose uptake in response to MA+VAP-1 was significantly reduced in the presence of the specific SSAO inhibitor BEA (Figure 4.7A).

We noted that the glucose responses in HSEC from different donors and at different passages were very variable, which we considered likely to reflect variable amounts of VAP-1 in these cells. Therefore we over expressed VAP-1 in HSEC and repeated the glucose uptake experiments. We transfected HSEC with viral constructs overexpressing enzymatically active or inactive VAP-1 and used empty vector containing LACZ alone as an additional control. The enzyme activity of these vectors has previously been confirmed (Liaskou et al., 2011). The expression of VAP-1 after transfection was confirmed by flow cytometric analysis (Figure 4.7B). We only observed an increase in glucose uptake following methylamine treatment, in HSEC transfected with the active VAP-1 (Figure 4.7C).

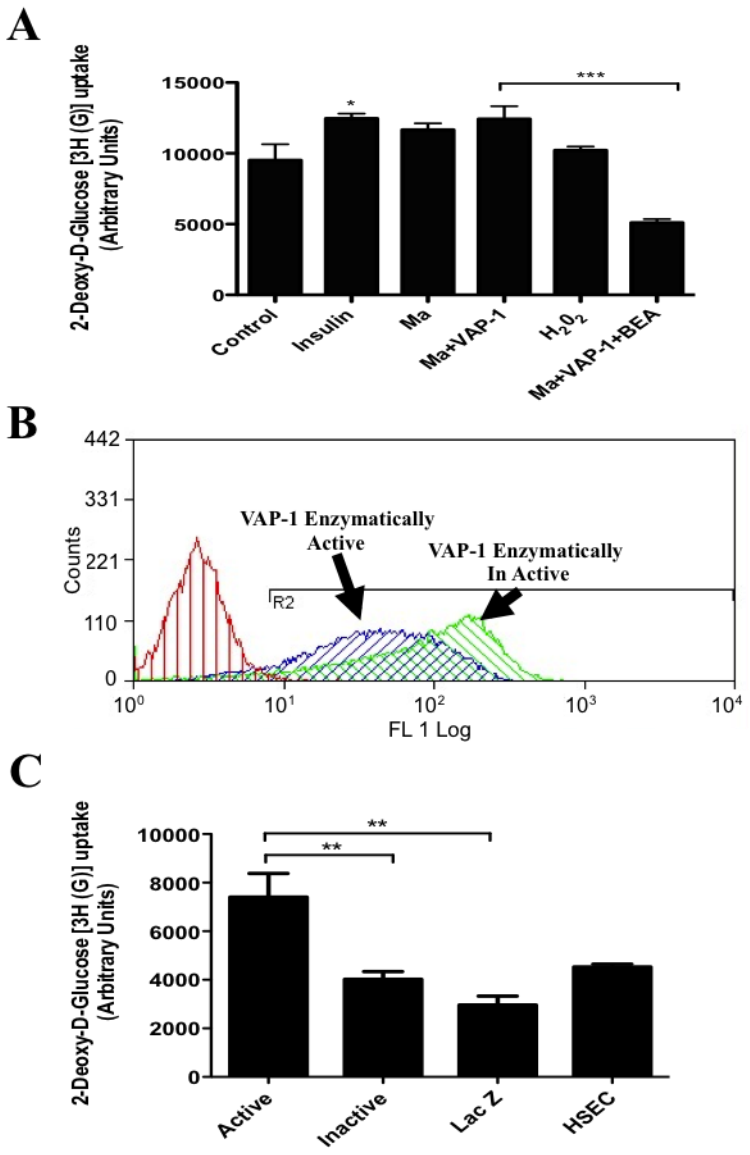

Figure 4.7: Assessment of glucose uptake after VAP-1 stimulation in HSEC
(A) Uptake of radiolabelled glucose after stimulation of HSEC with either insulin 0.10 IU, MA 200µm, VAP-1 500ng, H_2O_2 10µM, or in combination with MA+VAP-1, MA+VAP-1+BEA, for approximately 2 hours and 30 minutes and then 30 minutes with radiolabelled glucose. Cells were lysed and radioactivity measured. N=7 +/- SEM, significance expressed as * $p<0.05$, ***$p<0.001$ (B) FACS plot demonstrating surface expression of VAP-1 on transduced cells, representative image from N=3 cell isolates. HSEC were transfected with either an enzymatically active construct for VAP-1 (blue line), inactive construct (green line), or an empty vector containing LACZ (red line). (C) Uptake of radiolabelled glucose in transduced HSEC after stimulation. Cells transduced as described above and non-transfected HSEC were pre treated with MA 200µm for 2 hours and 30 minutes and then 30 minutes with radiolabelled glucose. Cells were lysed and radioactivity measured. N=3 +/- SEM, significance expressed as **$p<0.01$.

We conducted similar glucose uptake experiments using Huh7.5 and HepG2 cells. In Huh7.5 cells we found when cells were pre treated with MA, MA+VAP-1 there was a significant increase in glucose uptake compared to control. Furthermore the addition of MA+VAP-1+BEA significantly reduced glucose uptake compared to MA+VAP-1 treated cells (Figure 4.8A). Hydrogen peroxide also enhanced glucose uptake but this effect was not significant.

Interestingly when we compared the responses of the two cell lines we found that HepG2 cells had higher basal glucose uptake. Pretreatment of HepG2 with MA resulted in increased glucose uptake compared to control and MA+VAP-1/ hydrogen peroxide alone significantly increased glucose uptake whilst addition of MA+VAP-1+BEA significantly reduced glucose uptake compared to MA+VAP-1 treated cells (Figure 4.8B).

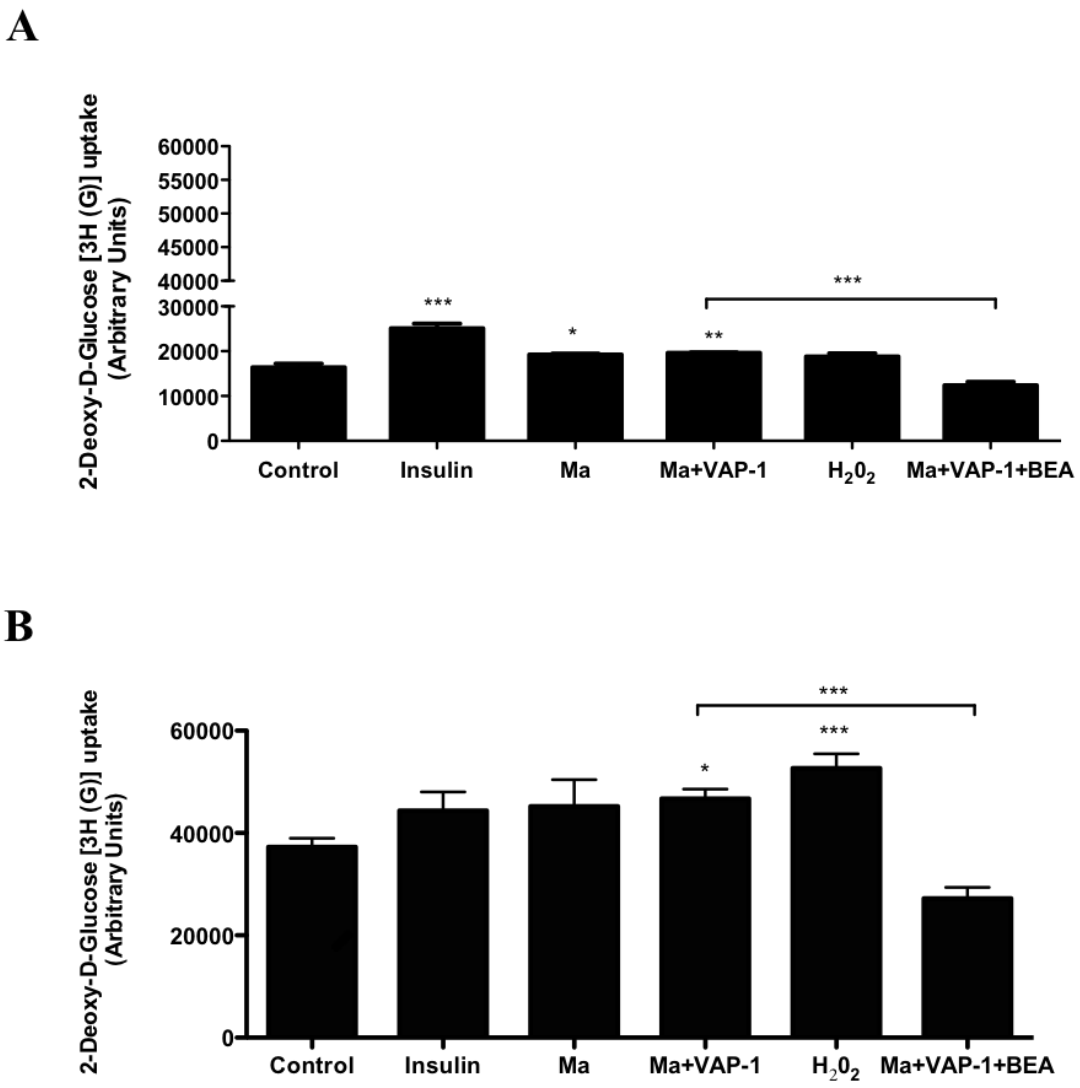

Figure 4.8: Assessment of glucose uptake after VAP-1 stimulation in Huh7.5 and HepG2 cells

(A) Uptake of radiolabelled glucose after stimulation of Huh7.5 or (B) HepG2. Cells were pretreated with either insulin 0.10 IU, MA 200µm, VAP-1 500ng, H_2O_2 10µM, or in combination with MA+VAP-1, MA+VAP-1+BEA, for approximately 2 hours and 30 minutes and then 30 minutes with radiolabelled glucose. Cells were lysed and radioactivity measured. For Huh7.5 N=3 +/- SEM, significance expressed * $p<0.05$, ** $p<0.01$, *** $p<0.001$ and for HepG2 N=4 +/- SEM, significance expressed * $p<0.05$, *** $p<0.001$.

4.3.3 Use of PCLS to model glucose and lipid homeostasis in human liver

Rather than limit our analyses to cultured cell lines, which may not accurately reflect the *in vitro* situation, we sought to investigate whether SSAO activity might modulate glucose uptake in a more physiological, multicellular context. Thus we developed a model based upon organ culture of human liver specimens. Normal resected tissue and on occasion cirrhotic tissue was used to generate 8mm tissue cores (Figure 4.9C), which were aseptically cut to generate 240μm thick PCLS (Figure 4.9D) using a Krumdieck tissue slicer (Figure 4.9A). We began by optimizing our culture methods and testing performance of the system.

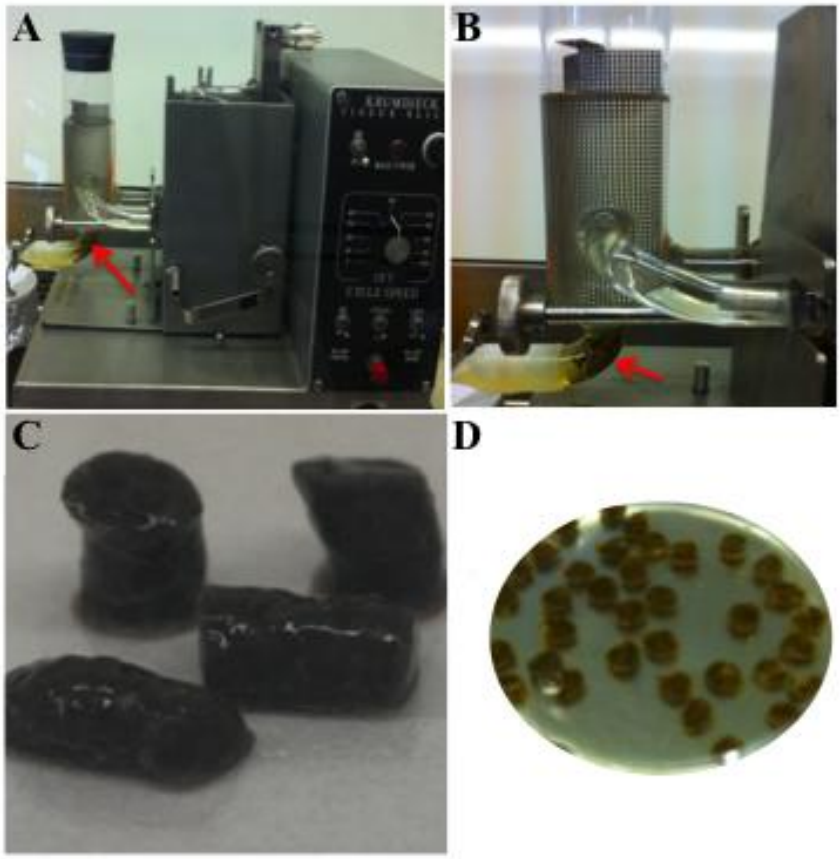

Figure 4.9: Generation of PCLS using a Krumdieck tissue slicer
(A) Image of a functional Krumdieck tissue slicer, (arrow indicates collection of PCLS in the collecting tube), (B) Magnified image of Krumdieck tissue slicer collecting tube (arrow indicates collection of PCLS in the collecting tube), (C) Tissue cores obtained from explanted liver (D) Representative images of PCLS in a petri dish.

PCLS weights were generally consistent between different experiments (Figure 4.10A), and use of MTT confirmed that slices retained viability in culture for up to 48 hours. However there was a significant reduction in viability between 24 and 48 hours (Figure 4.10B). Morphological assessment of cryosections cut from PCLS after H&E staining (Figure 4.11) suggested maintenance of intact tissue morphology in culture. Functional activity of tissue was demonstrated by albumin production (Figure 4.12A), although we noted a decrease at 24 hours. Similarly Hoechst staining (Figure 4.12C) was suggestive of maintenance of nuclear integrity at 24 hours in static culture, with a decline thereafter. This was confirmed by quantification using Image J (Figure 4.12B), which also showed that a loss of nuclear integrity was noted in central areas after prolonged culture (Figure 4.12B and image in Figure 4.12C). Importantly PCLS retained the ability to respond to insulin (Figure 4.12D) after 24 hours in culture and maintained the presence of glycogen granules. However these too decreased with increasing culture time (Figure 4.12E) (Karim et al., 2013).

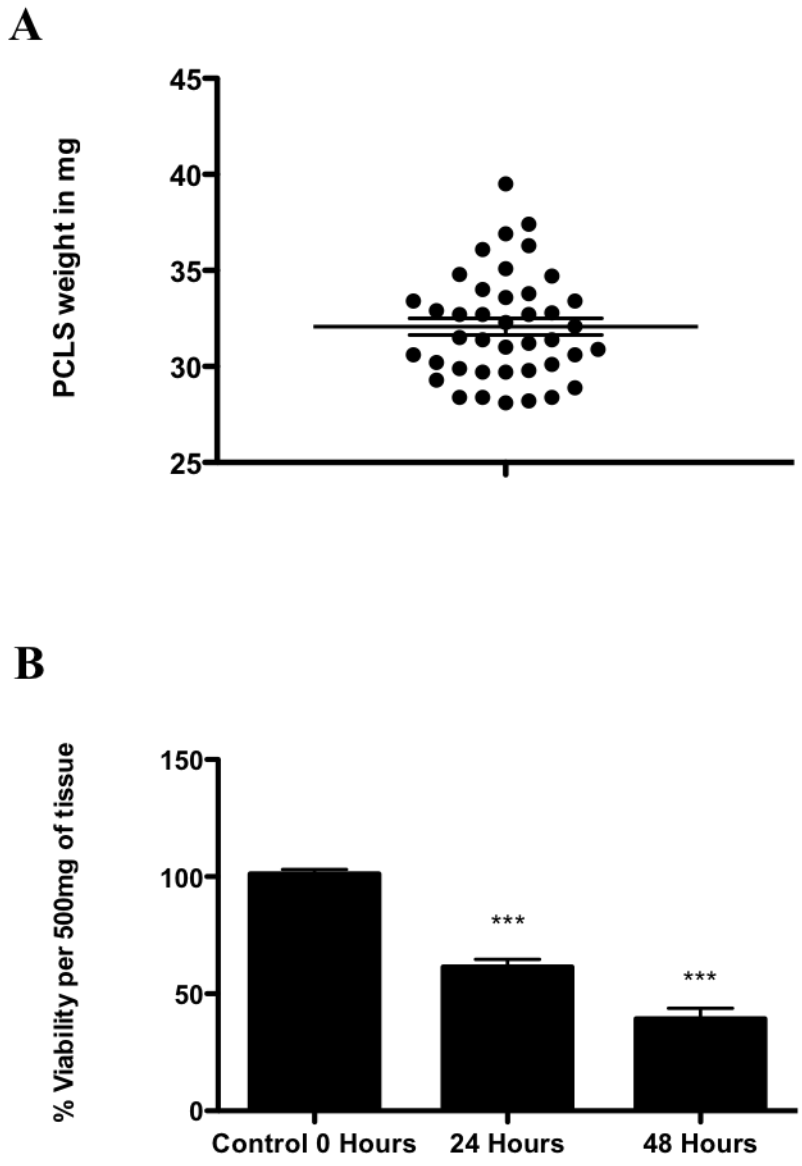

Figure 4.10: Assessment of PCLS reproducibility and viability
(A) XY scatter plot of mean PCLS weights, bold line represents the mean and thinner lines represent the mean +/- SEM, typical slice weights from N=6 41 slices, +/- SEM. (B) Viability of PCLS in culture using the MTT assay. MTT signal was normalized per 500mg of tissue and data is represented as % viability compared to control at 0 hours. Data generated from N=4 from resected normal livers with 27 replicate slices in total +/- SEM. Significance represented as *** $p<0.001$.

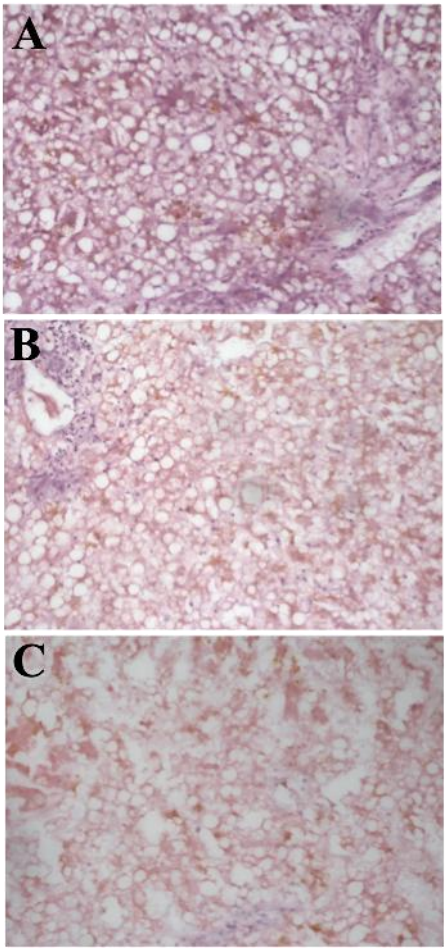

Figure 4.11: H&E staining of Cultured PCLS confirms loss of morphology over time

(A) H&E stained image of PCLS at 0 hours, (B) 24 hours and (C) 48 hours. Fresh PCLS or PCLS cultured in media for 24 or 48 hours were fixed and cryosectioned for H&E staining. Representative images are shown from N=3 resected/donor livers, 10X original magnification.

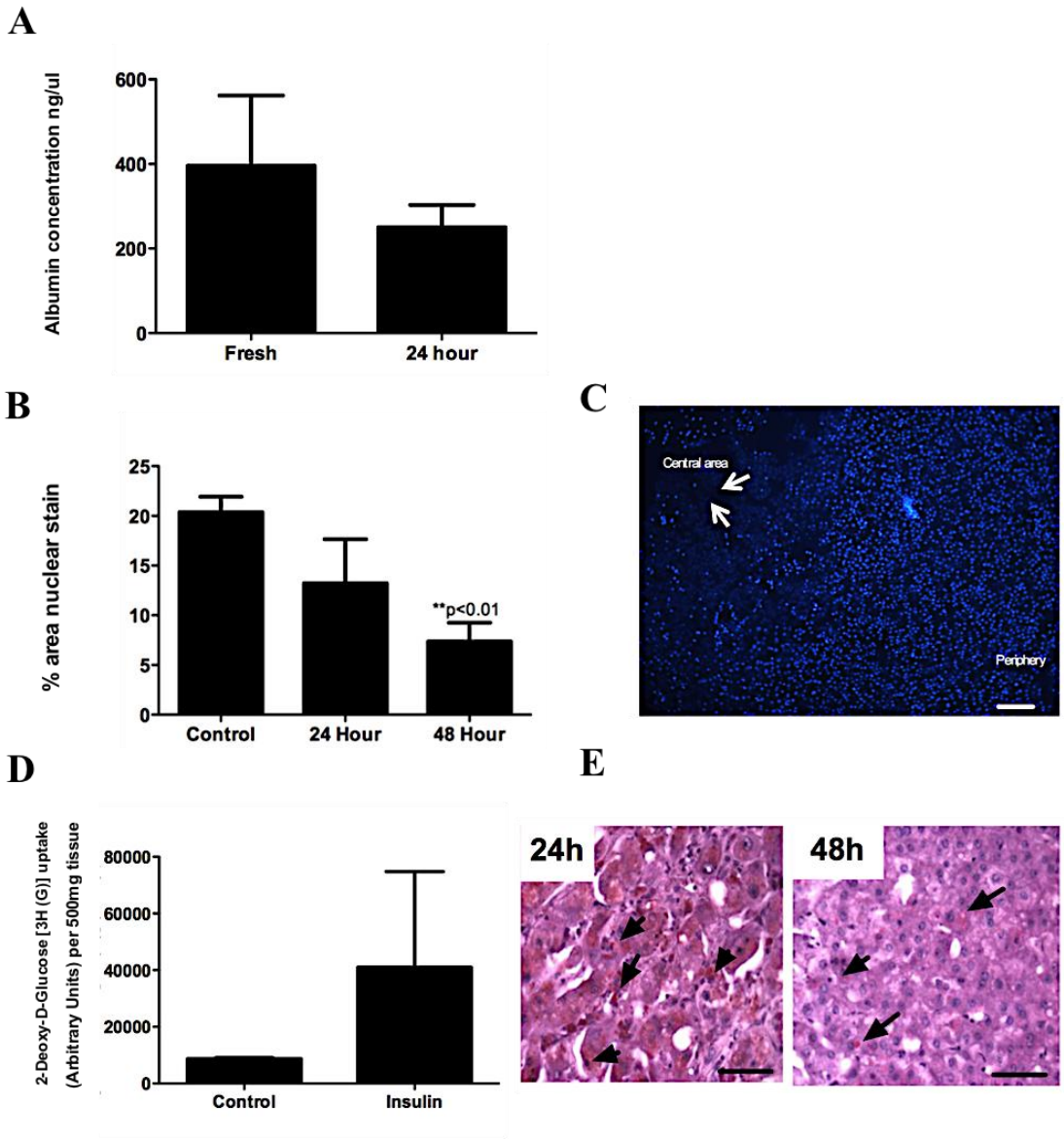

Figure 4.12: Functional assessment of cultured PCLS

(A) Production of albumin by PCLS, measured by captured ELISA, N=3 with 6 replicate slices, (B) Image J quantification of nuclear integrity of PCLS cultured for up to 48 hours, sections were stained with Bisbenzimide to visualize nuclear integrity, and images were taken of representative fields of view, data represented as the % area stained positive in five high power fields +/- SEM and N=4 with 2 replicate slices. Statistical analysis revealed a significant reduction in nuclear number at 48 hours $p<0.01$, (C) Representative image of PCLS cultured for 48 hours and stained with Bisbenzimide and arrows indicate loss in nuclear integrity in the central area compared to periphery, bar represents 100µm. (D) Uptake of radiolabelled glucose after insulin treatment of PCLS, data represents +/- SEM from 6 replicate slices and (E) Representative Images of PCLS cultured for 24 and 48 hours and stained with Periodic Acid Schiff stain, arrows indicate presence of glycogen which stains reddish purple and bar represents 50µm.

Next we wanted to ensure our *ex vivo* system was specifically optimised for our glucose uptake assays which require use of low glucose DMEM instead of Williams E Media. Thus we performed viability assays to ensure our PCLSs would be viable in this media. Our MTT assays confirmed a similar level of viability for both medias at all time points with a general decrease in viability over time as before (Figure 4.13).

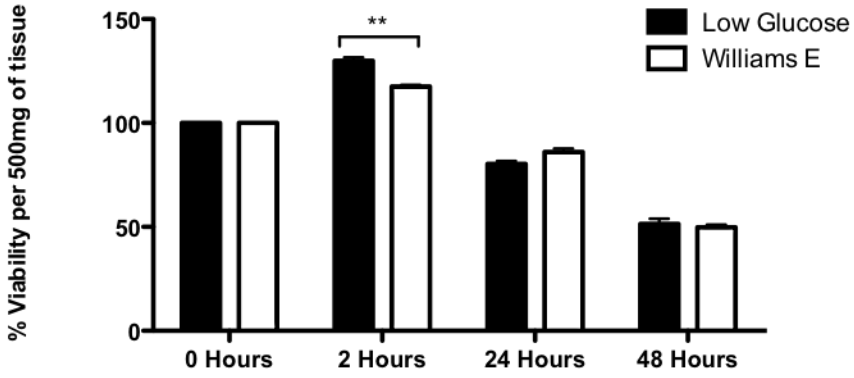

Figure 4.13: Assessment of PCLS viability in different media
Viability of PCLS after culture in low glucose DMEM or Williams E media using the MTT assay. The MTT signal was normalized per 500mg of tissue and data are represented as % viability compared to control at 0 hours. N=2 from resected normal livers 6 replicate slices in total. +/- SEM, significance represented as **$p<0.01$.

4.3.4 VAP-1 and its substrate methylamine regulate glucose uptake in liver tissue

Next we used our PCLS model, for glucose uptake experiments. We found that by supplying an exogenous substrate (methylamine, MA) to endogenous VAP-1 in the PCLS, or exogenous VAP-1 for possible endogenous substrates, we increased glucose uptake compared to control. Furthermore the combination of MA+VAP-1 significantly increased glucose uptake compared to control and more than when either were added in alone; this response was inhibited by BEA, an inhibitor of SSAO activity, which had a modest effect when used alone. Furthermore, addition of hydrogen peroxide one of the metabolites produced when VAP-1 interacts with its substrates also significantly enhanced glucose uptake compared to control (Figure 4.14A).

Since we observed a significant increase in glucose uptake in PCLS when pretreated with MA+VAP-1, we wanted to see whether the activity of SSAO had any effects on trafficking of GLUT4. Thus we stained for GLUT4 in our treated PCLS using immunofluorescent protocols. In the control slices we observed diffuse cytoplasmic staining for GLUT4 in hepatocytes, and following MA+VAP-1 treatment there appeared to be a relocalisation into cytoplasmic vesicles (shown by arrows, Figure 4.14B) with a tendency to appear more concentrated at the periphery of the cells. These droplets disappeared when the slices were treated with MA+VAP-1 in the presence of BEA (Figure 4.14B). We did note some background staining of cells within the sinusoids in all samples, but we did not see any change in this staining following treatment (Figure 4.14B).

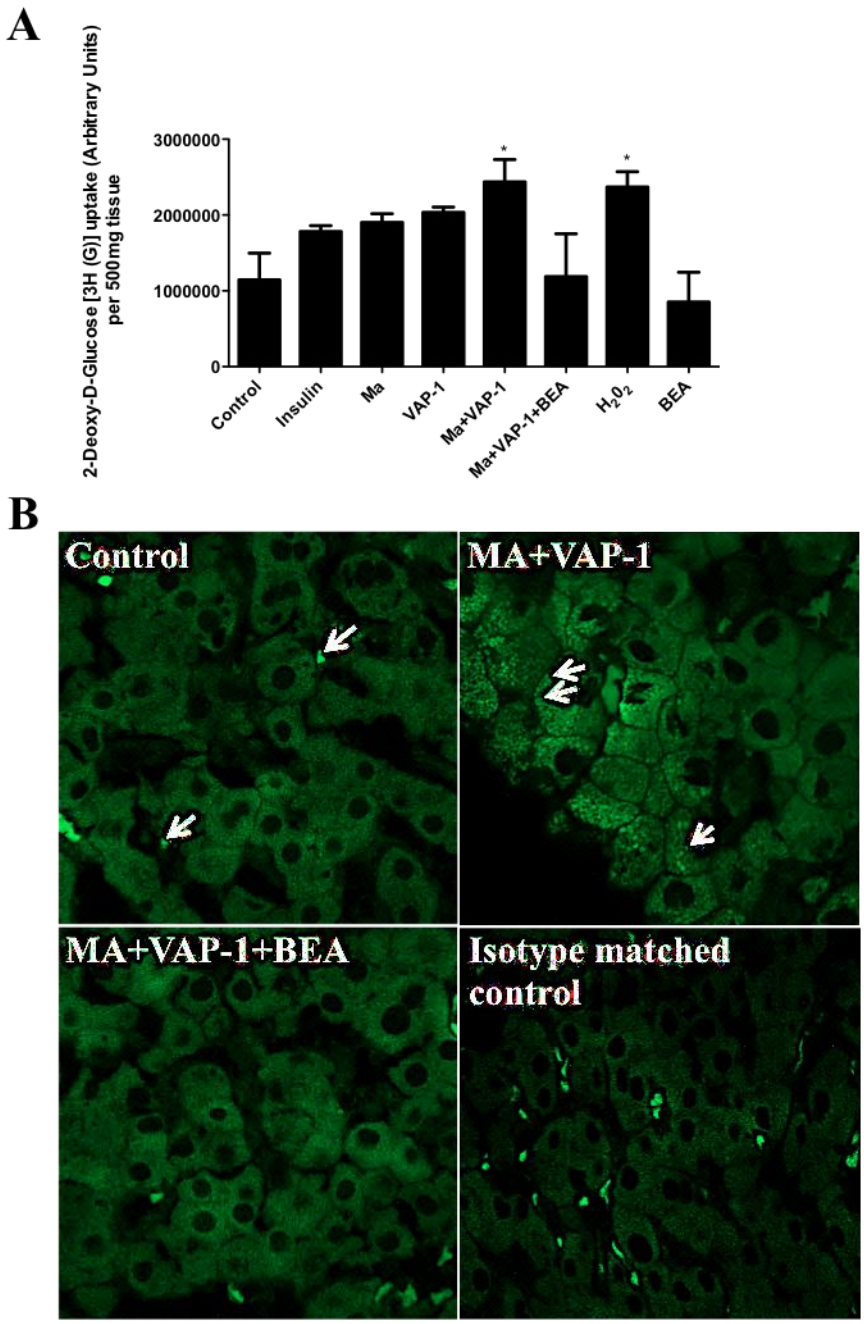

Figure 4.14: Assessment of glucose uptake after VAP-1 stimulation in PCLS
(A) Uptake of radiolabelled glucose after VAP-1 stimulation. PCLS were pretreated with either insulin 0.10 IU, methylamine 200µm, VAP-1 500ng, H_2O_2 10µM, BEA 400µm, or in combination with methylamine+VAP-1, methylamine+VAP-1+BEA, for approximately 2 hours and 30 minutes and then 30 minutes with radiolabelled glucose. PCLS were lysed, radioactivity was measured and signal normalized per 500mg of tissue. N=3 from resected normal livers +/- SEM. Significance expressed as * $p<0.05$ (B) Localization of GLUT4 in PCLS which were pretreated for 2 hours and 30 minutes with either methylamine+VAP-1 or methylamine+VAP-1+BEA, PCLSs were then fixed and cryosectioned and stained using GLUT4 antibody. Representative images from N=3 resected livers. Arrows in control indicate possible immune cell staining, and arrows in methylamine+VAP-1 PCLS sample indicate presence of large droplets at the periphery of the cell.

4.3.5 SSAO activity causes activation of NF-κB in PCLS

Our group has previously demonstrated that the SSAO activity of VAP1 leads to PI3-K dependent activation of NF-κB in cultured hepatic cells (Lalor et al., 2007). Thus we used a human NF-κB signaling pathway PCR array to determine whether we observed similar activation in PCLS following treatment. In PCLS treated with MA+VAP-1 compared to control we found many genes associated with the NF-κB signaling pathway altered. These included NF-κB1, IL6, IL8, IL10, ICAM-1 and TLR4 (Figures 4.15 and 4.16).

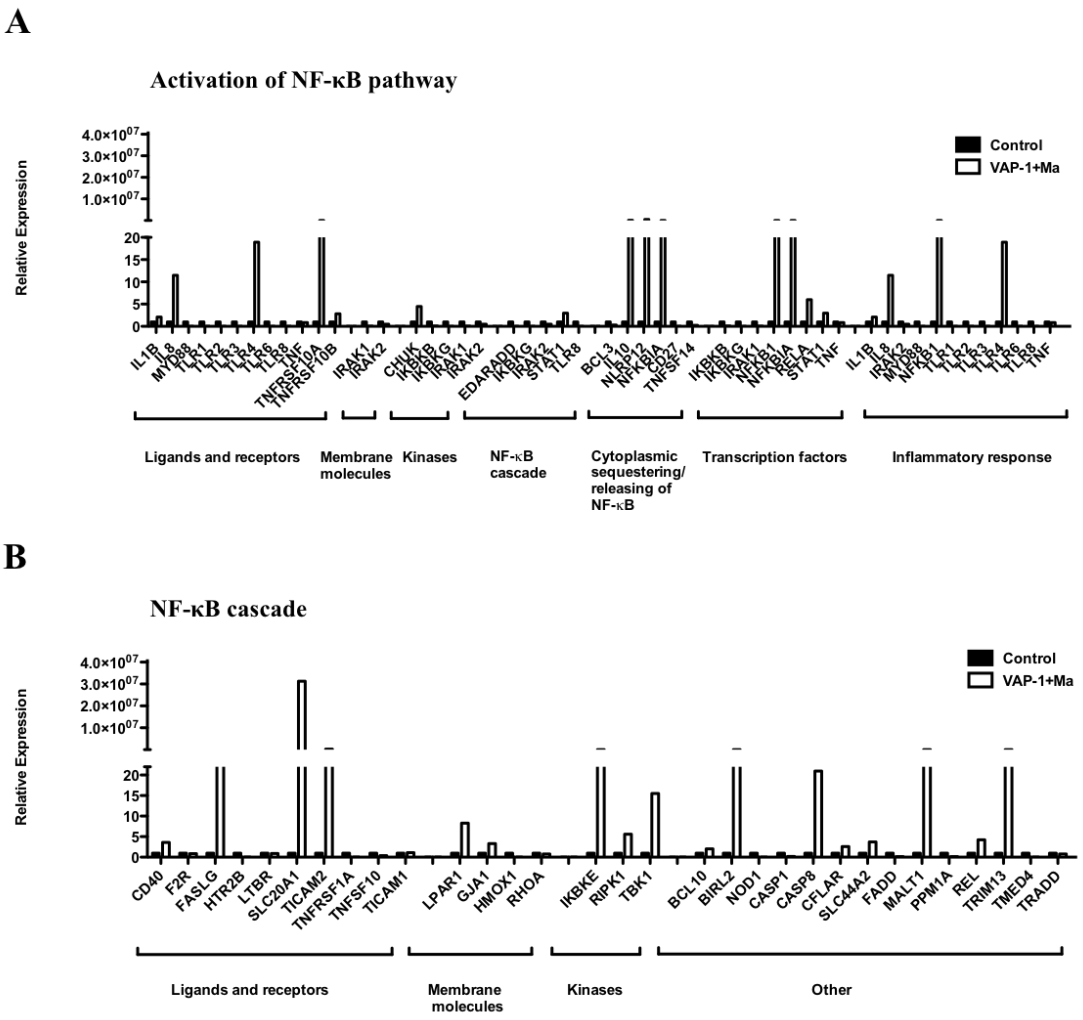

Figure 4.15: Analysis of NF-κB signaling pathway after VAP-1 treatment in PCLS

mRNA profiles of the expression of key genes related to NF-κB mediated signal transduction after VAP-1 stimuli treatment, involved in (A) Activation of NF-κB pathway and (B) NF-κB cascade. PCLS were treated with methylamine 200μm+VAP-1 500ng for approximately 2.5 hours. RNA was extracted and mRNA expression was carried out using a Human NF-κB Signaling Pathway RT²*Profiler*™ PCR Array. Results are expressed as the mean fold change in gene expression normalized to endogenous control GAPDH relative to control livers defined as 1. N=1

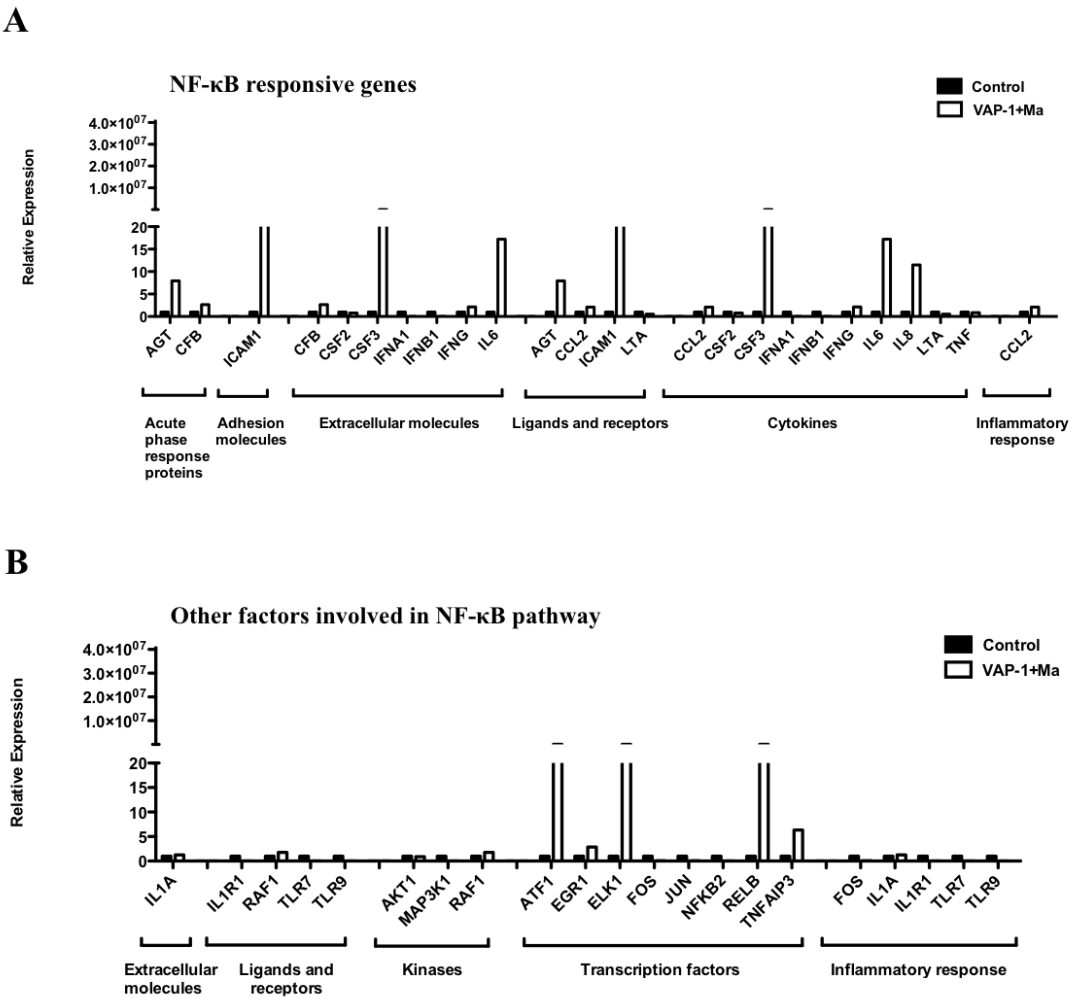

Figure 4.16: Analysis of NF-κB signaling pathway after VAP-1 treatment in PCLS

mRNA profiles of the expression of key genes related to NF-κB mediated signal transduction after VAP-1 stimuli treatment, involved in (A) NF-κB responsive genes and (B) other factors involved in NF-κB pathway. PCLS were treated with methylamine 200μm+VAP-1 500ng for approximately 2.5 hours. RNA was extracted and mRNA expression was carried out using a Human NF-κB Signaling Pathway RT²*Profiler*™ PCR Array. Results are expressed as the mean fold change in gene expression normalized to endogenous control GAPDH relative to control livers defined as 1. N=1

4.3.6 VAP1 and its substrate methylamine may alter the expression of GLUT proteins in PCLS

Next we used qPCR to investigate whether mRNA transcript levels for the GLUT transporters 1-13 were altered by MA pretreatment of PCLS. Results were normalized to the house keeping genes β-actin and GAPDH and expressed relative to control PCLS, which were set as 1. Pretreatment of PCLS with methylamine alone resulted in an increase in mRNA expression of GLUT4, GLUT10 and GLUT13, GLUT1, GLUT2, GLUT3 and GLUT7 remain unchanged compared to normal and all others were down regulated (Figure 4.17).

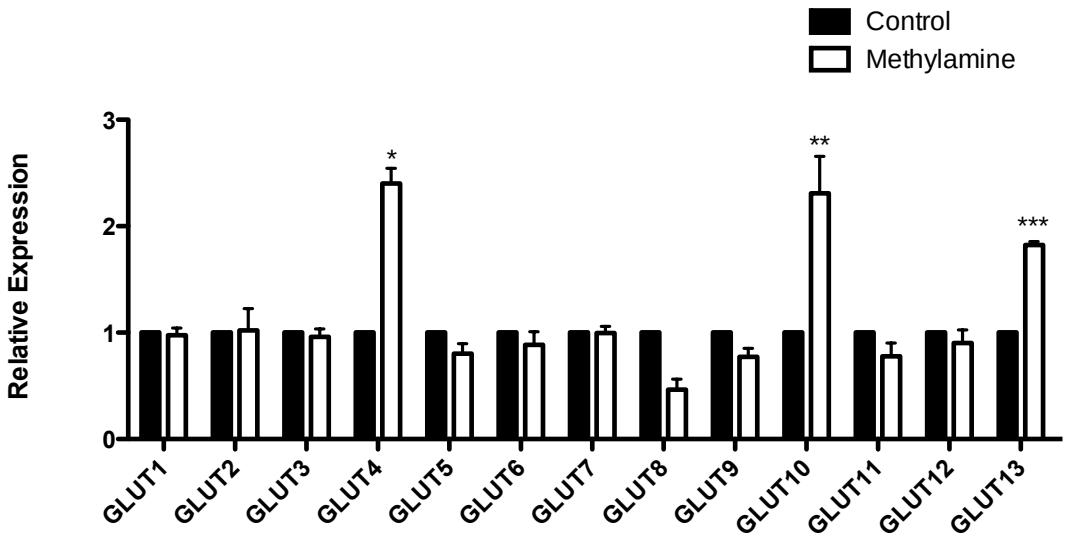

Figure 4.17: Analysis of GLUT mRNA in PCLS after VAP-1 stimulation by quantitative qPCR analysis
PCLS were treated with methylamine 200μm for approximately 4.5 hours. RNA was extracted and mRNA expression was carried out using a fluidigm qPCR array® run on triplicate arrays. Results are expressed as the mean fold change in gene expression normalized to pooled endogenous controls (β-actin and GAPDH) relative to control livers defined as 1 +/- SEM with means from two normal resected livers. Significance expressed as * $p<0.05$, ** $p<0.01$, *** $p<0.001$ using a one way ANOVA with Bonferroni correction.

4.3.7 VAP-1 null mice show altered glucose responses

Finally we generated PCLS from WT and VAP-1 KO mice fed on a normal diet in order to assess glucose response in these animals. Initially it was difficult to obtain reproducible PCLS from a multi lobed liver, but we were able to generate slices by stacking the liver and coring. Insulin was used as a positive control and indeed treatment of WT slices caused a robust increase in glucose uptake, which was less marked in the KO animals. Interestingly the KO animals also had a higher basal glucose uptake than the WT controls. In the WT mice we observed an increase in glucose uptake when the PCLS were pre treated with MA, VAP-1, MA+VAP-1, and hydrogen peroxide, although this was only significant with hydrogen peroxide (Figure 4.18A). Furthermore combination with BEA reduced the effect of MA+VAP-1 treatment. In the KO mice in contrast, we did not observe an increase in glucose uptake when slices were pretreated with MA, VAP-1, or MA+VAP-1, although hydrogen peroxide again enhanced uptake (Figure 4.18B).

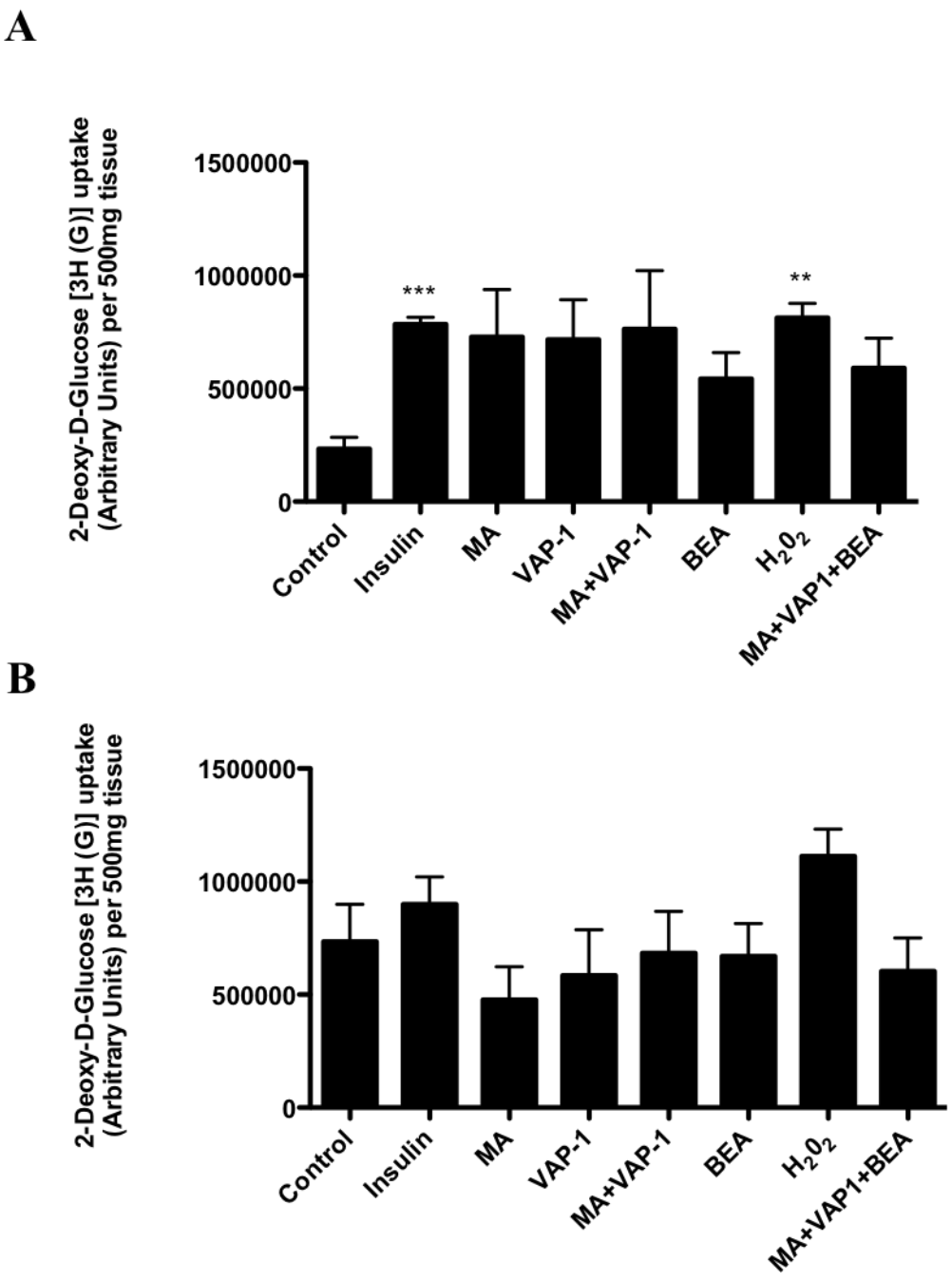

Figure 4.18: Assessment of glucose uptake after VAP-1 stimulation in PCLS from livers of WT and VAP-1 KO mice

(A) Uptake of radiolabelled glucose after stimulation of PCLS from WT mice and (B) VAP-1 KO mice. PCLS from WT and VAP-1 KO were pretreated with either insulin 0.10 IU, methylamine 200µm, VAP-1 500ng, H_2O_2 10µM, BEA 400µm, or in combination with methylamine+VAP-1, methylamine+VAP-1+BEA, for approximately 2 hours and 30 minutes and then 30 minutes with radiolabelled glucose. PCLS were lysed and radioactivity measured and signal normalized to per 500mg of tissue. N=3 +/- SEM. Significance expressed as **p<0.01, ***p<0.001 (mouse livers obtained from Lee Claridge).

4.4 Discussion

VAP-1 is highly expressed in adipose tissue where it has been shown to regulate glucose uptake. Since this protein has also been shown to be upregulated in inflammatory liver disease and diabetes, this chapter set out to examine whether it has a role in hepatic glucose homeostasis. Firstly we report increased expression of VAP-1/SSAO in NASH and ALD livers. We then performed functional studies using a novel *ex vivo* model of liver culture. We show for the first time global activation of hepatic NF-κB and transcription of target genes in response to activation of VAP-1. Importantly we demonstrated that VAP-1/SSAO activity stimulated glucose uptake with possible mobilization of hepatic GLUT4 and enhanced expression of GLUT10 and GLUT13.

4.4.1 VAP-1/SSAO expression and functional activity is upregulated in diseased livers

We found expression of VAP-1 to be upregulated in chronically inflamed NASH, ALD and PBC livers supporting previous findings from our group (Claridge L C, 2009). Stolen et al have previously shown increased VAP-1 expression in transgenic mice encoding human VAP-1 (hVAP-1) is associated with increase in SSAO activity in the liver (Stolen et al., 2004a) and others have correlated serum SSAO activity with sVAP-1 concentration in patients with liver disease (Kurkijarvi et al., 2000, Kurkijarvi et al., 1998). Kurkijarvi et al showed increase SSAO activity in chronic liver disease for example in ALD and PBC (Kurkijarvi et al., 2000). In agreement with these observations, our increase in mRNA and protein for VAP-1 in liver disease equated to increased SSAO activity in liver homogenates and could be inhibited by BEA a specific inhibitor of VAP-1/SSAO activity.

In contrast we found a down regulation of protein and mRNA in steatotic livers but no significant change in SSAO activity when compared to normal livers. Whilst to our knowledge this is the first study to report this finding in steatotic human liver, fatty adipose tissue biopsies from obese men (Body Mass Index (BMI) 32.6) in comparison to lean men (BMI 23.3) also show that VAP-1/SSAO activity remains unchanged (Visentin et al., 2004). Since the authors did not show VAP-1 protein expression in this study, the unchanged SSAO activity may be reflective of similar protein expression or altered activity in the presence of altered expression. In our study, we saw decreased VAP-1 mRNA but no change in SSAO activity or histological protein expression in steatosis. This may suggest that duration of expression or recycling of VAP-1 protein is modified during steatosis and so transcription of new VAP-1 protein may be reduced to minimize activity. However it must be noted that the samples we classed as steatotic in our study were fatty donor samples rather than true pathologically graded NAFLD samples. Analysis of VAP-1 expression and subcellular localization in normal and correctly classified NAFLD samples would therefore be important.

At the cellular level VAP-1 was expressed in HSEC as previously reported (Salmi et al., 1993), (McNab et al., 1996). In addition VAP-1 expression on HSEC increased in diseased livers for example in NASH and ALD, and interestingly our group has previously shown serum from ALD patients increases expression of VAP-1 on HSEC (Lalor et al., 2002) suggesting either a soluble stimulatory factor or presentation of sVAP-1 by HSEC. In support of previous data (Claridge L C, 2009) we also found that VAP-1 was expressed at the mRNA level in liver fibroblasts and protein colocalized to fibrotic regions and sinusoidal areas in tissue sections. This is

consistent with sinusoidal expression on HSCs, which is increased upon differentiation to activated myofibroblast cells in fibrosis.

One key finding from this chapter was that we did not see VAP-1 protein expression in hepatocytes in sections, however we document mRNA expression in HepG2 cells and Huh7.5. Although VAP-1 expression has been reported in rat hepatocytes (Martelius et al., 2000) these cells have generally been considered not to express VAP-1. This may suggest that the malignant transformation of hepatocytes in cancer could be associated with ability to express VAP-1, and certainly HCC is associated with particularly high sVAP-1 levels (Kemik et al., 2010). Additionally a role for VAP-1 in tumor angiogenesis has been reported where SSAO activity leads to recruitment of myeloid cells to tumors (Marttila-Ichihara et al., 2009), (Marttila-Ichihara et al., 2010), (Ferjancic et al., 2013) and numbers of these cells are reduced by small molecule inhibitors of VAP-1 (Marttila-Ichihara et al., 2010). Our group has also shown (Yoong et al., 1998) that inflammatory cells are recruited into tumors using VAP-1. Thus VAP-1 likely plays important roles in tumor biology, and it is likely that expression is altered in this context.

4.4.2 The role of amine oxidases in the pathogenesis of NASH

4.4.2.1 MAO

The deamination of amines by VAP-1 and other amine oxidases such as MAOA, MAOB and LOX results in the production of ammonia, aldehyde and hydrogen peroxide, (O'Sullivan et al., 2004), (Carpene et al., 2005) thus we felt it was important to study the expression patterns of all of these amine oxidases in the liver in addition

to VAP-1. The expression of MAOA and MAOB has previously been confirmed in fetal (Lewinsohn et al., 1980) and adult livers (Rodriguez et al., 2001). However disease specific expression has not been reported. Interestingly we found a decrease in all AO in the steatotic livers, which again supports data from adipose tissue where MAO activity is reduced in obese men compared to lean men (Visentin et al., 2004). It is possible that this downregulation may reflect changes in substrate availability with obesity/steatosis or mitochondrial dysfunction (Visentin et al., 2004). Regardless of cause, this suggests that the onset of oxidative stress which may trigger progression from simple steatosis to NASH may not be linked to MAO activity, or that a compensatory downregulation of expression is designed to protect against oxidative stress in this context. However, with advanced disease, expression increases and we found AO mRNAs upregulated in NASH and ALD and at the cellular level we have shown mRNA expression for MAOA and MAOB in hepatocytes and BEC. This has previously been reported at the protein level (Rodriguez et al., 2001) and in patients with NASH (Nocito et al., 2007). The mechanism leading to alterations in MAO expression with disease stage need to be characterized, but evidence from other organs such as the uterus (Zhang et al., 2011a) and cells such as platelets (Zellner et al., 2011) point to hormonal regulation, high protein diet, homocysteine levels and B12 deficiency. This has interesting implications for NASH in particular where homocystein levels are reduced and linked to metabolism of vitamin B12 (Polyzos et al., 2012).

Elevated MAO expression in NASH is of relevance because a study has shown that patients with NASH experience depression and anxiety (Elwing et al., 2006), and there is an established link between MAO and depression, with MAOA inhibitors

providing therapeutic efficacy. Interestingly depression has also been linked to markers of inflammation (Penninx et al., 2003), (Miller et al., 2003), (Sutherland et al., 2003) providing further evidence linking depression and the pathogenesis of NASH. Thus in the present study we provide evidence for elevated hepatic expression of MAO which may lead to depression in individuals, with implications including lack of motivation and a change in appetite. This could increase calorific intake and providing further substrates to fuel disease pathogenesis. Thus MAO inhibitors may have dual benefit by targeting psychological and pathological mechanisms and indeed administration of chlorgyline to animals with NASH induced by methionine-choline deficient diets improved both pathology and circulating liver enzymes (Nocito et al., 2007).

4.4.2.2 LOX

We report elevated expression of LOX in chronically inflamed and fibrotic NASH, ALD and PBC livers. Oxidation of lysine by, LOX leads to cross linking of collagen and elastin and remodeling of the extracellular matrix (Smith-Mungo and Kagan, 1998), and thus it makes sense that we see elevated expression associated with fibrotic injuries. LOX has previously been found in human liver (Kagan and Li, 2003) and in rat liver with an increase in activity associated with fibrosis and injury (Siegel et al., 1978), (Perepelyuk et al., 2013) furthermore serum activity levels of this enzyme have been indicated as markers for detecting liver fibrosis (Murawaki et al., 1991). However disease specific expression has only been reported for PBC (Vadasz et al., 2005) with no reported expression in NASH or ALD.

We found LOX was more abundant in NASH and ALD than PBC and this may be reflective of the local environment in these disease specific conditions since specific cytokines such as Transforming Growth Factor-β (TGFβ) have been shown to regulate LOX activity. At the cellular level it was expressed in all cells studied with particular abundance in HSEC, fibroblasts and hepatocyte cell lines. This is in agreement with reported expression in rat HSCs, portal fibroblasts, human hepatocytes and BEC (Perepelyuk et al., 2013), (Vadasz et al., 2005), (Wakasaki and Ooshima, 1990). Of note our elevated expression in the two hepatocyte cell lines may again be linked to the malignant origin of these cells since LOX is also elevated in tumors (Xiao and Ge, 2012) and a reduction in tumor mass can occur through its inhibition (Kanapathipillai et al., 2012).

4.4.3 Activation of VAP-1 stimulates glucose uptake in hepatic cells

We report for the first time that pretreatment of HSEC with MA, MA+VAP-1 or hydrogen peroxide stimulates glucose uptake, although similar responses have previously been reported in other cells for example rat and human adipocytes (Enrique-Tarancon et al., 1998), (Morin et al., 2001), VSMCs (El Hadri et al., 2002) and F422A cells (Fontana et al., 2001). Of note this effect was observed in the absence of vanadate, which has been required in addition to substrates of VAP-1 in other cells to stimulate glucose uptake (Enrique-Tarancon et al., 1998). We noticed when exogenous VAP-1+MA was added this resulted in a marked increase in glucose uptake, which was inhibited on addition of BEA suggesting specificity for VAP-1. Furthermore we found the addition of VAP-1+MA had a more potent effect in stimulating glucose uptake than when hydrogen peroxide was added in alone. One reason for this may be that a single dose of exogenously added hydrogen peroxide

may be less effective in causing the mobilization of insulin stimulated GLUTS and hence uptake of glucose than locally generated oxidants produced by VAP-1 catalysis. It is also likely that our hydrogen peroxide would be broken down by endogenous peroxidases. Certainly in other studies from our group, upregulation of Mucosal Addressin Cell Adhesion Molecule-1 (MAdCAM-1) by hydrogen peroxide when modeling products of VAP-1 catalysis required multiple re-stimulations over an incubation period for maximal effect (Liaskou et al., 2011). We found variable responses in HSEC which could be due to patient variability, for example whether cells were isolated from a diseased liver like ALD where endothelial VAP-1 expression is high or from a normal liver were expression is low, or due to loss of expression in culture. However we are confident that VAP-1 stimulates glucose uptake in HSEC in a manner dependent upon SSAO activity, since overexpression of enzymatically competent VAP-1 using virally encoded constructs led to increased glucose uptake upon exposure to substrate.

Glucose uptake in response to SSAO activity in rat adipocytes has been reported as being GLUT4-dependent (Enrique-Tarancon et al., 1998) and GLUT1 dependent in VSMCs (El Hadri et al., 2002) were in some cases the mechanism is based on tyrosine phosphorylation of IRS-1 and IRS-3 and activation of PI3-K (Enrique-Tarancon et al., 2000). Although we have not shown which GLUT is responsible for the observed effect. We feel this effect may have a possible contribution from the four insulin stimulated transporters GLUT4, GLUT8 (Schurmann et al., 2002), (Carayannopoulos et al., 2000), GLUT10 (Lee et al., 2010) or GLUT12 (Stuart et al., 2009) all of which we have shown to be expressed in HSEC (see Chapter 3) as they may be sensitive to signals likely to be replicated by VAP-1.

Interestingly, despite evidence, which suggests that hepatocyte-cells lack VAP-1, we observed similar effects with the two cell lines Huh7.5 and HepG2. However we found that HepG2 cells had higher basal glucose uptake. The higher basal glucose uptake seen in HepG2 may be reflective of the nature of this tumor-derived cell line and its demand for energy. The methylamine- driven stimulation of glucose uptake in these cells may be due to the presence of endogenous VAP-1, which was more abundant at message level in this cell line (Figure 4.3A). It would be important to try and reproduce these effects in isolated primary hepatocytes, but the data suggest that should a local source of VAP-1 and endogenous substrate be present within the liver microenvironment, proximal hepatocytes can respond in a manner similar to that reported for other cell types.

4.4.4 Development of an *ex vivo* human model of liver for the functional study of VAP-1 in glucose and lipid homeostasis

Although cell lines are easily available and can be expanded without restrictions and are used in many studies there are differences between cell lines and primary cells as shown by our current study and by others (Pan et al., 2009), (Tolosa et al., 2013). Thus whole animal models are commonly used in the study of liver disease pathogenesis (reviewed in (Billerbeck et al., 2013), (Ko et al., 2013), (Takahashi et al., 2012)). These models too are inherently different from human liver disease and do not completely reconstitute disease patterns seen in humans for example in the methionine choline deficient model the metabolic profile does not constitute the human NASH metabolic profile with peripheral insulin sensitivity and weight decrease (Takahashi et al., 2012). Thus since it is important to recreate the

multicellular interactions present in the human liver we sought to develop an *ex vivo* based model to study the effects of VAP-1 activity in a multicellular, physiologically relevant human model.

Previous studies have used human PCLS to investigate hepatic metabolism and hepatotoxicity (Connors et al., 1990), (Wishnies et al., 1991), (Price et al., 1996), (Kirby et al., 2004), (Guyot et al., 2007), however the functional activity of PCLS in culture has not been addressed by many studies and thus we felt it was vital to fully characterize the functional capability of PCLS in culture before performing any interventions.

We report that our PCLS culture system retains viability for up to 48 hours, and this is supported by albumin secretion, glucose uptake, MTT reduction, glycogen storage and morphological evidence in terms of visual integrity (Karim et al., 2013). Furthermore we adapted this system to our functional assays for measuring glucose uptake. Importantly we incorporate visual assessment of PCLS integrity, which is not carried out in all published studies, and our PCLS culture system is amenable to culture for up to 48 hours which extends the time point suggested by many studies using human and rodent PCLS for metabolic and toxicological studies (Connors et al., 1990), (Price et al., 1996), (Mortensen and Dale, 1995, Price et al., 1996, Naik et al., 2004). However we did note a gradual decrease in viability between 24 and 48 hours and this was accompanied with a decrease in albumin secretion and formation of glycogen droplets, loss of morphological structure and nuclear integrity. We also observed necrosis in the center of these slices compared to the periphery (Karim et al., 2013). This was probably because the periphery of PCLS where able to maintain

gaseous exchange and media perfusion. Similar studies have also reported loss in expression over time in culture for example of cytochrome P450 (Martin et al., 2003). This model could be further enhanced to improve tissue integrity and architecture at 48 hours as well as maintain viability over 48 hours by introducing a dynamic flow perfusion system for example using microchamber perfusion devices (van Midwoud et al., 2010a), (van Midwoud et al., 2010b) or immobilizing PCLS in inserts and allowing gaseous exchange in rotary culture (Clouzeau-Girard et al., 2006), (Guyot et al., 2007), (Klassen et al., 2008), (Schaffert et al., 2010). However within the confines of the current study all our functional experiments were carried out within 24 hours to ensure maximal viability of PCLS (Karim et al., 2013), (Liaskou et al., 2011).

4.4.5 Activated VAP-1 regulates glucose uptake in PCLS

Our group has previously confirmed that activation of SSAO activity drives activation of NF-κB in endothelial cells and induces transcription of IL-8, ICAM-1 and E-selectin (Lalor et al., 2007). Thus, in order to check whether our PCLS would respond to stimulation of VAP-1 we performed an analysis of NF-κB activity using a custom qPCR array. This included genes, which were up in the NF-κB activation pathway, cascade and NF-κB responsive genes IL8, IL6, IL10, ICAM1 and TLR4 which are involved in the inflammatory response and fits with the picture observed in NAFLD. Thus this data suggests stimulation of VAP-1 in PCLS is successful.

We report for the first time, hepatic glucose uptake in response to methylamine treatment of PCLS. This was due to activation of endogenous VAP-1 within tissue, which was likely expressed on HSEC, HSCs and possibly on fibroblastic cells.

However since the tissue predominantly used in the generation of PCLS was from resected non-fibrotic, normal liver the major contribution would likely be from HSEC and HSCs. Presence of shed sVAP-1 should also be considered since biological stress for example from the cutting procedure, may lead to shedding of catalytically active VAP-1 from HSEC or other cells. For example experimentally induced diabetes leads to shedding of VAP-1 from HSEC (Stolen et al., 2004a). Thus shed VAP-1 from systemic blood or hepatic cells could have local insulinomimetic effects on hepatocytes and other liver cells.

Although other studies have shown VAP-1 substrates to stimulate glucose in cells (El Hadri et al., 2002), (Fontana et al., 2001), (Enrique-Tarancon et al., 1998), (Morin et al., 2001) this is the first study that has shown methylamine to stimulate glucose uptake in firstly the human liver and secondly in a multicellular environment using an *ex vivo* based model. Of note, despite our cellular expression data we obviated the need to use inhibitors for other amine oxidases in the PCLS system by choice of substrate, since methylamine is not deaminated by the other AO (Lyles, 1996), (Yu, 1990). Our observation of an increase in glucose uptake when VAP-1 was added alone to PCLS suggests the presence of endogenous ligands. These could be endogenous amines such as methylamine, which is found in food and cigarette smoke or from the oxidation of adrenaline by MAO (O'Sullivan et al., 2004). Or amines such as leucine and valine which are metabolized by the liver (Holecek et al., 1998).

The addition of endogenous methylamine and VAP-1 resulted in a marked increase in glucose uptake, which returned to control levels on addition of BEA and was recapitulated on addition of hydrogen peroxide a metabolite known to mimic the

effects of insulin (Mahadev et al., 2001) as previously shown in different systems (Enrique-Tarancon et al., 1998), (Marti et al., 1998), (El Hadri et al., 2002). The presence of a large amount of exogenous VAP-1 in our system means there is an abundance of the enzyme available for the catalytic conversion of methylamine to hydrogen peroxide hence stimulating glucose uptake. Even so we found variable responses with different PCLS in this system, which may reflect donor genetic differences or variables such as tissue age and processing time prior to experimentation. Thus whilst we have confirmed that activation of SSAO activity increases glucose uptake by normal liver specimens, it would be interesting to see the responses of PCLS from steatotic and NASH patients, particularly in light of our observations on basal glucose transporter expression in these situations.

4.4.6 The role of GLUT4 and other glucose transporters in VAP-1 stimulated glucose transport

We then went on to examine whether the enhanced uptake of glucose as a result of VAP-1 activity was linked to activity of GLUT4, which has been shown previously in rat adipocytes (Enrique-Tarancon et al., 1998). We noted the appearance of large cytoplasmic GLUT4-containing droplets concentrated towards the periphery of hepatocytes in PCLS treated with VAP-1+MA. This effect was not seen in the control or VAP-1+MA+BEA treated PCLS and thus we are confident that this effect is a genuine observation as a result of VAP-1 activation. Certainly in adipocytes GLUT4 becomes enriched in membrane fractions after VAP-1 substrate stimulation (Enrique-Tarancon et al., 1998) and thus a similar mechanism may be in operation. We did notice some staining in the IgG control-treated PCLS, but this did not have the appearance of large cytoplasmic droplets. Thus the staining observed in the IgG

control could be due to autofluorescence of selected cells within the PCLS or non-specific binding of staining reagents. The bright cells in the sinusoids are likely to be macrophages or similar which bind antibody non-specifically.

It is interesting that the responsive cells are the hepatocytes which we have not found VAP-1 protein expression for and thus lack VAP-1 yet we see possible changes in GLUT4 in PCLS thus this implies that activation of VAP-1 by another cell caused the response in hepatocytes. Although we did not use specific cell labeling antibodies to identify for example the hepatocytes, morphologically these cells do appear to be hepatocytes. Interestingly we did not see the presence of these GLUT4 droplets in HSEC. This may be because the sections were to thin so hard to visualize or the HSEC were non responsive because the PCLS were bathed in treatment rather than it being delivered through the vasculature. A further explanation could be that we may have missed the endothelial response and rather saw the subsequent hepatocyte response due to a longer time point used, for example in adipocytes GLUT4 recruitment is seen within 1 hour of treatment (Enrique-Tarancon et al., 1998). However other studies have shown that changes in protein expression for example GLUT1 can be detected as early as 1 hour and persist as long as the cells are exposed to the amine (El Hadri et al., 2002).

Furthermore it most be noted that in addition to GLUT4 there are other insulin sensitive transporters which may be sensitive to signals likely to be replicated by insulinomimetic response of VAP-1 as suggested earlier for example GLUT8 (Schurmann et al., 2002), (Carayannopoulos et al., 2000), GLUT10 (Lee et al., 2010) and GLUT12. Our data confirms that human liver expresses these insulin- sensitive

transporters (see Chapter 3) and so VAP-1 activity may also stimulate glucose uptake by regulating the expression of these proteins. Thus future experiments should consider confocal staining for these GLUTS in isolated cells and treated liver sections to quantify cellular distribution. GLUT4-independent responses to VAP-1 stimulation have been demonstrated in VSMCs. Here SSAO activity causes the accumulation of GLUT1 at the cell membrane and not GLUT4 (El Hadri et al., 2002) as it does in other cells (Enrique-Tarancon et al., 1998) confirming that VAP-1 stimulates different GLUTS in different cells. Furthermore in some cells it can increase expression of multiple GLUTS for example GLUT1 and GLUT4 in 3T3 F442A cells (Fontana et al., 2001). We document elevated expression for GLUT8, GLUT10 and GLUT12 in NASH and ALD compared to normal livers and importantly these livers also have elevated levels of VAP-1. This suggests that VAP-1 may be implicated in their expression and also implies that GLUT8, GLUT10 and GLUT12 could be more important than GLUT-4 for VAP-1 stimulated glucose uptake in the diseased liver. However this would need further investigation.

One line of evidence supporting this hypothesis is that we have demonstrated increased expression of message for GLUT4, GLUT10, and GLUT13 in human PCLS following methylamine treatment. We also found increase in expression of GLUT1 in one sample studied. Increased expression for GLUT4 and GLUT1 by other amines such as tyramine and benzylamine has previously been reported in 3T3 F442A cells (Fontana et al., 2001) and also GLUT1 in VSMCs (El Hadri et al., 2002).

It was interesting to note that methylamine increased expression of GLUT10 which may be involved in protecting the cell from oxidative stress which arises as a direct

result of activated VAP-1 generating hydrogen peroxide or through lipid peroxidation. Certainly mitochondrial GLUT10 in smooth muscle cells has been shown to have a functional role in protecting cells from oxidative damage (Lee et al., 2010). Of note the NF-κB array data also showed that we induced activation of NF-κB1 and its target gene IL-10, both of which have anti-inflammatory roles for example IL-10 can prevent transcription of inflammatory cytokines (Cao et al., 2006), and inhibits IL-2 production in T lymphocytes thus inhibiting their growth (de Vries, 1995), whilst NF-κB1 has been shown to reduce the expression of TNFα and hence infiltration of immune cells (Oakley et al., 2005). In addition GLUT13 a H^+/myo-inositol co transporter (Zhao and Keating, 2007), (Uldry et al., 2001), (Scheepers et al., 2004) was also upregulated. Inositol can act as an insulin sensitizer (Giordano et al., 2011) which could precipitate glucose uptake in the context of IR. Additionally dietary supplementation with inositol has been shown to improve features of the MetS, for example a decrease in serum TAG and blood pressure (Giordano et al., 2011). Thus whilst VAP-1 activity has clear metabolic consequences, and can drive tissue inflammation in the context of disease (Lalor et al., 2007), and can regulate expression of ICAM-1 and IL-8 (Figure 4.15 and 4.16), there is also a suggestion that activation of protective mechanisms linked to antioxidant responses and anti-inflammatory gene expression are also induced.

4.4.7 VAP-1 KO mice show altered glucose responses

Our data from the human system suggests that VAP-1 activity has a profound ability to modify glucose uptake. To interrogate this further we used tissue from C57BL/6 mice lacking the VAP-1 gene to compare glucose responses in *ex vivo* murine PCLS. This strain of mice irrespective of diet develops obesity and IR with age (Anstee and

Goldin, 2006) and exhibit increased SSAO activity when compared to other mouse strains (Yu and Deng, 1998). Interestingly we found VAP-1 KO mice had a higher basal glucose uptake compared to WT, which may be a compensatory mechanism. Furthermore the addition of MA did not stimulate glucose uptake in contrast to WT animals. This confirms the specificity of our MA responses in the human tissue, and the requirement for endogenous VAP-1 to drive MA stimulated glucose uptake. Interestingly in the VAP-1 KO PCLS most other treatments did not enhance glucose uptake even when exogenous VAP-1 was added. This suggests that in the murine system, endogenous VAP-1 is more effective at recruiting GLUTS and driving glucose uptake than exogenous VAP-1. This may reflect an inability of murine ligands to respond to human VAP-1, but these proteins are conserved between mouse and human and thus unlikely. Importantly when we supplied hydrogen peroxide directly to the PCLS, we saw responses in both WT and VAP-1-deficient tissue, which suggests that signaling machinery downstream of VAP-1 is intact in both animals. Certainly mouse tissues engineered to overexpress human GLUT-4 show enhanced glucose uptake and fatty acid metabolism (Belke et al., 2001). Whilst this data strengthens the role of hepatic VAP-1 in glucose uptake, it must be noted that the responses were very variable in this system. This may simply reflect limitations in our *ex-vivo* assay for studies using mouse tissues. For example media constituents may need altering and optimizing for mouse tissues, and it was more difficult to slice the multi-lobed mouse livers than human samples. However it is important to remember that mice have high metabolic rates (Andrikopoulos et al., 2008) and different immune systems (Liu et al., 2013) than humans and a tendency to ingest calories at night (Andrikopoulos et al., 2008) all of which might alter responses in our assays.

4.4.8 The Functional significance of VAP-1 in chronic liver disease

In all this is the first study to document the role of VAP-1 in stimulation of glucose uptake in hepatic cells and the human and mouse liver using a novel *ex-vivo* model. Many patients diagnosed with NASH exhibit cardinal features collectively grouped together under the MetS, which include IR. Our data supports the hypothesis that in an IR patient suffering from NASH or other chronic inflammatory disease, an increase in VAP-1 expression is concomitant with levels of insulin in an attempt to regulate blood glucose levels. For example Salmi et al showed elevated levels of sVAP-1 in diabetic patients and this appeared to be regulated by levels of insulin which increased the shedding of VAP-1 (Salmi et al., 2002). In addition induction of experimental diabetes in mice overexpressing VAP-1 levels leads to elevated levels of sVAP-1 (Stolen et al., 2004a). Thus VAP-1 may be overexpressed in cells in an attempt to make them insulin sensitive. However it can be argued that this may not be restricted to VAP-1 since the deamination of amines by other AO can also result in the formation of hydrogen peroxide, which is key to mimic the insulin like effects. However we have shown MA, which is specific for VAP-1, stimulates glucose uptake in hepatic cells and PCLS, and further evidence suggesting VAP-1 colocalizes in intracellular vesicles with GLUT4 points to a specific role in glucose transport (Enrique-Tarancon et al., 1998). Thus VAP-1 has positive effects on diabetes by enhancing muscle glucose utilization however it is also associated with late complications of diabetes for example glomerulosclerosis and atherosclerosis, (Stolen et al., 2004a). Furthermore the extra fuel in the form of glucose could be used for DNL and hence drive steatosis, whilst activation of NF-κB may lead to inflammation and fibrosis in NASH.

In addition we have shown the liver expresses specific insulin-sensitive GLUTS, which are also upregulated in NASH and ALD livers. Thus it is possible that activated VAP-1 may also regulate glucose uptake through GLUT8, GLUT10 and GLUT12 in the diseased liver. Furthermore the enhanced expression of GLUT10 and GLUT13 by methylamine as shown by this study may represent a compensatory mechanism to protect against oxidative stress similar to that of GLUT10 in smooth muscle cells (Lee et al., 2010). GLUT13 can ameliorate conditions associated with the metabolic syndrome by transporting inositol which has roles in insulin signaling (Larner, 2002) and as an insulin sensitizer (Giordano et al., 2011). Although we did not find this transporter upregualted in NASH it was in ALD and thus may be associated with disease severity or exhibit disease specific expression. A schematic illustrating the roles of each GLUT discussed is below.

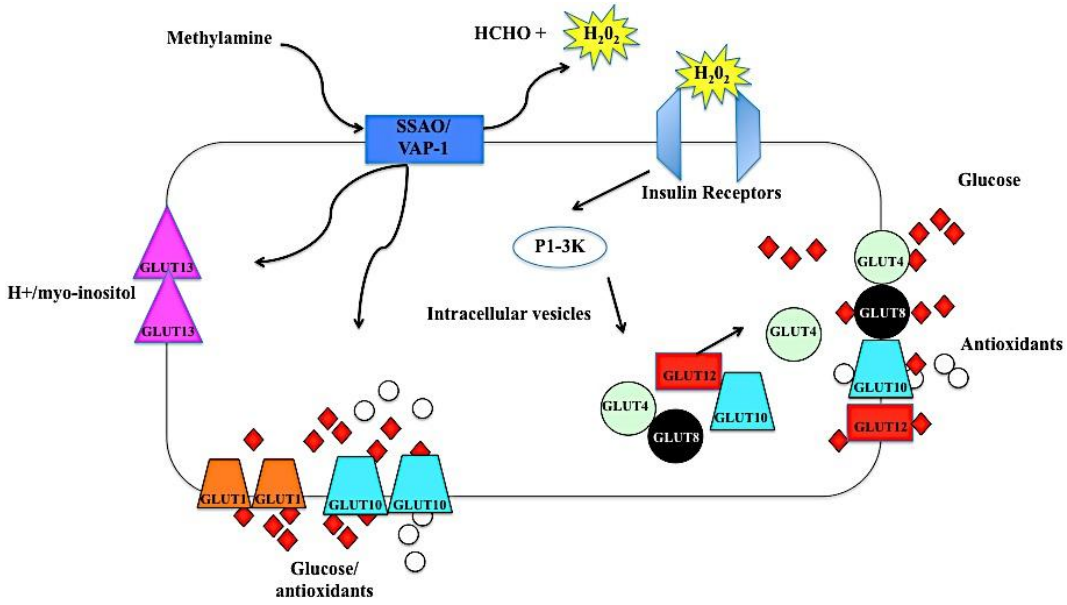

Figure 4.19: Schematic showing VAP-1/SSAO related glucose uptake in the human liver

We have shown activated VAP-1 leads to glucose stimulation through GLUT4, however in the liver it is not limited to GLUT4 but may include GLUT8, GLUT10 and GLUT12 which are elevated in disease. Addition of methylamine to PCLS leads to enhanced expression of GLUT13, which transports inositol and could have roles in sensitizing the insulin resistant liver in NASH and GLUT10, which protects the cell from oxidative damage as observed in NASH.

Finally it is important to acknowledge that excess uptake of glucose drives lipogenesis and such further evidence to support the insulinomimetic effects of VAP-1 have been described in adipocytes (Fontana et al., 2001), (Morin et al., 2001). Thus could the 'adipocyte like' differentiation of hepatocytes to make them store TAG a possible consequence of VAP-1 activity. Whether this occurs in the liver, and may cause or exacerbate disease pathogenesis needs further investigation. Thus the contribution of VAP-1 to lipid storage by the liver is investigated in the next chapter.

CHAPTER 5

5 IS THERE A ROLE FOR VAP-1 IN HEPATIC LIPID HOMEOSTASIS?

5.1 Introduction

Our studies thus far have demonstrated that activation of hepatic VAP-1 in whole liver and isolated cells leads to activation of NF-κB-dependent signaling cascades, translocation of GLUT-4 and enhanced glucose uptake. Of note VAP-1/SSAO-dependent deamination of amines not only regulates glucose uptake in cells but has also been shown to posses other insulin-like effects and can modify lipid metabolism (Morin et al., 2001), increase TAG storage (Fontana et al., 2001) and drive adipocyte differentiation (Morin et al., 2001). For example, chronic administration of VAP-1/SSAO substrates such as methylamine, leads to a development of fatty streaks in the aortae in mice fed on a high cholesterol diet (Yu et al., 2002) and these substrates have also been shown to activate differentiation in adipocytes (Fontana et al., 2001), (Carpene et al., 2006), (Mercier et al., 2001), (Subra et al., 2003), (Bour et al., 2005) as well as stimulating lipogenesis (Carpene et al., 2006). Treatment of diabetic rats with benzylamine and vanadate also causes a 45% increase in adipose tissue fat deposition (Marti et al., 2001), and transgenic mice overexpressing VAP-1/SSAO chronically supplemented with methylamine have increased BMI and abdominal fat pad weight (Stolen et al., 2004a). These data imply that VAP-1 has a potent ability to regulate not only glucose homeostasis but also the storage and distribution of lipids.

Our initial findings suggest that NASH and chronic liver diseases are associated with marked changes in hepatocellular lipid transport proteins, as has been noted in some other investigations and discussed in our initial chapter. Whilst speculations as to the mechanisms underlying these responses have been made, and links with disease susceptibility and progression have been noted (Westerbacka et al., 2007), (Doege et al., 2006), to our knowledge no one has considered the impact of amine oxidase

activity on liver lipid traffic. It is surprising that the link between obesity, VAP-1/SSAO and more strikingly fatty liver has received little attention. Of note, the increased dietary consumption patterns in western world have likely increased the availability of substrates such as methylamine which are abundantly found in food (Pirisino et al., 2001), cigarette smoke (Zhang et al., 2012) and are formed endogenously from the metabolism of adrenaline (Yu et al., 1997). This coupled with the direct portal connection between the gut and liver, may deliver increasing concentrations of substrate to the hepatic environment (Liaskou et al., 2011) and impact upon local production of hydrogen peroxide and other SSAO metabolites. Since hydrogen peroxide has insulinomimetic effects it could regulate lipid transporters for example CD36 and FATP1 (Stahl et al., 2002), (Schwenk et al., 2010), which are reported to be insulin sensitive and hence contribute to lipid accumulation, oxidative stress and further damage to the cell. Furthermore hydrogen peroxide could potentially drive endogenous lipogenesis and inhibit lipolysis just like insulin.

Thus the major aims of this chapter were:

(I) To develop *in vitro* and *ex-vivo* based models to investigate the role of VAP-1 in regulating lipid accumulation in the liver.

(II) To investigate the role of VAP-1 in regulating lipid accumulation in hepatic cells in culture

(III) To investigate the impact of SSAO activity on lipid transporter expression

5.2 Methods

For methods pertinent to this chapter please refer to the general methods p51-54.

5.3 Results

5.3.1 Quantification of lipid accumulation in cultured cells

Since excess lipid accumulation has reported toxic effects (Malhi et al., 2006), (Ricchi et al., 2009), (Malhi et al., 2007) we began by performing pilot experiments to test effects of different doses of both saturated and unsaturated FFAs on cultured Huh7.5 and HSEC. Cells were treated with varying concentrations of OA and PA (250μm, 500μm, 1500μm) for 3, 6 and 24 hours, the lipid was visualized by ORO a dye that stains neutral TAG and lipids red and images were taken of cells (see representative images in Figure 5.1). The ORO dye was then solubilized and quantified. We found in the Huh7.5 cells there were increased lipid accumulations with increasing incubation time with OA and accumulation appeared more pronounced with OA than PA see images in Figure 5.1 and Figure 5.2 ORO values, however this was also associated with increased cell loss with time (see images in Figure 5.1). Furthermore there appeared to be presence of both macro and microvesicular accumulation of lipids in cells, (macrovesicular steatosis shown by black arrow and microvesicular shown by blue arrow in Figure 5.1). Raw ORO values revealed that at 6 hours there was a significant increase in OA accumulation at all concentrations.

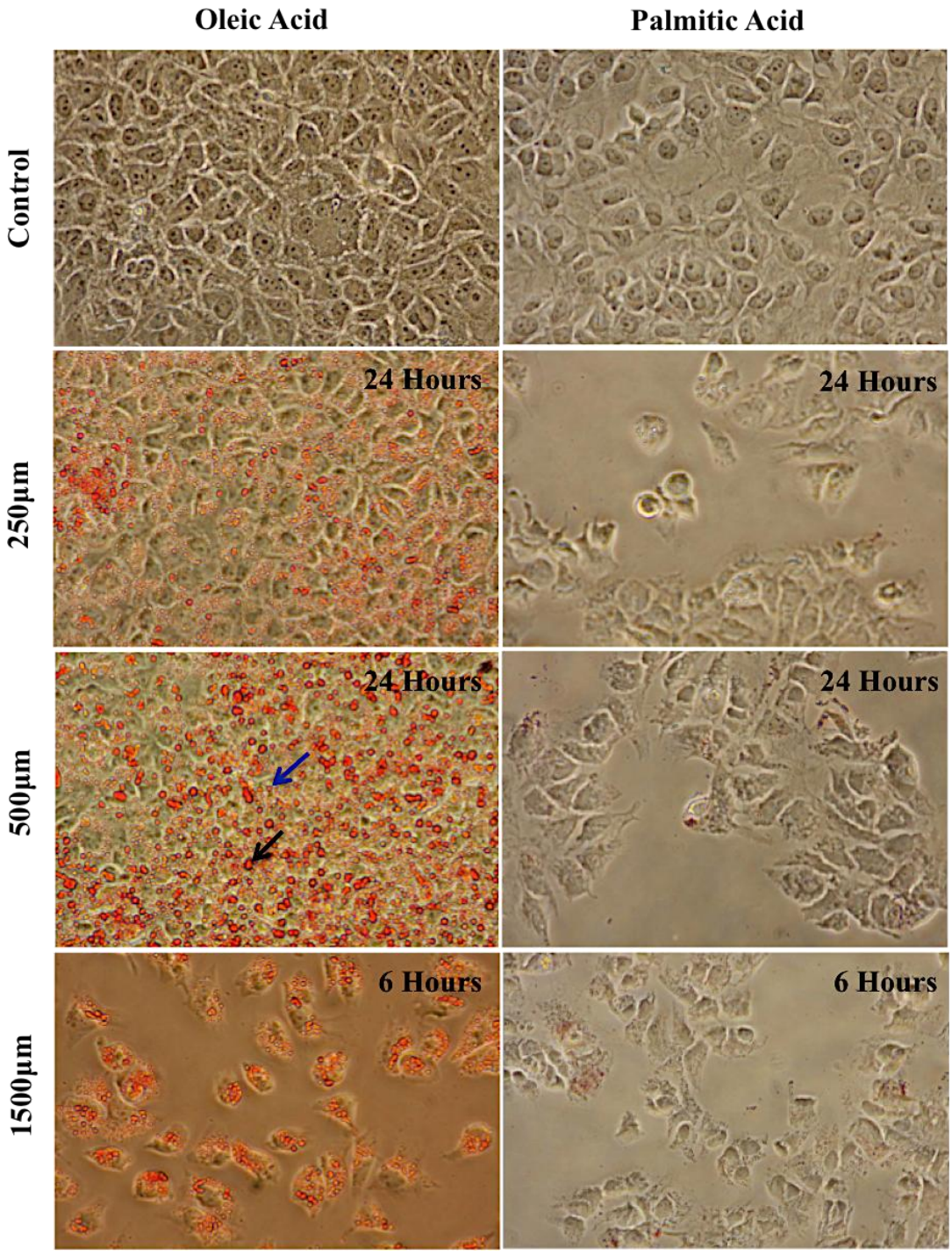

Figure 5.1: Accumulation of free fatty acids in Huh7.5 cells
Accumulation of FFAs and ORO staining in Huh7.5 cells. Cells were treated with OA or PA at 250µm, 500µm and 1500µm for 6 or 24 hours. Cells were fixed, and stained with ORO. Representative pictures from N=4, black arrow in oleic acid treated at 500µm for 24 hours indicates presence of macrovesicular steatosis and blue arrow indicates microvesicular steatosis. Pictures captured at 40X original magnification.

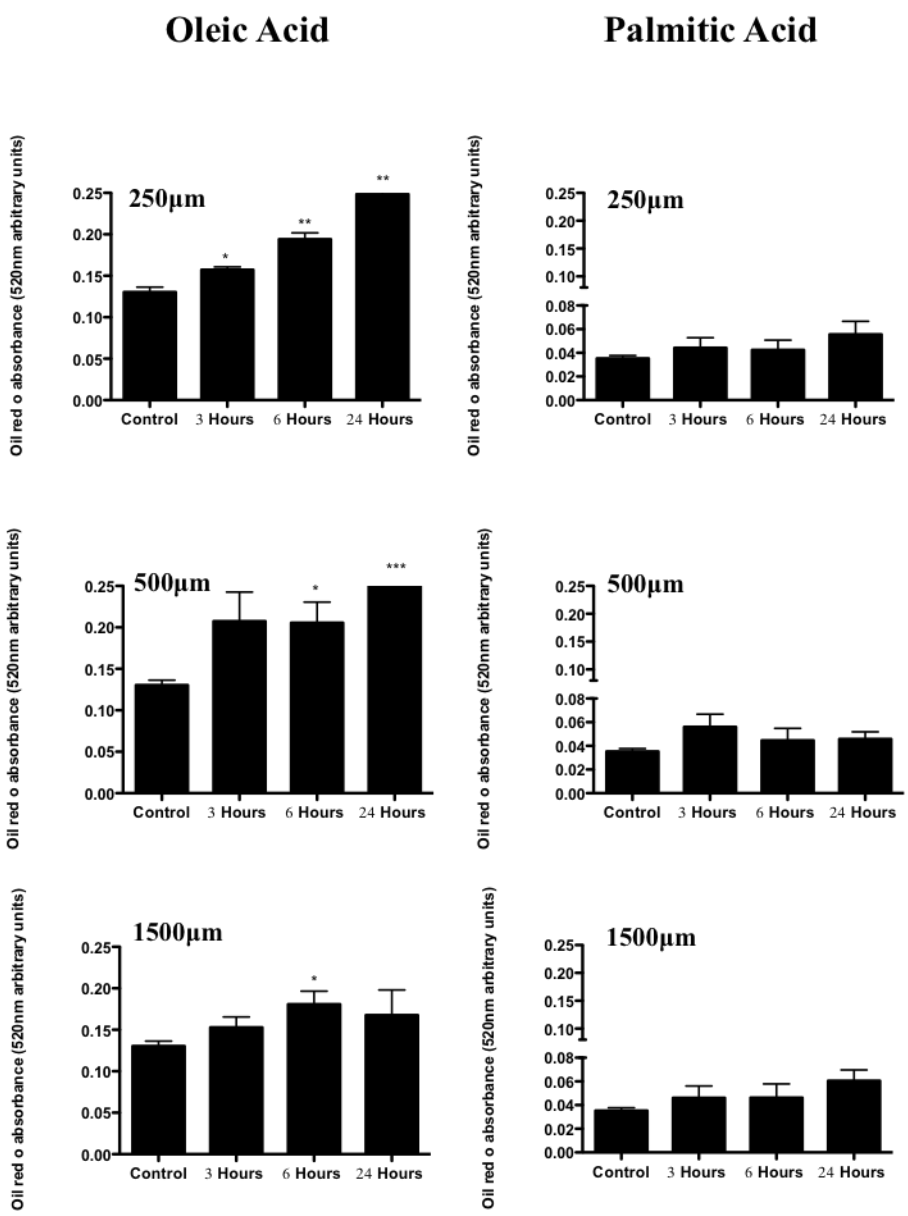

Figure 5.2: Dose and time dependent accumulation of free fatty acids in Huh7.5
Huh7.5 cells were treated with OA or PA at 250µm, 500µm and 1500µm for 3, 6 or 24 hours. Cells were fixed, and stained with ORO. ORO was then solubilized and quantified on a spectrophotometer. Representative graphs from N=3 +/- SEM. Significance expressed as * $p<0.05$, ** $p<0.01$, *** $p<0.001$.

The same response was noted for endothelium, which incorporated a smaller amount of lipid than the hepatocytes but still exhibited toxicity at high concentrations (see representative images for OA uptake in Figure 5.3). Here raw ORO values revealed an increase in uptake with time which was significant at 250µm for 24 hours, 500µm 3 hours and 1500µm 3 and 6 hours (Figure 5.4). HSEC were also treated with PA

however this was associated with toxicity even at the lowest dose 250µm at all time points (data not shown).

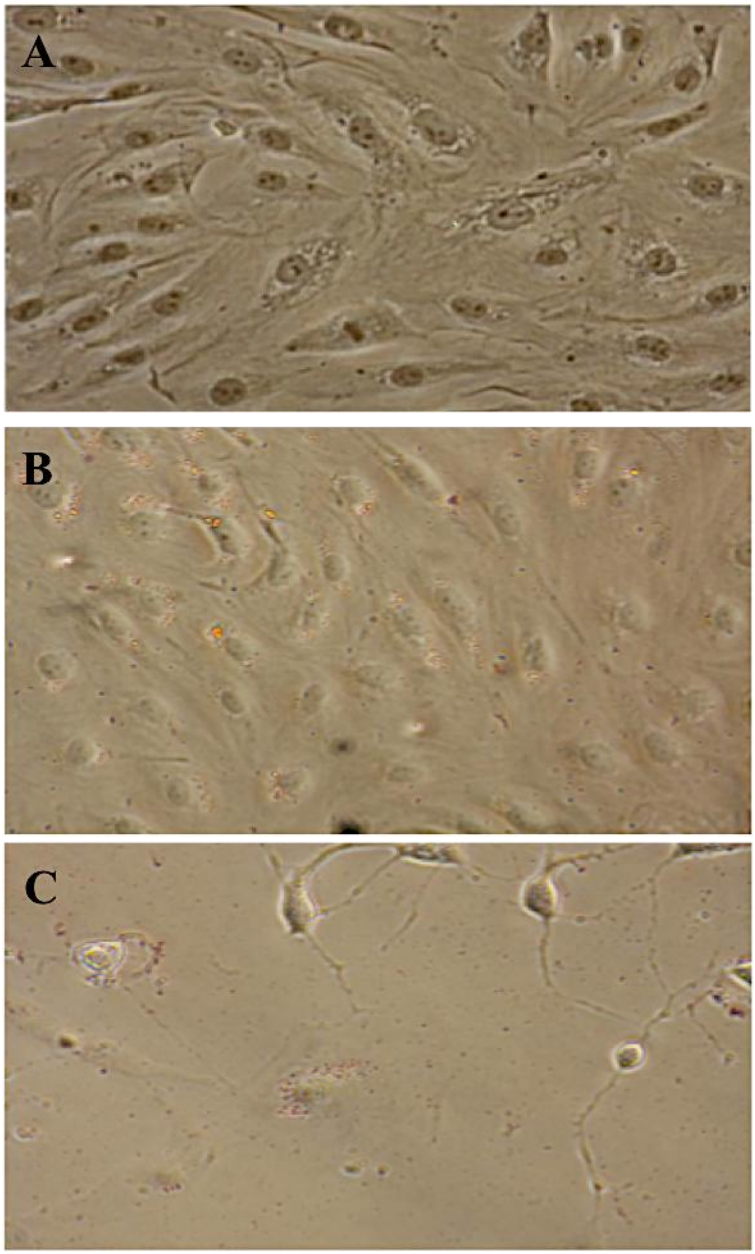

Figure 5.3: Accumulation of oleic acid in HSEC
Accumulation of OA and ORO staining in HSEC. (A) control, (B) 250µm and (C) 500µm OA treatment for 24 hours. Cells were fixed and stained with ORO. Representative pictures from N=4. Pictures captured at 40X original magnification

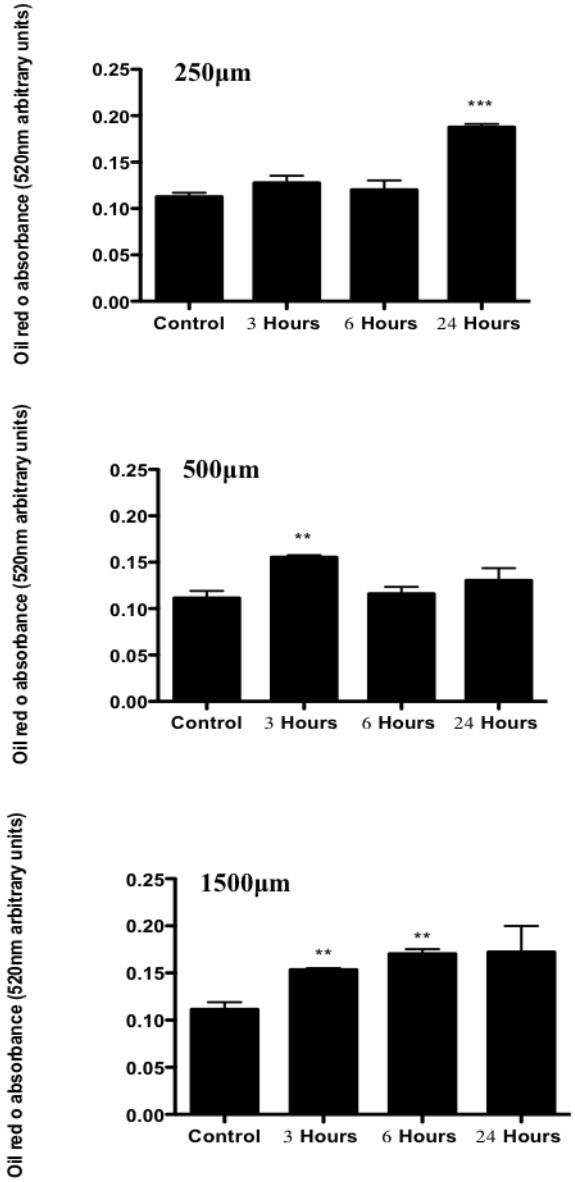

Figure 5.4: Dose and time dependent accumulation of oleic acid in HSEC
HSEC cells were treated with OA at 250µm, 500µm and 1500µm for 3, 6 or 24 hours. Cells were fixed, and stained with ORO. ORO was then solubilized and quantified on a spectrophotometer. Representative graphs from N=3 +/- SEM. Significance expressed as * $p<0.05$, ** $p<0.01$, *** $p<0.001$.

Although the raw ORO values allowed us to see that OA was more potent in accumulating in cells than PA, our visual assessment (Figure 5.1) clearly revealed cell loss and thus these results made it necessary for us to incorporate assessment of cell number into our FFA accumulation assays to permit normalization to number of cells. Therefore we constructed cell number calibration curves for cells grown at densities

ranging from 8000 to 100,000 cells per well and labeled with Hoechst dye. Graphs of cell number versus fluorescent signal were generated and then used to check cell numbers following treatments to permit adjustment for any loss of cells. Representative calibration curves for Huh7.5 and HSEC are shown in Figure 5.5.

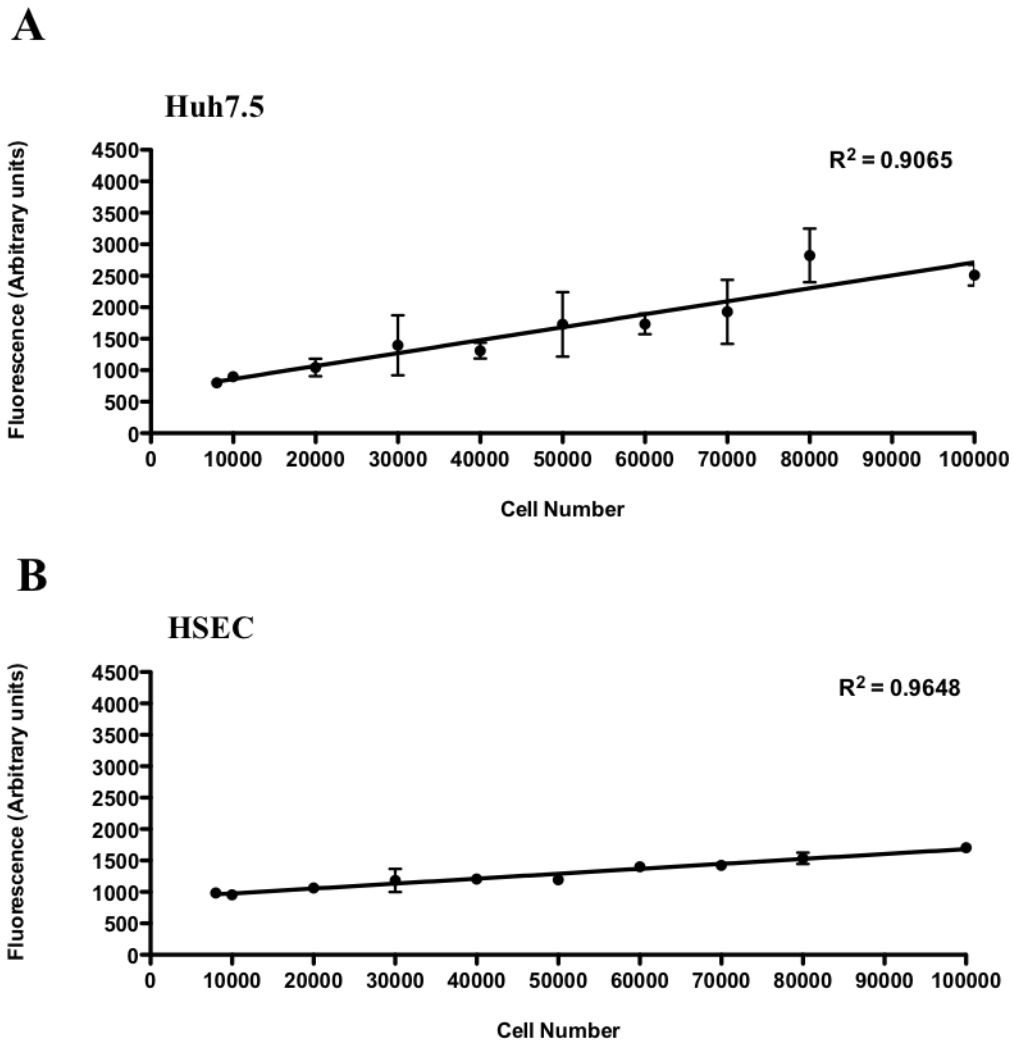

Figure 5.5: Determination of cell number using Hoechst dye
(A) Huh7.5 or (B) HSEC cells were seeded at densities ranging from 8000 to 100,000 cells per well for 24 hours. Cells were fixed and stained with Hoechst dye. A standard curve was generated as above and only used if the R^2 value was ≥ 0.9. Representative graphs from N=3 +/- SEM.

Next we treated Huh7.5 with 250μm, 500μm and 1500μm OA or PA for up to 3, 6 and 24 hours to determine normalized lipid accumulation within the cells. The corrected ORO values for Huh7.5 (obtained using Hoechst dye calibration curves) treated with OA show that there is an increase in OA uptake with time and concentration and at 500μm there seems to be a reduction in lipid uptake compared to 250μm at 24hours in the PA treated Huh7.5 (Figure 5.6B). This was not clear from the raw ORO values obtained earlier (Figure 5.2). For all concentrations the greatest uptake seems to be at 24 hours (Figure 5.6, data for 1500μm not shown). A similar trend was seen were OA appeared to be more potent in accumulating in cells than PA (Figure 5.6). The corrected ORO values for HSEC suggest there is greater accumulation of OA at 250μm and 500μm for 24 hours (Figure 5.7) and although the images in Figure 5.3 show cell loss, HSEC do appear to have lipid in them (see images in Figure 5.3).

Thus for all subsequent experiments we choose 250μm as our concentration as there was minimal cell death and good accumulation of FFAs with a time point of 6 and 24 hours for either functional assays or gene analysis.

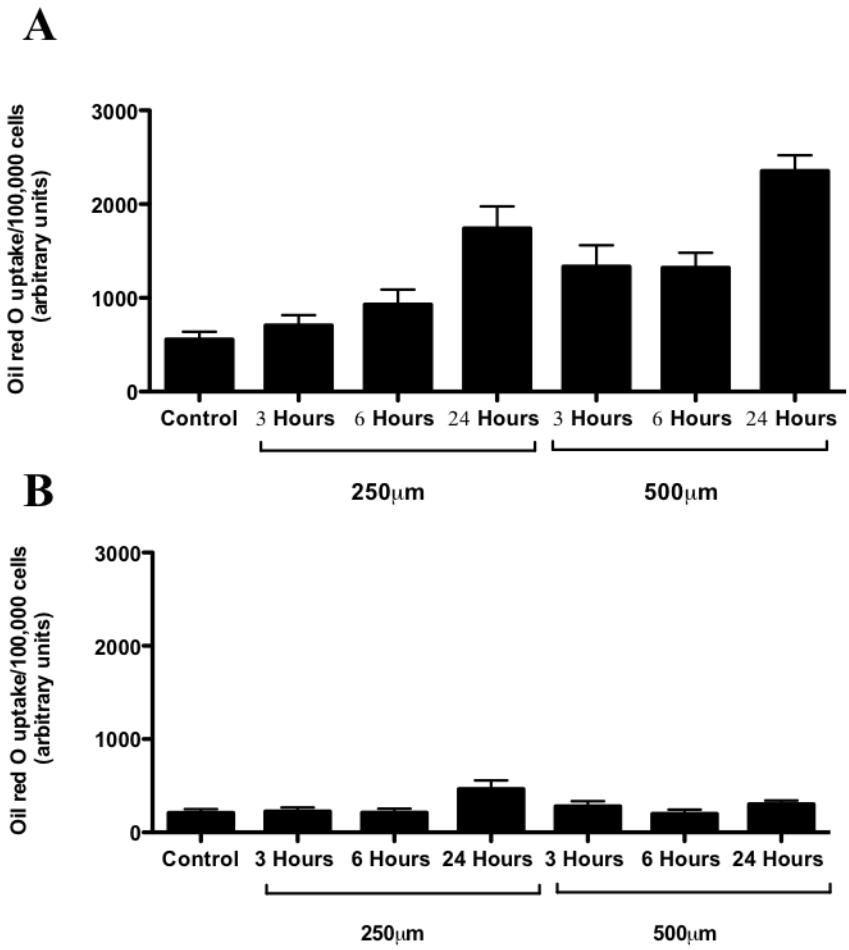

Figure 5.6: Quantification of free fatty acids in Huh7.5
Huh7.5 cells were treated with (A) OA or (B) PA at 250μm or 500μm for 3, 6 or 24 hours. Cells were fixed and stained with ORO or Hoechst dye. ORO was solubilized and quantified on a spectrophotometer and fluorescent readings taken of Hoechst dye treated plates. The ORO values were then manipulated to express the amount of ORO taken per 100,000 cells using the Hoechst dye readings. Representative graphs from N=3 +/- SEM. Significance expressed as $p<0.001$*** using a two way ANOVA.

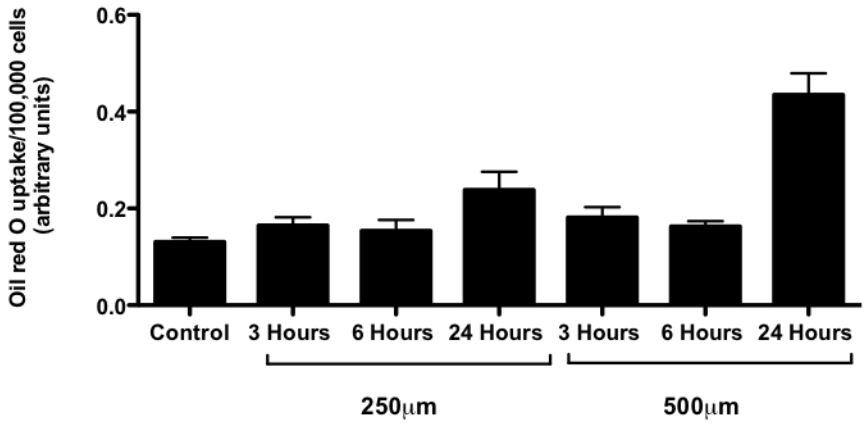

Figure 5.7: Quantification of oleic acid in HSEC
HSEC cells were treated with OA or PA at 250μm, 500μm for 3, 6 or 24 hours. Cells were fixed and stained with ORO or Hoechst dye. ORO was solubilized and quantified on a spectrophotometer and fluorescent readings taken of Hoechst dye treated plates. The ORO values were then manipulated to express the amount of ORO taken per 100,000 cells using the Hoechst dye readings. Representative graphs from N=4 +/- SEM. Significance expressed as $p<0.001$*** using a two way ANOVA.

5.3.2 Expression of Lipid transporters alters after treatment of cells with free fatty acids

We have demonstrated that 24 hours treatment with either OA or PA treatment at 250μm results in accumulation of lipid in cells and minimal cell death OA>PA (Figures 5.6 and 5.7). Thus we collected RNA from Huh7.5 treated with either 250μm OA or PA for 24 hours and used qPCR to measure transcript levels of FATPs 1-6, FABPs 1-7, CAV1, CD36, LRP1, LRP2 and LRP8. Results were normalized to the house keeping genes β-actin and GAPDH and expressed relative to untreated Huh7.5, which was set as 1. Pretreatment of Huh7.5 with unsaturated FA (OA) resulted in significant increase in CAV1, LRP1, LRP2, LRP8 and FATP6 mRNA (Figure 5). In contrast use of saturated FA (PA) resulted in mRNA for most transporter proteins being downregulated or unchanged, except FATP6 and FATP3 (Figure 5.8B). A notable exception was FATP6, which was highly upregulated by both FA.

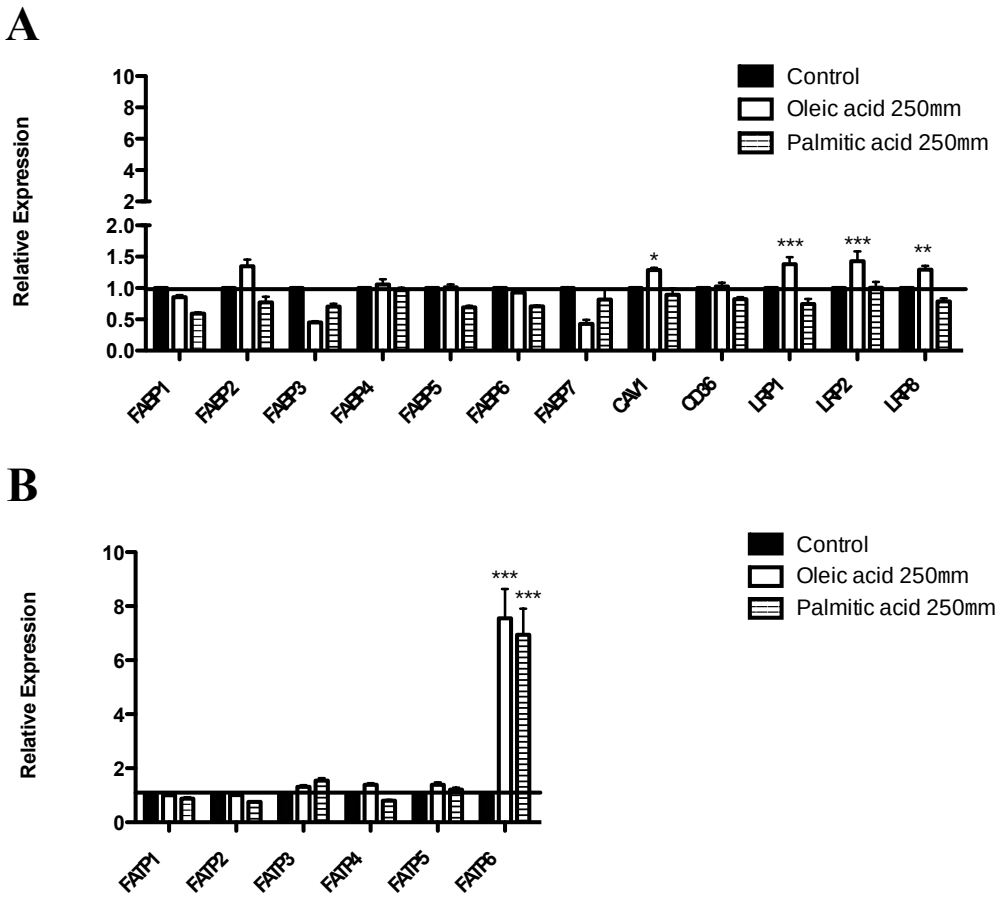

Figure 5.8: Analysis of fatty acid trafficking proteins in Huh7.5 after treatment with free fatty acids by quantitative qPCR analysis

mRNA expression of (A) FABP1-7, CAV1, CD36, LRP1, LRP2, LRP8 and (B) FATP1-6 after FFA treatment. Huh7.5 were treated with OA or PA at 250μm for 24 hours. RNA was extracted and mRNA expression was carried out using a fluidigm qPCR array® and run on triplicate arrays. Results are expressed as the mean fold change in gene expression normalized to pooled endogenous controls β-actin and GAPDH relative to control Huh7.5 defined as 1. N=3 +/- SEM. Significance expressed as * $p<0.05$, ** $p<0.01$, *** $p<0.001$ using a one way ANOVA with Bonferroni post correction.

5.3.3 VAP-1 regulates lipid accumulation in Huh7.5

Next we tested whether VAP-1 enzyme activity was able to modulate the way Huh7.5 responded to supply of exogenous FAs. We chose to test only OA in these experiments, since the pilot studies (Figure 5.1 and Figure 5.6A) suggested this had the greatest and most reliable effect on lipid accumulation. Therefore Huh7.5 were pretreated with MA, VAP-1 and hydrogen peroxide, and combinations of specific enzyme inhibitors for MAO and LOX prior to provision of OA for 6 hours. Figure 5.9 shows that methylamine+VAP-1, and the by-product of SSAO activity hydrogen peroxide all result in enhanced lipid accumulation in hepatocyte cells. This is confirmed by the representative images in Figure 5.10. Specific inhibition of SSAO using BEA had only a modest inhibitory effect, but interestingly when the inhibitors for MAOA and MAOB were added in combination with methylamine+VAP-1 there was a significant increase in lipid accumulation. Furthermore combination of methylamine+VAP-1+BAPN resulted in a decrease in OA uptake when compared to methylamine+VAP-1 alone.

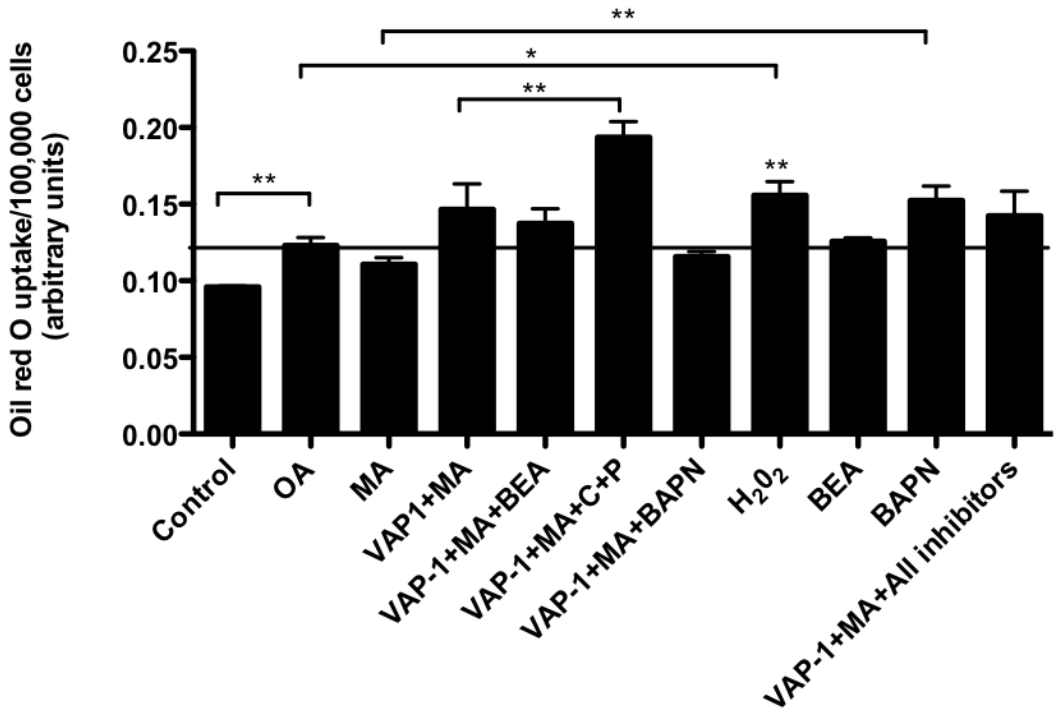

Figure 5.9: Assessment of oleic acid accumulation after VAP-1 stimuli
Accumulation of OA after VAP-1 stimulation. Huh7.5 were pretreated with either methylamine 200µm, H_2O_2 10µM, BEA 400µm, BAPN 250µm, or in combination with methylamine+VAP-1, methylamine+VAP-1+BEA, methylamine+VAP-1+C+P (C+P at 200µm), methylamine+VAP-1+BAPN, methylamine+VAP-1+BEA+C+P+BAPN for approximately 18 hours and then 6 hours with 250µm OA. Huh7.5 cells were fixed and stained with either ORO or Hoechst dye. ORO was solubilized and signal normalized to per 100,000 cells. N=3 from +/- SEM. Significance expressed as * $p<0.05$, ** $p<0.01$.

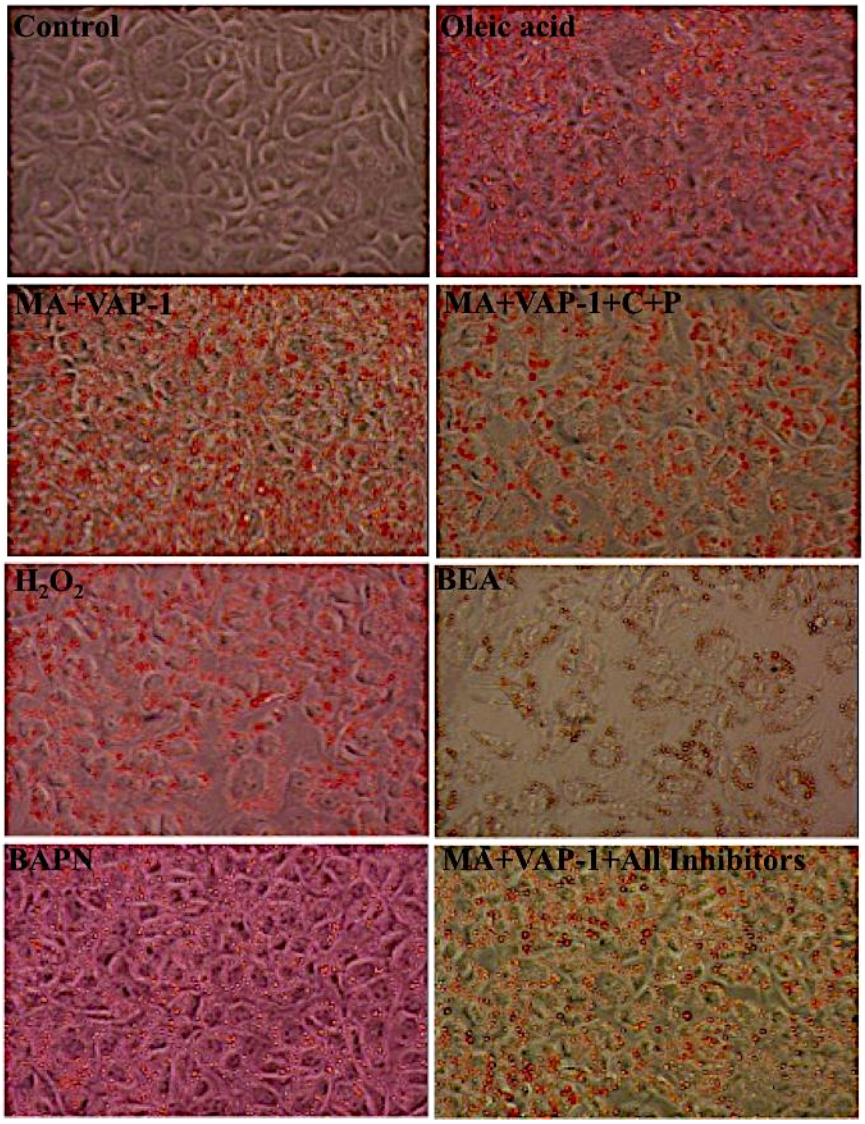

Figure 5.10: Visual assessment of oleic acid accumulation after VAP-1 stimulation

Huh7.5 were pretreated with either H_2O_2 10µM, BEA 400µm, BAPN 250µm, or in combination with methylamine (200µm)+VAP1 (500ng), methylamine+VAP-1+C+P (C+P at 200µm), methylamine+VAP-1+BEA+C+P+BAPN for approximately 18 hours and then 6 hours with 250µm OA. Huh7.5 cells were fixed and stained with ORO and representative images were captured at 40X original magnification. N=3.

5.3.4 Lipid deposits can be visualized in freshly harvested tissue specimens

Before we assessed the role of VAP-1 in lipid accumulation in our novel *ex-vivo* model we began by identifying the morphological appearance of normal and diseased tissue (normal, steatotic, NASH, ALD and PBC) using H&E and visualization of lipid deposits by ORO. H&E staining revealed normal liver architecture in the normal liver (hepatocytes shown by arrow, Figure 5.11). In contrast, the steatotic liver shows presence of macro (shown by black arrow, Figure 5.11) and microvesicular steatosis (shown by red arrow, Figure 5.11), which was confirmed with ORO (macrovesicular steatosis shown by black arrow and microvesicular steatosis, shown by blue arrow, Figure 5.11). The NASH and ALD livers show presence of inflammatory cells (shown by black arrows, Figure 5.11) and steatosis (shown by red arrows, Figure 5.11). PBC livers revealed loss of normal liver architecture and presence of bile in the liver parenchyma (shown by arrow, Figure 5.11). In Sirius red stained NASH, ALD and PBC livers, arrows indicate presence of large fibrotic tissue. In support of this, Image J analysis revealed significant more lipids in steatotic, NASH, ALD and PBC livers compared to normal based on the sampled area in five fields of view for each disease (Figure 5.12).

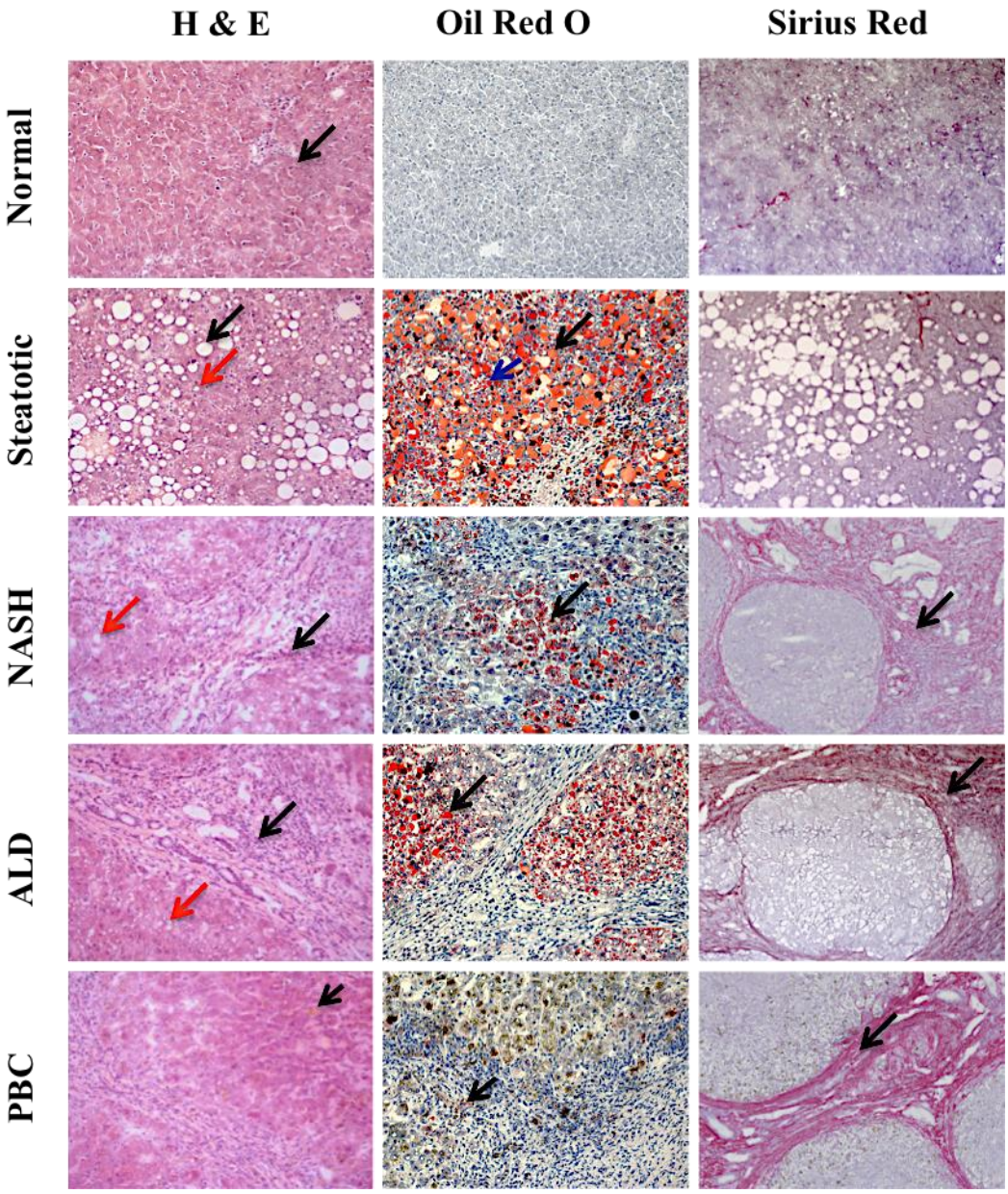

Figure 5.11: Morphological appearance of normal and diseased liver tissue.
Histological staining on acetone fixed frozen normal, steatotic, NASH, ALD and PBC livers with H&E, ORO staining and Sirius red staining. Images were captured at 20X original magnification. Images shown are representative from N=4 for ALD and N=3 for all other diseases. Arrows in H&E stained normal liver represents normal hepatocytes, in steatotic liver black arrow indicates macrovesicular steatosis and red arrow microvesicular, black arrows in NASH and ALD show inflammatory cells, red arrows indicate presence of steatosis. In PBC livers black arrow indicates bile. Black arrow in ORO stained steatotic liver indicates macrovesicular steatosis and blue arrow indicates microvesicular steatosis, black arrows in all other diseases indicate presence of steatosis. In Sirius red stained NASH, ALD and PBC livers arrows indicate presence of large fibrotic tissue.

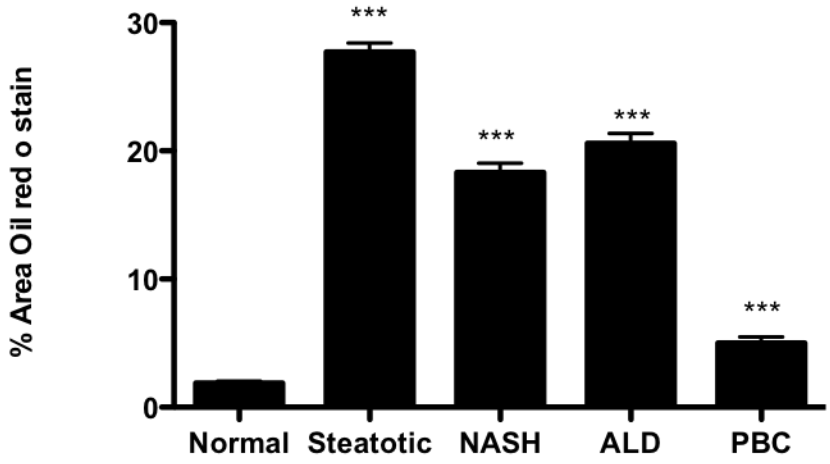

Figure 5.12: Image J analysis of lipid in normal and diseased tissue
Normal, steatotic, NASH, ALD and PBC livers were stained with ORO. Images were taken of representative fields of view, and amount of ORO staining was quantified by threshold analysis using Image J. Data represented as the % area stained positive in five high power fields, from N=4 for ALD and N=3 for all other diseases +/- SEM. Significance expressed as ***$p<0.001$.

5.3.5 Use of PCLS to model lipid homeostasis in human liver

5.3.5.1 PCLS can accumulate lipid in culture

Since this thesis set out to examine potential regulators of lipid accumulation we wanted to ensure our novel *ex-vivo* system responded to lipids. We chose to use OA only in these initial experiments, since our earlier data suggested this had the greatest and most reliable effect on lipid accumulation. Thus we added exogenous OA to the PCLS culture media and assessed whether we could regulate accumulation. MTT assay revealed viability of slices was not reduced following incubation with either 250μm or 500μm OA and if anything we observed an increase (Figure 5.13). Viability was maintained after treatment with OA at 500μm and of note also increased significantly compared to control (Figure 5.13B). ORO staining and solubilisation of fixed PCLS revealed significant uptake of 250μm OA at 6 and 24 hours which

increased with time (Figure 5.14A), similarly OA at 500μm also caused significant uptake compared to control at 3 and 24 hours, however 500μm of OA at 6 hours resulted in less uptake compared to the other two time points (Figure 5.14B). Maintenance of viability following treatment was confirmed by morphological assessment of PCLS. Figure 5.15 shows, that architecture of tissue were maintained at 3, 6 and 24 hours after 250μm OA treatment. Furthermore ORO staining revealed that although endogenous lipid was present in the liver samples (shown by arrow, Figure 5.15) there was presence of microvesicular droplets at 6 hours (shown by arrows, Figure 5.15) and both micro (shown by blue arrow, Figure 5.15) and macro vesicular droplets at 24 hours (shown by black arrow, Figure 5.15). In addition when PCLS were treated with 500μm OA the presence of large lipid filled vacuoles were evident (shown by arrows on H+E stains in, Figure 5.16). This accumulation of lipid following treatment was confirmed by ORO staining (shown by black arrows, Figure 5.16) and quantification (Figure 5.14B) suggesting increase in accumulation at both 250μm and 500μm at 24 hours with indication of earlier accumulation at 3 hours with 500μm OA.

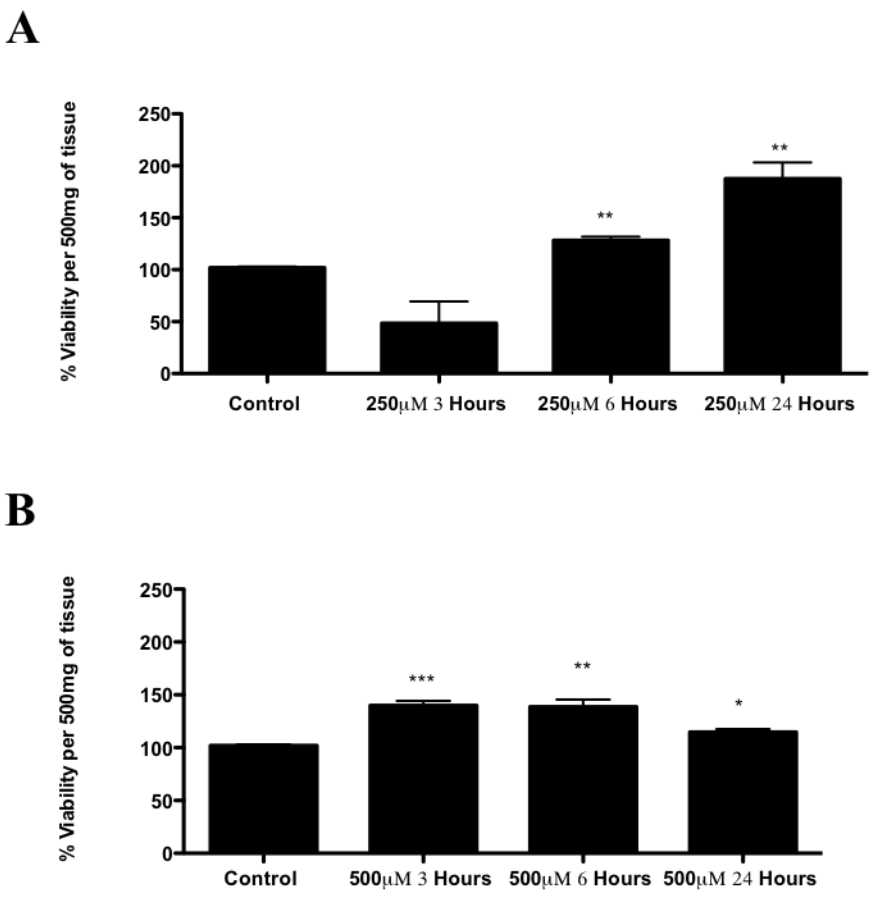

Figure 5.13: Viability of PCLS after free fatty acid treatment
Viability of PCLS in culture after treatment with OA at (A) 250μM and (B) 500μM OA for 3, 6 and 24 hours using the MTT assay. MTT signal normalized to per 500mg of tissue and data represented as % viability compared to control at 0 hours. N=3 from resected normal livers +/- SEM. Significance expressed as * $p<0.05$, ** $p<0.01$, ***$p<0.001$.

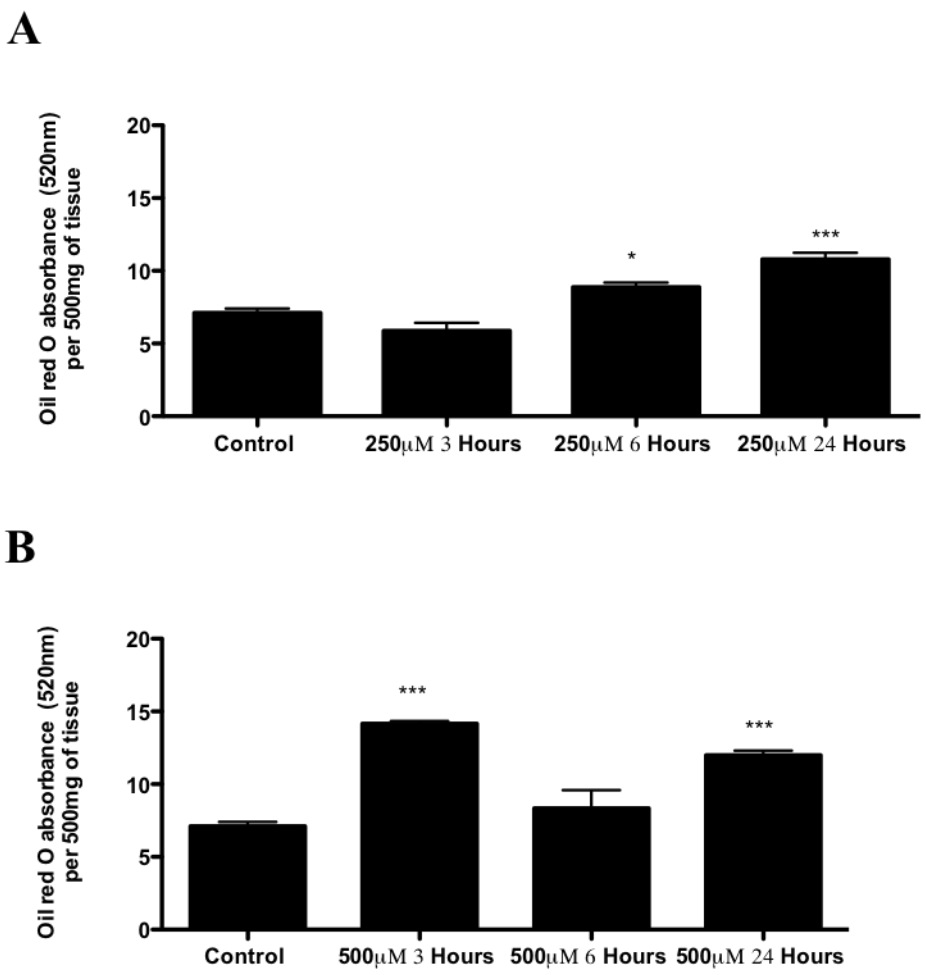

Figure 5.14: Assessment of lipid accumulation in PCLS
(A) Accumulation of OA at 250μM and (B) 500μM for 3, 6 and 24 hours. PCLS were cultured with OA with the indicated time points. PCLS were fixed and stained with ORO. ORO was solubilized and signal normalized to per 500mg of tissue. N=3 from resected normal livers +/- SEM. Significance expressed as * $p<0.05$, ***$p<0.001$.

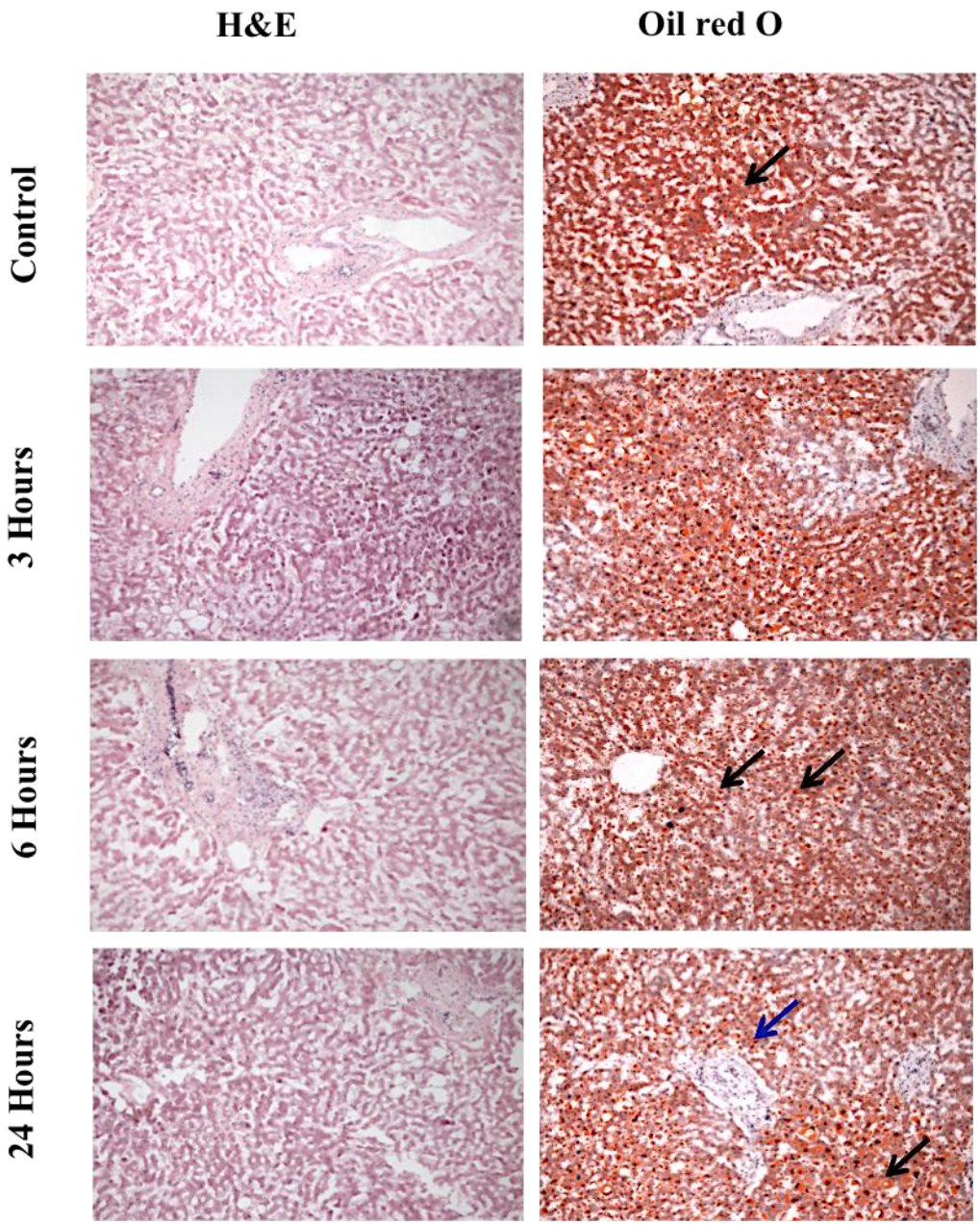

Figure 5.15: Morphological appearance of PCLS after 250µm oleic acid treatment

Histological staining of PCLS at time 0 (control), 3, 6 and 24 hours treated with 250µm OA and stained with H&E and ORO. Control stained with ORO, arrow indicates presence of endogenous lipid. Black arrows at 6 hours and blue arrow at 24 hours indicate microvesicular steatosis and also macrovesicular steatosis at 24 hours indicated by black arrow. Representative images were captured at 20X original magnification from N=3 resected livers.

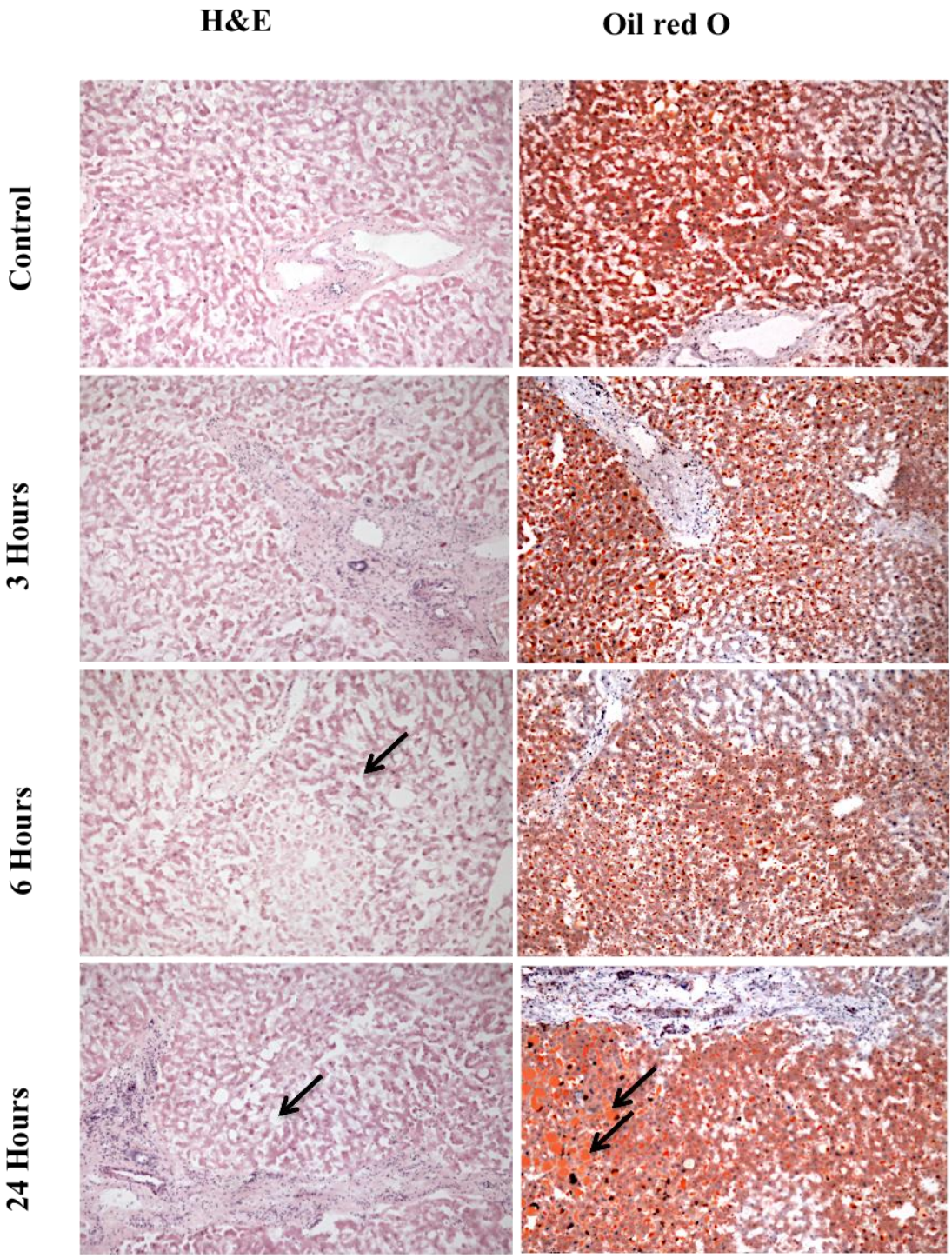

Figure 5.16: Morphological appearance of PCLS after 500µm oleic acid treatment

Histological staining of PCLS at time 0 (control), 3, 6 and 24 hours treated with 500µm OA and stained with H&E and ORO. Arrow in H&E stained PCLS at 6 hours indicates loss of cellular architecture and arrow at 24 hour indicates presence of large vacuoles confirmed as macrovesicular steatosis with ORO staining, shown by arrows. Representative images were captured at 20X original magnification from N=3 resected livers

5.3.5.2 VAP-1 and its substrate methylamine modify lipid accumulation in PCLS

Next we used the FA exposure model to test whether VAP-1 enzyme activity had any impact upon hepatic lipid accumulation. We began by using histology to confirm that our treatments were not toxic. Figure 5.17 confirms maintenance of tissue architecture in a representative normal liver following treatment with recombinant VAP-1 or methylamine or in combination with VAP-1+methylamine.

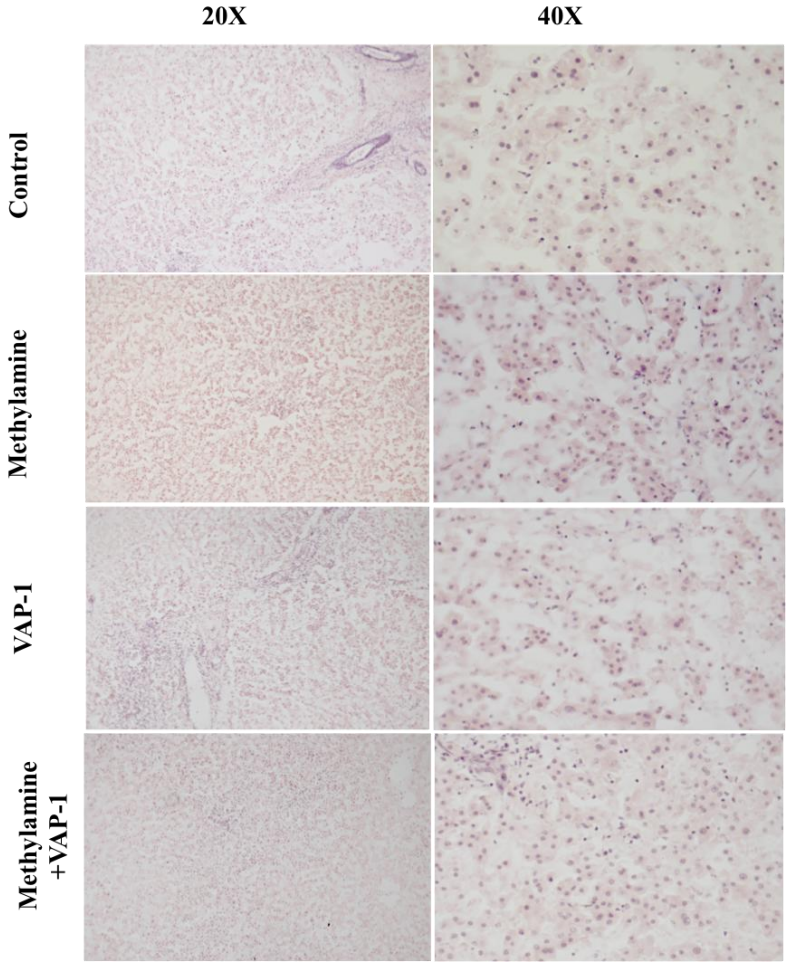

Figure 5.17: Morphological appearance of Cultured PCLS after VAP-1 stimulation
PCLS were cultured with either methylamine 200μm or VAP-1 500ng alone or in combination with methylamine and VAP-1 for approximately 18 hours. Controls were cultured in media alone for 18 hours. They were then fixed and cryosectioned for H&E staining. Images were captured at 20X and 40X original magnification. Representative images from N=3 resected/donor livers.

We tested the optimal time for which we should expose slices to FFAs after stimulation with VAP-1 reagents (since this may be different in a multi cellular environment than our single cell based system earlier) in order to determine effects on lipid accumulation. Both OA and PA were examined at 250μm for 3, 6 and 24 hours, Figure 5.18 shows that there was a significant increase in lipid accumulation compared to control after pretreatment with VAP-1 or a combination of VAP-1+MA at 6 hours for both OA and PA (Figure 5.18), this effect disappeared following longer lipid exposures (24 hours, data not shown). Treatment with methylamine alone had little effect on lipid accumulation at 6 or 24 hours, but we did note an effect at very early time points (3 hours, data not shown), which also occurred if VAP-1 was used in isolation.

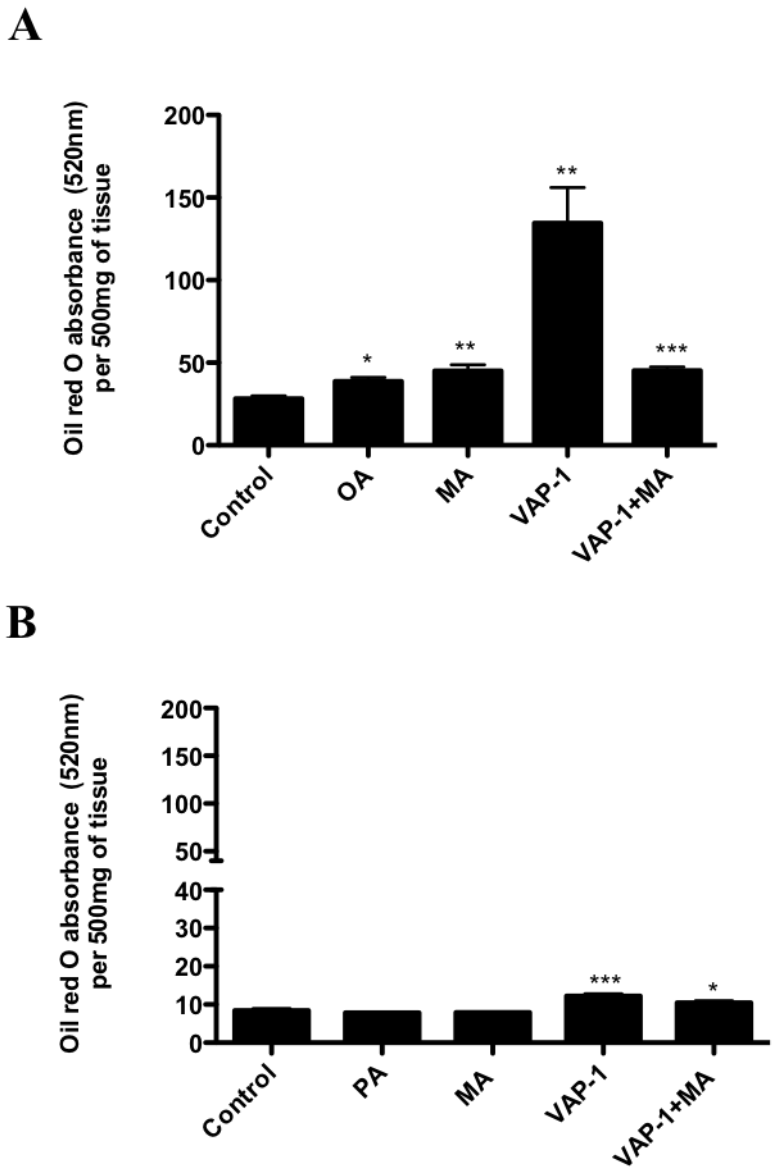

Figure 5.18: Assessment of 250µm oleic and palmitic acid accumulation after VAP-1 stimulation.
(A**)** Accumulation of 250µm OA and (B) PA after stimulation for 6 hours. PCLS were pretreated with either methylamine 200µm or VAP-1 500ng or a combination of VAP-1+methylamine for approximately 18 hours and then for 6 hours with 250µm OA or PA. PCLS were fixed, and stained with ORO. ORO was solubilized and signal normalized to per 500mg of tissue. N=3 from resected normal livers +/- SEM. Significance expressed as * $p<0.05$, ** $p<0.01$, *** $p<0.001$.

The specificity of this response was then tested by exposing PCLS to substrates for VAP-1 (MA: methylamine and BA: benzylamine), by products of VAP-1 enzyme activity (hydrogen peroxide) and specific inhibitors of both VAP-1/SSAO (BEA),

(BAPN: LOX inhibitor), and other MAOs Chlorgyline (C) and Pargyline (P) (inhibitors of MAOA and B respectively). Insulin treatment was also used as a positive control to stimulate lipogenesis within the PCLS.

Figure 5.19 shows that OA and insulin pretreatment leads to lipid accumulation in PCLS. BA appeared to be more potent in accumulating lipid than MA (Figure 5.19, panel A and B). VAP-1 added in alone appeared to be very potent at driving lipid accumulation and although MA/BA+VAP-1 treatment led to greater accumulation when compared to OA alone there was an interesting reduction versus VAP-1 alone. BEA specifically inhibited the MA/BA+VAP-1 response, and hydrogen peroxide had a modest effect. Furthermore pretreatment with MA/BA+VAP-1 with either BAPN or C and P did not result in an inhibition and if anything we saw an increase in accumulation with MA/BA+VAP-1+C+P (Figure 5.19 panel A and B). Interestingly when the inhibitors were added in alone there was an increase in lipid uptake compared to OA (Figure 5.19, panel C).

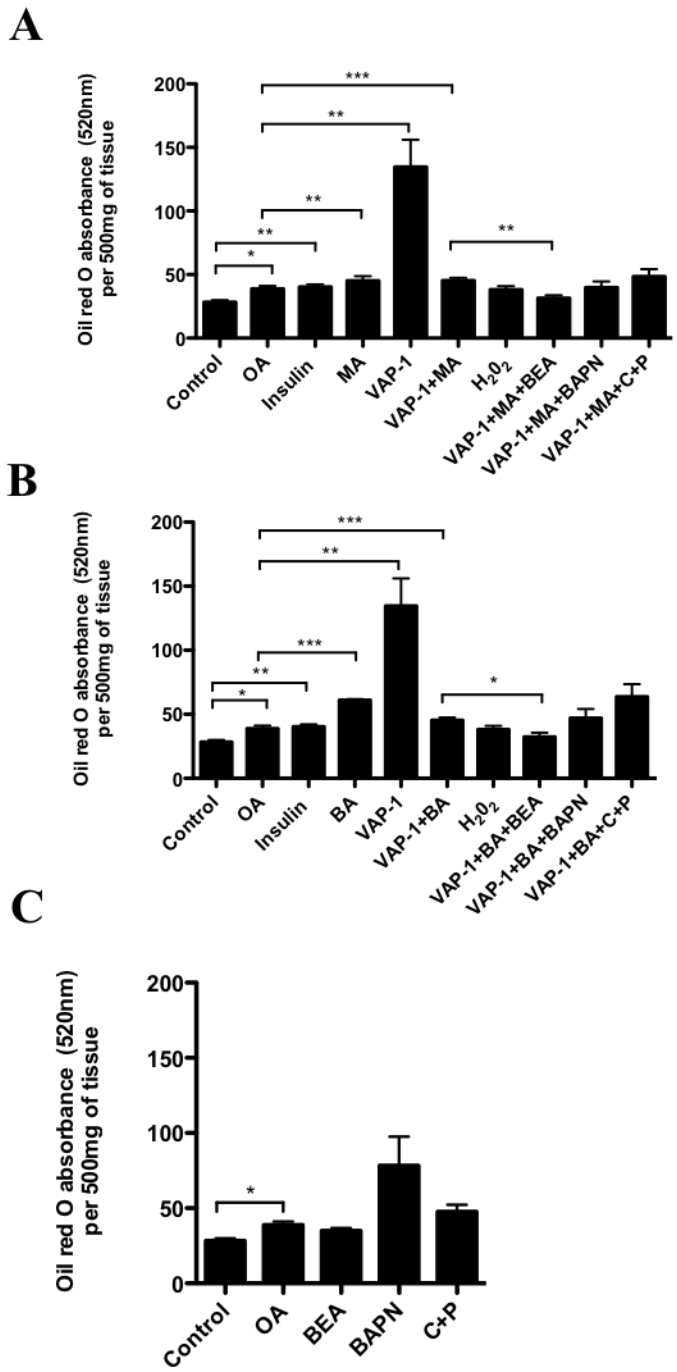

Figure 5.19: Assessment of oleic acid accumulation after VAP-1 activation
Accumulation of OA after VAP-1 stimulation using (A) methylamine, (B) benzylamine or (C) inhibitors alone. PCLS were pretreated with either insulin 0.10 IU, methylamine 200µm, benzylamine 200µm, VAP-1 500ng, H_2O_2 10µM, BEA 400µm, BAPN 250µm, C+P both at 200µm or in combination with methylamine+VAP-1, methylamine+VAP-1+BEA, methylamine+VAP-1+BAPN, methylamine+VAP-1+C+P, benzylamine+VAP-1, benzylamine+VAP-1+BEA, benzylamine+VAP1+BAPN, benzylamine+VAP-1+C+P for approximately 18 hours and then 6 hours with 250µm OA. PCLS were fixed, and stained with ORO. ORO was solubilized and signal normalized to per 500mg of tissue. N=3 from resected normal livers +/- SEM. Significance expressed as * $p<0.05$, ** $p<0.01$, *** $p<0.001$.

Interestingly when we used the saturated FA, PA we found that there was a small effect of VAP-1 alone compared to when unsaturated OA was used, however there was still a significant accumulation of lipid versus PA alone (Figure 5.20). Furthermore we found that BAPN and not BEA or C+P inhibited the VAP-1+MA response and interestingly we found that when BA was used as the substrate in combination with VAP-1+BA+BAPN or VAP-1+BA+C+P there was a significant increase in lipid accumulation compared to when VAP-1+BA was added in alone. Thus we tested whether the inhibitors themselves had any effect on lipid accumulation (Figure 5.19 panel C and Figure 5.20 Panel C), and interestingly we found that BAPN and C+P enhanced lipid accumulation compared to either OA or PA added in alone and that OA effects were more potent, however this effect was significant in PA treated PCLS only. Overall when comparing the pretreatment of PCLS with VAP-1 and its substrates/metabolites and subsequent stimulation of OA and PA we found that those treated with OA resulted in the largest accumulation (Figure 5.19).

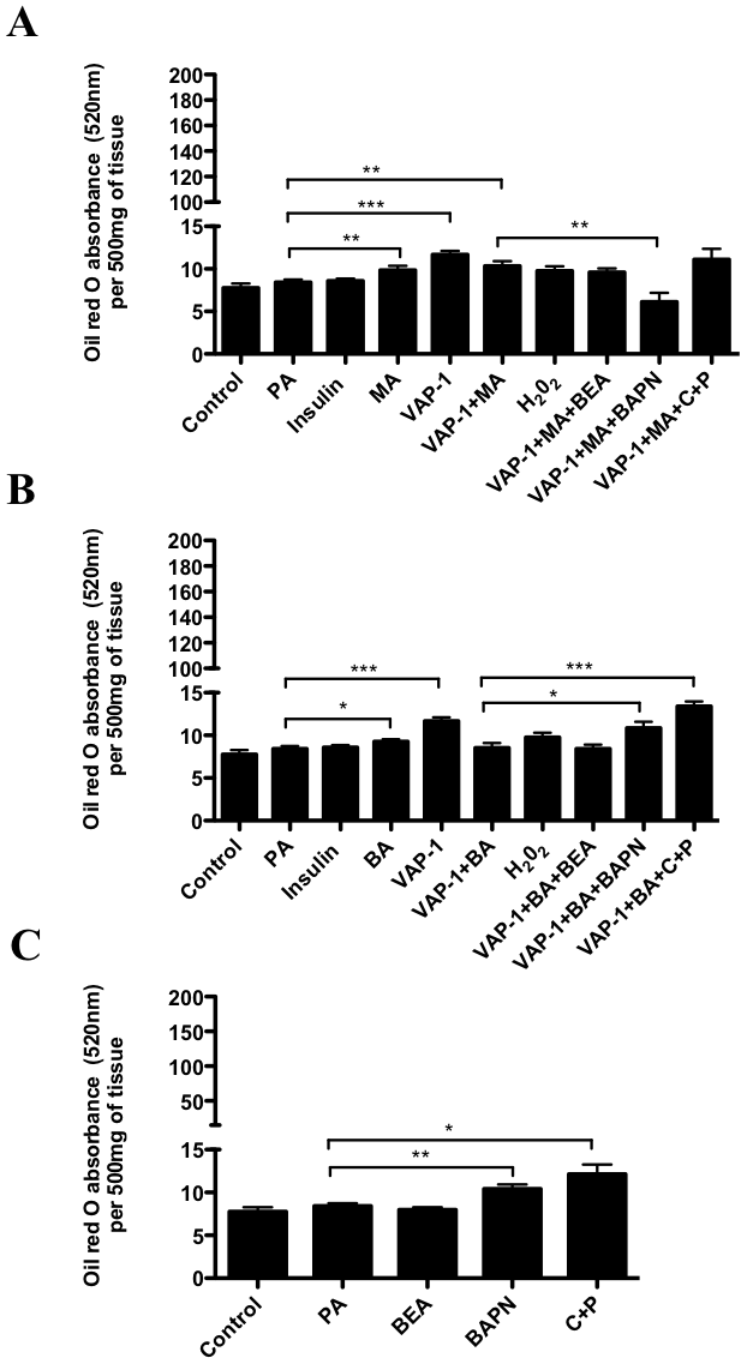

Figure 5.20: Assessment of palmitic acid accumulation after VAP-1 activation
Accumulation of PA after VAP-1 stimulation using (A) methylamine, (B) benzylamine or (C) inhibitors alone. PCLS were pretreated with either insulin 0.10 IU, methylamine 200µm, benzylamine 200µm, VAP-1 500ng, H_2O_2 10µM, BEA 400µm, BAPN 250µm, C+P both at 200µm or in combination with methylamine+VAP-1, methylamine+VAP-1+BEA, methylamine+VAP-1+BAPN, methylamine+VAP-1+C+P, benzylamine+VAP-1, benzylamine+VAP-1+BEA, benzylamine+VAP1+BAPN, benzylamine+VAP-1+C+P for approximately 18 hours and then 6 hours with 250µm PA. PCLS were fixed, and stained with ORO. ORO was solubilized and signal normalized to per 500mg of tissue. N=3 from resected normal livers +/- SEM. Significance expressed as * $p<0.05$, ** $p<0.01$, *** $p<0.001$.

5.3.5.3 Quantification of triglyceride secretion in PCLS after VAP-1 stimulation

In order to assess whether the increase in accumulation after VAP-1 and its stimuli was due to a decrease in triglyceride secretion we carried out a triglyceride secretion assay. We tested supernatants from samples where FFA accumulation had been tested with PA and pretreatment with MA, VAP-1, hydrogen peroxide or combination of VAP-1+MA, VAP-1+MA+BEA, VAP-1+MA+C+P, VAP-1+BA. We found that compared to control in all treatments tested there was a decrease in triglyceride secretion and addition of specific inhibitors for example in VAP-1+MA+BEA treated samples there appeared to be more triglyceride secretion compared to VAP-1+MA this is supportive of our earlier data (see Figure 5.20A) were there is a small decrease in accumulation when comparing VAP-1+MA and VAP-1+MA+BEA. Furthermore supernatants from VAP-1+MA and VAP-1+MA+C+P had similar levels of triglyceride secretion again supporting our earlier data (see Figure 5.20A).

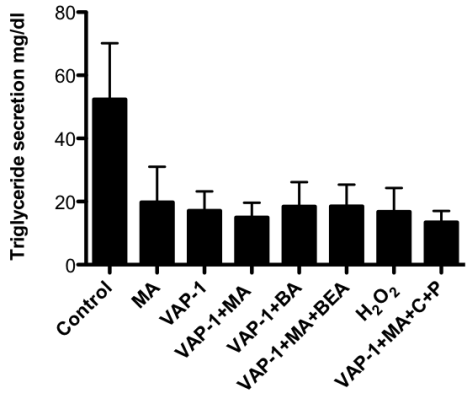

Figure 5.21: Assessment of triglyceride secretion after VAP-1 stimulation in PCLS
PCLS were pretreated with either, methylamine 200µm, VAP-1 500ng, H_2O_2 10µM, or in combination with methylamine+VAP-1, benzylamine+VAP-1, methylamine+VAP-1+BEA, methylamine+VAP-1+C+P, for approximately 18 hours and then 6 hours with 250µm PA. Supernatants were collected after treatments and triglyceride secretion quantified. N=3 from resected normal livers +/- SEM.

5.3.6 VAP-1 deficient animals exhibit reduced steatosis in response to a high fat diet

Next we wanted to check whether VAP-1 deficient mice had altered lipid accumulation compared to WT mice fed on a HFD. Interestingly ORO staining and quantification of WT and VAP-1 KO mice revealed a significant reduction of lipid in the VAP-1 deficient mice (Figure 5.22A) and this was also evident visually (Figure 5.22B).

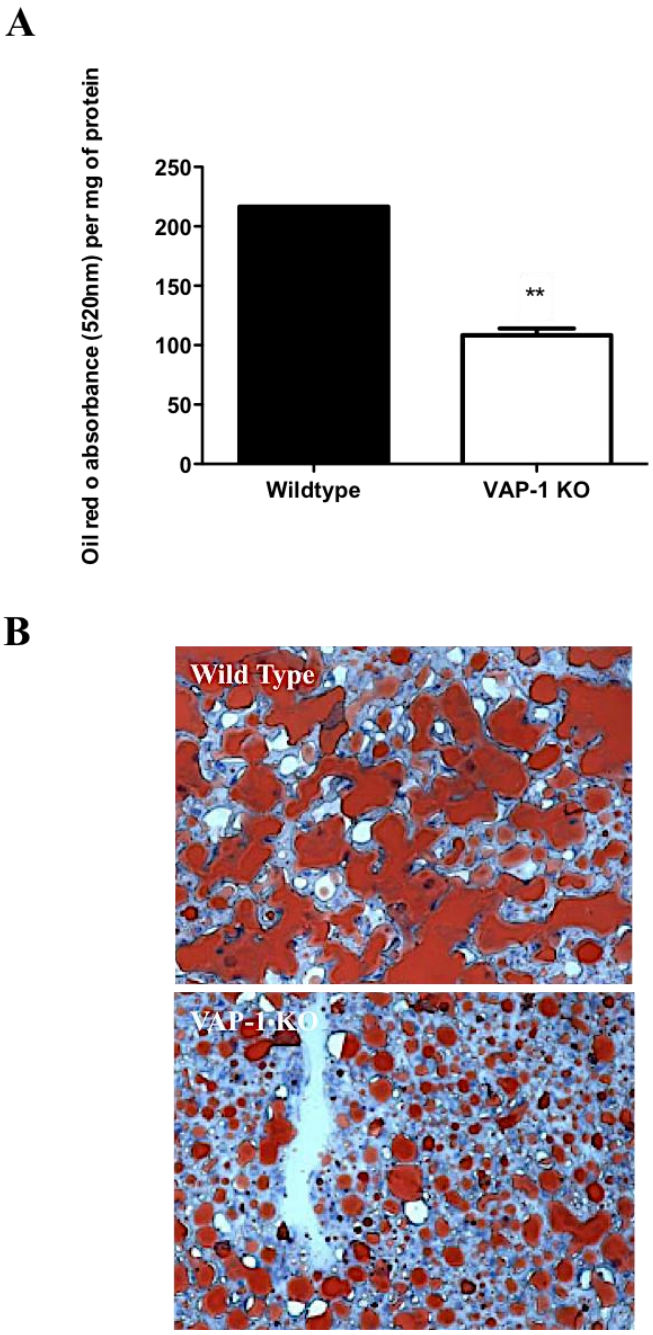

Figure 5.22: Assessment of lipid accumulation in WT and VAP-1 KO mice
Accumulation of lipid in WT and VAP-1 KO mice fed on a high fat diet for 12 weeks. (A) Livers from WT and VAP-1 KO mice were stained with ORO, which was then solubilized and expressed relative to protein concentration for each group of mice, +/- SEM. Significance expressed as **p<0.01. (B) ORO images of WT and VAP-1 KO mice, representative images from N=3 (Mouse samples obtained from Lee Claridge).

5.3.7 VAP-1 and methylamine alter the expression of fatty acid trafficking proteins in PCLS

In order to begin to determine the mechanism by which VAP-1 and methylamine resulted in increased lipid accumulation in tissue slices after FA exposure we used qPCR to measure the mRNA transcript levels of the FATP1-6, FABP1-7, CAV1, CD36, LRP1, LRP2 and LRP8 in PCLS after treatment (VAP-1 interventions only). Results were normalized to the house keeping genes β-actin and GAPDH and expressed relative to control PCLS, which were set as 1. Pretreatment of PCLS with methylamine resulted in an increase in mRNA expression of FABP2 and LRP1 and there was a trend for downreguation of all other transporters except FABP4, which remained unchanged (Figure 5.23), methylamine also caused an increase in mRNA expression for FATP3 and FATP6, with a suggestion of increased FATP4.

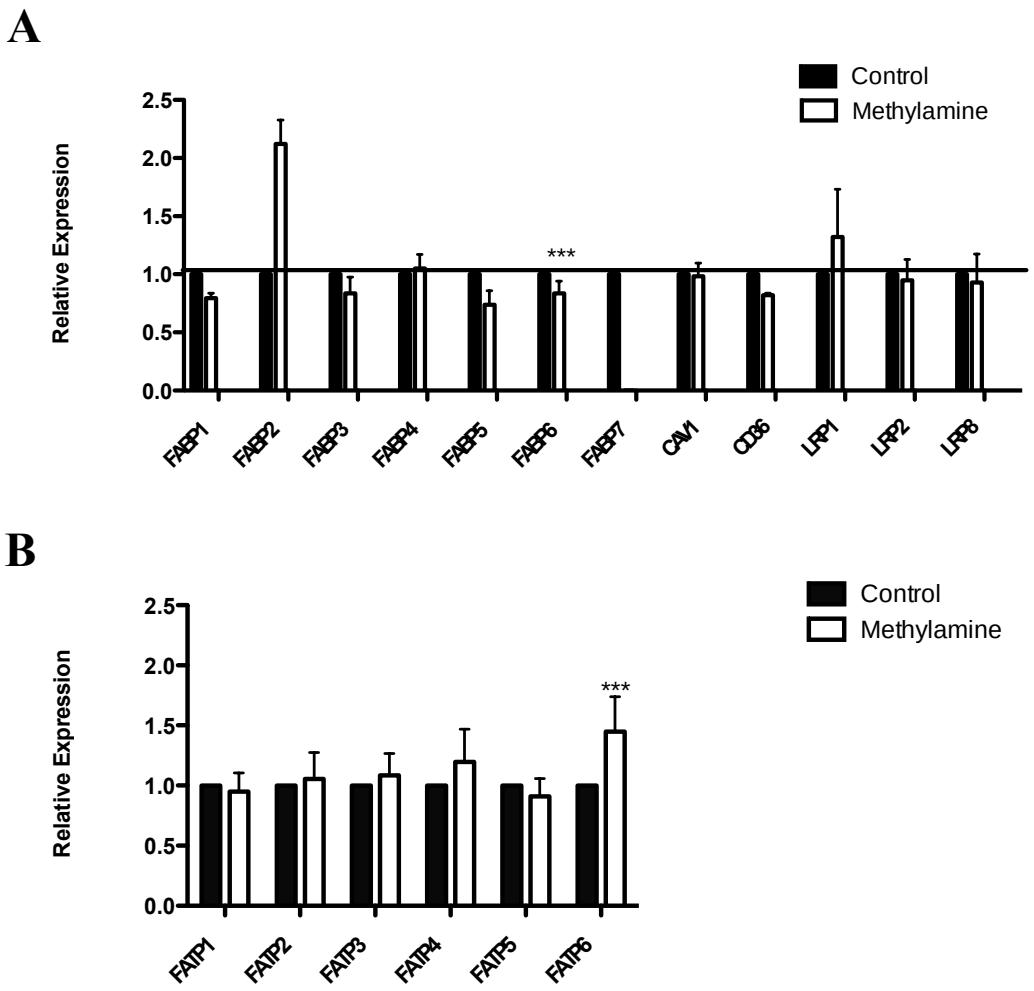

Figure 5.23: Analysis of fatty acid trafficking proteins in PCLS after methylamine treatment by quantitative qPCR analysis

mRNA expression of the fatty acid trafficking proteins (A) FABP1-7, CAV1, CD36, LRP1, LRP2 and LRP8 and (B) FATP1-6 after VAP-1 stimulation with methylamine. PCLS were treated with methylamine 200μm for approximately 4.5 hours. RNA was extracted and mRNA expression was carried out using a fluidigm qPCR array® run on triplicate arrays. Results are expressed as the mean fold change in gene expression normalized to pooled endogenous controls β-actin and GAPDH relative to control livers defined as 1 +/- SEM with means from two normal resected livers. Significance expressed as ***$p<0.001$ using a one way ANOVA with Bonferroni post correction.

5.4 Discussion

VAP-1 has been shown to have a role in storage and distribution of lipids (Yu et al., 2002), (Carpene et al., 2006), (Marti et al., 2001), (Stolen et al., 2004a) thus this thesis set out to examine the potential contribution of VAP-1 in accumulating lipid in the liver. In this chapter we show that VAP-1 has the ability to regulate lipid accumulation in Huh7.5 cells and in human PCLS. Furthermore VAP-1 deficient mice show reduced steatosis fed on a HFD and endogenous activation of VAP-1 by its substrate MA enhances expression of FABP2, LRP1, FATP2, FATP3, FATP4 and FATP6 in liver tissue.

5.4.1 Free fatty acids induce altered levels of steatosis

The hallmark of NAFLD is the presence of TAG in the liver and although the roots of these lipids is unknown there have been many speculations that the pathophysiology of NAFLD and NASH is due to an influx of FFA from adipocytes (Chen et al., 1987), (Frayn, 2001) as result of inhibition of lipolysis in the IR state or from increase flux of FFA from the diet. In particular two FFA the monounsaturated OA and saturated PA have been found at high levels in NAFLD and NASH patient serum (de Almeida et al., 2002), (Araya et al., 2004) and are abundantly available in serum and via the diet, thus we wanted to study the effects of these two FFA in particular.

We found that there was a clear time and dose dependent increase in FFA accumulation in Huh7.5 cells however this was associated with increasing cell loss with, increasing time and concentration for example at 1500μm. These toxic effects have been reported previously (Malhi et al., 2007), (Malhi et al., 2006), (Ricchi et al., 2009). Furthermore using our basic ORO colorimetric method and visual assessment

OA appeared to be more steatogenic and less toxic than PA. These findings support others where PA has been shown to induce apoptosis in cells (Ahn et al., 2013), and has been shown to poorly incorporate lipid in droplets (Mei et al., 2011). Furthermore combined treatment of OA and PA has been shown to protect cells from apoptosis (Ahn et al., 2013) suggesting a protective role for OA. In support of this PCLS treated with OA, if anything have an increase in viability (Figure 5.13). Interestingly we noticed presence of both macro and microvesicular steatosis in Huh7.5 treated with OA and this finding is consistent with clinical features of NAFLD and NASH and may be due to the presence of PAT proteins which have been associated with different sizes of lipid droplets (Straub et al., 2008).

We also looked at the effects of OA on HSEC since HSEC and hepatocytes are in close proximity *in vivo* and their unique fenestrations allows passage of materials to hepatocytes they have the ability to exacerbate disease pathogenesis. We found for the first time that human HSEC accumulated lipid with minimal toxicity at the lowest dose tested for the longest time point. Overall lipid accumulation was less than that seen in hepatocytes which may suggest that FAs would normally be rapidly utilized or possibly passed on to underlying cells via the fenestrations. Studies suggest that uptake of lipids by endothelium is sensitive to VEGFB (Hagberg et al., 2010), which would be abundant in the liver environment, and subsequently passed onto the surrounding tissue for use for example Hagberg et el showed that VEGFB regulates the transcription of FATP through PI3-K dependent pathway and thus the subsequent uptake of LCFA, in addition they showed VEGFB KO mice showed reduced lipid accumulation in the liver, heart, muscle, and brown adipose tissue and that surplus lipids were shunted to white adipose tissue (Hagberg et al., 2010).

5.4.2 FFA induce expression of fatty acid trafficking proteins in Huh7.5

FFAs provide fuel for the accumulation of TAG in the liver and pathogenesis of NAFLD and NASH, and so understanding the regulation of their uptake may have clinical relevance. We found that OA induced expression of FABP2, CAV1, LRP1, LRP2, LRP8 and FATP4 whilst both OA and PA induced expression of FATP3, FATP5 and FATP6, and in contrast FABP3 was down regulated by OA. To our knowledge this is the first study to document the effects of OA or PA on fatty acid trafficking proteins in Huh7.5 cells. However OA induced expression of LRP1 has been reported in adipocytes were OA activates PPARγ-induced expression of LRP1 (Gauthier et al., 2003). FABPs have the ability to partition lipids intracellularly to various metabolic fates for example FABP2 has been suggested to have a role in TAG synthesis (Hardwick et al., 2009), whilst FABP3 has a role in β-oxidation (Hardwick et al., 2009) and FATP4 in TAG synthesis and β-oxidation (Hardwick et al., 2009). This fits with our observations where OA increased expression of FABP2 resulting in intracellular accumulation of TAG and in contrast FABP2 was down regulated in PA treated Huh7.5 cells which had poor accumulation of TAG. The down regulation of FABP3 fits with storage of lipid rather than oxidation. In contrast FATP4 may initially regulate TAG synthesis, which then switches to β-oxidation when the cell requires energy. FATP3, FATP5 and FATP6 were upregulated by both OA and PA but the functions of these are unknown. However it is speculated that FATP3 may be involved in FA activation rather than transport (Pei et al., 2004), whilst FATP5 increase expression has been shown to increase hepatic FA uptake (Doege and Stahl, 2006), this fits with our results were we see increase expression of FATP5 and hence more intracellular lipid accumulation in OA treated cells compared to PA. Of note in Chapter 3 we found FATP6 mRNA expression upregulated in NASH and ALD livers,

but in the absence of mRNA in the cultured cell types we studied. We speculated that expression is only turned on in disease or restricted to cells, which we have not studied. However here we show that both OA and PA acid induced expression of FATP6 in Huh7.5. Since FATP6 has been shown to have a role in LCFA transport (Gimeno et al., 2003) this suggests that its directly implicated in disease pathogenesis via FA induced expression.

5.4.3 The activity of VAP-1 regulates lipid accumulation in Huh7.5

Since sVAP-1 levels are elevated in liver disease it is possible that circulating sVAP-1 and amines could have local insulinomimetic effects in hepatocytes. During hepatic steatosis it is the hepatocytes which become fatty, and since our initial data in Chapter 3 indicated there was a possibility Huh7.5 could express VAP-1 we felt it was prudent to use Huh7.5 as a test cell type to investigate the role of VAP-1 activity. We found that an exogenous supply of VAP-1+MA and the by-product of VAP-1 activity hydrogen peroxide all enhanced lipid accumulation in Huh7.5 cells. This is supported by other studies which have shown a role for VAP-1 in lipid accumulation for example in the 3T3-L1 pre adipocyte cell line were administration of methylamine promotes adipocyte differentiation (Mercier et al., 2001) and in 3T3 F442A preadipocyte cells VAP-1 substrates have been shown to enhance lipid accumulation (Fontana et al., 2001). Further studies have also shown antilipolytic effects of activated VAP-1 (Morin et al., 2001) which would also lead to accumulation within cells. Interestingly we found that this effect was only modestly reduced on addition of BEA. Here it could be argued that BEA is not as potent an inhibiter as for example such as semicarbazide. However we have shown it effectively blocks VAP-1 activity in our glucose assays (Chapter 4) and its potency and specificity have been confirmed

by others (Yu et al., 2001). Thus to rule out contribution from other AO we used specific inhibitors for these, and found that on addition of C+P to our samples we saw a further increase in lipid accumulation. This increased accumulation when MAO-A and B are inhibited suggested that these amine oxidases probably do not contribute to lipid uptake upon deamination of methylamine. These inhibitors could instead be increasing viability of cells, as reported for other MAO inhibitors (Johnson et al., 2010) or causing a compensatory upregulation of VAP-1. Of note however, inhibition of LOX with BAPN resulted in a decrease in VAP+MA stimulated lipid accumulation. This could suggest that LOX can deaminate MA, but this is not supported by evidence in the literature and rather LOX has more of a role in remodeling of the extracellular matrix by oxidation of lysine (Smith-Mungo and Kagan, 1998). However the variability in effects of enzyme inhibitors in isolation, and when combined in the presence of exogenous VAP-1 suggests that alternate approaches with exclusively specific inhibitors and substrates, or selective KO of key enzymes would be worthwhile.

The other important issue to clarify is the modest effects of methylamine when used in isolation. This may suggest a lack of endogenous VAP-1 expression by Huh7.5 cells, which disagrees with our qPCR findings but would fit with lack of hepatocyte staining in liver tissue. It is possible that other endogenous or model amines such as benzylamine or tyramine are better substrates for VAP-1 in this system, or it may well be that an acute treatment of 18 hours is not sufficient to see effect. Certainly a more chronic treatment, for example between 7-8 days may be more potent as shown by some studies, which have used 3T3 F442A and 3T3-L1 cells to measure TAG content (Fontana et al., 2001), (Mercier et al., 2001).

5.4.4 The role of VAP-1 in altering lipid accumulation in PCLS

Our staining data confirmed as expected that normal/resected livers contained minimal endogenous lipid thus these livers were used for functional experiments. Treatment with either exogenous FFAs increased viability which could be due to enhanced proliferation of cells as has been reported previously, (Wicha et al., 1979), (Maedler et al., 2001). Certainly the degree of lipid accumulation in PCLS corresponded with viability. It must be noted that there are problems in using physiological specimens for analysis of mechanisms leading to fat accumulation since it can be hard to distinguish between endogenous and newly synthesized lipids. Nevertheless we are confident this method worked well since we observed presence of both micro and macrovesicular steatosis after OA treatment. Future studies using BODIPY labeled FFA would allow us to distinguish between endogenous and exogenous lipids and our use of MALDI imaging and GC in the next chapter is also informative.

We found both MA and BA enhanced lipid accumulation in PCLS and this was most likely due to activation of endogenous VAP-1. These results are the first to be reported in the liver although VAP-1/SSAO substrate effects have been reported in single cell systems as discussed earlier (Mercier et al., 2001), (Fontana et al., 2001), (Morin et al., 2001). Importantly similar results have been reported *in vivo* where benzylamine and vanadate causes a 45% increase in adipose tissue fat deposition in diabetic rats (Marti et al., 2001), and transgenic mice overexpressing VAP-1/SSAO chronically supplemented with methylamine have increased BMI and abdominal fat pad weight (Stolen et al., 2004a). This supports the idea that the SSAO activity of VAP-1 influences the disposal of lipid at a variety of sites.

Interestingly we found that BA appeared to be more potent than MA, suggesting that BA may have a higher specificity/affinity for VAP-1 than MA as has been shown for other substrates (Yraola et al., 2006). In agreement, MA has been proposed as having the lowest affinity of some endogenous substrates such as histamine, dopamine and also synthetic BA for VAP-1 (Lyles, 1995). Certainly benzylamine is used in *in vitro* experiments because of its potency, but it is not a physiological ligand and thus this is why MA was used as it's found in cigarette smoke and food and thus may be in the liver from the gut. We noticed that when extra VAP-1 was added into the PCLS system there was a stark increase in lipid accumulation, which suggests the presence of unidentified endogenous substrates, which have higher affinity over MA for example such as tyramine, histamine or dopamine (Lyles, 1995). However when both VAP-1+MA are added, the excess of MA may permit it to function as a preferential substrate or a competitor with higher affinity over endogenous substrates, but is not able to induce the most potent effects. This is analogous to studies by Salmi et al who have shown that addition of BA reduces VAP-1-dependent lymphocyte binding to endothelial cells. Thus they suggested BA was a competitor for the actual endogenous substrate for VAP-1 (Salmi et al., 2001). However regardless of substrate specificity in our experiments the finding that BEA specifically inhibited the MA/BA+VAP-1 effect, confirms that VAP-1 is altering lipid accumulation in PCLS. Furthermore hydrogen peroxide elicited an effect, albeit modest, and as reiterated earlier this may be because of lack of bioavailability in the tissue media due to evaporation, breakdown by peroxidases or that a single dose of exogenously added hydrogen peroxide may be less effective in causing the mobilization of insulin stimulated fatty acid trafficking proteins and hence accumulation of lipid than locally generated oxidants produced by VAP-1 catalysis.

Further evidence that the observed lipid accumulation is due to VAP-1 and not other AO arose through addition of BAPN, C or P in combination with MA/BA+VAP-1. These inhibitors did not lead to inhibition of lipid accumulation, and if anything caused an increase. We observed the same effect in Huh7.5 with MA suggesting substrate, FFA and possibly cell specific effects of inhibitors. Interestingly when the inhibitors BAPN/C/P were added in alone we found an increase in lipid accumulation compared to OA alone. These effects have not been reported previously but its possible as suggested earlier that blocking of AO leads to upregulation of VAP-1 activity, or these inhibitors may be causing allosteric effects in VAP-1 thus increasing enzyme activity and hence increasing lipid accumulation. Of note, presence of the LOX inhibitor BAPN did cause a small decrease in lipid accumulation in PCLS and Huh7.5 in the presence of MA but not BA. This may suggest either that SSAO-dependent deamination of MA is also inhibited by BAPN, that LOX can use MA as a substrate or that there are other non-specific effects of BAPN. Since administration of BAPN does not reduce weight gain in rat models (Mercier et al., 2009), its seems unlikely that LOX is involved in lipid accumulation which points to substrate specific, off-target effects of BAPN.

Importantly the net accumulation of lipids after VAP-1 interventions fits with our triglyceride export data, which shows reduced triglyceride secretion after VAP-1 interventions and this fits with Aalto et al study who showed an inverse relationship between VAP-1 and triglyceride levels in serum (Aalto et al., 2012). Thus the likely cell fate of lipids may be that they are either being oxidized or stored within the cell.

The strongest evidence for a role of VAP-1 in lipid homeostasis was supplied by our VAP-1 null mouse experiments. Here we found reduced steatosis when VAP-1-/- mice were fed on a HFD compared to WT mice. This fits with studies where specific inhibition of VAP-1/SSAO activity leads to a decrease in subcutaneous fat deposition in obese Zucker rats (Prevot et al., 2007) and that inhibition of both MAO and VAP-1/SSAO reduces calorific intake, weight gain and also fat accumulation (Carpene et al., 2007). Similarly blockade of VAP-1/SSAO activity with potent inhibitors and semicarbazide in mice leads to a reduction in weight gain (Yu et al., 2004), (Mercader et al., 2011). Here the authors speculated that reduced weight gain was linked to both reduced glucose uptake and lipogenesis, which fits well with both our glucose uptake data and this chapter. Furthermore fatty streaks in aortae developed due to chronic treatment with methylamine in mice fed on a high cholesterol diet are decreased when these mice are administered with inhibitors of SSAO activity (Yu et al., 2002). In addition VAP-1/SSAO inhibitors in mice have been shown to decrease the levels of the toxic aldehyde malondialdehyde (MDA) which is elevated in diabetes and causes protein cross linking (Slatter et al., 2000). It is a marker of oxidative stress and also a by product of lipid oxidation (Yu et al., 2002) mainly derived from arachidonic acid (Esterbauer et al., 1990).

5.4.5 Activity of VAP-1 alters expression of lipid trafficking proteins

In order to begin to understand the possible mechanism by which VAP-1 may be altering lipid accumulation in PCLS we assessed the levels of various fatty acid trafficking proteins, which we previously documented in Chapter 3. Since VAP-1 has insulinomimetic effects its possible that VAP-1 activity may be accumulating lipid by translocation of either FATP1 or LRP1 which are both insulin sensitive transporters

(Stahl et al., 2002) and we have shown Huh7.5 express both. Furthermore FATP1 has been reported to be expressed in the endoplasmic reticulum in Huh7.5 cells (Krammer et al., 2011) an organelle were the bulk of neutral lipid synthesis occurs (Sturley and Hussain, 2012). Furthermore as discussed earlier OA induces expression of a number of fatty acid trafficking proteins for example FABP2.

Similarly for the PCLS system we assessed changes in transporter expression after MA treatment in the absence of exogenous FAs thereby minimizing confounding effects from exogenously added lipid. We found FABP2, LRP1, FATP2, FATP3, FATP4 and FATP6 were upregulated in response to MA treatment. As discussed in Chapter 3 many of these proteins have implications in the development of fatty liver. For example the Ala54Thr polymorphism of FABP2 has been associated with increased risk of fatty liver disease. In mice livers, FATP2 KO results in improved insulin sensitivity and a reduction in hepatic steatosis (Falcon et al., 2010). Similarly FATP4 which has been associated with obesity and IR (Gertow et al., 2004), is overexpressed in rat fatty liver (Feng and Chen, 2005). Furthermore in hepatocytes from mice lacking LRP1, HDL export is reduced (Basford et al., 2011) and in adipocytes lacking LRP1 lipid uptake is impaired and lipids are directed to the liver resulting in hepatosteatosis (Terrand et al., 2009). Thus it is possible that in the *in vivo* environment LRP-1 in the liver is upregulated in an attempt to remove VLDLP rich in TAG in the IR state.

Thus a possible mechanism explaining VAP-1 derived lipid accumulation could be that upregulation of LRP1 leads to endocytosis and breakdown of TAG rich VLDLP and chylomicron remnants (Terrand et al., 2009) leading to cellular accumulation of

lipid. However with almost 40 ligands for LRP1 (Herz and Strickland, 2001) further work would be needed to examine which ligand binds as a result of VAP-1 activity. Certainly in the post absorptive state, hepatic LRP1 has been shown to increase clearance of chylomicron remnants when it translocates to the plasma membrane in response to insulin (Laatsch et al., 2009). In addition upregulation of FATP2 and FATP6 leads to enhanced uptake of LCFA (Gimeno et al., 2003), (Krammer et al., 2011). The subsequent FA would then need to be activated via FATPs by their ACS leading to targeting for storage or β-oxidation to the mitochondria. For example FATP3 has been reported to have a preferential role in activation of FA (Pei et al., 2004). Since knockdown of FATP3 in rat hepatocytes results in a decrease in lipogenic transcription factors (Bu et al., 2009) disease-induced upregulation could contribute to steatogenesis. The activated FA destined for storage is then associated with FABP2 or FATP4 which have reported roles in TAG synthesis (Hardwick et al., 2009), with a role in β oxidation for FATP4 (Hardwick et al., 2009). Furthermore FABP2 overexpression in cell lines has been linked to reduced lipoprotein export (Levy et al., 2009) probably due to defective trafficking of FA to regions of lipoprotein assimilation (Levy et al., 2009). Of note, we found that many of these transporters were upregulated in NASH and ALD livers (Chapter 3).

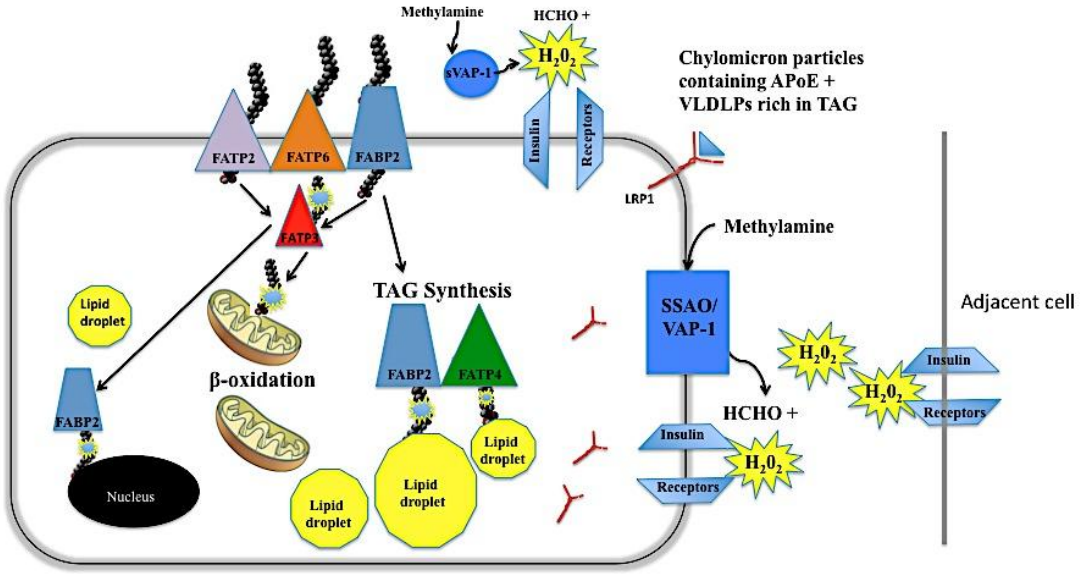

Figure 5.24: Schematic showing the hypothesized role of lipid transporters in liver, which are elevated as a result of VAP-1 activity

Membrane bound VAP-1-dependent catalysis of methylamine leads to production of hydrogen peroxide, which possibly stimulates tyrosine phosphorylation of insulin receptors. This leads to LRP1 translocation to the cell membrane in a manner similar to insulin were it picks up chylomicron remnants and VLDLPs rich in TAG. The activity of VAP-1 also leads to upregulation of FATP2, FATP6 and FABP2 which take up FA, these are then activated by FATP3 and targeted to either β-oxidation or storage were FABP2 and FATP4 have a role in formation of TAG synthesis. Activated FA can also be transported to nuclear receptors such as PPARs and NF-κB hence regulating genes, which are involved in metabolic and inflammatory processes. sVAP-1 and membrane bound VAP-1 production of hydrogen peroxide may also have local insulinomimetic effects on neighboring cells.

In all we have shown that the activity of VAP-1 alters development of hepatic steatosis in mice and, has a role in lipid accumulation in Huh7.5 and human PCLS, with changes in transporter expression induced by both FFA and VAP-1 activity. In Chapter 4 we have shown that VAP-1 regulates glucose uptake in isolated hepatic cells and PCLS thus taking these Chapters together it suggests that VAP-1 in the liver may have the ability to drive endogenous lipogenesis through glucose uptake and modification of fat uptake and disposal thus exacerbating disease pathogenesis. There are glucose and lipid transporters such as GLUT4, 8, 10, 12, FATP1 and LRP1 that are insulin sensitive, and it is likely that the activity of VAP-1 would be able to regulate these transporters in a manner similar to insulin. In addition there is evidence to suggest these proteins work together to achieve glucose and lipid homeostasis, for example GLUT4 and its association with FATP1 and CD36 suggest glucose and lipid transport is closely regulated (Stahl et al., 2002), (Schwenk et al., 2010). Interestingly SSAO, CD36, and Caveolin 1 have been found as major constituents of caveolae (Pilch et al., 2007), (Souto et al., 2003) and there is speculation caveolae are involved in GLUT4 trafficking (Scherer et al., 1994), (Gustavsson et al., 1996), (Ros-Baro et al., 2001), (Karlsson et al., 2002). This provides evidence of parallel regulation of pathways for glucose and lipid uptake as well as driving endogenous lipogenesis from excess imported glucose. It would be interesting to see whether there are differences in the lipid composition of VAP-1 deficient mice and PCLS treated with VAP-1 and their possible anatomical location and thus these are investigated in the next chapter.

CHAPTER 6

6 USE OF MASS SPECTROMETRY AND MALDI IMAGING TO DETECT PATHOLOGICAL CHANGES IN NASH

6.1 Introduction

NAFLD and NASH are a growing concern with approximately 25%-30% of the general population in western countries said to be suffering from the condition (Bhala et al., 2013), with prevalence of NASH in 3%-5% in the general population (Vernon et al., 2011) thus understanding of the key regulatory mechanisms is of vital importance, especially with difficulties in identifying and discriminating between these conditions. In the preceding chapters we have illustrated the pathological appearance of livers from patients with NASH and quantified associated changes in glucose transporter molecules and components of the lipid transporter pathway. We have also confirmed that the SSAO activity of VAP-1 can modulate hepatic glucose uptake and lipid accumulation and that livers from VAP-1 null mice have reduced steatosis on a HFD compared to WT controls.

Alterations in transporter expression and activity of VAP-1/SSAO may result in an altered lipid composition and deposition in the diseased liver. For example steatosis consists of both micro and macrovesicular steatosis (Kleiner et al., 2005), with macrovesicular steatosis associated with a poorer donor recipient outcome (de Graaf et al., 2012) and IR. Whilst some lipids for example TAG are reported as "good fats" (Yamaguchi et al., 2007) and others as pathologically "bad fats" for example sphingolipids ceramide and unsaturated FA (Fujiwaki et al., 2006), (Ma et al., 2007), (Cowart, 2009), (Huwiler and Pfeilschifter, 2009), (Stachowska et al., 2004). Thus we wanted to use techniques firstly to characterize what is happening in NASH versus simple steatosis and then how SSAO activity may impact on this, and thus these may provide potential for biomarker discovery.

Thus in this chapter we have performed pilot, proof of concept experiments to assess the validity of mass spectrometric approaches such as gas chromatography (GC), Matrix Assisted Laser Desorption Ionization Mass Spectrometry (MALDI-MS) and Matrix Assisted Laser Desorption Ionization Mass Spectrometry Imaging (MALDI-MSI) to identify the lipidomic profiles of normal, Steatotic, NASH, ALD and PBC livers. We have also determined whether SSAO activity results in quantifiable changes in hepatic lipid profiles. We begin with some background to the technology used.

6.1.1 MALDI

MALDI (Karas and Hillenkamp, 1988) is a technology which provides a means for fast, high throughput analysis of biomolecules within a sample with high sensitivity and spatial resolution (Koeniger et al., 2011). It is a combinatorial technique encompassing MALD-MS, which allows identification of component profiles in sample mixtures, and MALDI-MSI which provides information as to their spatial localization in thin tissue sections by desorption and ionization of samples (Zimmerman et al., 2008). MALDI-MS/MSI are powerful techniques, which have been used to find disease biomarkers in brain for Alzheimer's disease, epithelial ovarian cancer and IgA nephropathy (Rohner et al., 2005), (Huang et al., 2012), (Surin et al., 2013). Importantly, MALDI-MSI allows the unbiased visualization and direct analysis of biomolecules within tissue (Reyzer and Caprioli, 2007), (Bunch et al., 2004), (Fonville et al., 2013) without disrupting cellular integrity and architecture and thus avoids the need for extraction and purification of samples, which is essential for MALDI-MS (Shrivas et al., 2010). In comparison to conventional immunohistochemistry MALDI-MSI allows the detection of multiple targets in a

single test without the need for labeling (Bunch et al., 2004), (Caprioli et al., 1997), (Chaurand et al., 1999). Furthermore these two techniques can be combined to correlate spectral data to histological features in a given tissue and by using this combined approach has led to the identification of novel protein and lipid biomarkers in disease (Chaurand et al., 2006), (Johnson et al., 2006), (Sparvero et al., 2012). However we are specifically interested in lipids in this chapter. The most common lipids detected in MALDI experiments to date are the phospholipids as they easily ionize and are the most abundant in physiological specimens (Carter et al., 2011).

6.1.1.1 Sample collection and preparation

Sample collection for MALDI generally involves the immediate preservation and storage of samples by flash freezing in liquid nitrogen in order to prevent the degradation of tissue and rearrangement of species of interest. For MALDI-MS a specialized method for extracting lipids from tissue is employed (Folch et al., 1957) and can be optimized for the extraction of lipids for some tissues (Abbott et al., 2013), (Kulkarni et al., 2012). For MALDI-MSI tissue blocks are not digested and are usually mounted intact on to a cryostat cutting block using water rather than the conventional method of using OCT since this interferes with ion formation and mass spectra (Schwartz et al., 2003). Thin tissue sections are then cut and mounted on to MALDI target plates. At its simplest, sample preparation for MALDI experiments involves mixing the sample with an organic matrix and causing co-crystallization of both substances, also referred to as 'dried droplet' analysis in MALDI-MS. In contrast in the case of MALDI-MSI the matrix is usually deposited on top of a thin tissue section using an air brush (Hayasaka et al., 2009) as well as other methods such as

electrospray, inkjet printing and the use of automated acoustic multispotters (Baluya et al., 2007), (Aerni et al., 2006), (Altelaar et al., 2006). The matrix-sample complex is then irradiated using either ultraviolet (Holle et al., 2006) or infrared lasers (Park and Murray, 2012), which causes ionization of molecules. Ionization of molecules generally leads to protonated positive $[M+H]^+$ and negative ions $[M+H]^-$ which can include matrix ions and matrix-sample ions, however $[M+Na]^+$, $[M+Na]^-$ and $[M+K]^+$ $[M+K]^-$ ions can also be formed due to salts or other compounds within the sample (Schwartz et al., 2003). These ions are then detected using a mass spectrometer, usually a time of flight mass spectrometer (ToF-MS), (Chaurand et al., 2005) based on their mass to charge (*m/z*). Thus a typical mass spectrometer has three basic components, an ionization source, *m/z* analyzer and a detector (Zimmerman et al., 2008).

Sample ions can be identified using several approaches. The simplest is by comparing the *m/z* of a test ion to that of a known control compound ionized under identical conditions. This can also be supported by the use of molecular mass, mass spectrometry MS/MS which involves the fragmentation of the parent ion to further characterize the component parts of complex chemicals. This method can also be used to identify novel species. In particular MS/MS can be combined with MALDI-MSI (also referred to as tandem MSI) to form a very powerful technique for example to track the distribution of drugs and their metabolites (Khatib-Shahidi et al., 2006).

The successful formation of ions depends on the type and thickness of matrix used, the tissue surface and the formation of good quality homogenous crystals (Pol et al., 2011) thus all these parameters are usually optimized before any MALDI experiments

are carried out. There are several commonly used matrices employed in MALDI, which include 3,5-dimethoxy-4-hydroxycinnamic acid (SA) used in the study of proteins and peptides (Low et al., 2004), 2-5,dihydroxybenzoic acid (DHB), for the study of small oligo nucleotides, glycopeptides and glycoproteins (Andersson et al., 2008) and finally α-cyano-4-hydroxycinnamic acid (CHCA) which is used in the study of small proteins, peptides and glycoproteins (Gorka et al., 2012).

6.1.1.2 Data collection and processing

In MALDI-MSI, the mass spectrum of a given tissue is taken at each pixel location thus generating a large amount of raw data (Zimmerman et al., 2008). This data can be converted to produce an Analyze 7.5 dataset (Zimmerman et al., 2008) to aid analysis and data handling. This information can then used to form ion images of interest using specific software packages such as Matlab (Clerens et al., 2006) (Stoeckli et al., 2002) or Biomap. Although MALDI-MSI is a qualitative method (Koeniger et al., 2011) due to problems in sample homogeneity, for some molecules quantitative evaluation has been reported by normalization of signal to an internal standard (Ostrowski et al., 2007), (Goodwin et al., 2010).

In order to infer differences between normal and diseased samples with such large data sets the use of statistical, data clustering methods such as PCA, is essential (Zimmerman et al., 2008). PCA, which is commonly used for large sets of genomic information (Parsonage et al., 2003) allows the reduction and graphical visualization of the data set (Zaima et al., 2009) and has been successfully used in MALDI experiments to identify biomarkers (Zaima et al., 2009).

A further technique which can also be used to separate components of mixtures is GC which allows the rapid identification of volatile compounds and can serve as a non invasive tool for the analysis of disease biomarkers for example in breath (Dadamio et al., 2012), and serum (Hasokawa et al., 2012). For example in a recent study several compounds were identifiable in patients with liver cirrhosis which were not present in control subjects using GC (Dadamio et al., 2012). Briefly for lipid analysis using GC lipids are derived in to their methyl esters and injected in to the GC apparatus where they interact with the GC column and are retained until the inert gas carrier elutes them. The RT of lipids is based upon their chemical properties, and data is acquired as a chromatogram representing peaks for the different RT. These are then compared to RT to a known standard to assign a lipid identity to each peak; furthermore GC can separate isomers.

6.1.2 Use of mass spectrometry in the study of human liver disease

The ability for rapid unbiased assessment of compounds within valuable material from patients has led to an increase in the number of studies using mass spectrometry to assess liver disease pathogenesis. For example in a recent study several compounds were identifiable in patients with liver cirrhosis which were not present in control subjects using GC (Dadamio et al., 2012). Similarly descriptions of such techniques for identifying novel biomarkers in NASH have been reported (Solga et al., 2006), (Feldstein et al., 2004), (Feldstein et al., 2003), (Ratziu et al., 2000) with a specific focus on indicators of inflammation, oxidative stress and fibrosis. Furthermore some studies have identified circulating lipid profiles in NASH using MS (Feldstein et al., 2010). However to our knowledge little evidence of hepatic localization of potential biomarkers using MALDI-MSI has been reported (Wattacheril et al., 2013).

Therefore in this chapter we have used such technology to confirm whether patients with NASH have distinct lipidomic profiles, whether it is possible to use MALDI-MSI to localize species expression, and whether this technology can be used to assess any contribution of SSAO activity to lipidomic profiles.

Thus the major aims of this chapter were:

(I) To describe the lipidomic profiles of normal and diseased liver tissue using mass spectrometry techniques

(II) To assess the validity of using MALDI-MSI on human liver tissue

III) To identify the lipidomic profiles of WT and VAP-1/SSAO KO mice fed on a high fat diet

6.2 Methods

For methods pertinent to this chapter please refer to the general methods p67-70.

6.3 Results

6.3.1 Identification of lipid species in normal and diseased livers using Gas Chromatography (GC)

In the previous chapters we have reported altered profiles of lipid trafficking proteins in disease in combination with altered amounts of steatosis within our tissue samples. This steatotic accumulation of TAG along with native lipids such as signaling lipids and membrane phospholipids will constitute the lipid signature of each tissue. Thus initially we wanted to identify the profile of lipids in the normal human liver and to see how this changes in disease. This would form the basis to inform our understanding of how signaling via SSAO activity may alter this lipidomic signature. Thus we extracted lipids from lysates made of whole liver tissue and used GC to examine the profile of lipids present in normal and diseased liver. Figure 6.1 represents an overview of this.

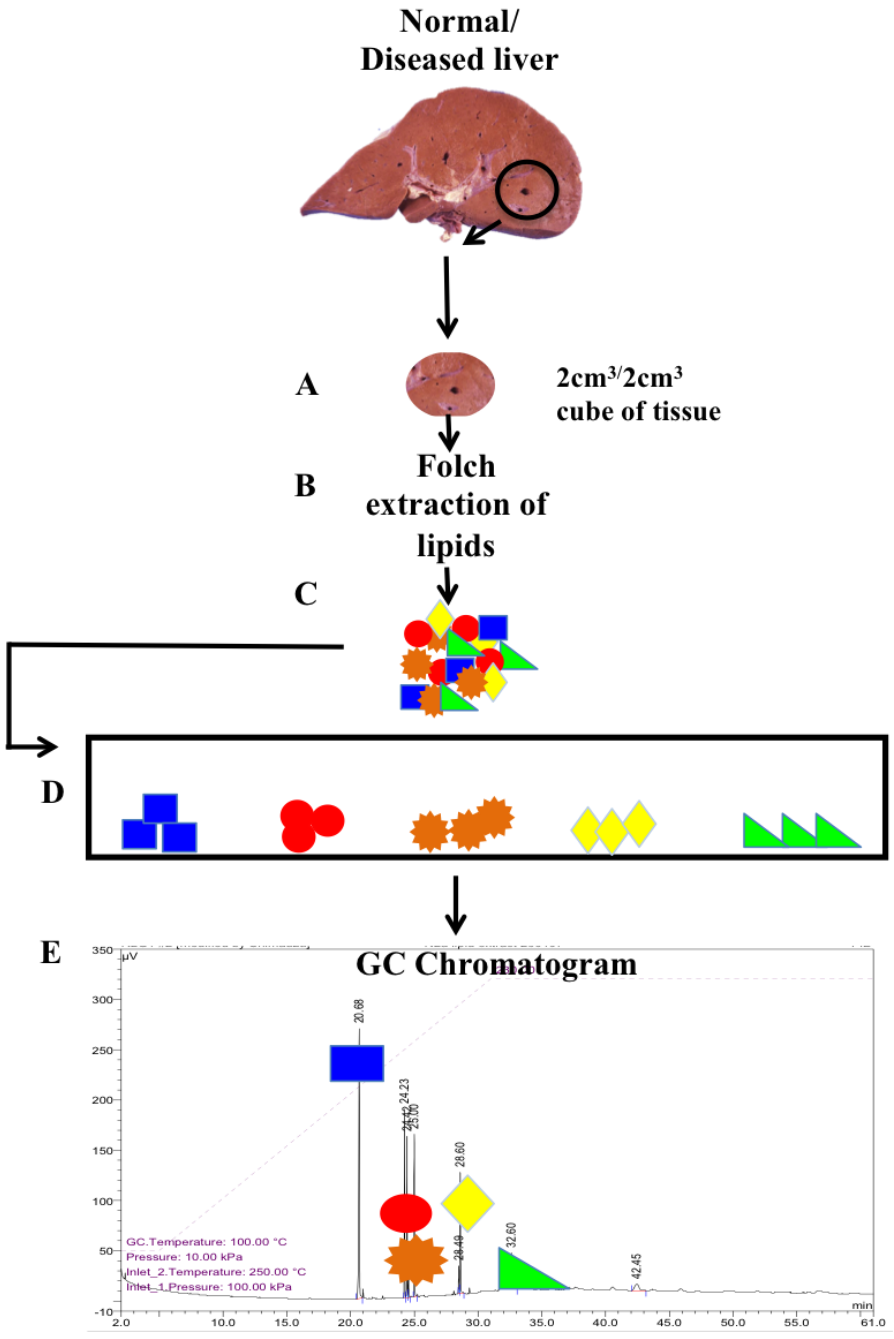

Figure 6.1: Schematic representation of workflow and of data acquired by gas chromatography

Normal and diseased liver were used for the extraction of lipids. (A) Small pieces of liver approximately $2cm^{3}/2cm^{3}$ were collected from freshly harvested livers and immediately snap frozen. Upon requirement samples were mechanically disrupted and homogenized, (B) lipids were then extracted using the Folch method, this mixture of lipids (C) was then injected in to the Gas Chromatograph (D). The methyl ester derivatives of the lipids interacted with the walls of the column inside the Gas Chromatograph causing the lipids to elute at different time points. The retention time data acquired is shown as a chromatogram (E) with peaks for the different retention times of individual lipids, these are then compared to retention times of a known standard analyzed under identical conditions to assign a lipid identity to each peak.

Our pilot GC analysis of lipid extracts from normal and diseased livers confirmed that this method was useful for analysis of human samples and revealed some key differences in lipid composition. Figure 6.2A shows a representative chromatogram from normal liver with red circles highlighting species present in normal but not NASH liver, see chromatogram in Figure 6.2B. For example the saturated FA myristate and the polyunsaturated FA gamma linolenate were detected in only steatotic livers, as well as a further lipid with a RT of 20.83 (Figure 6.2C). Furthermore a lipid with RT of 20.48/20.49 was only detected in normal livers (Figure 6.2C). Interestingly we found a lipid species with an RT of 32.6, which was present in all liver samples except NASH. Unfortunately these lipids with RT of 20.83, 20.48/20.49 and 32.6 could not be assigned as they, were not present in the standards we used (Figure 6.2C). We were only able to perform this analysis on limited numbers of samples and interestingly we found some lipid species, which were not detected in both samples from the same disease state. For example palmitoleate and a lipid with an RT of 24.53 were detected in normal liver 1 only and Gamma linolenate was detected in only one steatotic sample. (Figure 6.2C).

A

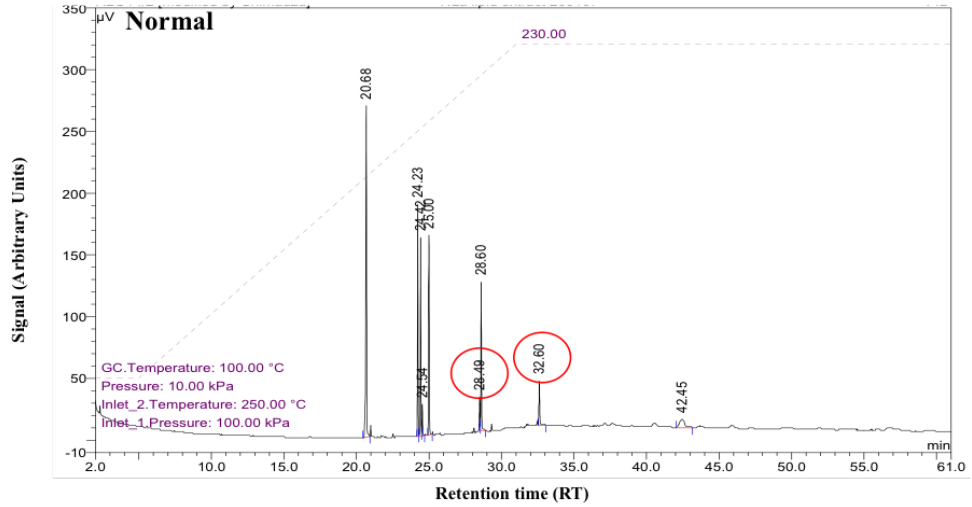

B

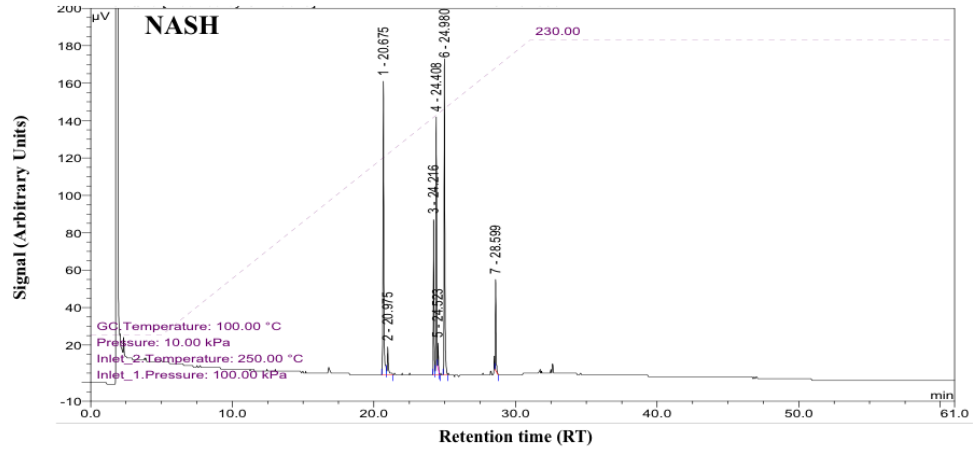

C

Disease								
Normal 1	Normal 2	Steatotic 1	Steatotic 2	NASH	ALD	PBC	Methyl Ester name	Other names
		16.74	16.74				Methyl tetradecanoate	Myristate
20.67	20.68	20.69	20.7	20.67	20.67	20.67	Methyl hexadecanoate	Palmitate
		20.83	20.83				Not in standard	
20.97		20.97	20.97	20.97	20.98	20.98	Methyl cis-9-hexadecenoate	Palmitoleate
24.22	24.23	24.23	24.23	24.22	24.22	24.22	Methyl octadecanoate	Stearate
24.41	24.43	24.44	24.43	24.41	24.41	24.41	Cis/Trans	Oleate/elaidate
24.53		24.53	24.53	24.53	24.54	24.53	Not in standard	
			25.74				Methyl cis-6,9,12-Octadecatrienoate	Gamma Linolenate
28.48	28.49						Not in standard	
28.59	28.6	28.6	28.6	28.6	28.6	28.6	Methyl cis-5,8,11,14-eicosatetraenoate	Arachidonate
32.6	32.6	32.6	32.6		32.6	32.6	Not in standard	

Figure 6.2: Analysis of fatty acid components of lipids in normal and diseased livers using GC

Lipid extracts of normal, steatotic, NASH, ALD and PBC livers were derived to methyl esters and analysis of lipid components was carried out using GC. Typical examples of GC chromatograms from normal (A) and NASH liver lipid extracts are shown. Red circles in the normal chromatogram (A) indicate peaks, which are present in normal but not NASH liver. A standard solution containing 37 methyl esters was also run along side the liver extracts and the RT time for each eluate (normal and diseased) was assigned to lipids by comparing with the standard. A summary table of RT of FA in normal and diseased livers with their lipid assignments is also shown (C). RT indicated in red are those found in the particular disease state. Data shown are from several livers (normal N=2, Steatotic N=2, NASH N=1, ALD N=1 and PBC N=1) with triplicate values determined for each sample.

6.3.2 Can Gas Chromatography identify any lipid compositional change in PCLS treated with VAP-1?

Our data in chapter 5 (Figures 5.19 and 5.20) showed that SSAO activity resulted in accumulation of lipid within liver slices and that VAP-1 null animals had reduced steatosis on a HFD. Next we wanted to examine whether the activity of SSAO was able to alter the composition of lipid species observed in the diseased livers. We found on the whole that there were very few compositional differences between treatments. However in PCLS treated with H_20_2 we found a lipid species with an RT of 9.59, which was absent from the other samples. Again this lipid was not represented in our generic standard and therefore could not be assigned. Similarly a lipid species with an RT of 24.62, which was detected in both MA and MA+VAP-1+BEA treated PCLS could not be assigned. Of note, we again found that there was variability between samplings of extracts made from the same liver samples in this analysis, for example the unique lipid species detected in the H_20_2 treated sample was not detected in all repeats (Figure 6.3).

A

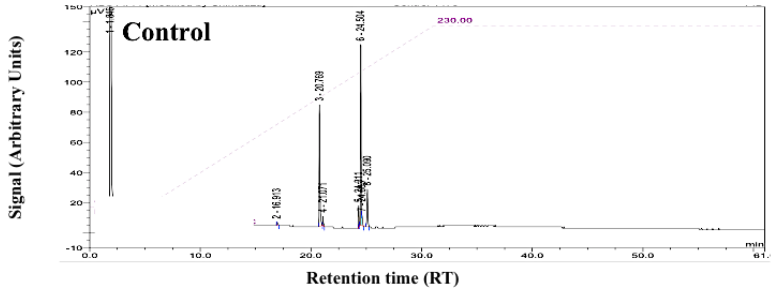

B

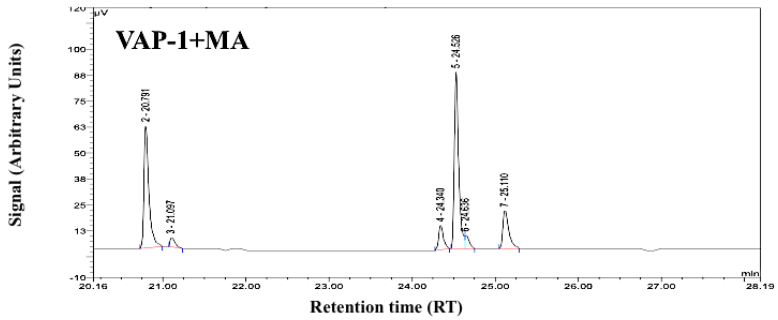

C

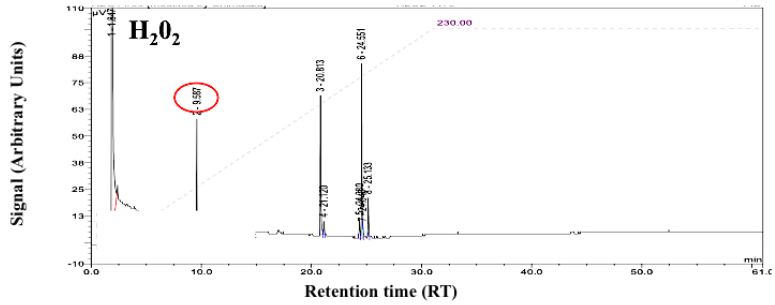

D

Treatment							
Control	MA	VAP-1	MA+VAP-1	MA+VAP-1+BEA	H_20_2	Methyl Ester name	Other names
1.85	1.85	1.85	1.85	1.85	1.85	Solvent	
					9.59	Not in standard	
16.91	16.89	16.9	16.89	16.88	16.91	Methyl tetradecanoate	Myristate
20.77	20.79	20.76	20.79	20.77	20.77	Methyl Hexadecanoate	Palmitate
21.07	21.09	21.07	21.1	21.07	21.07	Methyl cis-9-hexadecenoate	Palmitoleate
24.31	24.34	24.34	24.34	24.31	24.31	Methyl octadecanoate	Stearate
24.5	24.54	24.53	24.54	24.54	24.55	Cis/trans	Oleate/elaidate
	24.62			24.62		Not in standard	
25.12	25.07	25.08	25.11	25.06	25.13	Methyl cis-9,12-octadidecenoate	Linoleate

Figure 6.3: GC analysis of fatty acid components in PCLS after stimulation of VAP-1

PCLS were pretreated with either methylamine 200µm, VAP-1 500ng, H_2O_2 10µM, or a combination of methylamine+VAP-1, and methylamine+VAP-1+BEA for approximately 18 hours and then for 6 hours with 250µm PA. PCLS were then fixed and lipid was extracted using Folch method, derived to methyl esters and analysis of lipid components was carried out using GC. A standard containing 37 methyl esters was run alongside the liver extracts and RT times for each eluate (control and treated) was assigned to lipids by comparing to the standard. Typical GC chromatogram of lipid extracts from control PCLS (A) and slices after exposure to either VAP-1+MA (B) or H_20_2 (C) are shown. The red circle in the H_2O_2 chromatogram (C) indicates a peak, which is absent in the control sample. A Table of RT with lipid assignments for FA in PCLS treated with all stimuli (D) is also shown. Here RT indicated in red are those found in a particular treatment only. Data shown is from triplicate analyses for a single donor liver.

6.3.3 Identification of lipid species in normal and diseased livers using Matrix Assisted Laser Desorption Ionization-Mass Spectrometry (MALDI-MS)

Whilst our pilot chromatographic analyses hinted at compositional differences in treated liver samples, and showed promise for detection of disease-specific signatures, we were limited by availability of standard lipids and inter-sample variation. We were also unable to define the cellular origin of identified lipids. MALDI-MS allows the analysis of the full spectrum of lipids in a sample based upon structural information and can be combined with imaging to begin to assign species to cellular origin. Thus we continued our analysis using these approaches and Figure 6.4 represents an overview of this.

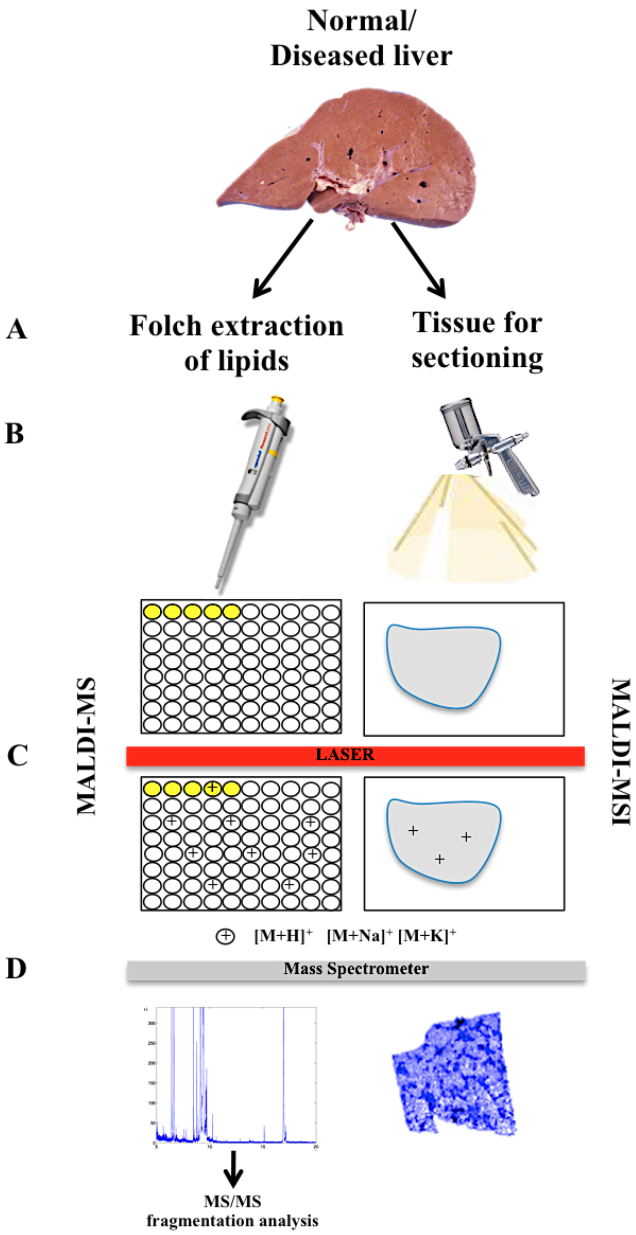

Figure 6.4: Schematic representation of workflow and of data acquired using MALDI-MS and MALDI-MSI

Normal or diseased livers were used for the extraction of lipids or for generation of tissue sections. Lipids were extracted using the Folch method and spotted on to a steel MALDI target plate or thin tissue sections were cut onto a MALDI target (A). The matrix CHCA was applied on top of the lipid extracts using a pipette, whilst an artist's brush was used to apply a homogenous layer of matrix onto tissue sections (B). The samples were pulsed with a laser which causes the generation of positively charged ions which can arise in a variety of positively charged forms such as the H^+, Na^+ and K^+ ions (C) These ions were detected by the spectrometer which generates *m/z* spectra allowing identification of differences between normal and diseased livers. Further structural information was also obtained by fragmenting a particular ion via MS/MS (D). MALDI-MSI allows the generation of ion images where the number of counts for each *m/z* peak are, displayed pixel wise according to location of sample origin on the section.

In order to analyze our samples using MALDI-MS we firstly optimized conditions necessary to run the experiment. A range of different matrix components, were analyzed to see which would give the highest ion counts in the lipid range of the spectra by MALDI-MS. We found that the CHCA matrix gave the highest ion counts and thus this matrix was employed for all future experiments (data not shown). The most commonly detected phospholipids (Astigarraga et al., 2008) in positive ion mode by MALDI-MS are phosphocholine-containing species, which are detected in the *m/z* 700-900 region. Furthermore MALDI-MS can give rise to three different ionic states of the same lipids detected in a sample, the $[M+H]^+$, $[M+Na]^+$ and $[M+K]^+$ forms. An example of a typical MALDI-MS spectrum we obtained from a normal liver is represented in Figure 6.5A, with an enlargement of the 700-840 region containing commonly detected phosphocholine-containing species (Astigarraga et al., 2008), which were also abundant in our specimens, phospholipids are highlighted on the spectrum and indicated in a table (Figure 6.5B and 6.5C).

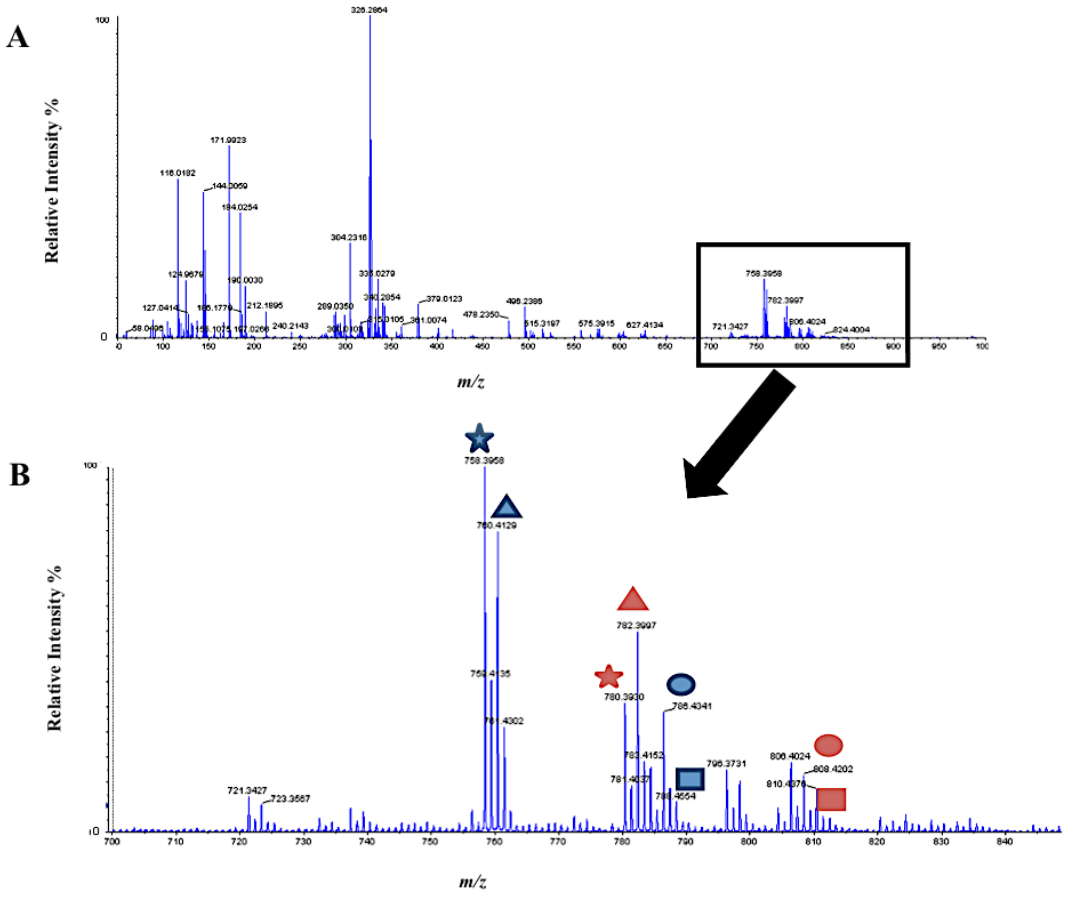

C

m/z Value	Assignment	Spectral label
758	PC 34:2 $[M+H]^+$	★
760	PC 34:1 $[M+H]^+$	▲
786	PC 36:2 $[M+H]^+$	●
788	PC 36:1 $[M+H]^+$	■
780	PC 34:2 $[M+Na]^+$	★
782	PC 34:1 $[M+Na]^+$	▲
808	PC 36:2 $[M+Na]^+$	●
810	PC 36:1 $[M+Na]^+$	■

Figure 6.5: Typical analysis of abundantly detected phosphocholines in normal liver lipid extracts using MALDI-MS

Folch extract samples of normal liver were spotted on to a multi well MALDI target plate, overlaid with a matrix solution (CHCA) and samples were analyzed on a hybrid TOF-MS and data were acquired in positive reflectron mode. (A) Representative spectra from normal liver in the *m/z* 50-1000 range with inset box indicating the *m/z* 700-840 region (B) enlarged spectrum of the *m/z* 700-840 region with symbols indicating typical phosphocholine lipids as shown in (C) a table of abundantly detected phosphocholine lipids in human liver. Data shown is representative spectra from normal livers N=2, with 10 replicate spots for each sample.

Next, Folch extracts from samples of normal and diseased liver were spotted onto the MALDI target plate and representative MALDI-MS spectra from normal, steatotic, NASH, ALD and PBC are presented in Figure 6.6. The inset pictures highlight the spectra from the lipid region (*m/z* 700-900), and whilst many peaks are apparent in all samples, there are clear differences between disease types. Our initial analysis revealed that there was some key compositional differences observed between samples, which included peaks at *m/z* 304 (Arachidonyl amine), 326 (10-nitro-9Z,12Z,octadecadienoic acid), 478 (glycerophospholipid), 502, (glycerophospholipid), 734 (glycerophospholipid), and 810 (Acetyl Co-A) (326 indicated on spectrum, Figure 6.6), which will be discussed in more detail below.

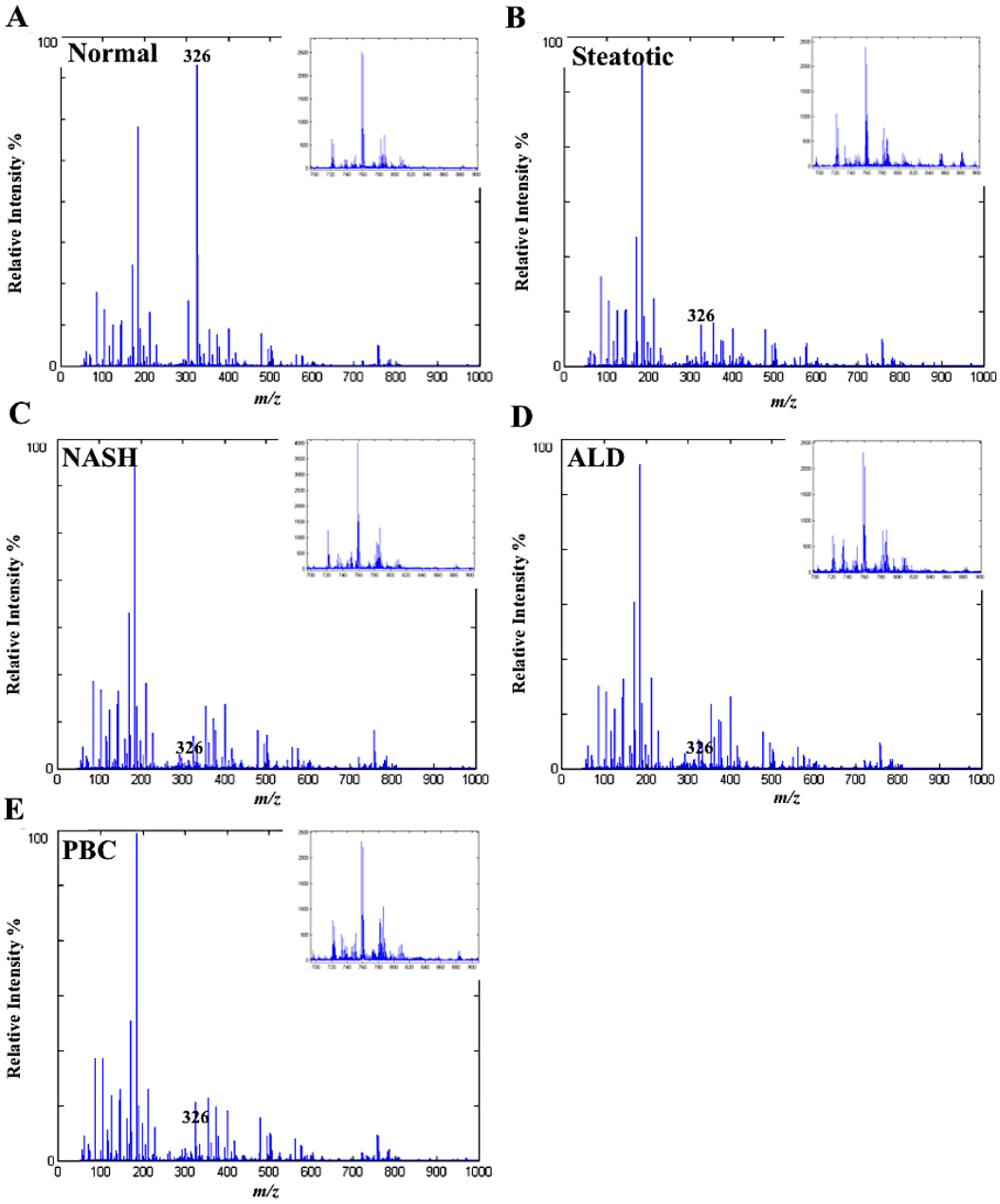

Figure 6.6: Analysis of normal and diseased liver lipid extracts using MALDI-MS

Folch extract samples of liver were spotted on to a multi well MALDI target plate, overlaid with a matrix solution (CHCA) and samples were analyzed on a hybrid TOF-MS and data were acquired in positive reflectron mode. MALDI-MS spectra shown represent phospholipids in (A) normal, (B) steatotic, (C) NASH, (D) ALD and (E) PBC liver extracts. Data shown are spectra from *m/z* region 50-1000 with inset regions at *m/z* 700-900 and are representative spectra from normal N=2, Steatotic N=2, NASH N=1, ALD N=1 and PBC N=1 livers with 10 replicate spots for each sample.

The ability to discriminate these and other species, which distinguish disease types, led us to perform PCA on our dataset. Restricting analysis to the first principle component showed that normal livers could be completely separated from the diseased livers (steatotic, NASH, ALD and PBC, see Figure 6.7A) and if analysis was extended to three components diseased livers were clearly separable from each other (Figure 6.7B). Importantly diseases that are difficult to discriminate histologically (NASH and ALD) were separable, and there was clear distinction between simple steatosis and NASH. An example of some of the data, which contributed to this analysis, is shown in Figure 6.8. We found that peaks for *m/z* 326 and 304 were most abundantly detected in normal livers compared to diseased livers whilst peaks *m/z* 478 and 502 were abundantly detected in NASH and Figure 6.8 and 6.9 show overlay of the mass spectra for *m/z* 326, 304, 478 and 502 in normal and diseased livers.

We then analyzed the spectrum for normal and disease states specifically in the region 700-900 since most phosphocholine-containing lipids are detected in this region. Interestingly we found a peak at *m/z* 734, which was more abundant in NASH and ALD liver than steatotic and normal samples. This is demonstrated by an overlay of *m/z* 734 in normal and diseased livers (Figure 6.10A), in order to try and identify this peak we carried out MS/MS fragmentation analysis to try and obtain some structural information we found presence of *m/z* 184 and *m/z* 86 in MS/MS fragmentation analysis (see inset in Figure 6.10A) suggesting this peak is a phosphocholine lipid, which contains two palmitic acid side chains. In addition we found peak *m/z* 810 was more abundant in NASH, ALD and PBC livers.

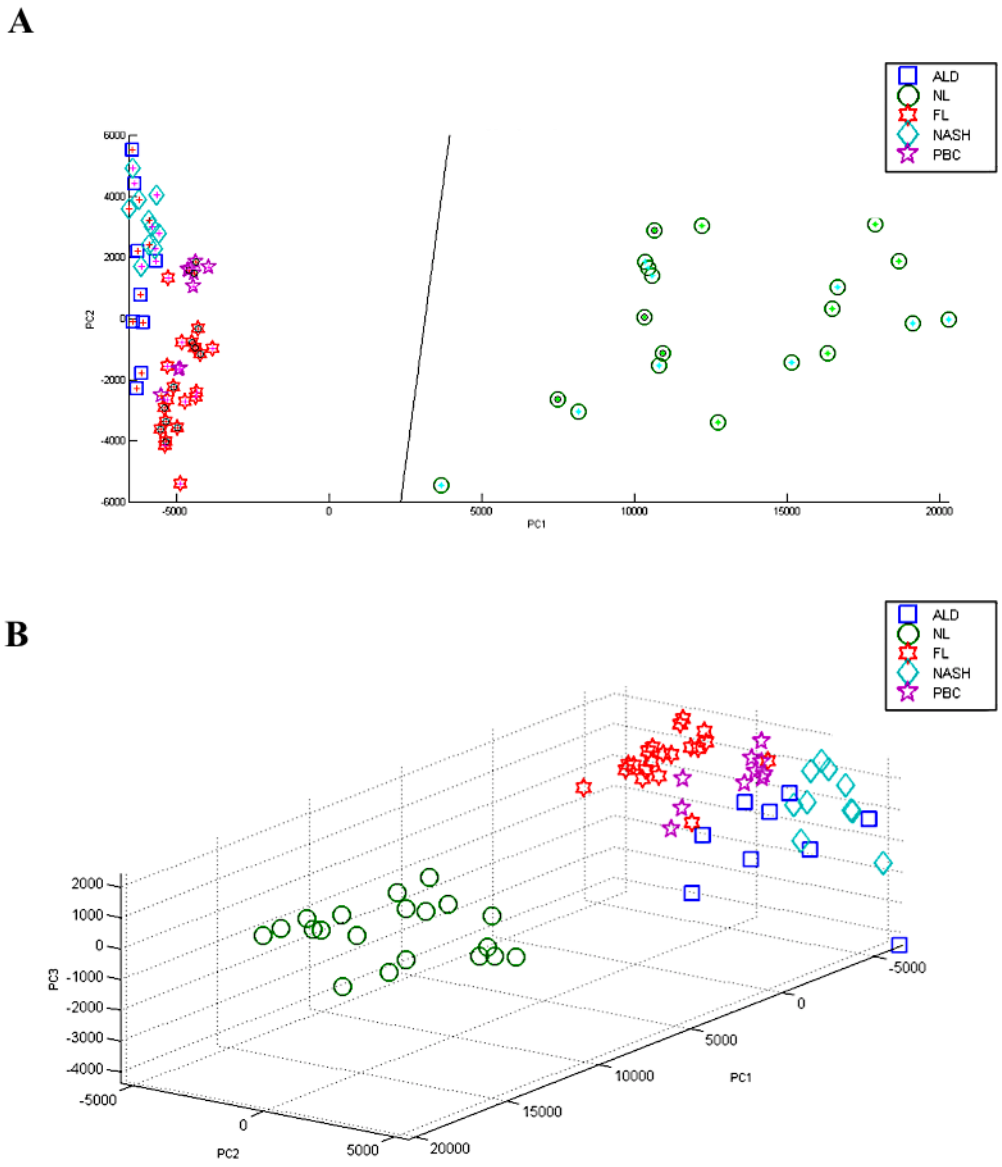

Figure 6.7: Principle component analysis of normal and diseased liver lipid extracts

PCA was performed on data generated from MALDI-MS spectra of normal, steatotic, NASH, ALD and PBC lipid liver extracts. Folch extract samples were spotted on to a multi well MALDI target plate, overlaid with matrix solution (CHCA) and analyzed on a hybrid TOF-MS, data acquired was in positive reflectron mode and data shown are from normal N=2, Steatotic N=2, NASH N=1 (established cirrhosis), ALD N=1 and (established cirrhosis with type II diabetes), PBC N=1 (biliary cirrhosis), with 10 replicate spots for each sample. (A) PCA analysis of normal and diseased liver based on the first two-principle components (B) PCA analysis of normal and diseased lipid liver extracts based on the first three principle components. PCA analysis was performed by Alan M Race.

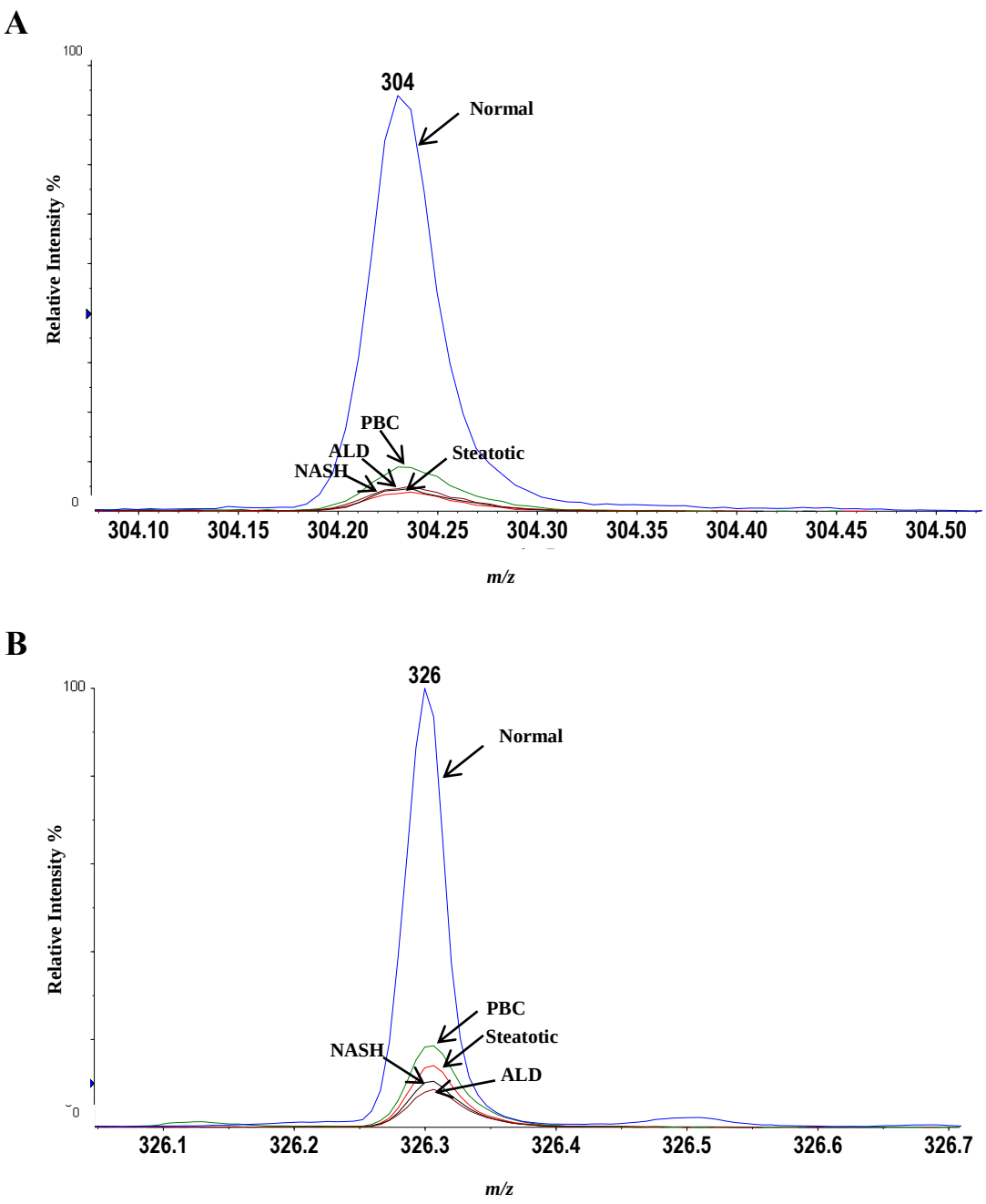

Figure 6.8: Analysis of *m/z* peak 304 and 326 in normal and disease lipid extracts using MALDI-MS

Folch extract samples from each disease state were spotted on to a multi well MALDI target plate, overlaid with matrix solution (CHCA) and analyzed on a hybrid TOF-MS, data acquired was in positive reflectron mode. (A) Overlay of mass spectra for peak *m/z* 326 in normal, steatotic, NASH, ALD and PBC lipid liver extracts, Overlay spectra shows more abundance of this ion in normal (B) Overlay of mass spectra for peak *m/z* 304 in normal, steatotic, NASH, ALD and PBC lipid liver extracts, Overlay spectra shows more abundance of this ion in normal. Data shown are representative spectra from normal N=2, steatotic N=2, NASH N=1, ALD N=1 and PBC N=1 livers with 10 replicate spots for each sample

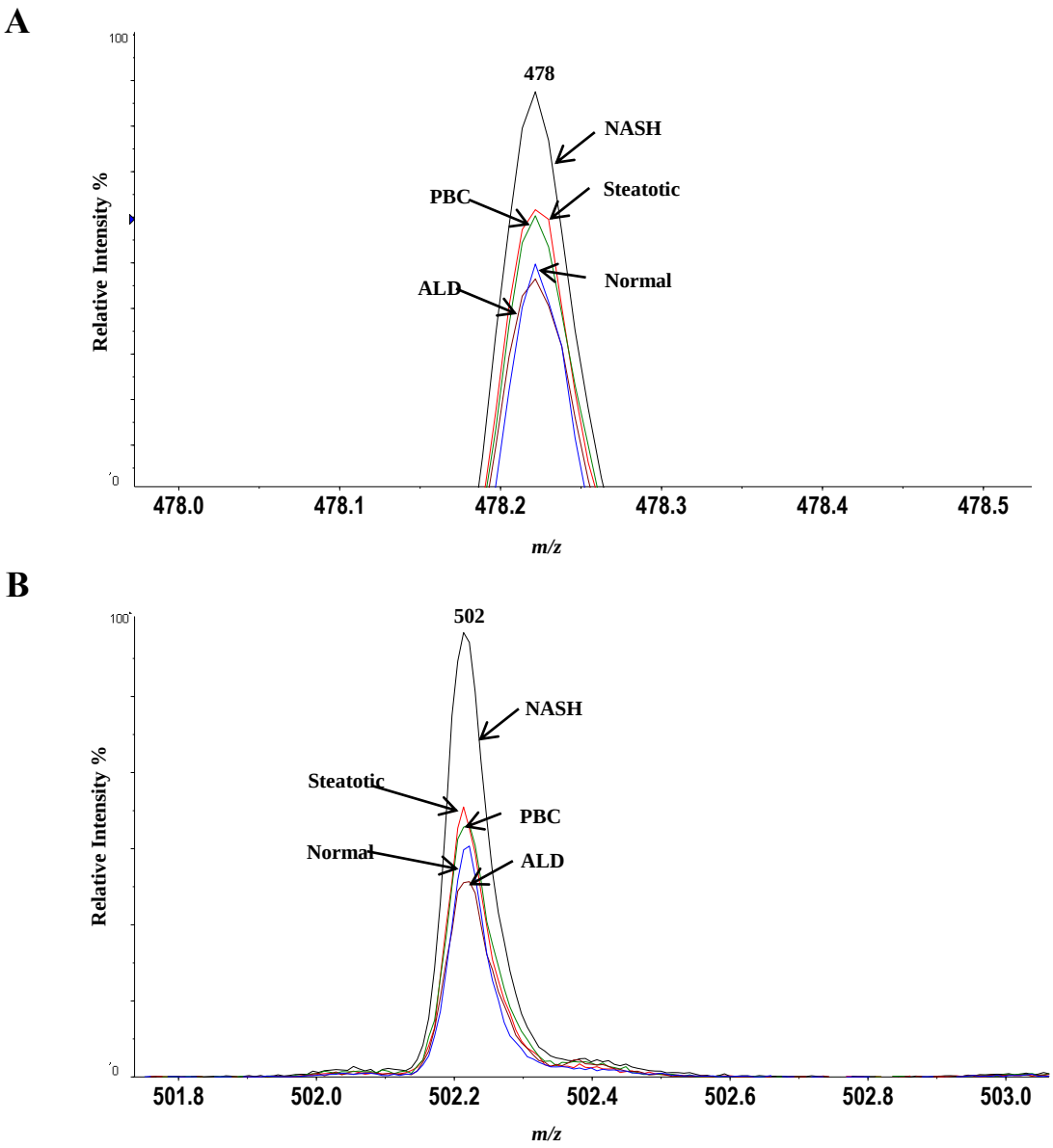

Figure 6.9: Analysis of *m/z* peak 478 and 502 in normal and disease lipid extracts using MALDI-MS

Folch extract samples from each disease state were spotted on to a multi well MALDI target plate, overlaid with matrix solution (CHCA) and analyzed on a hybrid TOF-MS, data acquired was in positive reflectron mode. (A) Overlay of mass spectra for peak *m/z* 478 in normal, steatotic, NASH, ALD and PBC lipid liver extracts, (B) overlay spectrum for ion *m/z* 502. Data shown are representative spectra from normal N=2, Steatotic N=2, NASH N=1, ALD N=1 and PBC N=1 livers with 10 replicate spots for each sample.

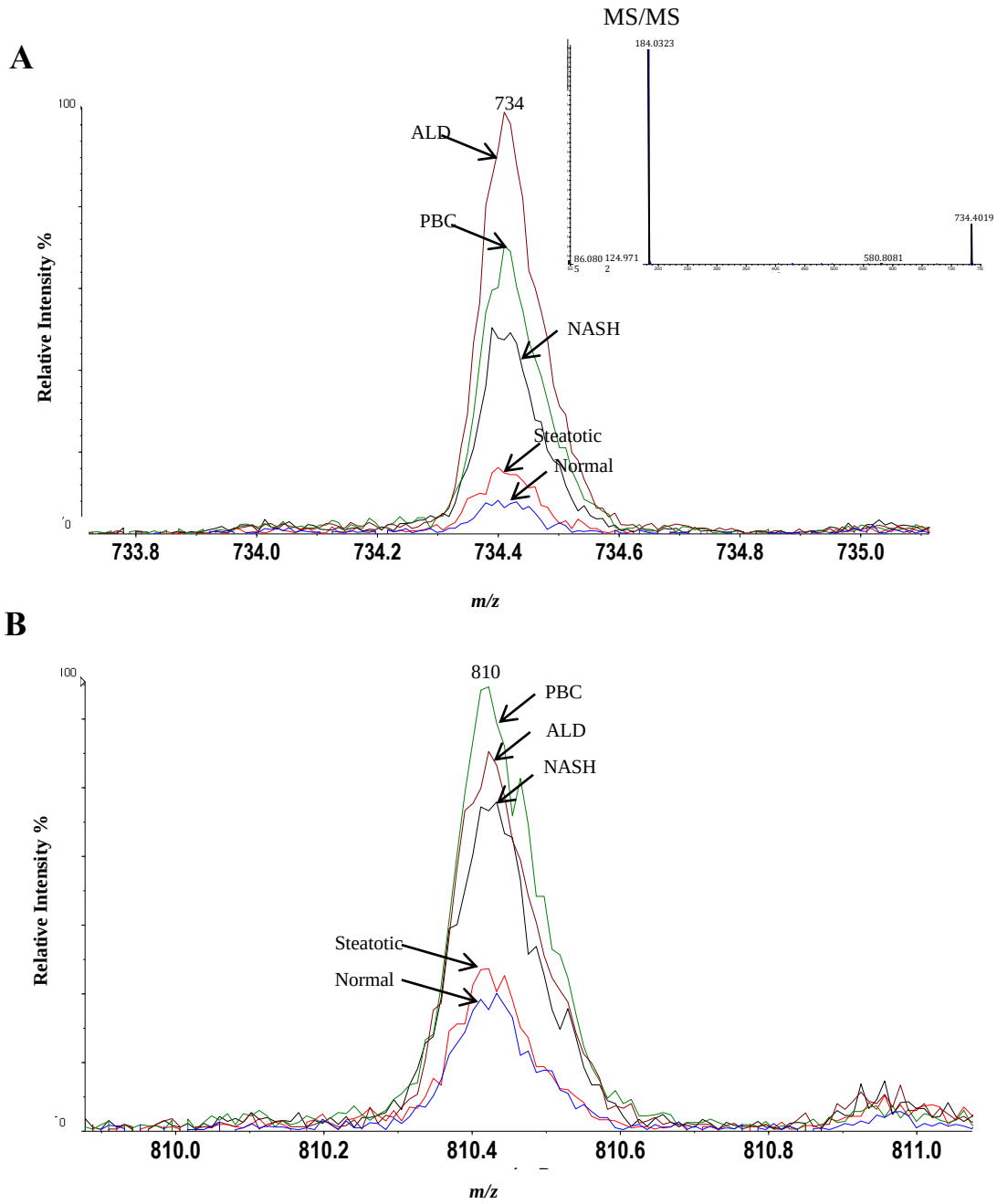

Figure 6.10: Analysis of *m/z* peak 734 and 810 in normal and disease lipid extracts using MALDI-MS

Folch extract samples from each disease states were spotted on to a multi well MALDI target plate, overlaid with matrix solution (CHCA) and analyzed on a hybrid TOF-MS, data acquired was in positive reflectron mode. (A) Overlay of mass spectra for peak *m/z* 734 in normal, steatotic, NASH, ALD and PBC lipid liver extracts, with inset spectrum showing MS/MS data for this ion suggesting this peak is a phosphocholine lipid and (B) Overlay spectrum for ion *m/z* 810. Data shown are representative spectra from normal N=2, steatotic N=2, NASH N=1, ALD N=1 and PBC N=1 livers with 10 replicate spots for each sample.

6.3.4 Identification of lipid species in wild type and VAP-1 KO mice using Matrix Assisted Laser Desorption Ionization-Mass Spectrometry (MALDI-MS)

Our pilot data from human tissue suggested that MALDI-MS could be used to assess global compositional changes in hepatic lipid profiles in disease and that we could identify some of the component lipids by MS/MS. Next we wanted to evaluate the livers from our VAP-1 null animals on a HFD to see if reduced steatosis was accompanied by compositional change in resident lipids. We also wondered whether these studies would show whether livers from mice fed a HFD reflect the picture seen in human steatosis or NASH.

Figure 6.11 shows a typical mass spectrum generated from normal mouse liver fed on a HFD with key phosphocholine containing lipids indicated and highlighted in the table. Of note again the most abundant species identified are the same as those found in the human livers and several ionic forms of each are present.

A

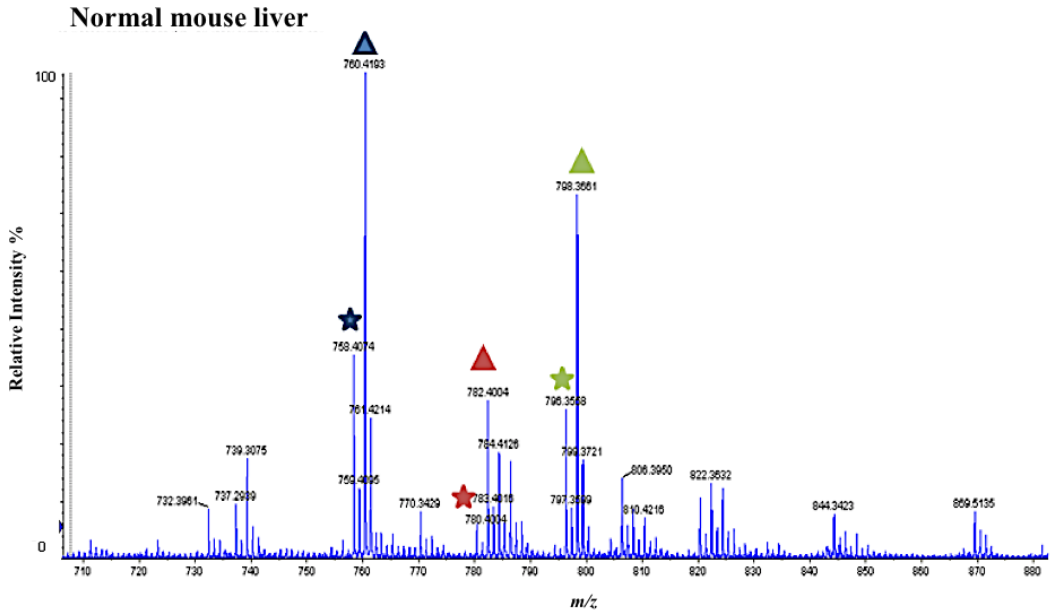

B

m/z Value	Assignment	Spectral label
758	PC 34:2 $[M+H]^+$	★
760	PC 34:1 $[M+H]^+$	▲
780	PC 34:2 $[M+Na]^+$	★
782	PC 34:1 $[M+Na]^+$	▲
796	PC 34:2 $[M+K]^+$	★
798	PC 34:1 $[M+K]^+$	▲

Figure 6.11: MALDI-MS Analysis of phosphocholine lipids present in normal mouse liver lipid extracts

Folch extract samples were spotted on to a multi well MALDI target plate, overlaid with matrix solution (CHCA) and analyzed on a hybrid TOF-MS, data acquired was in positive reflectron mode. (A) A representative spectra from the lipid region (*m/z* 700-880) of normal mouse liver fed on a HFD, with symbols indicating key phosphocholine lipids, which are highlighted in the table below (B) Data shown is representative of spectra from normal mouse liver (N=3), with 10 replicate spots for each sample spotted.

Interestingly by examination of spectra obtained from WT and VAP-1 KO mice fed on a HFD we found key differences between the samples. Thus some *m/z* peaks were present in WT but not VAP-1 KO mice and some *m/z* peaks were present in VAP-1 KO but not WT mice. These findings are summarized in Table 6.1 and also on spectra as highlighted see Figure 6.12 and 6.13. Furthermore the peak at *m/z* 326, which we observed to be most abundant in normal compared to other diseases in human specimens, was only detected in VAP-1 KO mice (highlighted on spectrum with a red circle, Figure 6.12B). We also identified a peak at *m/z* 782, which was present in VAP-1 KO mice only. Finally we performed PCA analysis on the entire MALDI-MS datasets, which showed that the two groups could not be separated (Figure 6.14A) and MALDI-MSI image of *m/z* 782 did not reveal any clear differences between WT and VAP-1 KO mice (Figure 6.14B).

m/z	Wild Type	VAP-1 Knock Out
250	✔	
475	✔	
505	✔	
522	✔	
534	✔	
639	✔	
822	✔	
866	✔	
972	✔	
326		✔
232		✔
582		✔
655		✔
824		✔
892		✔
968		✔
444	✔	
405	✔	
449	✔	
476	✔	
487	✔	
475	✔	
639	✔	
687	✔	
784	✔	
800 (TAG)	✔	
806 (TAG)	✔	
822 (TAG)	✔	
866 (TAG)	✔	
419		✔
423		✔
481		✔
499		✔
582		✔
703		✔
713		✔
737		✔
772		✔
763		✔
782		✔
786		✔
812		✔
824		✔
848		✔

Table 6.1: Table of *m/z* peaks present in WT and VAP-1 KO mice
Table of *m/z* peaks indicating those which are present in WT mice but absent from VAP-1 KO mice or those present in VAP-1 KO but absent in WT mice. Folch extract samples of each mouse group were spotted on to a multi well MALDI target plate, followed by a matrix solution (CHCA) and samples were analyzed on a hybrid TOF-MS, data acquired was in positive reflectron mode. Data shown are *m/z* values obtained from representative spectra from WT N=3 and VAP-1 KO N=3 with 10 replicate spots for each sample spotted.

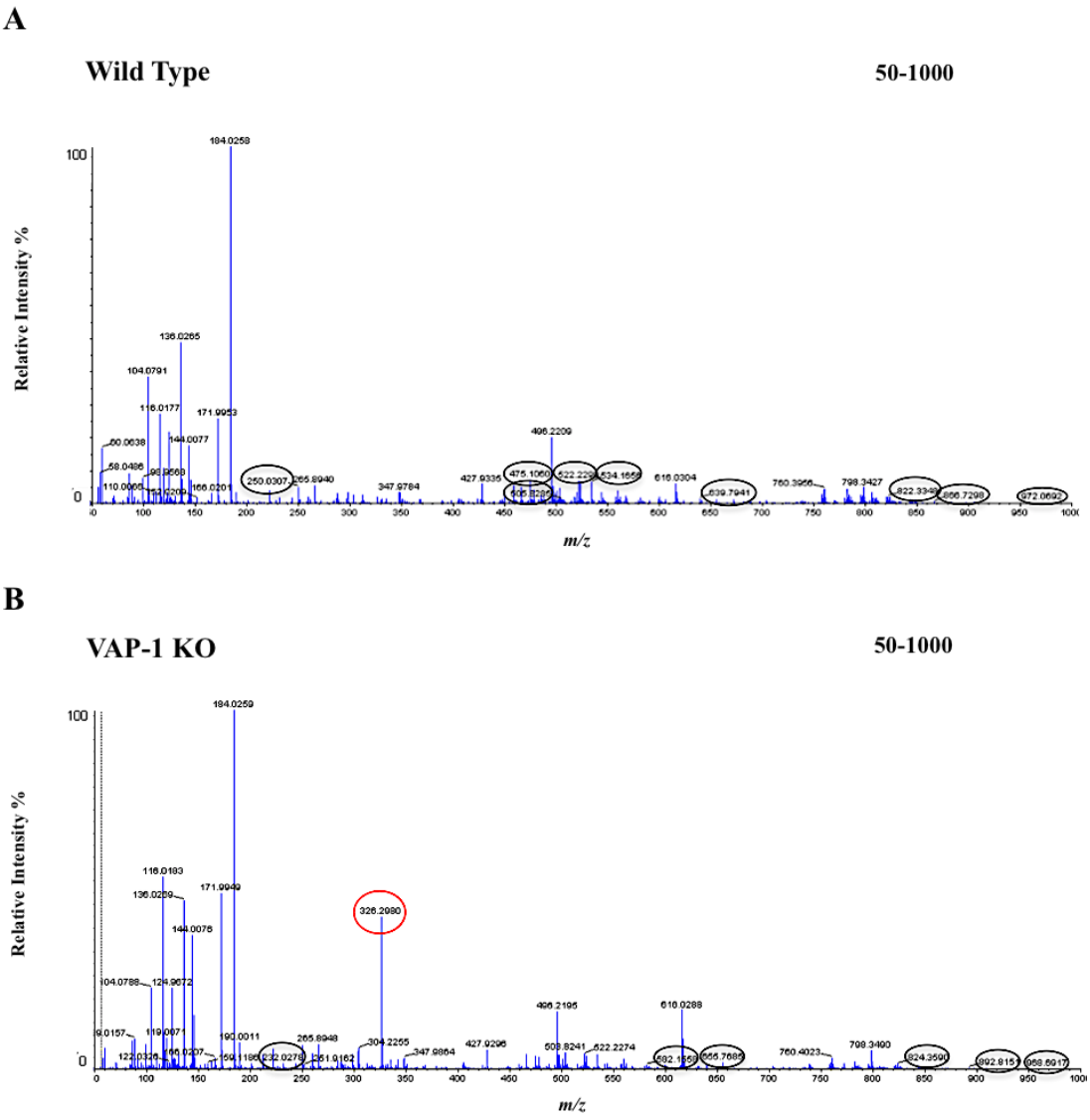

Figure 6.12: MALDI-MS analysis of hepatic lipid composition of WT and VAP-1 KO mice in *m/z* region 50-1000

Folch extract samples from each mouse group were spotted on to a multi well MALDI target plate, overlaid with matrix solution (CHCA) and analyzed on a hybrid TOF-MS, data acquired was in positive reflectron mode. Images show entire MALDI-MS spectra from *m/z* region 50-1000 in (A) WT and (B) VAP-1 KO mice lipid liver extracts. Data shown are representative spectra from wild type N=3 and VAP-1 KO N=3 livers with 10 replicate spots for each sample. The black circles in (A) indicate *m/z* peaks which are only present in WT mice and in (B) *m/z* peaks which are only present in VAP-1 KO mice, and the red circle in (B) indicates peak with *m/z* 326 which is only present in VAP-1 KO and was most abundant in normal human livers.

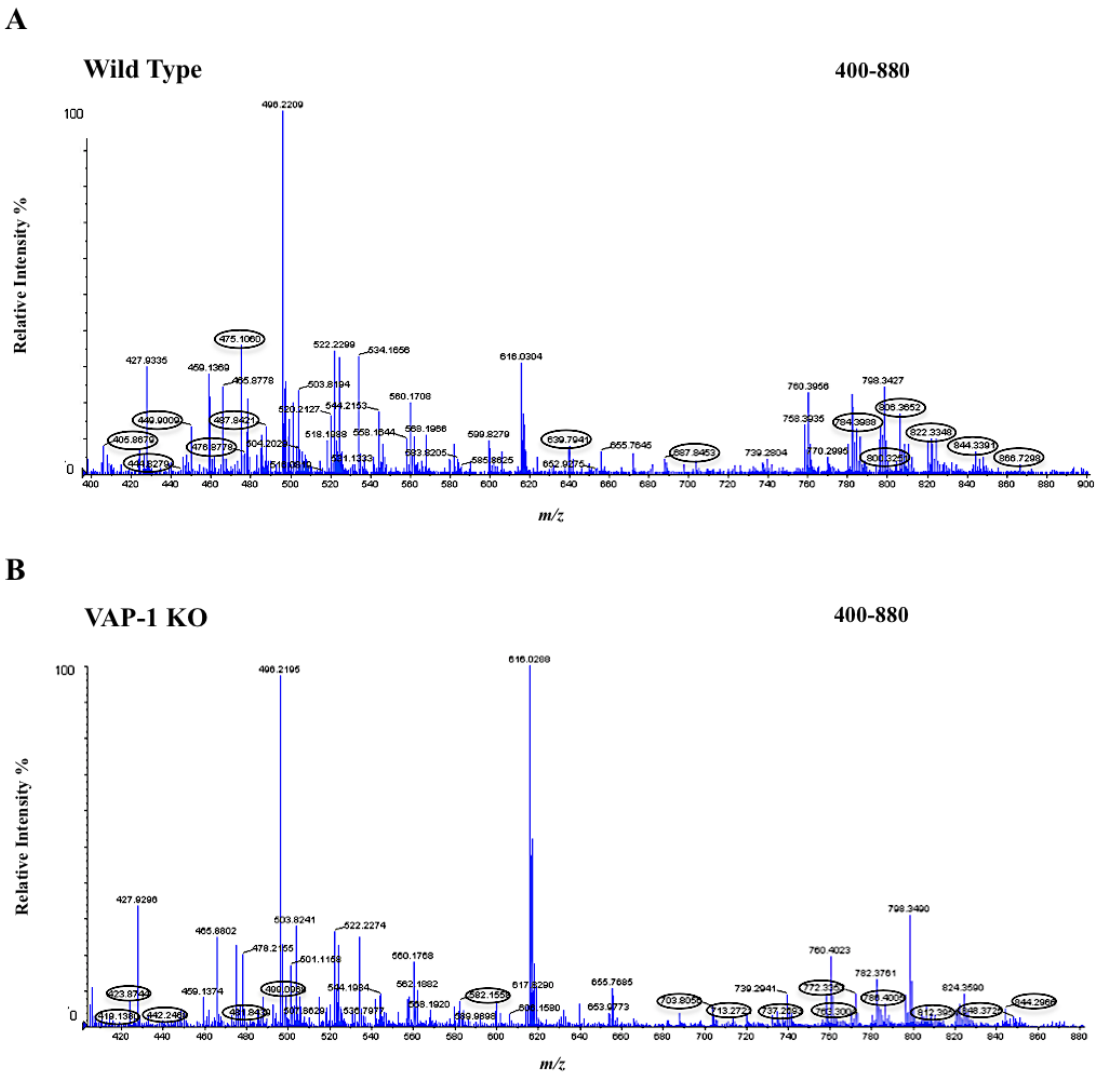

Figure 6.13: MALDI-MS analysis of hepatic lipid composition of wild type and VAP-1 KO mice in *m/z* region 400-880

Folch extract samples from each mouse group were spotted on to a multi well MALDI target plate, overlaid with matrix solution (CHCA) and analyzed on a hybrid TOF-MS, data acquired was in positive reflectron mode. Images show enlarged MALDI-MS spectra from *m/z* region 400-880 in (A) WT and (B) VAP-1 KO mice lipid liver extracts. Data shown are representative spectra from WT N=3 and VAP-1 KO N=3 livers with 10 replicate spots for each sample. Black circles in (A) indicate *m/z* peaks, which are only present in WT mice and in (B) *m/z* peaks, which are only present in VAP-1 KO mice.

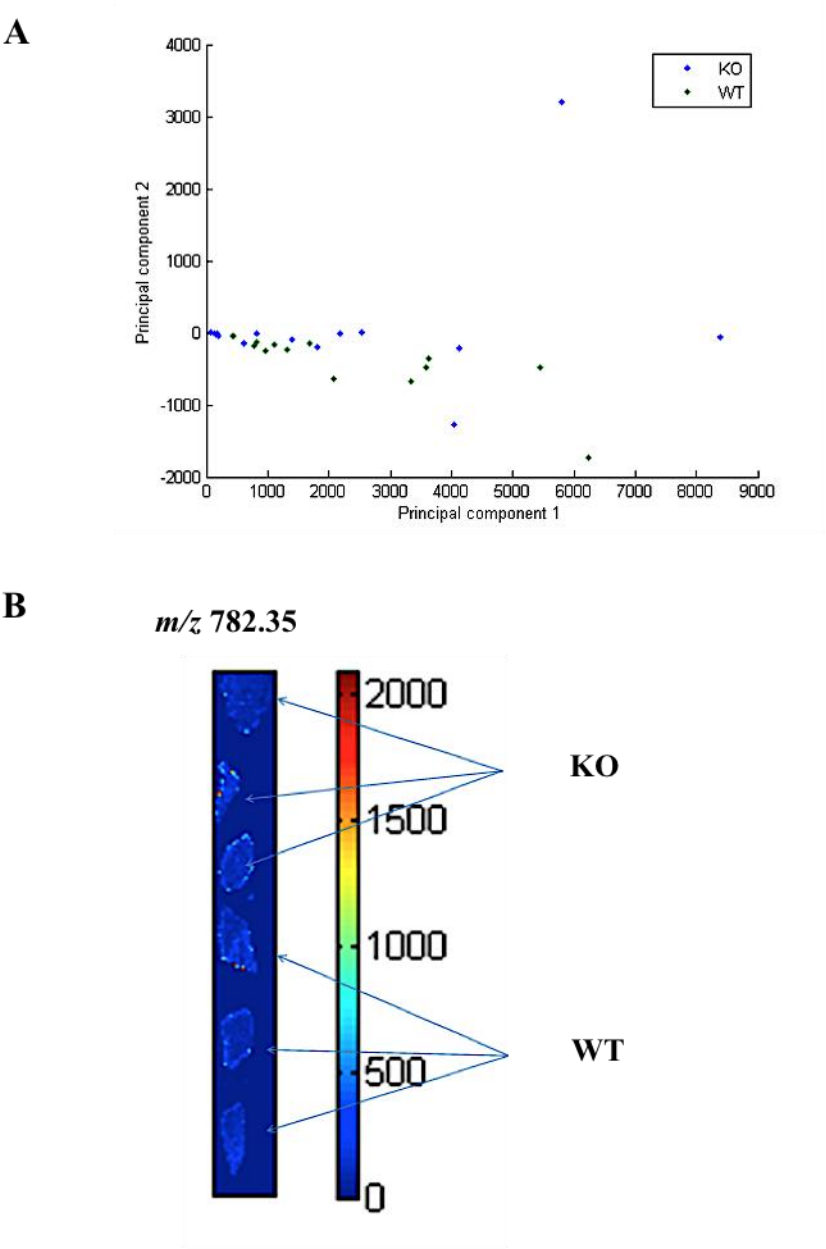

Figure 6.14: Principle component analysis of wild type and VAP-1 KO mice liver lipid extracts

Tissue sections from WT and VAP-1 KO mouse livers were placed on a MALDI target plate, overlaid with matrix solution (CHCA) and analyzed on a hybrid TOF-MS, data acquired was in positive reflectron mode. Ion images for *m/z* 782 were generated using oMALDI 5.1 (AB Sciex). PCA was performed on data generated from WT and VAP-1 KO liver lipid extracts. (A) PCA analysis of WT and VAP-1 KO mice lipid liver extracts based on the first two principle components, (B) ion images showing localization of *m/z* 782.35 in WT and VAP-1 KO mouse livers. Data shown was generated from representative spectra and images from WT N=3 and VAP-1 KO N=3 livers with 10 replicate spots for each sample in the MALDI-MS analysis. PCA analysis was performed by Alan M Race.

6.3.5 Imaging of lipid species in normal and diseased livers using Matrix Assisted Laser Desorption Ionization-Mass Spectrometry Imaging (MALDI-MSI)

Finally we wanted to examine whether we would be able to spatially locate the origins of the *m/z* peaks using MALDI-MSI where the spatial distribution of a particular peak can be visualized by plotting the intensity of that peak to generate an ion image. We were particularly interested in the MALDI-MS peak at *m/z* 734 since it was most abundant in NASH compared to normal liver. Thus MALDI-MSI images of *m/z* 772 (the most abundant peak in extracts is the $[M+H]^+$ state which corresponds to *m/z* 734 whilst in tissue the most abundant peak is the $[M+K]^+$ state which corresponds to *m/z* 772) were generated for normal, steatotic, NASH, ALD and PBC livers (Figure 6.15B). Panel A shows the spectra for this peak in all tissues and again confirms the abundance in NASH liver and presence in all liver samples. The inset shows the MS/MS fragmentation analysis. This molecule is identified as PC: 32:0 $[M+H]^+$.

The normal liver tissue distribution appeared homogenous for this peak with some intense signals in the perivascular areas of the steatotic specimen (indicated by arrows in Figure 6.15B). In contrast in the NASH liver there was intense detection of this peak within fibrotic regions (indicated by arrow in Figure 6.15B), which was also reciprocated in the ALD and PBC livers (indicated by arrows in Figure 6.15.B for each disease state), although not to the extent seen in the NASH sample. If we combined and overlaid the ion image of *m/z* 772 in NASH liver with an optical image of a serial H&E stained section, we noted excellent correlation (indicated by black arrow in ion image of 772 in NASH, white arrow in H&E stained NASH, and white

arrow in NASH H&E and ion image overlay, Figure 6.15C) of the ion localization and obvious gross histological features. These co-localizations are in an orientation suggestive of areas of extensive fibrosis in the NASH specimens (see Figure 5.11, Chapter 5) and of note tend to be the same areas where we see extensive VAP-1 protein expression (Figure 4.5, Chapter 4).

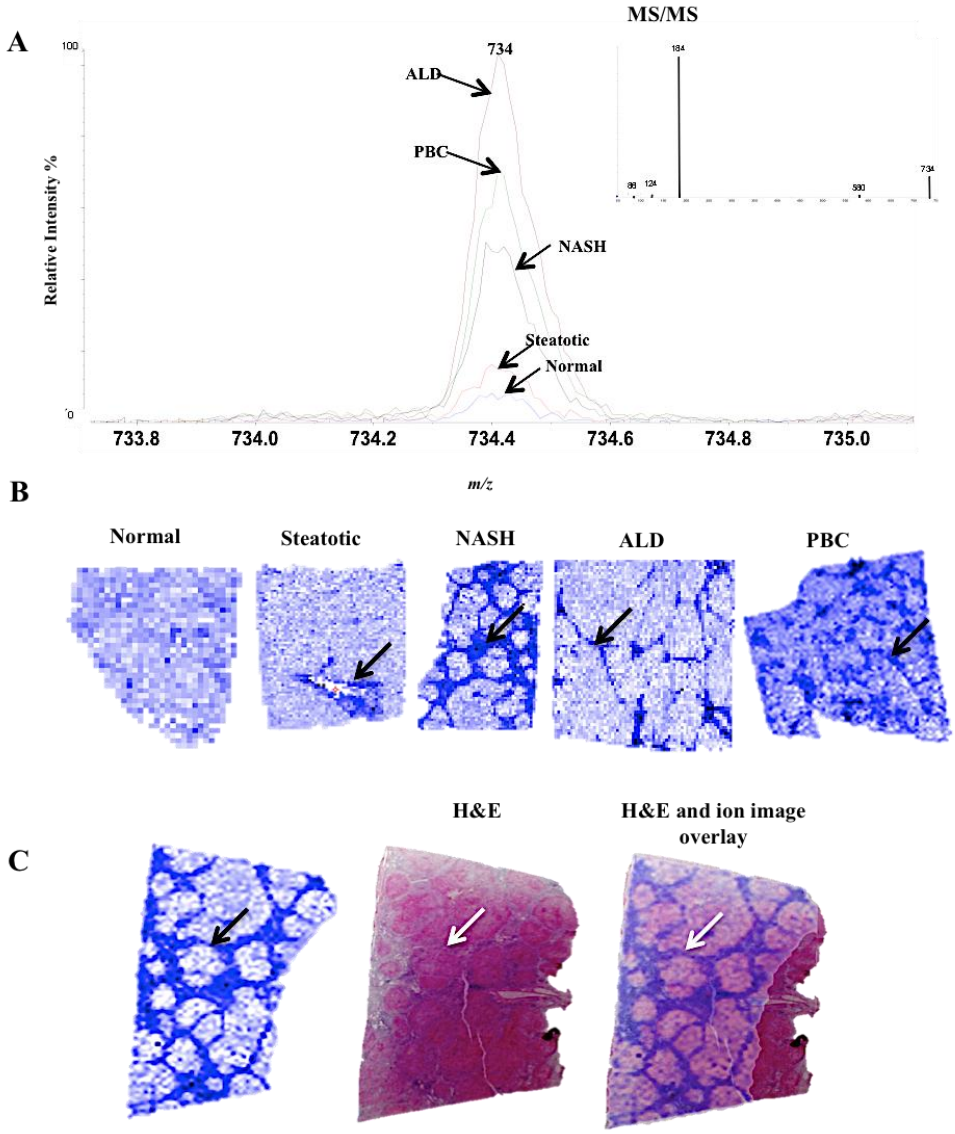

Figure 6.15: MALDI-MS and MALDI-MSI analysis of *m/z* 734 peak in normal and diseased liver extracts

Folch extracts from each liver were spotted on to a multi well MALDI target plate, overlaid with matrix solution (CHCA) and analyzed on a hybrid TOF-MS. Data acquired was in positive reflectron mode, and then MS/MS fragmentation analysis was carried out on this ion. Ion images were generated by mounting tissue sections onto a MALDI target plate, CHCA matrix was applied with an artistic brush and tissue sections were analyzed using a TOF-MS (oMALDI 5.1 (AB Sciex). (A) Shows the overlay of mass spectra for peak *m/z* 734 in normal, steatotic, NASH, ALD and PBC lipid liver extracts, with inset spectrum showing MS/MS data for this ion. (B) Shows representative MALDI-MSI images for this ion in normal and diseased livers and (C) is an overlay of MALDI-MSI for ion 772 generated using GNU image manipulation program 2.6, and a H&E image of a serial section of NASH liver. The arrows in (B) highlight areas with high intensity for this ion and the white arrows in overlay images (C) shows good correlation with histological features. Data shown are representative spectra and images from normal N=2, Steatotic N=2, NASH N=1, ALD N=1 and PBC N=1 livers with 10 replicate spots for each sample for the MALDI-MS analysis. Image manipulation, was performed by Dr Josephine Bunch.

6.4 Discussion

Thus far this thesis has established a role for VAP-1 in glucose uptake and lipid accumulation and altered expression of both glucose and lipid transporters, which may give, rise to a distinct lipid signature in diseased tissues with different basal VAP-1 activities, or in tissues where we have triggered VAP-1 activity exogenously. Therefore we were interested to investigate whether there were any compositional lipid differences in PCLS treated with VAP-1 or from livers from VAP-1 KO and WT mice and whether pathological changes could be detected in this chapter using mass spectrometry. In summary using MS we detected compositional differences between normal and diseased tissue and in WT and VAP-1 KO mice fed on a HFD using GC and MALDI-MS. In particular MALDI-MSI allowed visualization of *m/z* 734 phosphocholine containing lipid species distinctly located in fibrotic regions of NASH.

6.4.1 Gas chromatography reveals compositional lipid differences in normal and diseased livers.

To begin we used GC to examine the compositional lipid differences in normal and diseased tissue. We found that GC was effective in providing qualitative differences between tissues. GC identified the saturated FA Myristate and the polyunsaturated gamma linolenate to be present only in steatotic livers. Interestingly gamma linolenate which was only present in one steatotic liver has been previously shown to be elevated in NAFLD and NASH (Puri et al., 2009) and has also been shown to suppress weight regain in previously obese individuals (Schirmer and Phinney, 2007). Salt esters of palmitic, stearic, oleic and arachidonic acid were present in normal and diseased livers. Stearic acid has been shown to increase markers of ER stress (Zhang

et al., 2011b), whilst PA has been shown to induce ER stress and apoptosis (Wei et al., 2006), (Listenberger et al., 2001) which is reduced by the presence of some lipids for example α-Linolenic and Oleate acid (Zhang et al., 2011b), (Wei et al., 2006). These findings suggest there are distinct lipid species between normal and diseased livers, however these may reflect changes in the liver during organ collection or tissue processing, and support the abundance of PA and OA in tissue and our use in *in vitro* uptake assays.

Puri et al have shown arachidonic acid to be decreased in NASH (Puri et al., 2007) and its oxidized products are elevated (Puri et al., 2009). We found it was present in normal and NASH however we could not quantify it and thus it could be less in NASH livers. Furthermore in support of our data a HFD on obese mice resulted in an increase in palmitic, stearic and oleic acid identified using GC/MS (Kim et al., 2011). GC can be used to identify quantitative differences however appropriate calibration of GC needs to be carried out which was beyond the scope of this investigation. Thus although we have not quantified the levels of these FA we propose there may be a complex interplay between the different quantities of these FAs, which may change as a result of affording the cell protection or damage. It is important to note that there were four unidentified species, which were present only in steatotic or normal livers or not present in NASH as the standard used in this assay was unable to assign lipids to some retention times, as they were not present in the standard. Similar difficulties in identifying lipid species has been reported previously (Kim et al., 2011) and highlight the importance of standard selections in such technologies.

The Advantages of using GC are that it is fast, only a small amount of sample is needed thus this method with the appropriate set up would be excellent in a hospital setting in the non invasive diagnosis of NASH. In this investigation we have used liver tissue, however we would need to check blood for correlates however it is important to check for markers via all routes in pilot investigations to look for good serological markers. Diagnosis of NASH in many cases requires biopsy and histological examination (Brunt et al., 1999), (Kleiner et al., 2005) which in some cases can be associated with complications (Bravo et al., 2001), (Piccinino et al., 1986). Certainly a recent report has successfully used GC and exhaled breath samples to discriminate between patients with NASH and those without (Verdam et al., 2013). Thus GC of blood or other easily collected samples may provide a rapid and non-invasive method for the diagnosis of NASH in conjunction with other non invasive methods such as ultrasonography, transient elastography and FibroMeter (Festi et al., 2013).

6.4.2 Gas chromatography reveals compositional lipid differences in PCLS treated with VAP-1 and its metabolites

Next we wanted to examine whether we could identify compositional lipid differences resulting from VAP-1/SSAO activity in PCLS. On the whole we found that there were very few compositional differences which could reflect the short time point used in this study in comparison to other studies looking at a role for SSAO in lipid homeostasis which have used more chronic exposures (Marti et al., 2001), (Fontana et al., 2001), (Mercier et al., 2001), (Stolen et al., 2004a) and could also be reflective of the FA used as a source in these experiments. Nevertheless we did observe presence of two separate species one which was present in the hydrogen peroxide treated

sample only and the second that was only present in VAP-1+MA and VAP-1+MA+BEA treated PCLS, since hydrogen peroxide can also be produced by other reactions careful interpretation is needed. In addition the species detected in hydrogen peroxide treated samples was not detected in all repeats thus this result would need to be further validated, and again limitations in the standard used means that the identity of these species remains unknown. However this data suggests that interventions using PCLS can be detected and examined using GC.

6.4.3 Use of MALDI-MS to detect pathological changes in normal and diseased livers

We found that the matrix CHCA gave the highest ion counts in comparison to other commonly employed MALDI matrices used in lipid analysis (Schiller et al., 2001), (Schiller et al., 2007) this suggests that tissues from different organs or species give variable ion counts based on different matrix used. We found that our samples contained abundantly detected phosphocholine phospholipids as shown previously (Emerson et al., 2010). Interestingly MALDI-MS also revealed there were some compositional differences between normal and diseased livers for example normal liver most abundantly expressed peaks at *m/z* 326 and *m/z* 304 compared to all other diseases tested. Although these peaks could not be quantified, overlay spectra did show clear abundance reflective of ion counts. It is interesting to note that *m/z* 326 is a 10-nitro-9Z, 12Z, octadecadienoic acid. Other octadecadienoic acids such as 13-oxo-9-11-octadecadienoic acid have been shown to decrease hepatic TAG in obese mice by acting as a PPARα agonist (Kim et al., 2012) and it is interesting to speculate whether our species with *m/z* 326 could behave in a similar manner. Furthermore we then analyzed spectra in the region 700-900 since most phosphocholine containing

lipids are detected in this region and almost 65% of the TAG pool is said to be derived from phosphatidylcholines (van der Veen et al., 2012) which may have implications in NASH pathogenesis. We were able to identify peaks with increased abundance in NASH, which hints at distinct lipodomic profiles in NASH identifiable via MALDI-MS. For example *m/z* 810 may be Acetyl Co-A, an intermediate metabolite of both glucose and lipid metabolism, which was abundantly, detected in the NASH, ALD and PBC livers. Furthermore the MALDI-MSI peak of *m/z* 772 has also recently been detected by Wattacheril et al in NASH (Wattacheril et al., 2013).

The *ms/ms* analysis of *m/z* 734 revealed this was a phosphocholine lipid containing 2 PA side chains. This is interesting to note since activation of the inflammasome in macrophages/kupffer cells has recently been shown to be jointly activated by palmitic acid and Toll Like Receptor 2 (TLR2) and hence contributing to the development of NASH (Miura et al., 2013). Furthermore incubation of hepatocytes with PA has been shown to increase expression of IL-8 giving further support for the role of PA in the inflammatory process in NASH (Joshi-Barve et al., 2007). It must be noted that phospholipids are the most abundantly detected lipids in tissue since they are major constituents of lipid membranes. However these have also been shown to suppress signal from other lipids in MALDI analysis (Petkovic et al., 2001), thus its possible that we may not be detecting some mechanistically important lipids in these samples. Amendments to the current protocol for example using phospholipase treatment, may overcome this problem (Sparvero et al., 2012) and further lipid analysis could be improved by using additives such as nitrates (Griffiths and Bunch, 2012).

Regardless of our current technical limitations, PCA analysis on our data set allowed complete separation of normal and diseased livers. This confirms that there are distinct lipodomic profiles between normal and diseased liver and in addition between each disease state (e.g steatosis and NASH were separable). However it must be noted factors such as age and sex of donors as well as grade of fibrosis or cirrhosis may influence the separation of data in the PCA analysis. Although our results are preliminary and we acknowledge our samples numbers would need to be greatly enhanced before any clear distinctions can be made, it is clear that MALDI-MS can be used to identify distinct lipidomic profiles in NASH and hence possibly be used in disease diagnosis as reported previously (Zaima et al., 2009). Although our analysis has focused on invasive procedure involving tissue biopsy a less invasive method for example blood collecting would improve the utility of MALDI-MS as a clinical tool. For example other MS techniques have been used with non-invasively collected methods such as breath samples in both humans and animal models for distinguishing NASH (Millonig et al., 2010), (Aprea et al., 2012).

6.4.4 Use of MALDI-MSI to detect changes in lipid species in wild type and VAP-1 knock out mice

Using MALDI-MSI we were able to identify a number of lipid species, which differed between WT and VAP-1 KO mice, suggesting that the presence of VAP-1 not only alters lipid levels as shown in Chapter 5 but also the composition of lipids. This is consistent with other MS studies, which have shown altered lipid composition in NAFLD and NASH patients for example Wattacheril et al showed altered abundance of PC (Wattacheril et al., 2013), whilst Feldstein et al have shown increased oxidized lipid products in plasma of patients with NASH (Feldstein et al.,

2010). Furthermore we identified *m/z* peaks, which were present in WT but not VAP-1 KO mice, which suggests that VAP-1 activity may lead to oxidation or metabolism of parent lipids, which is possibly why we do not see them in the VAP-1 KO mice. Certainly some studies have reported presence of oxidized lipid in blood collected from NASH patients (Feldstein et al., 2010), however the origins of blood lipids and identification of oxidized lipids in the liver remains to be clarified. VAP-1 may provide a mechanistic link explaining sources of oxidized lipids and lipid metabolites. Certainly the presence of peaks in VAP-1 KO mice but not WT (for example *m/z* 326, which was also abundant in normal liver), suggest that VAP-1 could be suppressing key lipid species, or metabolizing them which could generate pathogenic derivatives or act as a protective mechanism against injury. For example we found *m/z* 326, a possible sodium adduct of arachidonic acid, to be present in VAP-1 KO but not WT mice and levels of its oxidized product 11-HETE have been shown to be elevated in NASH (Puri et al., 2009).

Whilst we were able to identify individual compositional changes, our PCA analysis revealed that the WT and VAP-1 KO livers could not be separated. This may reflect the ranking system used for the PCA, and high variability between individual samples. This type of analysis works best with samples with low signal to noise ratios, large variances and is a non-parametric analysis system. It is possible that stricter selection of the components could lead to a significant difference with PCA in future studies. However a disadvantage of using PCA is that complicated relationships may be missed. Furthermore TAGs are neutral molecules and hard to ionize thus it is possible we may be missing some lipid species in our analysis, which would significantly enhance sample separation by PCA.

6.4.5 MALDI-MSI allows visualization of lipid species in distinct anatomical locations in normal and diseased livers

Finally we analyzed the spatial distribution of peaks identified by our MALDI analysis. In particular here we focussed on *m/z* 734 (corresponds to peak *m/z* 772 in MALDI-MS) using MALDI-MSI since this was most abundant in NASH. As stated earlier this was a phosphocholine lipid containing 2 palmitic acid side chains, and MALDI-MSI confirmed this lipid species was most abundant in NASH and in particular in fibrotic regions of NASH, ALD and PBC livers. Of note these are also areas for which we have reported extensive VAP-1 expression (see Chapter 4), (Claridge L C, 2009). Thus it is clear from the MALDI-MS and MALDI-MSI data that this lipid species in particular is abundant and distinctly located in NASH as shown also by Wattacheril et al (Wattacheril et al., 2013). Here it is possible that ROS generated as a result of VAP-1 activity attack cellular lipids (for example the lipid species in question), which could lead to activation of the inflammatory response for example in kupffer cells which PA has been shown to induce (Miura et al., 2013). Its interesting to note that other studies using MS approaches have identified oxidized lipid products distinct in NASH (Feldstein et al., 2010) and have speculated these may be a result of free radicals. Thus whether oxidized products of this species are detected in NASH would need further investigation. Furthermore there is growing evidence of distinct localization of various lipids in NAFLD and NASH (Le Naour et al., 2009, Wattacheril et al., 2013) suggesting cellular damage in NASH may be an orchestrated event related to the type of fat and proteins present in particular anatomical locations.

This technique serves as a powerful tool for detecting pathological changes in NASH as recently shown by (Wattacheril et al., 2013) and thus may aid in biomarker discovery for NASH treatment. In contrast to MALDI-MS, MALDI-MSI avoids the need for extraction and purification of samples and the ability to perform tandem MS or fragmentation of the ionized samples may permit identification of molecules without recourse to standard preparations. Thus biopsy samples taken from NASH patients could help identify whether there are key disease biomarkers present. Furthermore in contrast to standard histology the identity of hundreds of proteins can be observed in a single measurement, reducing time constraints and requirement for pre-available detection reagents.

In all it is clear from our study and those of others that these applications can provide useful insight into possible disease pathogenesis, progression and diagnosis of NAFLD and NASH (Gorden et al., 2011), (Feldstein et al., 2010), (Verdam et al., 2013), (Wattacheril et al., 2013). With a recent report suggesting the potential of using a single section of tissue for both lipid and protein analysis (Steven and Bunch, 2013), MS represents a powerful technique reducing time and material requirements. Although there are some limitations to these technologies, for example identification of molecules is often based on known libraries of species which may not include every species detected thus some molecules are not identified for example in our study and by other investigators (Zaima et al., 2009), and statistical analysis which are often required for such large multivariate data sets may shone some differences we feel the advantages outweigh the disadvantages.

Future experiments should include identifying for example the glucose and fatty acid trafficking proteins which we have shown altered in disease, in a single measurement by color coding *m/z* spectra as shown in a recent method by Fonville et al (Fonville et al., 2013). Furthermore identification of the lipidomic profiles of isolated cells from NAFLD or NASH patients would aid in identifying which cells are responsible for the disease signature and use of laser microdissection of specific regions of liver would be beneficial in assessing disease pathogenesis since phospholipid zonation has been suggested to be associated with NASH pathogenesis (Wattacheril et al., 2013). This could be applied to using MALDI-MSI to detect possible localization of lipid species after VAP-1 intervention in PCLS. Furthermore with growing evidence that oxidative stress and ROS species lead to development of NASH, and with some MS studies linking volatile organic compounds in NASH (Verdam et al., 2013), it would be interesting to see of these are VAP-1-derived since VAP-1 is elevated in NASH. Thus identifying ROS generated by VAP-1 and their resultant lipid peroxidation products could be useful in biomarker discovery and diagnosis for NASH.

CHAPTER 7

7 CONCLUSIONS & FUTURE WORK

7.1 Overview

VAP-1 has a well established role in glucose (Enrique-Tarancon et al., 1998), (Morin et al., 2001), (El Hadri et al., 2002), (Fontana et al., 2001), (Marti et al., 1998) and lipid homeostasis (Morin et al., 2001), (Fontana et al., 2001), (Yu et al., 2002), (Carpene et al., 2006), (Mercier et al., 2001), (Subra et al., 2003), (Bour et al., 2005), (Marti et al., 2001), (Stolen et al., 2004a) as well as in inflammation (Salmi et al., 1993), (Tohka et al., 2001), (Merinen et al., 2005), (Lalor et al., 2002), (Lalor et al., 2007). VAP-1 levels are increased in NASH, (see Chapter 4), (Claridge L C, 2009) but its roles in hepatic glucose and lipid homeostasis were unknown up until this thesis (Figures 4.14, 5.19 and 5.20). In the liver it is able to recruit specific subset of cells during the inflammatory process. For example CD16+ monocytes are targeted to inflamed and fibrotic locations (Aspinall et al., 2010), whilst it also supports transcellular migration of CD4 lymphocytes (Shetty et al., 2011). Furthermore VAP-1 has potential roles in fibrosis for example sVAP-1 levels correlate with fibrosis scores (Claridge L C, 2009) and VAP-1 has been implicated in extracellular matrix remodeling by activating HSCs (unpublished observations, Centre for Liver Research). We have shown stimulation of VAP-1 leads to global activation of hepatic NF-κB and transcription of target genes (Figures 4.15 and 4.16), and in support of data in this thesis, our laboratory has shown that VAP-1 null mice have reduced steatosis and fibrosis after exposure to a high fat diet or CCL4 injury (unpublished observations, Centre for Liver Research). Hence VAP-1 has multiple roles in liver disease. NF-κB activation drives inflammatory and fibrotic liver disease, since it has been coupled to HSC activation (Elsharkawy et al., 1999) and Watson et al have shown that inhibition of NF-κB signaling leads to HSC apoptosis and reversal of fibrosis (Watson et al., 2008). Increased NF-κB activation has been reported in ALD

patients (Ribeiro et al., 2004) where it is associated with inflammation and fibrosis. Our data for VAP-1 activation of NF-κB suggests regulation of key genes such as ICAM-1, IL-6 and IL-10 which are associated with the activated HSC phenotype (Mann and Smart, 2002). Hence VAP-1 is a potential regulator of chronic disease through modulation of inflammation and fibrosis in addition to the metabolic consequences we describe in this thesis.

7.1.1 Physiological relevance of VAP-1 derived glucose and lipid accumulation in NASH

Since this multifunctional protein may do many things in long-term disease processes, it presents an interesting therapeutic target. It may initially afford protection to the cell, since VAP-1 signaling leads to accumulation of FFAs in PCLS, and TAG accumulation in the liver. Hepatocytes may be able to respond directly, or more likely we propose sVAP-1 or membrane bound VAP-1 on neighboring cells could promote local insulinomimetic effects on hepatocytes in this context. Furthermore it could also be recruiting in regulatory T cells (Shetty et al., 2011) or resolution promoting cells (Bonder et al., 2005), which can clear up acute inflammatory responses.

In NAFLD upregulation of hepatic VAP-1 could mimic or replace ineffective insulin signaling when hepatic IR prevails due to toxic ceramides and diacylglycerol (Samuel et al., 2010), in an attempt to regulate and restore glucose and lipid homeostasis systemically. Thus targeting of VAP-1 could potentially be used in ameliorating IR in adipose and muscle tissue by using cell directed therapy, or VAP-1 substrates could be used in the formulation of anti-diabetic drugs (Bonaiuto et al., 2010). However careful consideration needs to be taken since overexpression of VAP-1 is also

associated with diabetes like complications (Stolen et al., 2004a). The supply of exogenous lipids and FA from the diet or from adipose tissue depot overloads in an IR state could mean there is an increased requirement for VAP-1 activity to mop up excess and drive storage. Glucose would either be used for glycogen synthesis or storage, however when glycogen stores are overwhelmed glucose may enter glycolysis producing acetyl Co-A and hence used for DNL were the FA may enter further oxidation or storage and have potential in causing liver damage. The intermediate metabolite acetyl Co-A intricately links these two pathways. Increase in FFA influx and DNL using glucose as a substrate could potentially add further lipotoxicity to the cell. This would lead to generation of ROS, lipid peroxidation products, ER, and oxidative stress (Sanyal et al., 2001), (Neuschwander-Tetri, 2010), (Fu et al., 2011). Furthermore autophagy can lead to liberation of FA from lipid droplets (Singh et al., 2009), whilst glucose itself has been shown to induce apoptosis in hepatic cells (Chandrasekaran et al., 2010). Activation of HSCs and NF-κB would initiate the immune response, which would eventually lead to fibrosis, cirrhosis and even HCC (Feldstein, 2010), (De Minicis et al., 2013), (White et al., 2012), (Fares and Peron, 2013), although HCC is associated with cirrhosis, VAP-1 itself has been implicated in tumor angiogenesis (Marttila-Ichihara et al., 2009), (Marttila-Ichihara et al., 2010), (Ferjancic et al., 2013). Thus could this process cause upregulation of VAP-1 in hepatocytes, fuelling malignant transformation and growth thus linking NASH and HCC; this may explain why we have noted Huh7.5 and HepG2 display VAP-1 expression and not primary hepatocytes and thus may increase the risk for liver failure and mortality.

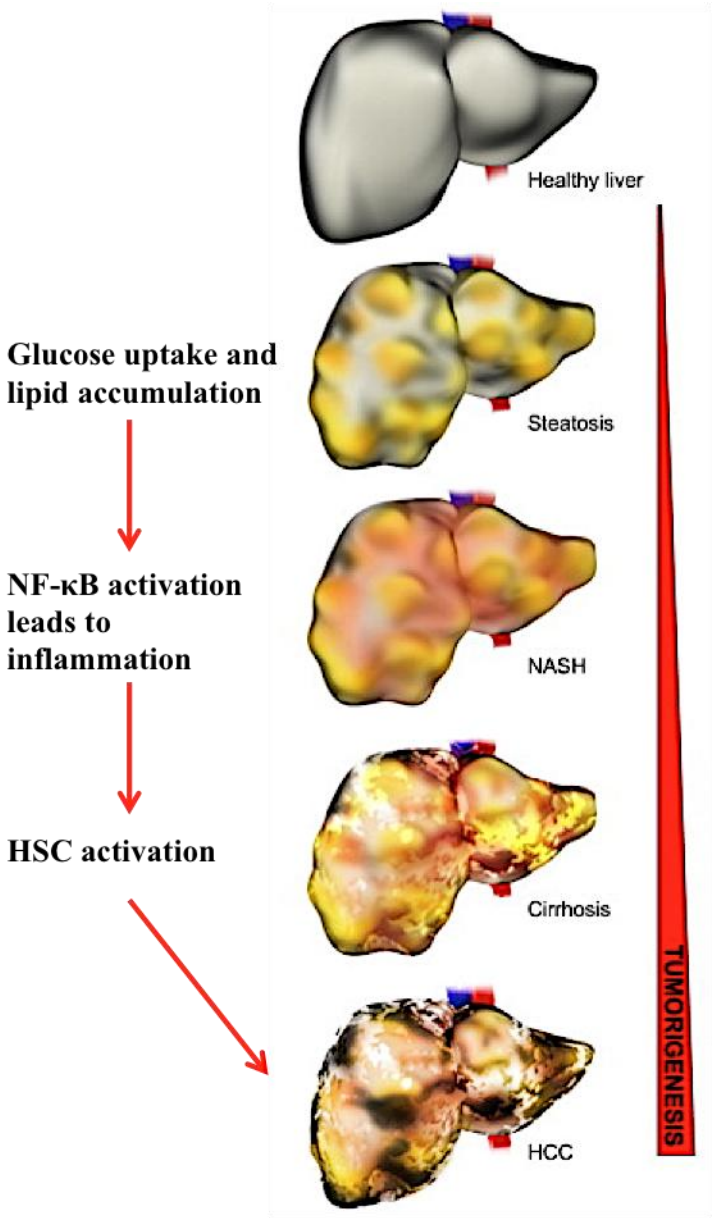

Figure 7.1: The hypothesized role of VAP-1 in the spectrum of NAFLD
Extra hepatic IR leads to excess FFA to the liver, which can eventually become IR, VAP-1 acts as a compensator to insulin by modulating glucose and lipid homeostasis, this eventually leads to further lipid loading in the liver, activation of NF-κB not only recruits inflammatory mediators but also promotes HSC activation and subsequent fibrosis which can eventually lead to HCC were VAP-1 can also increase recruitment of myeloid cells.

Thus VAP-1 may represent a valuable hepatic therapeutic target against lipid-induced damage by ROS, inflammation, and fibrosis, which ultimately progresses, to NASH, cirrhosis and HCC. Additionally blockade of VAP-1 may have beneficial effects in other tissues and interestingly some of these tissues are involved in late complications of diabetes. For example VAP-1 is expressed in brain (Hernandez-Guillamon et al., 2012) and associated with brain damage, eye (Almulki et al., 2010) where it is involved in diabetic retinopathy (Noda et al., 2009), kidney with involvement in nephropathy (Stolen et al., 2004a) and the heart and circulatory system (Salmi and Jalkanen, 2006) where its been shown to have a role in atherosclerosis (Stolen et al., 2004a). This widens the pool of organs where anti-VAP-1 therapy could be targeted, for example VAP-1 inhibition has been shown to prevent endotoxin induced uveitis (Noda et al., 2008). Thus the use of VAP-1 in therapy could be exploited by using cell directed therapy with vectors targeting VAP-1. Since the activation of NF-κB is important during fibrosis (Sunami et al., 2012), (Xiao et al., 2013) direct blocking of VAP-1 will also inhibit fibrosis and inflammation and targeting key genes in the NF-κB pathway may dampen down key responses.

However careful consideration for treatment needs to be considered since if a patient with fibrosis was targeted with therapeutics directed against VAP-1, these may also block the influx of resolution-promoting macrophages. Certainly in our lab clinical trials testing impact of anti-VAP-1 therapy are being planned. In one, PBC transplant patients will be administered with a bolus of VAP-1 antibody to prevent early leukocyte recruitment to the graft, outcomes linked to allograft rejection will be assessed along with safety endpoints. In a similar vein, small molecule inhibitors of VAP-1 reduce recruitment of myeloid cells to tumors (Marttila-Ichihara et al., 2010)

and clinical trials involving oral administration of VAP-1 antagonist in psoriasis and rheumatoid arthritis have begun (http://www.proximagen.com/docs/Proximagen%20VAP-1.pdf). The trials to date have focused on small molecule inhibitors or humanized monoclonal antibodies for therapy, but a recent study reports new thiazole derivatives for inhibiting VAP-1 in the treatment of diabetic macula edema (Inoue et al., 2013).

Our data also supports enhanced expression of MAO other than VAP-1 during liver disease (Figure 4.2). These enzymes have been linked to depression and inhibitors such as selegiline, which targets MAOB, are used in the treatment of depression and Parkinson's disease. Thus treatment for NAFLD and NASH could be combined with existing MAO inhibitors to improve psychological ie: improve sedentary lifestyle and pathological mechanisms (Nocito et al., 2007) and possibly MAO derived glucose and lipid uptake (Gres et al., 2013).

We accept there are limitations to our study, for example use of PCLS from patients or donors where external factors such as insulin state, recent meal patterns and whether the person was a deceased organ donor, may impact upon our biological readouts. Furthermore we found variable responses to hydrogen peroxide, which could be a deficiency in our experimental design where the use of repeated dosing may have overcome local antioxidant defense or it may be that other metabolites of VAP-1 which this study has not investigated may initiate responses for example a recent report has found similar responses, and have shown oxidation products of serotonin such as 5-hydroxyindoleacetic acid (HIAA) have the ability to bind to PPARϒ and regulate genes involved in lipid and glucose handling such as FABP4,

CD36 and GLUT1 thus leading to lipid storage in adipose tissue (Gres et al., 2013). This suggests other AO, and oxidation products other than hydrogen peroxide have the ability to regulate glucose and lipid handling in extra hepatic tissue and impact on the pathogenesis of NAFLD and NASH.

7.1.2 Hepatic expression of glucose and fatty acid trafficking transporter proteins and implications in NASH

We have documented differential expression of carbohydrate transporters (GLUTS), FABPs, FATPs, CAV-1 and members of the LRP receptor family in NASH and ALD and in particular in isolated hepatic cells (Chapter 3) which have roles in LCFA uptake, FA activation, TAG synthesis, β-oxidation, which may contribute to global changes in disease. Although protein identification for some remains to be confirmed this suggests that there are distinct GLUT and lipid trafficking protein signatures for hepatic cells and thus disease pathogenesis may not be restricted to one cell alone. Thus this study provides a basic framework for future studies focusing on metabolic aspects of liver disease looking in to mechanistic links and also as therapeutic targets.

In addition this study identified presence of several GLUTS and fatty acid trafficking proteins upregulated in NASH, which in Chapters 4 and 5 were not upregulated due to VAP-1 activation. This suggests mechanisms independent of VAP-1 alter transporter proteins, which could be adding further damage to the liver and exacerbating disease pathogenesis. Thus these transporters may serve as potential therapeutic or diagnostic targets. For example GLUT5 may serve as an attractive therapeutic target in NAFLD and NASH since its substrate fructose is widely used in the manufacturing of food and drinks and has the potential to induce disease progression from NAFLD to

NASH. Fructose metabolism leads to formation of free radicals, and fructose consumption has been implicated in NAFLD (Vila et al., 2008), (Ouyang et al., 2008), (Zelber-Sagi et al., 2007) and fibrosis severity (Abdelmalek et al., 2010). Fructose affects transcription factors ChREBP and SREBP-1c by activating and increasing expression of key enzymes involved in DNL thus promoting hepatic steatogenesis (Lim et al., 2010). Specific pharmacological inhibitors are not available, however interestingly a dietary supplement (Anthocyanin) prepared from some berries has been shown to reduce expression of fructose transporters GLUT5 and GLUT2 (F. Alzaid, 2010). This serves as an effective treatment strategy for preventing fructose-induced steatosis. Furthermore blockade of GLUTS could not only hinder onset of HCC but also progression due to decreased fuel intake, which is a requirement for tumor growth since tumors require a lot of fuel and this enters through GLUT transporters, thus blocking these would potentially hinder HCC progression.

Furthermore FABP1 and FABP4 expression was increased in NASH and ALD patients and thus may serve as a potential diagnostic biomarkers since these two proteins are found in the circulation (Xu et al., 2007), (Xu et al., 2006), (Pelsers et al., 2002). In addition FABP1 may be useful in distinguishing NAFLD from NASH since its elevated levels in serum have been reported to be related to hepatocellular damage (Pelsers et al., 2002). Also FABP4 has been reported as an early indicator for MetS (Xu et al., 2007), (Tso et al., 2007), (Stejskal and Karpisek, 2006). To note this transporter may be beneficial as both a diagnostic and therapeutic target since adipocytes lacking FABP4 have reduced lipolysis (Coe et al., 1999) this means that blocking this transporter would result in a decrease in FFA flux to the liver. Giving this exciting avenue care must be taken since single KO mice for FABP4 and FABP5

only show modest sensitivity to insulin and do not protect from fatty liver (Maeda et al., 2003), (Hotamisligil et al., 1996) whilst double KO mice for FABP4 and FABP5 show increased protection from fatty liver (Maeda et al., 2005). Therapies, using small inhibitor molecules against FABP4 in mice have already proven to be successful against type II diabetes and atherosclerosis (Furuhashi et al., 2007). Thus mechanisms such as VAP-1 activity, which may underlie regulation of FABPs, could have potential for therapy.

Similarly elevated expression for FATPs in NASH may be therapeutically relevant, since for example knockdown of FATP3 in rat hepatocytes results in a decrease in lipogenic transcription factors (Bu et al., 2009) and thus disease-induced upregulation could contribute to steatogenesis. However care must be taken before strategies targeting these proteins are tested since inhibition for example of FATP5 may lead to cholestasis (Musso et al., 2009) since FATP5 deficient mice have been shown to have defective bile acid conjugation (Hubbard et al., 2006).

Therefore standard current clinical diagnosis protocols could be used in combination with serum detection of some of these soluble proteins we report to, improve stratification of patients with hepatic disease. sVAP-1 levels already show promise for potential as a serological marker of fibrosis stage (Claridge L C, 2009). FABP-1 could distinguish between NAFLD and NASH, FABP4 expression may identify individuals at risk of developing NAFLD and LOX, which is reported to be elevated in disease, could be used as a serum marker together with sVAP-1 for detecting liver fibrosis (Murawaki et al., 1991). In the clinical setting these proteins could be easily detected in serum using GC.

7.1.3 Use of GC and MALDI-MS/MSI in diagnosis and biomarker discovery in NASH

This study has shown that MS techniques have the potential to identify differences between diseases, in particular the histologically hard to distinguish NASH and ALD. To date our analysis has been restricted to the use of liver samples and further studies would need to search for serological correlates, which could be screened with non-invasively collected material. Our sample numbers need to be increased further to assess the validity of our approach but these techniques have much potential for use in diagnostics and also biomarker discovery. For example using these techniques two protein biomarkers Carbamoyl phosphate synthase 1 (CPS1) and 78kDa glucose-regulated protein (GRP78) have been identified as differentially expressed in NASH (Rodriguez-Suarez et al., 2010). Furthermore our analysis and reported studies (Wattacheril et al., 2013) has identified the *m/z* 772 species specifically targeted to fibrous septae areas were we find extensive VAP-1 expression. It would be interesting to see if this species is detected in serum. Thus this species could be a signaling molecule and its functional importance needs further investigation. Furthermore isolated cells, PCLS, and MALDI-MSI could be combined to find markers or mechanisms linked to spectrum progression in NAFLD.

To conclude, the progression from NAFLD to NASH involves multiple, complex mechanisms. However the hallmark is oxidative stress and ROS generation, which arise due to lipid overload in the hepatocytes. We propose VAP-1 as a likely contributor to this process since in the liver its expression and activity are increased in NASH, thus VAP-1 is the "moral molecule" with bad side effects. On the one hand it attempts to do "good" by regulating systemic glucose and lipid homeostasis by

mimicking insulinomimetic effects and at the same time activating protective mechanisms for example GLUT10, NF-κB1 and IL-10 which have anti-inflammatory and ROS mopping up roles. On the other hand the "bad" side of VAP-1 function leads to lipotoxicity to the cell, which ultimately leads to cellular damage, and in the long-term liver failure. These findings suggest an interesting role for VAP-1 in the liver and future studies will shed more light on this multifunctional protein.

Investigations, which are a direct consequence of our current data, are outlined below.

7.1.4 Future work

Use of our ex-vivo model to study the effects of VAP-1 intervention in PCLS

- It would be interesting to see how PCLS from NASH and ALD patients would respond to an exogenous supply of VAP-1 and to examine glucose and FA transporter expression within them after treatment. We observed differences in basal glucose uptake in VAP-1 null animals and it would be useful to know if similar changes in baseline responses are evident in human disease.
- Silencing of specific transporters highlighted in the present study as a result of VAP-1 activation. We need to determine whether the changes we noted are functionally relevant. Thus if we knock key genes down do we impair our effects of VAP-1 stimulation?
- It would be interesting to see if the activity of VAP-1 is increasing levels of enzymes involved in DNL in PCLS.
- Use of fructose in glucose uptake assays, and to examine if it drives endogenous lipogenesis in the absence of lipid in the liver. The metabolism of

fructose is of key importance in the western diet-induced increase in NAFLD and our assays could provide an important means to dissect these effects.

- Using our *ex-vivo* model (Karim et al., 2013) our studies could be taken further by studying inter organ interactions by taking tissue slices from adipose and liver tissue or even muscle. In a manner similar to a recently published report using liver and intestinal slices (van Midwoud et al., 2010b).
- Efficacy of potential drugs or antibodies targeted against VAP-1 could be studied directly in the liver or other organs by using our novel *ex-vivo* model.

Use of MALDI in diagnostic and biomarker discovery for NASH

- Using our *ex-vivo* model and combining it with Liquid Extraction Surface Analysis Mass Spectrometry LESA-MS for identification of lipids and protein biomarker discovery. For example we could use MALDI-MSI to validate our qPCR data at the protein level in a single measurement, furthermore we could analyze serum from patients with normal liver, with NASH, or diabetes and then follow this with PCA and see if we can find a discriminator which predicts NAFLD or NASH such as FABP4 which has been shown to predict MetS.
- LESA-MS analysis of liver to see if glucose and lipid transporters are expressed relative to the zonation of liver.
- Identification of lipidomic profiles of cells isolated from NAFLD and NASH patients to identify cells with specific disease signature.
- Labeling of FFA and using MALDI-MSI to identify where FFA are distributed and incorporated into PCLS after VAP-1 intervention.

Other studies

- It would be interesting to see if there are elevated levels of VAP-1 and sVAP-1 in the pediatric population where there have been reported cases of NASH (Baldridge et al., 1995), (Rashid and Roberts, 2000). This would further provide direct evidence for a link between VAP-1 and NASH.
- Further more it would be of interest to see if VAP-1 colocalizes with any of the glucose or fatty acid trafficking proteins highlighted in this thesis.

LIST OF REFERENCES

2001. Executive Summary of The Third Report of The National Cholesterol Education Program (NCEP) Expert Panel on Detection, Evaluation, And Treatment of High Blood Cholesterol In Adults (Adult Treatment Panel III). *Jama.,* 285**,** 2486-97.

AALTO, K., MAKSIMOW, M., JUONALA, M., VIIKARI, J., JULA, A., KAHONEN, M., JALKANEN, S., RAITAKARI, O. T. & SALMI, M. 2012. Soluble vascular adhesion protein-1 correlates with cardiovascular risk factors and early atherosclerotic manifestations. *Arterioscler Thromb Vasc Biol.,* 32**,** 523-32. doi: 10.1161/ATVBAHA.111.238030. Epub 2011 Nov 23.

ABBOTT, S. K., JENNER, A. M., MITCHELL, T. W., BROWN, S. H., HALLIDAY, G. M. & GARNER, B. 2013. An improved high-throughput lipid extraction method for the analysis of human brain lipids. *Lipids.,* 48**,** 307-18. doi: 10.1007/s11745-013-3760-z. Epub 2013 Jan 26.

ABDELMALEK, M. F., SUZUKI, A., GUY, C., UNALP-ARIDA, A., COLVIN, R., JOHNSON, R. J. & DIEHL, A. M. 2010. Increased fructose consumption is associated with fibrosis severity in patients with nonalcoholic fatty liver disease. *Hepatology.,* 51**,** 1961-71. doi: 10.1002/hep.23535.

ABDELWAHAB, S. A., OWADA, Y., KITANAKA, N., IWASA, H., SAKAGAMI, H. & KONDO, H. 2003. Localization of brain-type fatty acid-binding protein in Kupffer cells of mice and its transient decrease in response to lipopolysaccharide. *Histochem Cell Biol.,* 119**,** 469-75. Epub 2003 Jun 11.

ABELLA, A., GARCIA-VICENTE, S., VIGUERIE, N., ROS-BARO, A., CAMPS, M., PALACIN, M., ZORZANO, A. & MARTI, L. 2004. Adipocytes release a soluble form of VAP-1/SSAO by a metalloprotease-dependent process and in a regulated manner. *Diabetologia.,* 47**,** 429-38. Epub 2004 Feb 13.

ADAMS, L. A., WHITE, S. W., MARSH, J. A., LYE, S. J., CONNOR, K. L., MAGANGA, R., AYONRINDE, O. T., OLYNYK, J. K., MORI, T. A., BEILIN, L. J., PALMER, L. J., HAMDORF, J. M. & PENNELL, C. E. 2013. Association between liver-specific gene polymorphisms and their expression levels with nonalcoholic fatty liver disease. *Hepatology.,* 57**,** 590-600. doi: 10.1002/hep.26184.

ADIDA, A. & SPENER, F. 2002. Intracellular lipid binding proteins and nuclear receptors involved in branched-chain fatty acid signaling. *Prostaglandins Leukot Essent Fatty Acids.,* 67**,** 91-8.

ADINOLFI, L. E. & RESTIVO, L. 2011. Does vitamin E cure nonalcoholic steatohepatitis? *Expert Rev Gastroenterol Hepatol.,* 5**,** 147-50. doi: 10.1586/egh.11.27.

AERNI, H. R., CORNETT, D. S. & CAPRIOLI, R. M. 2006. Automated acoustic matrix deposition for MALDI sample preparation. *Anal Chem.,* 78**,** 827-34.

AGELLON, L. B., DROZDOWSKI, L., LI, L., IORDACHE, C., LUONG, L., CLANDININ, M. T., UWIERA, R. R., TOTH, M. J. & THOMSON, A. B. 2007. Loss of intestinal fatty acid binding protein increases the susceptibility of male mice to high fat diet-induced fatty liver. *Biochim Biophys Acta.,* 1771**,** 1283-8. Epub 2007 Aug 22.

AGULLEIRO, M. J., ANDRE, M., MORAIS, S., CERDA, J. & BABIN, P. J. 2007. High transcript level of fatty acid-binding protein 11 but not of very low-density lipoprotein receptor is correlated to ovarian follicle atresia in a teleost fish (Solea senegalensis). *Biol Reprod.,* 77**,** 504-16. Epub 2007 Jun 6.

AHIMA, R. S. & FLIER, J. S. 2000. Adipose tissue as an endocrine organ. *Trends Endocrinol Metab.,* 11**,** 327-32.

AHN, J., LEE, H., JUNG, C. H. & HA, T. 2012. Lycopene inhibits hepatic steatosis via microRNA-21-induced downregulation of fatty acid-binding protein 7 in mice fed a high-fat diet. *Mol Nutr Food Res,* 12**,** 201200182.

AHN, J. H., KIM, M. H., KWON, H. J., CHOI, S. Y. & KWON, H. Y. 2013. Protective Effects of Oleic Acid Against Palmitic Acid-Induced Apoptosis in Pancreatic AR42J Cells and Its Mechanisms. *Korean J Physiol Pharmacol.,* 17**,** 43-50. doi: 10.4196/kjpp.2013.17.1.43. Epub 2013 Feb 14.

AIRENNE, T. T., NYMALM, Y., KIDRON, H., SMITH, D. J., PIHLAVISTO, M., SALMI, M., JALKANEN, S., JOHNSON, M. S. & SALMINEN, T. A. 2005. Crystal structure of the human vascular adhesion protein-1: unique structural features with functional implications. *Protein Sci.,* 14**,** 1964-74.

AITHAL, G. P., THOMAS, J. A., KAYE, P. V., LAWSON, A., RYDER, S. D., SPENDLOVE, I., AUSTIN, A. S., FREEMAN, J. G., MORGAN, L. & WEBBER, J. 2008. Randomized, placebo-controlled trial of pioglitazone in nondiabetic subjects with nonalcoholic steatohepatitis. *Gastroenterology.,* 135**,** 1176-84. doi: 10.1053/j.gastro.2008.06.047. Epub 2008 Jun 25.

AKCAM, M., BOYACI, A., PIRGON, O., KOROGLU, M. & DUNDAR, B. N. 2013. Importance of the liver ultrasound scores in pubertal obese children with nonalcoholic fatty liver disease. *Clin Imaging.,* 37**,** 504-8. doi: 10.1016/j.clinimag.2012.07.011. Epub 2012 Sep 3.

ALBERTI, K. G. & ZIMMET, P. Z. 1998. Definition, diagnosis and classification of diabetes mellitus and its complications. Part 1: diagnosis and classification of diabetes mellitus provisional report of a WHO consultation. *Diabet Med.,* 15**,** 539-53.

ALLER, R., DE LUIS, D. A., FERNANDEZ, L., CALLE, F., VELAYOS, B., IZAOLA, O., GONZALEZ SAGRADO, M., CONDE, R. & GONZALEZ, J. M. 2009. Influence of Ala54Thr polymorphism of fatty acid-binding protein 2 on histological alterations and insulin resistance of non alcoholic fatty liver disease. *Eur Rev Med Pharmacol Sci.,* 13**,** 357-64.

ALLER, R., DE LUIS, D. A., FERNANDEZ, L., CALLE, F., VELAYOS, B., OLCOZ, J. L., IZAOLA, O., SAGRADO, M. G., CONDE, R. & GONZALEZ, J. M. 2008. Influence of insulin resistance and adipokines in the grade of steatosis of nonalcoholic fatty liver disease. *Dig Dis Sci.,* 53**,** 1088-92. Epub 2007 Oct 13.

ALMULKI, L., NODA, K., NAKAO, S., HISATOMI, T., THOMAS, K. L. & HAFEZI-MOGHADAM, A. 2010. Localization of vascular adhesion protein-1 (VAP-1) in the human eye. *Exp Eye Res.,* 90**,** 26-32. doi: 10.1016/j.exer.2009.09.005. Epub 2009 Sep 15.

ALTELAAR, A. F., KLINKERT, I., JALINK, K., DE LANGE, R. P., ADAN, R. A., HEEREN, R. M. & PIERSMA, S. R. 2006. Gold-enhanced biomolecular surface imaging of cells and tissue by SIMS and MALDI mass spectrometry. *Anal Chem.,* 78**,** 734-42.

ALVES-COSTA, F. A., DENOVAN-WRIGHT, E. M., THISSE, C., THISSE, B. & WRIGHT, J. M. 2008. Spatio-temporal distribution of fatty acid-binding protein 6 (fabp6) gene transcripts in the developing and adult zebrafish (Danio rerio). *Febs J.,* 275**,** 3325-34. Epub 2008 May 19.

AMANN, T., MAEGDEFRAU, U., HARTMANN, A., AGAIMY, A., MARIENHAGEN, J., WEISS, T. S., STOELTZING, O., WARNECKE, C.,

SCHOLMERICH, J., OEFNER, P. J., KREUTZ, M., BOSSERHOFF, A. K. & HELLERBRAND, C. 2009. GLUT1 expression is increased in hepatocellular carcinoma and promotes tumorigenesis. *Am J Pathol.*, 174**,** 1544-52. Epub 2009 Mar 12.

ANDERSSON, M., GROSECLOSE, M. R., DEUTCH, A. Y. & CAPRIOLI, R. M. 2008. Imaging mass spectrometry of proteins and peptides: 3D volume reconstruction. *Nat Methods.*, 5**,** 101-8. doi: 10.1038/nmeth1145.

ANDRIKOPOULOS, S., BLAIR, A. R., DELUCA, N., FAM, B. C. & PROIETTO, J. 2008. Evaluating the glucose tolerance test in mice. *Am J Physiol Endocrinol Metab.*, 295**,** E1323-32. doi: 10.1152/ajpendo.90617.2008. Epub 2008 Sep 23.

ANSTEE, Q. M. & GOLDIN, R. D. 2006. Mouse models in non-alcoholic fatty liver disease and steatohepatitis research. *Int J Exp Pathol.*, 87**,** 1-16.

APREA, E., MORISCO, F., BIASIOLI, F., VITAGLIONE, P., CAPPELLIN, L., SOUKOULIS, C., LEMBO, V., GASPERI, F., D'ARGENIO, G., FOGLIANO, V. & CAPORASO, N. 2012. Analysis of breath by proton transfer reaction time of flight mass spectrometry in rats with steatohepatitis induced by high-fat diet. *J Mass Spectrom.*, 47**,** 1098-103. doi: 10.1002/jms.3009.

ASCHENBACH, J. R., STEGLICH, K., GABEL, G. & HONSCHA, K. U. 2009. Expression of mRNA for glucose transport proteins in jejunum, liver, kidney and skeletal muscle of pigs. *J Physiol Biochem.*, 65**,** 251-66.

ASPINALL, A. I., CURBISHLEY, S. M., LALOR, P. F., WESTON, C. J., LIASKOU, E., ADAMS, R. M., HOLT, A. P. & ADAMS, D. H. 2010. CX(3)CR1 and vascular adhesion protein-1-dependent recruitment of CD16(+) monocytes across human liver sinusoidal endothelium. *Hepatology.*, 51**,** 2030-9. doi: 10.1002/hep.23591.

ASTIGARRAGA, E., BARREDA-GOMEZ, G., LOMBARDERO, L., FRESNEDO, O., CASTANO, F., GIRALT, M. T., OCHOA, B., RODRIGUEZ-PUERTAS, R. & FERNANDEZ, J. A. 2008. Profiling and imaging of lipids on brain and liver tissue by matrix-assisted laser desorption/ ionization mass spectrometry using 2-mercaptobenzothiazole as a matrix. *Anal Chem.*, 80**,** 9105-14. doi: 10.1021/ac801662n.

ATSHAVES, B. P., MARTIN, G. G., HOSTETLER, H. A., MCINTOSH, A. L., KIER, A. B. & SCHROEDER, F. 2010. Liver fatty acid-binding protein and obesity. *J Nutr Biochem.*, 21**,** 1015-32.

AUINGER, A., HELWIG, U., PFEUFFER, M., RUBIN, D., LUEDDE, M., RAUSCHE, T., EDDINE EL MOKHTARI, N., FOLSCH, U. R., SCHREIBER, S., FREY, N. & SCHREZENMEIR, J. 2012. A variant in the heart-specific fatty acid transport protein 6 is associated with lower fasting and postprandial TAG, blood pressure and left ventricular hypertrophy. *Br J Nutr.*, 107**,** 1422-8. doi: 10.1017/S0007114511004727. Epub 2011 Sep 16.

AUINGER, A., VALENTI, L., PFEUFFER, M., HELWIG, U., HERRMANN, J., FRACANZANI, A. L., DONGIOVANNI, P., FARGION, S., SCHREZENMEIR, J. & RUBIN, D. 2010. A promoter polymorphism in the liver-specific fatty acid transport protein 5 is associated with features of the metabolic syndrome and steatosis. *Horm Metab Res.*, 42**,** 854-9. Epub 2010 Oct 13.

AXELROD, J. D. & PILCH, P. F. 1983. Unique cytochalasin B binding characteristics of the hepatic glucose carrier. *Biochemistry.*, 22**,** 2222-7.

BABAEV, V. R., RUNNER, R. P., FAN, D., DING, L., ZHANG, Y., TAO, H., ERBAY, E., GORGUN, C. Z., FAZIO, S., HOTAMISLIGIL, G. S. & LINTON, M. F. 2011. Macrophage Mal1 deficiency suppresses atherosclerosis in low-density lipoprotein receptor-null mice by activating peroxisome proliferator-activated receptor-gamma-regulated genes. *Arterioscler Thromb Vasc Biol.,* 31**,** 1283-90. doi: 10.1161/ATVBAHA.111.225839. Epub 2011 Apr 7.

BAIER, L. J., SACCHETTINI, J. C., KNOWLER, W. C., EADS, J., PAOLISSO, G., TATARANNI, P. A., MOCHIZUKI, H., BENNETT, P. H., BOGARDUS, C. & PROCHAZKA, M. 1995. An amino acid substitution in the human intestinal fatty acid binding protein is associated with increased fatty acid binding, increased fat oxidation, and insulin resistance. *J Clin Invest.,* 95**,** 1281-7.

BALDRIDGE, A. D., PEREZ-ATAYDE, A. R., GRAEME-COOK, F., HIGGINS, L. & LAVINE, J. E. 1995. Idiopathic steatohepatitis in childhood: a multicenter retrospective study. *J Pediatr.,* 127**,** 700-4.

BALKAU, B. & CHARLES, M. A. 1999. Comment on the provisional report from the WHO consultation. European Group for the Study of Insulin Resistance (EGIR). *Diabet Med.,* 16**,** 442-3.

BALUYA, D. L., GARRETT, T. J. & YOST, R. A. 2007. Automated MALDI matrix deposition method with inkjet printing for imaging mass spectrometry. *Anal Chem.,* 79**,** 6862-7. Epub 2007 Jul 21.

BARTHEL, A., SCHMOLL, D. & UNTERMAN, T. G. 2005. FoxO proteins in insulin action and metabolism. *Trends Endocrinol Metab.,* 16**,** 183-9.

BASFORD, J. E., WANCATA, L., HOFMANN, S. M., SILVA, R. A., DAVIDSON, W. S., HOWLES, P. N. & HUI, D. Y. 2011. Hepatic deficiency of low density lipoprotein receptor-related protein-1 reduces high density lipoprotein secretion and plasma levels in mice. *J Biol Chem.,* 286**,** 13079-87. doi: 10.1074/jbc.M111.229369. Epub 2011 Feb 22.

BASS, N. M., MANNING, J. A., OCKNER, R. K., GORDON, J. I., SEETHARAM, S. & ALPERS, D. H. 1985. Regulation of the biosynthesis of two distinct fatty acid-binding proteins in rat liver and intestine. Influences of sex difference and of clofibrate. *J Biol Chem.,* 260**,** 1432-6.

BATALLER, R. & BRENNER, D. A. 2005. Liver fibrosis. *J Clin Invest.,* 115**,** 209-18.

BECHMANN, L. P., HANNIVOORT, R. A., GERKEN, G., HOTAMISLIGIL, G. S., TRAUNER, M. & CANBAY, A. 2012. The interaction of hepatic lipid and glucose metabolism in liver diseases. *J Hepatol.,* 56**,** 952-64. doi: 10.1016/j.jhep.2011.08.025. Epub 2011 Dec 13.

BEISIEGEL, U., WEBER, W., IHRKE, G., HERZ, J. & STANLEY, K. K. 1989. The LDL-receptor-related protein, LRP, is an apolipoprotein E-binding protein. *Nature.,* 341**,** 162-4.

BELFORT, R., HARRISON, S. A., BROWN, K., DARLAND, C., FINCH, J., HARDIES, J., BALAS, B., GASTALDELLI, A., TIO, F., PULCINI, J., BERRIA, R., MA, J. Z., DWIVEDI, S., HAVRANEK, R., FINCKE, C., DEFRONZO, R., BANNAYAN, G. A., SCHENKER, S. & CUSI, K. 2006. A placebo-controlled trial of pioglitazone in subjects with nonalcoholic steatohepatitis. *N Engl J Med.,* 355**,** 2297-307.

BELKE, D. D., LARSEN, T. S., GIBBS, E. M. & SEVERSON, D. L. 2001. Glucose metabolism in perfused mouse hearts overexpressing human GLUT-4 glucose transporter. *Am J Physiol Endocrinol Metab.,* 280**,** E420-7.

BELL, G. I., KAYANO, T., BUSE, J. B., BURANT, C. F., TAKEDA, J., LIN, D., FUKUMOTO, H. & SEINO, S. 1990. Molecular biology of mammalian glucose transporters. *Diabetes Care.,* 13**,** 198-208.

BHALA, N., JOUNESS, R. I. & BUGIANESI, E. 2013. Epidemiology and Natural History of Patients with NAFLD. *Curr Pharm Des,* 4**,** 4.

BHOGAL, R. H., HODSON, J., BARTLETT, D. C., WESTON, C. J., CURBISHLEY, S. M., HAUGHTON, E., WILLIAMS, K. T., REYNOLDS, G. M., NEWSOME, P. N., ADAMS, D. H. & AFFORD, S. C. 2011. Isolation of primary human hepatocytes from normal and diseased liver tissue: a one hundred liver experience. *PLoS One.,* 6**,** e18222. doi: 10.1371/journal.pone.0018222.

BIEGHS, V., VERHEYEN, F., VAN GORP, P. J., HENDRIKX, T., WOUTERS, K., LUTJOHANN, D., GIJBELS, M. J., FEBBRAIO, M., BINDER, C. J., HOFKER, M. H. & SHIRI-SVERDLOV, R. 2012. Internalization of modified lipids by CD36 and SR-A leads to hepatic inflammation and lysosomal cholesterol storage in Kupffer cells. *PLoS One.,* 7**,** e34378. doi: 10.1371/journal.pone.0034378. Epub 2012 Mar 28.

BILIR, B. M., GONG, T. W., KWASIBORSKI, V., SHEN, C. S., FILLMORE, C. S., BERKOWITZ, C. M. & GUMUCIO, J. J. 1993. Novel control of the position-dependent expression of genes in hepatocytes. The GLUT-1 transporter. *J Biol Chem.,* 268**,** 19776-84.

BILLERBECK, E., DE JONG, Y., DORNER, M., DE LA FUENTE, C. & PLOSS, A. 2013. Animal models for hepatitis C. *Curr Top Microbiol Immunol.,* 369:49-86**.,** 10.1007/978-3-642-27340-7_3.

BLACHIER, M., LELEU, H., PECK-RADOSAVLJEVIC, M., VALLA, D. C. & ROUDOT-THORAVAL, F. 2013. The burden of liver disease in Europe: a review of available epidemiological data. *J Hepatol.,* 58**,** 593-608. doi: 10.1016/j.jhep.2012.12.005.

BLOMHOFF, R. & BLOMHOFF, H. K. 2006. Overview of retinoid metabolism and function. *J Neurobiol.,* 66**,** 606-30.

BONAIUTO, E., LUNELLI, M., SCARPA, M., VETTOR, R., MILAN, G. & DI PAOLO, M. L. 2010. A structure-activity study to identify novel and efficient substrates of the human semicarbazide-sensitive amine oxidase/VAP-1 enzyme. *Biochimie.,* 92**,** 858-68. doi: 10.1016/j.biochi.2010.03.006. Epub 2010 Mar 16.

BONDER, C. S., NORMAN, M. U., SWAIN, M. G., ZBYTNUIK, L. D., YAMANOUCHI, J., SANTAMARIA, P., AJUEBOR, M., SALMI, M., JALKANEN, S. & KUBES, P. 2005. Rules of recruitment for Th1 and Th2 lymphocytes in inflamed liver: a role for alpha-4 integrin and vascular adhesion protein-1. *Immunity.,* 23**,** 153-63.

BONEN, A., CHABOWSKI, A., LUIKEN, J. J. & GLATZ, J. F. 2007. Is membrane transport of FFA mediated by lipid, protein, or both? Mechanisms and regulation of protein-mediated cellular fatty acid uptake: molecular, biochemical, and physiological evidence. *Physiology (Bethesda).* 22**,** 15-29.

BOOMSMA, F., DE KAM, P. J., TJEERDSMA, G., VAN DEN MEIRACKER, A. H. & VAN VELDHUISEN, D. J. 2000. Plasma semicarbazide-sensitive amine

oxidase (SSAO) is an independent prognostic marker for mortality in chronic heart failure. *Eur Heart J.,* 21**,** 1859-63.

BOOMSMA, F., VAN DEN MEIRACKER, A. H., WINKEL, S., AANSTOOT, H. J., BATSTRA, M. R., MAN IN 'T VELD, A. J. & BRUINING, G. J. 1999. Circulating semicarbazide-sensitive amine oxidase is raised both in type I (insulin-dependent), in type II (non-insulin-dependent) diabetes mellitus and even in childhood type I diabetes at first clinical diagnosis. *Diabetologia.,* 42**,** 233-7.

BOOMSMA, F., VAN VELDHUISEN, D. J., DE KAM, P. J., MAN IN'T VELD, A. J., MOSTERD, A., LIE, K. I. & SCHALEKAMP, M. A. 1997. Plasma semicarbazide-sensitive amine oxidase is elevated in patients with congestive heart failure. *Cardiovasc Res.,* 33**,** 387-91.

BOORD, J. B., FAZIO, S. & LINTON, M. F. 2002. Cytoplasmic fatty acid-binding proteins: emerging roles in metabolism and atherosclerosis. *Curr Opin Lipidol.,* 13**,** 141-7.

BOUR, S., VISENTIN, V., GRES, S., SAULNIER-BLACHE, J. S., WABITSCH, M. & CARPENE, C. 2005. Tyramine, benzylamine, and to a lesser extent histamine, partially mimic the adipogenic effect of insulin in a human preadipocyte cell strain. *Inflamm Res.,* 54**,** S60-1.

BOUWENS, L. & WISSE, E. 1992. Pit cells in the liver. *Liver.,* 12**,** 3-9.

BRADBURY, M. W. 2006. Lipid metabolism and liver inflammation. I. Hepatic fatty acid uptake: possible role in steatosis. *Am J Physiol Gastrointest Liver Physiol.,* 290**,** G194-8.

BRAVO, A. A., SHETH, S. G. & CHOPRA, S. 2001. Liver biopsy. *N Engl J Med.,* 344**,** 495-500.

BROWNING, J. D., SZCZEPANIAK, L. S., DOBBINS, R., NUREMBERG, P., HORTON, J. D., COHEN, J. C., GRUNDY, S. M. & HOBBS, H. H. 2004. Prevalence of hepatic steatosis in an urban population in the United States: impact of ethnicity. *Hepatology.,* 40**,** 1387-95.

BRUNT, E. M. 2001. Nonalcoholic steatohepatitis: definition and pathology. *Semin Liver Dis.,* 21**,** 3-16.

BRUNT, E. M., JANNEY, C. G., DI BISCEGLIE, A. M., NEUSCHWANDER-TETRI, B. A. & BACON, B. R. 1999. Nonalcoholic steatohepatitis: a proposal for grading and staging the histological lesions. *Am J Gastroenterol.,* 94**,** 2467-74.

BRUUN, J. M., LIHN, A. S., VERDICH, C., PEDERSEN, S. B., TOUBRO, S., ASTRUP, A. & RICHELSEN, B. 2003. Regulation of adiponectin by adipose tissue-derived cytokines: in vivo and in vitro investigations in humans. *Am J Physiol Endocrinol Metab.,* 285**,** E527-33. Epub 2003 May 7.

BU, L., SALTO, L. M., DE LEON, K. J. & DE LEON, M. 2011. Polymorphisms in fatty acid binding protein 5 show association with type 2 diabetes. *Diabetes Res Clin Pract.,* 92**,** 82-91. doi: 10.1016/j.diabres.2011.01.005. Epub 2011 Feb 1.

BU, S. Y., MASHEK, M. T. & MASHEK, D. G. 2009. Suppression of long chain acyl-CoA synthetase 3 decreases hepatic de novo fatty acid synthesis through decreased transcriptional activity. *J Biol Chem.,* 284**,** 30474-83. doi: 10.1074/jbc.M109.036665. Epub 2009 Sep 8.

BUNCH, J., CLENCH, M. R. & RICHARDS, D. S. 2004. Determination of pharmaceutical compounds in skin by imaging matrix-assisted laser

desorption/ionisation mass spectrometry. *Rapid Commun Mass Spectrom.,* 18**,** 3051-60.

BURCHELL, A. 1998. A re-evaluation of GLUT 7. *Biochem J.,* 331**,** 973.

CANBAY, A., BECHMANN, L. & GERKEN, G. 2007. Lipid metabolism in the liver. *Z Gastroenterol.,* 45**,** 35-41.

CAO, S., ZHANG, X., EDWARDS, J. P. & MOSSER, D. M. 2006. NF-kappaB1 (p50) homodimers differentially regulate pro- and anti-inflammatory cytokines in macrophages. *J Biol Chem.,* 281**,** 26041-50. Epub 2006 Jul 11.

CAPRIOLI, R. M., FARMER, T. B. & GILE, J. 1997. Molecular imaging of biological samples: localization of peptides and proteins using MALDI-TOF MS. *Anal Chem.,* 69**,** 4751-60.

CARAYANNOPOULOS, M. O., CHI, M. M., CUI, Y., PINGSTERHAUS, J. M., MCKNIGHT, R. A., MUECKLER, M., DEVASKAR, S. U. & MOLEY, K. H. 2000. GLUT8 is a glucose transporter responsible for insulin-stimulated glucose uptake in the blastocyst. *Proc Natl Acad Sci U S A.,* 97**,** 7313-8.

CARPENE, C., BOUR, S., VISENTIN, V., PELLATI, F., BENVENUTI, S., IGLESIAS-OSMA, M. C., GARCIA-BARRADO, M. J. & VALET, P. 2005. Amine oxidase substrates for impaired glucose tolerance correction. *J Physiol Biochem.,* 61**,** 405-19.

CARPENE, C., DAVIAUD, D., BOUCHER, J., BOUR, S., VISENTIN, V., GRES, S., DUFFAUT, C., FONTANA, E., TESTAR, X., SAULNIER-BLACHE, J. S. & VALET, P. 2006. Short- and long-term insulin-like effects of monoamine oxidases and semicarbazide-sensitive amine oxidase substrates in cultured adipocytes. *Metabolism.,* 55**,** 1397-405.

CARPENE, C., IFFIU-SOLTESZ, Z., BOUR, S., PREVOT, D. & VALET, P. 2007. Reduction of fat deposition by combined inhibition of monoamine oxidases and semicarbazide-sensitive amine oxidases in obese Zucker rats. *Pharmacol Res.,* 56**,** 522-30. Epub 2007 Sep 26.

CARTER, C. L., MCLEOD, C. W. & BUNCH, J. 2011. Imaging of phospholipids in formalin fixed rat brain sections by matrix assisted laser desorption/ionization mass spectrometry. *J Am Soc Mass Spectrom.,* 22**,** 1991-8. doi: 10.1007/s13361-011-0227-4. Epub 2011 Sep 1.

CAZANAVE, S. C. & GORES, G. J. 2010. Mechanisms and clinical implications of hepatocyte lipoapoptosis. *Clin Lipidol.,* 5**,** 71-85.

CAZANAVE, S. C., MOTT, J. L., ELMI, N. A., BRONK, S. F., WERNEBURG, N. W., AKAZAWA, Y., KAHRAMAN, A., GARRISON, S. P., ZAMBETTI, G. P., CHARLTON, M. R. & GORES, G. J. 2009. JNK1-dependent PUMA expression contributes to hepatocyte lipoapoptosis. *J Biol Chem.,* 284**,** 26591-602. doi: 10.1074/jbc.M109.022491. Epub 2009 Jul 28.

CHANDRASEKARAN, K., SWAMINATHAN, K., CHATTERJEE, S. & DEY, A. 2010. Apoptosis in HepG2 cells exposed to high glucose. *Toxicol In Vitro.,* 24**,** 387-96. doi: 10.1016/j.tiv.2009.10.020. Epub 2009 Nov 3.

CHANG, C. Y., ARGO, C. K., AL-OSAIMI, A. M. & CALDWELL, S. H. 2006. Therapy of NAFLD: antioxidants and cytoprotective agents. *J Clin Gastroenterol.,* 40**,** S51-60.

CHANG, J., HISAMATSU, T., SHIMAMURA, K., YONENO, K., ADACHI, M., NARUSE, H., IGARASHI, T., HIGUCHI, H., MATSUOKA, K., KITAZUME, M. T., ANDO, S., KAMADA, N., KANAI, T. & HIBI, T. 2012. Activated hepatic stellate cells mediate the differentiation of macrophages. *Hepatol Res,* 28.

CHARLTON, M., KRISHNAN, A., VIKER, K., SANDERSON, S., CAZANAVE, S., MCCONICO, A., MASUOKO, H. & GORES, G. 2011. Fast food diet mouse: novel small animal model of NASH with ballooning, progressive fibrosis, and high physiological fidelity to the human condition. *Am J Physiol Gastrointest Liver Physiol.,* 301**,** G825-34. doi: 10.1152/ajpgi.00145.2011. Epub 2011 Aug 11.

CHARLTON, M., VIKER, K., KRISHNAN, A., SANDERSON, S., VELDT, B., KAALSBEEK, A. J., KENDRICK, M., THOMPSON, G., QUE, F., SWAIN, J. & SARR, M. 2009a. Differential expression of lumican and fatty acid binding protein-1: new insights into the histologic spectrum of nonalcoholic fatty liver disease. *Hepatology.,* 49**,** 1375-84.

CHARLTON, M., VIKER, K., KRISHNAN, A., SANDERSON, S., VELDT, B., KAALSBEEK, A. J., KENDRICK, M., THOMPSON, G., QUE, F., SWAIN, J. & SARR, M. 2009b. Differential expression of lumican and fatty acid binding protein-1: new insights into the histologic spectrum of nonalcoholic fatty liver disease. *Hepatology.,* 49**,** 1375-84. doi: 10.1002/hep.22927.

CHAURAND, P., NORRIS, J. L., CORNETT, D. S., MOBLEY, J. A. & CAPRIOLI, R. M. 2006. New developments in profiling and imaging of proteins from tissue sections by MALDI mass spectrometry. *J Proteome Res.,* 5**,** 2889-900.

CHAURAND, P., SCHWARTZ, S. A., REYZER, M. L. & CAPRIOLI, R. M. 2005. Imaging mass spectrometry: principles and potentials. *Toxicol Pathol.,* 33**,** 92-101.

CHAURAND, P., STOECKLI, M. & CAPRIOLI, R. M. 1999. Direct profiling of proteins in biological tissue sections by MALDI mass spectrometry. *Anal Chem.,* 71**,** 5263-70.

CHEESEMAN, C. 2008. GLUT7: a new intestinal facilitated hexose transporter. *Am J Physiol Endocrinol Metab.,* 295**,** E238-41. Epub 2008 May 13.

CHEN, L., ZHANG, W., ZHOU, Q. D., YANG, H. Q., LIANG, H. F., ZHANG, B. X., LONG, X. & CHEN, X. P. 2012. HSCs play a distinct role in different phases of oval cell-mediated liver regeneration. *Cell Biochem Funct.,* 30**,** 588-96. doi: 10.1002/cbf.2838. Epub 2012 Apr 26.

CHEN, Y. D., GOLAY, A., SWISLOCKI, A. L. & REAVEN, G. M. 1987. Resistance to insulin suppression of plasma free fatty acid concentrations and insulin stimulation of glucose uptake in noninsulin-dependent diabetes mellitus. *J Clin Endocrinol Metab.,* 64**,** 17-21.

CHIARELLI, N., RITELLI, M., ZOPPI, N., BENINI, A., BORSANI, G., BARLATI, S. & COLOMBI, M. 2011. Characterization and expression pattern analysis of the facilitative glucose transporter 10 gene (slc2a10) in Danio rerio. *Int J Dev Biol.,* 55**,** 229-36.

CHITTURI, S., FARRELL, G., FROST, L., KRIKETOS, A., LIN, R., FUNG, C., LIDDLE, C., SAMARASINGHE, D. & GEORGE, J. 2002. Serum leptin in NASH correlates with hepatic steatosis but not fibrosis: a manifestation of lipotoxicity? *Hepatology.,* 36**,** 403-9.

CHITTURI, S. & FARRELL, G. C. 2001. Etiopathogenesis of nonalcoholic steatohepatitis. *Semin Liver Dis.,* 21**,** 27-41.

CIARALDI, T. P., ABRAMS, L., NIKOULINA, S., MUDALIAR, S. & HENRY, R. R. 1995. Glucose transport in cultured human skeletal muscle cells. Regulation by insulin and glucose in nondiabetic and non-insulin-dependent diabetes mellitus subjects. *J Clin Invest.,* 96**,** 2820-7.

CLARIDGE L C, W. N., HAUGHTON E L 2009. Vascular Adhesion Protein 1 (VAP-1) is a novel biomarker and a potential anti inflammatory and anti fibrotic target in non alcoholic fatty liver disease (NAFLD). *Hepatology,* 50**,** 783A-84A.

CLARK, S. A., ANGUS, H. B., COOK, H. B., GEORGE, P. M., OXNER, R. B. & FRASER, R. 1988. Defenestration of hepatic sinusoids as a cause of hyperlipoproteinaemia in alcoholics. *Lancet.,* 2**,** 1225-7.

CLERENS, S., CEUPPENS, R. & ARCKENS, L. 2006. CreateTarget and Analyze This!: new software assisting imaging mass spectrometry on Bruker Reflex IV and Ultraflex II instruments. *Rapid Commun Mass Spectrom.,* 20**,** 3061-6.

CLOUZEAU-GIRARD, H., GUYOT, C., COMBE, C., MORONVALLE-HALLEY, V., HOUSSET, C., LAMIREAU, T., ROSENBAUM, J. & DESMOULIERE, A. 2006. Effects of bile acids on biliary epithelial cell proliferation and portal fibroblast activation using rat liver slices. *Lab Invest.,* 86**,** 275-85.

COBURN, C. T., HAJRI, T., IBRAHIMI, A. & ABUMRAD, N. A. 2001. Role of CD36 in membrane transport and utilization of long-chain fatty acids by different tissues. *J Mol Neurosci.,* 16**,** 117-21; discussion 151-7.

COE, N. R., SIMPSON, M. A. & BERNLOHR, D. A. 1999. Targeted disruption of the adipocyte lipid-binding protein (aP2 protein) gene impairs fat cell lipolysis and increases cellular fatty acid levels. *J Lipid Res.,* 40**,** 967-72.

COGGER, V. C., HILMER, S. N., SULLIVAN, D., MULLER, M., FRASER, R. & LE COUTEUR, D. G. 2006. Hyperlipidemia and surfactants: the liver sieve is a link. *Atherosclerosis.,* 189**,** 273-81. Epub 2006 Feb 2.

COKAKLI, M., ERDAL, E., NART, D., YILMAZ, F., SAGOL, O., KILIC, M., KARADEMIR, S. & ATABEY, N. 2009. Differential expression of Caveolin-1 in hepatocellular carcinoma: correlation with differentiation state, motility and invasion. *BMC Cancer.,* 9**,** 65.

CONNOLLY, M. K., BEDROSIAN, A. S., MALHOTRA, A., HENNING, J. R., IBRAHIM, J., VERA, V., CIEZA-RUBIO, N. E., HASSAN, B. U., PACHTER, H. L., COHEN, S., FREY, A. B. & MILLER, G. 2010. In hepatic fibrosis, liver sinusoidal endothelial cells acquire enhanced immunogenicity. *J Immunol.,* 185**,** 2200-8. doi: 10.4049/jimmunol.1000332. Epub 2010 Jul 16.

CONNORS, S., RANKIN, D. R., GANDOLFI, A. J., KRUMDIECK, C. L., KOEP, L. J. & BRENDEL, K. 1990. Cocaine hepatotoxicity in cultured liver slices: a species comparison. *Toxicology.,* 61**,** 171-83.

CONSIDINE, R. V., SINHA, M. K., HEIMAN, M. L., KRIAUCIUNAS, A., STEPHENS, T. W., NYCE, M. R., OHANNESIAN, J. P., MARCO, C. C., MCKEE, L. J., BAUER, T. L. & ET AL. 1996. Serum immunoreactive-leptin concentrations in normal-weight and obese humans. *N Engl J Med.,* 334**,** 292-5.

COOPER, A. D. 1997. Hepatic uptake of chylomicron remnants. *J Lipid Res.,* 38**,** 2173-92.

CORPE, C. P., BOVELANDER, F. J., MUNOZ, C. M., HOEKSTRA, J. H., SIMPSON, I. A., KWON, O., LEVINE, M. & BURANT, C. F. 2002. Cloning and functional characterization of the mouse fructose transporter, GLUT5. *Biochim Biophys Acta.,* 1576**,** 191-7.

COWART, L. A. 2009. Sphingolipids: players in the pathology of metabolic disease. *Trends Endocrinol Metab.,* 20**,** 34-42. doi: 10.1016/j.tem.2008.09.004. Epub 2008 Nov 13.

CRABB, D. W., GALLI, A., FISCHER, M. & YOU, M. 2004. Molecular mechanisms of alcoholic fatty liver: role of peroxisome proliferator-activated receptor alpha. *Alcohol.,* 34**,** 35-8.

CUTHBERTSON, D. J., IRWIN, A., GARDNER, C. J., DAOUSI, C., PUREWAL, T., FURLONG, N., GOENKA, N., THOMAS, E. L., ADAMS, V. L., PUSHPAKOM, S. P., PIRMOHAMED, M. & KEMP, G. J. 2012. Improved glycaemia correlates with liver fat reduction in obese, type 2 diabetes, patients given glucagon-like peptide-1 (GLP-1) receptor agonists. *PLoS One.,* 7**,** e50117. doi: 10.1371/journal.pone.0050117. Epub 2012 Dec 6.

DADAMIO, J., VAN DEN VELDE, S., LALEMAN, W., VAN HEE, P., COUCKE, W., NEVENS, F. & QUIRYNEN, M. 2012. Breath biomarkers of liver cirrhosis. *J Chromatogr B Analyt Technol Biomed Life Sci.,* 905:17-22**,** 10.1016/j.jchromb.2012.07.025. Epub 2012 Jul 31.

DAY, C. P. 2005. Natural history of NAFLD: remarkably benign in the absence of cirrhosis. *Gastroenterology.,* 129**,** 375-8.

DE ALMEIDA, I. T., CORTEZ-PINTO, H., FIDALGO, G., RODRIGUES, D. & CAMILO, M. E. 2002. Plasma total and free fatty acids composition in human non-alcoholic steatohepatitis. *Clin Nutr.,* 21**,** 219-23.

DE GRAAF, E. L., KENCH, J., DILWORTH, P., SHACKEL, N. A., STRASSER, S. I., JOSEPH, D., PLEASS, H., CRAWFORD, M., MCCAUGHAN, G. W. & VERRAN, D. J. 2012. Grade of deceased donor liver macrovesicular steatosis impacts graft and recipient outcomes more than the Donor Risk Index. *J Gastroenterol Hepatol.,* 27**,** 540-6. doi: 10.1111/j.1440-1746.2011.06844.x.

DE MINICIS, S., DAY, C. & SVEGLIATI-BARONI, G. 2013. From NAFLD to NASH and HCC: Pathogenetic Mechanisms and Therapeutic Insights. *Curr Pharm Des,* 4**,** 4.

DE VRIES, J. E. 1995. Immunosuppressive and anti-inflammatory properties of interleukin 10. *Ann Med.,* 27**,** 537-41.

DEBOSCH, B. J., CHI, M. & MOLEY, K. H. 2012. Glucose transporter 8 (GLUT8) regulates enterocyte fructose transport and global mammalian fructose utilization. *Endocrinology.,* 153**,** 4181-91. doi: 10.1210/en.2012-1541. Epub 2012 Jul 20.

DIRAISON, F., MOULIN, P. & BEYLOT, M. 2003. Contribution of hepatic de novo lipogenesis and reesterification of plasma non esterified fatty acids to plasma triglyceride synthesis during non-alcoholic fatty liver disease. *Diabetes Metab.,* 29**,** 478-85.

DOEGE, H., BAILLIE, R. A., ORTEGON, A. M., TSANG, B., WU, Q., PUNREDDY, S., HIRSCH, D., WATSON, N., GIMENO, R. E. & STAHL, A. 2006. Targeted deletion of FATP5 reveals multiple functions in liver metabolism: alterations in hepatic lipid homeostasis. *Gastroenterology.,* 130**,** 1245-58.

DOEGE, H. & STAHL, A. 2006. Protein-mediated fatty acid uptake: novel insights from in vivo models. *Physiology (Bethesda).* 21**,** 259-68.

DONGIOVANNI, P. & VALENTI, L. 2013. Peroxisome proliferator-activated receptor genetic polymorphisms and nonalcoholic Fatty liver disease: any role in disease susceptibility? *PPAR Res.,* 2013:452061.**,** 10.1155/2013/452061. Epub 2013 Feb 4.

DUAN, X. F., TANG, P., LI, Q. & YU, Z. T. 2013. Obesity, adipokines and hepatocellular carcinoma. *Int J Cancer,* 12**,** 28105.

DUGAIL, I. & POSTIC, C. 2010. Little caves ameliorate hepatic insulin signaling. Focus on "caveolin gene transfer improves glucose metabolism in diabetic mice". *Am J Physiol Cell Physiol.,* 298**,** C442-5. Epub 2009 Dec 23.

DURYEE, M. J., FREEMAN, T. L., WILLIS, M. S., HUNTER, C. D., HAMILTON, B. C., 3RD, SUZUKI, H., TUMA, D. J., KLASSEN, L. W. & THIELE, G. M. 2005. Scavenger receptors on sinusoidal liver endothelial cells are involved in the uptake of aldehyde-modified proteins. *Mol Pharmacol.,* 68**,** 1423-30. Epub 2005 Aug 16.

DUVNJAK, M., TOMASIC, V., GOMERCIC, M., SMIRCIC DUVNJAK, L., BARSIC, N. & LEROTIC, I. 2009. Therapy of nonalcoholic fatty liver disease: current status. *J Physiol Pharmacol.,* 60**,** 57-66.

EISENBERG, M. L., MAKER, A. V., SLEZAK, L. A., NATHAN, J. D., SRITHARAN, K. C., JENA, B. P., GEIBEL, J. P. & ANDERSEN, D. K. 2005. Insulin receptor (IR) and glucose transporter 2 (GLUT2) proteins form a complex on the rat hepatocyte membrane. *Cell Physiol Biochem.,* 15**,** 51-8.

EL HADRI, K., MOLDES, M., MERCIER, N., ANDREANI, M., PAIRAULT, J. & FEVE, B. 2002. Semicarbazide-sensitive amine oxidase in vascular smooth muscle cells: differentiation-dependent expression and role in glucose uptake. *Arterioscler Thromb Vasc Biol.,* 22**,** 89-94.

ELMASRI, H., KARAASLAN, C., TEPER, Y., GHELFI, E., WENG, M., INCE, T. A., KOZAKEWICH, H., BISCHOFF, J. & CATALTEPE, S. 2009a. Fatty acid binding protein 4 is a target of VEGF and a regulator of cell proliferation in endothelial cells. *Faseb J.,* 23**,** 3865-73. doi: 10.1096/fj.09-134882. Epub 2009 Jul 22.

ELMASRI, H., KARAASLAN, C., TEPER, Y., GHELFI, E., WENG, M., INCE, T. A., KOZAKEWICH, H., BISCHOFF, J. & CATALTEPE, S. 2009b. Fatty acid binding protein 4 is a target of VEGF and a regulator of cell proliferation in endothelial cells. *Faseb J.,* 23**,** 3865-73.

ELSHARKAWY, A. M., WRIGHT, M. C., HAY, R. T., ARTHUR, M. J., HUGHES, T., BAHR, M. J., DEGITZ, K. & MANN, D. A. 1999. Persistent activation of nuclear factor-kappaB in cultured rat hepatic stellate cells involves the induction of potentially novel Rel-like factors and prolonged changes in the expression of IkappaB family proteins. *Hepatology.,* 30**,** 761-9.

ELWING, J. E., LUSTMAN, P. J., WANG, H. L. & CLOUSE, R. E. 2006. Depression, anxiety, and nonalcoholic steatohepatitis. *Psychosom Med.,* 68**,** 563-9.

EMERSON, B., GIDDEN, J., LAY, J. O., JR. & DURHAM, B. 2010. A rapid separation technique for overcoming suppression of triacylglycerols by phosphatidylcholine using MALDI-TOF MS. *J Lipid Res.,* 51**,** 2428-34. doi: 10.1194/jlr.D003798. Epub 2010 May 5.

ENRIQUE-TARANCON, G., CASTAN, I., MORIN, N., MARTI, L., ABELLA, A., CAMPS, M., CASAMITJANA, R., PALACIN, M., TESTAR, X., DEGERMAN, E., CARPENE, C. & ZORZANO, A. 2000. Substrates of semicarbazide-sensitive amine oxidase co-operate with vanadate to stimulate tyrosine phosphorylation of insulin-receptor-substrate proteins, phosphoinositide 3-kinase activity and GLUT4 translocation in adipose cells. *Biochem J.,* 350**,** 171-80.

ENRIQUE-TARANCON, G., MARTI, L., MORIN, N., LIZCANO, J. M., UNZETA, M., SEVILLA, L., CAMPS, M., PALACIN, M., TESTAR, X., CARPENE, C. & ZORZANO, A. 1998. Role of semicarbazide-sensitive amine oxidase on

glucose transport and GLUT4 recruitment to the cell surface in adipose cells. *J Biol Chem.,* 273**,** 8025-32.

ESPIRITO SANTO, S. M., PIRES, N. M., BOESTEN, L. S., GERRITSEN, G., BOVENSCHEN, N., VAN DIJK, K. W., JUKEMA, J. W., PRINCEN, H. M., BENSADOUN, A., LI, W. P., HERZ, J., HAVEKES, L. M. & VAN VLIJMEN, B. J. 2004. Hepatic low-density lipoprotein receptor-related protein deficiency in mice increases atherosclerosis independent of plasma cholesterol. *Blood.,* 103**,** 3777-82. Epub 2004 Jan 22.

ESTERBAUER, H., DIEBER-ROTHENEDER, M., WAEG, G., STRIEGL, G. & JURGENS, G. 1990. Biochemical, structural, and functional properties of oxidized low-density lipoprotein. *Chem Res Toxicol.,* 3**,** 77-92.

ESTES, J. M., OLIVER, P. G., STRAUGHN, J. M., JR., ZHOU, T., WANG, W., GRIZZLE, W. E., ALVAREZ, R. D., STOCKARD, C. R., LOBUGLIO, A. F. & BUCHSBAUM, D. J. 2007. Efficacy of anti-death receptor 5 (DR5) antibody (TRA-8) against primary human ovarian carcinoma using a novel ex vivo tissue slice model. *Gynecol Oncol.,* 105**,** 291-8. Epub 2007 Feb 15.

F. ALZAID, K. P., P. A. SHARP, D. BAGCHI, V. R. PREEDY, H. WISEMAN 2010. Anthocyanin-rich berry-extract treatment decreases expression

of dietary glucose transporter genes in human intestinal Caco-2 cells. *Proceedings of the Nutrition Society,* (OCE4)**,** E326.

FALCON, A., DOEGE, H., FLUITT, A., TSANG, B., WATSON, N., KAY, M. A. & STAHL, A. 2010. FATP2 is a hepatic fatty acid transporter and peroxisomal very long-chain acyl-CoA synthetase. *Am J Physiol Endocrinol Metab.,* 299**,** E384-93. Epub 2010 Jun 8.

FARES, N. & PERON, J. M. 2013. [Epidemiology, natural history, and risk factors of hepatocellular carcinoma]. *Rev Prat.,* 63**,** 216-7, 220-2.

FEBBRAIO, M., HAJJAR, D. P. & SILVERSTEIN, R. L. 2001. CD36: a class B scavenger receptor involved in angiogenesis, atherosclerosis, inflammation, and lipid metabolism. *J Clin Invest.,* 108**,** 785-91.

FELDSTEIN, A. E. 2010. Novel insights into the pathophysiology of nonalcoholic fatty liver disease. *Semin Liver Dis.,* 30**,** 391-401. doi: 10.1055/s-0030-1267539. Epub 2010 Oct 19.

FELDSTEIN, A. E., CANBAY, A., GUICCIARDI, M. E., HIGUCHI, H., BRONK, S. F. & GORES, G. J. 2003. Diet associated hepatic steatosis sensitizes to Fas mediated liver injury in mice. *J Hepatol.,* 39**,** 978-83.

FELDSTEIN, A. E., LOPEZ, R., TAMIMI, T. A., YERIAN, L., CHUNG, Y. M., BERK, M., ZHANG, R., MCINTYRE, T. M. & HAZEN, S. L. 2010. Mass spectrometric profiling of oxidized lipid products in human nonalcoholic fatty liver disease and nonalcoholic steatohepatitis. *J Lipid Res.,* 51**,** 3046-54. doi: 10.1194/jlr.M007096. Epub 2010 Jul 14.

FELDSTEIN, A. E., WERNEBURG, N. W., CANBAY, A., GUICCIARDI, M. E., BRONK, S. F., RYDZEWSKI, R., BURGART, L. J. & GORES, G. J. 2004. Free fatty acids promote hepatic lipotoxicity by stimulating TNF-alpha expression via a lysosomal pathway. *Hepatology.,* 40**,** 185-94.

FELDSTEIN, A. E., WERNEBURG, N. W., LI, Z., BRONK, S. F. & GORES, G. J. 2006. Bax inhibition protects against free fatty acid-induced lysosomal permeabilization. *Am J Physiol Gastrointest Liver Physiol.,* 290**,** G1339-46. Epub 2006 Feb 16.

FENG, A. J. & CHEN, D. F. 2005. [The expression and the significance of L-FABP and FATP4 in the development of nonalcoholic fatty liver disease in rats]. *Zhonghua Gan Zang Bing Za Zhi.,* 13**,** 776-9.

FERJANCIC, S., GIL-BERNABE, A. M., HILL, S. A., ALLEN, P. D., RICHARDSON, P., SPAREY, T., SAVORY, E., MCGUFFOG, J. & MUSCHEL, R. J. 2013. VCAM-1 and VAP-1 recruit myeloid cells that promote pulmonary metastasis in mice. *Blood,* 13**,** 13.

FERNANDEZ, M. A., ALBOR, C., INGELMO-TORRES, M., NIXON, S. J., FERGUSON, C., KURZCHALIA, T., TEBAR, F., ENRICH, C., PARTON, R. G. & POL, A. 2006. Caveolin-1 is essential for liver regeneration. *Science.,* 313**,** 1628-32.

FESTI, D., SCHIUMERINI, R., MARZI, L., DI BIASE, A. R., MANDOLESI, D., MONTRONE, L., SCAIOLI, E., BONATO, G., MARCHESINI-REGGIANI, G. & COLECCHIA, A. 2013. Review article: the diagnosis of non-alcoholic fatty liver disease -- availability and accuracy of non-invasive methods. *Aliment Pharmacol Ther.,* 37**,** 392-400. doi: 10.1111/apt.12186. Epub 2012 Dec 20.

FOLCH, J., LEES, M. & SLOANE STANLEY, G. H. 1957. A simple method for the isolation and purification of total lipides from animal tissues. *J Biol Chem.,* 226**,** 497-509.

FONG, D. G., NEHRA, V., LINDOR, K. D. & BUCHMAN, A. L. 2000. Metabolic and nutritional considerations in nonalcoholic fatty liver. *Hepatology.,* 32**,** 3-10.

FONTANA, E., BOUCHER, J., MARTI, L., LIZCANO, J. M., TESTAR, X., ZORZANO, A. & CARPENE, C. 2001. Amine oxidase substrates mimic several of the insulin effects on adipocyte differentiation in 3T3 F442A cells. *Biochem J.,* 356**,** 769-77.

FONVILLE, J. M., CARTER, C. L., PIZARRO, L., STEVEN, R. T., PALMER, A. D., GRIFFITHS, R. L., LALOR, P. F., LINDON, J. C., NICHOLSON, J. K., HOLMES, E. & BUNCH, J. 2013. Hyperspectral visualization of mass spectrometry imaging data. *Anal Chem.,* 85**,** 1415-23. doi: 10.1021/ac302330a. Epub 2013 Jan 15.

FRANZESE, A., VAJRO, P., ARGENZIANO, A., PUZZIELLO, A., IANNUCCI, M. P., SAVIANO, M. C., BRUNETTI, F. & RUBINO, A. 1997. Liver involvement in obese children. Ultrasonography and liver enzyme levels at diagnosis and during follow-up in an Italian population. *Dig Dis Sci.,* 42**,** 1428-32.

FRASER, R., BOSANQUET, A. G. & DAY, W. A. 1978. Filtration of chylomicrons by the liver may influence cholesterol metabolism and atherosclerosis. *Atherosclerosis.,* 29**,** 113-23.

FRAYN, K. N. 2001. Adipose tissue and the insulin resistance syndrome. *Proc Nutr Soc.,* 60**,** 375-80.

FRENCH, S. W., NASH, J., SHITABATA, P., KACHI, K., HARA, C., CHEDID, A. & MENDENHALL, C. L. 1993. Pathology of alcoholic liver disease. VA Cooperative Study Group 119. *Semin Liver Dis.,* 13**,** 154-69.

FRIEDMAN, J. M., LEIBEL, R. L., SIEGEL, D. S., WALSH, J. & BAHARY, N. 1991. Molecular mapping of the mouse ob mutation. *Genomics.,* 11**,** 1054-62.

FRITSCHE, L., WEIGERT, C., HARING, H. U. & LEHMANN, R. 2008. How insulin receptor substrate proteins regulate the metabolic capacity of the liver--implications for health and disease. *Curr Med Chem.,* 15**,** 1316-29.

FROMENTY, B., ROBIN, M. A., IGOUDJIL, A., MANSOURI, A. & PESSAYRE, D. 2004. The ins and outs of mitochondrial dysfunction in NASH. *Diabetes Metab.,* 30**,** 121-38.

FU, S., YANG, L., LI, P., HOFMANN, O., DICKER, L., HIDE, W., LIN, X., WATKINS, S. M., IVANOV, A. R. & HOTAMISLIGIL, G. S. 2011. Aberrant lipid metabolism disrupts calcium homeostasis causing liver endoplasmic reticulum stress in obesity. *Nature.,* 473**,** 528-31. doi: 10.1038/nature09968. Epub 2011 May 1.

FUJIWAKI, T., TASAKA, M., TAKAHASHI, N., KOBAYASHI, H., MURAKAMI, Y., SHIMADA, T. & YAMAGUCHI, S. 2006. Quantitative evaluation of sphingolipids using delayed extraction matrix-assisted laser desorption ionization time-of-flight mass spectrometry with sphingosylphosphorylcholine as an internal standard. Practical application to cardiac valves from a patient with Fabry disease. *J Chromatogr B Analyt Technol Biomed Life Sci.,* 832**,** 97-102. Epub 2006 Jan 20.

FURUHASHI, M., TUNCMAN, G., GORGUN, C. Z., MAKOWSKI, L., ATSUMI, G., VAILLANCOURT, E., KONO, K., BABAEV, V. R., FAZIO, S., LINTON, M. F., SULSKY, R., ROBL, J. A., PARKER, R. A. & HOTAMISLIGIL, G. S. 2007. Treatment of diabetes and atherosclerosis by inhibiting fatty-acid-binding protein aP2. *Nature.,* 447**,** 959-65. Epub 2007 Jun 6.

GALIC, S., OAKHILL, J. S. & STEINBERG, G. R. 2010. Adipose tissue as an endocrine organ. *Mol Cell Endocrinol.,* 316**,** 129-39. doi: 10.1016/j.mce.2009.08.018. Epub 2009 Aug 31.

GAO, N., QU, X., YAN, J., HUANG, Q., YUAN, H. Y. & OUYANG, D. S. 2010. L-FABP T94A decreased fatty acid uptake and altered hepatic triglyceride and cholesterol accumulation in Chang liver cells stably transfected with L-FABP. *Mol Cell Biochem.,* 345**,** 207-14. doi: 10.1007/s11010-010-0574-7. Epub 2010 Aug 20.

GAUTHIER, A., VASSILIOU, G., BENOIST, F. & MCPHERSON, R. 2003. Adipocyte low density lipoprotein receptor-related protein gene expression and function is regulated by peroxisome proliferator-activated receptor gamma. *J Biol Chem.,* 278**,** 11945-53. Epub 2003 Jan 27.

GERTOW, K., PIETILAINEN, K. H., YKI-JARVINEN, H., KAPRIO, J., RISSANEN, A., ERIKSSON, P., HAMSTEN, A. & FISHER, R. M. 2004. Expression of fatty-acid-handling proteins in human adipose tissue in relation to obesity and insulin resistance. *Diabetologia.,* 47**,** 1118-25. Epub 2004 May 28.

GIMENO, R. E., ORTEGON, A. M., PATEL, S., PUNREDDY, S., GE, P., SUN, Y., LODISH, H. F. & STAHL, A. 2003. Characterization of a heart-specific fatty acid transport protein. *J Biol Chem.,* 278**,** 16039-44. Epub 2003 Jan 28.

GIORDANO, D., CORRADO, F., SANTAMARIA, A., QUATTRONE, S., PINTAUDI, B., DI BENEDETTO, A. & D'ANNA, R. 2011. Effects of myo-inositol supplementation in postmenopausal women with metabolic syndrome: a perspective, randomized, placebo-controlled study. *Menopause.,* 18**,** 102-4. doi: 10.1097/gme.0b013e3181e8e1b1.

GLATZ, J. F. & STORCH, J. 2001. Unravelling the significance of cellular fatty acid-binding proteins. *Curr Opin Lipidol.,* 12**,** 267-74.

GODOY, A., ULLOA, V., RODRIGUEZ, F., REINICKE, K., YANEZ, A. J., GARCIA MDE, L., MEDINA, R. A., CARRASCO, M., BARBERIS, S.,

CASTRO, T., MARTINEZ, F., KOCH, X., VERA, J. C., POBLETE, M. T., FIGUEROA, C. D., PERUZZO, B., PEREZ, F. & NUALART, F. 2006. Differential subcellular distribution of glucose transporters GLUT1-6 and GLUT9 in human cancer: ultrastructural localization of GLUT1 and GLUT5 in breast tumor tissues. *J Cell Physiol.,* 207**,** 614-27.

GONZALEZ-MUNOZ, E., LOPEZ-IGLESIAS, C., CALVO, M., PALACIN, M., ZORZANO, A. & CAMPS, M. 2009. Caveolin-1 loss of function accelerates glucose transporter 4 and insulin receptor degradation in 3T3-L1 adipocytes. *Endocrinology.,* 150**,** 3493-502. doi: 10.1210/en.2008-1520. Epub 2009 Apr 30.

GONZALEZ-RODRIGUEZ, A., NEVADO, C., ESCRIVA, F., SESTI, G., RONDINONE, C. M., BENITO, M. & VALVERDE, A. M. 2008. PTP1B deficiency increases glucose uptake in neonatal hepatocytes: involvement of IRA/GLUT2 complexes. *Am J Physiol Gastrointest Liver Physiol.,* 295**,** G338-47. Epub 2008 Jun 5.

GOODMAN, Z. D. & ISHAK, K. G. 1982. Occlusive venous lesions in alcoholic liver disease. A study of 200 cases. *Gastroenterology.,* 83**,** 786-96.

GOODWIN, R. J., SCULLION, P., MACINTYRE, L., WATSON, D. G. & PITT, A. R. 2010. Use of a solvent-free dry matrix coating for quantitative matrix-assisted laser desorption ionization imaging of 4-bromophenyl-1,4-diazabicyclo(3.2.2)nonane-4-carboxylate in rat brain and quantitative analysis of the drug from laser microdissected tissue regions. *Anal Chem.,* 82**,** 3868-73. doi: 10.1021/ac100398y.

GORDEN, D. L., IVANOVA, P. T., MYERS, D. S., MCINTYRE, J. O., VANSAUN, M. N., WRIGHT, J. K., MATRISIAN, L. M. & BROWN, H. A. 2011. Increased diacylglycerols characterize hepatic lipid changes in progression of human nonalcoholic fatty liver disease; comparison to a murine model. *PLoS One.,* 6**,** e22775. doi: 10.1371/journal.pone.0022775. Epub 2011 Aug 9.

GORKA, J., BAHR, U. & KARAS, M. 2012. Graphite supported preparation (GSP) of alpha-cyano-4-hydroxycinnamic acid (CHCA) for matrix-assisted laser desorption/ionization mass spectrometry (MALDI-MS) for peptides and proteins. *J Am Soc Mass Spectrom.,* 23**,** 1949-54. doi: 10.1007/s13361-012-0478-8. Epub 2012 Sep 20.

GOROVITS, N., CUI, L., BUSIK, J. V., RANALLETTA, M., HAUGUEL DE-MOUZON, S. & CHARRON, M. J. 2003. Regulation of hepatic GLUT8 expression in normal and diabetic models. *Endocrinology.,* 144**,** 1703-11.

GOUDRIAAN, J. R., DAHLMANS, V. E., TEUSINK, B., OUWENS, D. M., FEBBRAIO, M., MAASSEN, J. A., ROMIJN, J. A., HAVEKES, L. M. & VOSHOL, P. J. 2003. CD36 deficiency increases insulin sensitivity in muscle, but induces insulin resistance in the liver in mice. *J Lipid Res.,* 44**,** 2270-7. Epub 2003 Aug 16.

GOULD, G. W. & HOLMAN, G. D. 1993. The glucose transporter family: structure, function and tissue-specific expression. *Biochem J.,* 295**,** 329-41.

GRECO, D., KOTRONEN, A., WESTERBACKA, J., PUIG, O., ARKKILA, P., KIVILUOTO, T., LAITINEN, S., KOLAK, M., FISHER, R. M., HAMSTEN, A., AUVINEN, P. & YKI-JARVINEN, H. 2008. Gene expression in human NAFLD. *Am J Physiol Gastrointest Liver Physiol.,* 294**,** G1281-7. Epub 2008 Apr 3.

GREENWALT, D. E., LIPSKY, R. H., OCKENHOUSE, C. F., IKEDA, H., TANDON, N. N. & JAMIESON, G. A. 1992. Membrane glycoprotein CD36:

a review of its roles in adherence, signal transduction, and transfusion medicine. *Blood.,* 80**,** 1105-15.

GREENWAY, C. V. & STARK, R. D. 1971. Hepatic vascular bed. *Physiol Rev.,* 51**,** 23-65.

GRES, S., CANTEIRO, S., MERCADER, J. & CARPENE, C. 2013. Oxidation of high doses of serotonin favors lipid accumulation in mouse and human fat cells. *Mol Nutr Food Res,* 6**,** 201200681.

GRIFFITHS, R. L. & BUNCH, J. 2012. A survey of useful salt additives in matrix-assisted laser desorption/ionization mass spectrometry and tandem mass spectrometry of lipids: introducing nitrates for improved analysis. *Rapid Commun Mass Spectrom.,* 26**,** 1557-66. doi: 10.1002/rcm.6258.

GRODSKY, G. M. & BENNETT, L. L. 1966. Cation requirements for insulin secretion in the isolated perfused pancreas. *Diabetes.,* 15**,** 910-3.

GRYGLEWSKI, R. J., PALMER, R. M. & MONCADA, S. 1986. Superoxide anion is involved in the breakdown of endothelium-derived vascular relaxing factor. *Nature.,* 320**,** 454-6.

GUILLAM, M. T., BURCELIN, R. & THORENS, B. 1998. Normal hepatic glucose production in the absence of GLUT2 reveals an alternative pathway for glucose release from hepatocytes. *Proc Natl Acad Sci U S A.,* 95**,** 12317-21.

GUSTAVSSON, J., PARPAL, S. & STRALFORS, P. 1996. Insulin-stimulated glucose uptake involves the transition of glucose transporters to a caveolae-rich fraction within the plasma membrane: implications for type II diabetes. *Mol Med.,* 2**,** 367-72.

GUYOT, C., COMBE, C., BALABAUD, C., BIOULAC-SAGE, P. & DESMOULIERE, A. 2007. Fibrogenic cell fate during fibrotic tissue remodelling observed in rat and human cultured liver slices. *J Hepatol.,* 46**,** 142-50. Epub 2006 Oct 4.

HAGBERG, C. E., FALKEVALL, A., WANG, X., LARSSON, E., HUUSKO, J., NILSSON, I., VAN MEETEREN, L. A., SAMEN, E., LU, L., VANWILDEMEERSCH, M., KLAR, J., GENOVE, G., PIETRAS, K., STONE-ELANDER, S., CLAESSON-WELSH, L., YLA-HERTTUALA, S., LINDAHL, P. & ERIKSSON, U. 2010. Vascular endothelial growth factor B controls endothelial fatty acid uptake. *Nature.,* 464**,** 917-21. doi: 10.1038/nature08945. Epub 2010 Mar 14.

HAJRI, T., HAN, X. X., BONEN, A. & ABUMRAD, N. A. 2002. Defective fatty acid uptake modulates insulin responsiveness and metabolic responses to diet in CD36-null mice. *J Clin Invest.,* 109**,** 1381-9.

HALILBASIC, E., CLAUDEL, T. & TRAUNER, M. 2012. Bile acid transporters and regulatory nuclear receptors in the liver and beyond. *J Hepatol,* 8**,** 00622-8.

HAN, L. Q., LI, H. J., WANG, Y. Y., ZHU, H. S., WANG, L. F., GUO, Y. J., LU, W. F., WANG, Y. L. & YANG, G. Y. 2010. mRNA abundance and expression of SLC27A, ACC, SCD, FADS, LPIN, INSIG, and PPARGC1 gene isoforms in mouse mammary glands during the lactation cycle. *Genet Mol Res.,* 9**,** 1250-7.

HANDBERG, A., HOJLUND, K., GASTALDELLI, A., FLYVBJERG, A., DEKKER, J. M., PETRIE, J., PIATTI, P. & BECK-NIELSEN, H. 2012. Plasma sCD36 is associated with markers of atherosclerosis, insulin resistance and fatty liver in a nondiabetic healthy population. *J Intern Med.,* 271**,** 294-304. doi: 10.1111/j.1365-2796.2011.02442.x. Epub 2011 Sep 14.

HARDWICK, J. P., OSEI-HYIAMAN, D., WILAND, H., ABDELMEGEED, M. A. & SONG, B. J. 2009. PPAR/RXR Regulation of Fatty Acid Metabolism and

Fatty Acid omega-Hydroxylase (CYP4) Isozymes: Implications for Prevention of Lipotoxicity in Fatty Liver Disease. *PPAR Res.,* 2009:952734**.,** 10.1155/2009/952734. Epub 2010 Mar 16.

HARDY, O. T., KIM, A., CICCARELLI, C., HAYMAN, L. L. & WIECHA, J. 2013. Increased Toll-like receptor (TLR) mRNA expression in monocytes is a feature of metabolic syndrome in adolescents. *Pediatr Obes.,* 8**,** e19-23. doi: 10.1111/j.2047-6310.2012.00098.x. Epub 2012 Sep 19.

HASOKAWA, M., SHINOHARA, M., TSUGAWA, H., BAMBA, T., FUKUSAKI, E., NISHIUMI, S., NISHIMURA, K., YOSHIDA, M., ISHIDA, T. & HIRATA, K. 2012. Identification of biomarkers of stent restenosis with serum metabolomic profiling using gas chromatography/mass spectrometry. *Circ J.,* 76**,** 1864-73. Epub 2012 May 16.

HATIPOGLU, B. A. 2012. Cushing's syndrome. *J Surg Oncol.,* 106**,** 565-71. doi: 10.1002/jso.23197. Epub 2012 Jun 27.

HAYASAKA, T., GOTO-INOUE, N., ZAIMA, N., KIMURA, Y. & SETOU, M. 2009. Organ-specific distributions of lysophosphatidylcholine and triacylglycerol in mouse embryo. *Lipids.,* 44**,** 837-48. doi: 10.1007/s11745-009-3331-5. Epub 2009 Aug 15.

HAZLEHURST, J. M., GATHERCOLE, L. L., NASIRI, M., ARMSTRONG, M. J., BORROWS, S., YU, J., WAGENMAKERS, A. J., STEWART, P. M. & TOMLINSON, J. W. 2013. Glucocorticoids fail to cause insulin resistance in human subcutaneous adipose tissue in vivo. *J Clin Endocrinol Metab.,* 98**,** 1631-40. doi: 10.1210/jc.2012-3523. Epub 2013 Feb 20.

HELLEDIE, T., ANTONIUS, M., SORENSEN, R. V., HERTZEL, A. V., BERNLOHR, D. A., KOLVRAA, S., KRISTIANSEN, K. & MANDRUP, S. 2000. Lipid-binding proteins modulate ligand-dependent trans-activation by peroxisome proliferator-activated receptors and localize to the nucleus as well as the cytoplasm. *J Lipid Res.,* 41**,** 1740-51.

HERBERT, J. M., STEKEL, D., SANDERSON, S., HEATH, V. L. & BICKNELL, R. 2008. A novel method of differential gene expression analysis using multiple cDNA libraries applied to the identification of tumour endothelial genes. *BMC Genomics.,* 9:153**.,** 10.1186/1471-2164-9-153.

HERNANDEZ-GUILLAMON, M., SOLE, M., DELGADO, P., GARCIA-BONILLA, L., GIRALT, D., BOADA, C., PENALBA, A., GARCIA, S., FLORES, A., RIBO, M., ALVAREZ-SABIN, J., ORTEGA-AZNAR, A., UNZETA, M. & MONTANER, J. 2012. VAP-1/SSAO plasma activity and brain expression in human hemorrhagic stroke. *Cerebrovasc Dis.,* 33**,** 55-63. doi: 10.1159/000333370. Epub 2011 Dec 1.

HERRMANN, T., BUCHKREMER, F., GOSCH, I., HALL, A. M., BERNLOHR, D. A. & STREMMEL, W. 2001. Mouse fatty acid transport protein 4 (FATP4): characterization of the gene and functional assessment as a very long chain acyl-CoA synthetase. *Gene.,* 270**,** 31-40.

HERZ, J. & STRICKLAND, D. K. 2001. LRP: a multifunctional scavenger and signaling receptor. *J Clin Invest.,* 108**,** 779-84.

HIRSCH, D., STAHL, A. & LODISH, H. F. 1998. A family of fatty acid transporters conserved from mycobacterium to man. *Proc Natl Acad Sci U S A.,* 95**,** 8625-9.

HOLECEK, M., SPRONGL, L., TICHY, M. & PECKA, M. 1998. Leucine metabolism in rat liver after a bolus injection of endotoxin. *Metabolism.,* 47**,** 681-5.

HOLLAND, W. L., BROZINICK, J. T., WANG, L. P., HAWKINS, E. D., SARGENT, K. M., LIU, Y., NARRA, K., HOEHN, K. L., KNOTTS, T. A., SIESKY, A., NELSON, D. H., KARATHANASIS, S. K., FONTENOT, G. K., BIRNBAUM, M. J. & SUMMERS, S. A. 2007. Inhibition of ceramide synthesis ameliorates glucocorticoid-, saturated-fat-, and obesity-induced insulin resistance. *Cell Metab.,* 5**,** 167-79.

HOLLE, A., HAASE, A., KAYSER, M. & HOHNDORF, J. 2006. Optimizing UV laser focus profiles for improved MALDI performance. *J Mass Spectrom.,* 41**,** 705-16.

HORN, T., CHRISTOFFERSEN, P. & HENRIKSEN, J. H. 1987. Alcoholic liver injury: defenestration in noncirrhotic livers--a scanning electron microscopic study. *Hepatology.,* 7**,** 77-82.

HOTAMISLIGIL, G. S., JOHNSON, R. S., DISTEL, R. J., ELLIS, R., PAPAIOANNOU, V. E. & SPIEGELMAN, B. M. 1996. Uncoupling of obesity from insulin resistance through a targeted mutation in aP2, the adipocyte fatty acid binding protein. *Science.,* 274**,** 1377-9.

HOUTEN, S. M., WATANABE, M. & AUWERX, J. 2006. Endocrine functions of bile acids. *Embo J.,* 25**,** 1419-25. Epub 2006 Mar 16.

HUANG, H., LI, Y., LIU, J., ZHENG, M., FENG, Y., HU, K., HUANG, Y. & HUANG, Q. 2012. Screening and identification of biomarkers in ascites related to intrinsic chemoresistance of serous epithelial ovarian cancers. *PLoS One.,* 7**,** e51256. doi: 10.1371/journal.pone.0051256. Epub 2012 Dec 10.

HUBBARD, B., DOEGE, H., PUNREDDY, S., WU, H., HUANG, X., KAUSHIK, V. K., MOZELL, R. L., BYRNES, J. J., STRICKER-KRONGRAD, A., CHOU, C. J., TARTAGLIA, L. A., LODISH, H. F., STAHL, A. & GIMENO, R. E. 2006. Mice deleted for fatty acid transport protein 5 have defective bile acid conjugation and are protected from obesity. *Gastroenterology.,* 130**,** 1259-69.

HUGHES, A. L. & PIONTKIVSKA, H. 2011. Evolutionary diversification of the avian fatty acid-binding proteins. *Gene.,* 490**,** 1-5. Epub 2011 Oct 1.

HUI, A. Y. & FRIEDMAN, S. L. 2003. Molecular basis of hepatic fibrosis. *Expert Rev Mol Med.,* 5**,** 1-23.

HUI, J. M., HODGE, A., FARRELL, G. C., KENCH, J. G., KRIKETOS, A. & GEORGE, J. 2004. Beyond insulin resistance in NASH: TNF-alpha or adiponectin? *Hepatology.,* 40**,** 46-54.

HUMPHREYS, P., MCCARTHY, M., TUOMILEHTO, J., TUOMILEHTO-WOLF, E., STRATTON, I., MORGAN, R., REES, A., OWENS, D., STENGARD, J., NISSINEN, A. & ET AL. 1994. Chromosome 4q locus associated with insulin resistance in Pima Indians. Studies in three European NIDDM populations. *Diabetes.,* 43**,** 800-4.

HUWILER, A. & PFEILSCHIFTER, J. 2009. Lipids as targets for novel anti-inflammatory therapies. *Pharmacol Ther.,* 124**,** 96-112. doi: 10.1016/j.pharmthera.2009.06.008. Epub 2009 Jun 30.

ILTZ, J. L., BAKER, D. E., SETTER, S. M. & KEITH CAMPBELL, R. 2006. Exenatide: an incretin mimetic for the treatment of type 2 diabetes mellitus. *Clin Ther.,* 28**,** 652-65.

INOUE, T., MORITA, M., TOJO, T., NAGASHIMA, A., MORITOMO, A., IMAI, K. & MIYAKE, H. 2013. Synthesis and SAR study of new thiazole derivatives as vascular adhesion protein-1 (VAP-1) inhibitors for the treatment of diabetic macular edema: Part 2. *Bioorg Med Chem,* 14**,** 00193-4.

ITOH, S., YOUGEL, T. & KAWAGOE, K. 1987. Comparison between nonalcoholic steatohepatitis and alcoholic hepatitis. *Am J Gastroenterol.,* 82**,** 650-4.

IWAKIRI, Y. & GROSZMANN, R. J. 2006. The hyperdynamic circulation of chronic liver diseases: from the patient to the molecule. *Hepatology.,* 43**,** S121-31.

JAKOBSSON, E., NILSSON, J., OGG, D. & KLEYWEGT, G. J. 2005. Structure of human semicarbazide-sensitive amine oxidase/vascular adhesion protein-1. *Acta Crystallogr D Biol Crystallogr.,* 61**,** 1550-62. Epub 2005 Oct 19.

JALKANEN, S. & SALMI, M. 2001. Cell surface monoamine oxidases: enzymes in search of a function. *Embo J.,* 20**,** 3893-901.

JANEVSKI, M., RATNAYAKE, S., SILJANOVSKI, S., MCGLYNN, M. A., CAMERON-SMITH, D. & LEWANDOWSKI, P. 2012. Fructose containing sugars modulate mRNA of lipogenic genes ACC and FAS and protein levels of transcription factors ChREBP and SREBP1c with no effect on body weight or liver fat. *Food Funct.,* 3**,** 141-9. Epub 2011 Dec 9.

JARRAR, M. H., BARANOVA, A., COLLANTES, R., RANARD, B., STEPANOVA, M., BENNETT, C., FANG, Y., ELARINY, H., GOODMAN, Z., CHANDHOKE, V. & YOUNOSSI, Z. M. 2008. Adipokines and cytokines in non-alcoholic fatty liver disease. *Aliment Pharmacol Ther.,* 27**,** 412-21. Epub 2007 Dec 10.

JEONG, C. Y., HAH, Y. S., CHO, B. I., LEE, S. M., JOO, Y. T., JUNG, E. J., JEONG, S. H., LEE, Y. J., CHOI, S. K., HA, W. S., PARK, S. T. & HONG, S. C. 2012. Fatty acid-binding protein 5 promotes cell proliferation and invasion in human intrahepatic cholangiocarcinoma. *Oncol Rep.,* 28**,** 1283-92. doi: 10.3892/or.2012.1922. Epub 2012 Jul 19.

JEREMY M BERG, J. L. T., LUBERT STRYER 2002. Biochemistry 853-854.

JESSEN, N., BUHL, E. S., SCHMITZ, O. & LUND, S. 2006. Impaired insulin action despite upregulation of proximal insulin signaling: novel insights into skeletal muscle insulin resistance in liver cirrhosis. *J Hepatol.,* 45**,** 797-804. Epub 2006 Sep 28.

JOHNSON, M. D., FLOYD, J. L. & CAPRIOLI, R. M. 2006. Proteomics in diagnostic neuropathology. *J Neuropathol Exp Neurol.,* 65**,** 837-45.

JOHNSON, S., TAZIK, S., LU, D., JOHNSON, C., YOUDIM, M. B., WANG, J., RAJKOWSKA, G. & OU, X. M. 2010. The New Inhibitor of Monoamine Oxidase, M30, has a Neuroprotective Effect Against Dexamethasone-Induced Brain Cell Apoptosis. *Front Neurosci.,* 4:180**.,** 10.3389/fnins.2010.00180.

JOOST, H. G. & THORENS, B. 2001. The extended GLUT-family of sugar/polyol transport facilitators: nomenclature, sequence characteristics, and potential function of its novel members (review). *Mol Membr Biol.,* 18**,** 247-56.

JORNS, A., TIEDGE, M., SICKEL, E. & LENZEN, S. 1996. Loss of GLUT2 glucose transporter expression in pancreatic beta cells from diabetic Chinese hamsters. *Virchows Arch.,* 428**,** 177-85.

JOSHI-BARVE, S., BARVE, S. S., AMANCHERLA, K., GOBEJISHVILI, L., HILL, D., CAVE, M., HOTE, P. & MCCLAIN, C. J. 2007. Palmitic acid induces production of proinflammatory cytokine interleukin-8 from hepatocytes. *Hepatology.,* 46**,** 823-30.

JUNGERMANN, K. 1988. Metabolic zonation of liver parenchyma. *Semin Liver Dis.,* 8**,** 329-41.

K MAGYAR, Z. M., P. MÁTYUS 2001. Semicarbazide-sensitive amine oxidase. Its physiological significance. *Pure and Applied Chemistry* 73**,** 1393-1400.

KAGAN, H. M. & LI, W. 2003. Lysyl oxidase: properties, specificity, and biological roles inside and outside of the cell. *J Cell Biochem.,* 88**,** 660-72.

KANAPATHIPILLAI, M., MAMMOTO, A., MAMMOTO, T., KANG, J. H., JIANG, E., GHOSH, K., KORIN, N., GIBBS, A., MANNIX, R. & INGBER, D. E. 2012. Inhibition of mammary tumor growth using lysyl oxidase-targeting nanoparticles to modify extracellular matrix. *Nano Lett.,* 12**,** 3213-7. doi: 10.1021/nl301206p. Epub 2012 May 10.

KARANTH, S., DENOVAN-WRIGHT, E. M., THISSE, C., THISSE, B. & WRIGHT, J. M. 2008. The evolutionary relationship between the duplicated copies of the zebrafish fabp11 gene and the tetrapod FABP4, FABP5, FABP8 and FABP9 genes. *Febs J.,* 275**,** 3031-40. doi: 10.1111/j.1742-4658.2008.06455.x. Epub 2008 Apr 26.

KARAS, M. & HILLENKAMP, F. 1988. Laser desorption ionization of proteins with molecular masses exceeding 10,000 daltons. *Anal Chem.,* 60**,** 2299-301.

KARIM, S., ADAMS, D. H. & LALOR, P. F. 2012. Hepatic expression and cellular distribution of the glucose transporter family. *World J Gastroenterol.,* 18**,** 6771-81. doi: 10.3748/wjg.v18.i46.6771.

KARIM, S., LIASKOU, E., HADLEY, S., YOUSTER, J., FAINT, J., ADAMS, D. H. & LALOR, P. F. 2013. An In Vitro Model of Human Acute Ethanol Exposure That Incorporates CXCR3- and CXCR4-Dependent Recruitment of Immune Cells. *Toxicol Sci.,* 132**,** 131-41. doi: 10.1093/toxsci/kfs337. Epub 2013 Jan 8.

KARLSSON, M., THORN, H., PARPAL, S., STRALFORS, P. & GUSTAVSSON, J. 2002. Insulin induces translocation of glucose transporter GLUT4 to plasma membrane caveolae in adipocytes. *Faseb J.,* 16**,** 249-51. Epub 2001 Dec 14.

KATZ, N., TEUTSCH, H. F., JUNGERMANN, K. & SASSE, D. 1977a. Heterogeneous reciprocal localization of fructose-1,6-bisphosphatase and of glucokinase in microdissected periportal and perivenous rat liver tissue. *FEBS Lett.,* 83**,** 272-6.

KATZ, N., TEUTSCH, H. F., SASSE, D. & JUNGERMANN, K. 1977b. Heterogeneous distribution of glucose-6-phosphatase in microdissected periportal and perivenous rat liver tissue. *FEBS Lett.,* 76**,** 226-30.

KATZ, N. R. 1992. Metabolic heterogeneity of hepatocytes across the liver acinus. *J Nutr.,* 122**,** 843-9.

KAWAGUCHI, T., TAKENOSHITA, M., KABASHIMA, T. & UYEDA, K. 2001. Glucose and cAMP regulate the L-type pyruvate kinase gene by phosphorylation/dephosphorylation of the carbohydrate response element binding protein. *Proc Natl Acad Sci U S A.,* 98**,** 13710-5. Epub 2001 Nov 6.

KAYANO, T., BURANT, C. F., FUKUMOTO, H., GOULD, G. W., FAN, Y. S., EDDY, R. L., BYERS, M. G., SHOWS, T. B., SEINO, S. & BELL, G. I. 1990. Human facilitative glucose transporters. Isolation, functional characterization, and gene localization of cDNAs encoding an isoform (GLUT5) expressed in small intestine, kidney, muscle, and adipose tissue and an unusual glucose transporter pseudogene-like sequence (GLUT6). *J Biol Chem.,* 265**,** 13276-82.

KEECH, A., SIMES, R. J., BARTER, P., BEST, J., SCOTT, R., TASKINEN, M. R., FORDER, P., PILLAI, A., DAVIS, T., GLASZIOU, P., DRURY, P., KESANIEMI, Y. A., SULLIVAN, D., HUNT, D., COLMAN, P., D'EMDEN, M., WHITING, M., EHNHOLM, C. & LAAKSO, M. 2005. Effects of long-term fenofibrate therapy on cardiovascular events in 9795 people with type 2

diabetes mellitus (the FIELD study): randomised controlled trial. *Lancet.,* 366**,** 1849-61.

KEEMBIYEHETTY, C., AUGUSTIN, R., CARAYANNOPOULOS, M. O., STEER, S., MANOLESCU, A., CHEESEMAN, C. I. & MOLEY, K. H. 2006. Mouse glucose transporter 9 splice variants are expressed in adult liver and kidney and are up-regulated in diabetes. *Mol Endocrinol.,* 20**,** 686-97. Epub 2005 Nov 17.

KELLETT, G. L. & BROT-LAROCHE, E. 2005. Apical GLUT2: a major pathway of intestinal sugar absorption. *Diabetes.,* 54**,** 3056-62.

KEMIK, O., SUMER, A., KEMIK, A. S., ITIK, V., DULGER, A. C., PURISA, S. & TUZUN, S. 2010. Human vascular adhesion protein-1 (VAP-1): serum levels for hepatocellular carcinoma in non-alcoholic and alcoholic fatty liver disease. *World J Surg Oncol.,* 8:83**.,** 10.1186/1477-7819-8-83.

KHATIB-SHAHIDI, S., ANDERSSON, M., HERMAN, J. L., GILLESPIE, T. A. & CAPRIOLI, R. M. 2006. Direct molecular analysis of whole-body animal tissue sections by imaging MALDI mass spectrometry. *Anal Chem.,* 78**,** 6448-56.

KIM, H. J., KIM, J. H., NOH, S., HUR, H. J., SUNG, M. J., HWANG, J. T., PARK, J. H., YANG, H. J., KIM, M. S., KWON, D. Y. & YOON, S. H. 2011. Metabolomic analysis of livers and serum from high-fat diet induced obese mice. *J Proteome Res.,* 10**,** 722-31. doi: 10.1021/pr100892r. Epub 2010 Nov 24.

KIM, Y. I., HIRAI, S., GOTO, T., OHYANE, C., TAKAHASHI, H., TSUGANE, T., KONISHI, C., FUJII, T., INAI, S., IIJIMA, Y., AOKI, K., SHIBATA, D., TAKAHASHI, N. & KAWADA, T. 2012. Potent PPARalpha activator derived from tomato juice, 13-oxo-9,11-octadecadienoic acid, decreases plasma and hepatic triglyceride in obese diabetic mice. *PLoS One.,* 7**,** e31317. doi: 10.1371/journal.pone.0031317. Epub 2012 Feb 9.

KIRBY, T. O., RIVERA, A., REIN, D., WANG, M., ULASOV, I., BREIDENBACH, M., KATARAM, M., CONTRERAS, J. L., KRUMDIECK, C., YAMAMOTO, M., ROTS, M. G., HAISMA, H. J., ALVAREZ, R. D., MAHASRESHTI, P. J. & CURIEL, D. T. 2004. A novel ex vivo model system for evaluation of conditionally replicative adenoviruses therapeutic efficacy and toxicity. *Clin Cancer Res.,* 10**,** 8697-703.

KLASSEN, L. W., THIELE, G. M., DURYEE, M. J., SCHAFFERT, C. S., DEVENEY, A. L., HUNTER, C. D., OLINGA, P. & TUMA, D. J. 2008. An in vitro method of alcoholic liver injury using precision-cut liver slices from rats. *Biochem Pharmacol.,* 76**,** 426-36. doi: 10.1016/j.bcp.2008.05.012. Epub 2008 May 21.

KLEINER, D. E., BRUNT, E. M., VAN NATTA, M., BEHLING, C., CONTOS, M. J., CUMMINGS, O. W., FERRELL, L. D., LIU, Y. C., TORBENSON, M. S., UNALP-ARIDA, A., YEH, M., MCCULLOUGH, A. J. & SANYAL, A. J. 2005. Design and validation of a histological scoring system for nonalcoholic fatty liver disease. *Hepatology.,* 41**,** 1313-21.

KLINMAN, J. P. & MU, D. 1994. Quinoenzymes in biology. *Annu Rev Biochem.,* 63**,** 299-344.

KO, K. S., PENG, J. & YANG, H. 2013. Animal models of cholangiocarcinoma. *Curr Opin Gastroenterol,* 21**,** 21.

KOENIGER, S. L., TALATY, N., LUO, Y., READY, D., VOORBACH, M., SEIFERT, T., CEPA, S., FAGERLAND, J. A., BOUSKA, J., BUCK, W.,

JOHNSON, R. W. & SPANTON, S. 2011. A quantitation method for mass spectrometry imaging. *Rapid Commun Mass Spectrom.,* 25**,** 503-10. doi: 10.1002/rcm.4891.

KOH, J. H., SHIN, Y. G., NAM, S. M., LEE, M. Y., CHUNG, C. H. & SHIN, J. Y. 2009. Serum adipocyte fatty acid-binding protein levels are associated with nonalcoholic fatty liver disease in type 2 diabetic patients. *Diabetes Care.,* 32**,** 147-52. doi: 10.2337/dc08-1379. Epub 2008 Oct 3.

KONOPELSKA, S., KIENITZ, T., HUGHES, B., PIRLICH, M., BAUDITZ, J., LOCHS, H., STRASBURGER, C. J., STEWART, P. M. & QUINKLER, M. 2009. Hepatic 11beta-HSD1 mRNA expression in fatty liver and nonalcoholic steatohepatitis. *Clin Endocrinol (Oxf).* 70**,** 554-60. doi: 10.1111/j.1365-2265.2008.03358.x.

KOONEN, D. P., JACOBS, R. L., FEBBRAIO, M., YOUNG, M. E., SOLTYS, C. L., ONG, H., VANCE, D. E. & DYCK, J. R. 2007. Increased hepatic CD36 expression contributes to dyslipidemia associated with diet-induced obesity. *Diabetes.,* 56**,** 2863-71. Epub 2007 Aug 29.

KRAMMER, J., DIGEL, M., EHEHALT, F., STREMMEL, W., FULLEKRUG, J. & EHEHALT, R. 2011. Overexpression of CD36 and acyl-CoA synthetases FATP2, FATP4 and ACSL1 increases fatty acid uptake in human hepatoma cells. *Int J Med Sci.,* 8**,** 599-614. Epub 2011 Oct 7.

KULKARNI, B. V., WOOD, K. V. & MATTES, R. D. 2012. Quantitative and qualitative analyses of human salivary NEFA with gas-chromatography and mass spectrometry. *Front Physiol.,* 3:328.**,** 10.3389/fphys.2012.00328. Epub 2012 Aug 16.

KURATA, T., OGURI, T., ISOBE, T., ISHIOKA, S. & YAMAKIDO, M. 1999. Differential expression of facilitative glucose transporter (GLUT) genes in primary lung cancers and their liver metastases. *Jpn J Cancer Res.,* 90**,** 1238-43.

KURKIJARVI, R., ADAMS, D. H., LEINO, R., MOTTONEN, T., JALKANEN, S. & SALMI, M. 1998. Circulating form of human vascular adhesion protein-1 (VAP-1): increased serum levels in inflammatory liver diseases. *J Immunol.,* 161**,** 1549-57.

KURKIJARVI, R., YEGUTKIN, G. G., GUNSON, B. K., JALKANEN, S., SALMI, M., ADAMS, D. H., LEINO, R. & MOTTONEN, T. 2000. Circulating soluble vascular adhesion protein 1 accounts for the increased serum monoamine oxidase activity in chronic liver disease

Circulating form of human vascular adhesion protein-1 (VAP-1): increased serum levels in inflammatory liver diseases. *Gastroenterology.,* 119**,** 1096-103.

LAATSCH, A., MERKEL, M., TALMUD, P. J., GREWAL, T., BEISIEGEL, U. & HEEREN, J. 2009. Insulin stimulates hepatic low density lipoprotein receptor-related protein 1 (LRP1) to increase postprandial lipoprotein clearance. *Atherosclerosis.,* 204**,** 105-11. doi: 10.1016/j.atherosclerosis.2008.07.046. Epub 2008 Aug 29.

LAGO, R. M., SINGH, P. P. & NESTO, R. W. 2007. Congestive heart failure and cardiovascular death in patients with prediabetes and type 2 diabetes given thiazolidinediones: a meta-analysis of randomised clinical trials. *Lancet.,* 370**,** 1129-36.

LALOR, P. F., EDWARDS, S., MCNAB, G., SALMI, M., JALKANEN, S. & ADAMS, D. H. 2002. Vascular adhesion protein-1 mediates adhesion and

transmigration of lymphocytes on human hepatic endothelial cells. *J Immunol.,* 169**,** 983-92.

LALOR, P. F., LAI, W. K., CURBISHLEY, S. M., SHETTY, S. & ADAMS, D. H. 2006. Human hepatic sinusoidal endothelial cells can be distinguished by expression of phenotypic markers related to their specialised functions in vivo. *World J Gastroenterol.,* 12**,** 5429-39.

LALOR, P. F., SUN, P. J., WESTON, C. J., MARTIN-SANTOS, A., WAKELAM, M. J. & ADAMS, D. H. 2007. Activation of vascular adhesion protein-1 on liver endothelium results in an NF-kappaB-dependent increase in lymphocyte adhesion. *Hepatology.,* 45**,** 465-74.

LANGFORD, S. D., TRENT, M. B., BALAKUMARAN, A. & BOOR, P. J. 1999. Developmental vasculotoxicity associated with inhibition of semicarbazide-sensitive amine oxidase. *Toxicol Appl Pharmacol.,* 155**,** 237-44.

LARNER, J. 2002. D-chiro-inositol--its functional role in insulin action and its deficit in insulin resistance. *Int J Exp Diabetes Res.,* 3**,** 47-60.

LARTER, C. Z., YEH, M. M., WILLIAMS, J., BELL-ANDERSON, K. S. & FARRELL, G. C. 2008. MCD-induced steatohepatitis is associated with hepatic adiponectin resistance and adipogenic transformation of hepatocytes. *J Hepatol.,* 49**,** 407-16. doi: 10.1016/j.jhep.2008.03.026. Epub 2008 Apr 30.

LAVINE, J. E., SCHWIMMER, J. B., VAN NATTA, M. L., MOLLESTON, J. P., MURRAY, K. F., ROSENTHAL, P., ABRAMS, S. H., SCHEIMANN, A. O., SANYAL, A. J., CHALASANI, N., TONASCIA, J., UNALP, A., CLARK, J. M., BRUNT, E. M., KLEINER, D. E., HOOFNAGLE, J. H. & ROBUCK, P. R. 2011. Effect of vitamin E or metformin for treatment of nonalcoholic fatty liver disease in children and adolescents: the TONIC randomized controlled trial. *Jama.,* 305**,** 1659-68. doi: 10.1001/jama.2011.520.

LAZARIDIS, K. N., PHAM, L., VROMAN, B., DE GROEN, P. C. & LARUSSO, N. F. 1997. Kinetic and molecular identification of sodium-dependent glucose transporter in normal rat cholangiocytes. *Am J Physiol.,* 272**,** G1168-74.

LE NAOUR, F., BRALET, M. P., DEBOIS, D., SANDT, C., GUETTIER, C., DUMAS, P., BRUNELLE, A. & LAPREVOTE, O. 2009. Chemical imaging on liver steatosis using synchrotron infrared and ToF-SIMS microspectroscopies. *PLoS One.,* 4**,** e7408. doi: 10.1371/journal.pone.0007408.

LEE, R. G. 1995. Nonalcoholic steatohepatitis: tightening the morphological screws on a hepatic rambler. *Hepatology.,* 21**,** 1742-3.

LEE, Y. C., HUANG, H. Y., CHANG, C. J., CHENG, C. H. & CHEN, Y. T. 2010. Mitochondrial GLUT10 facilitates dehydroascorbic acid import and protects cells against oxidative stress: mechanistic insight into arterial tortuosity syndrome. *Hum Mol Genet.,* 19**,** 3721-33. Epub 2010 Jul 16.

LETURQUE, A., BROT-LAROCHE, E. & LE GALL, M. 2009. GLUT2 mutations, translocation, and receptor function in diet sugar managing. *Am J Physiol Endocrinol Metab.,* 296**,** E985-92. Epub 2009 Feb 17.

LEVY, E., MENARD, D., DELVIN, E., MONTOUDIS, A., BEAULIEU, J. F., MAILHOT, G., DUBE, N., SINNETT, D., SEIDMAN, E. & BENDAYAN, M. 2009. Localization, function and regulation of the two intestinal fatty acid-binding protein types. *Histochem Cell Biol.,* 132**,** 351-67. doi: 10.1007/s00418-009-0608-y. Epub 2009 Jun 5.

LEVY, E., MENARD, D., DELVIN, E., STAN, S., MITCHELL, G., LAMBERT, M., ZIV, E., FEOLI-FONSECA, J. C. & SEIDMAN, E. 2001. The polymorphism

at codon 54 of the FABP2 gene increases fat absorption in human intestinal explants. *J Biol Chem.*, 276**,** 39679-84. Epub 2001 Aug 3.

LEWINSOHN, R., GLOVER, V. & SANDLER, M. 1980. Development of benzylamine oxidase and monoamine oxidase A and B in man. *Biochem Pharmacol.*, 29**,** 1221-30.

LEWIS, J. R. & MOHANTY, S. R. 2010. Nonalcoholic fatty liver disease: a review and update. *Dig Dis Sci.*, 55**,** 560-78. doi: 10.1007/s10620-009-1081-0. Epub 2010 Jan 26.

LI, L., LIU, B., HAVERSEN, L., LU, E., MAGNUSSON, L. U., STAHLMAN, M., BOREN, J., BERGSTROM, G., LEVIN, M. C. & HULTEN, L. M. 2012. The importance of GLUT3 for de novo lipogenesis in hypoxia-induced lipid loading of human macrophages. *PLoS One.*, 7**,** e42360. Epub 2012 Aug 2.

LI, X., KIM, S. W., CHOI, J. S., LEE, Y. M., LEE, C. K., CHOI, B. H., KIM, T. H., CHOI, Y. I., KIM, J. J. & KIM, K. S. 2010. Investigation of porcine FABP3 and LEPR gene polymorphisms and mRNA expression for variation in intramuscular fat content. *Mol Biol Rep.*, 37**,** 3931-9. Epub 2010 Mar 19.

LI, Y. & GU, H. 2012. [Selective regulation of peroxisome proliferator-activated receptors on fatty acid binding protein-4 in human syncytiotrophoblast cells]. *Zhonghua Fu Chan Ke Za Zhi.*, 47**,** 726-9.

LIASKOU, E., KARIKOSKI, M., REYNOLDS, G. M., LALOR, P. F., WESTON, C. J., PULLEN, N., SALMI, M., JALKANEN, S. & ADAMS, D. H. 2011. Regulation of mucosal addressin cell adhesion molecule 1 expression in human and mice by vascular adhesion protein 1 amine oxidase activity. *Hepatology.*, 53**,** 661-72. doi: 10.1002/hep.24085. Epub 2011 Jan 10.

LIASKOU, E., WILSON, D. V. & OO, Y. H. 2012. Innate immune cells in liver inflammation. *Mediators Inflamm.*, 2012:949157**.,** 10.1155/2012/949157. Epub 2012 Aug 9.

LIEBERMAN, J. M., SACCHETTINI, J., MARKS, C. & MARKS, W. H. 1997. Human intestinal fatty acid binding protein: report of an assay with studies in normal volunteers and intestinal ischemia. *Surgery.*, 121**,** 335-42.

LILLIS, A. P., VAN DUYN, L. B., MURPHY-ULLRICH, J. E. & STRICKLAND, D. K. 2008. LDL receptor-related protein 1: unique tissue-specific functions revealed by selective gene knockout studies. *Physiol Rev.*, 88**,** 887-918. doi: 10.1152/physrev.00033.2007.

LIM, J. S., MIETUS-SNYDER, M., VALENTE, A., SCHWARZ, J. M. & LUSTIG, R. H. 2010. The role of fructose in the pathogenesis of NAFLD and the metabolic syndrome. *Nat Rev Gastroenterol Hepatol.*, 7**,** 251-64. Epub 2010 Apr 6.

LIN, Y. C., CHANG, P. F., CHANG, M. H. & NI, Y. H. 2013. A common variant in the peroxisome proliferator-activated receptor-gamma coactivator-1alpha gene is associated with nonalcoholic fatty liver disease in obese children. *Am J Clin Nutr.*, 97**,** 326-31. doi: 10.3945/ajcn.112.046417. Epub 2012 Dec 26.

LISANTI, M. P., SCHERER, P. E., VIDUGIRIENE, J., TANG, Z., HERMANOWSKI-VOSATKA, A., TU, Y. H., COOK, R. F. & SARGIACOMO, M. 1994. Characterization of caveolin-rich membrane domains isolated from an endothelial-rich source: implications for human disease. *J Cell Biol.*, 126**,** 111-26.

LISTENBERGER, L. L., ORY, D. S. & SCHAFFER, J. E. 2001. Palmitate-induced apoptosis can occur through a ceramide-independent pathway. *J Biol Chem.*, 276**,** 14890-5. Epub 2001 Feb 13.

LITHERLAND, G. J., HAJDUCH, E., GOULD, G. W. & HUNDAL, H. S. 2004. Fructose transport and metabolism in adipose tissue of Zucker rats: diminished GLUT5 activity during obesity and insulin resistance. *Mol Cell Biochem.,* 261**,** 23-33.

LIU, J. J., GLICKMAN, J. N., MASYUK, A. I. & LARUSSO, N. F. 2008. Cholangiocyte bile salt transporters in cholesterol gallstone-susceptible and resistant inbred mouse strains. *J Gastroenterol Hepatol.,* 23**,** 1596-602. doi: 10.1111/j.1440-1746.2008.05500.x. Epub 2008 Aug 20.

LIU, K. & CZAJA, M. J. 2013. Regulation of lipid stores and metabolism by lipophagy. *Cell Death Differ.,* 20**,** 3-11. doi: 10.1038/cdd.2012.63. Epub 2012 May 18.

LIU, Y., MEYER, C., XU, C., WENG, H., HELLERBRAND, C., TEN DIJKE, P. & DOOLEY, S. 2013. Animal models of chronic liver diseases. *Am J Physiol Gastrointest Liver Physiol.,* 304**,** G449-68. doi: 10.1152/ajpgi.00199.2012. Epub 2012 Dec 28.

LIVAK, K. J. & SCHMITTGEN, T. D. 2001. Analysis of relative gene expression data using real-time quantitative PCR and the 2(-Delta Delta C(T)) Method. *Methods.,* 25**,** 402-8.

LORD, G. 2002. Role of leptin in immunology. *Nutr Rev.,* 60**,** S35-8; discussion S68-84, 85-7.

LOUD, A. V. 1968. A quantitative stereological description of the ultrastructure of normal rat liver parenchymal cells. *J Cell Biol.,* 37**,** 27-46.

LOW, B. C., ROSS, I. K. & GRIGOR, M. R. 1992. Angiotensin II stimulates glucose transport activity in cultured vascular smooth muscle cells. *J Biol Chem.,* 267**,** 20740-5.

LOW, W., KANG, J., DIGRUCCIO, M., KIRBY, D., PERRIN, M. & FISCHER, W. H. 2004. MALDI-MS analysis of peptides modified with photolabile arylazido groups. *J Am Soc Mass Spectrom.,* 15**,** 1156-60.

LUDWIG, J., VIGGIANO, T. R., MCGILL, D. B. & OH, B. J. 1980. Nonalcoholic steatohepatitis: Mayo Clinic experiences with a hitherto unnamed disease. *Mayo Clin Proc.,* 55**,** 434-8.

LYLES, G. A. 1995. Substrate-specificity of mammalian tissue-bound semicarbazide-sensitive amine oxidase. *Prog Brain Res.,* 106**,** 293-303.

LYLES, G. A. 1996. Mammalian plasma and tissue-bound semicarbazide-sensitive amine oxidases: biochemical, pharmacological and toxicological aspects. *Int J Biochem Cell Biol.,* 28**,** 259-74.

MA, X., LIU, G., WANG, S., CHEN, Z., LAI, M., LIU, Z. & YANG, J. 2007. Evaluation of sphingolipids changes in brain tissues of rats with pentylenetetrazol-induced kindled seizures using MALDI-TOF-MS. *J Chromatogr B Analyt Technol Biomed Life Sci.,* 859**,** 170-7. Epub 2007 Oct 10.

MACSWEEN, R. N. & BURT, A. D. 1986. Histologic spectrum of alcoholic liver disease. *Semin Liver Dis.,* 6**,** 221-32.

MADRAZO, J. A. & KELLY, D. P. 2008. The PPAR trio: regulators of myocardial energy metabolism in health and disease. *J Mol Cell Cardiol.,* 44**,** 968-75. doi: 10.1016/j.yjmcc.2008.03.021. Epub 2008 Apr 4.

MAEDA, K., CAO, H., KONO, K., GORGUN, C. Z., FURUHASHI, M., UYSAL, K. T., CAO, Q., ATSUMI, G., MALONE, H., KRISHNAN, B., MINOKOSHI, Y., KAHN, B. B., PARKER, R. A. & HOTAMISLIGIL, G. S. 2005.

Adipocyte/macrophage fatty acid binding proteins control integrated metabolic responses in obesity and diabetes. *Cell Metab.,* 1**,** 107-19.

MAEDA, K., UYSAL, K. T., MAKOWSKI, L., GORGUN, C. Z., ATSUMI, G., PARKER, R. A., BRUNING, J., HERTZEL, A. V., BERNLOHR, D. A. & HOTAMISLIGIL, G. S. 2003. Role of the fatty acid binding protein mal1 in obesity and insulin resistance. *Diabetes.,* 52**,** 300-7.

MAEDLER, K., SPINAS, G. A., DYNTAR, D., MORITZ, W., KAISER, N. & DONATH, M. Y. 2001. Distinct effects of saturated and monounsaturated fatty acids on beta-cell turnover and function. *Diabetes.,* 50**,** 69-76.

MAHADEV, K., WU, X., ZILBERING, A., ZHU, L., LAWRENCE, J. T. & GOLDSTEIN, B. J. 2001. Hydrogen peroxide generated during cellular insulin stimulation is integral to activation of the distal insulin signaling cascade in 3T3-L1 adipocytes. *J Biol Chem.,* 276**,** 48662-9. Epub 2001 Oct 11.

MAKOWSKI, L., BRITTINGHAM, K. C., REYNOLDS, J. M., SUTTLES, J. & HOTAMISLIGIL, G. S. 2005. The fatty acid-binding protein, aP2, coordinates macrophage cholesterol trafficking and inflammatory activity. Macrophage expression of aP2 impacts peroxisome proliferator-activated receptor gamma and IkappaB kinase activities. *J Biol Chem.,* 280**,** 12888-95. Epub 2005 Jan 31.

MAKOWSKI, L. & HOTAMISLIGIL, G. S. 2004. Fatty acid binding proteins--the evolutionary crossroads of inflammatory and metabolic responses. *J Nutr.,* 134**,** 2464S-2468S.

MAKOWSKI, L. & HOTAMISLIGIL, G. S. 2005. The role of fatty acid binding proteins in metabolic syndrome and atherosclerosis. *Curr Opin Lipidol.,* 16**,** 543-8.

MALHI, H., BARREYRO, F. J., ISOMOTO, H., BRONK, S. F. & GORES, G. J. 2007. Free fatty acids sensitise hepatocytes to TRAIL mediated cytotoxicity. *Gut.,* 56**,** 1124-31. Epub 2007 Apr 30.

MALHI, H., BRONK, S. F., WERNEBURG, N. W. & GORES, G. J. 2006. Free fatty acids induce JNK-dependent hepatocyte lipoapoptosis. *J Biol Chem.,* 281**,** 12093-101. Epub 2006 Feb 27.

MANN, D. A. & SMART, D. E. 2002. Transcriptional regulation of hepatic stellate cell activation. *Gut.,* 50**,** 891-6.

MANSEGO, M. L., MARTINEZ, F., MARTINEZ-LARRAD, M. T., ZABENA, C., ROJO, G., MORCILLO, S., SORIGUER, F., MARTIN-ESCUDERO, J. C., SERRANO-RIOS, M., REDON, J. & CHAVES, F. J. 2012. Common variants of the liver fatty acid binding protein gene influence the risk of type 2 diabetes and insulin resistance in Spanish population. *PLoS One.,* 7**,** e31853. Epub 2012 Mar 2.

MARTELIUS, T., SALMI, M., WU, H., BRUGGEMAN, C., HOCKERSTEDT, K., JALKANEN, S. & LAUTENSCHLAGER, I. 2000. Induction of vascular adhesion protein-1 during liver allograft rejection and concomitant cytomegalovirus infection in rats. *Am J Pathol.,* 157**,** 1229-37.

MARTI, L., ABELLA, A., CARPENE, C., PALACIN, M., TESTAR, X. & ZORZANO, A. 2001. Combined treatment with benzylamine and low dosages of vanadate enhances glucose tolerance and reduces hyperglycemia in streptozotocin-induced diabetic rats. *Diabetes.,* 50**,** 2061-8.

MARTI, L., MORIN, N., ENRIQUE-TARANCON, G., PREVOT, D., LAFONTAN, M., TESTAR, X., ZORZANO, A. & CARPENE, C. 1998. Tyramine and vanadate synergistically stimulate glucose transport in rat adipocytes by amine

oxidase-dependent generation of hydrogen peroxide. *J Pharmacol Exp Ther.*, 285**,** 342-9.

MARTIN, H., SARSAT, J. P., DE WAZIERS, I., HOUSSET, C., BALLADUR, P., BEAUNE, P., ALBALADEJO, V. & LERCHE-LANGRAND, C. 2003. Induction of cytochrome P450 2B6 and 3A4 expression by phenobarbital and cyclophosphamide in cultured human liver slices. *Pharm Res.*, 20**,** 557-68.

MARTINI, F. H. 2006. Fundamentals of Anatomy and Physiology Chapter 24**,** P890-894.

MARTTILA-ICHIHARA, F., AUVINEN, K., ELIMA, K., JALKANEN, S. & SALMI, M. 2009. Vascular adhesion protein-1 enhances tumor growth by supporting recruitment of Gr-1+CD11b+ myeloid cells into tumors. *Cancer Res.*, 69**,** 7875-83. doi: 10.1158/0008-5472.CAN-09-1205. Epub 2009 Sep 29.

MARTTILA-ICHIHARA, F., CASTERMANS, K., AUVINEN, K., OUDE EGBRINK, M. G., JALKANEN, S., GRIFFIOEN, A. W. & SALMI, M. 2010. Small-molecule inhibitors of vascular adhesion protein-1 reduce the accumulation of myeloid cells into tumors and attenuate tumor growth in mice. *J Immunol.*, 184**,** 3164-73. doi: 10.4049/jimmunol.0901794. Epub 2010 Feb 12.

MASTRODONATO, M., CALAMITA, G., ROSSI, R., MENTINO, D., BONFRATE, L., PORTINCASA, P., FERRI, D. & LIQUORI, G. E. 2011. Altered distribution of caveolin-1 in early liver steatosis. *Eur J Clin Invest.*, 41**,** 642-51. doi: 10.1111/j.1365-2362.2010.02459.x. Epub 2011 Jan 20.

MASTRODONATO, M., PORTINCASA, P., MENTINO, D., ROSSI, R., RESTA, L., FERRI, D. & LIQUORI, G. E. 2012. Caveolin-1 and mitochondrial alterations in regenerating rat liver. *Microsc Res Tech.*, 75**,** 1026-32. doi: 10.1002/jemt.22027. Epub 2012 Mar 19.

MASUO, K., KAWAGUCHI, H., MIKAMI, H., OGIHARA, T. & TUCK, M. L. 2003. Serum uric acid and plasma norepinephrine concentrations predict subsequent weight gain and blood pressure elevation. *Hypertension.*, 42**,** 474-80. Epub 2003 Sep 2.

MATHYS, K. C., PONNAMPALAM, S. N., PADIVAL, S. & NAGARAJ, R. H. 2002. Semicarbazide-sensitive amine oxidase in aortic smooth muscle cells mediates synthesis of a methylglyoxal-AGE: implications for vascular complications in diabetes. *Biochem Biophys Res Commun.*, 297**,** 863-9.

MCBRAYER, S. K., CHENG, J. C., SINGHAL, S., KRETT, N. L., ROSEN, S. T. & SHANMUGAM, M. 2012. Multiple myeloma exhibits novel dependence on GLUT4, GLUT8, and GLUT11: implications for glucose transporter-directed therapy. *Blood.*, 119**,** 4686-97. doi: 10.1182/blood-2011-09-377846. Epub 2012 Mar 27.

MCCUSKEY, R. S. & MCCUSKEY, P. A. 1990. Fine structure and function of Kupffer cells. *J Electron Microsc Tech.*, 14**,** 237-46.

MCNAB, G., REEVES, J. L., SALMI, M., HUBSCHER, S., JALKANEN, S. & ADAMS, D. H. 1996. Vascular adhesion protein 1 mediates binding of T cells to human hepatic endothelium. *Gastroenterology.*, 110**,** 522-8.

MCVIE-WYLIE, A. J., LAMSON, D. R. & CHEN, Y. T. 2001. Molecular cloning of a novel member of the GLUT family of transporters, SLC2a10 (GLUT10), localized on chromosome 20q13.1: a candidate gene for NIDDM susceptibility. *Genomics.*, 72**,** 113-7.

MEI, S., NI, H. M., MANLEY, S., BOCKUS, A., KASSEL, K. M., LUYENDYK, J. P., COPPLE, B. L. & DING, W. X. 2011. Differential roles of unsaturated and

saturated fatty acids on autophagy and apoptosis in hepatocytes. *J Pharmacol Exp Ther.,* 339**,** 487-98. doi: 10.1124/jpet.111.184341. Epub 2011 Aug 19.

MERCADER, J., IFFIU-SOLTESZ, Z., BOUR, S. & CARPENE, C. 2011. Oral Administration of Semicarbazide Limits Weight Gain together with Inhibition of Fat Deposition and of Primary Amine Oxidase Activity in Adipose Tissue. *J Obes.,* 2011:475786**.,** 10.1155/2011/475786. Epub 2011 Feb 8.

MERCIER, N., KAKOU, A., CHALLANDE, P., LACOLLEY, P. & OSBORNE-PELLEGRIN, M. 2009. Comparison of the effects of semicarbazide and beta-aminopropionitrile on the arterial extracellular matrix in the Brown Norway rat. *Toxicol Appl Pharmacol.,* 239**,** 258-67. doi: 10.1016/j.taap.2009.06.005. Epub 2009 Jun 12.

MERCIER, N., MOLDES, M., EL HADRI, K. & FEVE, B. 2001. Semicarbazide-sensitive amine oxidase activation promotes adipose conversion of 3T3-L1 cells. *Biochem J.,* 358**,** 335-42.

MERINEN, M., IRJALA, H., SALMI, M., JAAKKOLA, I., HANNINEN, A. & JALKANEN, S. 2005. Vascular adhesion protein-1 is involved in both acute and chronic inflammation in the mouse. *Am J Pathol.,* 166**,** 793-800.

MERRIMAN, R. B., AOUIZERAT, B. E. & BASS, N. M. 2006. Genetic influences in nonalcoholic fatty liver disease. *J Clin Gastroenterol.,* 40**,** S30-3.

MESZAROS, Z., SZOMBATHY, T., RAIMONDI, L., KARADI, I., ROMICS, L. & MAGYAR, K. 1999. Elevated serum semicarbazide-sensitive amine oxidase activity in non-insulin-dependent diabetes mellitus: correlation with body mass index and serum triglyceride. *Metabolism.,* 48**,** 113-7.

MILLER, E. R., 3RD, PASTOR-BARRIUSO, R., DALAL, D., RIEMERSMA, R. A., APPEL, L. J. & GUALLAR, E. 2005a. Meta-analysis: high-dosage vitamin E supplementation may increase all-cause mortality. *Ann Intern Med.,* 142**,** 37-46. Epub 2004 Nov 10.

MILLER, G. E., FREEDLAND, K. E., CARNEY, R. M., STETLER, C. A. & BANKS, W. A. 2003. Pathways linking depression, adiposity, and inflammatory markers in healthy young adults. *Brain Behav Immun.,* 17**,** 276-85.

MILLER, P. J., FINUCANE, K. A., HUGHES, M. & ZHAO, F. Q. 2005b. Cloning and expression of bovine glucose transporter GLUT12. *Mamm Genome.,* 16**,** 873-83. Epub 2005 Nov 11.

MILLONIG, G., PRAUN, S., NETZER, M., BAUMGARTNER, C., DORNAUER, A., MUELLER, S., VILLINGER, J. & VOGEL, W. 2010. Non-invasive diagnosis of liver diseases by breath analysis using an optimized ion-molecule reaction-mass spectrometry approach: a pilot study. *Biomarkers.,* 15**,** 297-306. doi: 10.3109/13547501003624512.

MINOKOSHI, Y., KIM, Y. B., PERONI, O. D., FRYER, L. G., MULLER, C., CARLING, D. & KAHN, B. B. 2002. Leptin stimulates fatty-acid oxidation by activating AMP-activated protein kinase. *Nature.,* 415**,** 339-43.

MIQUILENA-COLINA, M. E., LIMA-CABELLO, E., SANCHEZ-CAMPOS, S., GARCIA-MEDIAVILLA, M. V., FERNANDEZ-BERMEJO, M., LOZANO-RODRIGUEZ, T., VARGAS-CASTRILLON, J., BUQUE, X., OCHOA, B., ASPICHUETA, P., GONZALEZ-GALLEGO, J. & GARCIA-MONZON, C. 2011. Hepatic fatty acid translocase CD36 upregulation is associated with insulin resistance, hyperinsulinaemia and increased steatosis in non-alcoholic steatohepatitis and chronic hepatitis C. *Gut.,* 60**,** 1394-402. doi: 10.1136/gut.2010.222844. Epub 2011 Jan 26.

MITSUYOSHI, H., YASUI, K., HARANO, Y., ENDO, M., TSUJI, K., MINAMI, M., ITOH, Y., OKANOUE, T. & YOSHIKAWA, T. 2009. Analysis of hepatic genes involved in the metabolism of fatty acids and iron in nonalcoholic fatty liver disease. *Hepatol Res.,* 39**,** 366-73. Epub 2008 Nov 25.

MIURA, K., YANG, L., VAN ROOIJEN, N., BRENNER, D. A., OHNISHI, H. & SEKI, E. 2013. Toll-like receptor 2 and palmitic acid cooperatively contribute to the development of nonalcoholic steatohepatitis through inflammasome activation in mice. *Hepatology.,* 57**,** 577-89. doi: 10.1002/hep.26081.

MOHANTY, S. R., TROY, T. N., HUO, D., O'BRIEN, B. L., JENSEN, D. M. & HART, J. 2009. Influence of ethnicity on histological differences in non-alcoholic fatty liver disease. *J Hepatol.,* 50**,** 797-804. doi: 10.1016/j.jhep.2008.11.017. Epub 2009 Jan 1.

MORIN, N., LIZCANO, J. M., FONTANA, E., MARTI, L., SMIH, F., ROUET, P., PREVOT, D., ZORZANO, A., UNZETA, M. & CARPENE, C. 2001. Semicarbazide-sensitive amine oxidase substrates stimulate glucose transport and inhibit lipolysis in human adipocytes. *J Pharmacol Exp Ther.,* 297**,** 563-72.

MORTENSEN, B. & DALE, O. 1995. Effects of hypothermia on the elimination of ethanol, diazepam and oxazepam in rat liver slice incubations. *Acta Anaesthesiol Scand.,* 39**,** 199-204.

MOYA, M., BENET, M., GUZMAN, C., TOLOSA, L., GARCIA-MONZON, C., PAREJA, E., CASTELL, J. V. & JOVER, R. 2012. Foxa1 reduces lipid accumulation in human hepatocytes and is down-regulated in nonalcoholic fatty liver. *PLoS One.,* 7**,** e30014. Epub 2012 Jan 6.

MUECKLER, M. 1990. Family of glucose-transporter genes. Implications for glucose homeostasis and diabetes. *Diabetes.,* 39**,** 6-11.

MUECKLER, M., CARUSO, C., BALDWIN, S. A., PANICO, M., BLENCH, I., MORRIS, H. R., ALLARD, W. J., LIENHARD, G. E. & LODISH, H. F. 1985. Sequence and structure of a human glucose transporter. *Science.,* 229**,** 941-5.

MURATA, M., PERANEN, J., SCHREINER, R., WIELAND, F., KURZCHALIA, T. V. & SIMONS, K. 1995. VIP21/caveolin is a cholesterol-binding protein. *Proc Natl Acad Sci U S A.,* 92**,** 10339-43.

MURAWAKI, Y., KUSAKABE, Y. & HIRAYAMA, C. 1991. Serum lysyl oxidase activity in chronic liver disease in comparison with serum levels of prolyl hydroxylase and laminin. *Hepatology.,* 14**,** 1167-73.

MUSSO, G., CASSADER, M., ROSINA, F. & GAMBINO, R. 2012. Impact of current treatments on liver disease, glucose metabolism and cardiovascular risk in non-alcoholic fatty liver disease (NAFLD): a systematic review and meta-analysis of randomised trials. *Diabetologia.,* 55**,** 885-904. doi: 10.1007/s00125-011-2446-4. Epub 2012 Jan 27.

MUSSO, G., GAMBINO, R. & CASSADER, M. 2009. Recent insights into hepatic lipid metabolism in non-alcoholic fatty liver disease (NAFLD). *Prog Lipid Res.,* 48**,** 1-26. Epub 2008 Sep 9.

MUZYKANTOV, V. R. 2001. Targeting of superoxide dismutase and catalase to vascular endothelium. *J Control Release.,* 71**,** 1-21.

NAIK, R. S., MUJUMDAR, A. M. & GHASKADBI, S. 2004. Protection of liver cells from ethanol cytotoxicity by curcumin in liver slice culture in vitro. *J Ethnopharmacol.,* 95**,** 31-7.

NAKAGAWA, T., HU, H., ZHARIKOV, S., TUTTLE, K. R., SHORT, R. A., GLUSHAKOVA, O., OUYANG, X., FEIG, D. I., BLOCK, E. R., HERRERA-ACOSTA, J., PATEL, J. M. & JOHNSON, R. J. 2006. A causal role for uric acid in fructose-induced metabolic syndrome. *Am J Physiol Renal Physiol.,* 290**,** F625-31. Epub 2005 Oct 18.

NAKAJIMA, K. 2012. Multidisciplinary pharmacotherapeutic options for nonalcoholic Fatty liver disease. *Int J Hepatol.,* 2012:950693**.,** 10.1155/2012/950693. Epub 2012 Dec 9.

NAKAMUTA, M., KOHJIMA, M., MORIZONO, S., KOTOH, K., YOSHIMOTO, T., MIYAGI, I. & ENJOJI, M. 2005. Evaluation of fatty acid metabolism-related gene expression in nonalcoholic fatty liver disease. *Int J Mol Med.,* 16**,** 631-5.

NAMIKAWA, C., SHU-PING, Z., VYSELAAR, J. R., NOZAKI, Y., NEMOTO, Y., ONO, M., AKISAWA, N., SAIBARA, T., HIROI, M., ENZAN, H. & ONISHI, S. 2004. Polymorphisms of microsomal triglyceride transfer protein gene and manganese superoxide dismutase gene in non-alcoholic steatohepatitis. *J Hepatol.,* 40**,** 781-6.

NEUSCHWANDER-TETRI, B. A. 2010. Hepatic lipotoxicity and the pathogenesis of nonalcoholic steatohepatitis: the central role of nontriglyceride fatty acid metabolites. *Hepatology.,* 52**,** 774-88. doi: 10.1002/hep.23719.

NEVADO, C., VALVERDE, A. M. & BENITO, M. 2006. Role of insulin receptor in the regulation of glucose uptake in neonatal hepatocytes. *Endocrinology.,* 147**,** 3709-18. Epub 2006 Apr 27.

NEWBERRY, E. P., XIE, Y., KENNEDY, S., HAN, X., BUHMAN, K. K., LUO, J., GROSS, R. W. & DAVIDSON, N. O. 2003. Decreased hepatic triglyceride accumulation and altered fatty acid uptake in mice with deletion of the liver fatty acid-binding protein gene. *J Biol Chem.,* 278**,** 51664-72. Epub 2003 Oct 8.

NIE, B., PARK, H. M., KAZANTZIS, M., LIN, M., HENKIN, A., NG, S., SONG, S., CHEN, Y., TRAN, H., LAI, R., HER, C., MAHER, J. J., FORMAN, B. M. & STAHL, A. 2012. Specific bile acids inhibit hepatic fatty acid uptake in mice. *Hepatology.,* 56**,** 1300-10. doi: 10.1002/hep.25797.

NOCITO, A., DAHM, F., JOCHUM, W., JANG, J. H., GEORGIEV, P., BADER, M., RENNER, E. L. & CLAVIEN, P. A. 2007. Serotonin mediates oxidative stress and mitochondrial toxicity in a murine model of nonalcoholic steatohepatitis. *Gastroenterology.,* 133**,** 608-18. Epub 2007 May 21.

NODA, K., MIYAHARA, S., NAKAZAWA, T., ALMULKI, L., NAKAO, S., HISATOMI, T., SHE, H., THOMAS, K. L., GARLAND, R. C., MILLER, J. W., GRAGOUDAS, E. S., KAWAI, Y., MASHIMA, Y. & HAFEZI-MOGHADAM, A. 2008. Inhibition of vascular adhesion protein-1 suppresses endotoxin-induced uveitis. *Faseb J.,* 22**,** 1094-103. Epub 2007 Nov 21.

NODA, K., NAKAO, S., ZANDI, S., ENGELSTADTER, V., MASHIMA, Y. & HAFEZI-MOGHADAM, A. 2009. Vascular adhesion protein-1 regulates leukocyte transmigration rate in the retina during diabetes. *Exp Eye Res.,* 89**,** 774-81. doi: 10.1016/j.exer.2009.07.010. Epub 2009 Jul 25.

NORDLIE, R. C., FOSTER, J. D. & LANGE, A. J. 1999. Regulation of glucose production by the liver. *Annu Rev Nutr.,* 19**,** 379-406.

O'SULLIVAN, J., UNZETA, M., HEALY, J., O'SULLIVAN, M. I., DAVEY, G. & TIPTON, K. F. 2004. Semicarbazide-sensitive amine oxidases: enzymes with quite a lot to do. *Neurotoxicology.,* 25**,** 303-15.

OAKLEY, F., MANN, J., NAILARD, S., SMART, D. E., MUNGALSINGH, N., CONSTANDINOU, C., ALI, S., WILSON, S. J., MILLWARD-SADLER, H., IREDALE, J. P. & MANN, D. A. 2005. Nuclear factor-kappaB1 (p50) limits the inflammatory and fibrogenic responses to chronic injury. *Am J Pathol.*, 166**,** 695-708.

OBIKA, M. & NOGUCHI, H. 2012. Diagnosis and evaluation of nonalcoholic fatty liver disease. *Exp Diabetes Res.*, 2012:145754**.,** 10.1155/2012/145754. Epub 2011 Oct 27.

OCHIAI, Y., ITOH, K., SAKURAI, E., ADACHI, M. & TANAKA, Y. 2006. Substrate selectivity of monoamine oxidase A, monoamine oxidase B, diamine oxidase, and semicarbazide-sensitive amine oxidase in COS-1 expression systems. *Biol Pharm Bull.*, 29**,** 2362-6.

OIE, C. I., APPA, R. S., HILDEN, I., PETERSEN, H. H., GRUHLER, A., SMEDSROD, B. & HANSEN, J. B. 2011. Rat liver sinusoidal endothelial cells (LSECs) express functional low density lipoprotein receptor-related protein-1 (LRP-1). *J Hepatol.*, 55**,** 1346-52. doi: 10.1016/j.jhep.2011.03.013. Epub 2011 Apr 13.

OLSON, A. L. & PESSIN, J. E. 1996. Structure, function, and regulation of the mammalian facilitative glucose transporter gene family. *Annu Rev Nutr.*, 16**,** 235-56.

OSTROWSKI, S. G., KURCZY, M. E., RODDY, T. P., WINOGRAD, N. & EWING, A. G. 2007. Secondary ion MS imaging to relatively quantify cholesterol in the membranes of individual cells from differentially treated populations. *Anal Chem.*, 79**,** 3554-60. Epub 2007 Apr 12.

OUDE ELFERINK, R. P. & GROEN, A. K. 2000. Mechanisms of biliary lipid secretion and their role in lipid homeostasis. *Semin Liver Dis.*, 20**,** 293-305.

OUYANG, X., CIRILLO, P., SAUTIN, Y., MCCALL, S., BRUCHETTE, J. L., DIEHL, A. M., JOHNSON, R. J. & ABDELMALEK, M. F. 2008. Fructose consumption as a risk factor for non-alcoholic fatty liver disease. *J Hepatol.*, 48**,** 993-9. doi: 10.1016/j.jhep.2008.02.011. Epub 2008 Mar 10.

PAN, C., KUMAR, C., BOHL, S., KLINGMUELLER, U. & MANN, M. 2009. Comparative proteomic phenotyping of cell lines and primary cells to assess preservation of cell type-specific functions. *Mol Cell Proteomics.*, 8**,** 443-50. doi: 10.1074/mcp.M800258-MCP200. Epub 2008 Oct 23.

PAREKH, S. & ANANIA, F. A. 2007. Abnormal lipid and glucose metabolism in obesity: implications for nonalcoholic fatty liver disease. *Gastroenterology.*, 132**,** 2191-207.

PARK, S. G. & MURRAY, K. K. 2012. Infrared laser ablation sample transfer for MALDI imaging. *Anal Chem.*, 84**,** 3240-5. doi: 10.1021/ac3006704. Epub 2012 Mar 22.

PARSONAGE, G., FALCIANI, F., BURMAN, A., FILER, A., ROSS, E., BOFILL, M., MARTIN, S., SALMON, M. & BUCKLEY, C. D. 2003. Global gene expression profiles in fibroblasts from synovial, skin and lymphoid tissue reveals distinct cytokine and chemokine expression patterns. *Thromb Haemost.*, 90**,** 688-97.

PASTUCHA, D., FILIPCIKOVA, R., HORAKOVA, D., RADOVA, L., MARINOV, Z., MALINCIKOVA, J., KOCVRLICH, M., HORAK, S., BEZDICKOVA, M. & DOBIAS, M. 2013. The incidence of metabolic syndrome in obese Czech children: the importance of early detection of insulin resistance using homeostatic indexes HOMA-IR and QUICKI. *Physiol Res,* 14**,** 14.

PEI, Z., FRAISL, P., BERGER, J., JIA, Z., FORSS-PETTER, S. & WATKINS, P. A. 2004. Mouse very long-chain Acyl-CoA synthetase 3/fatty acid transport protein 3 catalyzes fatty acid activation but not fatty acid transport in MA-10 cells. *J Biol Chem.,* 279**,** 54454-62. Epub 2004 Oct 6.

PELSERS, M. M., HERMENS, W. T. & GLATZ, J. F. 2005. Fatty acid-binding proteins as plasma markers of tissue injury. *Clin Chim Acta.,* 352**,** 15-35.

PELSERS, M. M., MOROVAT, A., ALEXANDER, G. J., HERMENS, W. T., TRULL, A. K. & GLATZ, J. F. 2002. Liver fatty acid-binding protein as a sensitive serum marker of acute hepatocellular damage in liver transplant recipients. *Clin Chem.,* 48**,** 2055-7.

PELTON, P. D., ZHOU, L., DEMAREST, K. T. & BURRIS, T. P. 1999. PPARgamma activation induces the expression of the adipocyte fatty acid binding protein gene in human monocytes. *Biochem Biophys Res Commun.,* 261**,** 456-8.

PENG, X., ZHANG, L., WANG, Q. & CUI, X. 2009. [Study on the relationship between FABP2 Ala54Thr polymorphism and the risk of non-alcoholic fatty liver diseases]. *Wei Sheng Yan Jiu.,* 38**,** 401-4.

PENG, X. E., WU, Y. L., LU, Q. Q., HU, Z. J. & LIN, X. 2012a. Two genetic variants in FABP1 and susceptibility to non-alcohol fatty liver disease in a Chinese population. *Gene.,* 500**,** 54-8. doi: 10.1016/j.gene.2012.03.050. Epub 2012 Mar 20.

PENG, X. E., WU, Y. L., LU, Q. Q., HU, Z. J. & LIN, X. 2012b. Two genetic variants in FABP1 and susceptibility to non-alcohol fatty liver disease in a Chinese population. *Gene.,* 500**,** 54-8. Epub 2012 Mar 20.

PENNINX, B. W., KRITCHEVSKY, S. B., YAFFE, K., NEWMAN, A. B., SIMONSICK, E. M., RUBIN, S., FERRUCCI, L., HARRIS, T. & PAHOR, M. 2003. Inflammatory markers and depressed mood in older persons: results from the Health, Aging and Body Composition study. *Biol Psychiatry.,* 54**,** 566-72.

PEREPELYUK, M., TERAJIMA, M., WANG, A. Y., GEORGES, P. C., JANMEY, P. A., YAMAUCHI, M. & WELLS, R. G. 2013. Hepatic stellate cells and portal fibroblasts are the major cellular sources of collagens and lysyl oxidases in normal liver and early after injury. *Am J Physiol Gastrointest Liver Physiol,* 17**,** 17.

PETKOVIC, M., SCHILLER, J., MULLER, J., MULLER, M., ARNOLD, K. & ARNHOLD, J. 2001. The signal-to-noise ratio as the measure for the quantification of lysophospholipids by matrix-assisted laser desorption/ionisation time-of-flight mass spectrometry. *Analyst.,* 126**,** 1042-50.

PICCININO, F., SAGNELLI, E., PASQUALE, G. & GIUSTI, G. 1986. Complications following percutaneous liver biopsy. A multicentre retrospective study on 68,276 biopsies. *J Hepatol.,* 2**,** 165-73.

PIEPER-FURST, U., HALL, R., HUSS, S., HOCHRATH, K., FISCHER, H. P., TACKE, F., WEISKIRCHEN, R. & LAMMERT, F. 2011. Expression of the megalin C-terminal fragment by macrophages during liver fibrogenesis in mice. *Biochim Biophys Acta.,* 1812**,** 1640-8. doi: 10.1016/j.bbadis.2011.09.003. Epub 2011 Sep 10.

PILCH, P. F., SOUTO, R. P., LIU, L., JEDRYCHOWSKI, M. P., BERG, E. A., COSTELLO, C. E. & GYGI, S. P. 2007. Cellular spelunking: exploring adipocyte caveolae. *J Lipid Res.,* 48**,** 2103-11. Epub 2007 May 11.

PILKIS, S. J. & GRANNER, D. K. 1992. Molecular physiology of the regulation of hepatic gluconeogenesis and glycolysis. *Annu Rev Physiol.,* 54**,** 885-909.

PIRISINO, R., GHELARDINI, C., BANCHELLI, G., GALEOTTI, N. & RAIMONDI, L. 2001. Methylamine and benzylamine induced hypophagia in mice: modulation by semicarbazide-sensitive benzylamine oxidase inhibitors and aODN towards Kv1.1 channels. *Br J Pharmacol.,* 134**,** 880-6.

PITTAS, A. G., JOSEPH, N. A. & GREENBERG, A. S. 2004. Adipocytokines and insulin resistance. *J Clin Endocrinol Metab.,* 89**,** 447-52.

POL, A., MARTIN, S., FERNANDEZ, M. A., FERGUSON, C., CAROZZI, A., LUETTERFORST, R., ENRICH, C. & PARTON, R. G. 2004. Dynamic and regulated association of caveolin with lipid bodies: modulation of lipid body motility and function by a dominant negative mutant. *Mol Biol Cell.,* 15**,** 99-110. Epub 2003 Oct 3.

POL, J., VIDOVA, V., HYOTYLAINEN, T., VOLNY, M., NOVAK, P., STROHALM, M., KOSTIAINEN, R., HAVLICEK, V., WIEDMER, S. K. & HOLOPAINEN, J. M. 2011. Spatial distribution of glycerophospholipids in the ocular lens. *PLoS One.,* 6**,** e19441. doi: 10.1371/journal.pone.0019441.

POLYZOS, S. A., KOUNTOURAS, J., PATSIAOURA, K., KATSIKI, E., ZAFEIRIADOU, E., DERETZI, G., ZAVOS, C., GAVALAS, E., KATSINELOS, P., MANE, V. & SLAVAKIS, A. 2012. Serum homocysteine levels in patients with nonalcoholic fatty liver disease. *Ann Hepatol.,* 11**,** 68-76.

POPOV, M. S. & POPOVA, I. V. 1986. [Primary biliary cirrhosis of the liver]. *Arkh Patol.,* 48**,** 81-7.

POSTIC, C. & GIRARD, J. 2008. Contribution of de novo fatty acid synthesis to hepatic steatosis and insulin resistance: lessons from genetically engineered mice. *J Clin Invest.,* 118**,** 829-38. doi: 10.1172/JCI34275.

PREITNER, F., BONNY, O., LAVERRIERE, A., ROTMAN, S., FIRSOV, D., DA COSTA, A., METREF, S. & THORENS, B. 2009. Glut9 is a major regulator of urate homeostasis and its genetic inactivation induces hyperuricosuria and urate nephropathy. *Proc Natl Acad Sci U S A.,* 106**,** 15501-6. Epub 2009 Aug 21.

PREVOT, D., SOLTESZ, Z., ABELLO, V., WANECQ, E., VALET, P., UNZETA, M. & CARPENE, C. 2007. Prolonged treatment with aminoguanidine strongly inhibits adipocyte semicarbazide-sensitive amine oxidase and slightly reduces fat deposition in obese Zucker rats. *Pharmacol Res.,* 56**,** 70-9. Epub 2007 May 1.

PRICE, R. J., MISTRY, H., WIELD, P. T., RENWICK, A. B., BEAMAND, J. A. & LAKE, B. G. 1996. Comparison of the toxicity of allyl alcohol, coumarin and menadione in precision-cut rat, guinea-pig, cynomolgus monkey and human liver slices. *Arch Toxicol.,* 71**,** 107-11.

PUIGSERVER, P., RHEE, J., DONOVAN, J., WALKEY, C. J., YOON, J. C., ORIENTE, F., KITAMURA, Y., ALTOMONTE, J., DONG, H., ACCILI, D. & SPIEGELMAN, B. M. 2003. Insulin-regulated hepatic gluconeogenesis through FOXO1-PGC-1alpha interaction. *Nature.,* 423**,** 550-5. Epub 2003 May 18.

PURCELL, S. H., AERNI-FLESSNER, L. B., WILLCOCKSON, A. R., DIGGS-ANDREWS, K. A., FISHER, S. J. & MOLEY, K. H. 2011. Improved insulin sensitivity by GLUT12 overexpression in mice. *Diabetes.,* 60**,** 1478-82. Epub 2011 Mar 25.

PURI, P., BAILLIE, R. A., WIEST, M. M., MIRSHAHI, F., CHOUDHURY, J., CHEUNG, O., SARGEANT, C., CONTOS, M. J. & SANYAL, A. J. 2007. A lipidomic analysis of nonalcoholic fatty liver disease. *Hepatology.,* 46**,** 1081-90.

PURI, P., WIEST, M. M., CHEUNG, O., MIRSHAHI, F., SARGEANT, C., MIN, H. K., CONTOS, M. J., STERLING, R. K., FUCHS, M., ZHOU, H., WATKINS, S. M. & SANYAL, A. J. 2009. The plasma lipidomic signature of nonalcoholic steatohepatitis. *Hepatology.,* 50**,** 1827-38. doi: 10.1002/hep.23229.

QUEIPO-ORTUNO, M. I., ESCOTE, X., CEPERUELO-MALLAFRE, V., GARRIDO-SANCHEZ, L., MIRANDA, M., CLEMENTE-POSTIGO, M., PEREZ-PEREZ, R., PERAL, B., CARDONA, F., FERNANDEZ-REAL, J. M., TINAHONES, F. J. & VENDRELL, J. 2012. FABP4 Dynamics in Obesity: Discrepancies in Adipose Tissue and Liver Expression Regarding Circulating Plasma Levels. *PLoS One.,* 7**,** e48605. doi: 10.1371/journal.pone.0048605. Epub 2012 Nov 5.

RACANELLI, V. & REHERMANN, B. 2006. The liver as an immunological organ. *Hepatology.,* 43**,** S54-62.

RADDATZ, D. & RAMADORI, G. 2007. Carbohydrate metabolism and the liver: actual aspects from physiology and disease. *Z Gastroenterol.,* 45**,** 51-62.

RAJU, T. N. 1999. The Nobel Chronicles. 1947: Carl Ferdinand Cori (1896-1984); Gerty Theresa Radnitz Cori (1896-1957); and Bernardo Alberto Houssay (1887-1971). *Lancet.,* 353**,** 1108.

RAKHA, E. A., ADAMSON, L., BELL, E., NEAL, K., RYDER, S. D., KAYE, P. V. & AITHAL, G. P. 2010. Portal inflammation is associated with advanced histological changes in alcoholic and non-alcoholic fatty liver disease. *J Clin Pathol.,* 63**,** 790-5. doi: 10.1136/jcp.2010.079145.

RAO, M. S., PAPREDDY, K., MUSUNURI, S. & OKONKWO, A. 2002. Prevention/reversal of choline deficiency-induced steatohepatitis by a peroxisome proliferator-activated receptor alpha ligand in rats. *In Vivo.,* 16**,** 145-52.

RAPPAPORT, A. M., BOROWY, Z. J., LOUGHEED, W. M. & LOTTO, W. N. 1954. Subdivision of hexagonal liver lobules into a structural and functional unit; role in hepatic physiology and pathology. *Anat Rec.,* 119**,** 11-33.

RASHID, M. & ROBERTS, E. A. 2000. Nonalcoholic steatohepatitis in children. *J Pediatr Gastroenterol Nutr.,* 30**,** 48-53.

RATZIU, V., DE LEDINGHEN, V., OBERTI, F., MATHURIN, P., WARTELLE-BLADOU, C., RENOU, C., SOGNI, P., MAYNARD, M., LARREY, D., SERFATY, L., BONNEFONT-ROUSSELOT, D., BASTARD, J. P., RIVIERE, M. & SPENARD, J. 2011. A randomized controlled trial of high-dose ursodesoxycholic acid for nonalcoholic steatohepatitis. *J Hepatol.,* 54**,** 1011-9. doi: 10.1016/j.jhep.2010.08.030. Epub 2010 Oct 31.

RATZIU, V., GIRAL, P., CHARLOTTE, F., BRUCKERT, E., THIBAULT, V., THEODOROU, I., KHALIL, L., TURPIN, G., OPOLON, P. & POYNARD, T. 2000. Liver fibrosis in overweight patients. *Gastroenterology.,* 118**,** 1117-23.

RAUTOU, P. E., MANSOURI, A., LEBREC, D., DURAND, F., VALLA, D. & MOREAU, R. 2010. Autophagy in liver diseases. *J Hepatol.,* 53**,** 1123-34. doi: 10.1016/j.jhep.2010.07.006. Epub 2010 Aug 1.

RAZANI, B., COMBS, T. P., WANG, X. B., FRANK, P. G., PARK, D. S., RUSSELL, R. G., LI, M., TANG, B., JELICKS, L. A., SCHERER, P. E. & LISANTI, M. P. 2002. Caveolin-1-deficient mice are lean, resistant to diet-induced obesity, and show hypertriglyceridemia with adipocyte abnormalities. *J Biol Chem.,* 277**,** 8635-47. Epub 2001 Dec 5.

REAVEN, G. M. 1988. Banting lecture 1988. Role of insulin resistance in human disease. *Diabetes.,* 37**,** 1595-607.

REAVEN, G. M. 1993. Role of insulin resistance in human disease (syndrome X): an expanded definition. *Annu Rev Med.,* 44**,** 121-31.

REDDY, J. K. & HASHIMOTO, T. 2001. Peroxisomal beta-oxidation and peroxisome proliferator-activated receptor alpha: an adaptive metabolic system. *Annu Rev Nutr.,* 21**,** 193-230.

REDDY, J. K. & RAO, M. S. 2006. Lipid metabolism and liver inflammation. II. Fatty liver disease and fatty acid oxidation. *Am J Physiol Gastrointest Liver Physiol.,* 290**,** G852-8.

RESHETNYAK, V. I. 2006. Concept on the pathogenesis and treatment of primary biliary cirrhosis. *World J Gastroenterol.,* 12**,** 7250-62.

REYNAERT, H., URBAIN, D. & GEERTS, A. 2008. Regulation of sinusoidal perfusion in portal hypertension. *Anat Rec (Hoboken).* 291**,** 693-8. doi: 10.1002/ar.20669.

REYZER, M. L. & CAPRIOLI, R. M. 2007. MALDI-MS-based imaging of small molecules and proteins in tissues. *Curr Opin Chem Biol.,* 11**,** 29-35. Epub 2006 Dec 20.

RIBEIRO, P. S., CORTEZ-PINTO, H., SOLA, S., CASTRO, R. E., RAMALHO, R. M., BAPTISTA, A., MOURA, M. C., CAMILO, M. E. & RODRIGUES, C. M. 2004. Hepatocyte apoptosis, expression of death receptors, and activation of NF-kappaB in the liver of nonalcoholic and alcoholic steatohepatitis patients. *Am J Gastroenterol.,* 99**,** 1708-17.

RICCHI, M., ODOARDI, M. R., CARULLI, L., ANZIVINO, C., BALLESTRI, S., PINETTI, A., FANTONI, L. I., MARRA, F., BERTOLOTTI, M., BANNI, S., LONARDO, A., CARULLI, N. & LORIA, P. 2009. Differential effect of oleic and palmitic acid on lipid accumulation and apoptosis in cultured hepatocytes. *J Gastroenterol Hepatol.,* 24**,** 830-40. doi: 10.1111/j.1440-1746.2008.05733.x. Epub 2009 Jan 13.

RINELLA, M. E., ELIAS, M. S., SMOLAK, R. R., FU, T., BORENSZTAJN, J. & GREEN, R. M. 2008. Mechanisms of hepatic steatosis in mice fed a lipogenic methionine choline-deficient diet*. *J Lipid Res.,* 49**,** 1068-76.

RING, A., LE LAY, S., POHL, J., VERKADE, P. & STREMMEL, W. 2006. Caveolin-1 is required for fatty acid translocase (FAT/CD36) localization and function at the plasma membrane of mouse embryonic fibroblasts. *Biochim Biophys Acta.,* 1761**,** 416-23. Epub 2006 Apr 19.

RIVAL, Y., STENNEVIN, A., PUECH, L., ROUQUETTE, A., CATHALA, C., LESTIENNE, F., DUPONT-PASSELAIGUE, E., PATOISEAU, J. F., WURCH, T. & JUNQUERO, D. 2004. Human adipocyte fatty acid-binding protein (aP2) gene promoter-driven reporter assay discriminates nonlipogenic peroxisome proliferator-activated receptor gamma ligands. *J Pharmacol Exp Ther.,* 311**,** 467-75. Epub 2004 Jul 23.

ROCKALL, A. G., SOHAIB, S. A., EVANS, D., KALTSAS, G., ISIDORI, A. M., MONSON, J. P., BESSER, G. M., GROSSMAN, A. B. & REZNEK, R. H.

2003. Hepatic steatosis in Cushing's syndrome: a radiological assessment using computed tomography. *Eur J Endocrinol.,* 149**,** 543-8.

RODRIGUEZ, M. J., SAURA, J., BILLETT, E. E., FINCH, C. C. & MAHY, N. 2001. Cellular localization of monoamine oxidase A and B in human tissues outside of the central nervous system. *Cell Tissue Res.,* 304**,** 215-20.

RODRIGUEZ-SUAREZ, E., DUCE, A. M., CABALLERIA, J., MARTINEZ ARRIETA, F., FERNANDEZ, E., GOMARA, C., ALKORTA, N., ARIZ, U., MARTINEZ-CHANTAR, M. L., LU, S. C., ELORTZA, F. & MATO, J. M. 2010. Non-alcoholic fatty liver disease proteomics. *Proteomics Clin Appl.,* 4**,** 362-71. doi: 10.1002/prca.200900119. Epub 2010 Feb 3.

ROH, M. S., JEONG, J. S., KIM, Y. H., KIM, M. C. & HONG, S. H. 2004. Diagnostic utility of GLUT1 in the differential diagnosis of liver carcinomas. *Hepatogastroenterology.,* 51**,** 1315-8.

ROHNER, T. C., STAAB, D. & STOECKLI, M. 2005. MALDI mass spectrometric imaging of biological tissue sections. *Mech Ageing Dev.,* 126**,** 177-85.

RONIS, M. J., BAUMGARDNER, J. N., SHARMA, N., VANTREASE, J., FERGUSON, M., TONG, Y., WU, X., CLEVES, M. A. & BADGER, T. M. 2013. Medium chain triglycerides dose-dependently prevent liver pathology in a rat model of non-alcoholic fatty liver disease. *Exp Biol Med (Maywood).* 238**,** 151-62. doi: 10.1258/ebm.2012.012303.

ROS-BARO, A., LOPEZ-IGLESIAS, C., PEIRO, S., BELLIDO, D., PALACIN, M., ZORZANO, A. & CAMPS, M. 2001. Lipid rafts are required for GLUT4 internalization in adipose cells. *Proc Natl Acad Sci U S A.,* 98**,** 12050-5. Epub 2001 Oct 2.

RUDERMAN, N., CHISHOLM, D., PI-SUNYER, X. & SCHNEIDER, S. 1998. The metabolically obese, normal-weight individual revisited. *Diabetes.,* 47**,** 699-713.

SALMI, M. & JALKANEN, S. 1992. A 90-kilodalton endothelial cell molecule mediating lymphocyte binding in humans. *Science.,* 257**,** 1407-9.

SALMI, M. & JALKANEN, S. 2001. VAP-1: an adhesin and an enzyme. *Trends Immunol.,* 22**,** 211-6.

SALMI, M. & JALKANEN, S. 2006. Developmental regulation of the adhesive and enzymatic activity of vascular adhesion protein-1 (VAP-1) in humans. *Blood.,* 108**,** 1555-61. Epub 2006 Mar 23.

SALMI, M., KALIMO, K. & JALKANEN, S. 1993. Induction and function of vascular adhesion protein-1 at sites of inflammation. *J Exp Med.,* 178**,** 2255-60.

SALMI, M., STOLEN, C., JOUSILAHTI, P., YEGUTKIN, G. G., TAPANAINEN, P., JANATUINEN, T., KNIP, M., JALKANEN, S. & SALOMAA, V. 2002. Insulin-regulated increase of soluble vascular adhesion protein-1 in diabetes. *Am J Pathol.,* 161**,** 2255-62.

SALMI, M., YEGUTKIN, G. G., LEHVONEN, R., KOSKINEN, K., SALMINEN, T. & JALKANEN, S. 2001. A cell surface amine oxidase directly controls lymphocyte migration. *Immunity.,* 14**,** 265-76.

SAMUEL, V. T., PETERSEN, K. F. & SHULMAN, G. I. 2010. Lipid-induced insulin resistance: unravelling the mechanism. *Lancet.,* 375**,** 2267-77. doi: 10.1016/S0140-6736(10)60408-4.

SANDOVAL, A., FRAISL, P., ARIAS-BARRAU, E., DIRUSSO, C. C., SINGER, D., SEALLS, W. & BLACK, P. N. 2008. Fatty acid transport and activation

and the expression patterns of genes involved in fatty acid trafficking. *Arch Biochem Biophys.,* 477**,** 363-71. Epub 2008 Jun 20.

SANYAL, A. J., CAMPBELL-SARGENT, C., MIRSHAHI, F., RIZZO, W. B., CONTOS, M. J., STERLING, R. K., LUKETIC, V. A., SHIFFMAN, M. L. & CLORE, J. N. 2001. Nonalcoholic steatohepatitis: association of insulin resistance and mitochondrial abnormalities. *Gastroenterology.,* 120**,** 1183-92.

SCHAFFERT, C. S., DURYEE, M. J., BENNETT, R. G., DEVENEY, A. L., TUMA, D. J., OLINGA, P., EASTERLING, K. C., THIELE, G. M. & KLASSEN, L. W. 2010. Exposure of precision-cut rat liver slices to ethanol accelerates fibrogenesis. *Am J Physiol Gastrointest Liver Physiol.,* 299**,** G661-8. doi: 10.1152/ajpgi.00287.2009. Epub 2010 Jul 1.

SCHEEPERS, A., JOOST, H. G. & SCHURMANN, A. 2004. The glucose transporter families SGLT and GLUT: molecular basis of normal and aberrant function. *JPEN J Parenter Enteral Nutr.,* 28**,** 364-71.

SCHEJA, L., MAKOWSKI, L., UYSAL, K. T., WIESBROCK, S. M., SHIMSHEK, D. R., MEYERS, D. S., MORGAN, M., PARKER, R. A. & HOTAMISLIGIL, G. S. 1999. Altered insulin secretion associated with reduced lipolytic efficiency in aP2-/- mice. *Diabetes.,* 48**,** 1987-94.

SCHERER, P. E., LISANTI, M. P., BALDINI, G., SARGIACOMO, M., MASTICK, C. C. & LODISH, H. F. 1994. Induction of caveolin during adipogenesis and association of GLUT4 with caveolin-rich vesicles. *J Cell Biol.,* 127**,** 1233-43.

SCHILLER, J., SUSS, R., FUCHS, B., MULLER, M., PETKOVIC, M., ZSCHORNIG, O. & WASCHIPKY, H. 2007. The suitability of different DHB isomers as matrices for the MALDI-TOF MS analysis of phospholipids: which isomer for what purpose? *Eur Biophys J.,* 36**,** 517-27. Epub 2006 Sep 20.

SCHILLER, J., ZSCHORNIG, O., PETKOVIC, M., MULLER, M., ARNHOLD, J. & ARNOLD, K. 2001. Lipid analysis of human HDL and LDL by MALDI-TOF mass spectrometry and (31)P-NMR. *J Lipid Res.,* 42**,** 1501-8.

SCHIRMER, M. A. & PHINNEY, S. D. 2007. Gamma-linolenate reduces weight regain in formerly obese humans. *J Nutr.,* 137**,** 1430-5.

SCHMITTGEN, T. D. & LIVAK, K. J. 2008. Analyzing real-time PCR data by the comparative C(T) method. *Nat Protoc.,* 3**,** 1101-8.

SCHURMANN, A., AXER, H., SCHEEPERS, A., DOEGE, H. & JOOST, H. G. 2002. The glucose transport facilitator GLUT8 is predominantly associated with the acrosomal region of mature spermatozoa. *Cell Tissue Res.,* 307**,** 237-42. Epub 2002 Jan 16.

SCHWARTZ, S. A., REYZER, M. L. & CAPRIOLI, R. M. 2003. Direct tissue analysis using matrix-assisted laser desorption/ionization mass spectrometry: practical aspects of sample preparation. *J Mass Spectrom.,* 38**,** 699-708.

SCHWENK, R. W., DIRKX, E., COUMANS, W. A., BONEN, A., KLIP, A., GLATZ, J. F. & LUIKEN, J. J. 2010. Requirement for distinct vesicle-associated membrane proteins in insulin- and AMP-activated protein kinase (AMPK)-induced translocation of GLUT4 and CD36 in cultured cardiomyocytes. *Diabetologia.,* 53**,** 2209-19. doi: 10.1007/s00125-010-1832-7. Epub 2010 Jun 26.

SCHWIMMER, J. B., BEHLING, C., NEWBURY, R., DEUTSCH, R., NIEVERGELT, C., SCHORK, N. J. & LAVINE, J. E. 2005. Histopathology of pediatric nonalcoholic fatty liver disease. *Hepatology.,* 42**,** 641-9.

SEILER, N. 2002. Ammonia and Alzheimer's disease. *Neurochem Int.,* 41**,** 189-207.

SENATES, E., COLAK, Y., YESIL, A., COSKUNPINAR, E., SAHIN, O., KAHRAMAN, O. T., ERKALMA SENATES, B. & TUNCER, I. 2012. Circulating resistin is elevated in patients with non-alcoholic fatty liver disease and is associated with steatosis, portal inflammation, insulin resistance and nonalcoholic steatohepatitis scores. *Minerva Med.,* 103**,** 369-76.

SHAH, V., TORUNER, M., HADDAD, F., CADELINA, G., PAPAPETROPOULOS, A., CHOO, K., SESSA, W. C. & GROSZMANN, R. J. 1999. Impaired endothelial nitric oxide synthase activity associated with enhanced caveolin binding in experimental cirrhosis in the rat. *Gastroenterology.,* 117**,** 1222-8.

SHAN, W. F., CHEN, B. Q., ZHU, S. J., JIANG, L. & ZHOU, Y. F. 2011. Effects of GLUT4 expression on insulin resistance in patients with advanced liver cirrhosis. *J Zhejiang Univ Sci B.,* 12**,** 677-82.

SHEILA SHERLOCK, J. D. 2002. Diseases of the liver and biliary system Chapter 1**,** P1-16.

SHEN, G. Q., LI, L., GIRELLI, D., SEIDELMANN, S. B., RAO, S., FAN, C., PARK, J. E., XI, Q., LI, J., HU, Y., OLIVIERI, O., MARCHANT, K., BARNARD, J., CORROCHER, R., ELSTON, R., CASSANO, J., HENDERSON, S., HAZEN, S. L., PLOW, E. F., TOPOL, E. J. & WANG, Q. K. 2007. An LRP8 variant is associated with familial and premature coronary artery disease and myocardial infarction. *Am J Hum Genet.,* 81**,** 780-91. Epub 2007 Aug 31.

SHEN, G. Q., LI, L. & WANG, Q. K. 2012. Genetic variant R952Q in LRP8 is associated with increased plasma triglyceride levels in patients with early-onset CAD and MI. *Ann Hum Genet.,* 76**,** 193-9. doi: 10.1111/j.1469-1809.2012.00705.x. Epub 2012 Mar 8.

SHETTY, S., WESTON, C. J., OO, Y. H., WESTERLUND, N., STAMATAKI, Z., YOUSTER, J., HUBSCHER, S. G., SALMI, M., JALKANEN, S., LALOR, P. F. & ADAMS, D. H. 2011. Common lymphatic endothelial and vascular endothelial receptor-1 mediates the transmigration of regulatory T cells across human hepatic sinusoidal endothelium. *J Immunol.,* 186**,** 4147-55. doi: 10.4049/jimmunol.1002961. Epub 2011 Mar 2.

SHIMADA, M., KAWAHARA, H., OZAKI, K., FUKURA, M., YANO, H., TSUCHISHIMA, M., TSUTSUMI, M. & TAKASE, S. 2007. Usefulness of a combined evaluation of the serum adiponectin level, HOMA-IR, and serum type IV collagen 7S level to predict the early stage of nonalcoholic steatohepatitis. *Am J Gastroenterol.,* 102**,** 1931-8. Epub 2007 May 19.

SHINODA, Y., SUZUKI, T., SUGAWARA-YOKOO, M., NAGAMATSU, S., KUWANO, H. & TAKATA, K. Expression of Sugar Transporters by In Vivo Electroporation and Particle Gun Methods in the Rat Liver : Localization to Specific Membrane Domains.

SHRIVAS, K., HAYASAKA, T., GOTO-INOUE, N., SUGIURA, Y., ZAIMA, N. & SETOU, M. 2010. Ionic Matrix for Enhanced MALDI Imaging Mass Spectrometry for Identification of Phospholipids in Mouse Liver and Cerebellum Tissue Sections. *Anal Chem,* 12**,** 12.

SIEGEL, R. C., CHEN, K. H., GREENSPAN, J. S. & AGUIAR, J. M. 1978. Biochemical and immunochemical study of lysyl oxidase in experimental hepatic fibrosis in the rat. *Proc Natl Acad Sci U S A.,* 75**,** 2945-9.

SINGH, R., KAUSHIK, S., WANG, Y., XIANG, Y., NOVAK, I., KOMATSU, M., TANAKA, K., CUERVO, A. M. & CZAJA, M. J. 2009. Autophagy regulates

lipid metabolism. *Nature.,* 458**,** 1131-5. doi: 10.1038/nature07976. Epub 2009 Apr 1.

SIREK, A. S., LIU, L., NAPLES, M., ADELI, K., NG, D. S. & JIN, T. 2009. Insulin stimulates the expression of carbohydrate response element binding protein (ChREBP) by attenuating the repressive effect of Pit-1, Oct-1/Oct-2, and Unc-86 homeodomain protein octamer transcription factor-1. *Endocrinology.,* 150**,** 3483-92. doi: 10.1210/en.2008-1702. Epub 2009 Apr 9.

SLATTER, D. A., BOLTON, C. H. & BAILEY, A. J. 2000. The importance of lipid-derived malondialdehyde in diabetes mellitus. *Diabetologia.,* 43**,** 550-7.

SMITH, D. J., SALMI, M., BONO, P., HELLMAN, J., LEU, T. & JALKANEN, S. 1998. Cloning of vascular adhesion protein 1 reveals a novel multifunctional adhesion molecule. *J Exp Med.,* 188**,** 17-27.

SMITH-MUNGO, L. I. & KAGAN, H. M. 1998. Lysyl oxidase: properties, regulation and multiple functions in biology. *Matrix Biol.,* 16**,** 387-98.

SMITS, M. M., IOANNOU, G. N., BOYKO, E. J. & UTZSCHNEIDER, K. M. 2013. Non-Alcoholic Fatty Liver Disease as an Independent Manifestation of the Metabolic Syndrome: Results of a U.S. National Survey in Three Ethnic Groups. *J Gastroenterol Hepatol,* 3**,** 12106.

SOLGA, S. F., ALKHURAISHE, A., COPE, K., TABESH, A., CLARK, J. M., TORBENSON, M., SCHWARTZ, P., MAGNUSON, T., DIEHL, A. M. & RISBY, T. H. 2006. Breath biomarkers and non-alcoholic fatty liver disease: preliminary observations. *Biomarkers.,* 11**,** 174-83.

SOLGA, S. F. & DIEHL, A. M. 2003. Non-alcoholic fatty liver disease: lumen-liver interactions and possible role for probiotics. *J Hepatol.,* 38**,** 681-7.

SOUTO, R. P., VALLEGA, G., WHARTON, J., VINTEN, J., TRANUM-JENSEN, J. & PILCH, P. F. 2003. Immunopurification and characterization of rat adipocyte caveolae suggest their dissociation from insulin signaling. *J Biol Chem.,* 278**,** 18321-9. Epub 2003 Mar 11.

SPARVERO, L. J., AMOSCATO, A. A., DIXON, C. E., LONG, J. B., KOCHANEK, P. M., PITT, B. R., BAYIR, H. & KAGAN, V. E. 2012. Mapping of phospholipids by MALDI imaging (MALDI-MSI): realities and expectations. *Chem Phys Lipids.,* 165**,** 545-62. doi: 10.1016/j.chemphyslip.2012.06.001. Epub 2012 Jun 9.

SPOLARICS, Z., PEKALA, P. H., BAGBY, G. J. & SPITZER, J. J. 1993. Brief endotoxemia markedly increases expression of GLUT1 glucose transporter in Kupffer, hepatic endothelial and parenchymal cells. *Biochem Biophys Res Commun.,* 193**,** 1211-5.

STACHOWSKA, E., GUTOWSKA, I., DOLEGOWSKA, B., CHLUBEK, D., BOBER, J., RAC, M., GUTOWSKI, P., SZUMILOWICZ, H. & TUROWSKI, R. 2004. Exchange of unsaturated fatty acids between adipose tissue and atherosclerotic plaque studied with artificial neural networks. *Prostaglandins Leukot Essent Fatty Acids.,* 70**,** 59-66.

STAHL, A., EVANS, J. G., PATTEL, S., HIRSCH, D. & LODISH, H. F. 2002. Insulin causes fatty acid transport protein translocation and enhanced fatty acid uptake in adipocytes. *Dev Cell.,* 2**,** 477-88.

STAHL, A., GIMENO, R. E., TARTAGLIA, L. A. & LODISH, H. F. 2001. Fatty acid transport proteins: a current view of a growing family. *Trends Endocrinol Metab.,* 12**,** 266-73.

STARLEY, B. Q., CALCAGNO, C. J. & HARRISON, S. A. 2010. Nonalcoholic fatty liver disease and hepatocellular carcinoma: a weighty connection. *Hepatology.,* 51**,** 1820-32. doi: 10.1002/hep.23594.

STEJSKAL, D. & KARPISEK, M. 2006. Adipocyte fatty acid binding protein in a Caucasian population: a new marker of metabolic syndrome? *Eur J Clin Invest.,* 36**,** 621-5.

STEVEN, R. T. & BUNCH, J. 2013. Repeat MALDI MS imaging of a single tissue section using multiple matrices and tissue washes. *Anal Bioanal Chem,* 21**,** 21.

STIRPE, F., DELLA CORTE, E., BONETTI, E., ABBONDANZA, A., ABBATI, A. & DE STEFANO, F. 1970. Fructose-induced hyperuricaemia. *Lancet.,* 2**,** 1310-1.

STOECKLI, M., STAAB, D., STAUFENBIEL, M., WIEDERHOLD, K. H. & SIGNOR, L. 2002. Molecular imaging of amyloid beta peptides in mouse brain sections using mass spectrometry. *Anal Biochem.,* 311**,** 33-9.

STOLEN, C. M., MADANAT, R., MARTI, L., KARI, S., YEGUTKIN, G. G., SARIOLA, H., ZORZANO, A. & JALKANEN, S. 2004a. Semicarbazide sensitive amine oxidase overexpression has dual consequences: insulin mimicry and diabetes-like complications. *Faseb J.,* 18**,** 702-4. Epub 2004 Feb 20.

STOLEN, C. M., YEGUTKIN, G. G., KURKIJARVI, R., BONO, P., ALITALO, K. & JALKANEN, S. 2004b. Origins of serum semicarbazide-sensitive amine oxidase. *Circ Res.,* 95**,** 50-7. Epub 2004 Jun 3.

STRAND, M., PERRY, J. & WANG, P. 2012. The association of metabolic syndrome with alcohol consumption among urban Chinese. *World Health Popul.,* 13**,** 5-14.

STRAUB, B. K., STOEFFEL, P., HEID, H., ZIMBELMANN, R. & SCHIRMACHER, P. 2008. Differential pattern of lipid droplet-associated proteins and de novo perilipin expression in hepatocyte steatogenesis. *Hepatology.,* 47**,** 1936-46. doi: 10.1002/hep.22268.

STROLIN BENEDETTI, M., TIPTON, K. F. & WHOMSLEY, R. 2007. Amine oxidases and monooxygenases in the in vivo metabolism of xenobiotic amines in humans: has the involvement of amine oxidases been neglected? *Fundam Clin Pharmacol.,* 21**,** 467-80.

STUART, C. A., HOWELL, M. E., ZHANG, Y. & YIN, D. 2009. Insulin-stimulated translocation of glucose transporter (GLUT) 12 parallels that of GLUT4 in normal muscle. *J Clin Endocrinol Metab.,* 94**,** 3535-42. Epub 2009 Jun 23.

STURLEY, S. L. & HUSSAIN, M. M. 2012. Lipid droplet formation on opposing sides of the endoplasmic reticulum. *J Lipid Res.,* 53**,** 1800-10. doi: 10.1194/jlr.R028290. Epub 2012 Jun 14.

SUBRA, C., FONTANA, E., VISENTIN, V., TESTAR, X. & CARPENE, C. 2003. Tyramine and benzylamine partially but selectively mimic insulin action on adipose differentiation in 3T3-L1 cells. *J Physiol Biochem.,* 59**,** 209-16.

SUMMERS, S. A. 2006. Ceramides in insulin resistance and lipotoxicity. *Prog Lipid Res.,* 45**,** 42-72. Epub 2005 Dec 19.

SUNAMI, Y., LEITHAUSER, F., GUL, S., FIEDLER, K., GULDIKEN, N., ESPENLAUB, S., HOLZMANN, K. H., HIPP, N., SINDRILARU, A., LUEDDE, T., BAUMANN, B., WISSEL, S., KREPPEL, F., SCHNEIDER, M., SCHARFFETTER-KOCHANEK, K., KOCHANEK, S., STRNAD, P. & WIRTH, T. 2012. Hepatic activation of IKK/NFkappaB signaling induces

liver fibrosis via macrophage-mediated chronic inflammation. *Hepatology.*, 56**,** 1117-28. doi: 10.1002/hep.25711. Epub 2012 Jul 10.

SUNG, R. Y., TONG, P. C., YU, C. W., LAU, P. W., MOK, G. T., YAM, M. C., LAM, P. K. & CHAN, J. C. 2003. High prevalence of insulin resistance and metabolic syndrome in overweight/obese preadolescent Hong Kong Chinese children aged 9-12 years. *Diabetes Care.*, 26**,** 250-1.

SURIN, B., SACHON, E., ROUGIER, J. P., STEVERLYNCK, C., GARREAU, C., LELONGT, B., RONCO, P. & PIEDAGNEL, R. 2013. LG3 fragment of endorepellin is a possible biomarker of severity in IgA nephropathy. *Proteomics.*, 13**,** 142-52. doi: 10.1002/pmic.201200267. Epub 2012 Dec 18.

SUTHERLAND, A. G., ALEXANDER, D. A. & HUTCHISON, J. D. 2003. Disturbance of pro-inflammatory cytokines in post-traumatic psychopathology. *Cytokine.*, 24**,** 219-25.

SUTHERLAND, J. P., MCKINLEY, B. & ECKEL, R. H. 2004. The metabolic syndrome and inflammation. *Metab Syndr Relat Disord.*, 2**,** 82-104. doi: 10.1089/met.2004.2.82.

TACKE, F. & YONEYAMA, H. 2013. From NAFLD to NASH to fibrosis to HCC: Role of dendritic cell (DC) populations in the liver. *Hepatology,* 20**,** 26405.

TAKAHASHI, Y., SOEJIMA, Y. & FUKUSATO, T. 2012. Animal models of nonalcoholic fatty liver disease/nonalcoholic steatohepatitis. *World J Gastroenterol.,* 18**,** 2300-8. doi: 10.3748/wjg.v18.i19.2300.

TAKANAGA, H., CHAUDHURI, B. & FROMMER, W. B. 2008. GLUT1 and GLUT9 as major contributors to glucose influx in HepG2 cells identified by a high sensitivity intramolecular FRET glucose sensor. *Biochim Biophys Acta.*, 1778**,** 1091-9. Epub 2007 Dec 14.

TAKATA, K., KASAHARA, T., KASAHARA, M., EZAKI, O. & HIRANO, H. 1990. Erythrocyte/HepG2-type glucose transporter is concentrated in cells of blood-tissue barriers. *Biochem Biophys Res Commun.,* 173**,** 67-73.

TAL, M., KAHN, B. B. & LODISH, H. F. 1991. Expression of the low Km GLUT-1 glucose transporter is turned on in perivenous hepatocytes of insulin-deficient diabetic rats. *Endocrinology.,* 129**,** 1933-41.

TAN, N. S., SHAW, N. S., VINCKENBOSCH, N., LIU, P., YASMIN, R., DESVERGNE, B., WAHLI, W. & NOY, N. 2002. Selective cooperation between fatty acid binding proteins and peroxisome proliferator-activated receptors in regulating transcription. *Mol Cell Biol.,* 22**,** 5114-27.

TANABE, K. K., LEMOINE, A., FINKELSTEIN, D. M., KAWASAKI, H., FUJII, T., CHUNG, R. T., LAUWERS, G. Y., KULU, Y., MUZIKANSKY, A., KURUPPU, D., LANUTI, M., GOODWIN, J. M., AZOULAY, D. & FUCHS, B. C. 2008. Epidermal growth factor gene functional polymorphism and the risk of hepatocellular carcinoma in patients with cirrhosis. *Jama.,* 299**,** 53-60. doi: 10.1001/jama.2007.65.

TANG, Y. & CHEN, A. 2010. Curcumin prevents leptin raising glucose levels in hepatic stellate cells by blocking translocation of glucose transporter-4 and increasing glucokinase. *Br J Pharmacol.,* 161**,** 1137-49. doi: 10.1111/j.1476-5381.2010.00956.x.

TARGHER, G., BERTOLINI, L., RODELLA, S., ZOPPINI, G., SCALA, L., ZENARI, L. & FALEZZA, G. 2006. Associations between plasma adiponectin concentrations and liver histology in patients with nonalcoholic fatty liver disease. *Clin Endocrinol (Oxf).* 64**,** 679-83.

TERRAND, J., BRUBAN, V., ZHOU, L., GONG, W., EL ASMAR, Z., MAY, P., ZURHOVE, K., HAFFNER, P., PHILIPPE, C., WOLDT, E., MATZ, R. L., GRACIA, C., METZGER, D., AUWERX, J., HERZ, J. & BOUCHER, P. 2009. LRP1 controls intracellular cholesterol storage and fatty acid synthesis through modulation of Wnt signaling. *J Biol Chem.*, 284**,** 381-8. doi: 10.1074/jbc.M806538200. Epub 2008 Nov 6.

THORENS, B., WEIR, G. C., LEAHY, J. L., LODISH, H. F. & BONNER-WEIR, S. 1990. Reduced expression of the liver/beta-cell glucose transporter isoform in glucose-insensitive pancreatic beta cells of diabetic rats. *Proc Natl Acad Sci U S A.*, 87**,** 6492-6.

TOBIN, V., LE GALL, M., FIORAMONTI, X., STOLARCZYK, E., BLAZQUEZ, A. G., KLEIN, C., PRIGENT, M., SERRADAS, P., CUIF, M. H., MAGNAN, C., LETURQUE, A. & BROT-LAROCHE, E. 2008. Insulin internalizes GLUT2 in the enterocytes of healthy but not insulin-resistant mice. *Diabetes.*, 57**,** 555-62. Epub 2007 Dec 5.

TOHKA, S., LAUKKANEN, M., JALKANEN, S. & SALMI, M. 2001. Vascular adhesion protein 1 (VAP-1) functions as a molecular brake during granulocyte rolling and mediates recruitment in vivo. *Faseb J.*, 15**,** 373-82.

TOLOSA, L., GOMEZ-LECHON, M. J., PEREZ-CATALDO, G., CASTELL, J. V. & DONATO, M. T. 2013. HepG2 cells simultaneously expressing five P450 enzymes for the screening of hepatotoxicity: identification of bioactivable drugs and the potential mechanism of toxicity involved. *Arch Toxicol,* 9**,** 9.

TOLWANI, R. J., HAMM, D. A., TIAN, L., SHARER, J. D., VOCKLEY, J., RINALDO, P., MATERN, D., SCHOEB, T. R. & WOOD, P. A. 2005. Medium-chain acyl-CoA dehydrogenase deficiency in gene-targeted mice. *PLoS Genet.*, 1**,** e23. Epub 2005 Aug 19.

TOMINAGA, K., KURATA, J. H., CHEN, Y. K., FUJIMOTO, E., MIYAGAWA, S., ABE, I. & KUSANO, Y. 1995. Prevalence of fatty liver in Japanese children and relationship to obesity. An epidemiological ultrasonographic survey. *Dig Dis Sci.,* 40**,** 2002-9.

TOMLINSON, J. W., FINNEY, J., GAY, C., HUGHES, B. A., HUGHES, S. V. & STEWART, P. M. 2008. Impaired glucose tolerance and insulin resistance are associated with increased adipose 11beta-hydroxysteroid dehydrogenase type 1 expression and elevated hepatic 5alpha-reductase activity. *Diabetes.,* 57**,** 2652-60. doi: 10.2337/db08-0495. Epub 2008 Jul 15.

TORRES, D. M. & HARRISON, S. A. 2012. Nonalcoholic steatohepatitis and noncirrhotic hepatocellular carcinoma: fertile soil. *Semin Liver Dis.,* 32**,** 30-8. doi: 10.1055/s-0032-1306424. Epub 2012 Mar 13.

TORSTENSEN, B. E., ESPE, M., STUBHAUG, I. & LIE, O. 2011. Dietary plant proteins and vegetable oil blends increase adiposity and plasma lipids in Atlantic salmon (Salmo salar L.). *Br J Nutr.,* 106**,** 633-47. doi: 10.1017/S0007114511000729. Epub 2011 May 3.

TRIGATTI, B. L., ANDERSON, R. G. & GERBER, G. E. 1999. Identification of caveolin-1 as a fatty acid binding protein. *Biochem Biophys Res Commun.,* 255**,** 34-9.

TSO, A. W., XU, A., SHAM, P. C., WAT, N. M., WANG, Y., FONG, C. H., CHEUNG, B. M., JANUS, E. D. & LAM, K. S. 2007. Serum adipocyte fatty acid binding protein as a new biomarker predicting the development of type 2 diabetes: a 10-year prospective study in a Chinese cohort. *Diabetes Care.,* 30**,** 2667-72. Epub 2007 Jul 9.

TSUKAMOTO, H. & LU, S. C. 2001. Current concepts in the pathogenesis of alcoholic liver injury. *Faseb J.*, 15**,** 1335-49.

TSUKIOKA, M., MATSUMOTO, Y., NORIYUKI, M., YOSHIDA, C., NOBEYAMA, H., YOSHIDA, H., YASUI, T., SUMI, T., HONDA, K. & ISHIKO, O. 2007. Expression of glucose transporters in epithelial ovarian carcinoma: correlation with clinical characteristics and tumor angiogenesis. *Oncol Rep.*, 18**,** 361-7.

ULDRY, M., IBBERSON, M., HORISBERGER, J. D., CHATTON, J. Y., RIEDERER, B. M. & THORENS, B. 2001. Identification of a mammalian H(+)-myo-inositol symporter expressed predominantly in the brain. *Embo J.*, 20**,** 4467-77.

UNGER, R. H., ZHOU, Y. T. & ORCI, L. 1999. Regulation of fatty acid homeostasis in cells: novel role of leptin. *Proc Natl Acad Sci U S A.*, 96**,** 2327-32.

UTZSCHNEIDER, K. M. & KAHN, S. E. 2006. Review: The role of insulin resistance in nonalcoholic fatty liver disease. *J Clin Endocrinol Metab.*, 91**,** 4753-61. Epub 2006 Sep 12.

VADASZ, Z., KESSLER, O., AKIRI, G., GENGRINOVITCH, S., KAGAN, H. M., BARUCH, Y., IZHAK, O. B. & NEUFELD, G. 2005. Abnormal deposition of collagen around hepatocytes in Wilson's disease is associated with hepatocyte specific expression of lysyl oxidase and lysyl oxidase like protein-2. *J Hepatol.*, 43**,** 499-507.

VAN DER VEEN, J. N., LINGRELL, S. & VANCE, D. E. 2012. The membrane lipid phosphatidylcholine is an unexpected source of triacylglycerol in the liver. *J Biol Chem.*, 287**,** 23418-26. doi: 10.1074/jbc.M112.381723. Epub 2012 May 18.

VAN MIDWOUD, P. M., GROOTHUIS, G. M., MEREMA, M. T. & VERPOORTE, E. 2010a. Microfluidic biochip for the perifusion of precision-cut rat liver slices for metabolism and toxicology studies. *Biotechnol Bioeng.*, 105**,** 184-94. doi: 10.1002/bit.22516.

VAN MIDWOUD, P. M., MEREMA, M. T., VERPOORTE, E. & GROOTHUIS, G. M. 2010b. A microfluidic approach for in vitro assessment of interorgan interactions in drug metabolism using intestinal and liver slices. *Lab Chip.*, 10**,** 2778-86. doi: 10.1039/c0lc00043d. Epub 2010 Sep 7.

VAN ROOYEN, D. M., LARTER, C. Z., HAIGH, W. G., YEH, M. M., IOANNOU, G., KUVER, R., LEE, S. P., TEOH, N. C. & FARRELL, G. C. 2011. Hepatic free cholesterol accumulates in obese, diabetic mice and causes nonalcoholic steatohepatitis. *Gastroenterology.*, 141**,** 1393-403, 1403.e1-5. doi: 10.1053/j.gastro.2011.06.040. Epub 2011 Jun 23.

VEAL, E. & DAY, A. 2011. Hydrogen peroxide as a signaling molecule. *Antioxid Redox Signal.*, 15**,** 147-51. doi: 10.1089/ars.2011.3968. Epub 2011 May 25.

VEERKAMP, J. H. & VAN MOERKERK, H. T. 1993. Fatty acid-binding protein and its relation to fatty acid oxidation. *Mol Cell Biochem.*, 123**,** 101-6.

VERDAM, F. J., DALLINGA, J. W., DRIESSEN, A., DE JONGE, C., MOONEN, E. J., VAN BERKEL, J. B., LUIJK, J., BOUVY, N. D., BUURMAN, W. A., RENSEN, S. S., GREVE, J. W. & VAN SCHOOTEN, F. J. 2013. Non-alcoholic steatohepatitis: a non-invasive diagnosis by analysis of exhaled breath. *J Hepatol.*, 58**,** 543-8. doi: 10.1016/j.jhep.2012.10.030. Epub 2012 Nov 7.

VERNON, G., BARANOVA, A. & YOUNOSSI, Z. M. 2011. Systematic review: the epidemiology and natural history of non-alcoholic fatty liver disease and non-

alcoholic steatohepatitis in adults. *Aliment Pharmacol Ther.,* 34**,** 274-85. doi: 10.1111/j.1365-2036.2011.04724.x. Epub 2011 May 30.

VILA, L., ROGLANS, N., ALEGRET, M., SANCHEZ, R. M., VAZQUEZ-CARRERA, M. & LAGUNA, J. C. 2008. Suppressor of cytokine signaling-3 (SOCS-3) and a deficit of serine/threonine (Ser/Thr) phosphoproteins involved in leptin transduction mediate the effect of fructose on rat liver lipid metabolism. *Hepatology.,* 48**,** 1506-16.

VISENTIN, V., PREVOT, D., DE SAINT FRONT, V. D., MORIN-CUSSAC, N., THALAMAS, C., GALITZKY, J., VALET, P., ZORZANO, A. & CARPENE, C. 2004. Alteration of amine oxidase activity in the adipose tissue of obese subjects. *Obes Res.,* 12**,** 547-55.

VISTISEN, B., ROEPSTORFF, K., ROEPSTORFF, C., BONEN, A., VAN DEURS, B. & KIENS, B. 2004. Sarcolemmal FAT/CD36 in human skeletal muscle colocalizes with caveolin-3 and is more abundant in type 1 than in type 2 fibers. *J Lipid Res.,* 45**,** 603-9. Epub 2004 Jan 16.

VITART, V., RUDAN, I., HAYWARD, C., GRAY, N. K., FLOYD, J., PALMER, C. N., KNOTT, S. A., KOLCIC, I., POLASEK, O., GRAESSLER, J., WILSON, J. F., MARINAKI, A., RICHES, P. L., SHU, X., JANICIJEVIC, B., SMOLEJ-NARANCIC, N., GORGONI, B., MORGAN, J., CAMPBELL, S., BILOGLAV, Z., BARAC-LAUC, L., PERICIC, M., KLARIC, I. M., ZGAGA, L., SKARIC-JURIC, T., WILD, S. H., RICHARDSON, W. A., HOHENSTEIN, P., KIMBER, C. H., TENESA, A., DONNELLY, L. A., FAIRBANKS, L. D., ARINGER, M., MCKEIGUE, P. M., RALSTON, S. H., MORRIS, A. D., RUDAN, P., HASTIE, N. D., CAMPBELL, H. & WRIGHT, A. F. 2008. SLC2A9 is a newly identified urate transporter influencing serum urate concentration, urate excretion and gout. *Nat Genet.,* 40**,** 437-42. Epub 2008 Mar 9.

WADDELL, I. D., ZOMERSCHOE, A. G., VOICE, M. W. & BURCHELL, A. 1992. Cloning and expression of a hepatic microsomal glucose transport protein. Comparison with liver plasma-membrane glucose-transport protein GLUT 2. *Biochem J.,* 286**,** 173-7.

WAKASAKI, H. & OOSHIMA, A. 1990. Immunohistochemical localization of lysyl oxidase with monoclonal antibodies. *Lab Invest.,* 63**,** 377-84.

WANG, D., WEI, Y. & PAGLIASSOTTI, M. J. 2006. Saturated fatty acids promote endoplasmic reticulum stress and liver injury in rats with hepatic steatosis. *Endocrinology.,* 147**,** 943-51. Epub 2005 Nov 3.

WANG, Q., YIN, J., XU, L., CHENG, H., ZHAO, X., XIANG, H., LAM, H. S., MI, J. & LI, M. 2013. Prevalence of metabolic syndrome in a cohort of Chinese schoolchildren: comparison of two definitions and assessment of adipokines as components by factor analysis. *BMC Public Health.,* 13:249**.,** 10.1186/1471-2458-13-249.

WANG, Y., SINGH, R., XIANG, Y. & CZAJA, M. J. 2010. Macroautophagy and chaperone-mediated autophagy are required for hepatocyte resistance to oxidant stress. *Hepatology.,* 52**,** 266-77. doi: 10.1002/hep.23645.

WANG, Y., ZHU, Q., ZHAO, X. L., YAO, Y. G. & LIU, Y. P. 2011. Age-related expression profile of the SLC27A1 gene in chicken tissues. *Mol Biol Rep.,* 38**,** 5139-45. Epub 2010 Dec 24.

WATSON, M. R., WALLACE, K., GIELING, R. G., MANAS, D. M., JAFFRAY, E., HAY, R. T., MANN, D. A. & OAKLEY, F. 2008. NF-kappaB is a critical

regulator of the survival of rodent and human hepatic myofibroblasts. *J Hepatol.,* 48**,** 589-97. doi: 10.1016/j.jhep.2007.12.019. Epub 2008 Jan 31.

WATTACHERIL, J., SEELEY, E. H., ANGEL, P., CHEN, H., BOWEN, B. P., LANCIAULT, C., R, M. C., ABUMRAD, N. & FLYNN, C. R. 2013. Differential intrahepatic phospholipid zonation in simple steatosis and nonalcoholic steatohepatitis. *PLoS One.,* 8**,** e57165. doi: 10.1371/journal.pone.0057165. Epub 2013 Feb 25.

WEI, Y., WANG, D., GENTILE, C. L. & PAGLIASSOTTI, M. J. 2009. Reduced endoplasmic reticulum luminal calcium links saturated fatty acid-mediated endoplasmic reticulum stress and cell death in liver cells. *Mol Cell Biochem.,* 331**,** 31-40. doi: 10.1007/s11010-009-0142-1. Epub 2009 May 15.

WEI, Y., WANG, D., TOPCZEWSKI, F. & PAGLIASSOTTI, M. J. 2006. Saturated fatty acids induce endoplasmic reticulum stress and apoptosis independently of ceramide in liver cells. *Am J Physiol Endocrinol Metab.,* 291**,** E275-81. Epub 2006 Feb 21.

WELSH, F. A. 1972. Changes in distribution of enzymes within the liver lobule during adaptive increases. *J Histochem Cytochem.,* 20**,** 107-11.

WESTERBACKA, J., KOLAK, M., KIVILUOTO, T., ARKKILA, P., SIREN, J., HAMSTEN, A., FISHER, R. M. & YKI-JARVINEN, H. 2007. Genes involved in fatty acid partitioning and binding, lipolysis, monocyte/macrophage recruitment, and inflammation are overexpressed in the human fatty liver of insulin-resistant subjects. *Diabetes.,* 56**,** 2759-65. Epub 2007 Aug 17.

WESTON, C. J. & ADAMS, D. H. 2011. Hepatic consequences of vascular adhesion protein-1 expression. *J Neural Transm.,* 118**,** 1055-64. doi: 10.1007/s00702-011-0647-0. Epub 2011 Apr 22.

WHITE, D. L., KANWAL, F. & EL-SERAG, H. B. 2012. Association between nonalcoholic fatty liver disease and risk for hepatocellular cancer, based on systematic review. *Clin Gastroenterol Hepatol.,* 10**,** 1342-1359.e2. doi: 10.1016/j.cgh.2012.10.001. Epub 2012 Oct 4.

WICHA, M. S., LIOTTA, L. A. & KIDWELL, W. R. 1979. Effects of free fatty acids on the growth of normal and neoplastic rat mammary epithelial cells. *Cancer Res.,* 39**,** 426-35.

WIECKOWSKA, A., PAPOUCHADO, B. G., LI, Z., LOPEZ, R., ZEIN, N. N. & FELDSTEIN, A. E. 2008. Increased hepatic and circulating interleukin-6 levels in human nonalcoholic steatohepatitis. *Am J Gastroenterol.,* 103**,** 1372-9. doi: 10.1111/j.1572-0241.2007.01774.x. Epub 2008 May 28.

WILLAERT, A., KHATRI, S., CALLEWAERT, B. L., COUCKE, P. J., CROSBY, S. D., LEE, J. G., DAVIS, E. C., SHIVA, S., TSANG, M., DE PAEPE, A. & URBAN, Z. 2012. GLUT10 is required for the development of the cardiovascular system and the notochord and connects mitochondrial function to TGFbeta signaling. *Hum Mol Genet.,* 21**,** 1248-59. Epub 2011 Nov 24.

WILMOT, C. M., HAJDU, J., MCPHERSON, M. J., KNOWLES, P. F. & PHILLIPS, S. E. 1999. Visualization of dioxygen bound to copper during enzyme catalysis. *Science.,* 286**,** 1724-8.

WISHNIES, S. M., PARRISH, A. R., SIPES, I. G., GANDOLFI, A. J., PUTNAM, C. W., KRUMDIECK, C. L. & BRENDEL, K. 1991. Biotransformation activity in vitrified human liver slices. *Cryobiology.,* 28**,** 216-26.

WISSE, E. 1970. An electron microscopic study of the fenestrated endothelial lining of rat liver sinusoids. *J Ultrastruct Res.,* 31**,** 125-50.

WISSE, E., BRAET, F., LUO, D., DE ZANGER, R., JANS, D., CRABBE, E. & VERMOESEN, A. 1996. Structure and function of sinusoidal lining cells in the liver. *Toxicol Pathol.,* 24**,** 100-11.

WISSE, E., LUO, D., VERMIJLEN, D., KANELLOPOULOU, C., DE ZANGER, R. & BRAET, F. 1997. On the function of pit cells, the liver-specific natural killer cells. *Semin Liver Dis.,* 17**,** 265-86.

WOLF, A. M., WOLF, D., AVILA, M. A., MOSCHEN, A. R., BERASAIN, C., ENRICH, B., RUMPOLD, H. & TILG, H. 2006. Up-regulation of the anti-inflammatory adipokine adiponectin in acute liver failure in mice. *J Hepatol.,* 44**,** 537-43. Epub 2005 Sep 23.

WOLFRUM, C., BORRMANN, C. M., BORCHERS, T. & SPENER, F. 2001. Fatty acids and hypolipidemic drugs regulate peroxisome proliferator-activated receptors alpha - and gamma-mediated gene expression via liver fatty acid binding protein: a signaling path to the nucleus. *Proc Natl Acad Sci U S A.,* 98**,** 2323-8. Epub 2001 Feb 20.

WOUDENBERG, J., REMBACZ, K. P., VAN DEN HEUVEL, F. A., WOUDENBERG-VRENKEN, T. E., BUIST-HOMAN, M., GEUKEN, M., HOEKSTRA, M., DEELMAN, L. E., ENRICH, C., HENNING, R. H., MOSHAGE, H. & FABER, K. N. 2010. Caveolin-1 is enriched in the peroxisomal membrane of rat hepatocytes. *Hepatology.,* 51**,** 1744-53.

WU, C. T., DAVIS, P. A., LUKETIC, V. A. & GERSHWIN, M. E. 2004. A review of the physiological and immunological functions of biliary epithelial cells: targets for primary biliary cirrhosis, primary sclerosing cholangitis and drug-induced ductopenias. *Clin Dev Immunol.,* 11**,** 205-13.

WU, Q., ORTEGON, A. M., TSANG, B., DOEGE, H., FEINGOLD, K. R. & STAHL, A. 2006. FATP1 is an insulin-sensitive fatty acid transporter involved in diet-induced obesity. *Mol Cell Biol.,* 26**,** 3455-67.

WU, T., PAN, T., ZHENG, Z., CHEN, T. & PAN, Y. 2008. [Relationship between Glut-1, Glut-3 expression and fluorodeoxyglucose uptake in NSCLC and benign pulmonary lesion.]. *Zhongguo Fei Ai Za Zhi.,* 11**,** 555-8.

WUNDERLICH, M. T., HANHOFF, T., GOERTLER, M., SPENER, F., GLATZ, J. F., WALLESCH, C. W. & PELSERS, M. M. 2005. Release of brain-type and heart-type fatty acid-binding proteins in serum after acute ischaemic stroke. *J Neurol.,* 252**,** 718-24. Epub 2005 Apr 18.

XIAO, J., HO, C. T., LIONG, E. C., NANJI, A. A., LEUNG, T. M., LAU, T. Y., FUNG, M. L. & TIPOE, G. L. 2013. Epigallocatechin gallate attenuates fibrosis, oxidative stress, and inflammation in non-alcoholic fatty liver disease rat model through TGF/SMAD, PI3 K/Akt/FoxO1, and NF-kappa B pathways. *Eur J Nutr,* 21**,** 21.

XIAO, Q. & GE, G. 2012. Lysyl oxidase, extracellular matrix remodeling and cancer metastasis. *Cancer Microenviron.,* 5**,** 261-73. doi: 10.1007/s12307-012-0105-z. Epub 2012 Apr 13.

XU, A., TSO, A. W., CHEUNG, B. M., WANG, Y., WAT, N. M., FONG, C. H., YEUNG, D. C., JANUS, E. D., SHAM, P. C. & LAM, K. S. 2007. Circulating adipocyte-fatty acid binding protein levels predict the development of the metabolic syndrome: a 5-year prospective study. *Circulation.,* 115**,** 1537-43.

XU, A., WANG, Y., KESHAW, H., XU, L. Y., LAM, K. S. & COOPER, G. J. 2003. The fat-derived hormone adiponectin alleviates alcoholic and nonalcoholic fatty liver diseases in mice. *J Clin Invest.,* 112**,** 91-100.

XU, A., WANG, Y., XU, J. Y., STEJSKAL, D., TAM, S., ZHANG, J., WAT, N. M., WONG, W. K. & LAM, K. S. 2006. Adipocyte fatty acid-binding protein is a plasma biomarker closely associated with obesity and metabolic syndrome. *Clin Chem.,* 52**,** 405-13. Epub 2006 Jan 19.

XU, C. S., JIANG, Y., ZHANG, L. X., CHANG, C. F., WANG, G. P., SHI, R. J. & YANG, Y. J. 2012. The role of Kupffer cells in rat liver regeneration revealed by cell-specific microarray analysis. *J Cell Biochem.,* 113**,** 229-37. doi: 10.1002/jcb.23348.

YAMAGUCHI, K., YANG, L., MCCALL, S., HUANG, J., YU, X. X., PANDEY, S. K., BHANOT, S., MONIA, B. P., LI, Y. X. & DIEHL, A. M. 2007. Inhibiting triglyceride synthesis improves hepatic steatosis but exacerbates liver damage and fibrosis in obese mice with nonalcoholic steatohepatitis. *Hepatology.,* 45**,** 1366-74.

YAMASHITA, H., TAKENOSHITA, M., SAKURAI, M., BRUICK, R. K., HENZEL, W. J., SHILLINGLAW, W., ARNOT, D. & UYEDA, K. 2001. A glucose-responsive transcription factor that regulates carbohydrate metabolism in the liver. *Proc Natl Acad Sci U S A.,* 98**,** 9116-21. Epub 2001 Jul 24.

YANG, L., LI, P., FU, S., CALAY, E. S. & HOTAMISLIGIL, G. S. 2010. Defective hepatic autophagy in obesity promotes ER stress and causes insulin resistance. *Cell Metab.,* 11**,** 467-78. doi: 10.1016/j.cmet.2010.04.005.

YANG, M. & BUTLER, M. 2002. Effects of ammonia and glucosamine on the heterogeneity of erythropoietin glycoforms. *Biotechnol Prog.,* 18**,** 129-38.

YANG, Y. J., HOPE, I. D., ADER, M. & BERGMAN, R. N. 1989. Insulin transport across capillaries is rate limiting for insulin action in dogs. *J Clin Invest.,* 84**,** 1620-8.

YODA-MURAKAMI, M., TANIGUCHI, M., TAKAHASHI, K., KAWAMATA, S., SAITO, K., CHOI-MIURA, N. H. & TOMITA, M. 2001. Change in expression of GBP28/adiponectin in carbon tetrachloride-administrated mouse liver. *Biochem Biophys Res Commun.,* 285**,** 372-7.

YOKOMORI, H., ODA, M., OGI, M., SAKAI, K. & ISHII, H. 2002. Enhanced expression of endothelial nitric oxide synthase and caveolin-1 in human cirrhosis. *Liver.,* 22**,** 150-8.

YOONG, K. F., MCNAB, G., HUBSCHER, S. G. & ADAMS, D. H. 1998. Vascular adhesion protein-1 and ICAM-1 support the adhesion of tumor-infiltrating lymphocytes to tumor endothelium in human hepatocellular carcinoma. *J Immunol.,* 160**,** 3978-88.

YOUNOSSI, Z. M., JARRAR, M., NUGENT, C., RANDHAWA, M., AFENDY, M., STEPANOVA, M., RAFIQ, N., GOODMAN, Z., CHANDHOKE, V. & BARANOVA, A. 2008. A novel diagnostic biomarker panel for obesity-related nonalcoholic steatohepatitis (NASH). *Obes Surg.,* 18**,** 1430-7. doi: 10.1007/s11695-008-9506-y. Epub 2008 May 24.

YRAOLA, F., GARCIA-VICENTE, S., FERNANDEZ-RECIO, J., ALBERICIO, F., ZORZANO, A., MARTI, L. & ROYO, M. 2006. New efficient substrates for semicarbazide-sensitive amine oxidase/VAP-1 enzyme: analysis by SARs and computational docking. *J Med Chem.,* 49**,** 6197-208.

YU, P. H. 1990. Oxidative deamination of aliphatic amines by rat aorta semicarbazide-sensitive amine oxidase. *J Pharm Pharmacol.,* 42**,** 882-4.

YU, P. H., DAVIS, B. A. & DENG, Y. 2001. 2-Bromoethylamine as a potent selective suicide inhibitor for semicarbazide-sensitive amine oxidase. *Biochem Pharmacol.,* 61**,** 741-8.

YU, P. H. & DENG, Y. L. 1998. Endogenous formaldehyde as a potential factor of vulnerability of atherosclerosis: involvement of semicarbazide-sensitive amine oxidase-mediated methylamine turnover. *Atherosclerosis.,* 140**,** 357-63.

YU, P. H., LAI, C. T. & ZUO, D. M. 1997. Formation of formaldehyde from adrenaline in vivo; a potential risk factor for stress-related angiopathy. *Neurochem Res.,* 22**,** 615-20.

YU, P. H., WANG, M., DENG, Y. L., FAN, H. & SHIRA-BOCK, L. 2002. Involvement of semicarbazide-sensitive amine oxidase-mediated deamination in atherogenesis in KKAy diabetic mice fed with high cholesterol diet. *Diabetologia.,* 45**,** 1255-62. Epub 2002 Aug 8.

YU, P. H., WANG, M., FAN, H., DENG, Y. & GUBISNE-HABERLE, D. 2004. Involvement of SSAO-mediated deamination in adipose glucose transport and weight gain in obese diabetic KKAy mice. *Am J Physiol Endocrinol Metab.,* 286**,** E634-41. Epub 2003 Dec 2.

ZAIMA, N., MATSUYAMA, Y. & SETOU, M. 2009. Principal component analysis of direct matrix-assisted laser desorption/ionization mass spectrometric data related to metabolites of fatty liver. *J Oleo Sci.,* 58**,** 267-73.

ZELBER-SAGI, S., NITZAN-KALUSKI, D., GOLDSMITH, R., WEBB, M., BLENDIS, L., HALPERN, Z. & OREN, R. 2007. Long term nutritional intake and the risk for non-alcoholic fatty liver disease (NAFLD): a population based study. *J Hepatol.,* 47**,** 711-7. Epub 2007 Aug 14.

ZELLNER, M., BABELUK, R., JAKOBSEN, L. H., GERNER, C., UMLAUF, E., VOLF, I., ROTH, E. & KONDRUP, J. 2011. A proteomics study reveals a predominant change in MaoB expression in platelets of healthy volunteers after high protein meat diet: relationship to the methylation cycle. *J Neural Transm.,* 118**,** 653-62. doi: 10.1007/s00702-011-0617-6. Epub 2011 Mar 20.

ZHANG, D., LEI, C. & ZHANG, W. 2011a. Up-regulated monoamine oxidase in the mouse uterus during the peri-implantation period. *Arch Gynecol Obstet.,* 284**,** 861-6. doi: 10.1007/s00404-010-1765-x. Epub 2010 Nov 24.

ZHANG, Y., DONG, L., YANG, X., SHI, H. & ZHANG, L. 2011b. alpha-Linolenic acid prevents endoplasmic reticulum stress-mediated apoptosis of stearic acid lipotoxicity on primary rat hepatocytes. *Lipids Health Dis.,* 10:81**.,** 10.1186/1476-511X-10-81.

ZHANG, Y., MAO, J., YU, P. H. & XIAO, S. 2012. A micro trapping system coupled with a high performance liquid chromatography procedure for methylamine determination in both tissue and cigarette smoke. *Anal Chim Acta.,* 752:106-11**.,** 10.1016/j.aca.2012.09.027. Epub 2012 Oct 1.

ZHAO, F. Q. & KEATING, A. F. 2007. Functional properties and genomics of glucose transporters. *Curr Genomics.,* 8**,** 113-28.

ZHOU, J., FEBBRAIO, M., WADA, T., ZHAI, Y., KURUBA, R., HE, J., LEE, J. H., KHADEM, S., REN, S., LI, S., SILVERSTEIN, R. L. & XIE, W. 2008. Hepatic fatty acid transporter Cd36 is a common target of LXR, PXR, and PPARgamma in promoting steatosis. *Gastroenterology.,* 134**,** 556-67. Epub 2007 Nov 28.

ZIMMERMAN, A. W. & VEERKAMP, J. H. 2002. New insights into the structure and function of fatty acid-binding proteins. *Cell Mol Life Sci.,* 59**,** 1096-116.

ZIMMERMAN, T. A., MONROE, E. B., TUCKER, K. R., RUBAKHIN, S. S. & SWEEDLER, J. V. 2008. Chapter 13: Imaging of cells and tissues with mass spectrometry: adding chemical information to imaging. *Methods Cell Biol.,* 89:361-90**.,** 10.1016/S0091-679X(08)00613-4.